CLIMATE CHANGE VULNERABILITY ASSESSMENT

FOR THE PANJ-AMU RIVER BASIN AFGHANISTAN

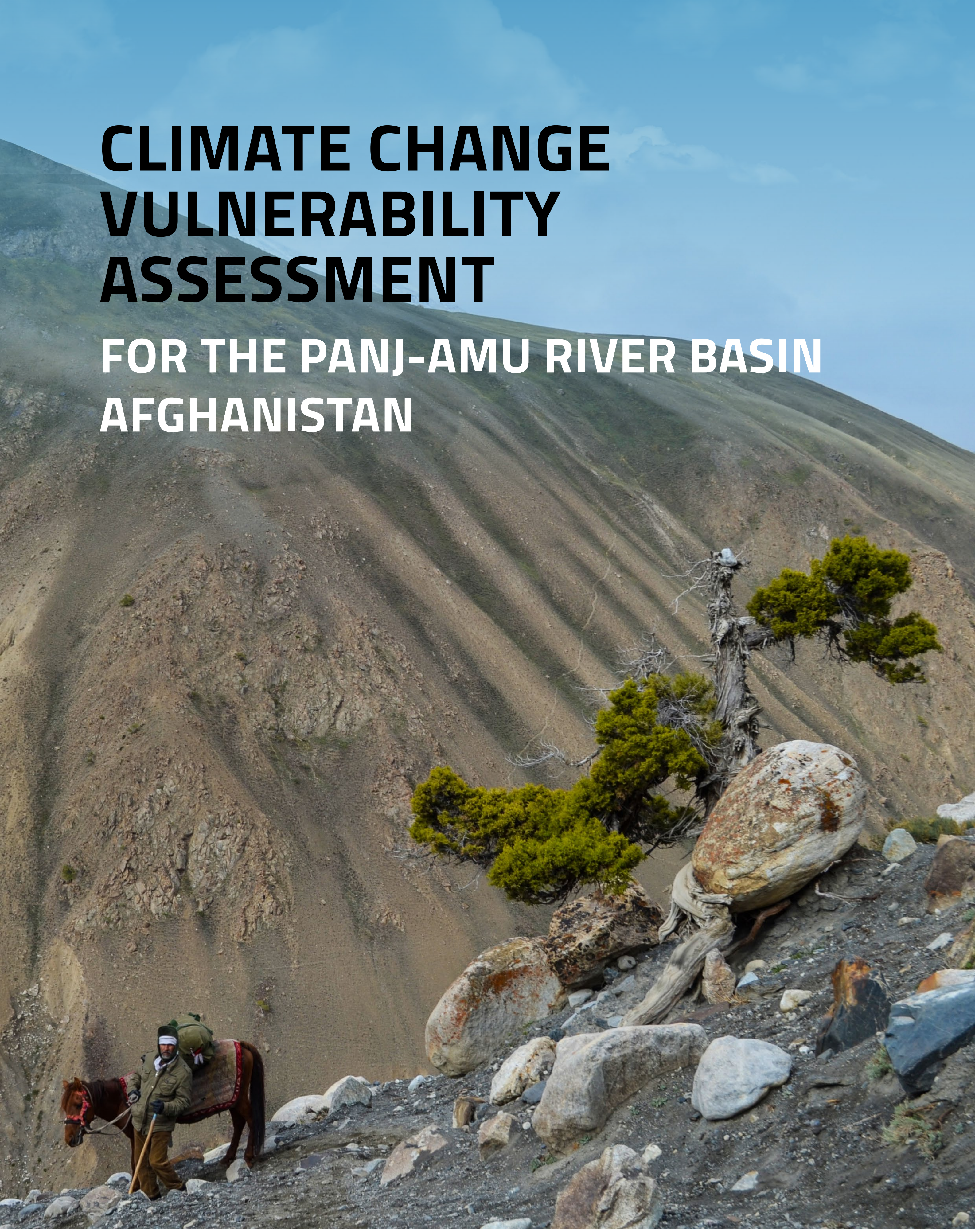

Funded by the European Union

Wildlife Conservation Society

AGA KHAN FOUNDATION

Edited by: Paul R. Elsen, Sorosh Poya Faryabi, Gautam Surya, and Hedley S. Grantham

Disclaimers:

This publication may be reproduced in whole or in part and in any form for educational or non-profit services without special permission from the copyright holder, provided acknowledgement of the source is made. The Wildlife Conservation Society would appreciate receiving a copy of any publication that uses this publication as a source.

Mention of a commercial company or product in this document does not imply endorsement by the Wildlife Conservation Society or the authors. The use of information from this document for publicity or advertising is not permitted. Trademark names and symbols are used in an editorial fashion with no intention on infringement of trademark or copyright laws.

This project was funded by the European Union. The views expressed in this publication do not necessarily reflect the views of the European Union, nor the Wildlife Conservation Society (WCS). Content in this publication developed by third parties for educational purposes does not constitute endorsement or recommendation by WCS or the European Union. We regret any errors or omissions that may have been unwittingly made.

© Maps, photos and illustrations as specified

DOI: https://doi.org/10.19121/2023.Report.45305

Design and layout: Ahmad Reza Amiri

Supporting organizations:

Columbia Climate School Center for Climate Systems Research

UCA University of Central Asia

CLIMATE CHANGE VULNERABILITY ASSESSMENT

FOR THE PANJ-AMU RIVER BASIN AFGHANISTAN

Edited by Paul R. Elsen, Sorosh Poya Faryabi, Gautam Surya, and Hedley S. Grantham

FOREWORD

The Panj-Amu River Basin (P-ARB) of northeastern Afghanistan is a spectacular landscape covering over 90,000 km^2 (approx. 14% of the area of Afghanistan). It is home to some of the world's most wondrous wildlife living alongside over 4.5 million people experiencing some of the highest rates of poverty in the country. Local communities within the P-ARB are characterized by their unique cultures and deep ties to the land. The tight bonds between the people and the landscape mean that the region's communities are heavily reliant on the P-ARB's ecosystems, biodiversity, and natural resources. More broadly, the P-ARB watersheds provide water and other critical ecological services to large swaths of Afghanistan's population. The natural and cultural significance of the P-ARB was recently codified by the creation of Band-e-Amir, Bamyan Plateau, and Wakhan National Parks, bringing both national and global recognition.

Yet climate change is poised to up-end this region and the interrelationships between local communities and the natural ecosystems on which they depend. Identified risks in the region include increases in the magnitude and frequency of natural disasters, changing water regimes, rangeland degradation caused by drought, and wildlife community shifts, among others.

The urgency of the risks posed by climate change in the P-ARB has necessitated a comprehensive evaluation of how and where climate impacts will be most acute on multiple sectors—ecosystems, hydrology, wildlife, and local communities. *The Panj-Amu River Basin Climate Change Vulnerability Assessment* presented here evaluates climate risk across all these dimensions. Tailored, downscaled climate models were specially developed to bring unprecedented detail to the evaluation and to link with impact models for these sectors and determine direct impacts from natural hazards.

While climate impacts will affect all portions of the P-ARB to some degree, provinces differ in their degree of exposure, sensitivity, and adaptive capacity, which ultimately determines their overall vulnerability to climate change. Takhar, Baghlan, and Bamyan, provinces are among the most vulnerable owing to high risks from natural hazards (particularly droughts and heat waves), low adaptive capacity of communities, widespread rangeland degradation, relative hydrological instability, and low projected stability of wildlife species, which could increase human-wildlife conflict. While Kunduz, Badakhshan, and Samangan are at relatively lower risk, they are still vulnerable to some natural hazards (particularly floods and decreased permafrost) and additional pressures on ecosystems and wildlife species.

The results of this assessment point to the clear need for action on multiple levels. This includes continuing to engage in climate mitigation measures, halting rangeland degradation and increasing ecosystem integrity, enhancing ecosystem restoration and protection, practicing sustainable management, and supporting human development initiatives. Without such actions, the threats from climate change will certainly be greater, and adaptive responses increasingly difficult and costly.

The *Panj-Amu River Basin Climate Change Vulnerability Assessment*, supported by the European Union, paves the way for ambitious action to combat negative climate impacts in this important region. The associated spatial datasets and included policy and management recommendations facilitate targeted actions to promote climate resilience. The assessment also serves as an important baseline for comparison with future changes, impacts, and trajectories, and can support further studies throughout the transboundary and interconnected portion of the P-ARB to enable a more comprehensive understanding of climate vulnerability. Sustained environmental monitoring and evaluation of climate impacts throughout the P-ARB will be critical to ensure positive outcomes.

Raffaella Iodice

Deputy Head of Delegation

EU Delegation

ACKNOWLEDGMENTS

Climate Vulnerability

The editors would like to thank Alex C. Ruane, Meridel Phillips, and Manishka De Mel for contributions related to analysis, figures, and written content adapted from the report "Climate Projections for the Panj-Amu River Basin" (Ruane et al., 2021).

Natural Hazards Vulnerability

The editors would like to thank Alex C. Ruane, Meridel Phillips, and Manishka De Mel for contributions related to analysis, figures, and written content adapted from the report "Climate Projections for the Panj-Amu River Basin" (Ruane et al., 2021); and Arnaud Caiserman, Ben Jarihani, Roy C. Sidle, and Evgenii Shibkov for contributions related to analysis, figures, and written content for subsections related to Avalanches and Landslides.

Ecosystem Vulnerability

The editors would like to thank Arnaud Caiserman for contributions related to analysis and written content for the Ecosystem Carbon subsection; Katarzyna Ewa Lewińska and Harald Zandler for contributions related to analysis and data collection in the Rangeland Condition subsection; Haqiq Rahmani for contributions related to analysis of the land cover map in the Rangeland Condition subsection; and Nasratullah Jahed, Ali Madad Rajabi, Hashim Rooyesh, Mirza Hussain, Rezayee Sayed Jalal Jafari, Rahmatullah Ahmadi, Shanbe Shirzad, Karmal Esa, Mohammed Amin, Sallahudin Ismaili, Mubarak Ali, Abdur Rahman Mominzada, and Aziz Ali Khan for contributions related to field data collection in the Rangeland Condition subsection.

Hydrologic Vulnerability

The editors would like to thank Jamal Shokory, Imran Sajid, and Ayoubi Tooryalay for contributions related to analysis, figures, and written content adapted from the report "Understanding current and future hydrological risk within the Panj-Amu River Basin" (ROD, 2022) and Roy C. Sidle, Ben Jarihani, Arnaud Caiserman, and Maksim Kulikov for contributions supporting the hydrological modeling analysis.

Wildlife Species Vulnerability

The editors would like to thank Ali Madad Rajabi, Hashim Rooyesh, Nasratullah Jahed, Mirza Hussain, Rezayee Sayed Jalal Jafari, Rahmatullah Ahmadi, Shanbe Shirzad, Karmal Esa, Aziz Bek Akbar, Ayan Bek Mohammed Amin, and Abdur Rahman Mominzada for contributions related to field data collection in the Changes in Mammal and Bird Range Size and Location subsections; and Nathalie Butt for contributions related to conceptualizing data analysis in the Mammal and Bird Species Sensitivity to Climate Change subsection.

Local Communities Vulnerability

The editors would like to thank Roman Mogilevskii, Bohdan Krawchenko, Aimal Ahmadzai, and Didar Ali Diar for contributions related to analysis and written content.

Data availability

The editors would like to thank all authors, organizations, and institutions that provided open source and freely available data that was used in this Report (citations are included in relevant sections).

Draft review

The editors would like to thank Stephane Ostrowski, Zalmai Moheb, Kharoosh Sahel, Humaira Daniel, Abdul Ahad, Roy C. Sidle, and Ben Jarihani, for reviewing sections and providing feedback that strengthened this report.

Photo Credits

Cover page: © Sorosh Poya-Faryabi; Second cover page: © Inayat Ali; pp. VII: © Inayat Ali; pp. 1: © WCS Afghanistan; pp. 12: © WCS Afghanistan; pp. 72: © Amruddin Sanjer; pp. 74: © Hafizullah Noori; pp. 74: © Amruddin Sanjer; pp.87:© Rob Craig; pp. 104: © Harald Zandler; p. 104: © Sarwar Pamiri; pp.107: © Amruddin Sanjer; pp.109: © John Winnie; pp.121: © Harald Zandler; pp. 135: © Ali Madad Rajabi; pp.135: © Chris Chank; pp.142: © Ali Madad Rajabi; pp. 170: © Harald Zandler; pp. 170:© Ali Madad Rajabi; pp. 172: © Harald Zandler; pp. 174: © Ali Madad Rajabi; pp.174: © Sayeed Naqib Mostafawi; pp.177: © Hashim Rooyesh; pp.177: © John Winnie; pp. 204: © Sayeed Naqib Mostafawi; pp. 204: © WCS Afghanistan; pp.213: © Harald Zandler; pp. 222: © Ali Madad Rajabi; pp. 222 © WCS Afghanistan; pp. 224: © Ali Madad Rajabi; pp. 224: © Sayeed Naqib Mostafawi; pp. 248: © Hamidullah Sahibi; pp. 248: © WCS Afghanistan; pp. 254: © Zalmai Moheb; pp. 265: © Zalmai Moheb; pp. Back cover: © WCS Afghanistan; © Beth Wald; © Ahmad Nabizada; © Ali Rajabi; © Fatima Baqiri; © Zalmai Moheb; © WCS Afghanistan.

COORDINATING ORGANIZATIONS

Wildlife Conservation Society

The Wildlife Conservation Society (WCS) is a global science-based conservation organization that has been established for over 125 years. WCS produces scientific information to support conservation efforts and management activities in wild places. WCS operates in over 60 countries, employs more than 250 PhD and DVM scientists, and provides educational and training opportunities. WCS works in partnership with government, local communities, and other organizations to support best practices that mitigate natural resource impacts in the context of rapid environmental and social change. WCS's efforts have led to the creation or expansion of 245 protected areas worldwide. WCS staff are leaders in conservation science, wildlife veterinary medicine, and curatorial research.

Since 2006, WCS has been effectively contributing to Afghanistan's capacity to conserve and sustainably manage its wildlife and natural resources and improve livelihoods for the benefit of the nation, with a focus on Wakhan District of Badakhshan, Afghanistan's central highlands, the eastern forests, and Kabul.

Aga Khan Foundation

The Aga Khan Foundation (AKF) seeks to improve the quality of life, promote pluralism, and enhance self-reliance in poor and marginalized communities in Africa, Asia, and the Middle East. AKF strives to enhance agriculture and food security, promote early childhood development and access to quality education, improve health and nutrition, advance economic inclusion, and strengthen civil society. Active in 18 countries, AKF is a member of the Aga Khan Development Network, one of the world's leading international development organizations.

In Afghanistan, AKF works with rural communities in mountainous, remote, or resource poor areas to improve quality of life in the areas of natural resource management, market development, governance, education, and health.

EXECUTIVE SUMMARY

Afghanistan is one of the most at-risk countries from climate change. Within the country, the Panj-Amu River Basin (P-ARB) in the northeast is particularly sensitive as it is characterized by remote and rugged topography, high elevation glaciers, and local communities with a high dependence on natural resources. Projections of climate change in the region show increased climate impacts on natural hazards including droughts, floods, landslides, and avalanches. In addition, warming temperatures and changes in rainfall will affect ecosystem productivity to support livestock, agriculture, and biodiversity. The latter is also directly impacted as climate change forces species to relocate to track suitable climate conditions and habitats.

The P-ARB is also a vital source of water for millions of people both in Afghanistan and in neighboring countries. Several important rivers, including the Amu Darya, originate in the P-ARB and are influenced by complex hydrological processes. These hydrological processes will also be directly impacted by climate change, as both increases and decreases in rainfall, and increased snow and glacier melt will contribute to additional runoff and discharge throughout the region. This will have both short- and long-term impacts on water availability for people (e.g., for irrigation) and for wildlife.

The local communities within the region depend on natural resources, such as productive rangelands, for grazing livestock and for fuel and firewood collection. In general, communities are characterized by low education, wealth and income, and limited opportunities and alternative livelihoods. As a result, this decreases the adaptive capacity of local communities to cope with climate change impacts.

In this report, we conduct a comprehensive climate change vulnerability assessment to determine the patterns and magnitude of climate change exposure, sensitivity, and adaptive capacity, which ultimately contribute to overall climate change vulnerability. The assessment in this report covers six main sectors: climate, natural hazards, ecosystems, hydrology, wildlife species, and local communities. For each sector, several indicators related to sector-specific vulnerability are analyzed using the best available data. The results are depicted as maps covering the entire P-ARB and are summarized by ecoregion and province (or sub-basin, in the case of hydrological analyses).

An overview of vulnerability rankings by province is depicted in the following table:

Vulnerability Rank by Sector								
Province	Climate	Hazards	Ecosystems	Hydrology	Species	Local communities	Mean vulnerability score	Overall vulnerability rank
Takhar	4	1	2	2	5	1	2.50	1
Baghlan	1	4	5	1	1	4	2.67	2
Bamyan	2	1	4	6	2	2	2.83	3
Kunduz	4	4	1	4	2	Not evaluated	3.00	4
Badakhshan	2	4	6	3	2	3	3.33	5
Samangan	6	1	3	5	5	Not evaluated	4.00	6

The results are intended to guide policy, management, and the conservation and sustainability of ecosystems and natural resources. Thus, each major section of the report is concluded with a dedicated subsection delivering policy and management recommendations. These can be broadly summarized by the following twelve actions:

1. Invest in nature-based solutions to joint climate mitigation-adaptation
2. Develop alternative strategies for energy generation and food production to reduce emissions and impacts on natural systems
3. Maintain ecosystem integrity through improved governance, management, and protection
4. Restore degraded landscapes
5. Develop wildlife conflict mitigation strategies
6. Educate the public about climate change and climate change impacts
7. Establish a long-term monitoring system covering all sectors
8. Create a natural hazard warning system
9. Invest in water conservation solutions
10. Strengthen livestock and agricultural management
11. Create opportunities for communities to diversify incomes
12. Support human development activities

Reducing vulnerability in the region will require immediate and sustained action across all sectors. The results presented in this report identify at-risk ecosystems, wildlife, and communities, and provide a blueprint for effective conservation and sustainable development action. The data outputs from this report will be made available to the public to facilitate further research and application in this fragile and important landscape.

TABLE OF CONTENTS

List of Figures

List of Tables

ACRONYMS AND ABBREVIATIONS

AC	Adaptive Capacity
AfDHS	Afghanistan Demographic and Health Survey
AGB	Aboveground Biomass
AKDN	Aga Khan Development Network
AKF	Aga Khan Foundation
AMD	Afghanistan Meteorological Department
AT	Air Temperature
BGB	Belowground Biomass
CCI	Climate Change Initiative
CCSR	Center for Climate Systems Research
CDC	Community Development Council
CEF	Cumulative Endmember Fraction
CGIAR-CSI	Consultative Group on International Agricultural Research-Consortium for Spatial Information
CHELSA	Climatologies at High Resolution for the Earth's Land Surface Area
CHILI	Continuous Heat-Insolation Load Index
CHIRPS	Climate Hazards group Infrared Precipitation with Stations
CMIP5	Coupled Model Intercomparison Project Phase 5
CMIP6	Coupled Model Intercomparison Project Phase 6
CORDEX-CORE	Coordinated Regional Downscaling Experiment-Coordinated Output for Regional Evaluations
CSO	Central Statistical Organization
DDA	District Development Association
DEM	Digital Elevation Model
DHS	Demographic and Health Survey
DPS	Deep Pore Storage
EcoSIS	Ecological Spectral Information System
ESA	European Space Agency
ET	Actual Evapotranspiration
ETM+	Enhanced Thematic Mapper Plus
EU	European Union
EVI	Enhanced Vegetation Index
FAO	Food and Agriculture Organization
FFS	Farmer Field Schools
GBAO	Gorno-Badakhshan Autonomous Oblast
GBIF	Global Biodiversity Information Facility
GCM	General Circulation Model
GE	Google Earth
GEE	Google Earth Engine
GHG	Greenhouse Gas
GHM	Global Human Modification

GIS	Geographic Information System
GISS	Goddard Institute for Space Studies
GLC	Global Landslide Catalog
GLI	Green Leaf Index
GLW	Gridded Livestock of the World
GOSAVI	Green Optimized Soil Adjusted Vegetation Index
GPM	Global Precipitation Measurement
GPS	Global Positioning System
hh	Household
HLI	Heat Load Index
HRU	Hydrological Response Unit
ICRAF	World Agroforestry Center
IDW	Inverse Distance Weighting
IMERG	Integrated Multi-satellite Retrievals for GPM
IOC	International Ornithological Congress
ISRIC	International Soil Reference and Information Centre
IUCN	International Union for Conservation of Nature
JAMS	Jena Adaptable Modeling System
LAI	Leaf Area Index
LHASA	Landslide Hazard Assessment for Situational Awareness
LPS	Large Pore Storage
LSU	Livestock Units
LULC	Land Use/Land Cover
MAE	Mean Absolute Error
MAIL	Ministry of Agriculture, Irrigation, and Livestock
MCE	Minimum Cumulative Exposure
MCTI	MERIS Terrestrial Chlorophyll Index
MED	Minimum Exposure Distance
MERIS	Medium Resolution Imaging Spectrometer
MIAD	Multi-Input Area Development
MODIS	Moderate Resolution Imaging Spectroradiometer
MoPH	Ministry of Public Health
MPS	Middle Pore Storage
NASA	National Aeronautics and Space Administration
NDMI	Normalized Difference Moisture Index
NDSI	Normalized Difference Snow Index
NDVI	Normalized Difference Vegetation Index
NDWI	Normalized Difference Water Index
NEPA	National Environmental Protection Agency
NGO	Non-Governmental Organization
NIR	Near Infrared
NRVI	Normalized Ratio Vegetation Index
NS	Nash-Sutcliffe
NSE	Nash-Sutcliffe Efficiency
NSIA	National Statistic and Information Authority
NWARA	National Water Affairs Regulation Authority
OECM	Other Effective Conservation Measure
OLI	Operational Land Imager

P-ARB	Panj-Amu River Basin
PA	Protected Area
PC	Principal Component
PCA	Principal Component Analysis
PDF	Portable Document Format
PET	Potential Evapotranspiration
PPS	Proportional to Population Size
PPT	Precipitation
PSU	Primary Sampling Unit
PTA	Parent-Teacher Association
QA	Quality Assessment
QoL	Quality of Life
RCM	Regional Climate Model
RCP	Representative Concentration Pathway
RH	Relative Humidity
RMSE	Root Mean Square Error
RO	Runoff
SAR	Synthetic Aperture Radar
SAVI	Soil Adjusted Vegetation Index
SD	Standard Deviation
SDG	Sustainable Development Goal
SDM	Species Distribution Model
SLR	Solar Radiation
SMA	Spectral Mixture Analysis
SMC	School Management Committee
SPOT	Satellite Pour L'Observation de la Terre
SRTM	Shuttle Radar Topography Mission
SWAT	Soil Water Assessment Tool
SWAT-CUP	Soil Water Assessment Tool Calibration Uncertainty Program
SWE	Snow Water Equivalent
TIRS	Thermal Infrared Sensor
UNESCO	United Nations Educational, Scientific, and Cultural Organization
USDA-ARS	United States Department of Agriculture-Agriculture Research Services
USGS	United States Geological Survey
VH	Vertical Transmit-Horizontal Receive Polarization
VNIR	Visible Near Infrared
VV	Vertical Transmit-Vertical Receive Polarization
WCS	Wildlife Conservation Society
WS	Wind Speed
WWF	World Wildlife Fund

1 INTRODUCTION

1.1 Background

The Panj-Amu River Basin Climate Change Vulnerability Assessment contributes to the EU funded project *Addressing Climate Change in Afghanistan through Sustainable Energy and Ecosystem Management.* The purpose of the vulnerability assessment is to identify ecosystems, regions, wildlife species, and communities at risk from climate change impacts. The geographic scope of the vulnerability assessment is the Panj-Amu River Basin (P-ARB) in northeastern Afghanistan.

This report describes expected future changes in climatic conditions and natural hazards in the P-ARB and associated vulnerabilities to ecosystems, hydrology, wildlife, natural resources, and local communities. Activities conducted to support this report included:

- A detailed literature review of all published and unpublished material relevant to climate change, ecosystems, hydrology, wildlife, natural resources, local communities, and vulnerability assessments in the P-ARB and Afghanistan more broadly (see Appendix 1)
- Meetings with national, subnational, and local governments and stakeholders in the P-ARB and in Kabul to identify the scope of the vulnerability assessment
- The development of a set of indicators used to determine vulnerability for each component of the assessment
- Production of a technical guidance document describing the analytical methodologies employed in this vulnerability assessment
- Field work in targeted intervention areas of the P-ARB by WCS and AKF field staff to collect data supporting the vulnerability assessment (see Appendix 2)
- The compilation and analysis of datasets related to climate, topography, land cover, hydrology, wildlife occurrences and distributions, and socio-economic factors available for the P-ARB
- An external review process by national, subnational, and local government and stakeholders in the P-ARB and in Kabul

This report includes recommendations for policy and management for each section in the assessment. Furthermore, the results outlined in this report support long-term monitoring decisions and priorities.

1.2 Geographic and Socio-ecological Context

The Panj-Amu River Basin (P-ARB) is located in north-eastern Afghanistan. The 90,692 km^2 ecosystem largely consists of grassland interspersed with patches of woodland (Figure 1). The P-ARB covers six main provinces in Afghanistan: Badakhshan, Takhar, Kunduz, Samangan, Baghlan, and Bamyan (Figure 2).

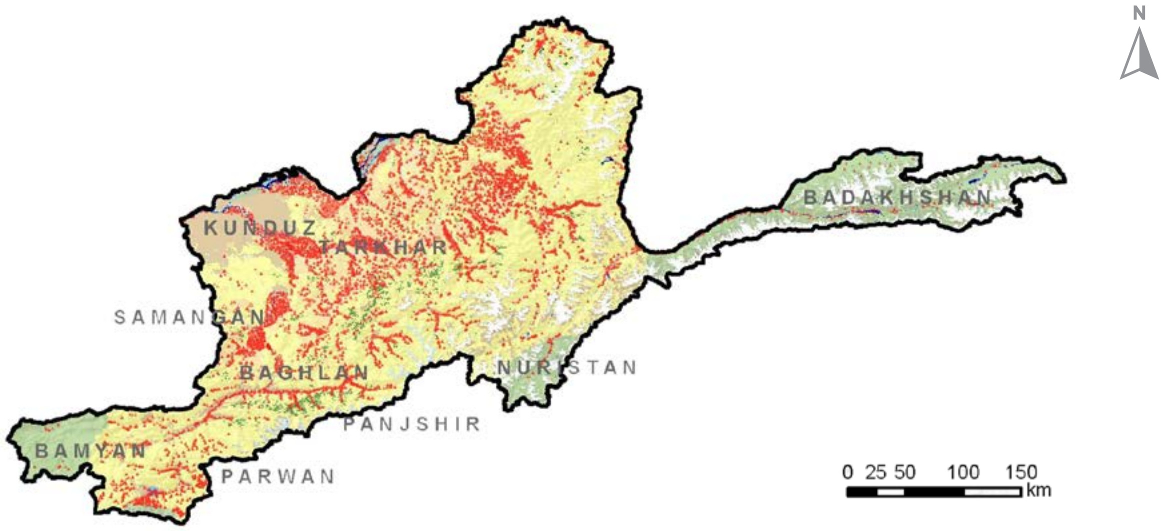

Figure 1. Map of the Panj-Amu River Basin (P-ARB) ecosystem depicting major habitat types, hydrological features, protected areas, settlements, and topography. Inset shows the position of the P-ARB within Afghanistan.

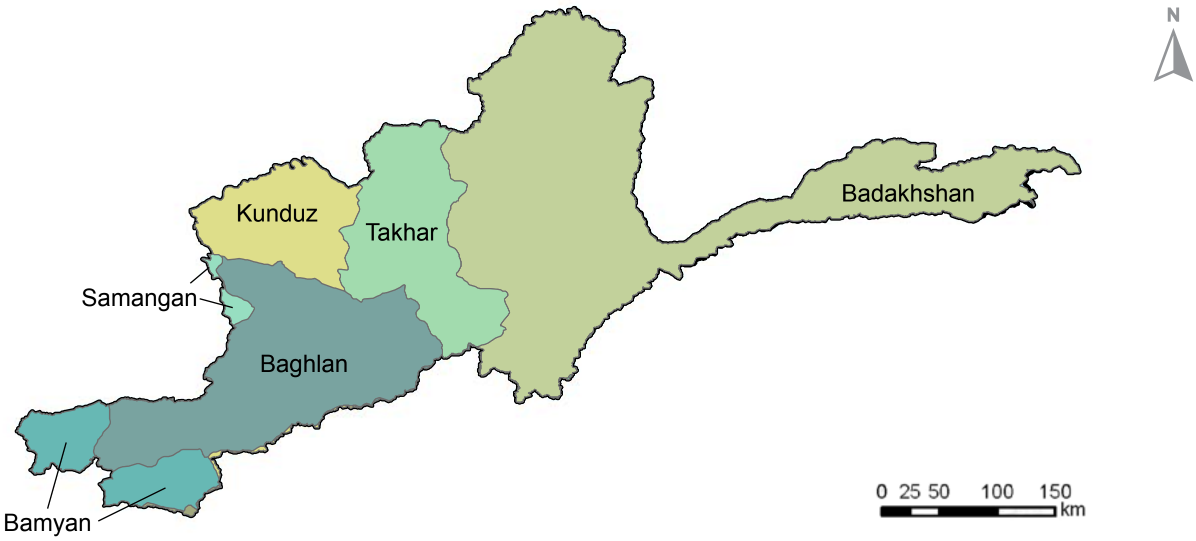

Figure 2. Major provinces located in the Panj-Amu River Basin.

The P-ARB is characterized by eight ecoregions, which are distinct biogeographical units. Ecoregions include multiple types of deserts and semi-deserts, steppe and meadows, and woodlands (Figure 3). For the purposes of summary plots (see "Format of the Vulnerability Assessment), they are numbered as follows:

Ecoregion 1: Pamir alpine desert and tundra

Ecoregion 2: Karakoram-West Tibetan Plateau alpine steppe

Ecoregion 3: Gissaro-Alai open woodlands

Ecoregion 4: Paropamisus xeric woodlands

Ecoregion 5: Ghorat-Hazarajat alpine meadow

Ecoregion 6: Hindu-Kush alpine meadow

Ecoregion 7: Afghan Mountains semi-desert

Ecoregion 8: Badghyz and Karabil semi-desert

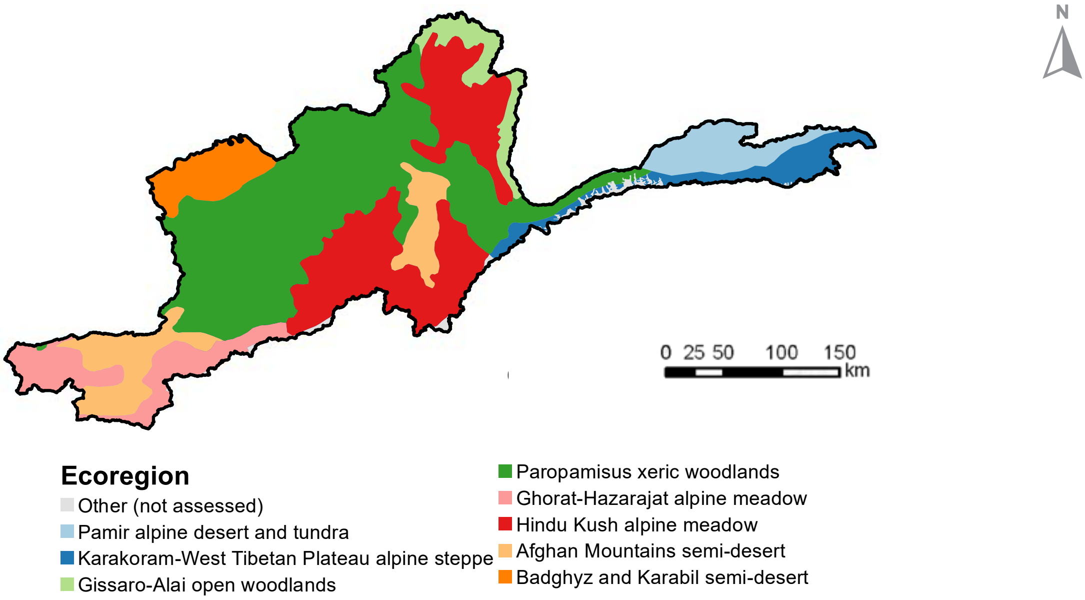

Figure 3. Ecoregions within the Panj-Amu River Basin.

Livestock grazing in rangelands is common throughout the landscape. The other dominant forms of land-use are rainfed and irrigated agriculture (Figure 4). Rapid growth in livestock numbers together with unsustainable grazing practices hinders the regeneration of harvested biomass and degrades vegetation cover, compacts the soil, reduces ground water replenishment, and increases erosion, including stream incision.

Woody vegetation from these ecosystems is the main source of energy for heating and cooking in rural households. Cutting of trees and collection of dwarf shrubs has led to dramatic shrinkage in woodland areas and removal of rangeland vegetation cover. Together, these practices have contributed to rangeland degradation and forest depletion.

Figure 4. Example of rainfed and irrigated agriculture among rangelands in the Panj-Amu River Basin. © P. R. Elsen.

The P-ARB landscape is mostly covered by complex topography due to the presence of several mountain ranges, including the Hindu-Kush, Karakorum, and Pamir Mountain ranges. Elevation ranges from 285 to 7,391 m (Figure 5), with the lowest elevation areas in Kunduz and the highest elevation areas in Badakhshan.

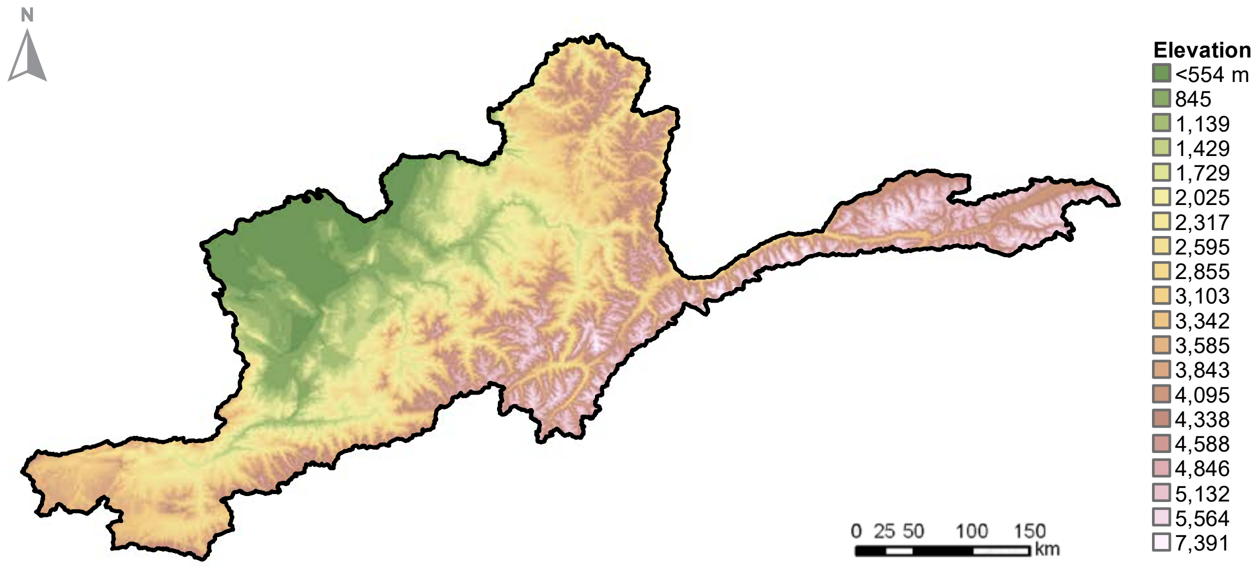

Figure 5. Elevation within the Panj-Amu River Basin.

Topography has a profound influence on the climate in the region. Mean annual temperatures range from -17 to 19.5 °C (Figure 6), with the warmest areas in Kunduz and the coldest areas in Badakhshan. Total annual precipitation ranges from 35 to 1,050 mm (Figure 7). Precipitation comes in the form of snowfall in winter (January-March) and rainfall in spring (February-April).

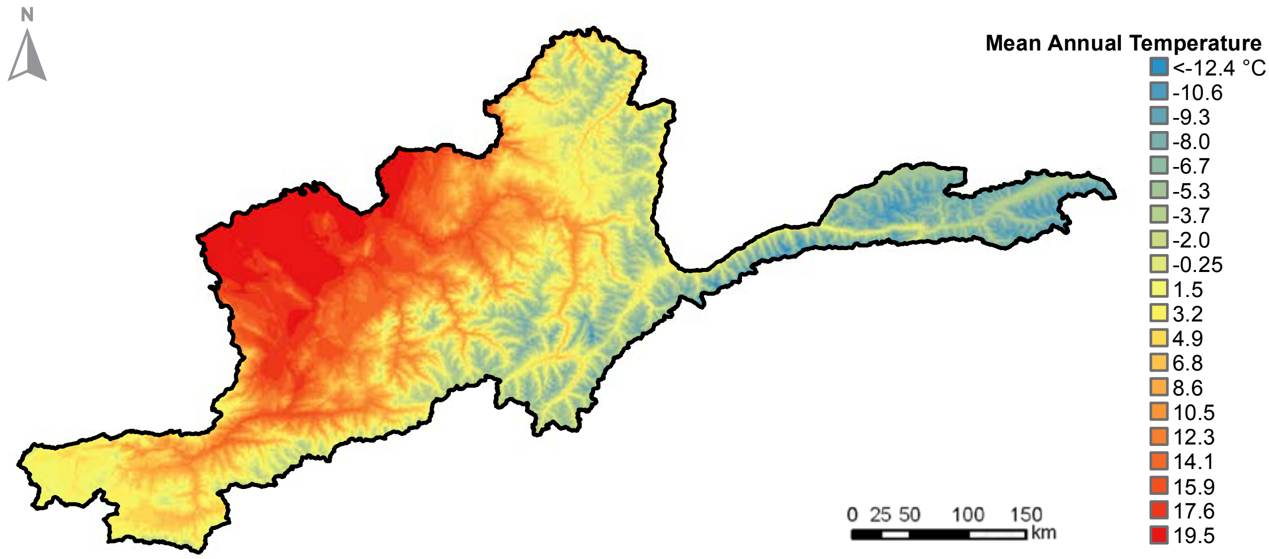

Figure 6. Mean annual temperature within the Panj-Amu River Basin.

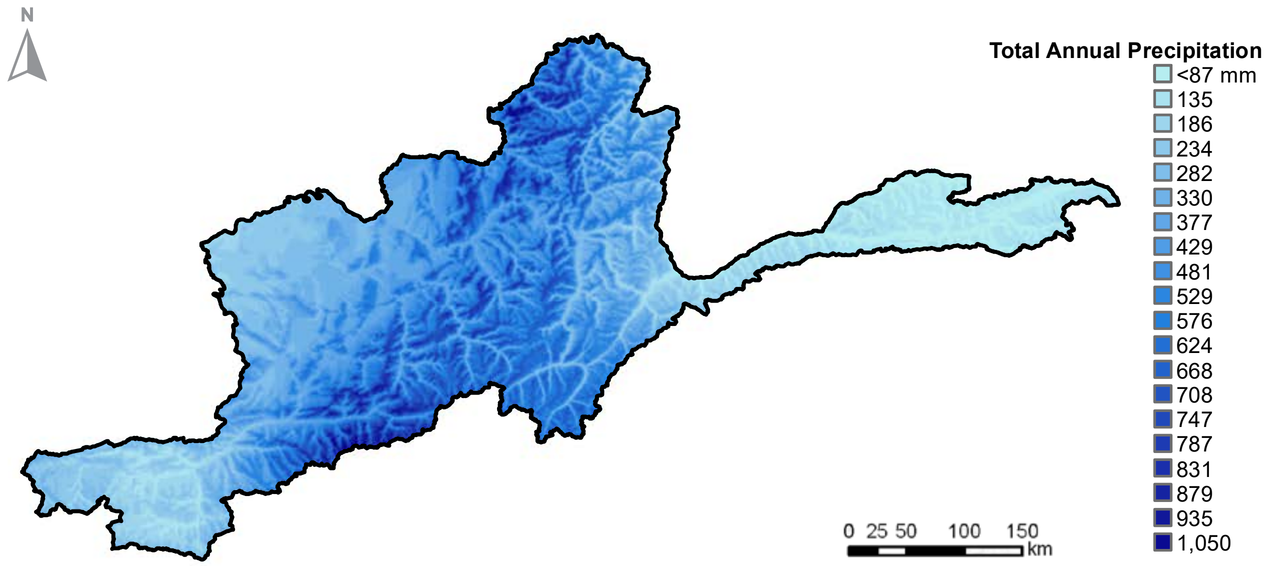

Figure 7. Total annual precipitation within the Panj-Amu River Basin.

The P-ARB consists of multiple sub-basins, which are similar in distribution to ecoregions (Figure 8). The upper catchment of the P-ARB is considered the main "water tower" for millions of people, not only in Afghanistan, but also in Tajikistan, Uzbekistan, and Turkmenistan as far as the Aral Sea (Figure 9).

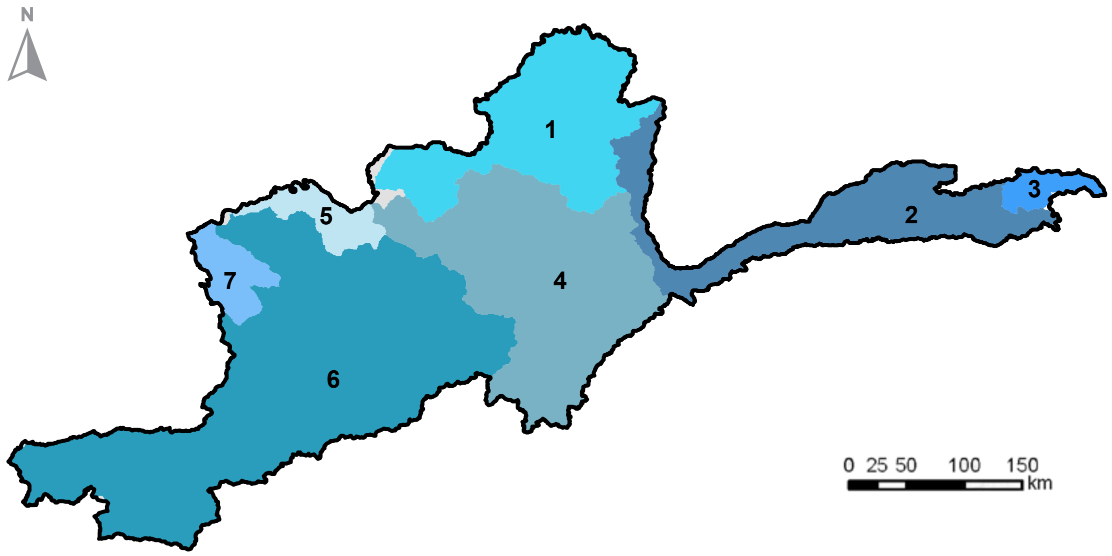

Figure 8. Sub-basins of the P-ARB. Sub-basin typology follows Pfaffstetter Level 6.

Figure 9. Sub-basins of Central Asia, with Afghanistan outlined in black and the Panj-Amu River Basin highlighted in yellow. Sub-basin typology follows Pfaffstetter Level 6 subdivisions.

The region also contains a variety of wildlife, including top predators (e.g., snow leopards, brown bear), meso-predators (e.g., Pallas's cat, Eurasian lynx), and herbivores (e.g., Marco polo sheep, urial). These species both rely on the landscape, compete with livestock for resources, and sometimes directly consume livestock.

Extreme weather events such as heat waves, floods and droughts, reduced snow cover, and subsequent glacial lake outflows are expected to increase in frequency and intensity under climate change. Over 80% of local communities living in this landscape depend on natural resources for their livelihoods, consequently, these hazards pose a serious threat to the local economy, stability, and food security. Degraded ecosystems and impoverished biodiversity resulting from unsustainable grazing, harvesting, and management are less resilient and offer less potential for adaptation under changing climate conditions. The region is generally characterized by protracted insecurity and high levels of poverty, which likely reduces adaptive capacity and increases vulnerability. Thus, the future health of ecosystems, wildlife, and people are intricately linked in this landscape, such that the vulnerability of the ecosystem will influence the vulnerability of the people and vice versa. Because of this, components of ecosystems, hydrology, wildlife, and local communities are all included in this vulnerability assessment.

Figure 10. Some of the wildlife found in the P-ARB. Clockwise from top left – Urial (*Ovis vignei*), Snow Leopard (*Panthera uncia*), Grey Wolf *(Canis lupus lupus*) and Argali (*Ovis ammon polii*). Photos courtesy Ali Madad Rajabi, Julie Larsen, and WCS.

1.3 Vulnerability Assessment Key Concepts and Definitions

The following terms are essential concepts and components of vulnerability assessments in the context of climate change and will be used throughout this report. The definitions are adapted from those outlined by Dawson et al. (2011), which were developed specifically for assessing vulnerability in the context of climate and biodiversity.

V **Vulnerability** is the extent to which a target (one or more of ecosystem, landscape feature, species, natural resource, or local community) is threatened with decline, degradation, stress, reduction in survival, reduction in resources or livelihoods, genetic loss, or extinction owing to climate change. Vulnerability has three components (Figure 11): exposure (which is positively related to vulnerability), sensitivity (positively related), and adaptive capacity (negatively related).

E **Exposure** refers to the extent of climate change likely to be experienced by a target. Exposure depends on the rate and magnitude of climate change (e.g., temperature, precipitation, flood frequency) in regions occupied by the target.

S **Sensitivity** is the degree to which the survival, persistence, fitness, performance, regeneration, or livelihood of a target is dependent on the prevailing climate, particularly on climate variables that are likely to undergo changes in the near future. Sensitivity depends on a variety of factors, including ecophysiology, life history/lifestyle, preferences, and behaviors.

AC **Adaptive capacity** refers to the capacity of a target to cope with climate change by persisting in situ, by shifting or migrating to more suitable locales, or by changing behaviors. Adaptive capacity depends on a variety of intrinsic factors, including phenotypic plasticity, genetic diversity, evolutionary rates, life history traits, dispersal and colonization ability, and general resource availability.

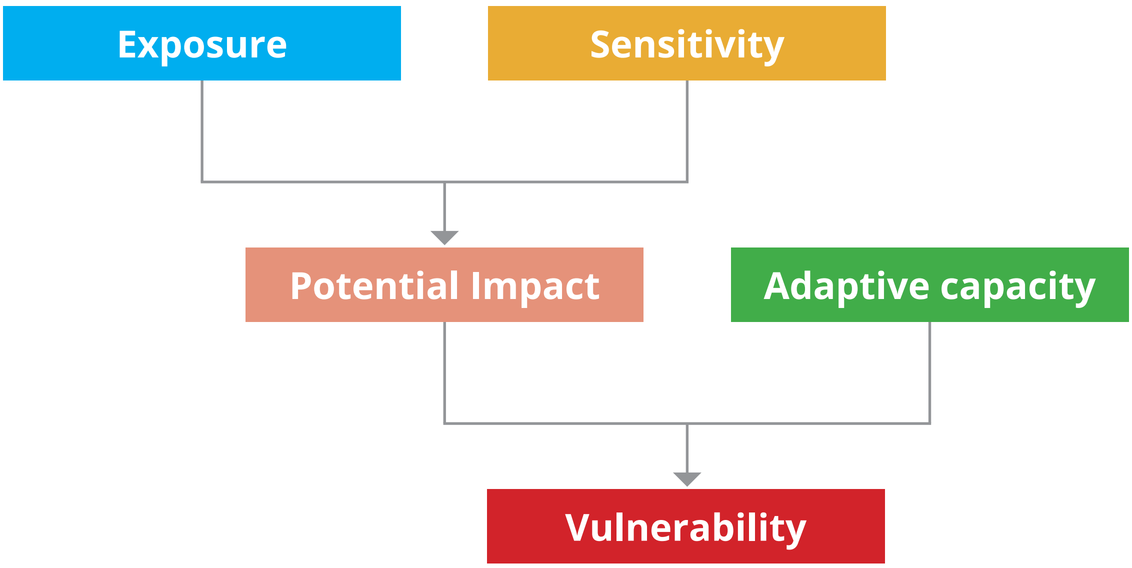

Figure 11. Relationships between the three components of vulnerability. Adapted from Stein et al. (2014).

1.4 Scope of the Vulnerability Assessment

The vulnerability assessment in this report covers aspects of climate, natural hazards, ecosystem, hydrology, wildlife species, and local communities. These aspects were included as they are the major components of the landscape in the P-ARB, and interactions between all these factors influence vulnerability.

Several indicators have been developed for each category, as outlined in Table 1. The full list of indicators is included in the table of contents.

Table 1. Overview of indicators included in the vulnerability assessment by category.

Category	Indicator	Vulnerability Component Assessed
Climate	Degree of exposure of 19 bioclimatic variables	Exposure
	Climatic dissimilarity	Exposure
	Climate velocity	Exposure
Natural hazards	Permafrost	Exposure
	Growing season length	Exposure
	Extreme heat (2 temperature thresholds)	Exposure
	Extreme precipitation (3 precipitation thresholds)	Exposure
	Snow water equivalent	Exposure
	Soil moisture drought (February and October)	Exposure
	Size and frequency of avalanches	Exposure
Ecosystem	Change in natural land cover extent	Exposure
	Ecosystem carbon	Exposure
	Change in NDVI	Exposure
	Change in rangeland condition	Exposure
	Ecosystem protection status	Adaptive Capacity
	Shifts in spatial distribution of ecoregions	Exposure
	Thermal heterogeneity	Adaptive Capacity
	Topographic heterogeneity	Adaptive Capacity
Hydrology	Change in river runoff and discharge rates	Exposure
Wildlife species	Change in species' range size and locations	Sensitivity, adaptive capacity
	Mammal and bird species sensitivity to climate change	Sensitivity, Adaptive Capacity
Local communities	Quantity of and access to biophysical resources	Sensitivity, Adaptive Capacity
	Demographic status	Sensitivity, Adaptive Capacity
	Socioeconomic status	Sensitivity, Adaptive Capacity

1.5 Format of the Vulnerability Assessment

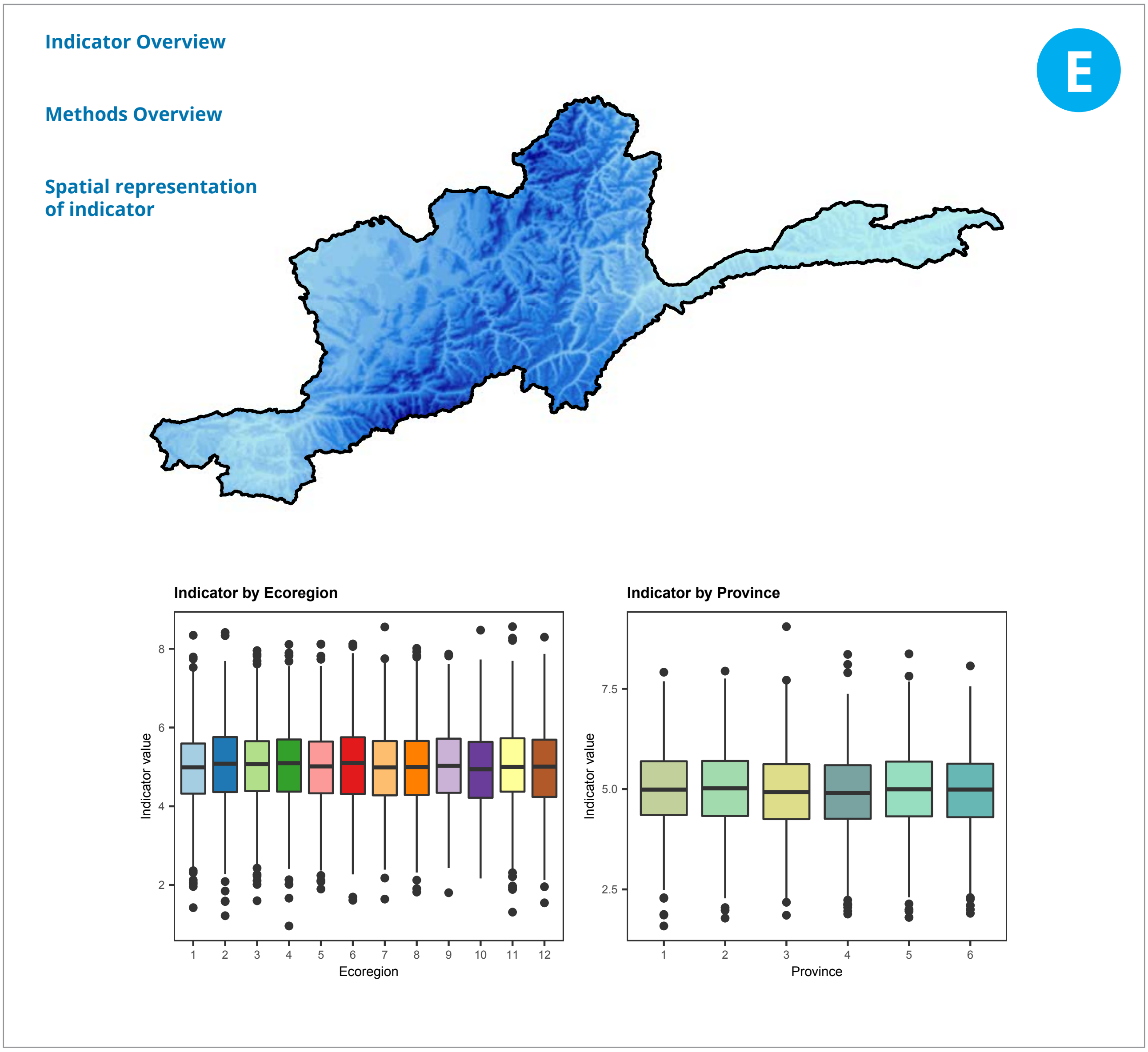

Figure 12. Example format of results for each indicator of the vulnerability assessment.

2 VULNERABILITY ASSESSMENT

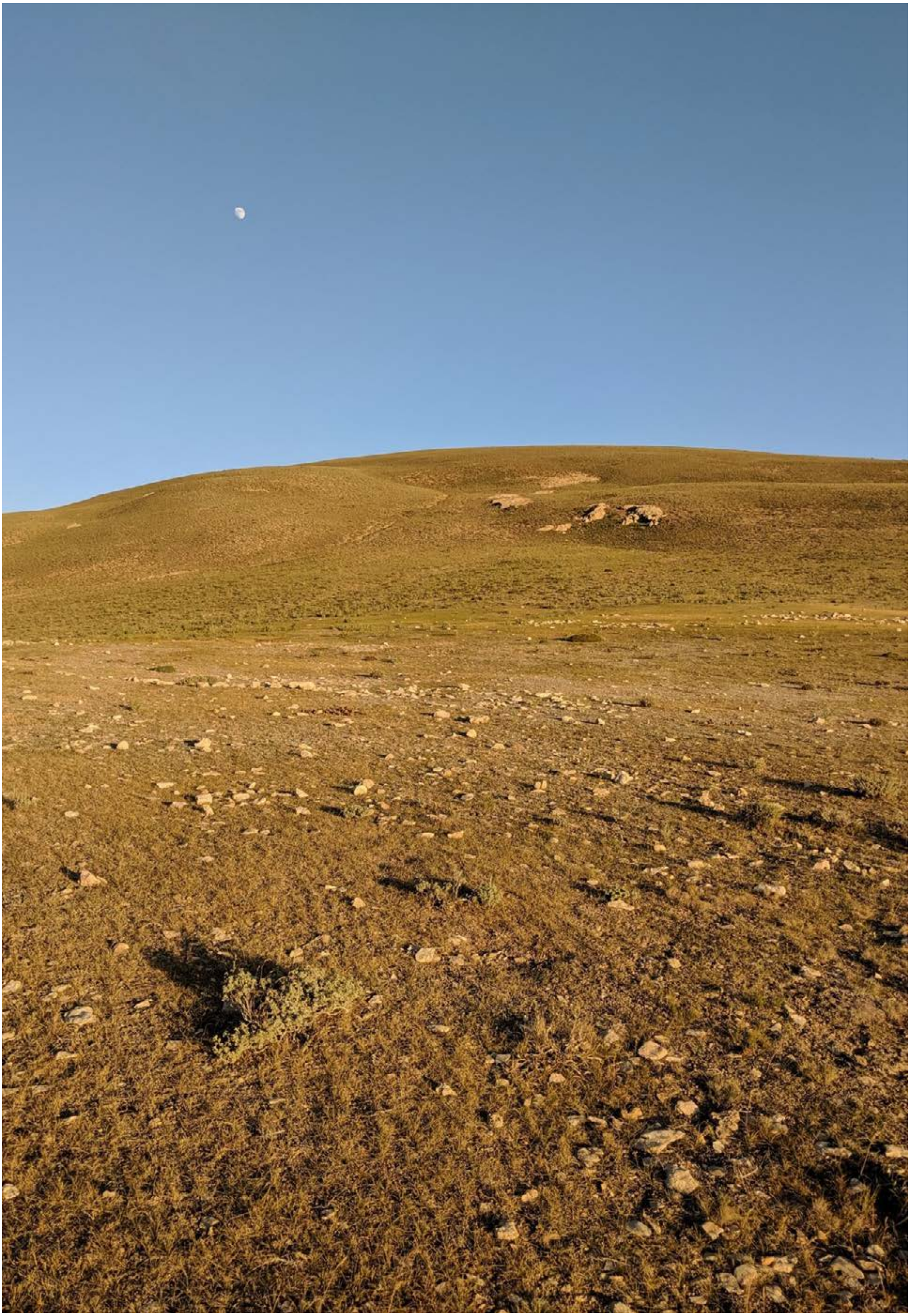

Figure 13. An example of a healthy rangeland ecosystem of Bamyan Plateau in the P-ARB. © P. R. Elsen.

Climate Vulnerability

2.1 Climate Vulnerability

Overview

Climate scenario analysis

- Historical climate datasets and an ensemble of climate projections have been downscaled and bias-adjusted to enable analysis of climate-driven hazards and risks to ecosystems, wildlife, hydrology, and communities in the Panj-Amu River Basin (P-ARB), Northeastern Afghanistan.

Overview of the changing climate

- Climate model projections indicate that climate change will impact a range of sectors and alter the bioclimatic conditions across the P-ARB. Climate-related hazards will also shift, as critical variables such as precipitation (total and intensity), temperatures, extreme heat, soil moisture, snow, and permafrost change over time.
- The balance of changes across average and extreme climate conditions suggests disruptive pressures on society and natural ecosystems, which are important to recognize in current and future planning for the P-ARB.
- As future climate is likely to be different from past and current conditions, incorporating a range of possible projections in planning and decision-making is essential to minimize impacts and build resilience. We present a range of results by using two climate change scenarios, RCP2.6 (a low emissions pathway) and RCP8.5 (a high emissions pathway), accounting for uncertainty by examining eight separate downscaled climate models.

Projected mean temperature changes

- Projected warming is uniformly higher under the higher emissions RCP8.5 scenario compared to a lower emissions (higher mitigation) RCP2.6 scenario.
- RCP2.6 has a temperature peak in the 2050s and then declines slightly by the 2080s due to a substantial decrease in greenhouse gas concentrations under this pathway. By end-century, P-ARB temperatures are projected to increase by approximately 2°C under RCP2.6 (compared to recent past).
- Warming under RCP8.5 continues throughout the 21st century, resulting in an average P-ARB temperature increase of approximately 6°C.
- Warming trends generally shift current temperature zones to higher elevations and lengthen the warmer seasons of the year.
- Projected warming is fairly uniform across the P-ARB, with important distinctions across ecoregions. Warming is highest in the eastern Paropamisus xeric woodlands, Ghorat-Hazarajat alpine meadow, Hindu Kush alpine meadow, and Afghan Mountains semi-desert ecoregions, and lowest in the Badghyz and Karabil semi-desert and western Paropamisus xeric woodlands ecoregions.

Projected total precipitation changes

- Projected precipitation varies widely across the P-ARB, with some regions becoming drier and others becoming wetter by end-century. The projected magnitude of changes is much greater under RCP8.5 compared to RCP2.6, although uncertainty across climate projections also increases.
- The eastern half of the P-ARB, including the Pamir alpine desert and tundra, Karakoram-West Tibetan Plateau alpine steppe, Gissaro-Alai open woodlands, and eastern portions of the Paropamisus xeric woodlands and Hindu Kush alpine meadow ecoregions, is projected to become wetter by 10-40% based on the ensemble mean (although individual models vary in magnitude and direction of precipitation change). The western half of the P-ARB, including the Ghorat-Hazarajat alpine meadow, Afghan Mountains semi-desert, Badghyz and Karabil semi-desert, and western portions of the Paropamisus xeric woodlands and Hindu Kush alpine meadow ecoregions, is projected to become drier by 10-40%.

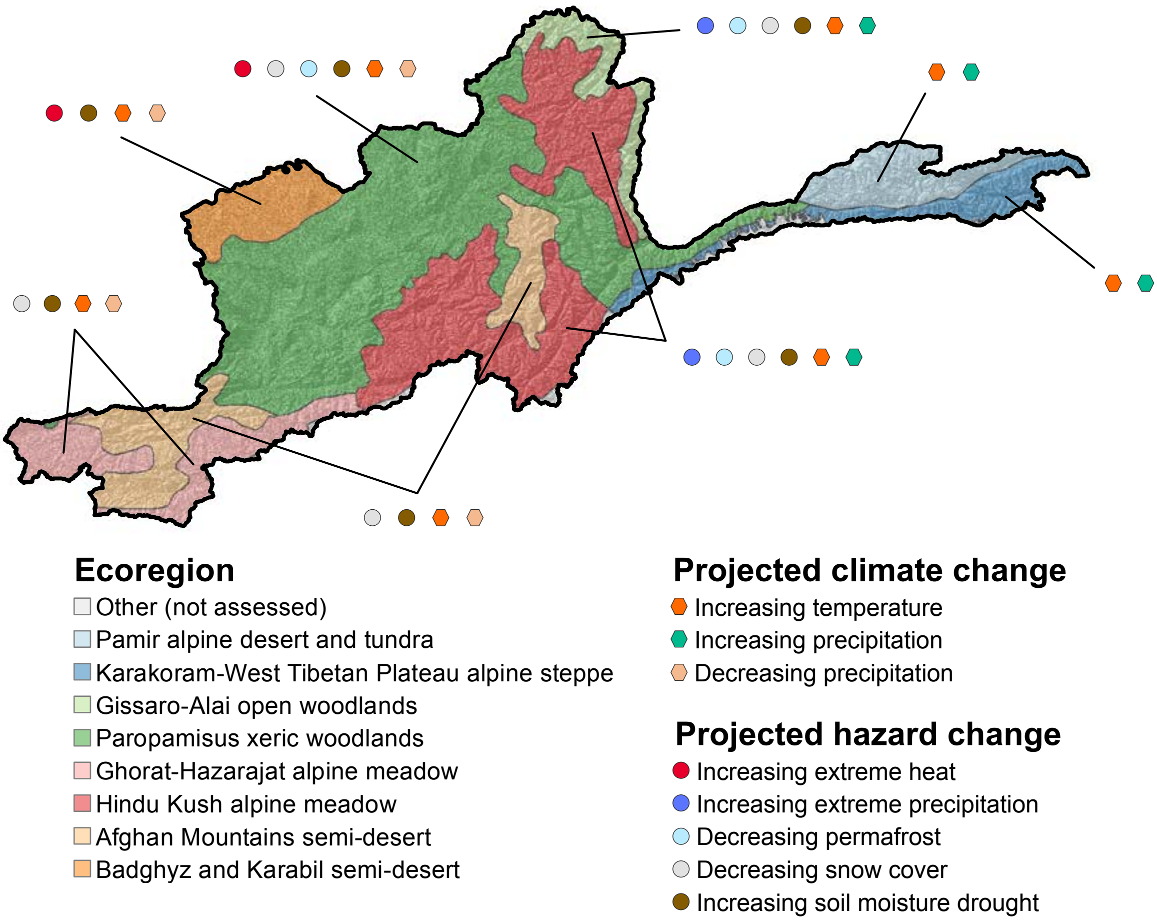

Figure 14. Overview of major projected hazards and climate changes within ecoregions of the Panj-Amu River Basin.

Background and Introduction

The Columbia University Center for Climate Systems Research (CCSR) has developed climate projection for the Wildlife Conservation Society (WCS) project on 'Improving participatory management and efficiency of rangeland and watershed focusing on Wakhan, Yakawlang, and Saighan Districts in Afghanistan.' These draft results are a component of the broader engagement that spans the entire Panj-Amu River Basin (P-ARB), for which tailored and bias-adjusted climate projections support a range of uses including ecosystem and species modeling, impacts of climate hazards on communities, and hydrology modeling in the project region. For example, the temperature and precipitation projections for several Bioclim variables are designed for potential use by rangeland and species distribution models to enable projections for climate change driven effects on ecosystems.

The project focuses on the P-ARB, however CCSR has developed downscaled, bias-adjusted climate projections for a broader Afghanistan domain that includes the entire country and partially covers neighboring countries including Iran, Turkmenistan, Uzbekistan, Tajikistan, China, India, and Pakistan. A sample map of ensemble mean annual baseline temperature, showing the full extent of CCSR outputs with the P-ARB boundaries highlighted, is shown in Figure 15.

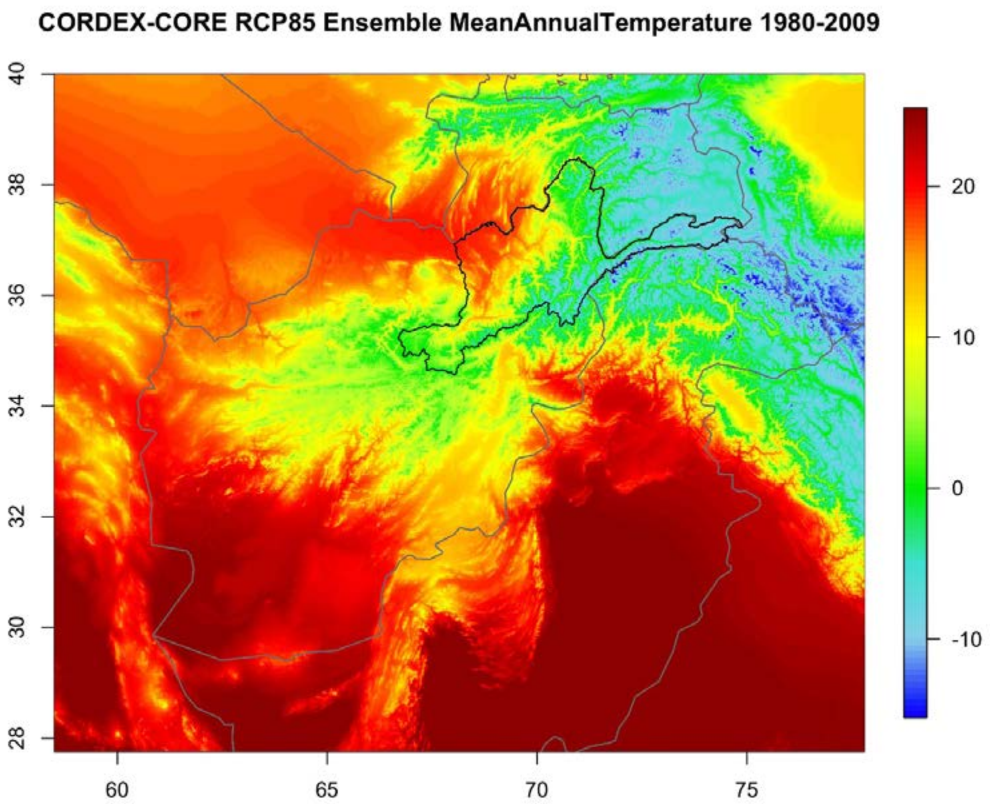

Figure 15. Ensemble mean annual temperature from eight CORDEX-CORE GCM-RCM combinations from 1980-2009. Country borders are shown in gray with the focus Panj-Amu River Basin region outlined in black. [Resolution: 30 arcsec = approximately 1 km].

About the Columbia University Center for Climate Systems Research

The Center for Climate Systems Research (CCSR) is the home of the cooperative relationship between Columbia University and the National Aeronautics and Space Administration Goddard Institute for Space Studies (NASA GISS) and a research center of The Earth Institute at Columbia University. CCSR was established with the objective of providing enhanced understanding of the Earth's climate and its impacts on key sectors and systems. The GISS Climate Impacts Group develops innovative methods to apply climate information to aid in impact forewarning, risk reduction and resilience building for climate hazards around the world.

CCSR also plays a large role in the dissemination of climate change research and information to governments, local and international organizations, educational institutions, and stakeholders.

Key climate hazards, impacts, and risk

Climate change has implications for several key sectors in Afghanistan, with focus here on ecosystems wildlife, hydrology, and communities. Some changes (e.g., mean temperature trends) create long term-pressures, while heatwaves and extreme precipitation are projected to cause more immediate and acute impacts depending on local vulnerability and exposure. Some risks are heightened when tolerance thresholds are crossed and system tipping points are surpassed. Climate change is also a threat multiplier and can have knock-on effects, exacerbating existing issues such as food security and ecosystem degradation. Compounding of extreme events, feedbacks, and other interactions can amplify physical impacts and need to be considered in planning and decision-making.

Table 2. Climate hazards, key impacts, and risks.

Climate hazard	Key impacts and risks
Mean temperature	Mean temperature trends can build slowly over time but can have implications for a number of sectors. Warming trends increase risk for ecosystems and species, especially for species with sensitive tolerance thresholds, predator-prey relationships, and range-restricted species that may not be able to keep up with the pace of climate change (e.g., climate velocity). Increasing mean temperature can cause phenological changes in ecosystems and agricultural crops. Increasing temperatures also have implications for disease vectors, resulting in health impacts to communities.
Mean precipitation	Complex changes to total and seasonal precipitation affect a number of sectors. Both too much or too little rain and snow can affect crop growth and farm yields and the seasonal timing of rainfall can shift agricultural growing seasons. Shifts in growth of native vegetation can also lead to phenological mismatches with species that depend on plant availability at specific times of the year. Plant and animal species are generally adapted to a region's precipitation, with changes affecting water availability. Communities also rely on consistent seasonal precipitation for water resource availability and may be threatened by flooding hazards when intense precipitation events occur over short time periods.

Purpose of this Draft Report

This report provides documentation of project methodologies and results for bias-adjusted temperature and precipitation scenarios as well as associated bioclimatic variables designed to facilitate ecosystem modeling. The outputs from the analyses will also inform water resource applications that are being provided by additional project partners.

This report provides a framework that CCSR and project partners may use to engage with project partners and stakeholders.

Methodology

Climate scenarios created for this report were designed to capture details of regional climate that are important to natural and human systems in the P-ARB and combine these with information about the ways that climate is changing due to the rise of greenhouse gas concentrations and changing aerosols in the atmosphere. In situ observational datasets, remotely sensed observations (e.g., from satellites), and observational products (which fill in observational gaps) were analyzed to understand current climate conditions. In addition, dynamically downscaled future climate models were utilized to provide information about projected climate changes. The combination of these two sets of information produced new climate scenarios that capture important regional aspects of climate across complex terrain while also capturing the effects of climate change and associated uncertainty.

Climate Model Bias Adjustment and Downscaling

All projections of future climate change in this report use the World Climate Research Programme Coordinated Regional Downscaling Experiment Coordinated Output for Regional Evaluations (CORDEX-CORE) dataset of downscaled global and regional climate models for the South Asia domain (Gutowski et al. 2016, Teichmann et al. 2021). After assessing other global climate datasets at lower resolutions (see "Also considered" below), CORDEX-CORE projections emerge as the most applicable and valuable climate modeling outputs in this region. CORDEX-CORE is a higher-resolution version of the regional dynamically downscaled CORDEX dataset, both driven by earth system model simulations from the Coupled Model Intercomparison Project Phase 5 (CMIP5) (Taylor et al. 2012). CORDEX-CORE provides the variables of interest (mean, minimum, and maximum temperature and total precipitation) for nine unique combinations of General Circulation Models (GCMs) and Regional Climate Models (RCMs) over the South Asia Domain for a high-emissions scenario, with eight of these combinations also available for a low-emissions scenario (Table 3). This project focuses primarily on the bounding higher greenhouse gas emissions pathway and the high mitigation pathway, known as Representative Concentration Pathways 8.5 and 2.6, respectively (RCP8.5 and RCP2.6) (Moss et al. 2010) because models using the mid-level emissions pathway (RCP4.5) scenario are unavailable from the higher-resolution CORDEX-CORE outputs. CORDEX-CORE regional model outputs are available on a spatial resolution of 0.22 degrees (~22 km x 22 km) from 1970-2100; this analysis uses projections from 1979-2100 to include the full baseline period of the target datasets (see sections 2.2 and 2.3 below).

Also considered: Global climate model projections are too coarse for application in this region of complex topography, with grid cells often several hundred kilometers across. Even with bias-adjustment, these model projections would miss important interactions between mountains and valleys, snow and snow-free land surfaces, and vegetative differences that can cause important gradients that shift under climate change and are therefore important to the project aims. The newer generation of CMIP6 models (Eyring et al. 2016) have not yet been dynamically downscaled under CORDEX, and the overall changes in patterns are not substantially different from CMIP5 to merit their use at coarser scale. Additional GCM/RCM combinations are available from the standard CORDEX outputs, but at an intermediate scale (~40km), and fewer simulations are available for the domain covering Afghanistan than for regions such as Europe, North America, and Africa. Inclusion of further GCM/RCM combinations is not practical given the resources and timeframe of this project, however, the sampling of multiple GCMs and RCMs provides important context for risk management in the region.

Table 3. Global and regional climate models available in CORDEX-CORE.

		Regional Climate Model (RCM)		
		RegCM4-7	REMO2015	COSMO-crCLIM
Global Climate Model (GCM)	MPI-ESM-LR		X	X
	MPI-ESM-MR	X		
	HadGEM2-ES		X	
	NorESM1-M	X	X	X
	MIROC5	X		

Temperature

Climate change projections of mean, minimum, and maximum temperature are based on CORDEX-CORE scenarios and bias-adjusted using the Climatologies at High resolution for the Earth's Land Surface Areas (CHELSA) dataset version 1.2 (Karger et al. 2017). CHELSA provides global precipitation and mean, minimum, and maximum temperature data at a high spatial resolution (30 arcsec or ~1 km) based on statistical downscaling of global reanalyses and GCM outputs. CHELSA data are available as climatological monthly means from 1979-2013, indicating the monthly mean of daily mean, minimum, or maximum temperature. CORDEX-CORE model outputs were linearly interpolated onto a 30 arcsec grid to match CHELSA, then a monthly correction value was calculated for each of the three temperature variables by subtracting CORDEX-CORE outputs on a monthly scale from the CHELSA climatology for the same period (using RCP8.5 for the years 2006-2013 as the CORDEX historical GCM simulations conclude in 2005). This monthly correction was then added to each corresponding month in CORDEX-CORE for the full 1979-2100 period to produce a high-resolution monthly time series for each GCM-RCM combination. Although the year 1979 is included in final outputs for consistency with the period of CHELSA climatological products, the baseline period in bioclimatic and hazard analysis is defined as the 30 years between 1980-2009 to match the length of future time slices.

Also considered: The CHELSA dataset is similar to WorldClim v1.4 temperature climatologies (Hijmans et al. 2005), but includes a more comprehensive downscaling procedure for precipitation that results in higher accuracy than WorldClim and the major patterns of regional and seasonal temperature differences were well captured in the CHELSA climatologies. Satellite-based land surface temperatures from MODIS were biased high as a surface skin temperature (compared to the standard 2-meter thermometer measure).

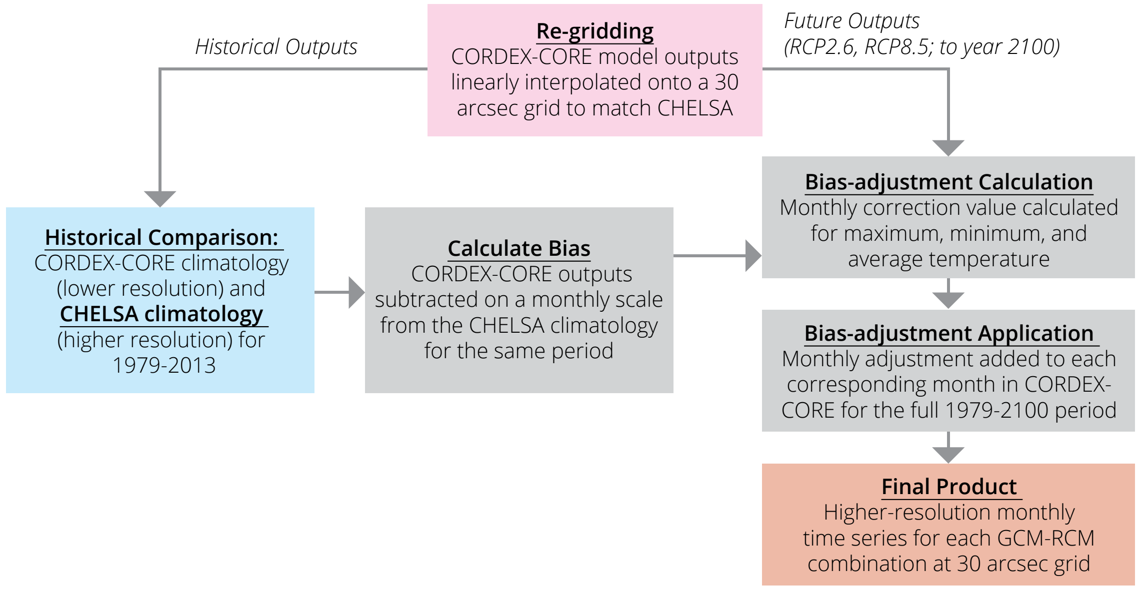

Figure 16. Overview of temperature bias-adjustment method.

Precipitation

For future projections of precipitation, CORDEX-CORE data were bias-adjusted using a combined target dataset (here referred to as “CHIRPS+”) that was developed using CHELSA precipitation as well as the Climate Hazards group InfraRed Precipitation with Station (CHIRPS) data, a global precipitation dataset using climatologies, satellite imagery, and in situ station data from 1981 to near-present (Funk et al. 2015). As a high-resolution, longer-term dataset combining multiple model and imaging products, CHIRPS provides an advantage over other climatological and satellite precipitation sources (see “Also considered” section below). CHIRPS data are available on a daily scale at a 0.05° spatial resolution (~5 km x 5 km); the CHIRPS dataset was used from 1981 to the most recent complete year, 2019. To develop the combined target dataset, CHIRPS was aggregated to monthly means, then linearly interpolated onto a 30 arcsec grid to match CHELSA. The monthly ratio between CHELSA climatological mean precipitation and CHIRPS monthly mean precipitation was calculated for the closest matching time period (1979-2013 in CHELSA; 1981-2013 in CHIRPS). To avoid infinite and missing values in correction ratios, several conditions were set in the calculation of a CHELSA/CHIRPS monthly ratio:

1. In months and for grid cells where CHIRPS indicated zero mean precipitation over the 1981-2013 period, the correction ratio was set equal to one. This was a simple step to preserve any CHIRPS precipitation data in the remaining years (2014-2019) in the final CHIRPS+ output.
2. In months and for grid cells where CHIRPS indicated less than 1 mm mean precipitation over the full 1981-2019 period, the value for all years in the output dataset was replaced with the corresponding CHELSA climatological value. This step preserves topographical detail in CHELSA in months and regions that were extremely dry, as lower-resolution CHIRPS could mask out CHELSA geography with anomalously high or low correction ratios.
3. In months and for grid cells where the correction ratio was greater than three, the ratio was changed to three to avoid anomalously high precipitation outputs. Bias correction factor truncation is common in precipitation bias-adjustment processes when multiple sets of observational products are used, given the difference in the inclusion of secondary factors that can contribute to overall precipitation amounts, and the tendency for correction ratios to be overexaggerated in areas with low amounts of precipitation.

These monthly correction ratios were applied to each month in CHIRPS from 1981 to 2019 to develop a monthly CHIRPS+ dataset at a 30 arcsec resolution with high-resolution CHELSA patterns.

This 30 arcsec CHIRPS+ dataset served as the target for CORDEX-CORE precipitation bias adjustment. To bias-adjust CORDEX-CORE precipitation, a quantile mapping approach was used, as precipitation distributions are more likely to contain systematic biases, and extreme precipitation events, or “tails” of the distributions, require quantile-specific bias adjustment. As the overlapping baseline time period contained just 39 years, only four quantiles or “quartiles” were used in the adjustment process.

For each CORDEX-CORE GCM-RCM combination, the corresponding time period (1981-2019) was selected, and data was linearly interpolated to match the CHIRPS+ target spatial grid. For each month in both CHIRPS+ and CORDEX-CORE, the distribution of 39 years was split into four quartiles based on the 0-25, 25-50, 50-75 and 75-100 percentile bins. In cases where the CHIRPS+ value was static due to replacement using the CHELSA climatological value, these bins were necessarily the same in the target data, and so a single correction factor was used rather than separate quartiles. A correction ratio between CHIRPS+ and CORDEX-CORE for each month and quartile in the 1981-2019 period was then calculated, applying similar conditions to avoid missing values:

1. In months and for grid cells where CORDEX-CORE indicated zero mean precipitation over the 1981-2019 period, the correction ratio was set equal to one to preserve potential CORDEX precipitation data in the remaining years (2020-2100) in the final output.
2. In months and for grid cells where the correction ratio was greater than three, the ratio was changed to three to avoid anomalously high precipitation outputs.

The quartile of future CORDEX-CORE precipitation data for the given month was calculated using the bin boundaries from the 1981-2019 period. The corresponding quartile's monthly correction ratios were then applied to each month in CORDEX-CORE from 1979 to 2100.

Finally, a decadal correction factor was applied to preserve CORDEX-CORE patterns in precipitation change. For each month, a percent change value was calculated between the non-bias-adjusted 1979-2005 period and each non-bias-adjusted decade in CORDEX-CORE future projections (beginning with 2006-2019 and ending with 2090-2100, with each decade in between consisting of 10 years). The corresponding percent change between bias-adjusted mean baseline month and the same month in the bias-adjusted mean future decade was then calculated. To produce the final precipitation output, each of the ~10 months in the decade was then multiplied by a decadal correction factor, replacing those grid cells where both bias-adjusted baseline and bias-adjusted future monthly mean was zero precipitation with a zero in the final precipitation output. This served to restore the bias-adjusted percent change to the initial percent change, maintaining CORDEX-CORE patterns of future precipitation changes while providing monthly precipitation output with high-resolution CHELSA topographical patterns out to 2100.

Also considered: Historical climatologies from CHELSA and WorldClim were also examined and considered to be similar, however the CHELSA product includes a more comprehensive downscaling procedure for precipitation that results in higher accuracy than WorldClim. Time series products derived from CHELSA were also considered, but these are often the result of physical models rather than a higher temporal-resolution version of CHELSA. The IMERG precipitation product (NASA 2020) was also considered alongside CHIRPS, with similar results but a shorter time coverage that would have limited the ability to create quartile bias-adjustment factors and capture the range of historical monthly extremes (which in turn would have affected future scenarios' temporal ranges). Although weather station data in the region is limited, a comparison of the CHELSA, CHIRPS, and IMERG products against monthly station data showed moderate agreement with annual totals (Figure 17). More agreement is seen between these three products than between any individual climate product and individual weather station sites.

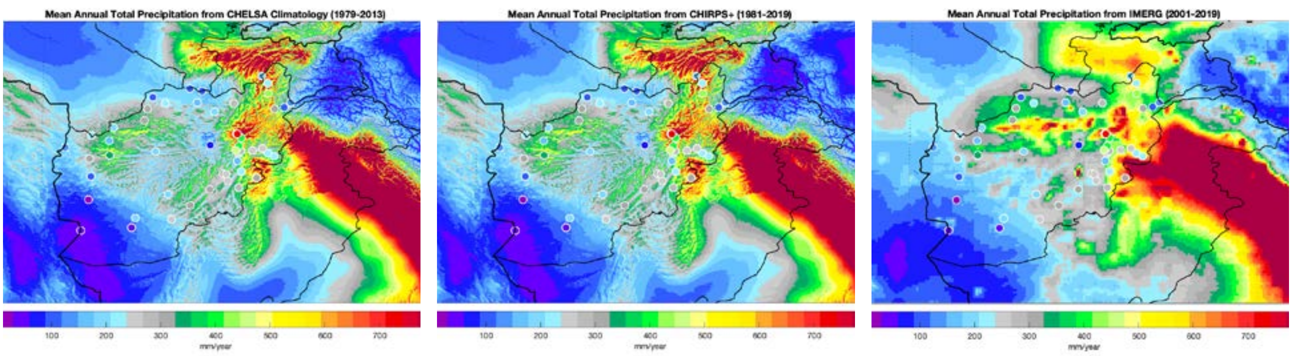

Figure 17. Mean annual total precipitation from CHELSA, CHIRPS and IMERG for available time periods, with annual total precipitation values from weather station data as overlaid points. [Resolution: CHELSA, 30 arcsec; CHIRPS, 0.05°, IMERG, 0.1°].

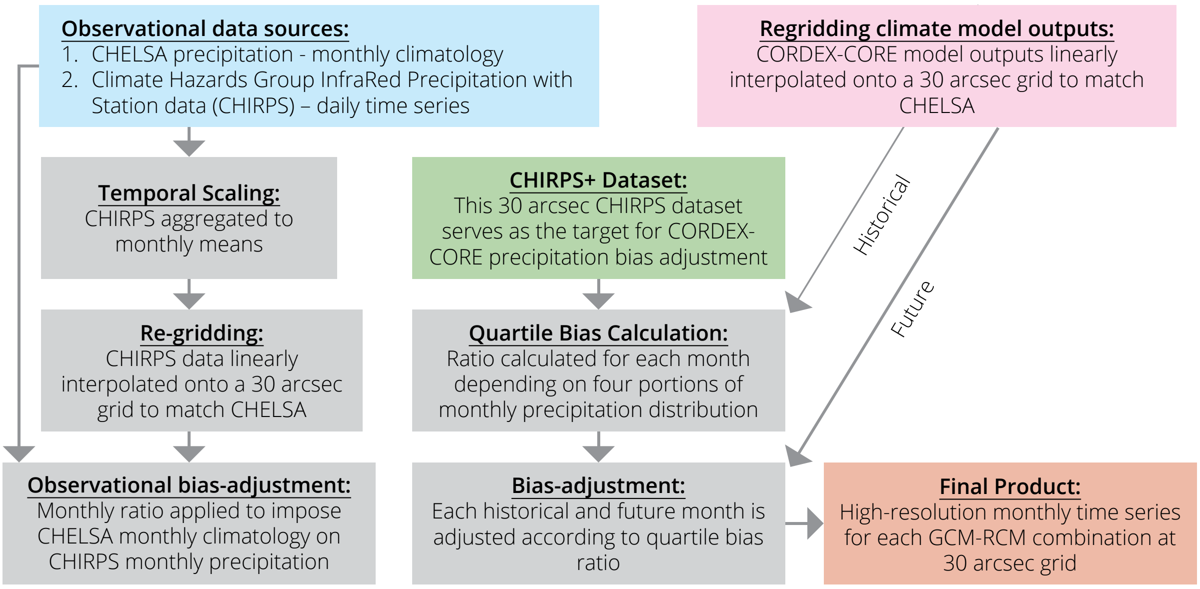

Figure 18. Precipitation bias adjustment method.

Projection Uncertainty

Like all future projections, climate projections have uncertainty embedded within them that must be factored into risk management and resilience planning. Sources of uncertainty include data and modeling constraints, the random nature of some parts of the climate system, and limited understanding of some physical processes. For this analysis, the levels of uncertainty are characterized using state-of-the-art climate models from CORDEX-CORE bias-correction, and multiple scenarios of future greenhouse gas concentrations (RCPs 2.6 and 8.5). The projections are not true probabilities, but instead represent environmental responses to plausible outcomes given socioeconomic and geopolitical decisions. The further employment of scenario-planning methods to manage the risks inherent in future climate is recommended.

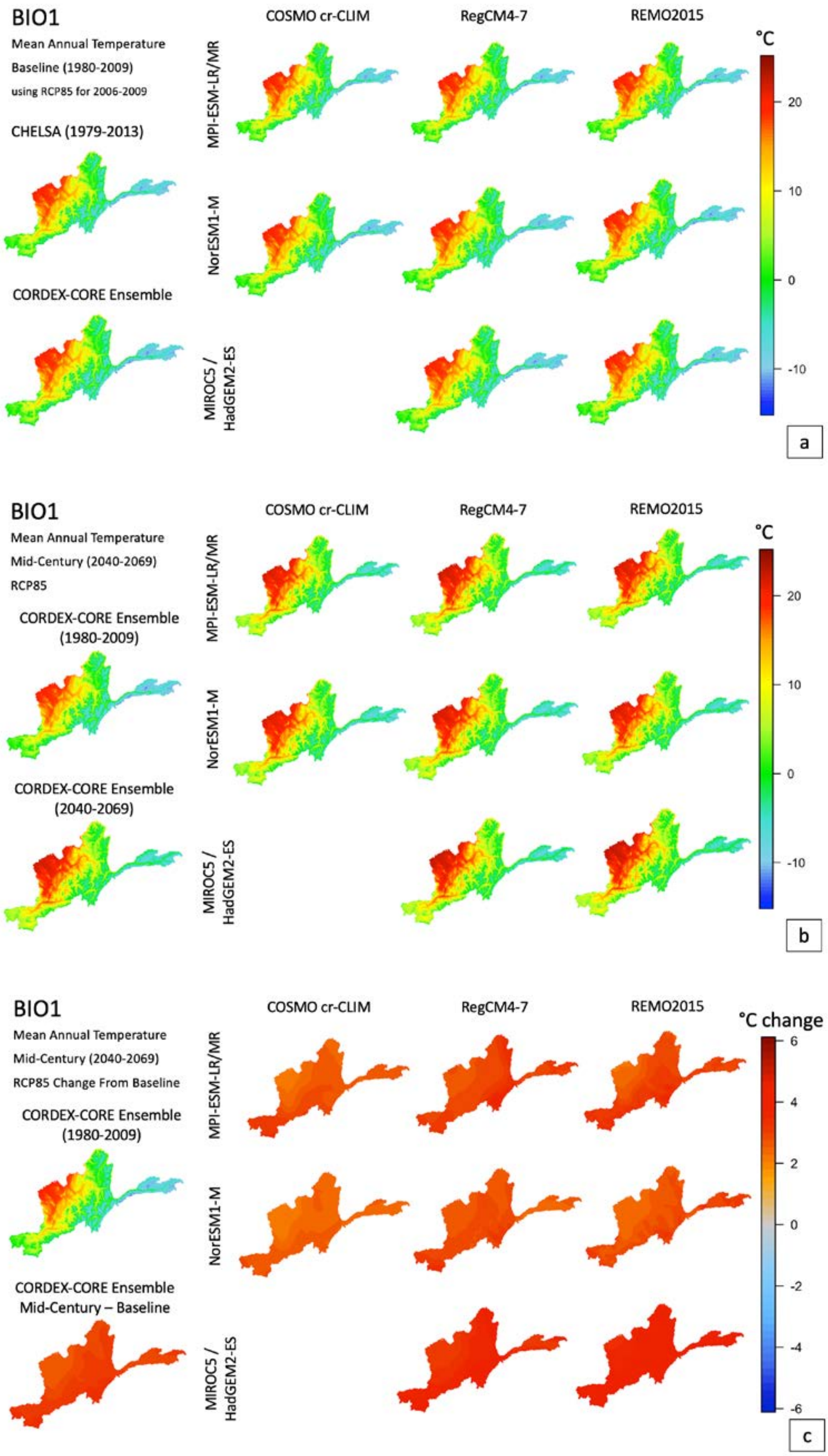

Figure 19. Individual GCM-RCM combinations showing mean annual temperature (BIO1) over the Panj-Amu River Basin for (a) baseline (1980-2009), (b) RCP8.5 mid-century (2040-2069), and (c) change from baseline to mid-century. [Resolution: 30 arcsec].

An overview of patterns in historical mean annual temperature shows that raw differences between individual GCM-RCM combinations are somewhat small after bias-adjustment; the overall temperature pattern in the region is largely determined by the mountains and valleys, as is also visible in CHELSA.

This pattern holds even in the future scenarios, as climate changes are still smaller than the temperature difference between valleys and high mountains. Climate effects are more clearly visualized by mapping the temperature changes between baseline and future periods for each model; this retains some features of elevational effects, but is not as pronounced as the raw values given the coarser resolution of the CORDEX-CORE simulations.

Substantial regional patterns show differences in warming across areas of the P-ARB, as well as more noticeable differences between GCM-RCMs. While some individual GCM-RCMs indicate a lower level of warming in the northwestern region than in the mountainous southeastern side of the basin, this gradient is somewhat reduced in the overall ensemble change. Stronger similarity in change patterns between GCM-RCMs that share underlying regional circulation models (i.e., maps in the same column of Figure 17) are seen, while those that share global circulation models (i.e., maps in the same row of Figure 17) tend to agree less on regional patterns and more on the general amount of warming.

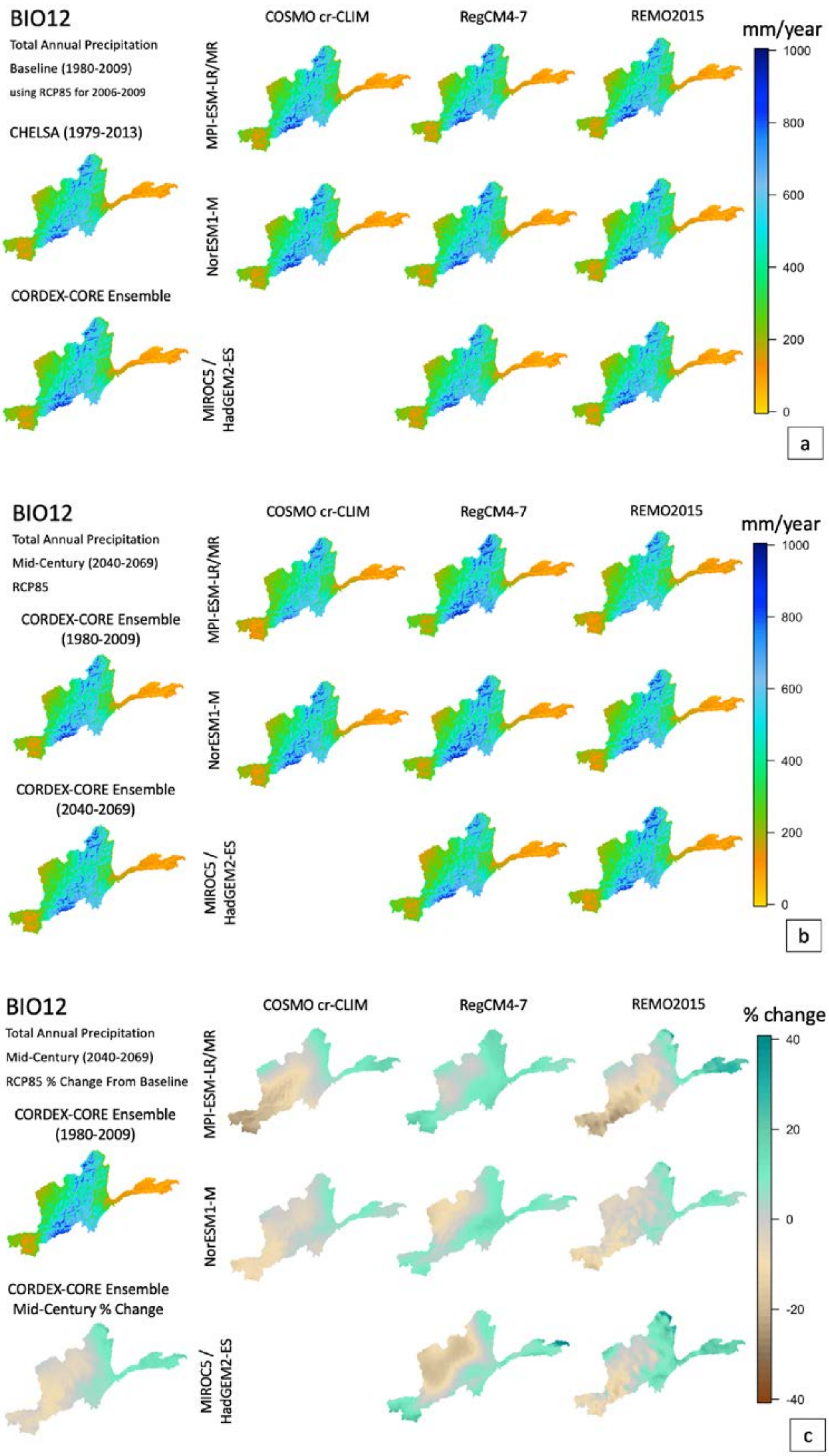

Figure 20. Individual GCM-RCM combinations showing total annual precipitation (BIO12) over the Panj-Amu River Basin for (a) baseline (1980-2009), (b) RCP8.5 mid-century (2040-2069), and (c) percent change from baseline to mid-century. [Resolution: 30 arcsec].

Differences in patterns of total annual precipitation are more subtle across GCM-RCM combinations, but a similar topographical pattern to that seen in the CHELSA climatology is clearly visible, with overall lower levels of total precipitation in the far northeast and southwest regions of the P-ARB.

Many of these patterns are consistent in future scenarios given bias-adjustment, but a stronger signal appears in future scenarios owing to the influence of CORDEX-CORE simulations. The types and level of agreement seen across underlying regional and global circulation models in precipitation changes are less obvious than those observed when examining temperature change, with the exception of some higher-contrast patterns in the REMO2015 regional model.

Every GCM-RCM combination projects precipitation increases in the mountainous northeast, while most show slight to moderate decreases in the southwestern side of the region (with the exception of the RegCM4-7 regional model). Overall, more substantial differences between GCM-RCM combinations are visible when examining mid-century precipitation changes, such as varying model agreement on the direction of change in the southwest corner of the river basin, indicating more complex interactions between climate change projections and local topography.

Figure 21 illustrates the importance of including multiple GCM-RCM combinations to capture uncertainty in global and regional climate model responses using an example location within the P-ARB (Taleqan, in the Takhar Province of northeastern Afghanistan). Uncertainty increases over time as model differences accumulate, as illustrated by increasing standard deviation across models in both temperature and precipitation over time, and the scenarios each include long-term trends embedded within large interannual variation, particularly for precipitation. Because of this variability, this report highlights model-based probabilistic projections for longer-term trends using a broad range of years, considering the full scope of individual GCM-RCM projections while focusing on ensemble average results. Hazard analyses focus on the conditions that occur at the intersection of trends and interannual extremes.

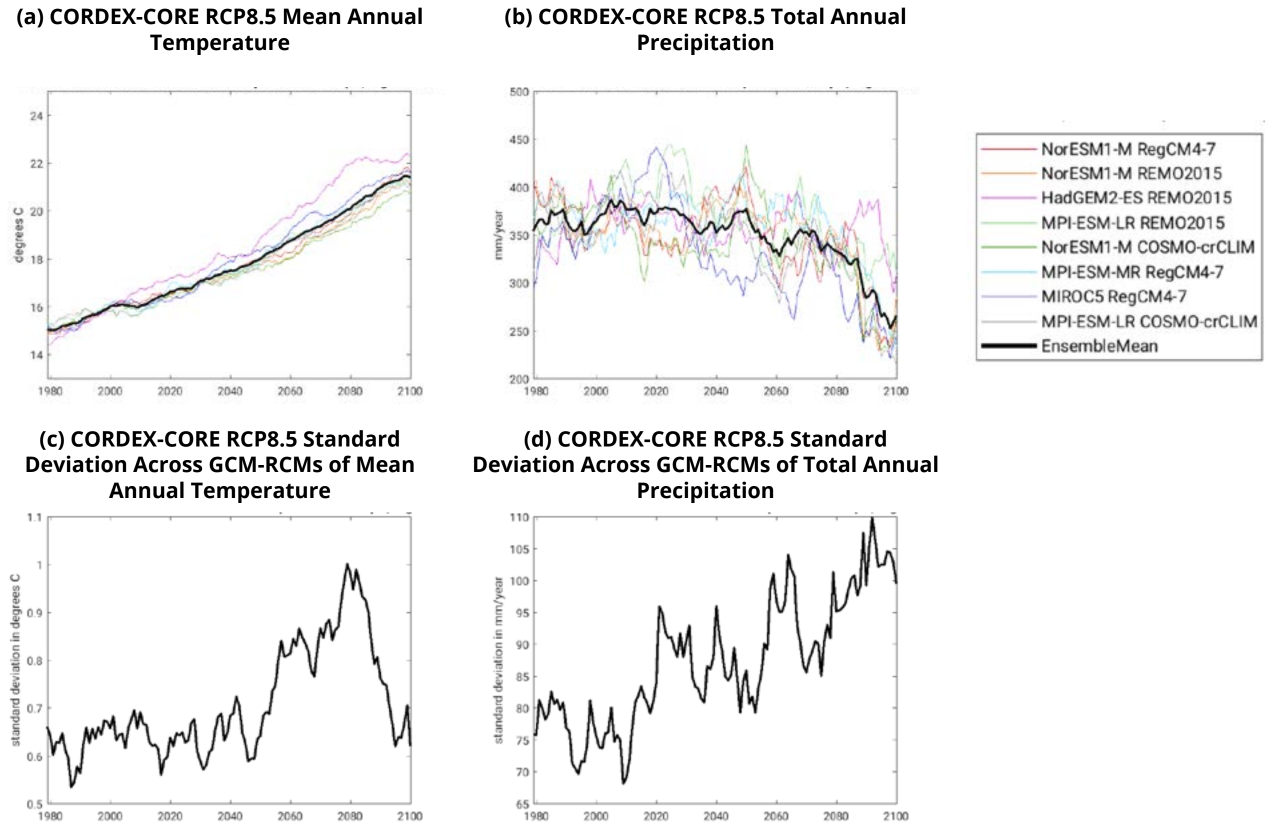

Figure 21. Time series of mean (a) temperature and (b) precipitation and standard deviation (c) temperature and (d) precipitation projections for each GCM-RCM combination from 1979-2100 for Taleqan, Afghanistan using bias-adjusted historical and RCP8.5 data.

Bioclimatic Projections

Bioclimatic variables are derived variables from the monthly mean, maximum, and minimum temperature as well as monthly precipitation totals. They are developed for species distribution modeling and related ecological applications as they represent key aspects of the long-term climate (e.g., mean annual temperature, total annual precipitation), its seasonality (e.g., annual range in temperature), and extreme or limiting environmental factors (e.g., temperature of the coldest and warmest month, and precipitation of the wet and dry quarters).

In this section, the bioclimatic projections are presented. In the following sections, baseline (1980-2009) climate conditions and future change projections from the ensemble mean of eight CORDEX-CORE GCM-RCM combinations for RCP8.5 in mid-century (2040-2069) and end-of-century (2070-2099) time horizons are shown. Differences are shown here to emphasize the climate changes, but scenarios provide raw data (including high-resolution features similar to what is seen in the baseline dataset) to connect with species models that rely on particular limits of acceptable or optimal conditions for species habitats or presence. Equations to calculate each bioclimatic variable are provided here based on those outlined in O'Donnell and Ignizio (2012).

BIO1 – Mean Annual Temperature

E

Bias-adjusted CORDEX Baseline (1980-2009) Mean Annual Temperature (ºC)

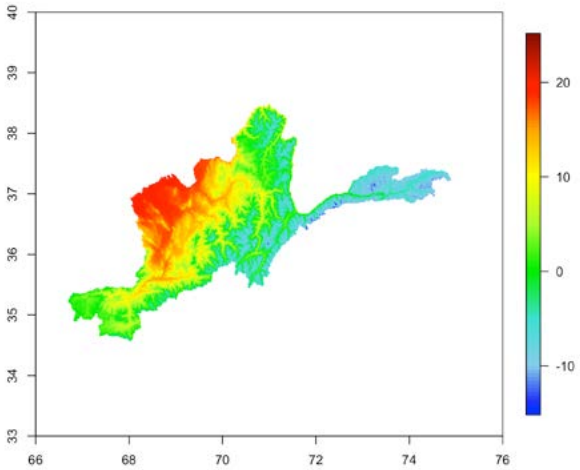

Low Emissions Pathway

RCP2.6 2050s Ensemble Mean
Annual Temperature Change (ºC)
CORDEX Future (2040-2069) – Baseline (1980-2009)

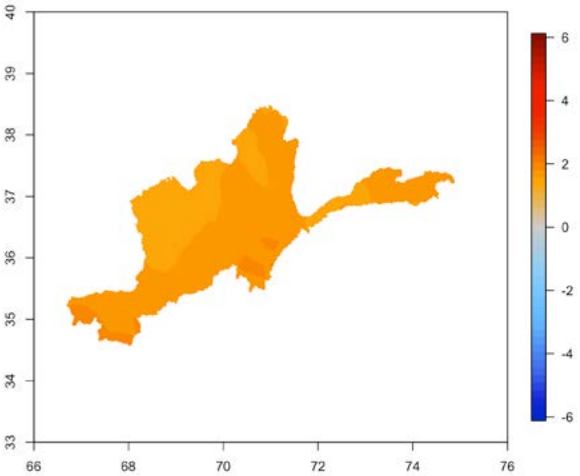

RCP2.6 2080s Ensemble Mean
Annual Temperature Change (ºC)
CORDEX Future (2070-2099) – Baseline (1980-2009)

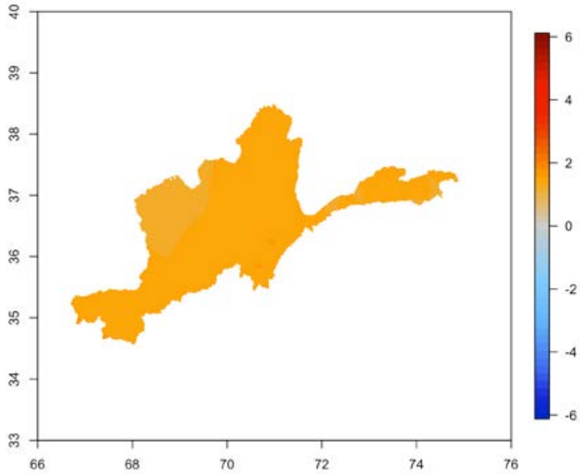

High Emissions Pathway

RCP8.5 2050s Ensemble Mean
Annual Temperature Change (ºC)
CORDEX Future (2040-2069) – Baseline (1980-2009)

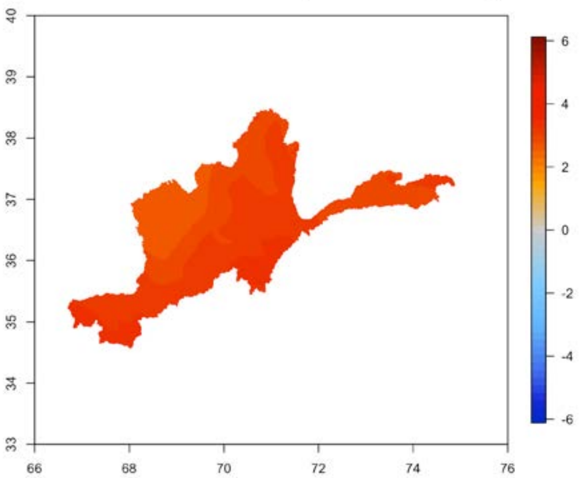

RCP8.5 2080s Ensemble Mean
Annual Temperature Change (ºC)
CORDEX Future (2070-2099) – Baseline (1980-2009)

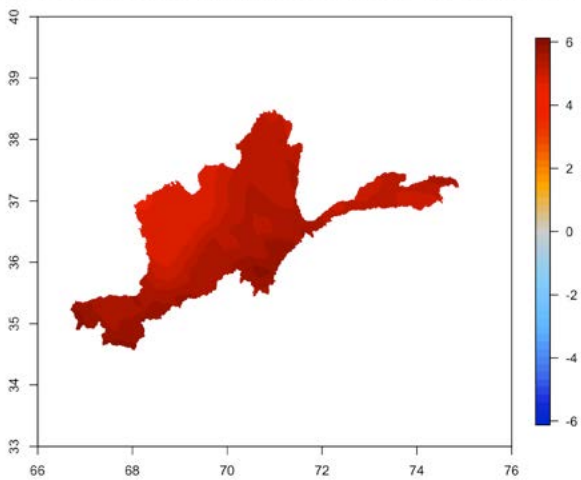

Figure 22. BIO1 – Mean Annual Temperature.

Mean annual temperature is calculated as the average across 12 monthly mean temperatures for each year (Eqn. 1):

$$BIO1 = \frac{\sum_{i=1}^{i=12} Tavg_i}{12} \tag{1}$$

where $Tavg_i$ represents the mean temperature for the given month i.

Mean annual temperature increases under RCP2.6 by the 2050s with similar levels of warming visible by the 2080s. Much of the warming in both time slices are seen in the southern, northern, and northeastern areas of the P-ARB (about 1-2°C of warming). These are the Pamir alpine desert and tundra, Karakoram-West Tibetan Plateau alpine steppe, Gissaro-Alai open woodlands, Paropamisus xeric woodlands, Ghorat-Hazarajat alpine meadow, Hindu Kush alpine meadow, Afghan Mountains semi-desert ecoregions. A similar pattern is seen in the 2080s and the warming seen in the two time slices are not too distinct in magnitude. In fact, the magnitude of change is very slightly higher in the 2050s than the 2080s, given that under RCP2.6 warming is projected to peak by mid-century before dipping slightly by the end of the century.

Mean annual temperature increases more rapidly under RCP8.5 (about 3-6°C of warming) than RCP2.6, with warming by the 2050s continuing to higher levels by the 2080s. Warming covers all regions, with higher increases in the same regions as RCP2.6 (southern, northern, and northeastern areas), generally following a pattern of greater warming at higher elevations.

BIO2 – Mean Diurnal Range

E

Bias-adjusted CORDEX Baseline (1980-2009) Mean Diurnal Range (ºC)

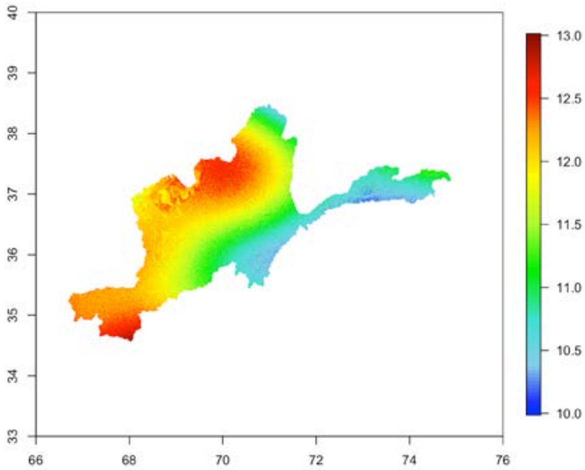

Low Emissions Pathway

RCP2.6 2050s Ensemble Mean
Change in Diurnal Range (ºC)
CORDEX Future (2040-2069) – Baseline (1980-2009)

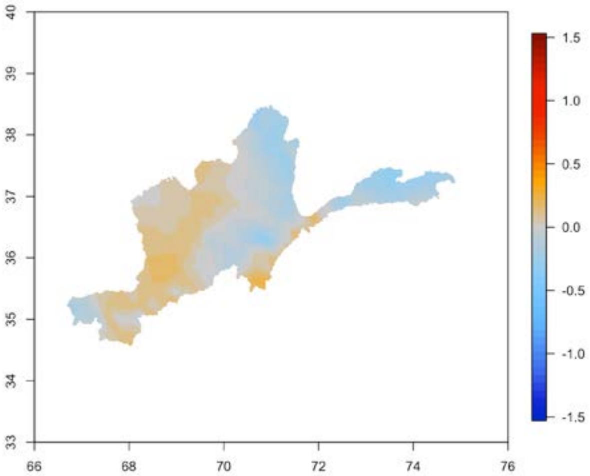

RCP2.6 2080s Ensemble Mean
Change in Diurnal Range (ºC)
CORDEX Future (2070-2099) – Baseline (1980-2009)

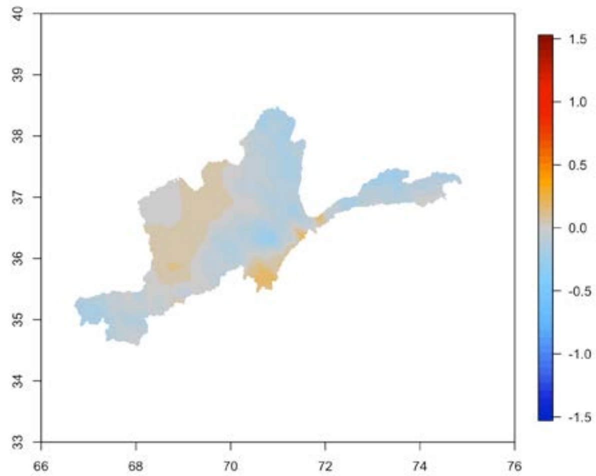

High Emissions Pathway

RCP8.5 2050s Ensemble Mean
Change in Diurnal Range (ºC)
CORDEX Future (2040-2069) – Baseline (1980-2009)

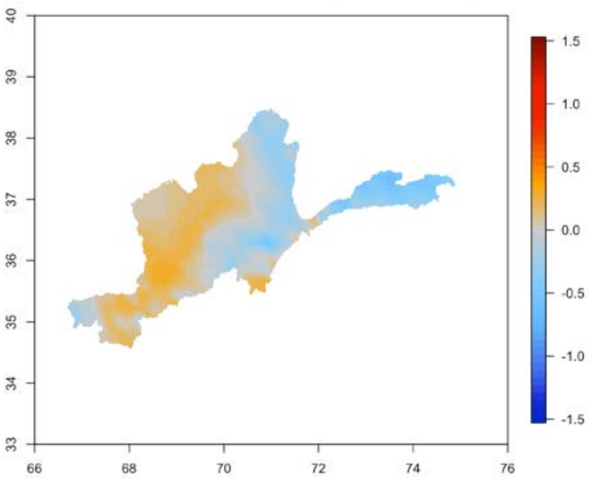

RCP8.5 2080s Ensemble Mean
Change in Diurnal Range (ºC)
CORDEX Future (2070-2099) – Baseline (1980-2009)

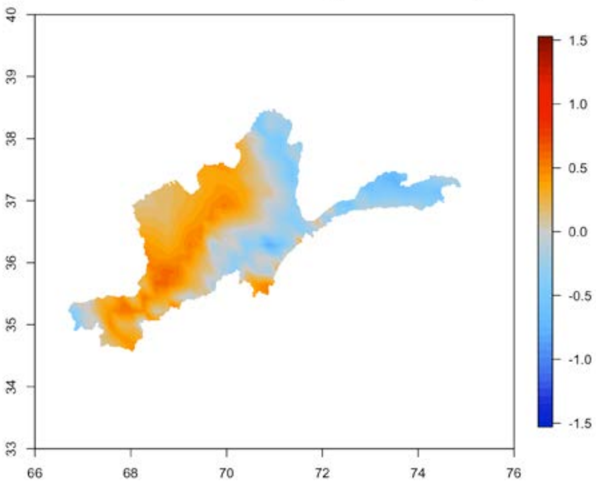

Figure 23. BIO2 – Mean Diurnal Range.

Diurnal range is calculated by subtracting mean minimum temperature from mean maximum temperature for each month. Mean diurnal range for each year was calculated by taking an average of these 12 diurnal range values (Eqn 2):

$$BIO2 = \frac{\sum_{i=1}^{i=12}(Tmax_i - Tmin_i)}{12} \tag{2}$$

where $Tmax_i$ represents the mean daily maximum temperature and $Tmin_i$ represents the mean daily minimum temperature for the given month *i*.

In all scenarios, both minimum and maximum temperatures are projected to increase compared to present day, but diurnal range reflects differences in mid-day highs and pre-dawn low temperatures.

Diurnal temperature range has only small changes under RCP2.6 2050s and RCP2.6 2080s. The change in diurnal range shows slight increases across much of the P-ARB under RCP8.5 2050s, with RCP8.5 2080s showing a heightened increase in northern, southern, eastern, and central areas. Small areas in the southern, central, and northern regions (Paropamisus xeric woodlands, Ghorat-Hazarajat alpine meadow, Hindu Kush alpine meadow, Afghan Mountains semi-desert, Badghyz and Karabil semi-desert) see a decrease in diurnal range. In the mountainous eastern region (Pamir alpine desert and tundra, Karakoram-West Tibetan Plateau alpine steppe), the range decreases across the entire region.

BIO3 – Isothermality

E

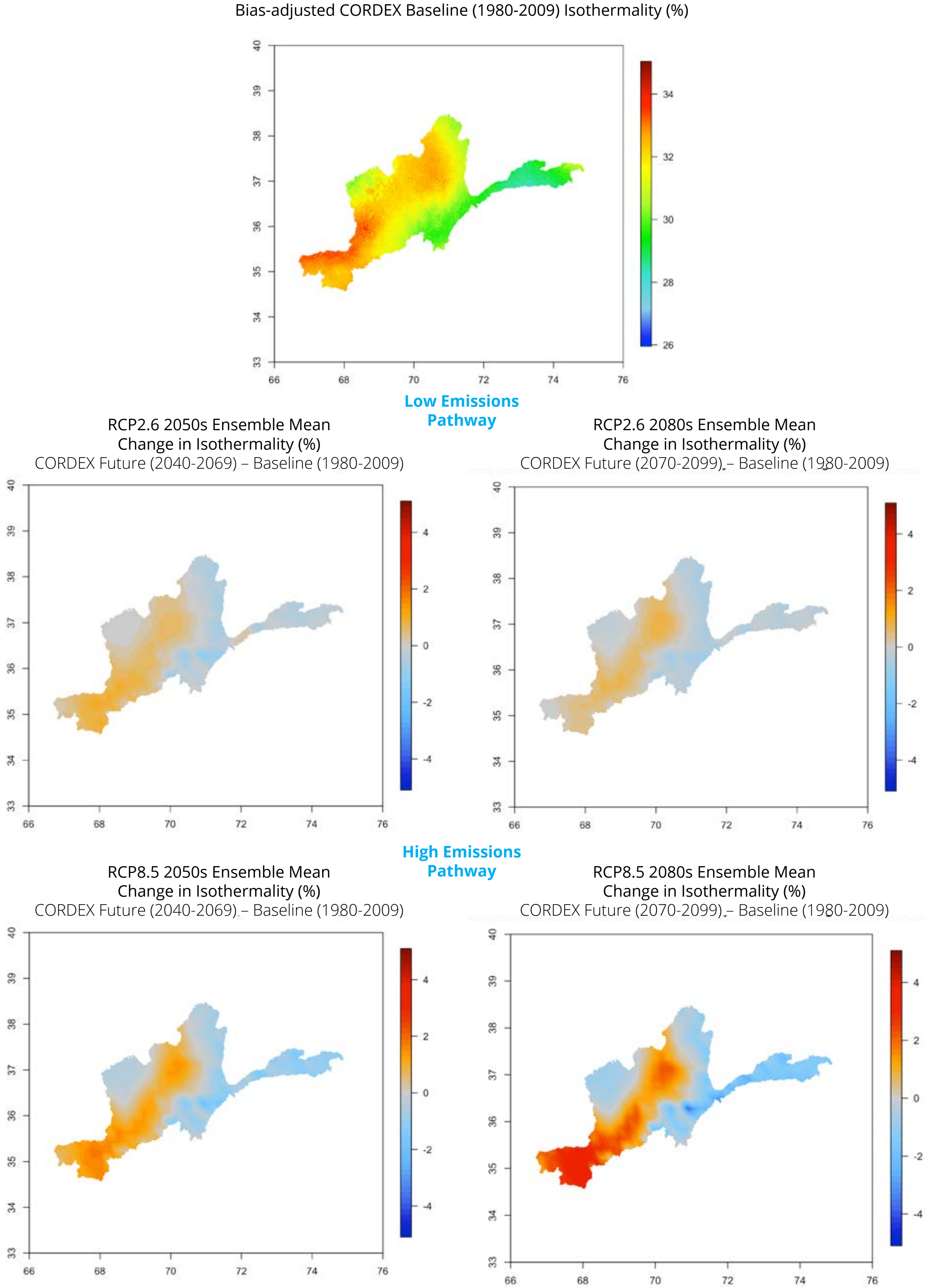

Figure 24. BIO3 – Isothermality.

Isothermality is a measure of how much daily temperatures fluctuate relative to annual temperature fluctuations. It is calculated for each year using BIO2 (Mean Diurnal Range, above) and BIO7 (Annual Temperature Range, below). Isothermality was calculated for each year as the mean diurnal range for that year divided by the annual temperature range for the year, multiplied 100%, as a measure of the relative amplitude of diurnal and annual variations (Eqn 3):

$$BIO3 = \frac{BIO2}{BIO7} \times 100 \qquad (3)$$

Isothermality is projected to increase across much of the P-ARB under RCP2.6 under both time slices, indicating more diurnal variation or reduced annual variation. By the 2050s, isothermality will increase in the northern, southern, western, and central regions (Paropamisus xeric woodlands, Ghorat-Hazarajat alpine meadow, Afghan Mountains semi-desert). Some localized areas in the southern, central, and northern regions see smaller increases in isothermality (Gissaro-Alai open woodlands, Paropamisus xeric woodlands, Hindu Kush alpine meadow, Afghan Mountains semi-desert, Badghyz and Karabil semi-desert). A similar pattern is seen by the 2080s and the increase seen in the two time slices is not too distinct in magnitude. In fact, the magnitude of change is very slightly higher by the 2050s than by the 2080s, given that under RCP2.6 warming is projected to peak by mid-century before dipping slightly by the end of the century.

Isothermality is projected to increase across much of the P-ARB under RCP8.5 by the 2050s with warming in the northern, southern, western, and central regions (Paropamisus xeric woodlands, Ghorat-Hazarajat alpine meadow, Afghan Mountains semi-desert). Small, localized areas in the southern, central, and northern regions (Gissaro-Alai open woodlands, Paropamisus xeric woodlands, Hindu Kush alpine meadow, Afghan Mountains semi-desert, Badghyz and Karabil semi-desert) see a decrease in isothermality, while much of the eastern mountainous region (Pamir alpine desert and tundra, Karakoram-West Tibetan Plateau alpine steppe) also sees a decrease. A similar, but intensified pattern is seen by the 2080s in all regions apart from the mountainous eastern region (Pamir alpine desert and tundra, Karakoram-West Tibetan Plateau alpine steppe), where isothermality decreases compared to the 2050s.

BIO4 – Temperature Seasonality

E

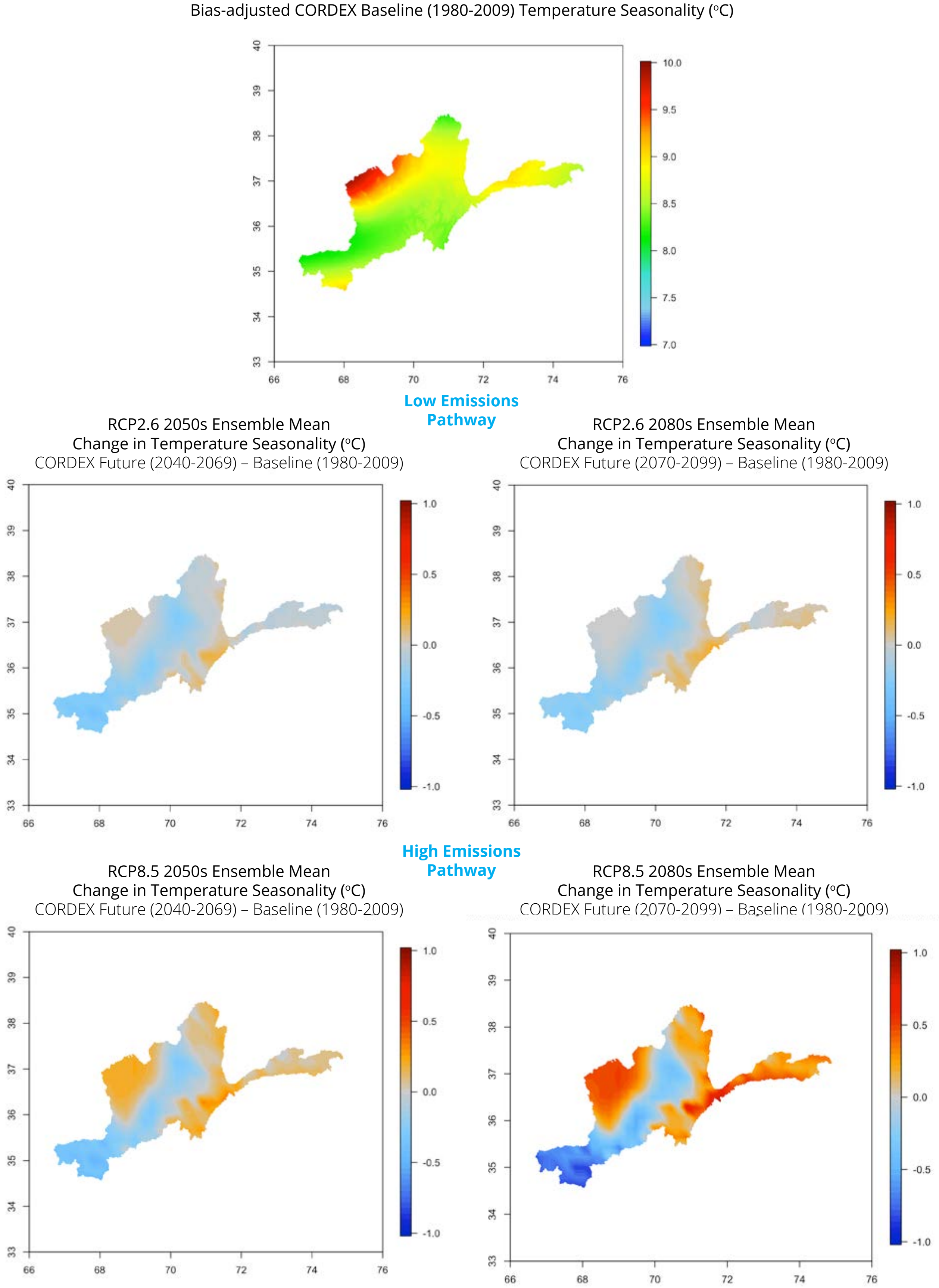

Figure 25. BIO4 – Temperature Seasonality.

Temperature seasonality is a measure of how much temperature changes month-to-month. To calculate temperature seasonality, the standard deviation across the monthly mean temperatures in each year was calculated (Eqn 4):

$$BIO4 = \sigma\{Tavg_1, \ldots, Tavg_{12}\} \tag{4}$$

where *Tavg* represents the mean of daily mean temperatures for each month.

Temperature seasonality projections indicate increases across much of the P-ARB under RCP2.6 by the 2050s, with the western region and some areas in the center seeing smaller increases (Paropamisus xeric woodlands, Ghorat-Hazarajat alpine meadow, Hindu Kush alpine meadow, Afghan Mountains semi-desert, Badghyz and Karabil semi-desert). A similar pattern is seen by the 2080s and the increase seen in the two time slices are not too distinct in magnitude. In fact, the magnitude of change is very slightly higher by the 2050s than by the 2080s, given that under RCP2.6 warming is projected to peak by mid-century before dipping slightly by the end of the century.

Temperature seasonality projections indicate increases across much of the P-ARB under RCP8.5 by the 2050s, except for the southwestern region and some areas in the center (Paropamisus xeric woodlands, Ghorat-Hazarajat alpine meadow, Hindu Kush alpine meadow, Afghan Mountains semi-desert, Badghyz and Karabil semi-desert), where it decreases. A similar, but intensified pattern is seen by the 2080s.

BIO5 – Maximum Temperature of Warmest Month

E

Bias-adjusted CORDEX Baseline (1980-2009) Max Temperature of Warmest Month (°C)

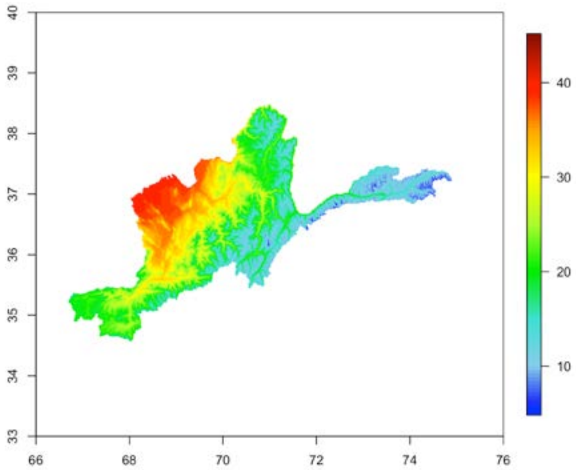

Low Emissions Pathway

RCP2.6 2050s Ensemble Mean
Change in Maximum Temperature of Warmest Month (°C)
CORDEX Future (2040-2069) – Baseline (1980-2009)

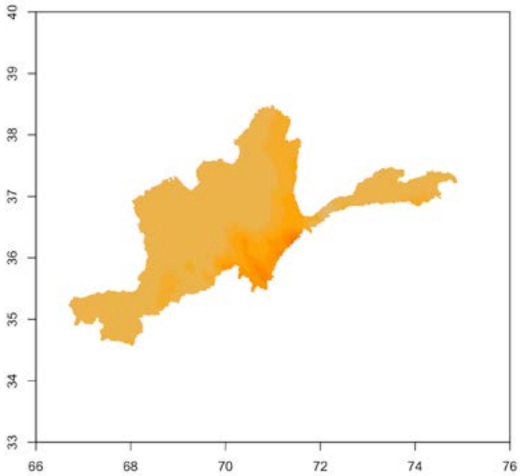

RCP2.6 2080s Ensemble Mean
Change in Maximum Temperature of Warmest Month (°C)
CORDEX Future (2070-2099) – Baseline (1980-2009)

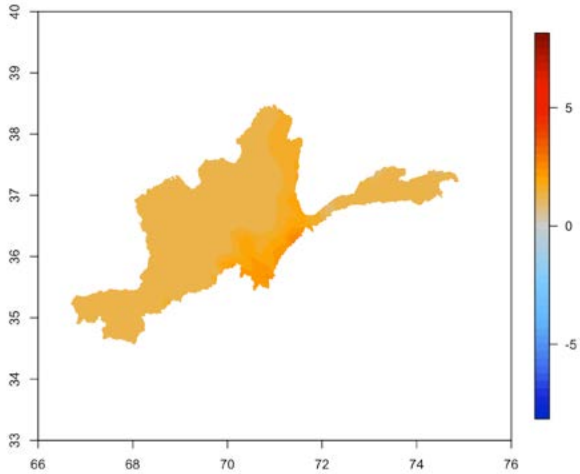

High Emissions Pathway

RCP8.5 2050s Ensemble Mean
Change in Maximum Temperature of Warmest Month (°C)
CORDEX Future (2040-2069) – Baseline (1980-2009)

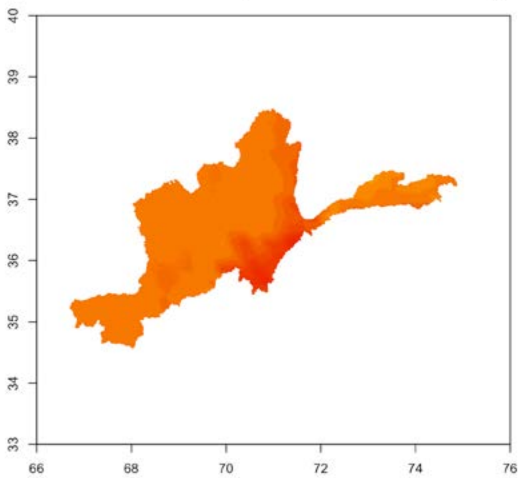

RCP8.5 2080s Ensemble Mean
Change in Maximum Temperature of Warmest Month (°C)
CORDEX Future (2070-2099) – Baseline (1980-2009)

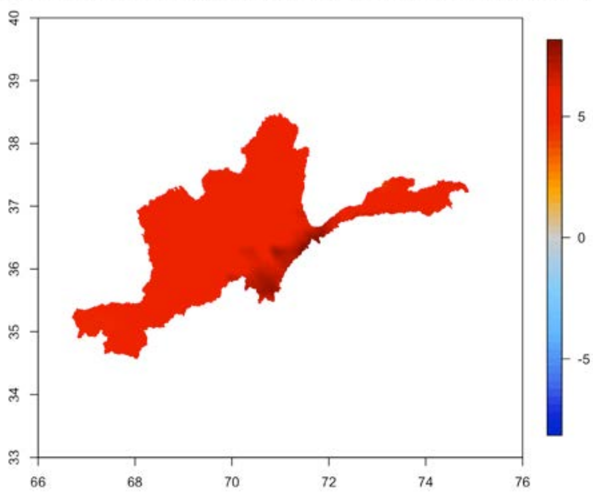

Figure 26. BIO5 – Maximum Temperature of Warmest Month.

Maximum temperature of the warmest month for each year was calculated by taking the maximum of the 12 monthly mean maximum temperature values (Eqn 5):

$$BIO5 = max\{Tmax_1, \dots, Tmax_{12}\} \qquad (5)$$

where *Tmax* represents the mean of daily maximum temperatures for each month.

The maximum temperature of the warmest month is projected to increase in a uniform pattern across the P-ARB under RCP2.6 by the 2050s, with some areas in the southern region (Hindu Kush alpine meadow). seeing higher levels of warming. A similar pattern is seen by the 2080s and the increase seen in the two time slices are not too distinct in magnitude. In fact, the magnitude of change is very slightly higher by the 2050s than by the 2080s, given that under RCP2.6 warming is projected to peak by mid-century before dipping slightly by the end of the century.

The maximum temperature of the warmest month is projected to increase in a uniform pattern across the P-ARB under RCP8.5 by the 2050s, with some areas in the southern region seeing higher levels of warming. By the 2080s, the warming is much higher and shows a similar pattern of distribution across the area.

BIO6 – Minimum Temperature of Coldest Month

E

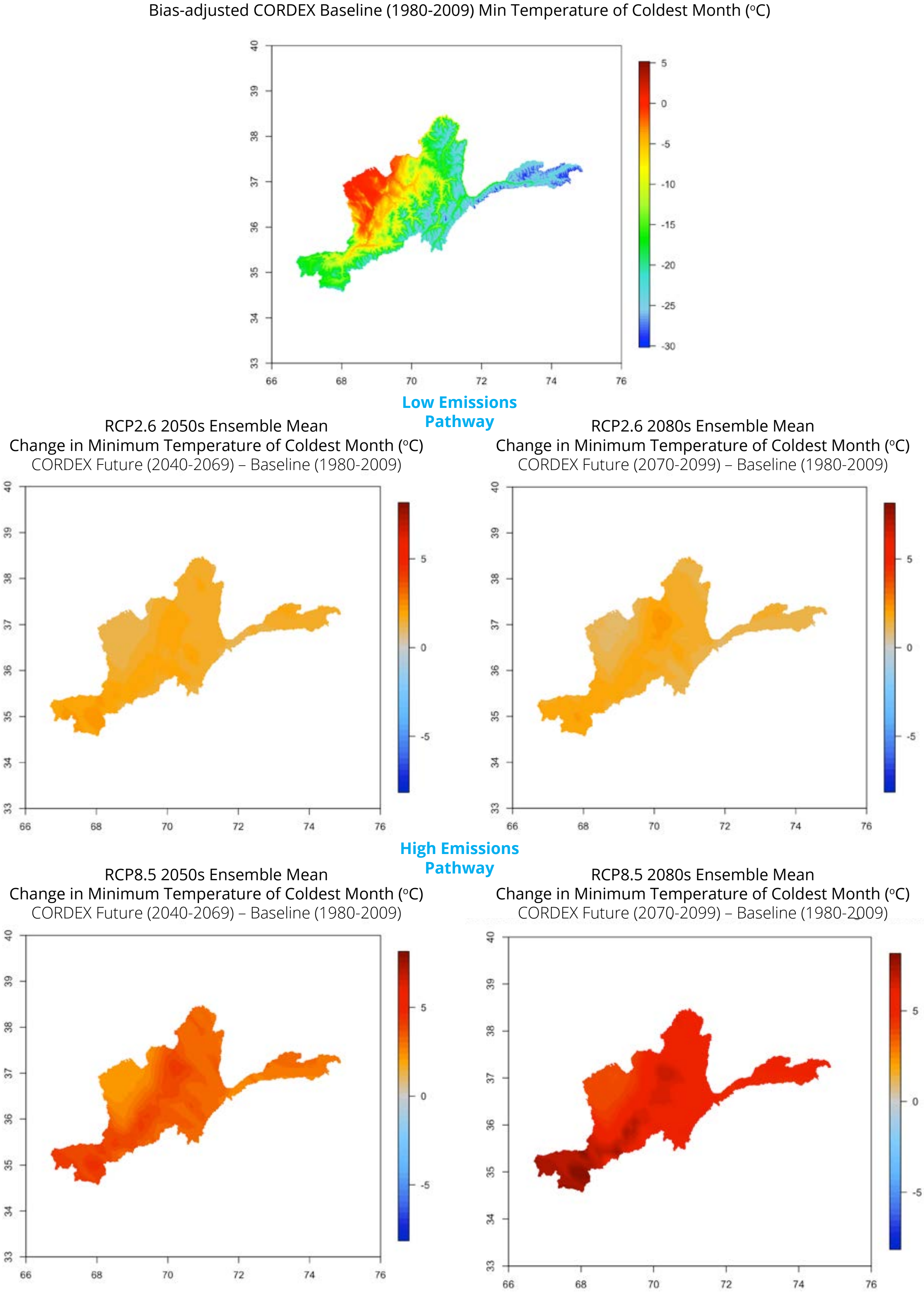

Figure 27. BIO6 – Minimum Temperature of Coldest Month.

Minimum temperature of the coldest month for each year was calculated by taking the minimum of the 12 monthly mean minimum temperature values (Eqn 6):

$$BIO6 = min\{Tmin_1, \dots, Tmin_{12}\} \qquad (6)$$

where *Tmin* represents the mean of daily minimum temperatures for each month.

The minimum temperature of the coldest month is projected to increase under RCP2.6 by the 2050s with some areas in the western and southern central regions (Paropamisus xeric woodlands, Ghorat-Hazarajat alpine meadow, Afghan Mountains semi-desert) seeing slightly more warming. The northwestern region (Badghyz and Karabil semi-desert) sees the least amount of warming, followed by the mountainous eastern region (Pamir alpine desert and tundra, Karakoram-West Tibetan Plateau alpine steppe). A similar pattern seen in the two time slices are not too distinct in magnitude. In fact, the magnitude of change is very slightly higher by the 2050s than by the 2080s, given that under RCP2.6 warming is projected to peak by mid-century before dipping slightly by the end of the century.

The minimum temperature of the coldest month is projected to increase under RCP8.5 by the 2050s with some areas in the western and southern central regions (Paropamisus xeric woodlands, Ghorat-Hazarajat alpine meadow, Afghan Mountains semi-desert) seeing more warming. The northwestern region (Badghyz and Karabil semi-desert) sees the least amount of warming, followed by the mountainous eastern region (Pamir alpine desert and tundra, Karakoram-West Tibetan Plateau alpine steppe). A similar, more intensified pattern of warming is seen by the 2080s, with the southwestern region seeing the most warming and the northwestern region seeing the least warming.

BIO7 – Temperature Annual Range

E

Bias-adjusted CORDEX Baseline (1980-2009) Annual Temperature Range (°C)

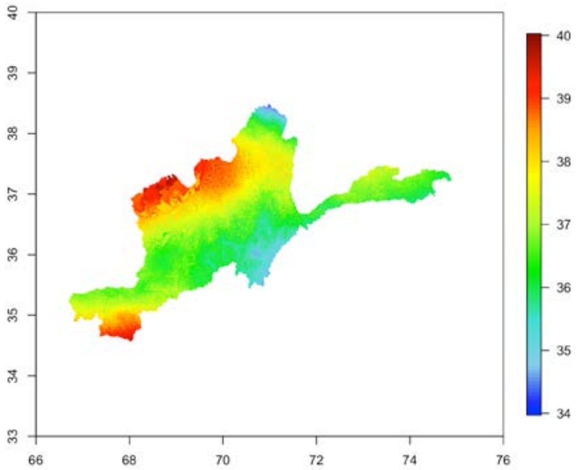

Low Emissions Pathway

RCP2.6 2050s Ensemble Mean
Change in Annual Temperature Range (°C)
CORDEX Future (2040-2069) – Baseline (1980-2009)

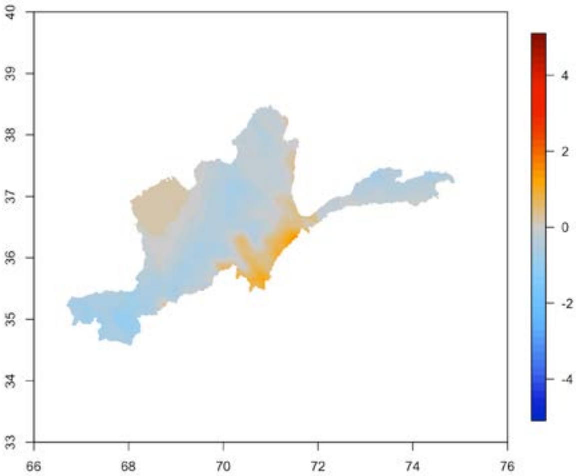

RCP2.6 2080s Ensemble Mean
Change in Annual Temperature Range (°C)
CORDEX Future (2070-2099) – Baseline (1980-2009)

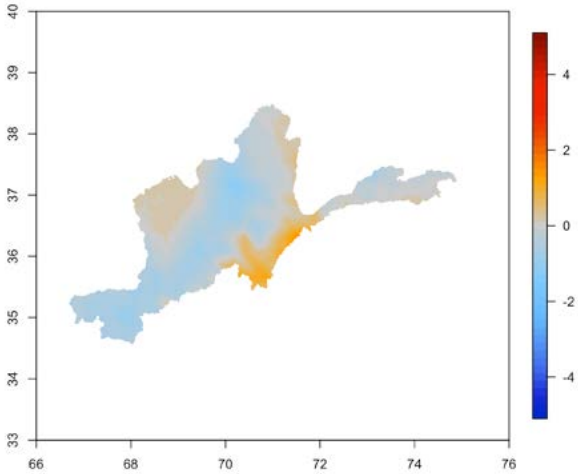

High Emissions Pathway

RCP8.5 2050s Ensemble Mean
Change in Annual Temperature Range (°C)
CORDEX Future (2040-2069) – Baseline (1980-2009)

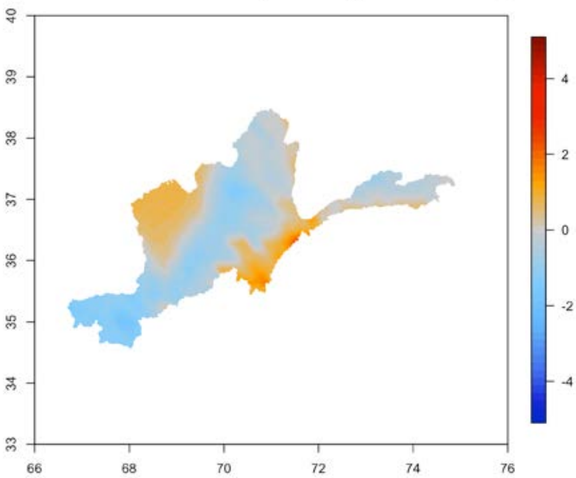

RCP8.5 2080s Ensemble Mean
Change in Annual Temperature Range (°C)
CORDEX Future (2070-2099) – Baseline (1980-2009)

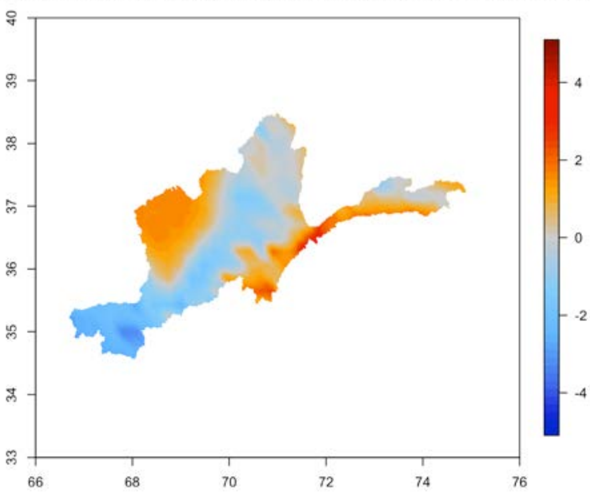

Figure 28. BIO7 – Temperature Annual Range.

Annual temperature range was calculated by subtracting BIO6 (minimum temperature of the coldest month) from BIO5 (maximum temperature of the warmest month) for each year (Eqn 7):

$$BIO7 = BIO5 - BIO6 \tag{7}$$

The annual temperature range is projected to increase across much of the P-ARB under RCP2.6 by the 2050s due to warming, except for the southwestern region and some areas in the center (Paropamisus xeric woodlands, Ghorat-Hazarajat alpine meadow, Afghan Mountains semi-desert), where the annual temperature range decreases slightly. A similar pattern and magnitude of change is seen in the two time slices. In fact, the magnitude of change is very slightly higher by the 2050s than by the 2080s, given that under RCP2.6 warming is projected to peak by mid-century before dipping slightly by the end of the century.

The annual temperature range is projected to increase across much of the P-ARB under RCP8.5 by the 2050s due to warming, except for the southwestern region and some areas in the center (Paropamisus xeric woodlands, Ghorat-Hazarajat alpine meadow, Afghan Mountains semi-desert), where the annual temperature range decreases. A similar, but intensified pattern is seen by the 2080s with the southwestern region seeing a decline in the annual temperature range.

BIO8 – Mean Temperature of Wettest Quarter

E

Bias-adjusted CORDEX Baseline (1980-2009) Mean Temperature of Wettest Quarter (°C)

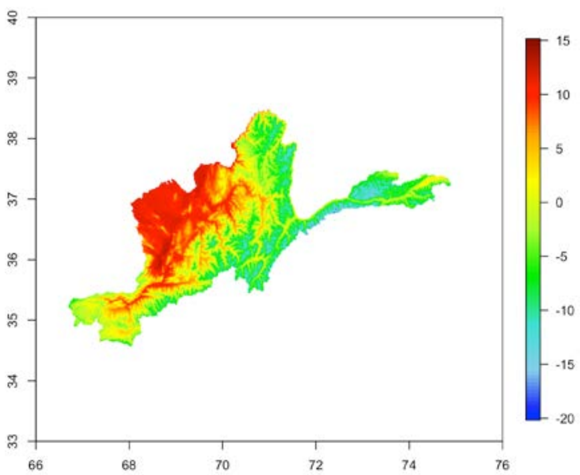

Low Emissions Pathway

RCP2.6 2050s Ensemble Mean
Change in Mean Temperature of Wettest Quarter (°C)
CORDEX Future (2040-2069) – Baseline (1980-2009)

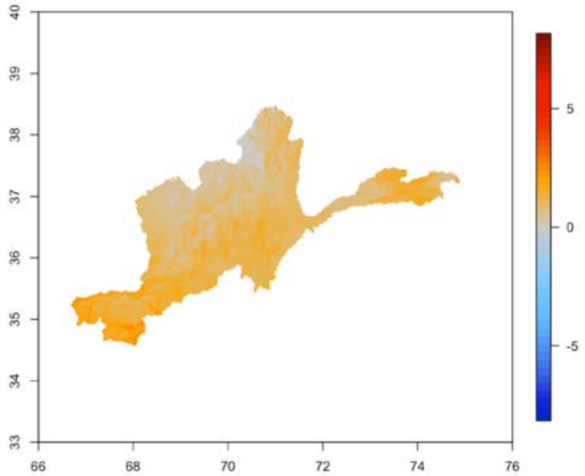

RCP2.6 2080s Ensemble Mean
Change in Mean Temperature of Wettest Quarter (°C)
CORDEX Future (2070-2099) – Baseline (1980-2009)

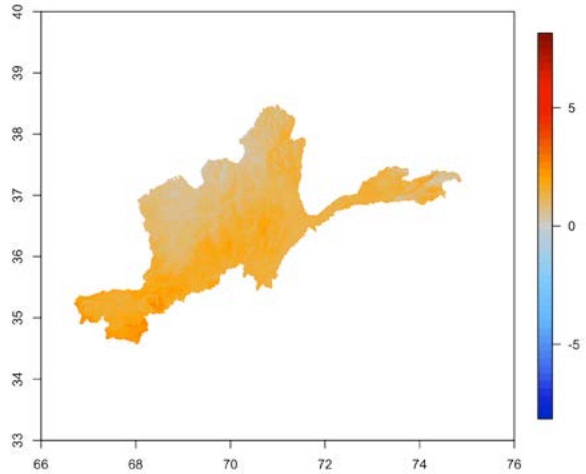

High Emissions Pathway

RCP8.5 2050s Ensemble Mean
Change in Mean Temperature of Wettest Quarter (°C)
CORDEX Future (2040-2069) – Baseline (1980-2009)

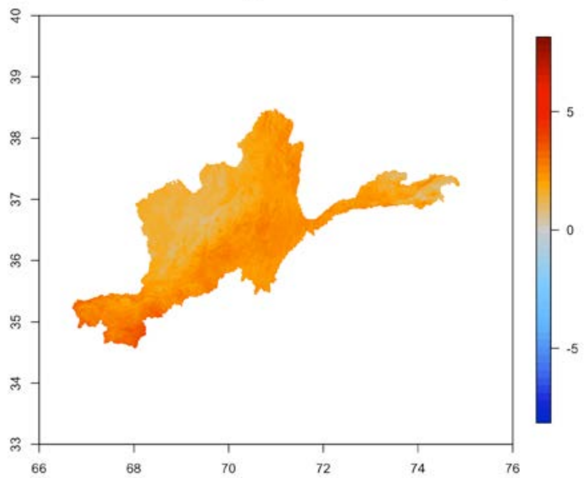

RCP8.5 2080s Ensemble Mean
Change in Mean Temperature of Wettest Quarter (°C)
CORDEX Future (2070-2099) – Baseline (1980-2009)

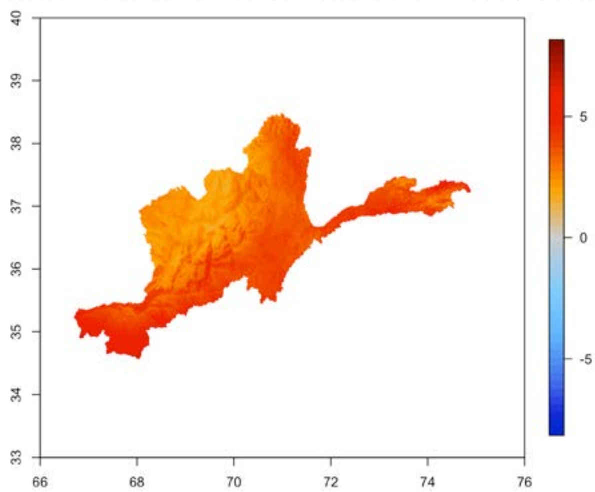

Figure 29. BIO8 – Mean Temperature of Wettest Quarter.

The total precipitation of each quarter was calculated as a sum over a 3-month period, with 12 consecutive sets of quarters in a year. For the final two quarters of each year, the 3-month period includes precipitation data from the subsequent year. Quarterly mean temperature was similarly calculated by taking an average over monthly mean temperatures for the same set of 12 rolling 3-month periods. To calculate the mean temperature of the wettest quarter, the quarter in which the maximum precipitation occurs (QPmax) in each year was identified (Eqn 8):

$$Q_{P_{max}} = max\{\sum_{i=1}^{i=3} P_i, \sum_{i=2}^{i=4} P_i, \ldots, \sum_{i=10}^{i=12} P_i, \sum_{i=11}^{i=1} P_i, \sum_{i=12}^{i=2} P_i\} \qquad (8)$$

where *P*i represents the total precipitation of each month in the rolling 3-month period. Then the average temperature for $Q_{P_{max}}$ was calculated (Eqn 9):

$$BIO8 = \frac{\sum_{i=x}^{i=y} Tavg_i}{3} \qquad (9)$$

where month indices *i=x* and *i=y* represent the months identified in $Q_{P_{max}}$.

The mean temperature of the wettest quarter is projected to increase under RCP2.6 by the 2050s. Much of the warming in both time slices is seen in the southern, north-eastern, and southwestern regions (Pamir alpine desert and tundra, Karakoram-West Tibetan Plateau alpine steppe, Gissaro-Alai open woodlands, Paropamisus xeric woodlands, Ghorat-Hazarajat alpine meadow, Hindu Kush alpine meadow, Afghan Mountains semi-desert). The northern region adjoining the central region (Badghyz and Karabil semi-desert, Paropamisus xeric woodlands) and parts of the mountainous east (Pamir alpine desert and tundra, Karakoram-West Tibetan Plateau alpine steppe) see the least warming during the wettest period. The increase seen in the two time slices are not too distinct in magnitude. In fact, the magnitude of change is very slightly higher by the 2050s than by the 2080s, given that under RCP2.6 warming is projected to peak by mid-century before dipping slightly by the end of the century.

The mean temperature of the wettest quarter is projected to increase under RCP8.5 by the 2050s with further warming by the 2080s. Much of the warming in both time slices is seen in the southern, northern (some localized areas), and northeastern regions (Pamir alpine desert and tundra, Karakoram-West Tibetan Plateau alpine steppe, Gissaro-Alai open woodlands, Paropamisus xeric woodlands, Ghorat-Hazarajat alpine meadow, Hindu Kush alpine meadow, Afghan Mountains semi-desert) of the P-ARB. The most warming is seen in the southwest Ghorat-Hazarajat alpine meadow, Afghan Mountains semi-desert). The northwestern region and the adjoining northern and central regions (Badghyz and Karabil semi-desert, Paropamisus xeric woodlands) and the far end of the mountainous east (Pamir alpine desert and tundra, Karakoram-West Tibetan Plateau alpine steppe) see the least warming. By the 2080s, the general pattern of warming remains, but the level of warming increases.

BIO9 – Mean Temperature of Driest Quarter

E

Bias-adjusted CORDEX Baseline (1980-2009) Mean Temperature of Driest Quarter (°C)

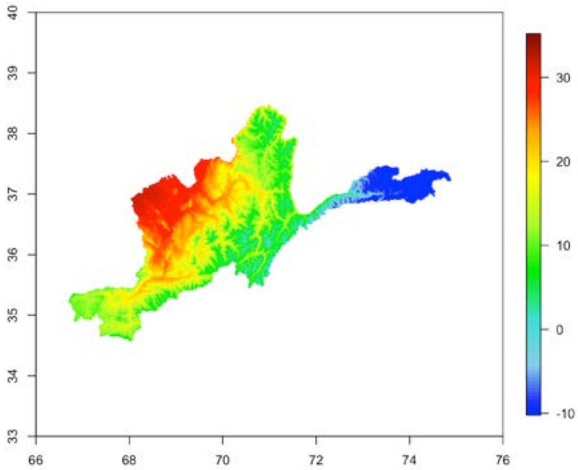

Low Emissions Pathway

RCP2.6 2050s Ensemble Mean
Change in Mean Temperature of Driest Quarter (°C)
CORDEX Future (2040-2069) – Baseline (1980-2009)

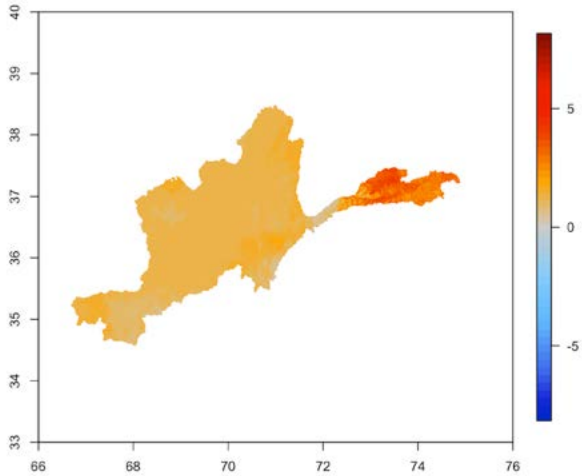

RCP2.6 2080s Ensemble Mean
Change in Mean Temperature of Driest Quarter (°C)
CORDEX Future (2070-2099) – Baseline (1980-2009)

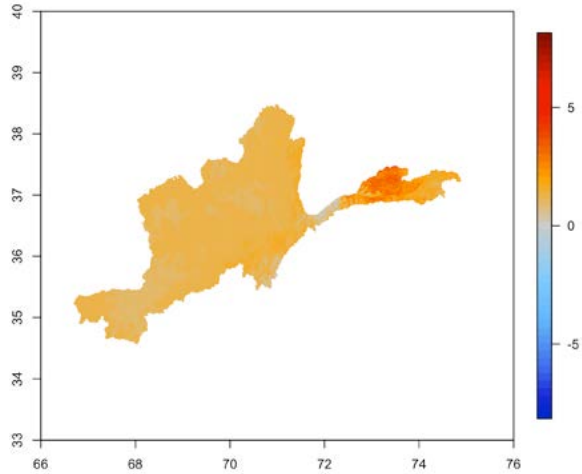

High Emissions Pathway

RCP8.5 2050s Ensemble Mean
Change in Mean Temperature of Driest Quarter (°C)
CORDEX Future (2040-2069) – Baseline (1980-2009)

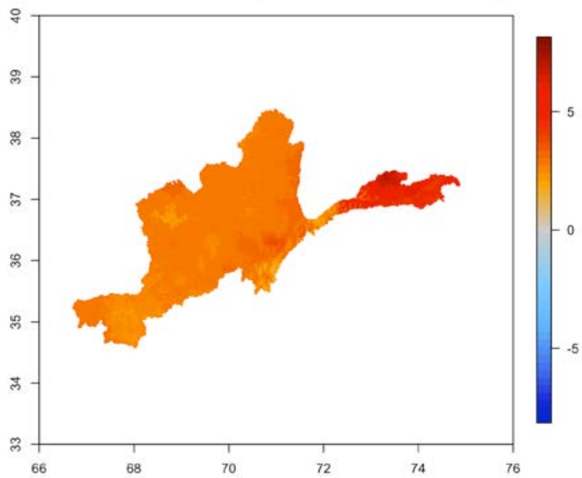

RCP8.5 2080s Ensemble Mean
Change in Mean Temperature of Driest Quarter (°C)
CORDEX Future (2070-2099) – Baseline (1980-2009)

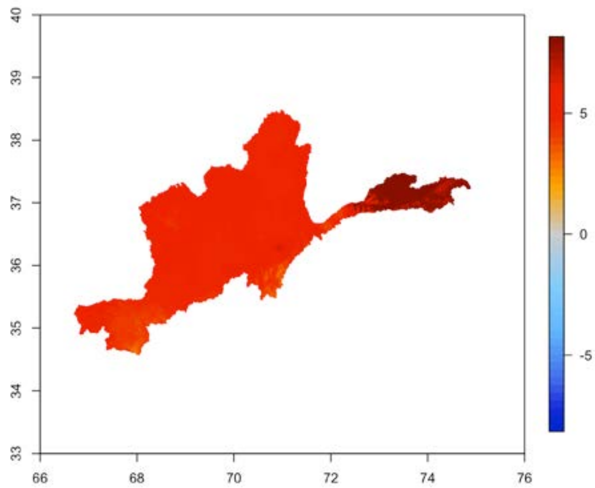

Figure 30. BIO9 – Mean Temperature of Driest Quarter.

The mean temperature of the driest quarter of each year was calculated similar to BIO8, by identifying the quarter with the minimum precipitation for each year (Eqn 10):

$$Q_{P_{min}} = min\{\sum_{i=1}^{i=3} P_i, \sum_{i=2}^{i=4} P_i, \ldots, \sum_{i=10}^{i=12} P_i, \sum_{i=11}^{i=1} P_i, \sum_{i=12}^{i=2} P_i\} \qquad (10)$$

where *Pi* represents the total precipitation of each month in the rolling 3-month period. Then the average temperature for $Q_{P_{min}}$ was calculated (Eqn 11):

$$BIO9 = \frac{\sum_{i=x}^{i=y} Tavg_i}{3} \qquad (11)$$

where month indices *i=x* and *i=y* represent the months identified in $Q_{P_{min}}$.

Projections indicate that the mean temperature of the driest quarter increases slightly under RCP2.6 by the 2050s with similar patterns of warming seen by the 2080s. The eastern mountainous areas (Pamir alpine desert and tundra, Karakoram-West Tibetan Plateau alpine steppe) warm more intensely than the rest of the region. The increase seen in the two time slices are not too distinct in magnitude. In fact, the magnitude of change is very slightly higher by the 2050s than by the 2080s, given that under RCP2.6 warming is projected to peak by mid-century before dipping slightly by the end of the century.

The mean temperature of the driest quarter increases under RCP8.5 by the 2050s with further warming by the 2080s. The eastern mountainous areas (Pamir alpine desert and tundra, Karakoram-West Tibetan Plateau alpine steppe) warm more intensely than the rest of the P-ARB. This general pattern continues by the 2080s, except with higher levels of warming.

BIO10 – Mean Temperature of Warmest Quarter

E

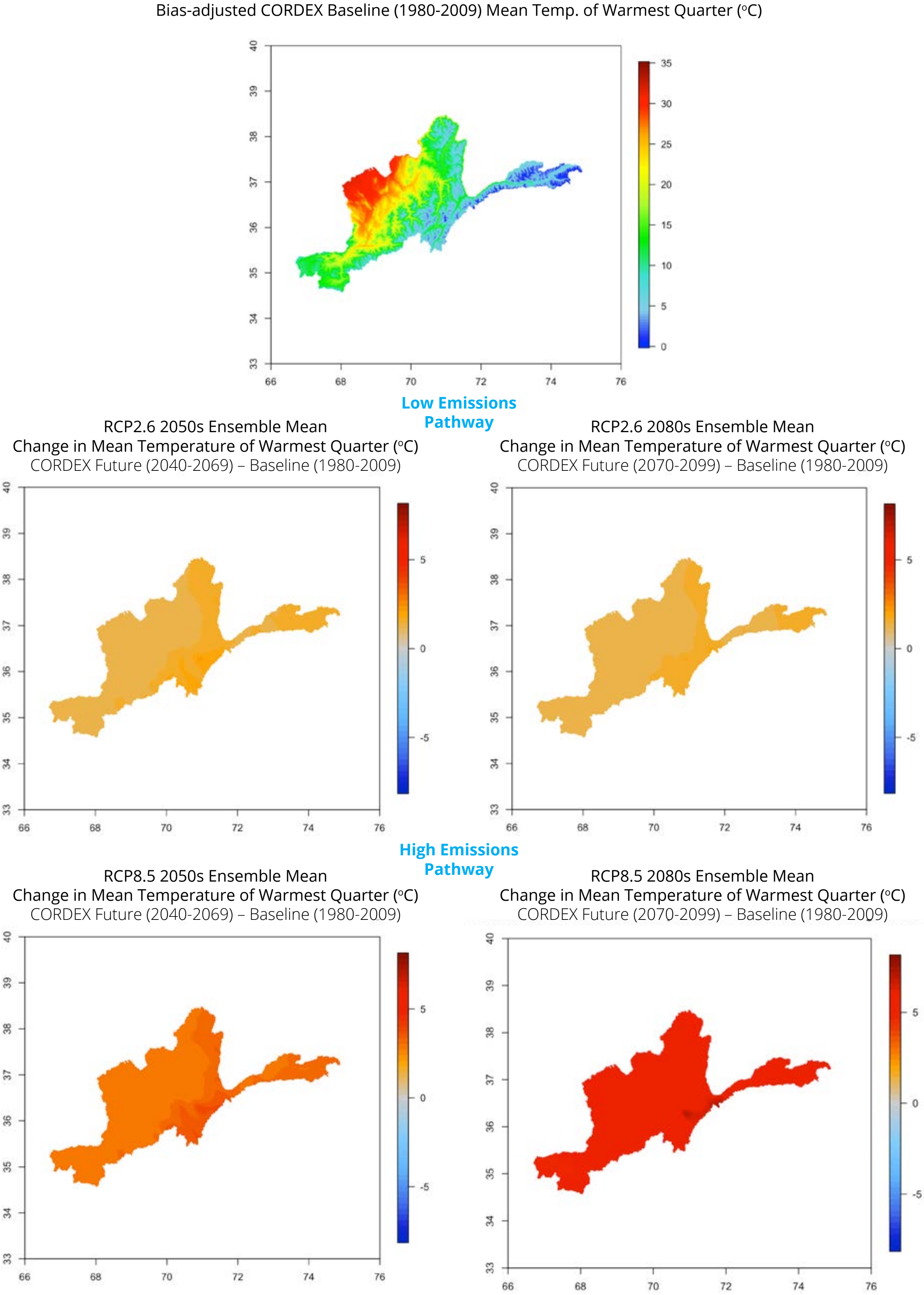

Figure 31. BIO10 – Mean Temperature of Warmest Quarter.

The mean temperature for each quarter as an average of monthly mean temperatures over a 3-month period was calculated, with 12 consecutive sets of quarters in a year, as with BIO8 and BIO9, with the maximum quarter being identified (Eqn 12):

$$Q_{T_{max}} = max\{\sum_{i=1}^{i=3} Tavg_i, \sum_{i=2}^{i=4} Tavg_i, \ldots, \sum_{i=10}^{i=12} Tavg_i, \sum_{i=11}^{i=1} Tavg_i, \sum_{i=12}^{i=2} Tavg_i\} \quad (12)$$

where $Tavg_i$ represents the mean of daily mean temperatures for each month in the rolling 3-month period. Then the average temperature for $Q_{T_{max}}$ was calculated (Eqn 13):

$$BIO10 = \frac{\sum_{i=x}^{i=y} Tavg_i}{3} \quad (13)$$

where month indices $i=x$ and $i=y$ represent the months identified in $Q_{P_{min}}$.

The mean temperature of the warmest quarter is projected to increase under RCP2.6 by the 2050s with somewhat similar patterns of warming seen by the 2080s. The warming across the P-ARB is slight and uniform with some very small regions in the south (Hindu Kush alpine meadow) seeing slightly higher levels of warming. The increase seen in the two time slices are not too distinct in magnitude. In fact, the magnitude of change is very slightly higher by the 2050s than by the 2080s, given that under RCP2.6 warming is projected to peak by mid-century before dipping slightly by the end of the century.

The mean temperature of the warmest quarter is projected to increase under RCP8.5 by the 2050s with further warming by the 2080s. The warming across the P-ARB is uniform with some very small regions in the south (Hindu Kush alpine meadow) seeing slightly higher levels of warming. This general pattern continues by the 2080s, except with higher levels of warming.

BIO11 – Mean Temperature of Coldest Quarter

E

Bias-adjusted CORDEX Baseline (1980-2009) Mean Temperature of Coldest Quarter (°C)

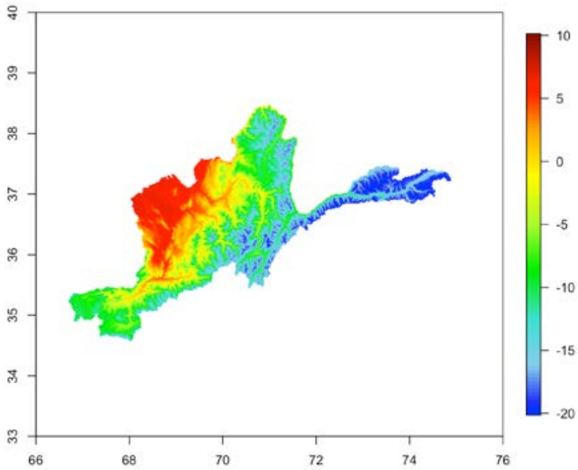

Low Emissions Pathway

RCP2.6 2050s Ensemble Mean
Change in Mean Temperature of Coldest Quarter (°C)
CORDEX Future (2040-2069) – Baseline (1980-2009)

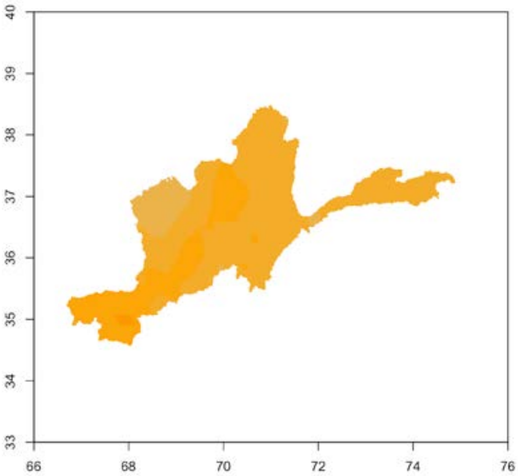

RCP2.6 2080s Ensemble Mean
Change in Mean Temperature of Coldest Quarter (°C)
CORDEX Future (2070-2099) – Baseline (1980-2009)

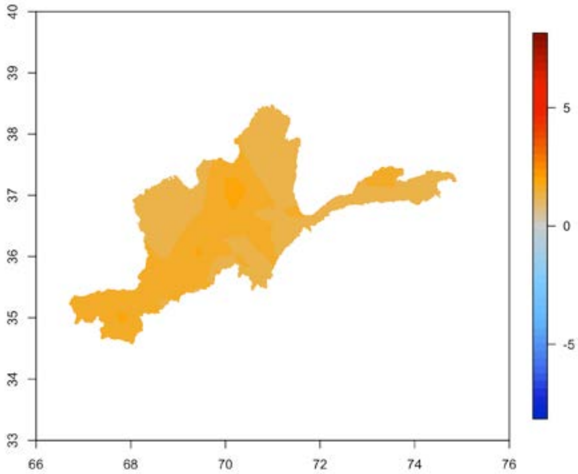

High Emissions Pathway

RCP8.5 2050s Ensemble Mean
Change in Mean Temperature of Coldest Quarter (°C)
CORDEX Future (2040-2069) – Baseline (1980-2009)

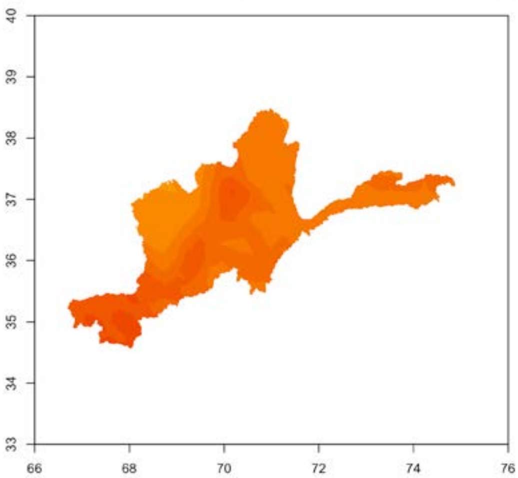

RCP8.5 2080s Ensemble Mean
Change in Mean Temperature of Coldest Quarter (°C)
CORDEX Future (2070-2099) – Baseline (1980-2009)

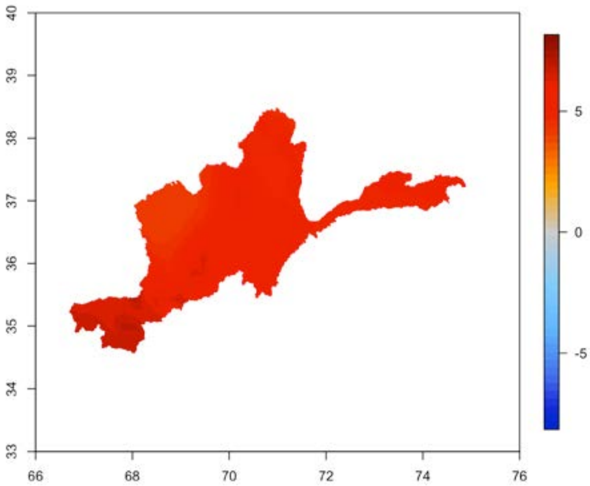

Figure 32. BIO11 – Mean Temperature of Coldest Quarter.

The mean temperature for each quarter as an average of monthly mean temperatures over a 3-month period was calculated, with 12 consecutive sets of quarters in a year, as with BIO10, with the minimum quarter being identified (Eqn 14):

$$Q_{T_{min}} = min\{\sum_{i=1}^{i=3} Tavg_i, \sum_{i=2}^{i=4} Tavg_i, \dots, \sum_{i=10}^{i=12} Tavg_i, \sum_{i=11}^{i=1} Tavg_i, \sum_{i=12}^{i=2} Tavg_i\} \qquad (14)$$

where $Tavg_i$ represents the mean of daily mean temperatures for each month in the rolling 3-month period. Then the average temperature for $Q_{T_{min}}$ was calculated (Eqn 15):

$$BIO11 = \frac{\sum_{i=x}^{i=y} Tavg_i}{3} \qquad (15)$$

where month indices $i{=}x$ and $i{=}y$ represent the months identified in $Q_{T_{min}}$.

The mean temperature of the coldest quarter slightly is projected to increase under RCP2.6 by the 2050s. The highest levels of warming are seen in the southwest (Ghorat-Hazarajat alpine meadow, Afghan Mountains semi-desert), followed by some areas in the center (Paropamisus xeric woodlands). The least warming is seen in the northwestern region (Badghyz and Karabil semi-desert). The increase seen in the two time slices are not too distinct in magnitude. In fact, the magnitude of change is very slightly higher by the 2050s than by the 2080s, given that under RCP2.6 warming is projected to peak by mid-century before dipping slightly by the end of the century.

The mean temperature of the coldest quarter is projected to increase under RCP8.5 by the 2050s with further warming by the 2080s. The highest levels of warming are seen in the southwest (Ghorat-Hazarajat alpine meadow, Afghan Mountains semi-desert), followed by some areas in the center (Paropamisus xeric woodlands). The least warming is seen in the northwestern region (Badghyz and Karabil semi-desert). This warming pattern continues by the 2080s, with higher levels of warming.

BIO12 – Annual Precipitation

E

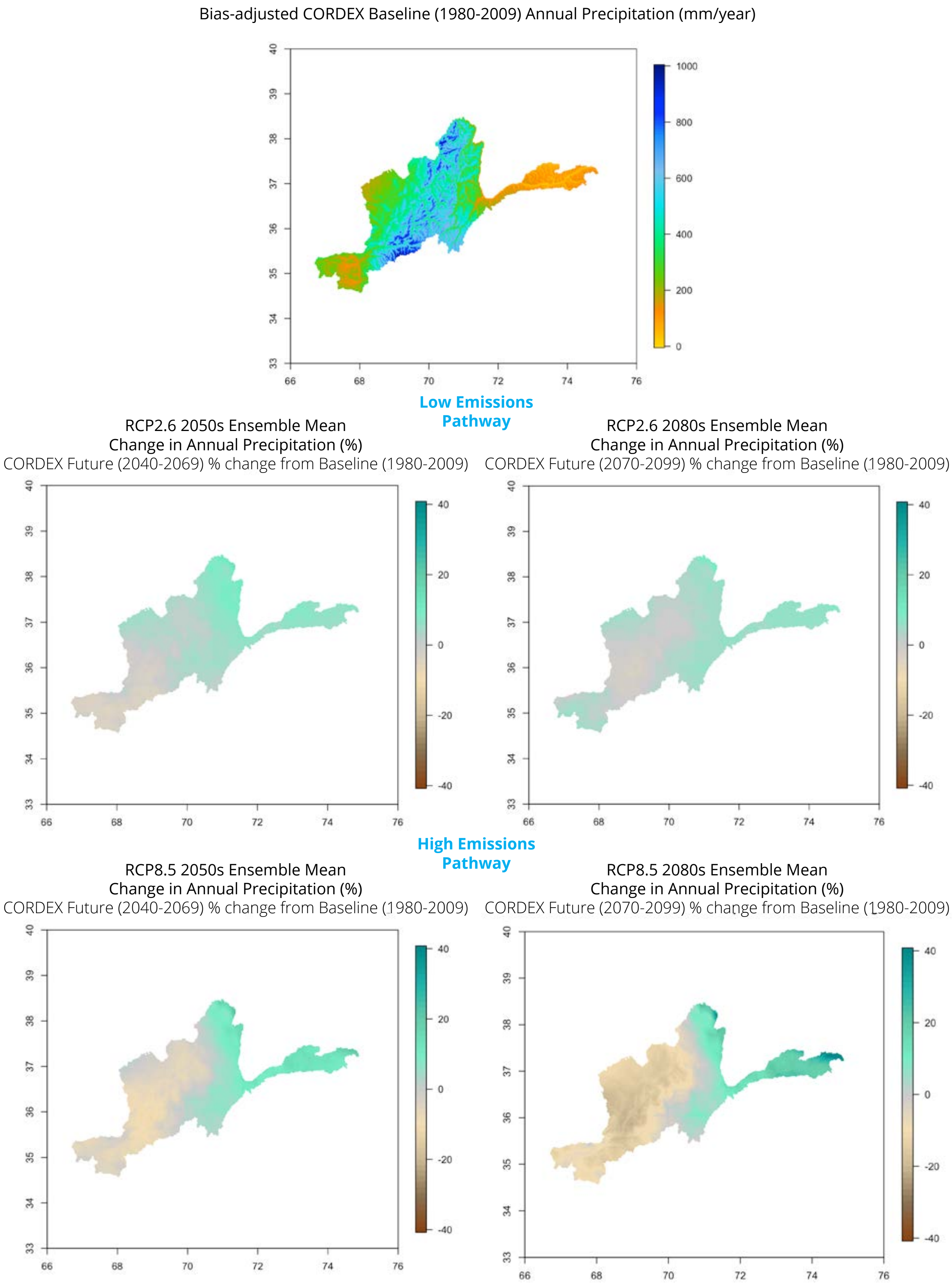

Figure 33. BIO12 – Annual Precipitation.

Total annual precipitation was calculated by taking the sum over total monthly precipitation values in each year (Eqn 16):

$$BIO12 = \sum_{i=1}^{i=12} P_i \qquad (16)$$

where P_i represents the total precipitation for the given month *i*.

Precipitation changes are more complex than temperature changes with the northern, northeastern, eastern, southern, and southeastern regions (Pamir alpine desert and tundra, Karakoram-West Tibetan Plateau alpine steppe, Gissaro-Alai open woodlands, Paropamisus xeric woodlands, Ghorat-Hazarajat alpine meadow, Hindu Kush alpine meadow, Afghan Mountains semi-desert) projected with the largest percentage increases under RCP2.6, while much of the central and western regions (Paropamisus xeric woodlands, Ghorat-Hazarajat alpine meadow, Afghan Mountains semi-desert, Badghyz and Karabil semi-desert) see a decrease. It should be noted that the baseline precipitation in the eastern mountainous region (Pamir alpine desert and tundra, Karakoram-West Tibetan Plateau alpine steppe) is low and percentage increases may not necessarily translate to large increases in absolute numbers. A similar pattern of rainfall changes is seen by the 2080s, with the southwestern region also seeing increases in precipitation.

Precipitation changes are more complex than temperature changes with the northeastern, eastern, and southeastern regions projected with the largest percentage increases under RCP8.5, while much of the central and western regions (Pamir alpine desert and tundra, Karakoram-West Tibetan Plateau alpine steppe, Gissaro-Alai open woodlands, Paropamisus xeric woodlands, Hindu Kush alpine meadow) see a decrease. It should be noted that the baseline precipitation in the eastern mountainous region (Pamir alpine desert and tundra, Karakoram-West Tibetan Plateau alpine steppe) is low and percentage increases may not necessarily translate to large increases in absolute numbers. A similar pattern of rainfall changes is seen by the 2080s.

BIO13 – Precipitation of Wettest Month

E

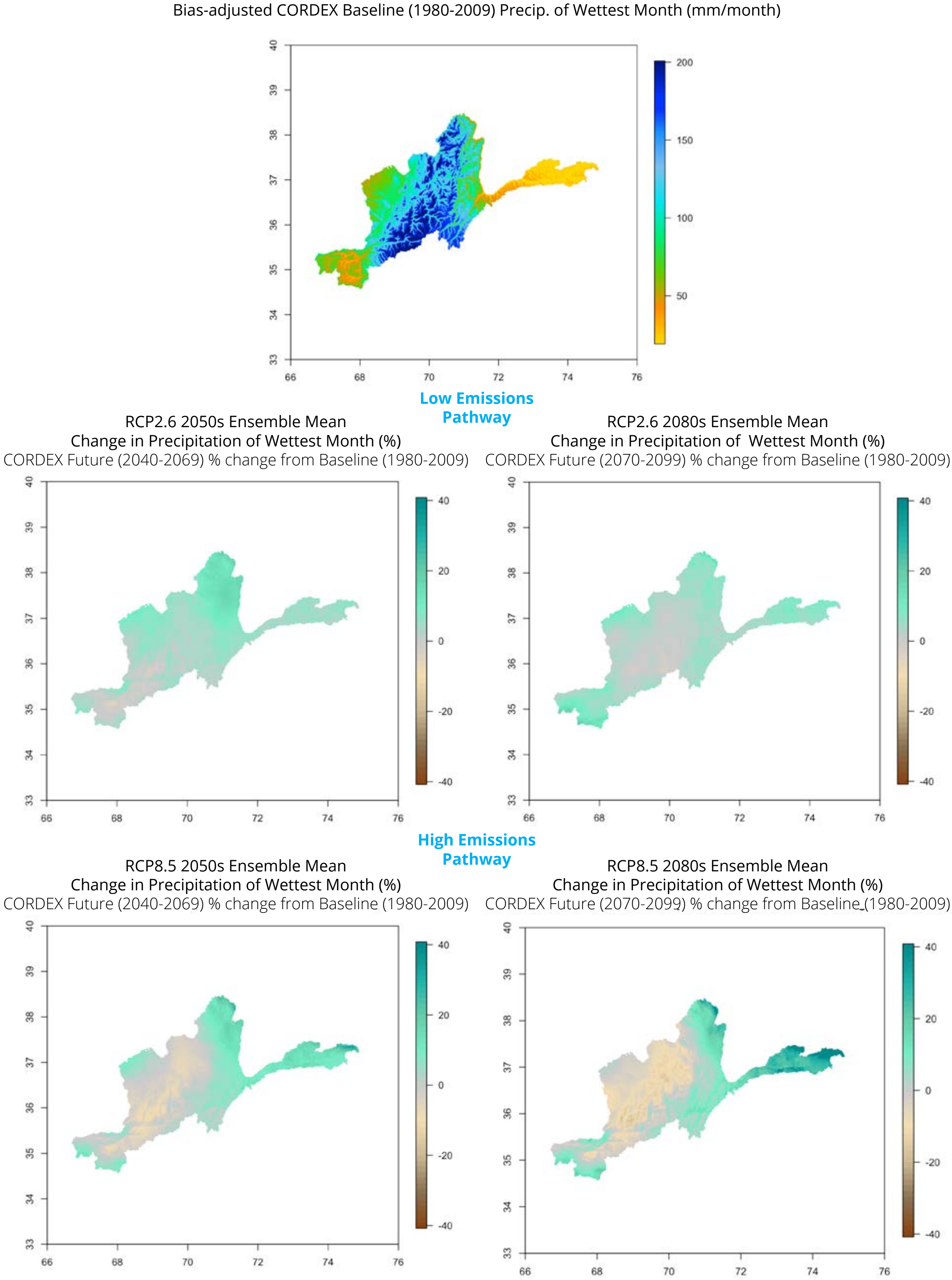

Figure 34. BIO13 – Precipitation of Wettest Month.

The total precipitation of the wettest month was calculated by finding the maximum value over total monthly precipitation values in each year (Eqn 17):

$$BIO13 = max\{P_1, \dots, P_{12}\} \tag{17}$$

where *P* represents the total precipitation for each month.

Precipitation changes in the wettest month are complex with the northeast, east, southeast, southwest, and tip of the northwest (Pamir alpine desert and tundra, Karakoram-West Tibetan Plateau alpine steppe, Gissaro-Alai open woodlands, Paropamisus xeric woodlands, Ghorat-Hazarajat alpine meadow, Hindu Kush alpine meadow, Afghan Mountains semi-desert, Badghyz and Karabil semi-desert) projected to show the largest percentage increases under RCP2.6, while much of the remaining area sees decreases. It should be noted that the baseline precipitation of the wettest month in the eastern mountainous region (Pamir alpine desert and tundra, Karakoram-West Tibetan Plateau alpine steppe) is low and percentage increases may not necessarily translate to large increases in absolute numbers. A similar pattern of changes is seen by the 2080s, with the exception of the northeastern tip, which sees a decline.

Precipitation changes in the wettest month are complex with the northeast, east, southeast, southwest, and tip of the northwest (Pamir alpine desert and tundra, Karakoram-West Tibetan Plateau alpine steppe, Gissaro-Alai open woodlands, Paropamisus xeric woodlands, Ghorat-Hazarajat alpine meadow, Hindu Kush alpine meadow, Afghan Mountains semi-desert, Badghyz and Karabil semi-desert) projected to show the largest percentage increases under RCP8.5, while much of the remaining area sees decreases. It should be noted that the baseline precipitation of the wettest month in the eastern mountainous region (Pamir alpine desert and tundra, Karakoram-West Tibetan Plateau alpine steppe) is low and percentage increases may not necessarily translate to large increases in absolute numbers. A similar pattern of changes is seen by the 2080s, with the exception of the northeastern tip, which sees a decline.

BIO14 – Precipitation of Driest Month

E

Bias-adjusted CORDEX Baseline (1980-2009) Precipitation of Driest Month (mm/month)

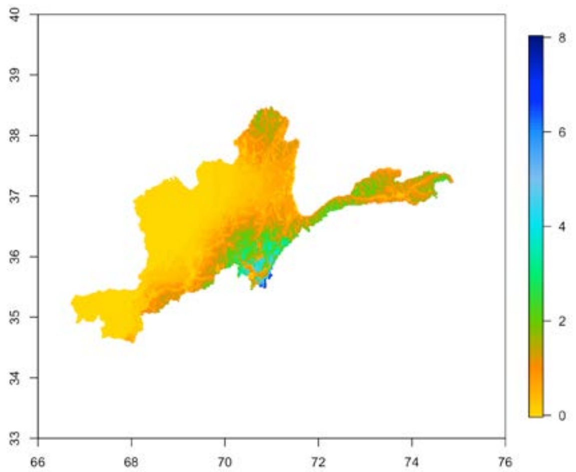

Low Emissions Pathway

RCP2.6 2050s Ensemble Mean
Change in Precipitation of Driest Month (%)
CORDEX Future (2040-2069) % change from Baseline (1980-2009)

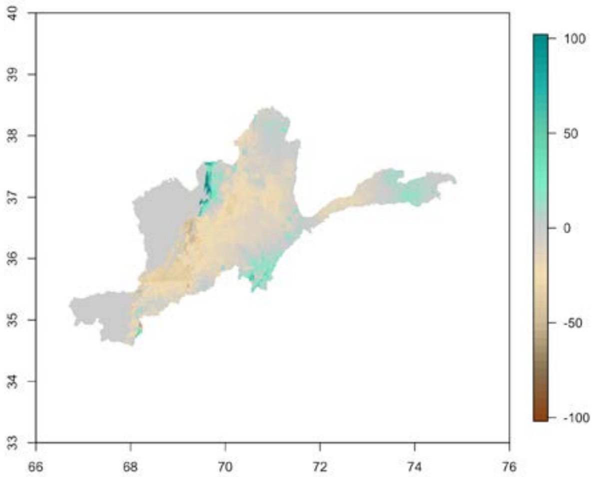

RCP2.6 2080s Ensemble Mean
Change in Precipitation of Driest Month (%)
CORDEX Future (2070-2099) % change from Baseline (1980-2009)

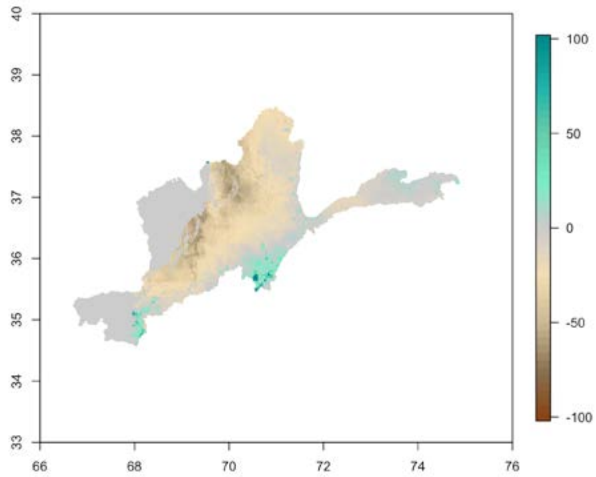

High Emissions Pathway

RCP8.5 2050s Ensemble Mean
Change in Precipitation of Driest Month (%)
CORDEX Future (2040-2069) % change from Baseline (1980-2009)

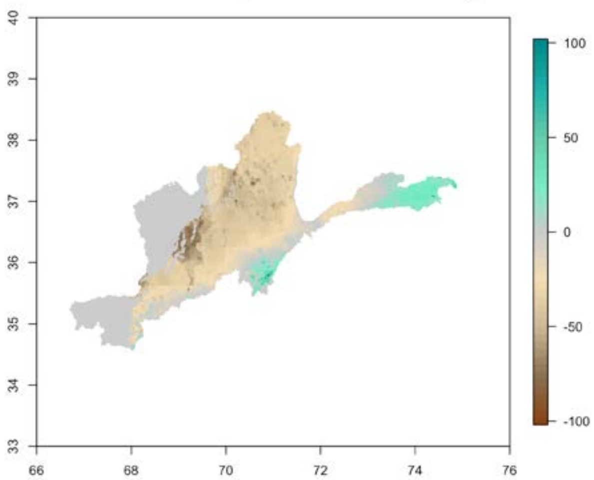

RCP8.5 2080s Ensemble Mean
Change in Precipitation of Driest Month (%)
CORDEX Future (2070-2099) % change from Baseline (1980-2009)

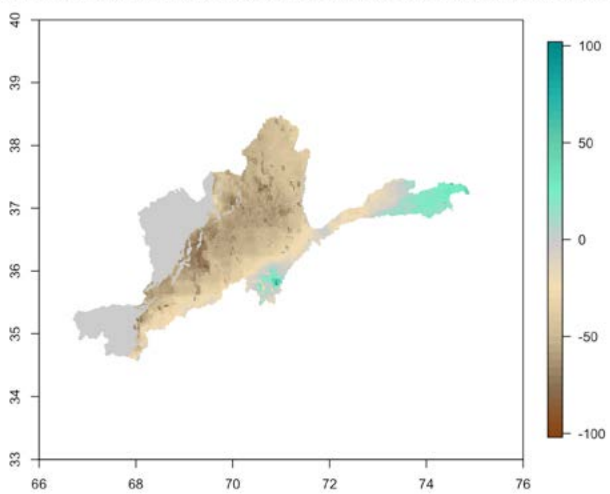

Figure 35. BIO14 – Precipitation of Driest Month.

The total precipitation of the driest month was calculated by finding the minimum value over total monthly precipitation values in each year (Eqn 18):

$$BIO14 = min\{P_1, \ldots, P_{12}\} \tag{18}$$

where *P* represents the total precipitation for each month.

Precipitation levels during the driest month are projected to decrease under RCP2.6 in much of the P-ARB except small parts of the far west (Ghorat-Hazarajat alpine meadow), northcentral (Paropamisus xeric woodlands in the 2050s), and tip of the southern region (Hindu Kush alpine meadow), which see increases. Large parts of the western, northern, and eastern regions (Pamir alpine desert and tundra, Karakoram-West Tibetan Plateau alpine steppe, Paropamisus xeric woodlands, Ghorat-Hazarajat alpine meadow, Afghan Mountains semi-desert, Badghyz and Karabil semi-desert) see no change, with the central region seeing declines. The precipitation pattern remains largely the same by the 2080s, with the north central region (Paropamisus xeric woodlands) experiencing decreases, although this region saw an increase in precipitation by the 2050s.

Precipitation levels during the driest month are projected to decrease under RCP8.5 in much of the P-ARB except in the tips of the southern (Hindu Kush alpine meadow) and eastern regions (Karakoram-West Tibetan Plateau alpine steppe), which see an increase. This pattern of precipitation change is apparent in both time slices, although by the 2080s the central region (Paropamisus xeric woodlands) sees further declines in dry-month precipitation. Large parts of the western and northwestern regions (Paropamisus xeric woodlands, Ghorat-Hazarajat alpine meadow, Afghan Mountains semi-desert, Badghyz and Karabil semi-desert) see no change. In much of the P-ARB, the baseline precipitation levels are very low during the driest month, and therefore even a large percentage change in precipitation does not necessarily mean large changes in terms of absolute numbers.

BIO15 – Precipitation Seasonality

E

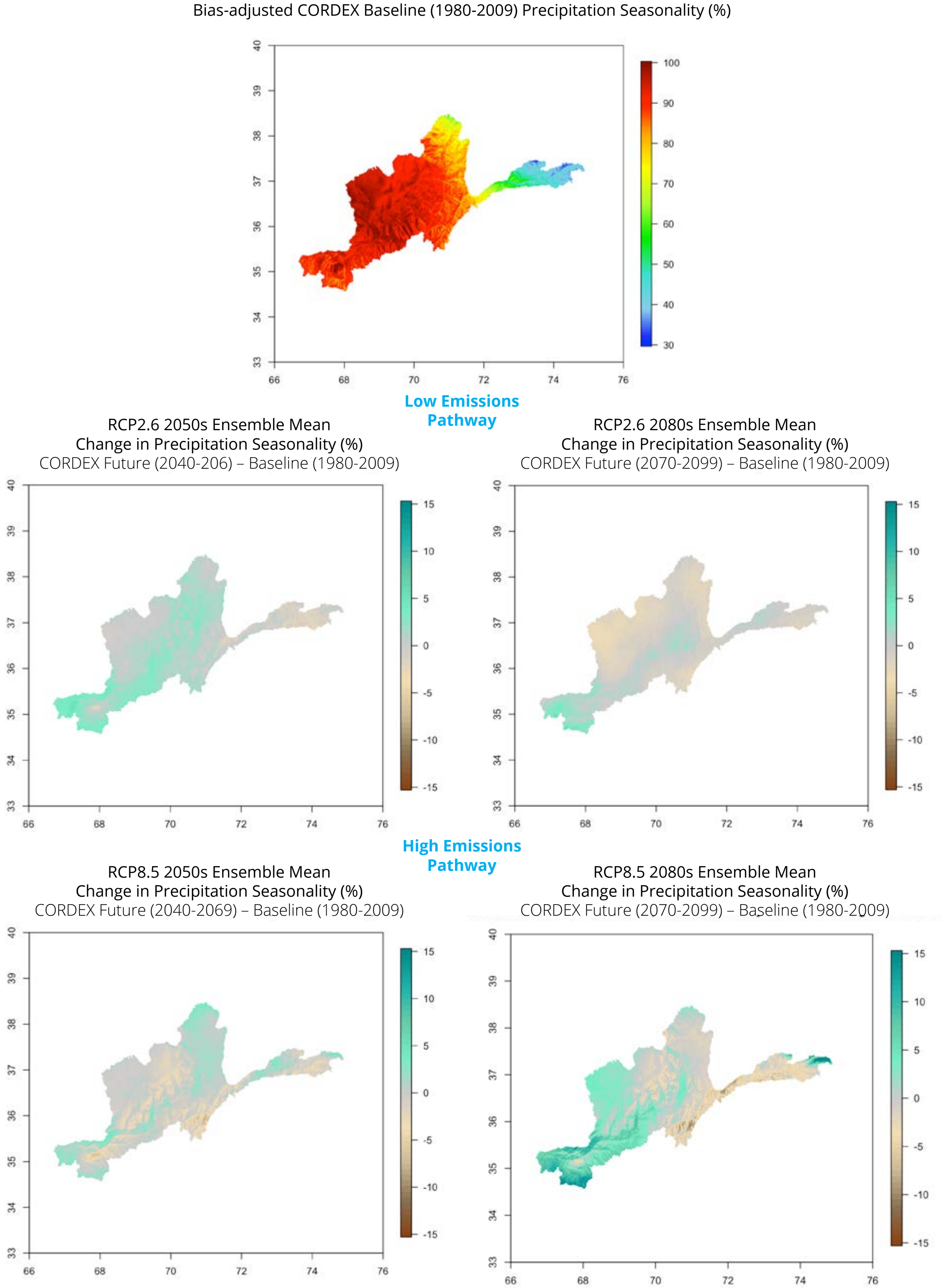

Figure 36. BIO15 – Precipitation Seasonality.

Precipitation seasonality was calculated by taking the standard deviation over monthly total precipitation values for each year and dividing by the mean monthly total precipitation for that year. One was added to the denominator to avoid regions where precipitation may be less than 1 mm (O'Donnell et al., 2012). The result was then multiplied by 100 to obtain units of percent (Eqn 19):

$$BIO15 = \frac{\sigma\{P_1, \ldots, P_{12}\}}{1 + \frac{BIO12}{12}} \times 100 \qquad (19)$$

where P represents the total precipitation for each month.

Precipitation seasonality projections show small increases in some parts of the western, southern, central, and northern regions (Gissaro-Alai open woodlands, Paropamisus xeric woodlands, Ghorat-Hazarajat alpine meadow, Hindu Kush alpine meadow, Afghan Mountains semi-desert,) under RCP2.6 by the 2050s, with other areas seeing slight decreases. By the 2080s, much of the P-ARB sees declines, with some parts of the western, central, and eastern regions (Pamir alpine desert and tundra, Paropamisus xeric woodlands, Ghorat-Hazarajat alpine meadow, Hindu Kush alpine meadow, Afghan Mountains semi-desert) seeing slight increases.

Precipitation seasonality projections indicate small levels of absolute change with the southwestern, northern central and eastern regions (Pamir alpine desert and tundra, Karakoram-West Tibetan Plateau alpine steppe, Gissaro-Alai open woodlands, Paropamisus xeric woodlands, Ghorat-Hazarajat alpine meadow, Hindu Kush alpine meadow, Afghan Mountains semi-desert) seeing small increases in precipitation seasonality under RCP8.5 by the 2050s. By the 2080s, much higher increases in precipitation seasonality are visible in the southwest (Ghorat-Hazarajat alpine meadow, Afghan Mountains semi-desert) and the far eastern edge (Pamir alpine desert and tundra, Karakoram-West Tibetan Plateau alpine steppe) of the P-ARB, while small declines are seen in the southcentral regions (Hindu Kush alpine meadow) and the western side of the Wakhan corridor (Pamir alpine desert and tundra, Karakoram-West Tibetan Plateau alpine steppe).

BIO16 – Precipitation of Wettest Quarter

E

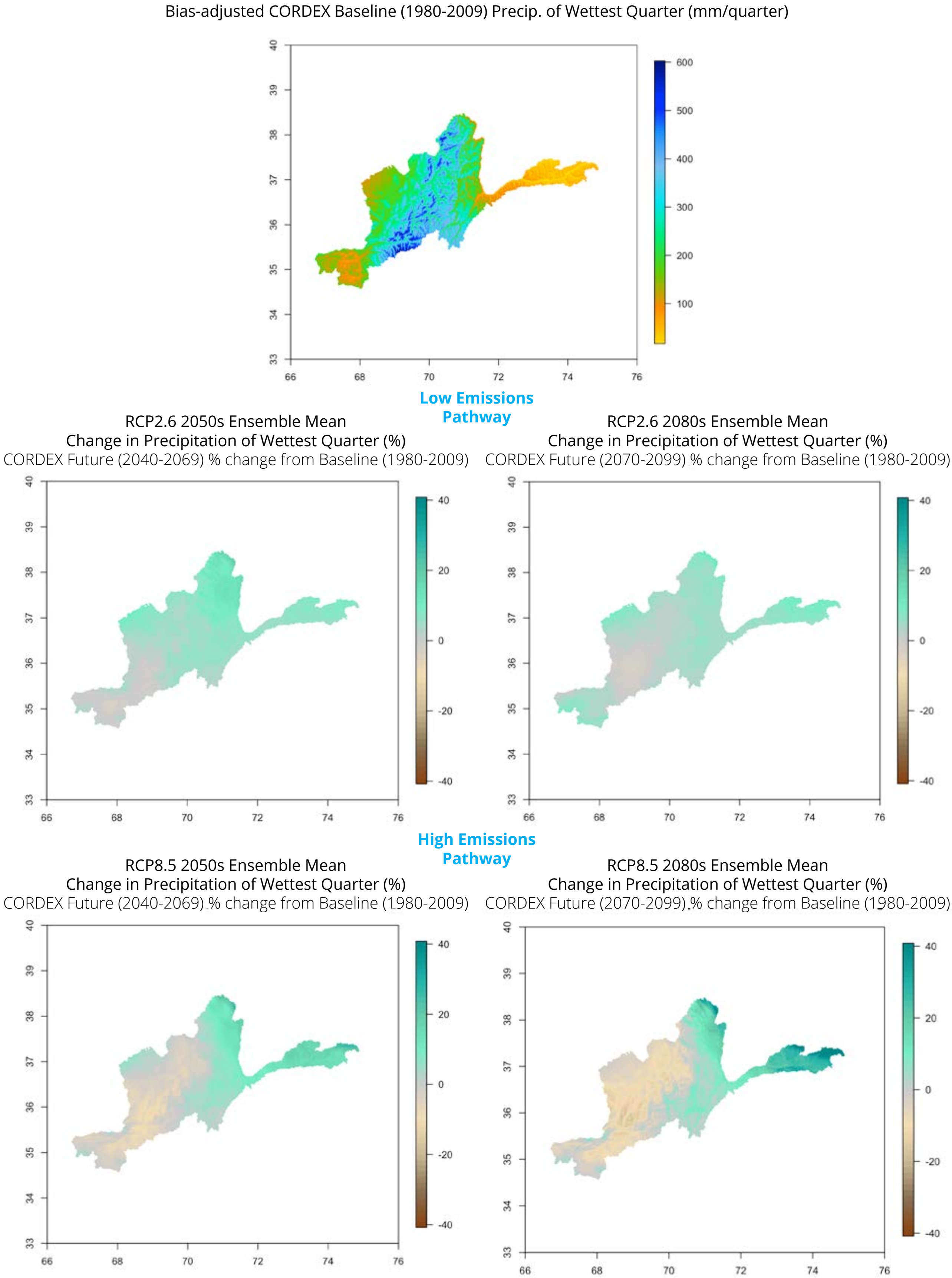

Figure 37. BIO16 – Precipitation of Wettest Quarter.

The total precipitation of each quarter was calculated as a sum over a 3-month period, with 12 consecutive sets of quarters in a year, as with BIO8 and BIO9. To calculate precipitation of the wettest quarter, the maximum total precipitation was calculated over the 12 rolling 3-month periods in each year (Eqn 20):

$$BIO16 = max\{\sum_{i=1}^{i=3} P_i, \sum_{i=2}^{i=4} P_i, \dots, \sum_{i=10}^{i=12} P_i, \sum_{i=11}^{i=1} P_i, \sum_{i=12}^{i=2} P_i\} \qquad (20)$$

where P_i represents the total precipitation of each month in the rolling 3-month period.

Precipitation in the wettest quarter sees increases broadly across most of the P-ARB under RCP2.6 by the 2050s, expect the western region and the adjoining central (Paropamisus xeric woodlands, Ghorat-Hazarajat alpine meadow, Afghan Mountains semi-desert). By the 2080s, the western region (Ghorat-Hazarajat alpine meadow, Afghan Mountains semi-desert) sees an increase, but there is a decline in the central region, compared with the 2050s.

Precipitation in the wettest quarter sees increases under RCP8.5 broadly across the east and the tip of the northwest (Pamir alpine desert and tundra, Karakoram-West Tibetan Plateau alpine steppe, Gissaro-Alai open woodlands, Paropamisus xeric woodlands, Hindu Kush alpine meadow, Badghyz and Karabil semi-desert), while much of the P-ARB sees a decrease. It should be noted that the baseline precipitation in the wettest quarter in the eastern mountainous region (Pamir alpine desert and tundra, Karakoram-West Tibetan Plateau alpine steppe) is low and percentage increases may not necessarily translate to large increases in absolute numbers. A similar pattern of changes is seen by the 2080s, with the exception of the northwestern tip (Badghyz and Karabil semi-desert), which sees a decline.

BIO17 – Precipitation of Driest Quarter

E

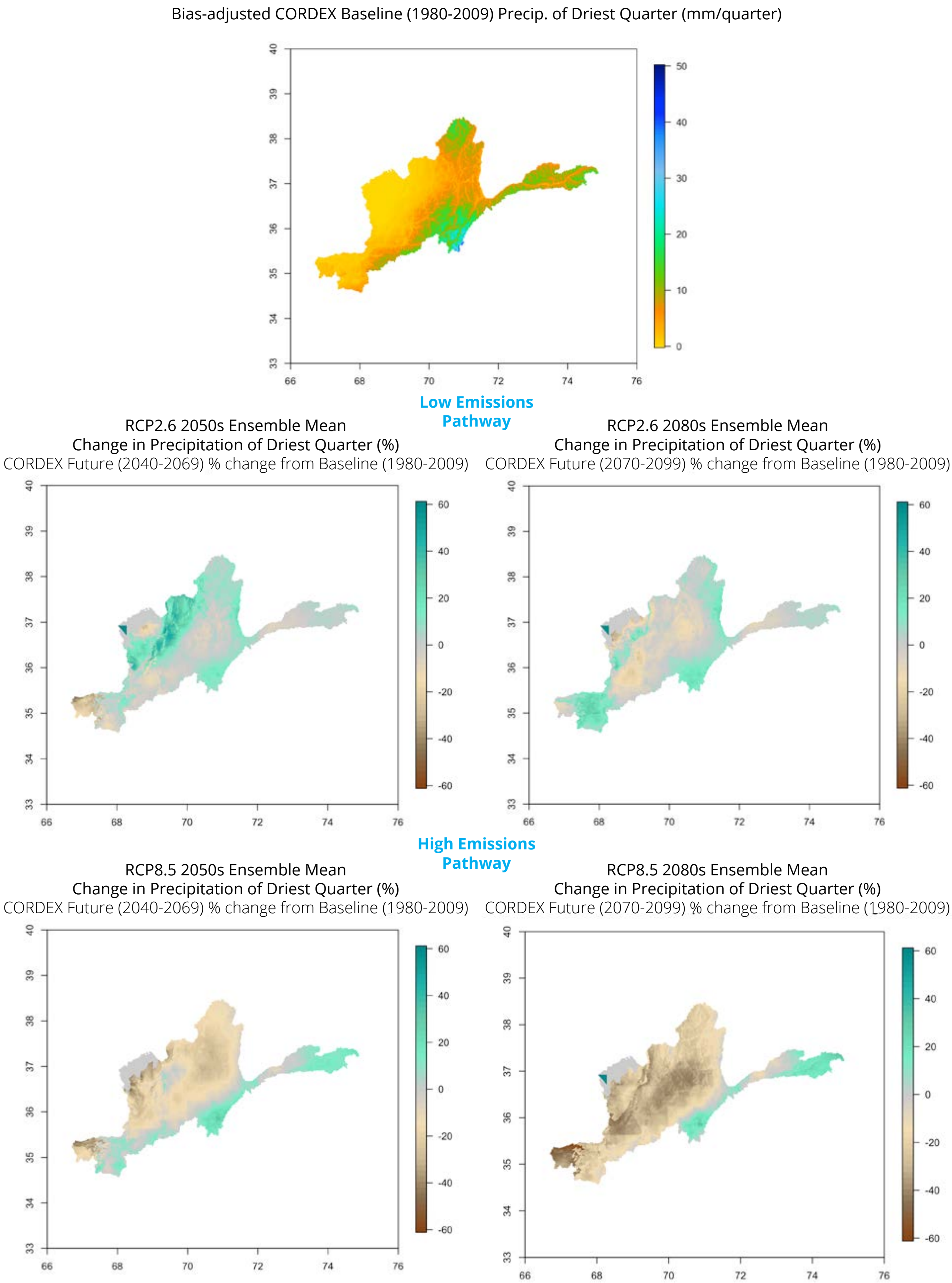

Figure 38. BIO17 – Precipitation of Driest Quarter.

The total precipitation of the driest quarter was calculated similar to BIO16, by finding the minimum total precipitation over the 12 rolling 3-month periods in each year (Eqn 21):

$$BIO17 = min\{\sum_{i=1}^{i=3} P_i, \sum_{i=2}^{i=4} P_i, \dots, \sum_{i=10}^{i=12} P_i, \sum_{i=11}^{i=1} P_i, \sum_{i=12}^{i=2} P_i\} \qquad (21)$$

where P_i represents the total precipitation of each month in the rolling 3-month period.

Precipitation in the driest quarter sees slight decreases across a large portion of the P-ARB under RCP2.6, especially the western and central regions (Paropamisus xeric woodlands, Ghorat-Hazarajat alpine meadow, Hindu Kush alpine meadow, Afghan Mountains semi-desert), with some small areas in the north, south, and far east (Gissaro-Alai open woodlands, Paropamisus xeric woodlands, Hindu Kush alpine meadow, Pamir alpine desert and tundra, Karakoram-West Tibetan Plateau alpine steppe). Increases are seen in some parts of the northern region and scattered areas in the south and east (Paropamisus xeric woodlands, Gissaro-Alai open woodlands, Hindu Kush alpine meadow, Pamir alpine desert and tundra, Karakoram-West Tibetan Plateau alpine steppe). The 2080s see a similar pattern, but with an increase in the far west (Ghorat-Hazarajat alpine meadow, Afghan Mountains semi-desert) and declines in north (Paropamisus xeric woodlands).

Precipitation in the driest quarter sees substantial decreases across much of the region under RCP8.5, except in the southern, southeastern, and southwestern regions (Pamir alpine desert and tundra, Karakoram-West Tibetan Plateau alpine steppe, Ghorat-Hazarajat alpine meadow, Hindu Kush alpine meadow, Afghan Mountains semi-desert), which see increases by the 2050s. The 2080s see a similar but stronger pattern. The increases are seen in the southern and southeastern regions (Hindu Kush alpine meadow, Pamir alpine desert and tundra, Karakoram-West Tibetan Plateau alpine steppe), with more regions seeing declining precipitation, which is also more intensified in the central regions and the western tip (Paropamisus xeric woodlands, Ghorat-Hazarajat alpine meadow) of the P-ARB. It should be noted that the baseline precipitation in the driest quarter in much of the P-ARB is low and percentage changes may not necessarily translate to large changes in absolute numbers.

BIO18 – Precipitation of Warmest Quarter

E

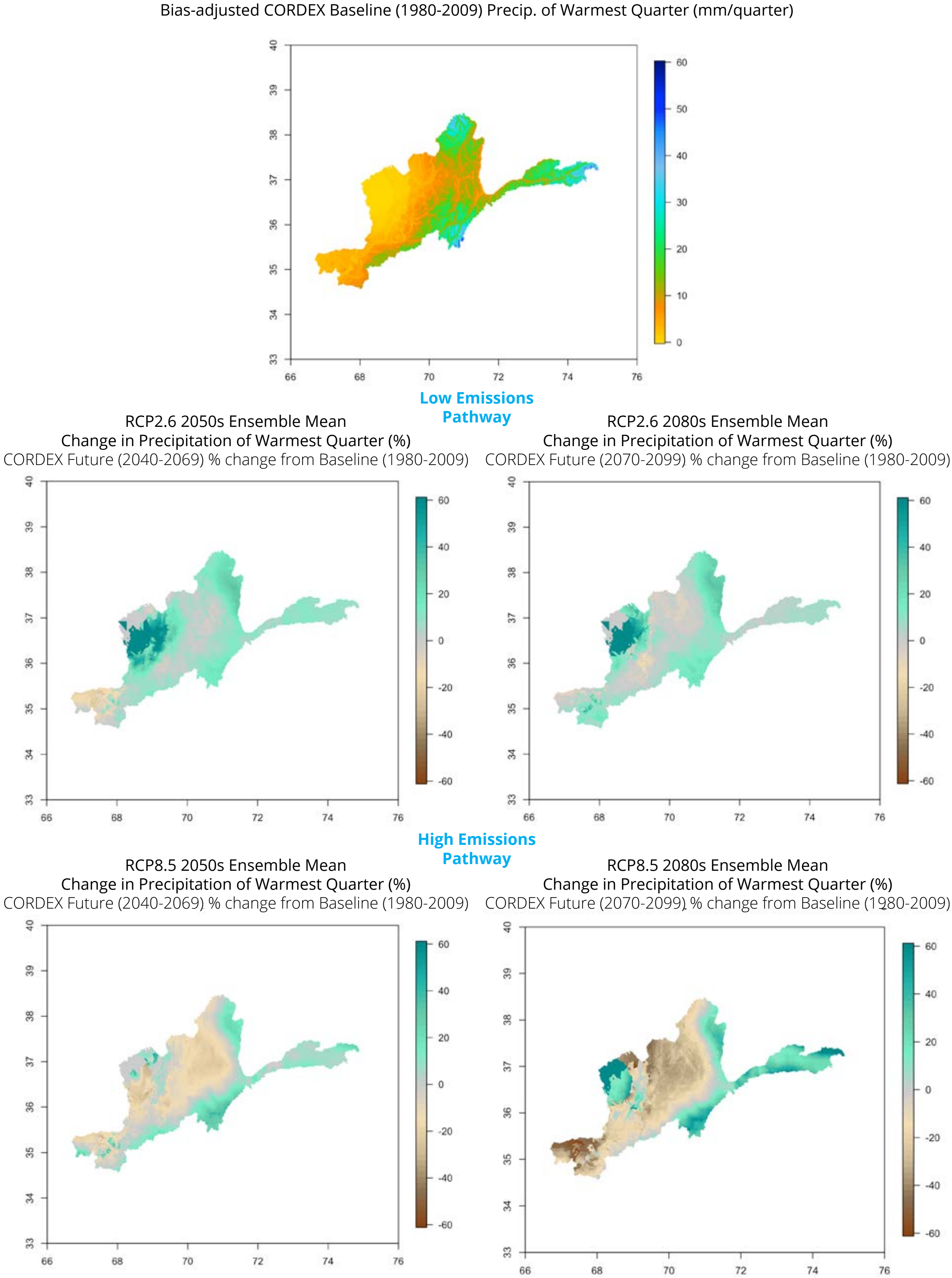

Figure 39. BIO18 – Precipitation of Warmest Quarter.

The total precipitation of the warmest quarter of each year was calculated by identifying the quarter with the maximum mean temperature (Eqn 22):

$$Q_{T_{max}} = max\{\sum_{i=1}^{i=3} Tavg_i, \sum_{i=2}^{i=4} Tavg_i, \dots, \sum_{i=10}^{i=12} Tavg_i, \sum_{i=11}^{i=1} Tavg_i, \sum_{i=12}^{i=2} Tavg_i\} \qquad (22)$$

where $Tavg_i$ represents the mean of daily mean temperatures for each month in the rolling 3-month period. Then the total precipitation for Q_{Tmax} was calculated (Eqn 23):

$$BIO18 = \sum_{i=x}^{i=y} P_i \qquad (23)$$

where month indices $i=x$ and $i=y$ represent the months identified in Q_{Tmax}.

Precipitation in the warmest quarter sees slight decreases under RCP2.6 across the western region, with the central region and small parts of the northwest seeing little or no decreases. The largest increases are seen in the northwest (Badghyz and Karabil semi-desert, Paropamisus xeric woodlands), though increases are also seen in large parts of the northern, eastern, and southern regions (Pamir alpine desert and tundra, Karakoram-West Tibetan Plateau alpine steppe, Gissaro-Alai open woodlands, Ghorat-Hazarajat alpine meadow, Hindu Kush alpine meadow, Afghan Mountains semi-desert). This pattern largely remains the same in the 2080s but a larger part of the central region (Paropamisus xeric woodlands, Hindu Kush alpine meadow sees little or no rain and the far west (Ghorat-Hazarajat alpine meadow, Afghan Mountains semi-desert) sees an increase.

Precipitation in the warmest quarter sees slight decreases across much of the P-ARB under RCP8.5, except in patches across the southern, southeastern, southwestern, northwestern, and northeastern regions (Pamir alpine desert and tundra, Karakoram-West Tibetan Plateau alpine steppe, Gissaro-Alai open woodlands, Ghorat-Hazarajat alpine meadow, Hindu Kush alpine meadow, Afghan Mountains semi-desert, Badghyz and Karabil semi-desert), which see increases by the 2050s. The 2080s see a similar pattern, but the increases are more substantial, especially in the northwestern region (Badghyz and Karabil semi-desert, Paropamisus xeric woodlands). It should be noted that the baseline precipitation for the warmest quarter in much of the P-ARB is low and percentage changes may not necessarily translate to large changes in absolute numbers.

BIO19 – Precipitation of Coldest Quarter

E

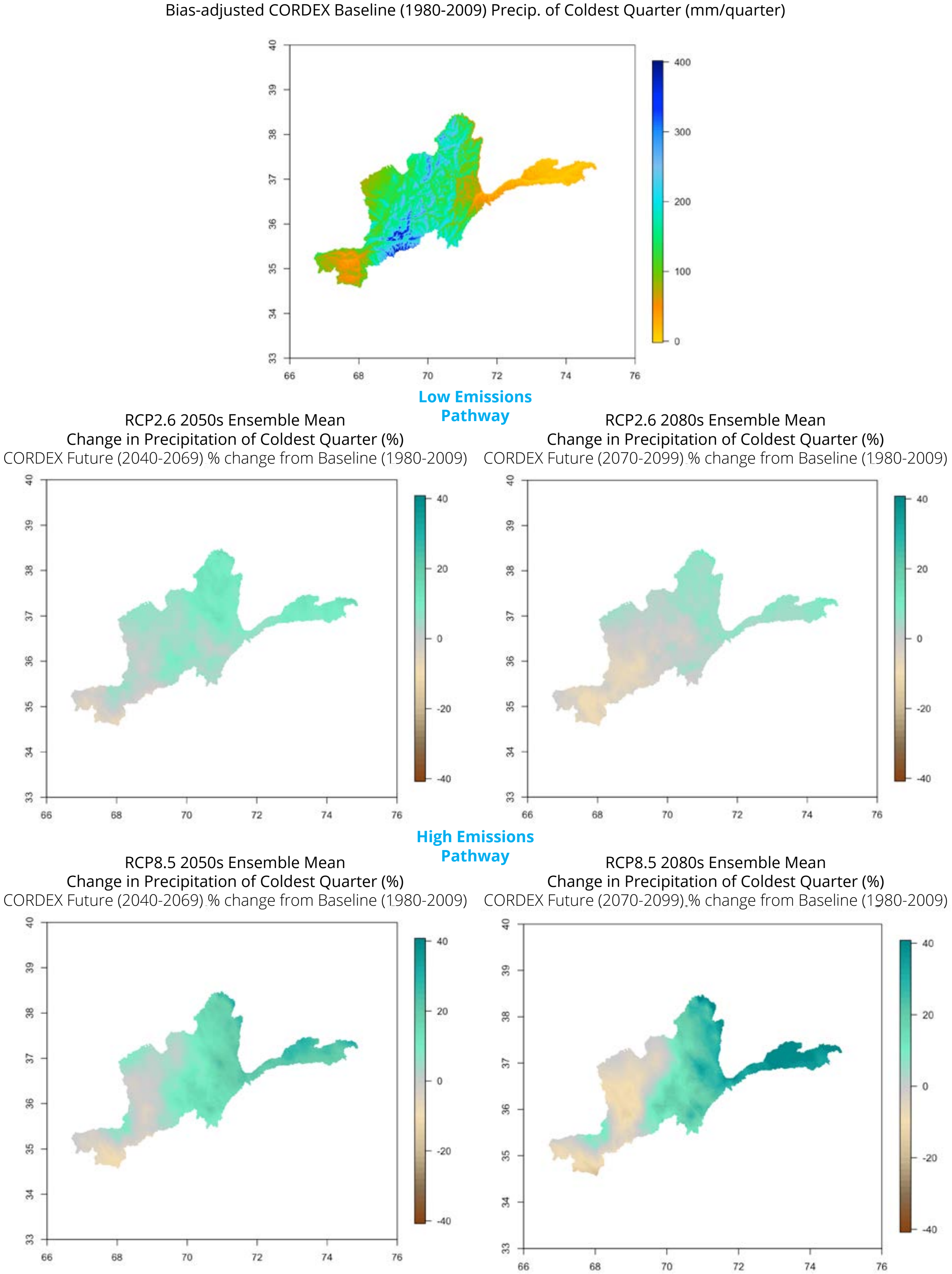

Figure 40. BIO19 – Precipitation of Coldest Quarter.

The total precipitation of the coldest quarter of each year was calculated by identifying the quarter with the minimum mean temperature (Eqn 24):

$$Q_{T_{min}} = min\{\sum_{i=1}^{i=3} Tavg_i, \sum_{i=2}^{i=4} Tavg_i, \ldots, \sum_{i=10}^{i=12} Tavg_i, \sum_{i=11}^{i=1} Tavg_i, \sum_{i=12}^{i=2} Tavg_i\} \qquad (24)$$

where $Tavg_i$ represents the mean of daily mean temperatures for each month in the rolling 3-month period. Then the total precipitation for $Q_{T_{min}}$ was calculated (Eqn 25):

$$BIO19 = \sum_{i=x}^{i=y} P_i \qquad (25)$$

where month indices $i=x$ and $i=y$ represent the months identified in $Q_{T_{min}}$.

Total precipitation projections for the coldest quarter show increases across much of the P-ARB under RCP2.6, except in patches in the western, southwestern, and central regions (Paropamisus xeric woodlands, Ghorat-Hazarajat alpine meadow, Hindu Kush alpine meadow, Afghan Mountains semi-desert) that see slight declines or no change by the 2050s. The 2080s see a similar pattern, but there are more decreases, especially in the western and central regions (Paropamisus xeric woodlands, Ghorat-Hazarajat alpine meadow, Hindu Kush alpine meadow, Afghan Mountains semi-desert).

Total precipitation projections for the coldest quarter show increases across much of the P-ARB under RCP8.5, except in patches in the western and southwestern regions (Paropamisus xeric woodlands, Ghorat-Hazarajat alpine meadow, Afghan Mountains semi-desert, Badghyz and Karabil semi-desert) that see slight declines by the 2050s. The 2080s see a similar pattern, but the increases are slightly higher, especially in the far eastern region (Pamir alpine desert and tundra, Karakoram-West Tibetan Plateau alpine steppe). It should be noted that the baseline precipitation for the coldest quarter in some regions (especially the eastern mountainous region – Pamir alpine desert and tundra, Karakoram-West Tibetan Plateau alpine steppe) is low and percentage changes may not necessarily translate to large changes in absolute numbers.

Climatic Dissimilarity

E

Indicator overview

Assessments of changes in individual bioclimatic variables describe the expected exposure to climate change on single climate axes. However, different areas may be more vulnerable to change in different aspects of climate. For example, areas in the P-ARB that are likely to experience the most change in mean annual temperature (BIO1) are not necessarily those that are likely to experience the most change in mean annual precipitation (BIO12). Therefore, a multivariate approach—referred to as climatic dissimilarity—is useful to characterize climate exposure more holistically.

Methods overview

The climatic dissimilarity metric was created by first conducting a principal component analysis (PCA) on the 19 bioclimatic variables described above, calculated as a multidecadal average. This produced a set of 19 rasters, each representing an orthogonal climate axis, for each GCM-RCM-RCP model, for the current, mid-century and end-century time periods. The weighted Euclidean distance was then calculated between current and future periods at each location, where weights represent the proportion of variance explained by each principal component axis (Grenier et al. 2013).

Spatial representation of indicator

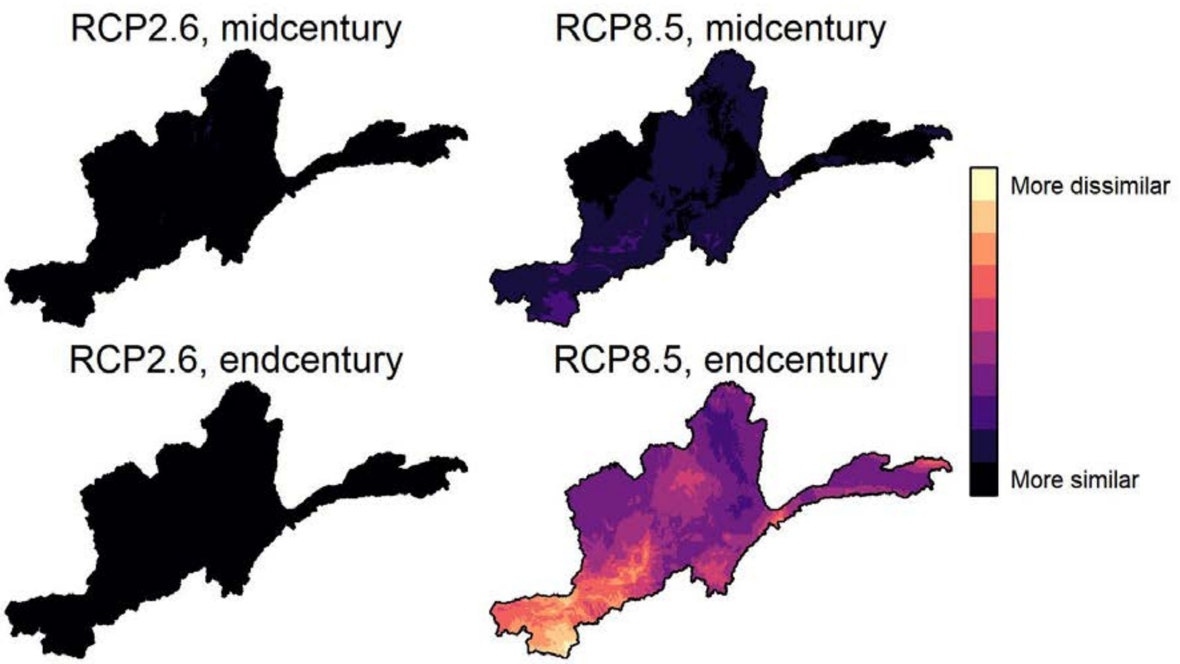

Figure 41. Multivariate climatic dissimilarity metric for the P-ARB, for low-emissions and high-emissions futures, mid-century and end-century compared to present.

Vulnerability Assessment

Summary plots of indicator by ecoregion and province

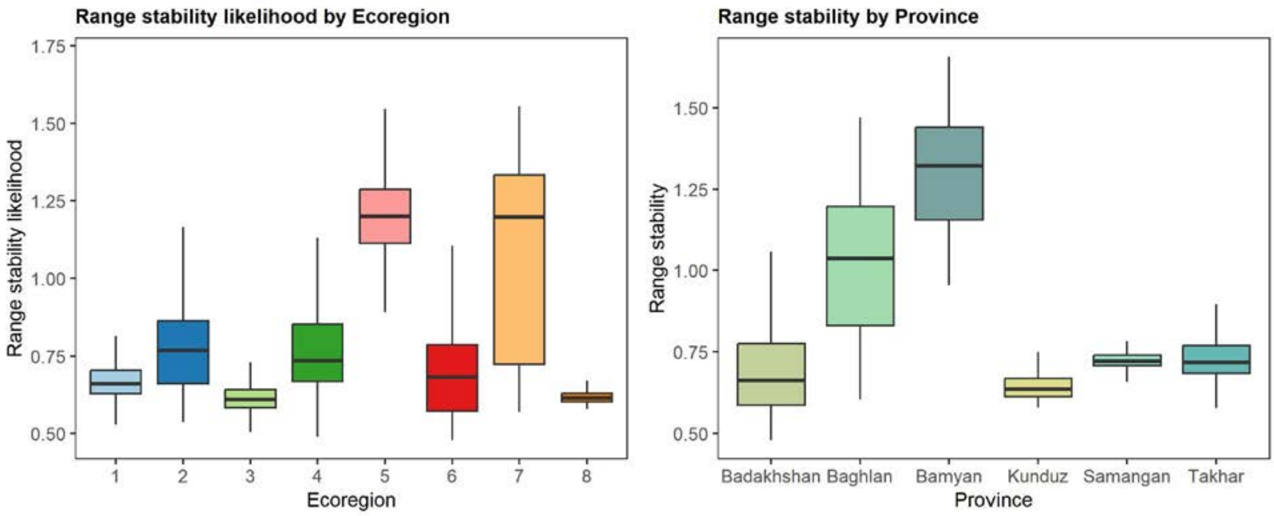

Figure 42. Summary of climatic dissimilarity index under RCP8.5 for end-century by ecoregion and province. Note that outlier values have been removed for visual clarity. Ecoregion legend: 1 – Pamir alpine desert and tundra; 2 – Karakorum-West Tibetan Plateau alpine steppe; 3 – Gissaro-Alai open woodlands; 4 – Paropamisus xeric woodlands; 5 – Ghorat-Hazarajat alpine meadow; 6 – Hindu-Kush alpine meadow; 7 – Afghan Mountains semi-desert; 8 - Badghyz and Karabil semi-desert

Results summary

The results in Figure 41 show clearly that overall climate dissimilarity is projected to be far higher in a high-emissions (RCP8.5) future than a low-emissions (RCP2.6) future, and that change under RCP8.5 even by mid-century will far exceed end-century change under RCP2.6. The overall climatic dissimilarity is highest in the southwestern portion of the P-ARB, indicating that this region is projected to have the greatest exposure to altered climate regimes. Dissimilarity is thus highest in Bamyan province, followed by Baghlan. The Ghorat-Hazarajat alpine meadow (ecoregion 5) and Afghan Mountains semi-desert (ecoregion 7) are projected to face the most exposure to climate change by this metric, while the Badghyz and Karabil semi-desert (ecoregion 8) are projected to face the least exposure (Figure 42).

Climate Velocity

E

Indicator overview

Climatic dissimilarity metrics, either univariate or multivariate, are a way to understand the amount of climate change that might occur at a fixed location. However, this is not the only way to quantify climate exposure. Another set of climate metrics involve climate velocity (Loarie et al. 2009). While dissimilarity metrics quantify change at a location, velocity metrics reverse this framing and ask how far an organism at a given location would have to travel to find a location with the same climate. High velocity values thus represent further distances that must be traversed to maintain suitable climate conditions, which increases vulnerability. As such, climate velocity provides a differing and complementary picture of climate vulnerability compared to climatic dissimilarity (Dobrowski and Parks 2016). Generally, velocity metrics are univariate, and the metric analyzed here are based on changes in mean annual temperature.

Methods overview

Two measures of climate velocity—minimum exposure distance (MED) and minimum cumulative exposure (MCE) (Hamann et al. 2014, Carroll et al. 2015)—were calculated. To calculate these metrics, a tolerance level of 1°C was used (i.e., for an organism originating at a specific location with a given mean annual temperature, all locations with future temperature within 1°C were considered as potential destinations). Least-cost paths were then derived based on a climate resistance grid between the origin cell and all possible destination cells (i.e., not necessarily the shortest possible path, but the path that would traverse the least non-analogous temperature conditions possible). The MED for a given location is calculated as the length of the shortest of these least-cost paths; the MCE for a given location is calculated as the degree of exposure to non-analogous temperatures along the MED path.

Spatial representation of indicator

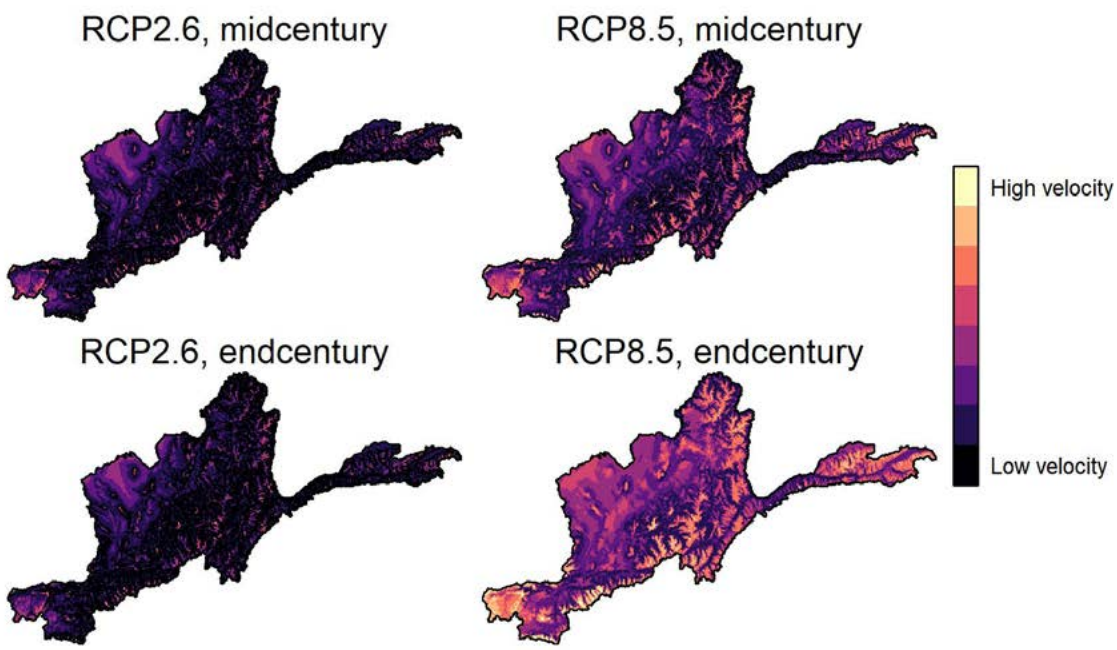

Figure 43. Minimum exposure distance (MED) for the P-ARB, for low-emissions and high-emissions futures, mid-century and end-century compared to present. Data have been log-transformed to aid legibility.

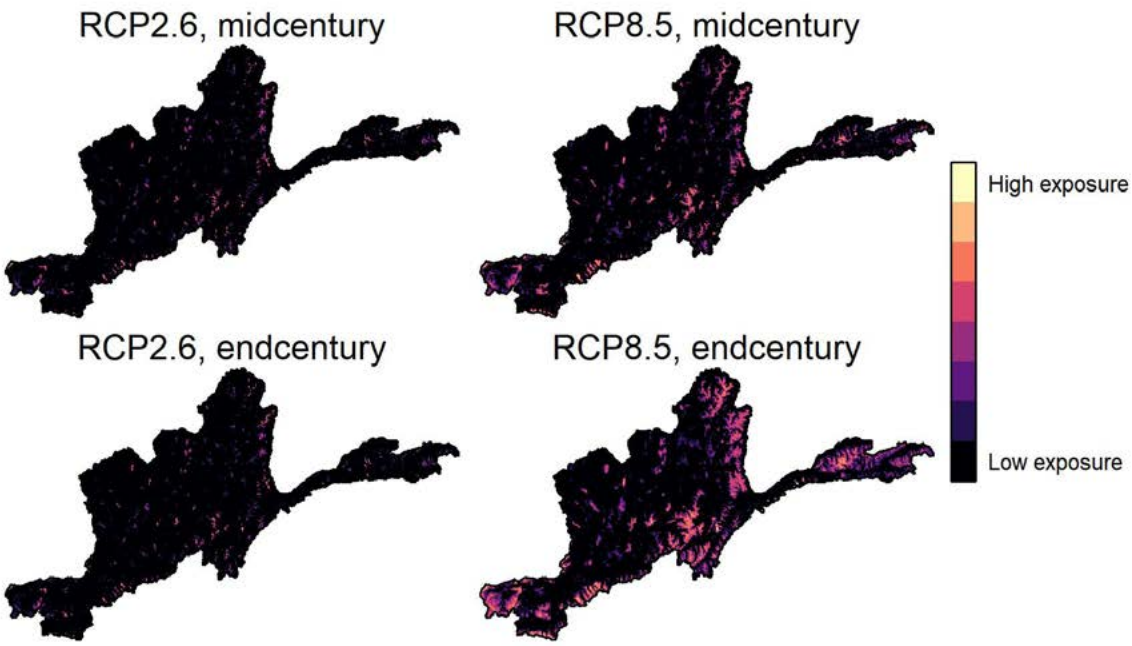

Figure 44. Minimum cumulative exposure (MCE) for the P-ARB, for low-emissions and high-emissions futures, mid-century and end-century compared to present. Data have been log-transformed to aid legibility.

Summary plots of indicator by ecoregion and province

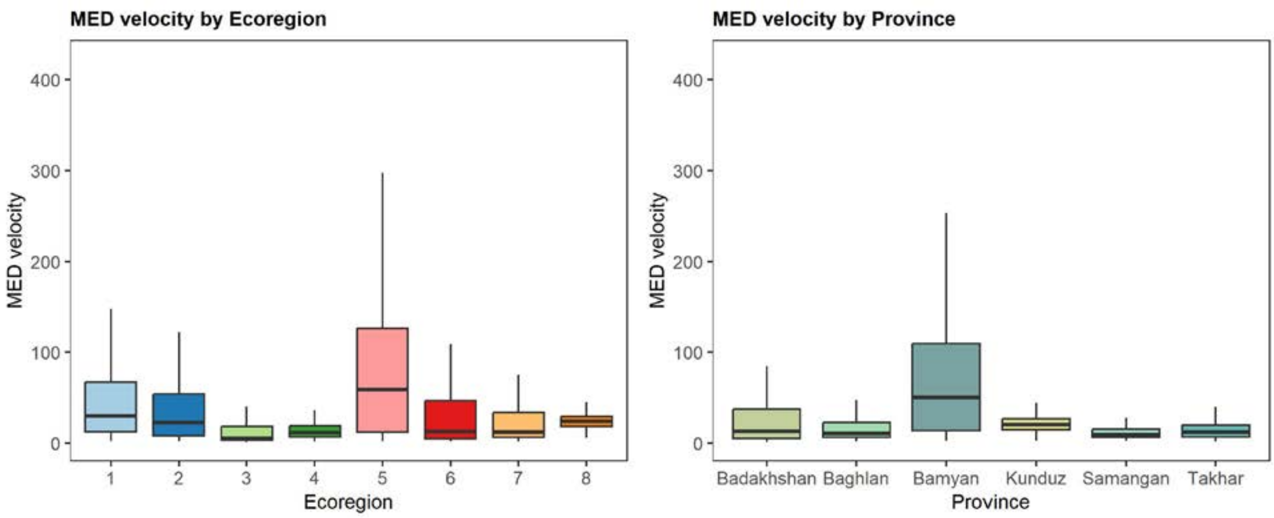

Figure 45. MED climate velocity for RCP8.5, end-century, summarized by province and ecoregion. Note that outlier values have been removed for visual clarity. Ecoregion legend: 1 – Pamir alpine desert and tundra; 2 – Karakorum-West Tibetan Plateau alpine steppe; 3 – Gissaro-Alai open woodlands; 4 – Paropamisus xeric woodlands; 5 – Ghorat-Hazarajat alpine meadow; 6 – Hindu-Kush alpine meadow; 7 – Afghan Mountains semi-desert; 8 - Badghyz and Karabil semi-desert.

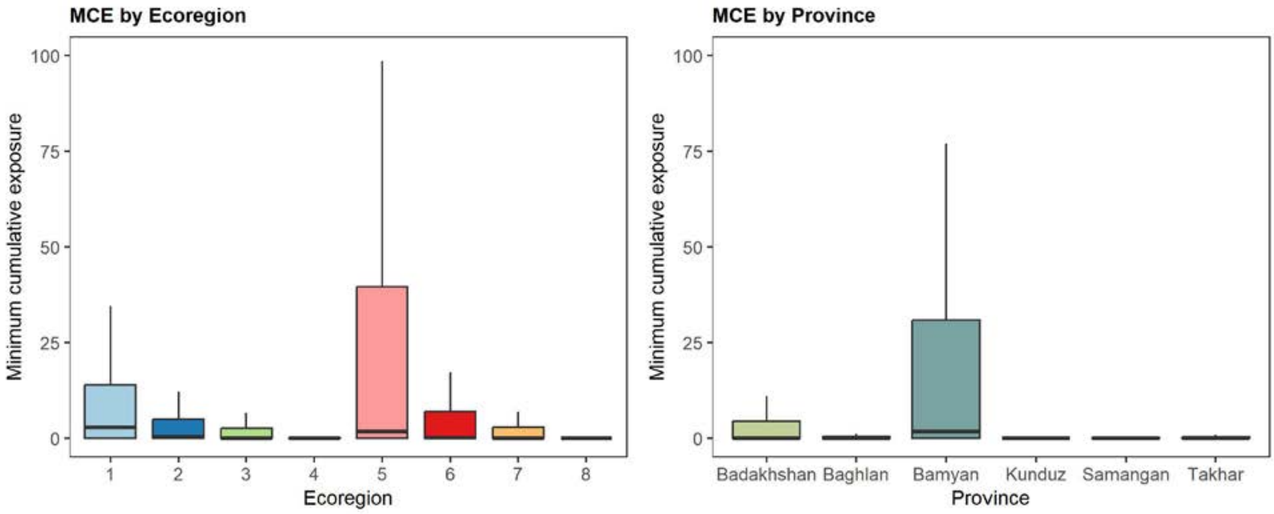

Figure 46. MCE climate velocity for RCP8.5, end-century, summarized by province and ecoregion. Note that outlier values have been removed for visual clarity, and the y-axis has been rescaled (outlier values far exceed the maximum shown here). Ecoregion legend: 1 – Pamir alpine desert and tundra; 2 – Karakorum-West Tibetan Plateau alpine steppe; 3 – Gissaro-Alai open woodlands; 4 – Paropamisus xeric woodlands; 5 – Ghorat-Hazarajat alpine meadow; 6 – Hindu-Kush alpine meadow; 7 – Afghan Mountains semi-desert; 8 - Badghyz and Karabil semi-desert.

Results summary

As with climatic dissimilarity, both MED and MCE are highest in a high-emissions future, and at mid-century compared to end-century (Figure 43 and Figure 44). However, there are clear differences in the distribution of high-exposure regions. The Bamyan province has the highest exposure to climate velocity (both MED and MCE), followed by Badakhshan. Among ecoregions, the Ghorat-Hazarajat alpine meadow (ecoregion 5), followed by the Pamir alpine desert and tundra (ecoregion 1) have the greatest exposure (Figure 45 and Figure 46).

Policy and Management Recommendations

Observations and projections of climate in the P-ARB of Afghanistan show a consistent message of climate changes that will affect average and extreme conditions in ways that could challenge ecosystems, water resources, and communities. Climate model projections indicate that climate change is likely to impact a range of sectors as critical variables such as precipitation (total and intensity), temperatures, extreme heat, soil moisture, snow and permafrost change over time.

The balance of changes across average and extreme climate conditions suggests disruptive pressures on society and natural ecosystems which are important to recognize in current and future planning for the P-ARB. The full extent of projected risks requires additional analysis of vulnerability, adaptive capacity, and exposure for each affected system. Information about the projected changes, their geographic patterns, temporal evolution, scenario dependence and relative levels of uncertainty is an important step toward developing specific adaptation and risk management strategies to protect these unique and fragile ecosystems and communities in the decades to come.

The results from the analysis of climate vulnerability point to several key recommendations for policy and management to mitigate consequences for ecosystems, biodiversity, and local communities and increase their resilience under climate change. These recommendations can be grouped into five domains:

1. Invest in nature-based solutions to joint climate mitigation-adaptation

- Maintain intact ecosystems to help buffer climate impacts and retain existing carbon stocks
- Slow rates of degradation to reduce emissions
- Recover areas identified as degraded to bolster carbon storage and increase adaptation potential
- Initiate tree planting campaigns to reforest communities
- Initiate grassland restoration activities in heavily degraded grasslands

2. Develop alternative strategies for energy generation to reduce emissions

- Utilize better technology, low energy savings and alternatives
- Invest in renewable energy sources
- Distribute or subsidize efficient cook stoves and heaters

3. Educate the public about climate change and climate change impacts

- Develop community education programs suitable for all ages
- Create courses and modules at the university level, including opportunities for research in climate science and climate adaptation
- Create jobs that utilize education and training for climate adaptation

4. Establish a system for long-term climate monitoring

- Ensure monitoring system uses both field-based and remote-sensing approaches
- Develop a glacier monitoring system
- Deploy weather stations across a representative sample of all terrestrial ecosystems at different elevations to monitor local climate changes and conditions
- Deploy Hydromet stations within a representative sample of rivers in all sub-catchments
- Establish regular monitoring of all terrestrial ecosystems, including rangelands, forests, and riparian vegetation to link climate change to changes in ecosystems
- Develop a system to monitor carbon emissions from activities across sectors

5. Create a natural hazard warning system

- Conduct real-time/near real-time analyses of natural hazards, such as floods, droughts, landslides, and avalanches
- Develop a system to announce emergency warnings to local communities via mobile communications

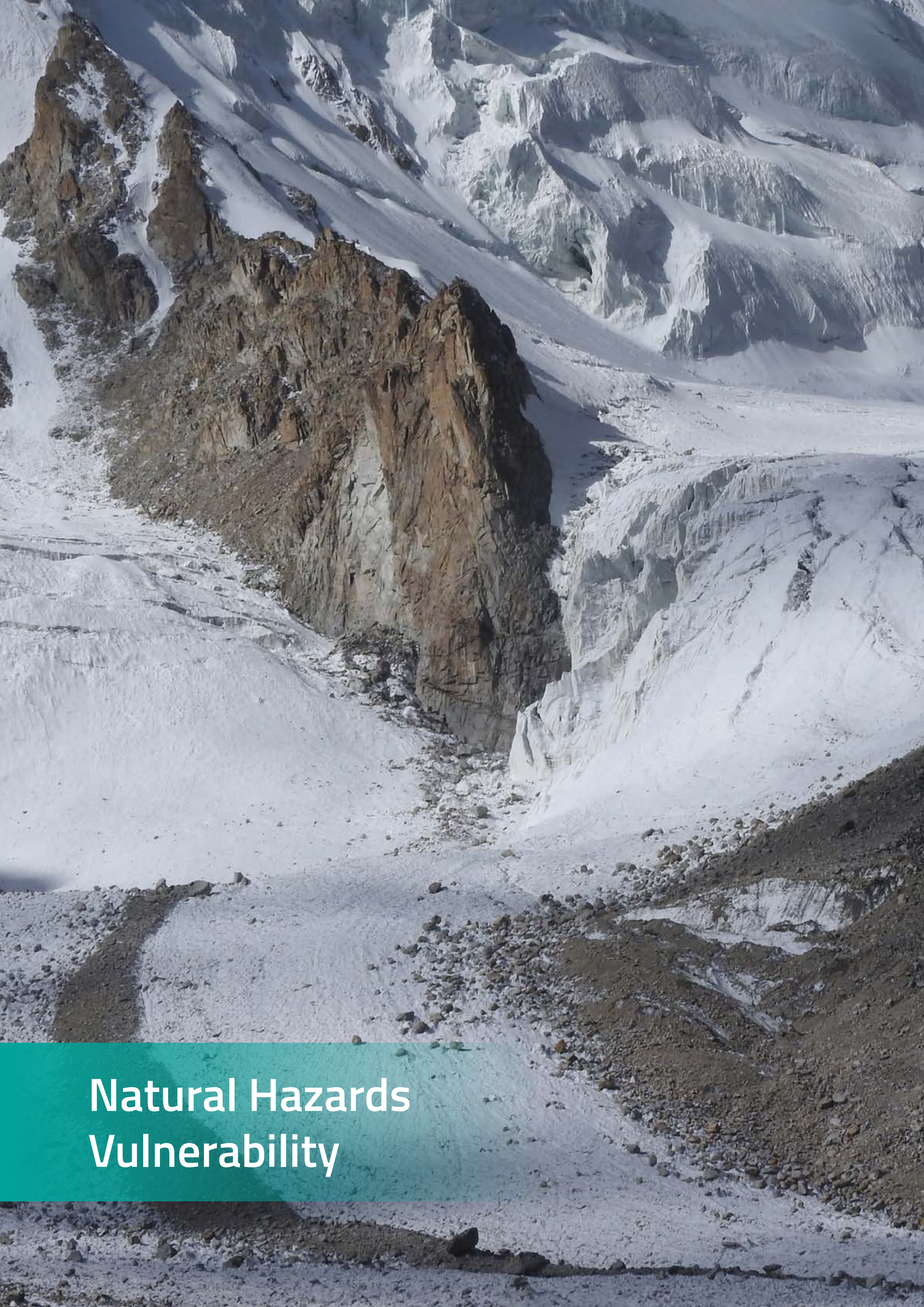

Natural Hazards Vulnerability

2.2 Natural Hazards Vulnerability

Overview

Analyses of historical and future projections of climate provide information on risks of natural hazards to ecosystems, wildlife, hydrology, and communities in the P-ARB.

Projected changes in natural hazards

Note: An overview of the projected climate changes is given in Section 2.1, along with a map of the geographic distribution of natural hazards in Figure 14.

- Extreme heat: The number of extreme heat days is projected to increase by mid-century in the western and central portions of the P-ARB. Changes are most pronounced in the northwest, including the Badghyz and Karabil semi-desert and the western portion of the Paropamisus xeric woodlands ecoregions, which may experience up to 40 more days per year above 30°C, with increases of higher thresholds showing a similar geographic pattern.
- Extreme precipitation: The frequency of extreme precipitation events is projected to increase by mid-century in the eastern half of the P-ARB, most prominently in the Gissaro-Alai open woodlands and Hindu Kush alpine meadow ecoregions. Here, the average number of 30 mm heavy daily precipitation events will increase by between 1-5 days per year under RCP 8.5.
- Permafrost: Temperature increases will lead to permafrost reductions in some areas currently that are currently conducive to permafrost conditions, most prominently in the Hindu Kush alpine meadow, Gissaro-Alai open woodland, and eastern-most portions of Paropamisus xeric woodlands ecoregions. Here, permafrost thaw and active layer thickness increases moving to higher elevations as warming continues.
- Snow cover: The number of days per year with snow will decline across the entire P-ARB by mid-century. Reductions are most pronounced in the northern, central, and southwestern regions, including the Gissaro-Alai open woodlands, Hindu Kush alpine meadow, Paropamisus xeric woodlands, Ghorat-Hazarajat alpine meadow, and Afghan Mountains semi-desert ecoregions. Here, snow cover could be reduced by as much as 50 days per year.
- Soil moisture drought: The frequency of rare, "1-in-10-year" drought events will increase over much of the P-ARB. Early spring (February) drought events will become 2-3 times more frequent in the southwest and northeast regions of the P-ARB (Afghan Mountains semi-desert, Ghorat-Hazarajat alpine meadow, Gissaro-Alai open woodlands, and northern Hindu Kush alpine meadow ecoregions). Late autumn (October) drought events will become 3-5 times more frequent in the central, west, and southwest regions (Paropamisus xeric woodlands, Badghyz and Karabil semi-desert, Afghan Mountains semi-desert, and Ghorat-Hazarajat alpine meadow ecoregions).
- Growing season length: The length of the growing season will increase across the P-ARB. The greatest increase (up to 50 days) is projected in the central and southern region (Hindu Kush alpine meadow, Afghan Mountains semi-desert, and portions of the Paropamisus xeric woodlands ecoregions). The northeastern and northwestern regions will experience fewer than 20 additional days of growing season.

Background, Introduction, and Methodology

To anticipate the types of challenges that will face ecosystems, hydrology and communities in the P-ARB, the following hazard metrics were analyzed:

- Near-surface permafrost boundary line changes, represented as regions where mean annual temperature is greater than 0°C
- Growing season length as the duration between the first occurrence after 1st January of at least six consecutive days with mean temperatures above 5°C and the first occurrence after 1st July of at least six consecutive days with mean temperatures below 5°C
- Extreme heat in days per year where maximum temperatures exceed 25°C or 30°C
- Extreme precipitation in days per year where precipitation exceeds 20, 30 or 50 mm

The glaciers of the Panj-Amu River Basin are melting at an alarming rate, posing a long-term threat to communities and their livelihoods.

Changes in snowmelt patterns affect the traditional land-use practices for pastoralists and agro-pastoralist communities across the Panj-Amu River Basin.

- Snow water equivalent in days per year where snow water equivalent (depth of water should snow melt) on the ground exceeds 0 mm
- Soil moisture drought showing the "1-in-10-year" (10th percentile) dry soil moisture event. Soil moisture drought metrics are presented for two months:
    - February, as the month before the peak precipitation month
    - October, as a month after the dry summer season representing more extreme water limitations

Detailed descriptions of the risks associated with each hazard are given in Table 4.

Table 4. Natural hazards, key impacts, and risks.

Climate hazard	Key impacts and risks
Permafrost	Changes in permafrost areas, particularly the thawing of near-surface permafrost, can affect the stability of existing ecosystems including trees and surface water ecosystems. Permafrost thawing and active layer thickness increases also have implications for the stability of infrastructure such as roads, bridges, and buildings, affecting community livelihoods and the economy.
Growing season length	The overall growing season length is projected to increase by mid-century, but this is not uniform across the region. The potential for seasonal expansion occurs in areas with relatively long baseline growing seasons. Warming can have negative effects on crops, although some crops can benefit from this. A longer growing season may also allow opportunities for farmers to diversify crops or have multiple harvests. However, the types of crops grown could be limited, increase in invasive species and weeds and increased demand for irrigation water. There could be disruptions in ecosystems, altering range and types of species in an area.
Extreme heat	The implications of extreme heat (e.g., heat waves) are often felt immediately given exceedance of biophysical or engineered tolerances. Heat waves can directly threaten individual and community health, especially the very young and the elderly who have lower tolerances to high temperatures and humidity levels that can lead to heatstroke and potentially result in death. Ecosystems and agricultural crops likewise have tolerance levels whereby productivity is decreased or plants begin to fail (e.g., leaf senescence or organ breakdown).

Extreme precipitation	Heavy precipitation events can lead to pluvial and flash flooding which can cause injury, death, and economic impacts. Heavy precipitation events may also destabilize hillslopes leading to mudflow and landslide hazards, particularly in mountainous regions. Heavy precipitation can also directly damage crops (e.g., through lodging) with acute impacts on crop production, rangelands, and food security.
Snow days/snow water equivalent	Warming temperatures reduce seasonal snowpack, which alters ecosystem dynamics (e.g., predator-prey camouflage dynamics), reduces natural water resource reservoirs, alters the timing of seasonal melt flows, and reduces natural insulation for sub-surface roots and burrowing animals. Reduced snow cover may also extend the season in which agricultural fields may be worked. Over time, snow cover and amount may decrease, with no snow in some areas due to increased warming.
Soil moisture droughts	A decline in soil moisture and increased episodic droughts are strongly connected to reduced available water resources and water stress for crops, rangelands, and natural ecosystems. Droughts can therefore drive acute food security and livelihood impacts.

This analysis focused on the RCP8.5 scenario (higher emissions) given the limited availability of only the RCP2.6 and RCP8.5 scenarios from CORDEX-CORE.

Of these hazard metrics, only the permafrost maps are able to be calculated with monthly bias-adjusted CORDEX-CORE data, so these are shown on a high-resolution 30 arcsec (~1 km) grid. The remaining hazards are calculated using daily CORDEX-CORE outputs, which were not available for bias-adjustment within the scope of this project and are presented here on the native CORDEX-CORE 0.22-degree (~22 km) grid.

For each hazard metric, four figures are presented (as applicable between differences in types of hazard variables and varying temporal resolutions):

1. Baseline ensemble mean value showing the current hazard map
2. Change in ensemble mean projections from baseline based on mid-century projections for the RCP8.5 emissions pathway
3. The timing of emergence, i.e., when a majority of models show the crossing of a particular climatic threshold representing historical averages or variability for the metric between ensemble baseline, 2050s, and 2080s
4. Model agreement showing the number of models (out of 8 GCM/RCM combinations in CORDEX-CORE) projecting a particular threshold crossing for the metric by the RCP8.5 mid-century time slice.

Permafrost

Threshold: Mean Annual Temperature > 0°C

E

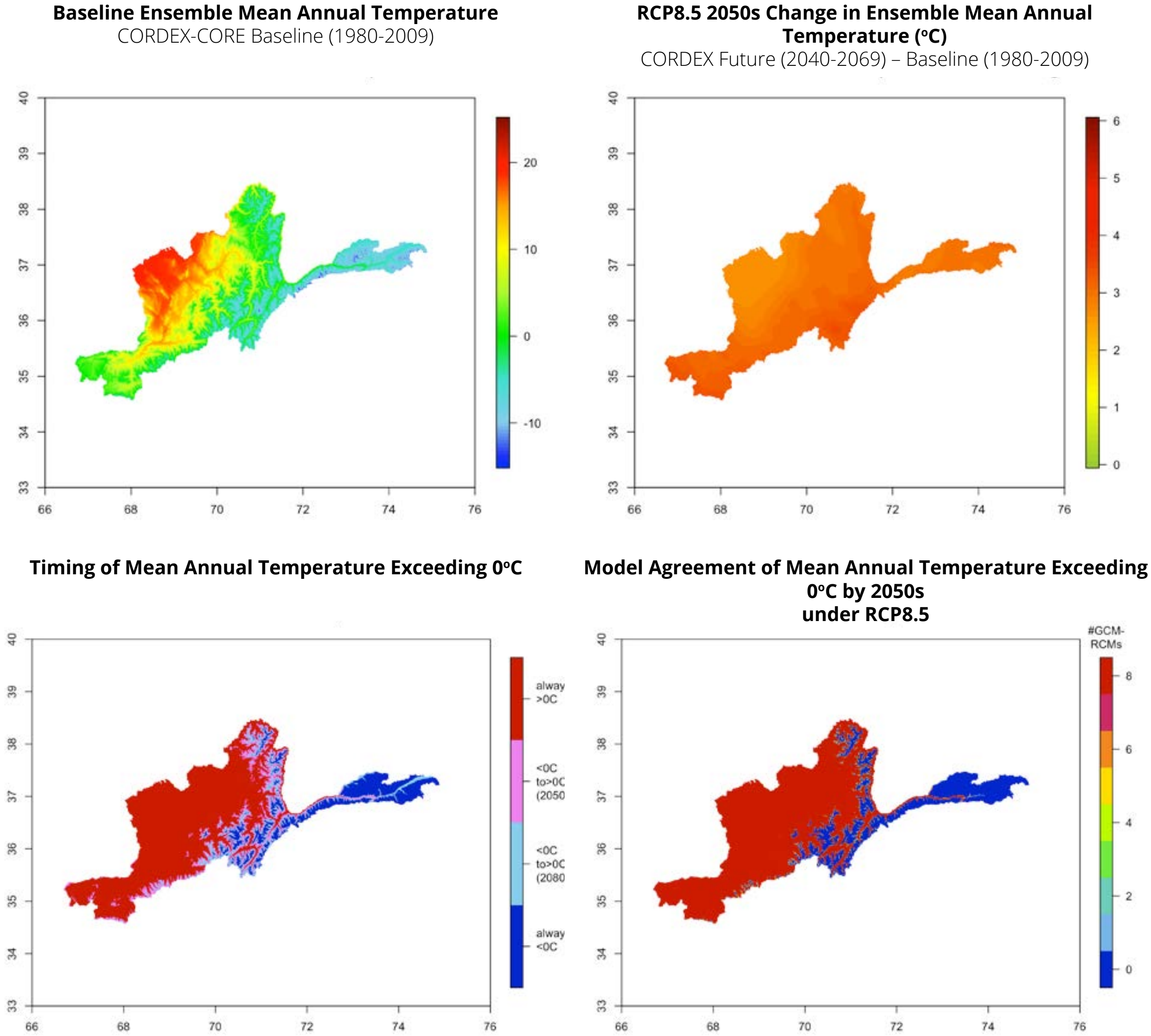

Figure 47. Permafrost.

Permafrost areas are defined as Earth surfaces that remain below 0ºC for at least two continuous years. Changes in permafrost areas, particularly the withdrawal of permafrost region boundaries with warming climates, can affect the stability of existing ecosystems, infrastructure, and communities (Romanovsky et al. 2002).

Permafrost results are shown in Figure 47. To assess changes in the permafrost boundary line, a categorical indicator was used, showing whether the bias-adjusted CORDEX-CORE ensemble mean annual temperature (top left) exceeds 0ºC. Changes in ensemble mean annual temperature between baseline and RCP8.5 mid-century (2040-2069) are shown in the top right panel as an indication of the overall warming.

The bottom left panel shows regions where the ensemble mean annual temperature is below 0ºC from the baseline out to 2100 (dark blue, indicating always conducive to near-surface permafrost), remains above 0ºC from the baseline out to 2100 (red, indicating never conducive to near-surface permafrost), or changes from below 0ºC in the baseline to above 0ºC (conducive to not conducive conditions) either by mid-century (pink) or by end-of-century (light blue). The pattern of temporal emergence closely matches the mountainous topography of the region, with the 0ºC boundary visible between warmer western regions (Paropamisus xeric woodlands, Ghorat-Hazarajat alpine meadow, Hindu Kush alpine meadow, Afghan Mountains semi-desert, Badghyz and Karabil semi-desert) and the colder mountains in the east (Pamir alpine desert and tundra, Karakoram-West Tibetan Plateau alpine steppe, Ghorat-Hazarajat alpine meadow, Hindu Kush alpine meadow). Further into the future, the 0ºC line moves from lower-elevation areas (always greater than 0ºC) to the smaller mountains and foothills, which warm to above 0ºC by mid-century. By the end of the century, the permafrost boundary retreats all the way to the tops of some mountain regions and to the larger valleys of the Wakhan corridor (Pamir alpine desert and tundra, Karakoram-West Tibetan Plateau alpine steppe). Large changes are also evident where conditions suitable to near-surface permafrost move all the way up a mountain and locally disappear.

The bottom right panel indicates the number of GCM-RCM combinations (out of the eight available) that agree on whether the mean annual temperature will exceed 0ºC in the RCP8.5 mid-century time period. A similar topographical pattern to the temporal emergence map is visible, with a unanimous model agreement (shown in red) on mean annual temperatures above 0ºC across the western side of the river basin, including some lower-elevation mountain regions. In areas with higher elevation, fewer models agree that permafrost will retreat to this extent by mid-century, with all models agreeing that mean annual temperature will remain below 0ºC in the most mountainous areas in the far east (Pamir alpine desert and tundra, Karakoram-West Tibetan Plateau alpine steppe).

Growing Season Length

E

Threshold: >150 Days Per Year Growing Season Length

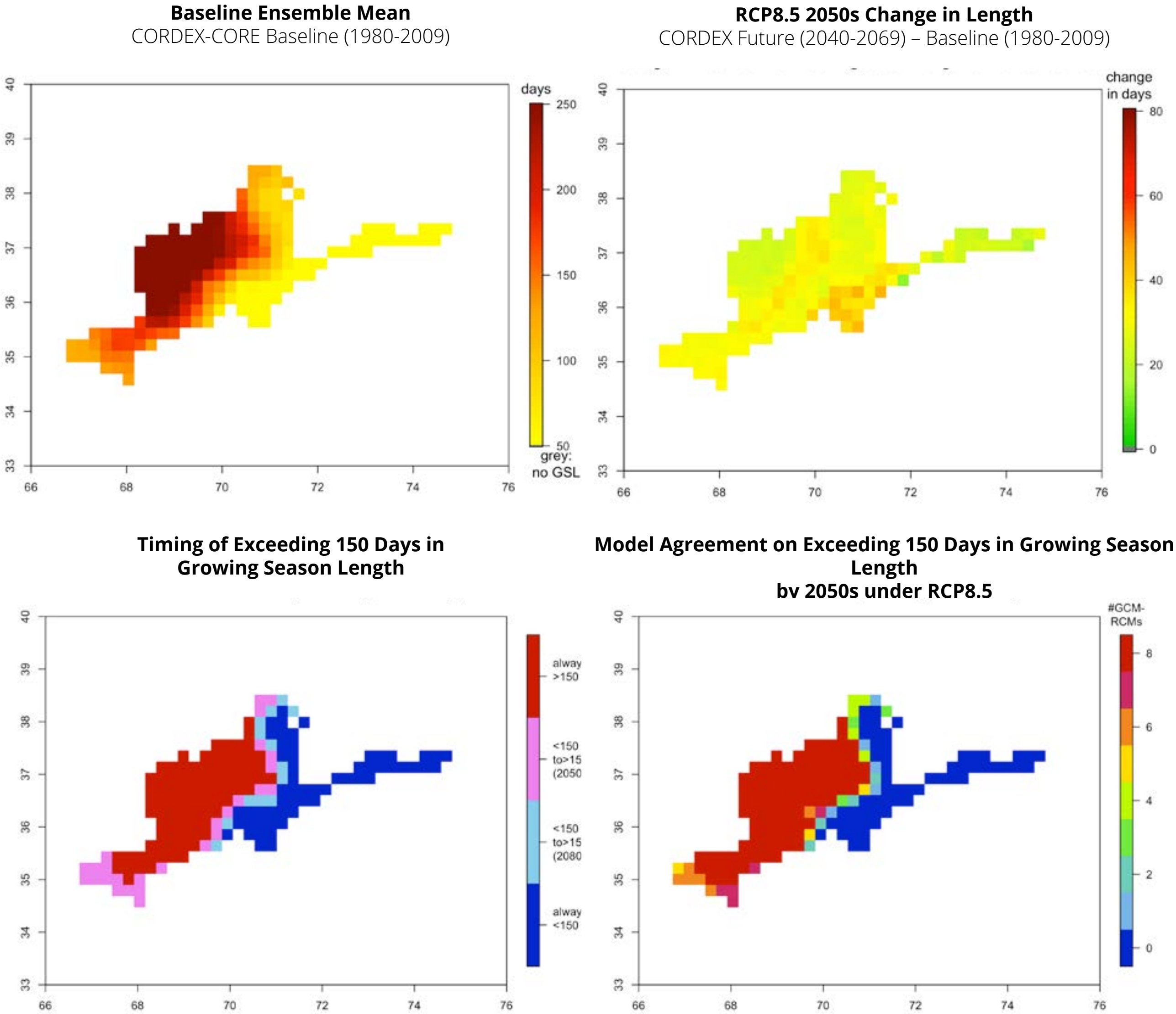

Figure 48. Growing Season Length.

Growing season length is defined as the length of time in days between the first occurrence of at least six consecutive days with mean daily temperatures above 5°C, and the first occurrence after 1st July (in the Northern Hemisphere) of at least six consecutive days with mean temperatures below 5°C. This metric captures the duration between early- and late-year conditions when the threat of frosts surrounds the agricultural growing season. Although the length of the growing season will depend on additional factors, including the cultivar, water availability, daylight hours, and additional socioeconomic factors, this indicator serves to highlight the limiting factor of temperature in determining seasonal planting and harvest windows.

Growing season length results are shown in Figure 48. The ensemble mean growing season length in CORDEX-CORE in the baseline period, seen in the top left panel, clearly follows the pattern of temperature in the region. Longer growing seasons of 250 days or more are visible in the warmer western areas (Badghyz and Karabil semi-desert, Paropamisus xeric woodlands) of the P-ARB, with shorter growing season lengths in the higher-elevation eastern region (Pamir alpine desert and tundra, Karakoram-West Tibetan Plateau alpine steppe). As temperatures increase broadly across the region under RCP8.5, the overall growing season length is projected to increase accordingly by mid-century, as seen in the top right panel. However, this increase is not uniform across the region, with the highest increases in growing season length occurring in the southern central area (Hindu Kush alpine meadow, Afghan Mountains semi-desert) of the river basin, where the season may extend by 40-50 days. The regions with the largest increases in growing season length are often on the threshold of those with relatively long baseline growing seasons, indicating the potential for seasonal expansion in those areas even while the coldest regions in the far east (Pamir alpine desert and tundra, Karakoram-West Tibetan Plateau alpine steppe) show relatively small increases in growing season length.

The bottom left panel shows the emergence of the threshold of a growing season length of 150 days across all time periods in RCP8.5. Regions in red, mostly in the west of the river basin (Paropamisus xeric woodlands, Ghorat-Hazarajat alpine meadow, Hindu Kush alpine meadow, Afghan Mountains semi-desert, Badghyz and Karabil semi-desert), show areas where the ensemble mean growing season length is projected to remain above 150 days for all time periods; regions in dark blue, in the east (Pamir alpine desert and tundra, Karakoram-West Tibetan Plateau alpine steppe, Gissaro-Alai open woodlands, Paropamisus xeric woodlands, Hindu Kush alpine meadow, Afghan Mountains semi-desert), show areas where the mean growing season length never exceeds 150 days at any point in the century. The threshold between these regions follows the spread of higher temperatures from west to east, as the mean growing season length expands to 150 days by mid-century first (in pink), followed by a smaller expansion further east by end-of-century (in light blue).

The bottom right panel shows model agreement on exceeding 150 days in growing season length by RCP8.5 mid-century. As with the bottom left panel, there is complete agreement that the growing season length in the warmer western region (Paropamisus xeric woodlands, Ghorat-Hazarajat alpine meadow, Hindu Kush alpine meadow, Afghan Mountains semi-desert, Badghyz and Karabil semi-desert) will continue to exceed 150 days by mid-century, but the season will remain under 150 days in the colder east (Pamir alpine desert and tundra, Karakoram-West Tibetan Plateau alpine steppe, Gissaro-Alai open woodlands, Paropamisus xeric woodlands, Hindu Kush alpine meadow, Afghan Mountains semi-desert). There is higher model agreement on this exceedance in the southwest (Ghorat-Hazarajat alpine meadow, Afghan Mountains semi-desert) of the P-ARB, but somewhat less model agreement on the threshold between east and west, with 50% or less of the GCM-RCMs agreeing on more than 150 days of growing season length by mid-century in the northernmost edge (Paropamisus xeric woodlands, Gissaro-Alai open woodlands) of the P-ARB.

Extreme Heat (25°C Threshold)

Threshold: >120 Days Per Year where Maximum Temperature > 25°C)

E

Baseline Ensemble Mean
CORDEX-CORE Baseline (1980-2009)

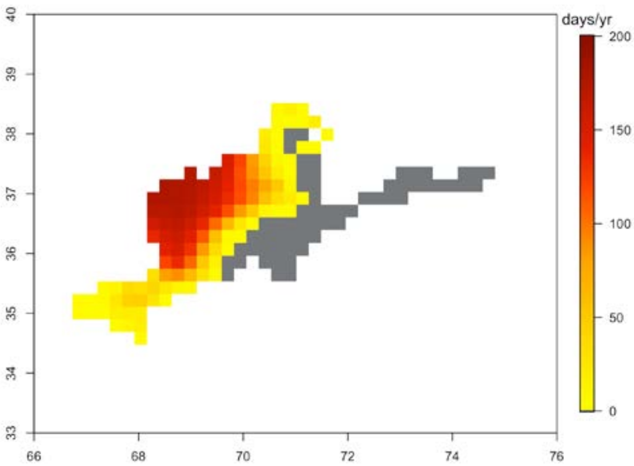

RCP8.5 2050s Change in Frequency
CORDEX Future (2040-2069) – Baseline (1980-2009)

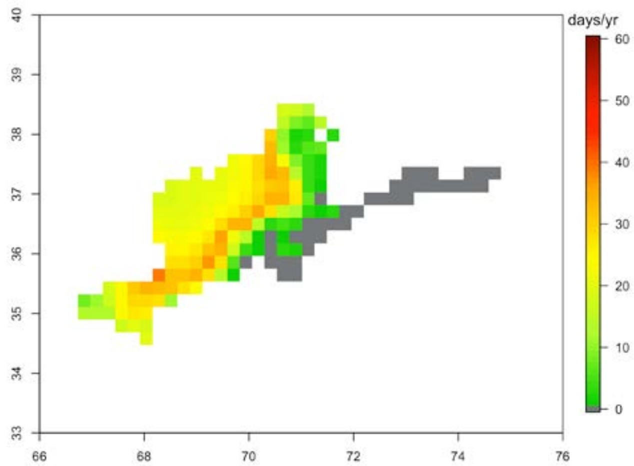

Timing of Exceeding 120 Days/Year with Max Temp > 25°C

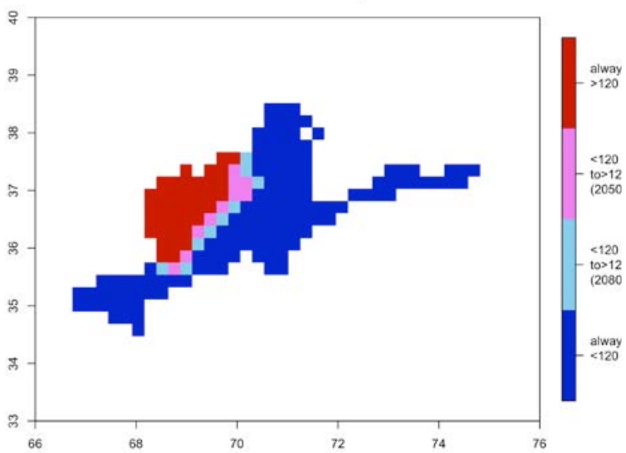

Model Agreement on Exceeding 120 Days/Year with Max Temp > 25°C bv 2050s under RCP8.5

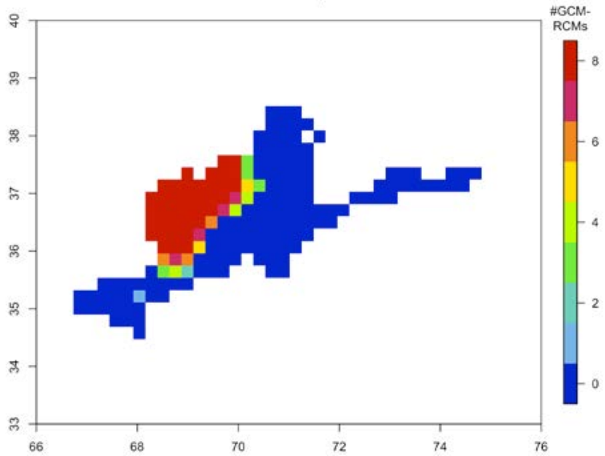

Figure 49. Extreme Heat (25°C Threshold).

Extreme heat can have a range on impacts on communities, ecosystems, and species and can trigger physical hazards due to rapid snow melt. The thresholds of 25°C and 30°C were selected to understand how climate change influences these hazards. In the baseline, much of the high-elevation northeastern parts of the region (Pamir alpine desert and tundra, Karakoram-West Tibetan Plateau alpine steppe, Gissaro-Alai open woodlands, Hindu Kush alpine meadow, Paropamisus xeric woodlands) never exceed 25°C; these areas are highlighted in grey.

Extreme heat results for the 25°C threshold results are shown in Figure 49. Parts of the north, central and southwestern regions (Gissaro-Alai open woodlands, Paropamisus xeric woodlands, Ghorat-Hazarajat alpine meadow, Hindu Kush alpine meadow, Afghan Mountains semi-desert) see between 0 and 50 days per year with temperatures over the threshold, while the northwestern region (Paropamisus xeric woodlands, Badghyz and Karabil semi-desert) sees 100-200 days that exceed 25°C. The top right panel highlights the changes in frequency of extreme heat days per year over 25°C, including a pattern of the most substantial increases along the edge of the mountains that indicates a region that already experienced sporadic heat events in the baseline, but moves to more regular seasonal heat hazards in the future. The coldest regions in the northeast and south (Pamir alpine desert and tundra, Karakoram-West Tibetan Plateau alpine steppe, Hindu Kush alpine meadow, Paropamisus xeric woodlands), again highlighted in grey, do not see any increase in frequency, but areas on the edge of these high-mountain regions do see a slight increase despite zero days per year above 25°C in the baseline. High-frequency areas in the baseline, such as the western side of the river basin (Paropamisus xeric woodlands, Badghyz and Karabil semi-desert), see lower increases than the center of the region (Hindu Kush alpine meadow, Paropamisus xeric woodlands), where the effects of increases in extreme heat days may be more pronounced due to lower baseline levels.

The likelihood of exceeding 120 days per year above 25°C, for each of the two future 30-year time slices, is shown in the bottom left panel for the ensemble mean. A majority of the P-ARB, such as the northern, northeastern, southern, central, and southwestern regions (Pamir alpine desert and tundra, Karakoram-West Tibetan Plateau alpine steppe, Gissaro-Alai open woodlands, Paropamisus xeric woodlands, Ghorat-Hazarajat alpine meadow, Hindu Kush alpine meadow, Afghan Mountains semi-desert), never exceeds 120 days per year above 25°C. The northwestern region (Paropamisus xeric woodlands, Badghyz and Karabil semi-desert) always exceeds 120 days per year with maximum temperatures above 25°C. Areas that did not exceed 120 days per year above 25°C in the baseline, but do exceed 120 days in the future, are shown in pink (exceedance by mid-century) or light blue (exceedance by the end of the century). The expansion of warmer areas, and with it an increase in extreme heat days, is visible here as the area with more than 120 days of maximum temperatures exceeding 25°C, which moves slightly east in the 2050s and further into the center of the P-ARB by the 2080s. This reflects a movement of extreme heat conditions toward higher elevations.

Model agreement on the number of days per year above 25°C exceeds 120 days in the RCP8.5 mid-century time period is shown in the bottom right panel. Most or all model combinations (75-100%) agree on a frequency of at least 120 days exceeding 25°C by mid-century in the northwestern region (Paropamisus xeric woodlands, Badghyz and Karabil semi-desert), as expected from the temporal emergence map on the bottom left. All models agree that the northern, central, southern, northeastern, and southwestern regions (Pamir alpine desert and tundra, Karakoram-West Tibetan Plateau alpine steppe, Gissaro-Alai open woodlands, Paropamisus xeric woodlands, Ghorat-Hazarajat alpine meadow, Hindu Kush alpine meadow, Afghan Mountains semi-desert) do not exceed 120 days per year above 25°.C by mid-century under RCP8.5. Between these two regions of high agreement, a higher number of GCM-RCM combinations agree on exceeding 120 days per year on the edge of the warmer western region (Paropamisus xeric woodlands, Badghyz and Karabil semi-desert), with fewer models agreeing with the movement into the central and southern areas (Paropamisus xeric woodlands).

Extreme Heat (30°C Threshold)

Threshold: >120 Days Per Year where Maximum Temperature > 30°C)

E

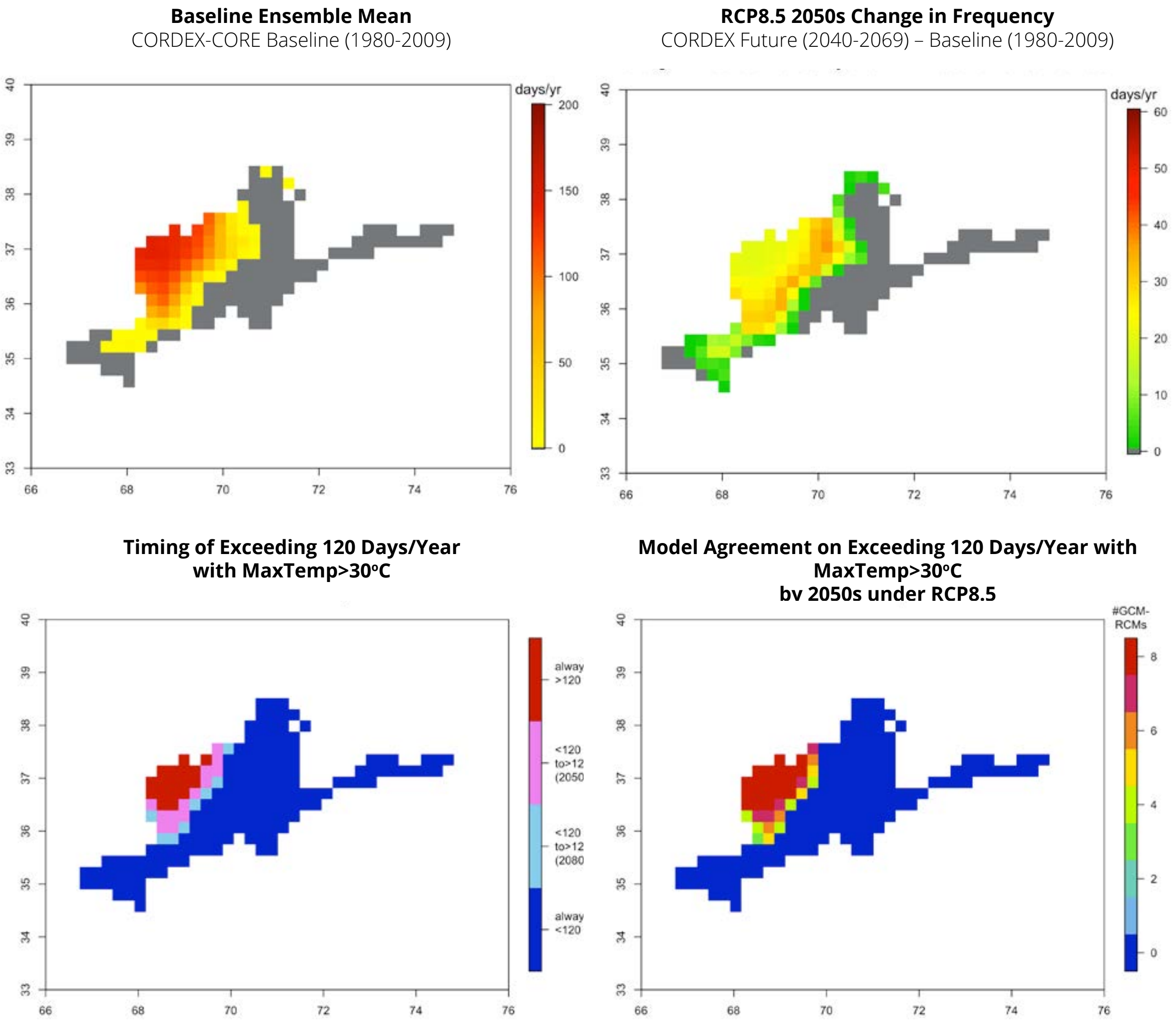

Figure 50. Extreme Heat (30°C Threshold).

Similar to the extreme heat analysis for the threshold of 25ºC, an analysis using the number of days per year that exceed 30ºC was also carried out. Extreme heat results for the 30ºC threshold results are shown in Figure 50. In the baseline, much of the high-elevation parts of the P-ARB, seen in grey in the top left panel, never exceed 30ºC, along with some areas in the southwest (Ghorat-Hazarajat alpine meadow, Afghan Mountains semi-desert). Parts of the north, central, and southwestern regions (Gissaro-Alai open woodlands, Paropamisus xeric woodlands, Ghorat-Hazarajat alpine meadow, Afghan Mountains semi-desert) see between 0 and 50 days per year with temperatures over the threshold, while the northwestern region (Paropamisus xeric woodlands, Badghyz and Karabil semi-desert) sees 100-200 days that exceed 30ºC. The top right panel highlights the changes in frequency of extreme heat days per year over 30ºC, which shows a similar pattern of larger changes along the mountain edges where extreme heat goes from sporadic to more regular. The coldest regions in the north, northeast, and south (Pamir alpine desert and tundra, Karakoram-West Tibetan Plateau alpine steppe, Gissaro-Alai open woodlands, Paropamisus xeric woodlands, Ghorat-Hazarajat alpine meadow, Hindu Kush alpine meadow), represented by grey areas in the map, do not see any increase in frequency, but areas on the western edges of these regions (Ghorat-Hazarajat alpine meadow, Afghan Mountains semi-desert) do see a slight increase despite zero days per year above 30ºC in the baseline. As with the 25ºC threshold, areas in the baseline with a very high count, such as the western side (Paropamisus xeric woodlands, Ghorat-Hazarajat alpine meadow, Afghan Mountains semi-desert, Badghyz and Karabil semi-desert) of the P-ARB, see lower increases than the center of the region (Paropamisus xeric woodlands), which may experience up to 40 more days per year above 30ºC.

The likelihood of exceeding 120 days per year above 30ºC, for each of the two future 30-year time slices, is shown in the bottom left panel for the ensemble mean. A majority of the P-ARB, such as the northern, northeastern, southern, central, and southwestern regions (Pamir alpine desert and tundra, Karakoram-West Tibetan Plateau alpine steppe, Gissaro-Alai open woodlands, Paropamisus xeric woodlands, Ghorat-Hazarajat alpine meadow, Hindu Kush alpine meadow, Afghan Mountains semi-desert), never exceeds 120 days per year above 30ºC. The northwestern region (Paropamisus xeric woodlands, Badghyz and Karabil semi-desert) always exceeds 120 days per year with maximum temperatures above 30ºC. Areas that did not exceed 120 days per year above 30ºC days in the baseline, but do exceed 120 days in the future, are shown in pink (exceedance by mid-century) or light blue (exceedance by the end of the century). With a higher threshold than the 25ºC threshold previously considered, the expansion of warmer areas is more limited, but a similar pattern is visible as the area with more than 120 days of maximum temperatures exceeding 30ºC moves slightly east in the 2050s and even further east by the 2080s.

Model agreement on whether the number of days per year above 30ºC exceeds 120 days in the RCP8.5 mid-century time period is shown in the bottom right panel. Most or all model combinations (75-100%) agree on a frequency of at least 120 days exceeding 30ºC by mid-century in the northwestern region (Paropamisus xeric woodlands, Badghyz and Karabil semi-desert), as expected from the temporal emergence map on the bottom left. All models agree that the majority of the P-ARB will not exceed 120 days per year above 30ºC by mid-century under RCP8.5. On the edge of the warmer western region (Paropamisus xeric woodlands), a smaller number of GCM-RCM combinations (between 25-75%) agree on exceeding 120 days per year above 30ºC.

Extreme Precipitation (20 mm Threshold)

Threshold: >5 Days Per Year where Daily Precipitation > 20 mm)

E

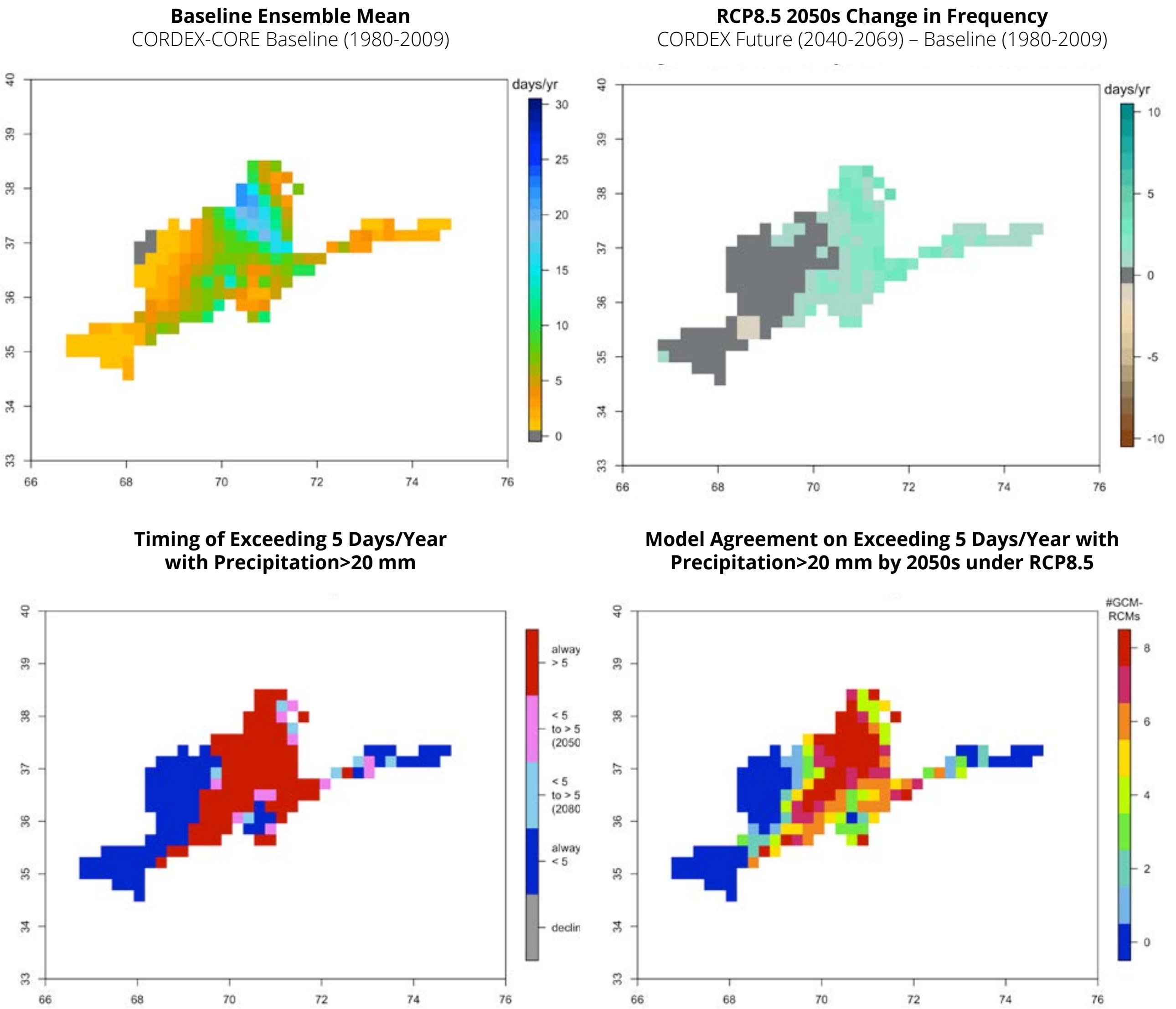

Figure 51. Extreme Precipitation (20 mm Threshold).

Extreme precipitation events are not only useful indicators of potential pluvial flooding and waterlogging, but can also be linked to other climate hazards, such as flash river floods, landslides, or avalanches. A range of precipitation thresholds for single-day events, from 20 mm to 50 mm were assessed, to provide a broad analysis of the risk of these hazards and in recognition that coarser model resolution reduces the magnitude of extreme event statistics that can be larger at localized scales. Extreme precipitation results for the 20 mm threshold results are shown in Figure 51. The number of 20 mm/day precipitation events per year, shown for the ensemble mean baseline in the top left panel, follows a similar pattern to total annual precipitation in the region (Figure 6). A higher number of these events are seen throughout the center (Paropamisus xeric woodlands, Hindu Kush alpine meadow) of the P-ARB and the largest number, nearly 30 days per year, is seen in the mountains (Paropamisus xeric woodlands, Hindu Kush alpine meadow) just south of Tajikistan. Throughout the P-ARB, the ensemble mean number of 20 mm daily precipitation events per year increases slightly by the RCP8.5 mid-century scenario, but only by 1-3 days per year in most areas, with the potential for a decrease by ~1 day per year in the mid-southern central region (Ghorat-Hazarajat alpine meadow, Afghan Mountains semi-desert). However, small increases for these heavy precipitation events in mountainous terrain, seen across the entire eastern side of the P-ARB and the Wakhan corridor (Pamir alpine desert and tundra, Karakoram-West Tibetan Plateau alpine steppe, Gissaro-Alai open woodlands, Paropamisus xeric woodlands, Hindu Kush alpine meadow, Afghan Mountains semi-desert), can still indicate an increased risk of rainfall-induced hazards, such as mudflows, erosion, flash floods, and landslides.

The likelihood of exceeding 5 days per year of extreme precipitation greater than 20 mm/year, for each of the two future 30-year time slices, is shown in the bottom left panel. Regions that never exceed 5 days per year of 20 mm precipitation events are shown in dark blue; those that exceed 5 days of 20 mm events from the baseline out to 2100 are shown in red, corresponding to higher-count areas in the baseline ensemble mean (top left). Areas that did not exceed 5 days per year of 20 mm events in the baseline, but do exceed 5 days in the future, are shown in pink (exceedance by mid-century) or light blue (exceedance by the end of the century). A slight expansion in the areas with more than 5 days is seen, and largely in the same regions that also see higher counts in the baseline; namely, the northern end (Gissaro-Alai open woodlands, Paropamisus xeric woodlands, Hindu Kush alpine meadow) of the P-ARB and the edges of those areas that always exceed 5 days. A further expansion is seen by the end of the century, with only a few more grid cells switching from below to above 5 days per year of 20 mm events.

Model agreement on whether the number of days per year of 20 mm precipitation events exceeds 5 days in the RCP8.5 mid-century time period is shown in the bottom right panel. As expected, the highest levels of model agreement are in areas where the temporal exceedance map shows the ensemble mean to be consistently above 5 days per year, from the baseline out into the future. When expanding from this central northern area (Gissaro-Alai open woodlands, Paropamisus xeric woodlands, Ghorat-Hazarajat alpine meadow, Hindu Kush alpine meadow, Afghan Mountains semi-desert), less GCM-RCM agreement is seen on whether or not the mid-century RCP8.5 time period will exceed 5 days per year of 20 mm events; around 50% of models agree on this exceedance in the northernmost part (Gissaro-Alai open woodlands, Hindu Kush alpine meadow) of the P-ARB below Tajikistan, as well as the south-central mountainous regions (Paropamisus xeric woodlands, Hindu Kush alpine meadow, Afghan Mountains semi-desert). As with the ensemble mean, all models agree that the lower-elevation southern and western areas (Paropamisus xeric woodlands, Ghorat-Hazarajat alpine meadow, Afghan Mountains semi-desert, Badghyz and Karabil semi-desert) will not exceed 5 days per year of 20 mm events by mid-century under RCP8.5. Model disagreement on the direction of precipitation change, and particularly the tails of daily precipitation distributions such as extreme single-day events, is not uncommon, as trends in precipitation can be sensitive to a variety of internal GCM and RCM dynamics and factors.

Extreme Precipitation (30 mm Threshold)

Threshold: >5 Days Per Year where Daily Precipitation > 30 mm)

E

Baseline Ensemble Mean
CORDEX-CORE Baseline (1980-2009)

RCP8.5 2050s Change in Frequency
CORDEX Future (2040-2069) – Baseline (1980-2009)

Timing of Exceeding 5 Days/Year with Precipitation>30 mm

Model Agreement on Exceeding 5 Days/Year with Precipitation>30 mm by 2050s under RCP8.5

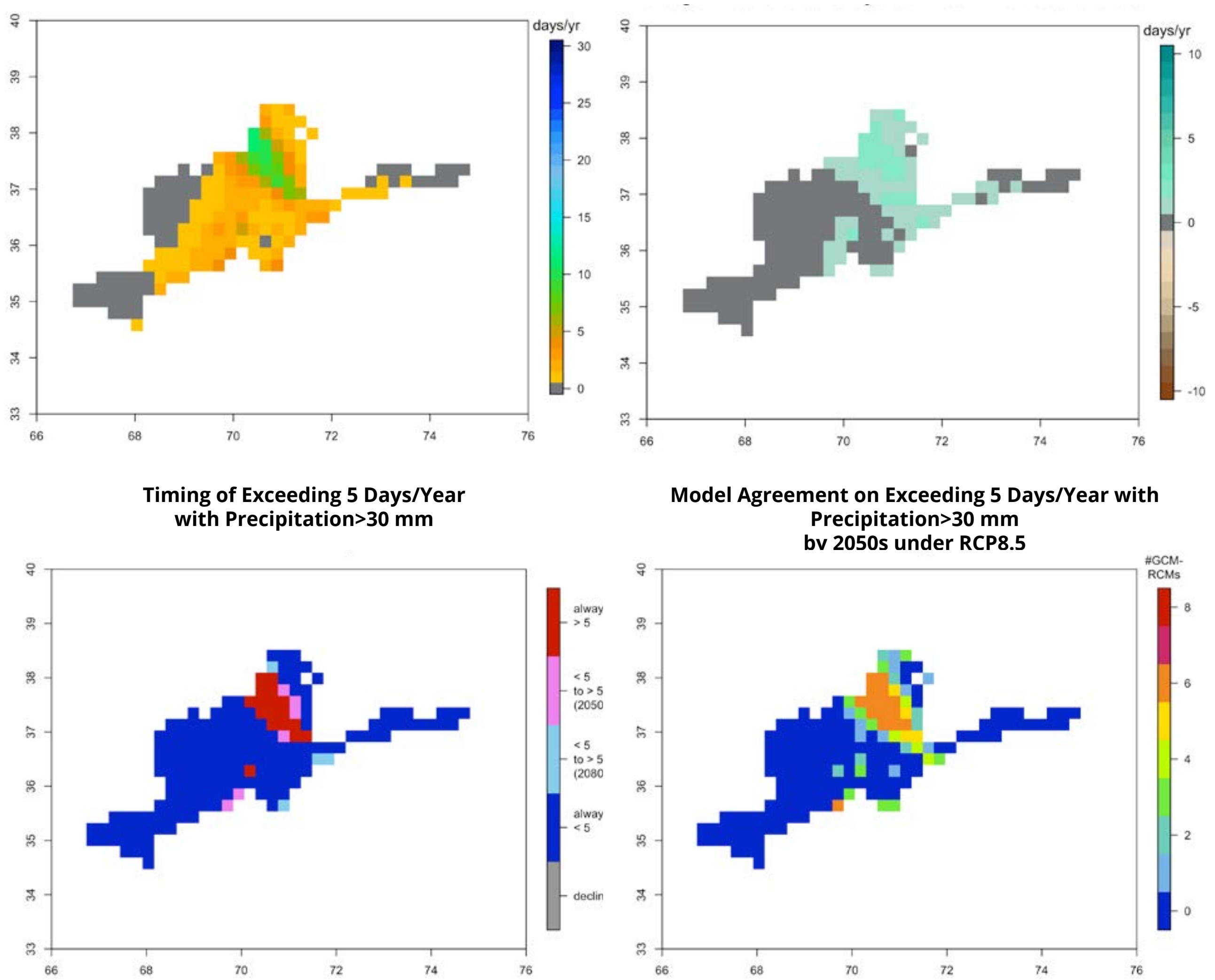

Figure 52. Extreme Precipitation (30 mm Threshold).

While precipitation brings much-needed water for agriculture and other crucial human uses, it can also lead to flash floods and landslides, which can be devastating for people living in rural areas.

Similar to the set of maps for days of extreme precipitation over 20 mm, the 30 mm threshold for single-day events is assessed to provide a broad analysis of the risk for precipitation-related hazards. Extreme precipitation results for the 30 mm threshold results are shown in Figure 52. The number of 30 mm/day precipitation events per year is shown for the ensemble mean baseline in the top left panel. A higher number of these events (~10) is seen in the north Paropamisus xeric woodlands, Hindu Kush alpine meadow, followed by areas with between zero and five days in much of the P-ARB, except the western, southwestern, and far eastern regions (Badghyz and Karabil semi-desert, Paropamisus xeric woodlands, Ghorat-Hazarajat alpine meadow, Pamir alpine desert and tundra, Karakoram-West Tibetan Plateau alpine steppe), which see no days with a threshold of 30 mm. In the northern, eastern, and southeastern regions (Pamir alpine desert and tundra, Karakoram-West Tibetan Plateau alpine steppe, Gissaro-Alai open woodlands, Paropamisus xeric woodlands, Hindu Kush alpine meadow, Afghan Mountains semi-desert), the ensemble mean number of 30 mm daily precipitation events per year increases slightly by the RCP8.5 mid-century scenario, but only by 1-3 days per year in most areas. However, small increases for these heavy precipitation events in mountainous terrain, seen across the entire eastern side of the P-ARB and the western side of the Wakhan corridor (Pamir alpine desert and tundra, Karakoram-West Tibetan Plateau alpine steppe, Gissaro-Alai open woodlands, Paropamisus xeric woodlands, Hindu Kush alpine meadow, Afghan Mountains semi-desert), can still indicate an increased risk of rainfall-induced hazards, such as mudflows, erosion, flash floods, and landslides. Much of the P-ARB does not see any change in 30 mm events.

The likelihood of exceeding 5 days per year, for each of the two future 30-year time slices, is shown in the bottom left panel. Regions that never exceed 5 days per year of 30 mm precipitation events are shown in dark blue; those that exceed 5 days of 30 mm events from the baseline out to 2100 are shown in red. Areas that did not exceed 5 days per year of 30 mm events in the baseline, but do exceed 5 days in the future, are shown in pink (exceedance by mid-century) or light blue (exceedance by the end of the century). Compared to the results using a threshold of 20 mm daily precipitation, there are fewer grid cells with more than 5 days of 30 mm events. The areas with 5 days of 30 mm events by the 2050s and 2080s are seen in just a few grid cells in the central northern area of the river basin and to a very small extent in the south (Gissaro-Alai open woodlands, Paropamisus xeric woodlands, Hindu Kush alpine meadow, Afghan Mountains semi-desert). Much of the region does not see an exceedance of 5 days per year of 30 mm precipitation events.

Model agreement on whether the number of days per year of 30 mm precipitation events exceeds 5 days in the RCP8.5 mid-century time period is shown in the bottom right panel. The highest levels of model agreement are in areas where the temporal exceedance map shows the ensemble mean to be consistently above or below 5 days per year, from the baseline out into the end of the century. However, unlike the 20 mm threshold, there are no areas where more than 75% of models agree that the mid-century time slice will exceed 5 days of 30 mm events. Throughout this central northern area (Gissaro-Alai open woodlands, Paropamisus xeric woodlands, Hindu Kush alpine meadow, Afghan Mountains semi-desert), there is less overall GCM-RCM agreement on whether the mid-century RCP8.5 scenario will exceed 5 days per year of 30 mm events.

Extreme Precipitation (50 mm Threshold)

Threshold: >5 Days Per Year where Daily Precipitation > 50 mm)

E

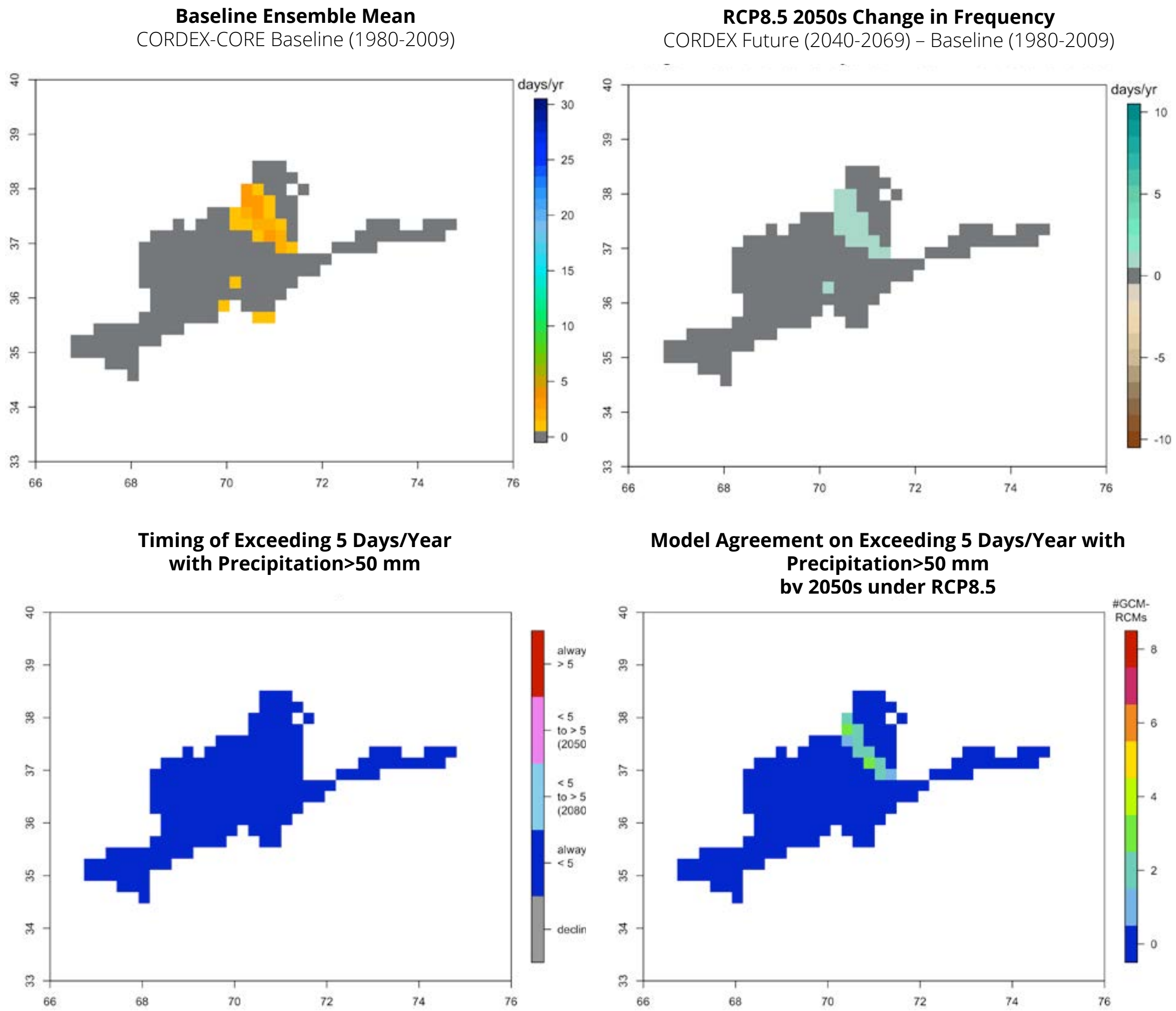

Figure 53. Extreme Precipitation (50 mm Threshold).

Similar to the set of maps for days of extreme precipitation over 20 and 30 mm, the 50 mm threshold is assessed for single-day events to provide a broad analysis of the risk for precipitation-related hazards. Extreme precipitation results for the 50 mm threshold results are shown in Figure 53. The number of 50 mm/day precipitation events per year is shown for the ensemble mean baseline in the top left panel. Very few grid cells with these events are seen and these are concentrated in the central north region of the P-ARB, with a few scattered grid cells in the south (Paropamisus xeric woodlands, Hindu Kush alpine meadow). Many of the areas with any daily 50 mm rainfall events see an increase in frequency by ~1 day per year under RCP8.5 by mid-century.

The likelihood of exceeding 5 days per year, for each of the two future 30-year time slices, is shown in the bottom left panel. For the ensemble mean across GCM-RCMs, there are no areas in the river basin region that exceed 5 days per year of 50 mm precipitation events at any point in the RCP8.5 projections, as shown in dark blue across the map.

Model agreement on whether the number of days per year of 50 mm precipitation events exceeds 5 days in the RCP8.5 mid-century time period is shown in the bottom right panel. There are one or two models that project at least 5 days of 50 mm events in the highest-precipitation areas in the central north of the region (Paropamisus xeric woodlands, Hindu Kush alpine meadow), but there is overall very little model agreement on exceeding this threshold. For the majority of the region, all models agree that daily precipitation events will not exceed 5 days above 50 mm by RCP8.5 mid-century.

Snow Water Equivalent

Threshold: <150 Days Per Year where SWE > 0 mm)

E

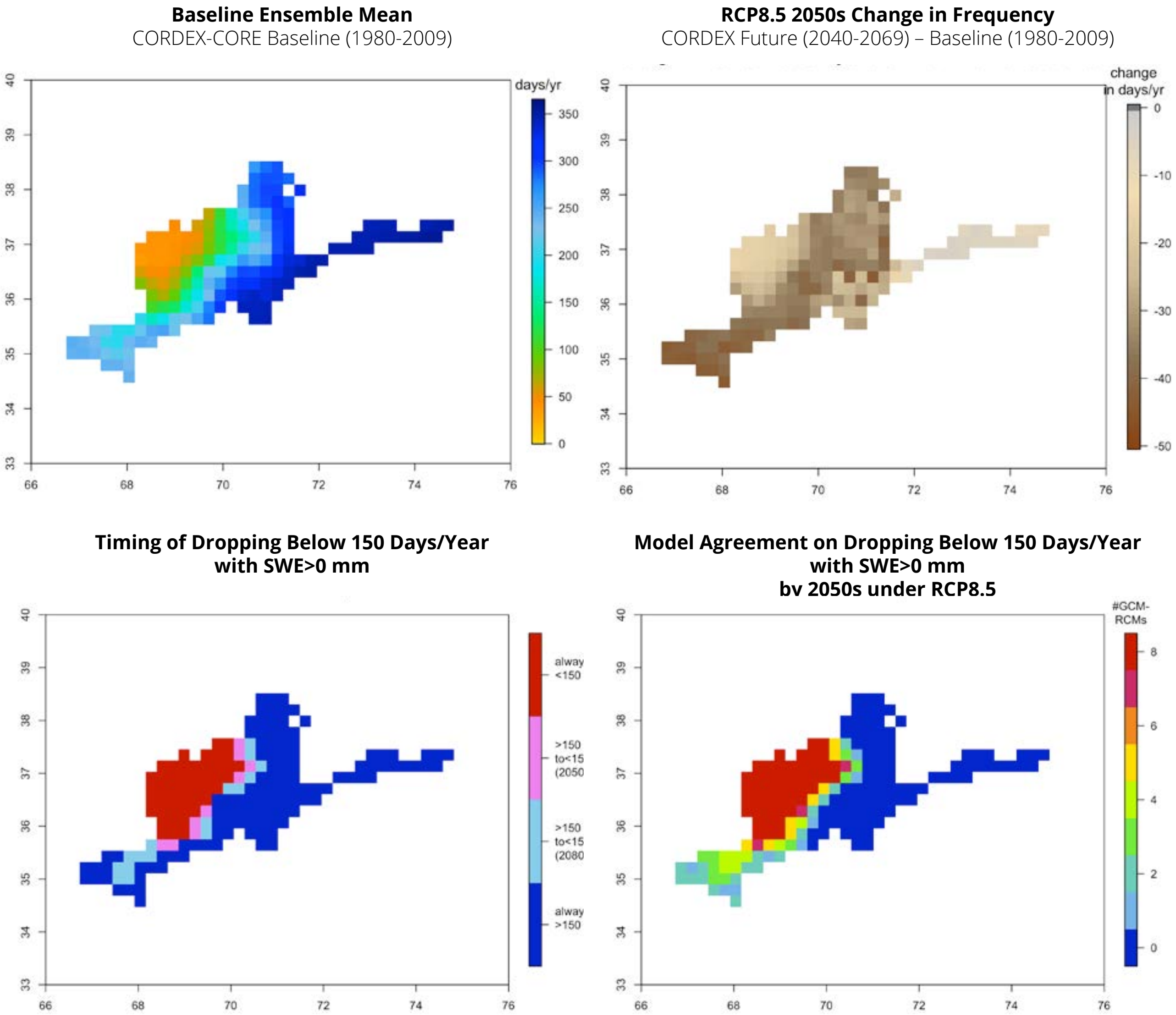

Figure 54. Snow Water Equivalent.

Snow water equivalent (SWE) is represented by the number of days per year with snow on the ground having SWE > 0 mm (representing, e.g., potential camouflage). Snow water equivalent results results are shown in Figure 54. The baseline ensemble mean is depicted in the top left panel, where the high mountain areas in the east and southeastern region (Pamir alpine desert and tundra, Karakoram-West Tibetan Plateau alpine steppe, Hindu Kush alpine meadow) of the P-ARB see year-round snow. Coarse model resolution at 0.22° likely obscures sub-grid-scale valleys that do not have year-round snow. Some areas of the northern, western, and southern regions see snow for much of the year, along with parts of the central and western regions (Pamir alpine desert and tundra, Karakoram-West Tibetan Plateau alpine steppe, Gissaro-Alai open woodlands, Paropamisus xeric woodlands, Ghorat-Hazarajat alpine meadow, Hindu Kush alpine meadow, Afghan Mountains semi-desert). The northwestern region (Badghyz and Karabil semi-desert, Paropamisus xeric woodlands) sees the least snow, with some areas almost free of snow. The top right panel displays the change in frequency of the number of days per year with snow. By mid-century, all regions see a decline in snow days, with northern, central, and southwestern regions seeing the largest decline (Gissaro-Alai open woodlands, Paropamisus xeric woodlands, Ghorat-Hazarajat alpine meadow, Hindu Kush alpine meadow, Afghan Mountains semi-desert), followed by the northeastern and northwestern regions (Pamir alpine desert and tundra, Karakoram-West Tibetan Plateau alpine steppe, Paropamisus xeric woodlands, Badghyz and Karabil semi-desert), although the low number of baseline snow days per year in the western side of the P-ARB means that there may be very few snow days per year in that area by RCP8.5 mid-century.

The bottom left panel depicts the likelihood of ensemble mean snow days falling below 150 days for each of the two future 30-year time slices. In mountainous areas with high amounts of snow in the baseline, such as the northern, northeastern regions and parts of the south and west (Pamir alpine desert and tundra, Karakoram-West Tibetan Plateau alpine steppe, Gissaro-Alai open woodlands, Paropamisus xeric woodlands, Ghorat-Hazarajat alpine meadow, Hindu Kush alpine meadow, Afghan Mountains semi-desert), the number of snow days per year never drops below 150, despite the ensemble mean decline in snow days by mid-century (top right). The northwestern region (Badghyz and Karabil semi-desert, Paropamisus xeric woodlands), which is the region with the least number of snow days in the baseline, always sees less than 150 snow days per year. When moving forward from the baseline to mid-century, the areas with less than 150 days of snow per year expands from those that are consistently below 150 for all time periods, with several grid cells dropping below 150 days by mid-century. A larger expansion is seen by the end of the century, with some southwestern regions (Ghorat-Hazarajat alpine meadow, Afghan Mountains semi-desert) also dropping below 150 days of snow per year.

The bottom right panel displays the model agreement on whether the number of snow days per year will fall below 150, with 75-100% of models agreeing that the western region (Badghyz and Karabil semi-desert, Paropamisus xeric woodlands) will see less than 150 days per year of snow, similar to the baseline map (top left). All models agree that the higher elevation regions in the north, northeast, and south (Pamir alpine desert and tundra, Karakoram-West Tibetan Plateau alpine steppe, Gissaro-Alai open woodlands, Paropamisus xeric woodlands, Hindu Kush alpine meadow, Afghan Mountains semi-desert) will see more than 150 days of snow by mid-century under RCP8.5. Model agreement varies in the central and southwestern regions (Paropamisus xeric woodlands, Ghorat-Hazarajat alpine meadow, Afghan Mountains semi-desert), with a greater number of models (between 50 and 75%) agreeing for those grid cells that are closest to the low-elevation areas, and model agreement declining further south and east.

Soil Moisture Drought (1-in-10 Year Event, February)

Threshold: Events 3x More Frequent

E

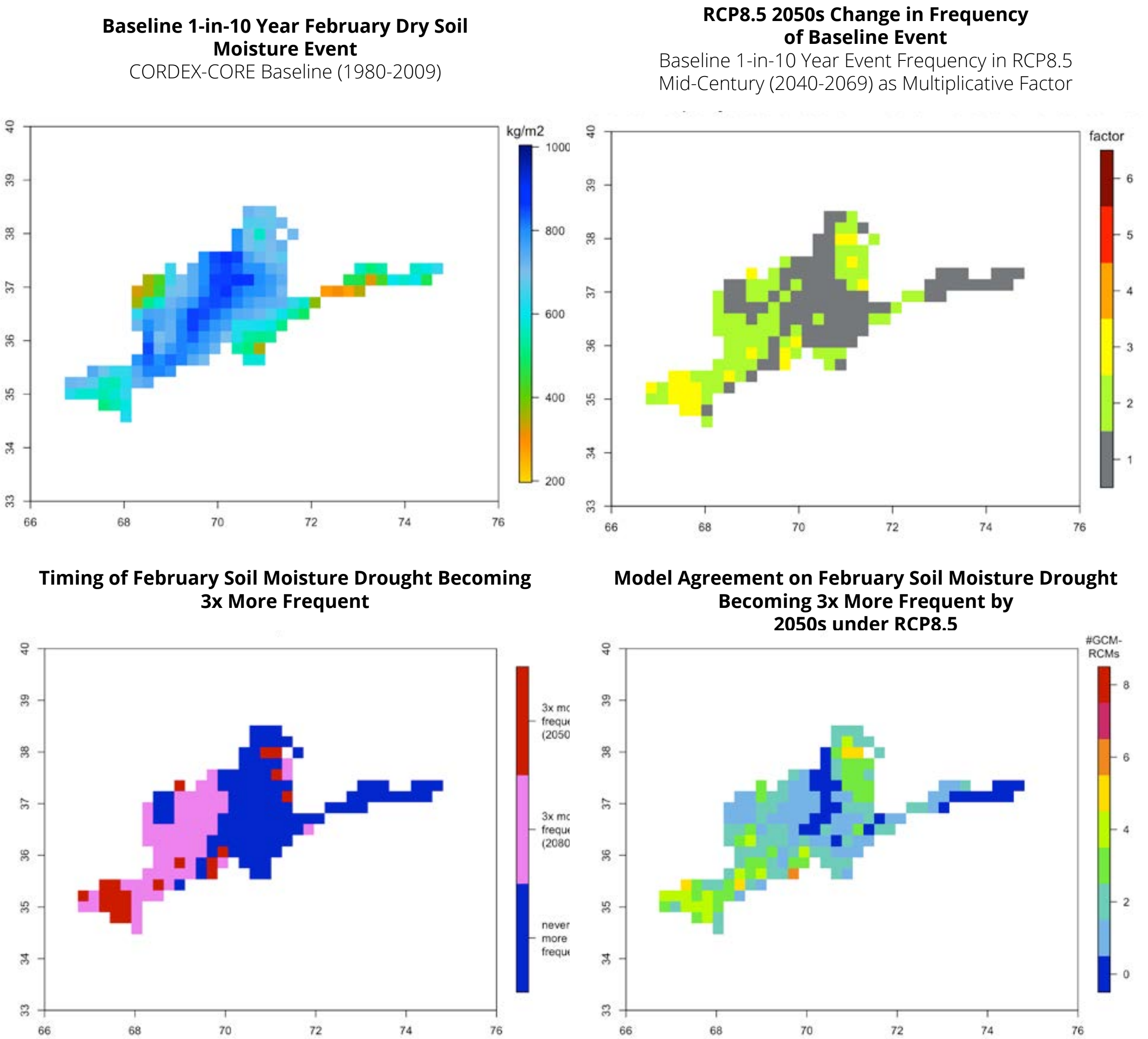

Figure 55. Soil Moisture Drought (1-in-10 Year Event, February).

The soil moisture "1-in-10 year" event is defined for each month in the 30-year baseline as the third-lowest soil moisture value for that month; this value is referred to as the "soil moisture drought" for that month. "1-in-10" soil moisture drought results for February are shown in Figure 55. The ensemble mean baseline soil moisture drought for the month of February—the month directly preceding the wettest period of the year—is presented in the top left panel, showing broadly wetter patterns throughout the center of the P-ARB and drier events in the northwest and eastern areas (Pamir alpine desert and tundra, Karakoram-West Tibetan Plateau alpine steppe, Badghyz and Karabil semi-desert), similar to the overall pattern of precipitation in the region (Figure 6). Rather than a standard change value between baseline and future soil moisture drought events, the frequency of the baseline drought in the future is analyzed by counting the number of times the future soil moisture for February falls below the baseline event in the 30-year future time period and dividing the result by three. The results for RCP8.5 mid-century are shown in the top right panel; a value of one indicates that the baseline drought event occurs at about the same frequency in the future (roughly once every ten years), while values of two and three scattered across the southwestern region and mountainous north (Karakoram-West Tibetan Plateau alpine steppe, Gissaro-Alai open woodlands, Paropamisus xeric woodlands, Ghorat-Hazarajat alpine meadow, Hindu Kush alpine meadow, Afghan Mountains semi-desert, Badghyz and Karabil semi-desert) indicate that the baseline drought event is twice or three times more frequent for this future scenario, respectively. Uncertainty across models limits the level of actionable detail for changing drought frequency in this region, as shown in the bottom right panel.

The bottom left panel shows the emergence of the "three times more frequent" scenario across future time periods. Areas in dark blue show regions where the baseline February soil moisture drought event never becomes three times more frequent in either RCP8.5 future; areas in pink show regions where that baseline event is three times more frequent by the 2080s under RCP8.5; and areas in red show regions where the baseline event is three times more frequent by mid-century under RCP8.5, matching the pattern in the top right panel. Some areas with very low drought events in the baseline, such as the northwestern area (Badghyz and Karabil semi-desert) of the P-ARB or the western side of the Wakhan corridor (Pamir alpine desert and tundra, Karakoram-West Tibetan Plateau alpine steppe), may not become much more frequent in the future due to already-low baseline values. However, mid-range (between 600 and 800 kg/m^2) baseline soil moisture values appear in areas with the potential for large reductions in soil moisture in the future, such as the low-elevation western-central region (Paropamisus xeric woodlands, Ghorat-Hazarajat alpine meadow, Afghan Mountains semi-desert, Badghyz and Karabil semi-desert), and therefore these events often become three times more frequent by the end of the century, if not earlier.

The bottom right panel shows model agreement on the emergence of the "three times more frequent" scenario by RCP8.5 mid-century. Categories are organized by the overall percent of model agreement, with dark blue areas (largely in the highest-elevation zones - Pamir alpine desert and tundra, Karakoram-West Tibetan Plateau alpine steppe, Paropamisus xeric woodlands), showing regions where no models project three times the frequency of the baseline event. For the February soil moisture drought event, although the ensemble mean in the top right panel shows some grid cells with three times the frequency of the baseline drought, there are no regions where more than 75% of models agree with this projection. Most of the P-ARB shows less than 50% of models agreeing that the baseline drought will be three times more frequent, indicating that most agree it will not; only a handful of grid cells show that 50-75% of the GCM-RCM combinations agree on the drought frequency increase by mid-century.

Soil Moisture Drought (1-in-10 Year Event, October)

Threshold: Events 3x More Frequent

E

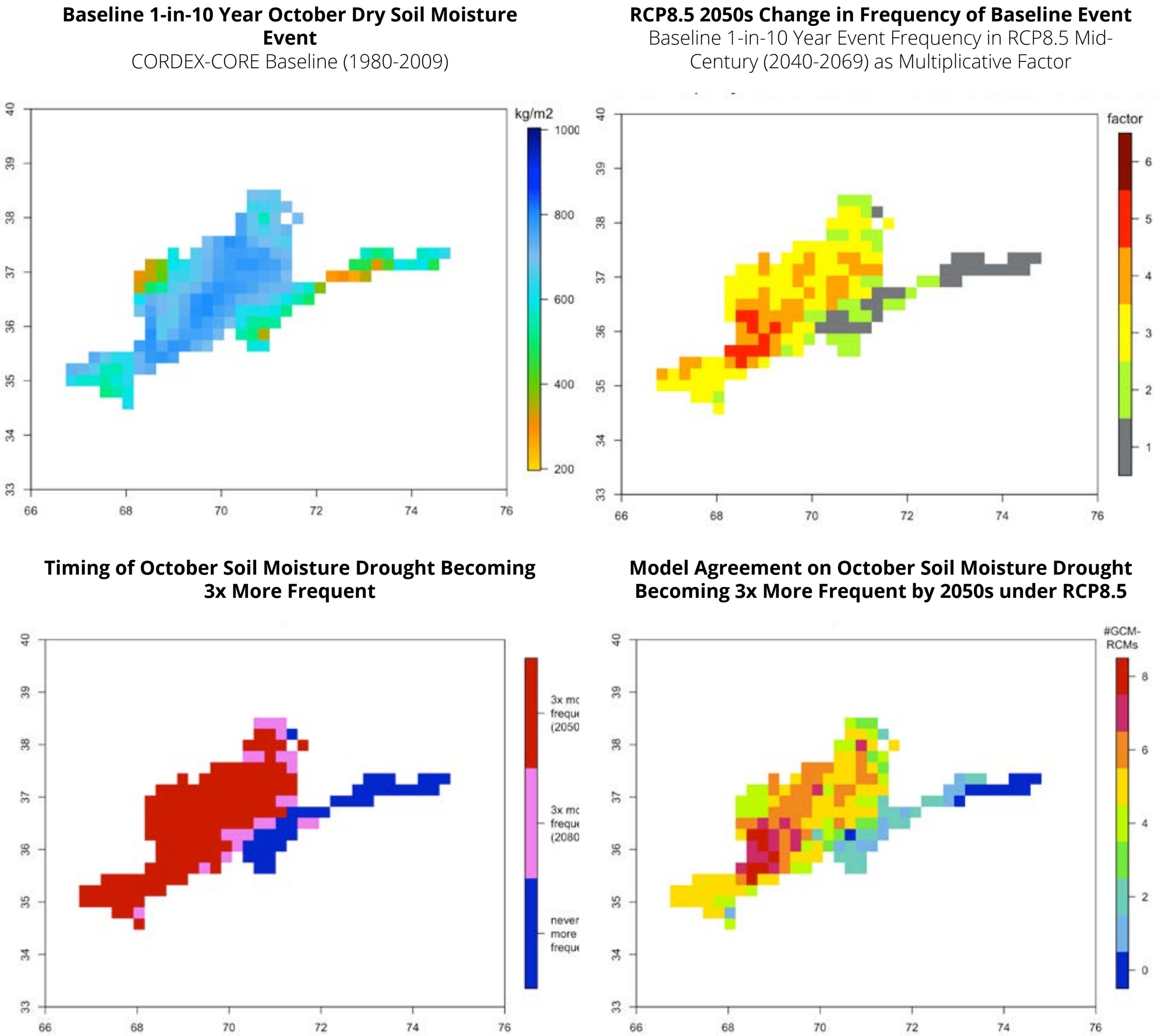

Figure 56. Soil Moisture Drought (1-in-10 Year Event, October).

Vulnerability Assessment

Similar to the previous set of soil moisture "1-in-10 year" event maps, this set of analyses focuses on the month of October—a month after the dry summer season. "1-in-10" soil moisture drought results for October are shown in Figure 56.

The ensemble mean baseline soil moisture drought for the month of October is presented in the top left panel, showing broadly wetter patterns throughout the center of the P-ARB and drier events in the northwest and eastern areas, similar to the overall pattern of precipitation in the region (Figure 6). This is also similar to the February pattern, although somewhat drier than the February soil moisture drought metric. In the analysis on the frequency of the baseline drought in the future, similar to the previous set of maps, this is developed by counting the number of times the future soil moisture for October falls below the baseline event in the 30-year future time period and dividing the result by three. The results for RCP8.5 mid-century are shown in the top right panel; a value of one indicates that the baseline drought event occurs at about the same frequency in the future (roughly once every ten years), which is seen in the high mountain regions in and around Wakhan (Pamir alpine desert and tundra, Karakoram-West Tibetan Plateau alpine steppe). Large parts of the P-ARB see values of two and three, mostly across the northern, central, and southwestern regions (Gissaro-Alai open woodlands, Paropamisus xeric woodlands, Ghorat-Hazarajat alpine meadow, Hindu Kush alpine meadow, Afghan Mountains semi-desert, Badghyz and Karabil semi-desert). Values of 4 and 5 are seen scattered across the central and southwestern regions (Paropamisus xeric woodlands, Ghorat-Hazarajat alpine meadow, Hindu Kush alpine meadow, Afghan Mountains semi-desert, Badghyz and Karabil semi-desert), indicating that the baseline drought event is four or five times more frequent for this future scenario. Uncertainty across models limits the level of actionable detail for changing drought frequency in this region, as shown in the bottom right panel.

The bottom left panel shows the emergence of the "three times more frequent" scenario across time periods. Areas in dark blue show regions where the baseline October soil moisture drought event never becomes three times more frequent in the RCP8.5 future. These areas are seen in the eastern region in and around Wakhan (Pamir alpine desert and tundra, Karakoram-West Tibetan Plateau alpine steppe, Paropamisus xeric woodlands, Hindu Kush alpine meadow). Areas in pink show regions where that baseline event is three times more frequent by the 2080s under RCP8.5, which are seen in a few scattered areas in the northern and southern regions (Gissaro-Alai open woodlands, Paropamisus xeric woodlands, Hindu Kush alpine meadow, Afghan Mountains semi-desert). Areas in red show regions where the baseline event is three times more frequent by mid-century under RCP8.5. Large regions of the P-ARB fall into this category, including the northern, central, and southwestern regions (Gissaro-Alai open woodlands, Paropamisus xeric woodlands, Ghorat-Hazarajat alpine meadow, Hindu Kush alpine meadow, Afghan Mountains semi-desert, Badghyz and Karabil semi-desert). Some areas with very low soil moisture drought in the baseline, such as the western side of the Wakhan corridor (Pamir alpine desert and tundra, Karakoram-West Tibetan Plateau alpine steppe), may not become much more frequent in the future due to already-low baseline values. However, mid-range (between 600 and 800 kg/m^2) baseline drought values appear in areas with the potential for large reductions in soil moisture in the future, such as the low-elevation western-central region (Paropamisus xeric woodlands, Ghorat-Hazarajat alpine meadow, Hindu Kush alpine meadow, Afghan Mountains semi-desert, Badghyz and Karabil semi-desert), and therefore these events often become three times more frequent by mid-century.

The bottom right panel shows model agreement on the emergence of the "three times more frequent" scenario by RCP8.5 mid-century. Similar to above, categories are organized by the overall percent of model agreement, with dark blue areas, largely in the highest-elevation zones (Pamir alpine desert and tundra, Karakoram-West Tibetan Plateau alpine steppe), showing regions where no models project three times the frequency of the baseline event. For the October soil moisture drought event, there are a few grid cells with at least three times the frequency of the baseline drought by this scenario with more than 75% model agreement. These areas are mostly seen in the southwestern and central regions (Paropamisus xeric woodlands, Afghan Mountains semi-desert) with a couple of scattered grid cells in other areas. Most of the P-ARB shows 50-75% of models agreeing that the baseline drought will be at least three times more frequent by mid-century, indicating that most agree on the drought frequency increase.

Avalanches

E

Key findings and outputs

- Avalanches annually cover 1.23% of the Panj-Amu River Basin (mean over 30 years)
- 604 villages are vulnerable to avalanches
- 5.47% of the road network is exposed to avalanches
- The 10 most vulnerable districts include Shighnan, Ishkashim, Darwaz, Kuran Wa Munjan, Khwahan, Kuran Wa Munjan, Fayzabad, Ragh, Jurm, and Shibar
- The number of avalanches per year did not significantly increase during the last 30 years

Indicator overview

Afghanistan is one of the most mountainous countries in the world, with half of its land above 2000 m (Asad Sarwar 2002), which creates a high level of risk for avalanches. In Central Asia, Afghanistan, especially the mountainous terrain of the Panj-Amu River Basin, contains a population at high risk of avalanches from December to March (Chabot and Kaba 2016, Mohanty et al. 2019). However, the location, frequency, and size of avalanches are key information that are not well known. The objective of this analysis was to assess the frequency of avalanches and how they affect local communities and infrastructure (roads and road travellers) to better characterize vulnerability at more local scales.

Because the P-ARB is very large and an analysis of the frequency of avalanches requires historical data, satellite images and remote sensing techniques have been used to address the objectives. Landsat satellite data offer an archive of 30 years of imagery. The use of remotely sensed data is still not widespread for avalanche monitoring, although recent studies tend to use automated detection methods (Bühler 2012, Eckerstorfer et al. 2019). Here, Google Earth Engine was used to first calculate the Normalized Difference Snow Index (NDSI) from open-access Landsat satellite images. Next, a temporal approach was used to automate the identification of avalanches during the last 30 years.

Methods overview

Google Earth Engine was used to create annual maps of avalanches in the P-ARB from 1990 to 2021. The core idea of the algorithm is to select a period of time within a year that only shows the avalanche coverage. This method does not distinguish between wet and dry avalanches, but targets all snow packages that remain riverbanks and valley bottoms for a few weeks after the end of winter. Indeed, snow packages of avalanches are distinct after the proximate, less compacted snow cover has melted. To identify those late snow packages, the NDSI is computed on each image from May up to July every year. Different date ranges were chosen depending on elevation to accommodate slightly different periods of snowfall and snow persistence at different elevations. Snow cover around avalanches persists longer at higher elevations than at low elevations. A reclassification of NDSI was used to distinguish among bare soil, water bodies, and snow cover (Table 5). The workflow used in this analysis is outlined in Figure 57.

Once the avalanche dataset was assembled, the number of avalanches, classified per unit area (30 m resolution), was counted within villages and road rights-of-way. Avalanches were also enumerated per sub catchment to highlight the most vulnerable areas.

Table 5. Range values to distinguish snow cover, bare soil, and water bodies.

Coverage	NDSI values
Bare soil	-1 to -0.05
Water bodies	-0.051 to 0.30
Snow cover	0.31 to 1

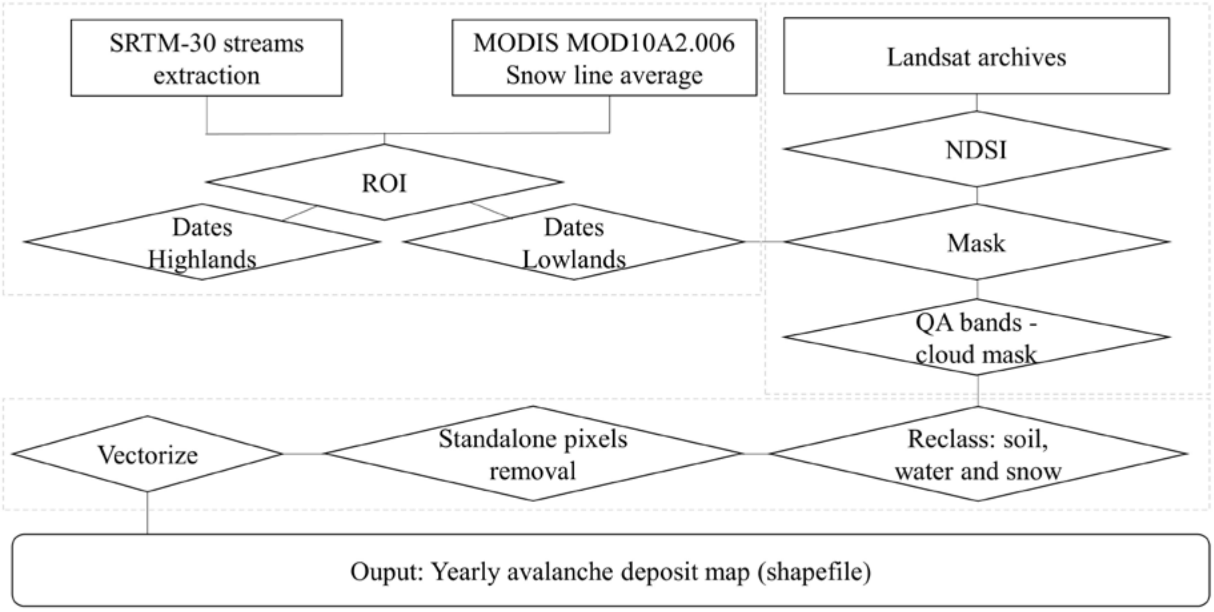

Figure 57. Workflow of avalanche identification using NDSI in Google Earth Engine.

The identification of avalanches was validated by verifying the locations of the avalanches extracted from Google Earth Engine against the GPS locations of known avalanches collected in the field. In late winter of 2021, six GPS were collected along the border of the Panj River where there were significant avalanches (Figure 58). All six had temporary blocked the road. The six avalanches that were visible in the field were also correctly identified through the analysis. The identified avalanches were represented by a few pixels, while in the field, their areas were larger. However, this gives confidence that the approach can reasonably determine the location of avalanches and their importance through an assessment of the number of pixels identified as having avalanches. In addition, it is possible that the approach used identifies avalanches in locations where none actually occurred. This could be due to remaining snow cover or, in some cases, confusion with some water bodies, such as very large flood areas or lakes. However, the avalanches identified remain reliable and depict both their locations and the frequency of avalanches in a given area. Further validation with more GPS points is needed to provide a more comprehensive validation, but the results of the model are encouraging it provides significant information about vulnerable areas from avalanches.

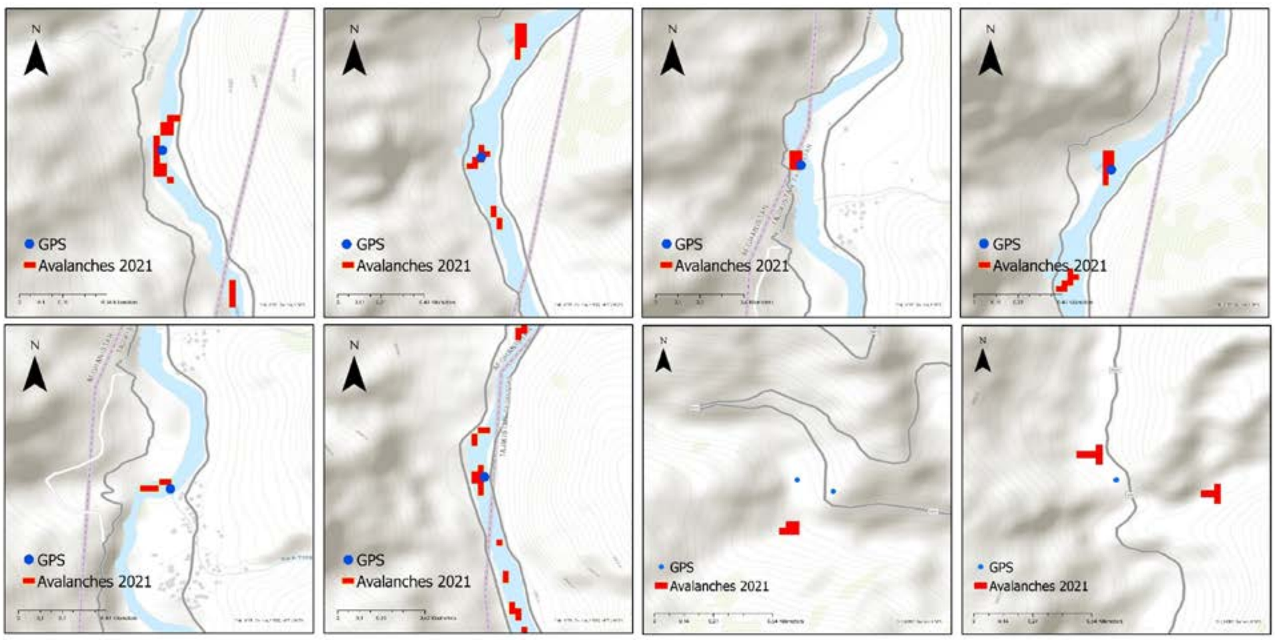

Figure 58. Examples of avalanche validations along the Panj River in winter 2021.

Spatial representation of indicator

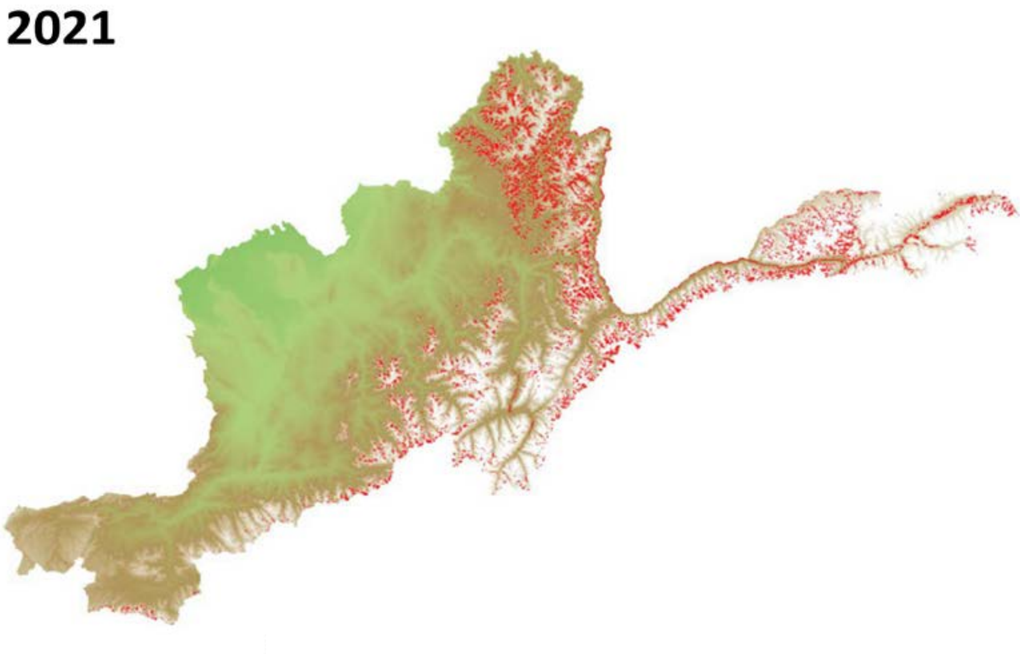

Figure 59. The spatial distribution of snow avalanches (red) in the P-ARB in 2021.

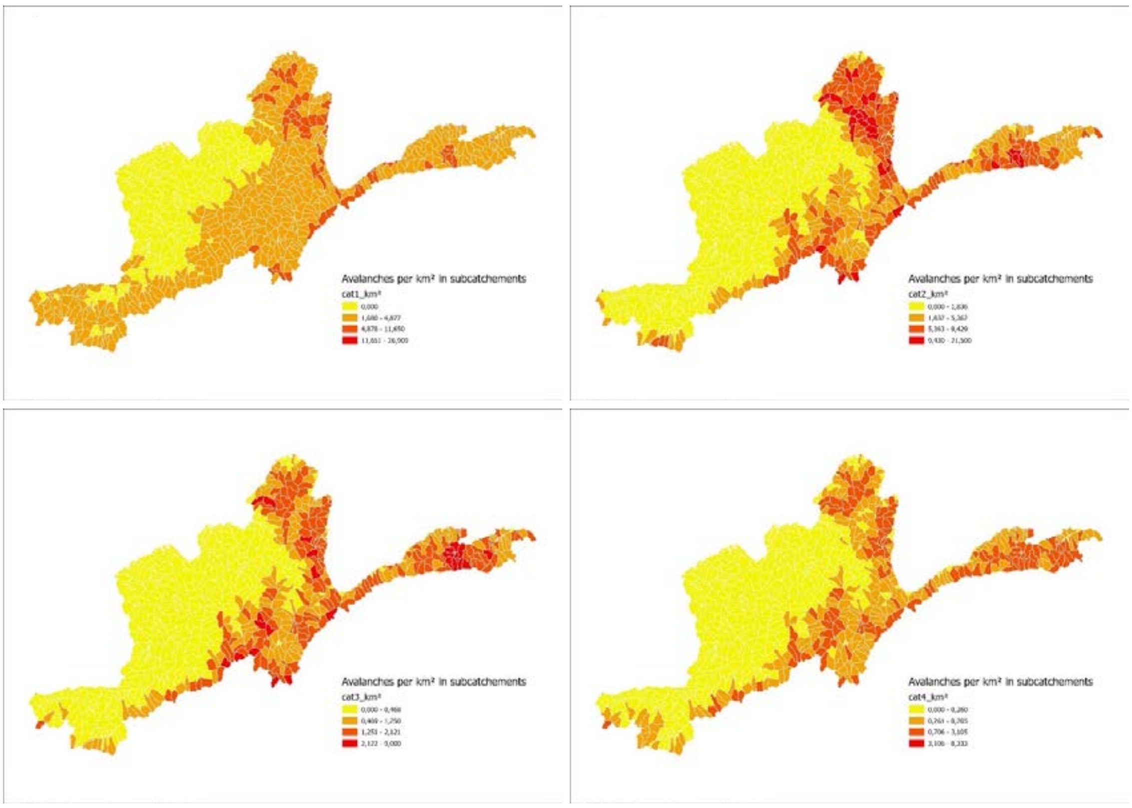

Figure 60. Total avalanches per square km per sub-catchments over the past 30 years by category.

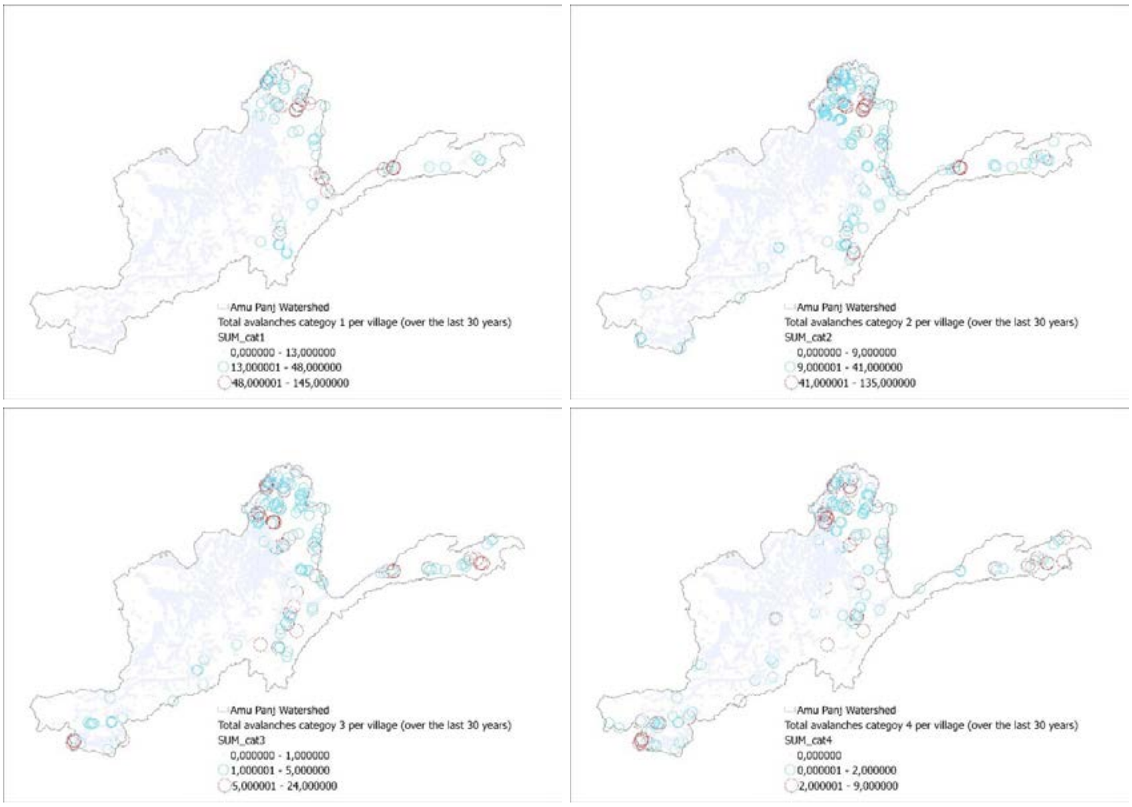

Figure 61. Total avalanches per village over the past 30 years by category.

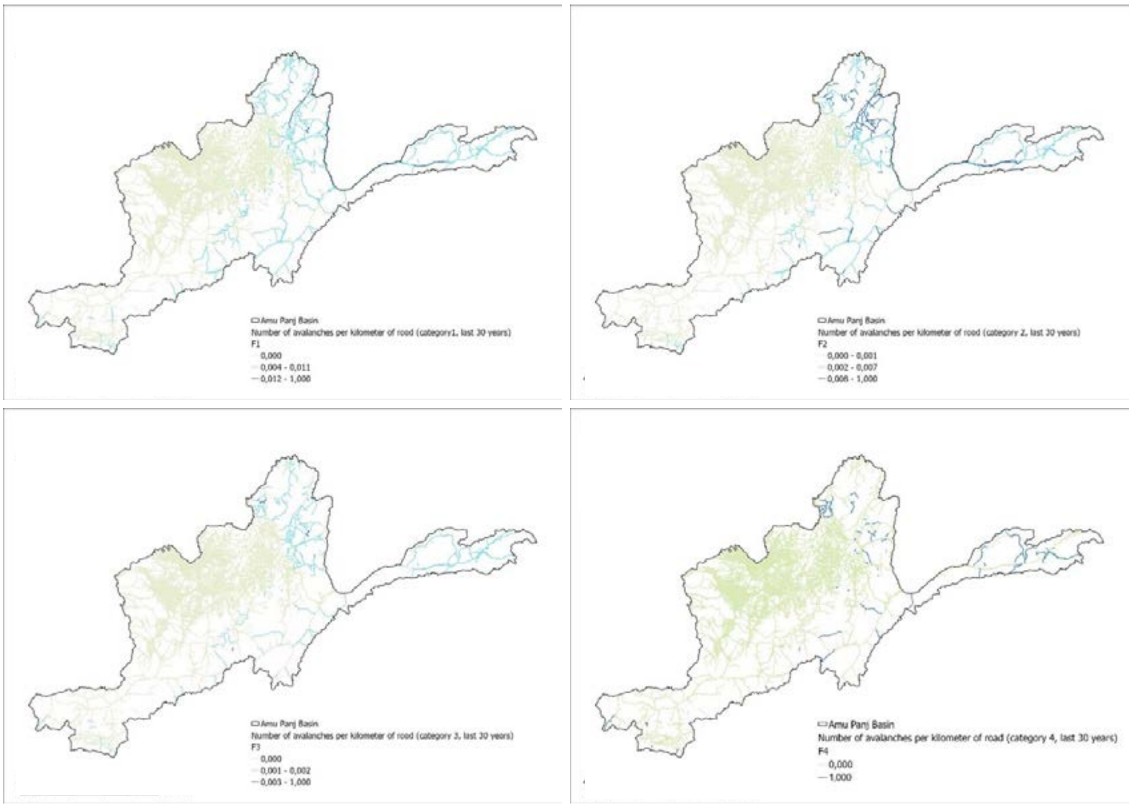

Figure 62. Total avalanches per km of road over the past 30 years by category.

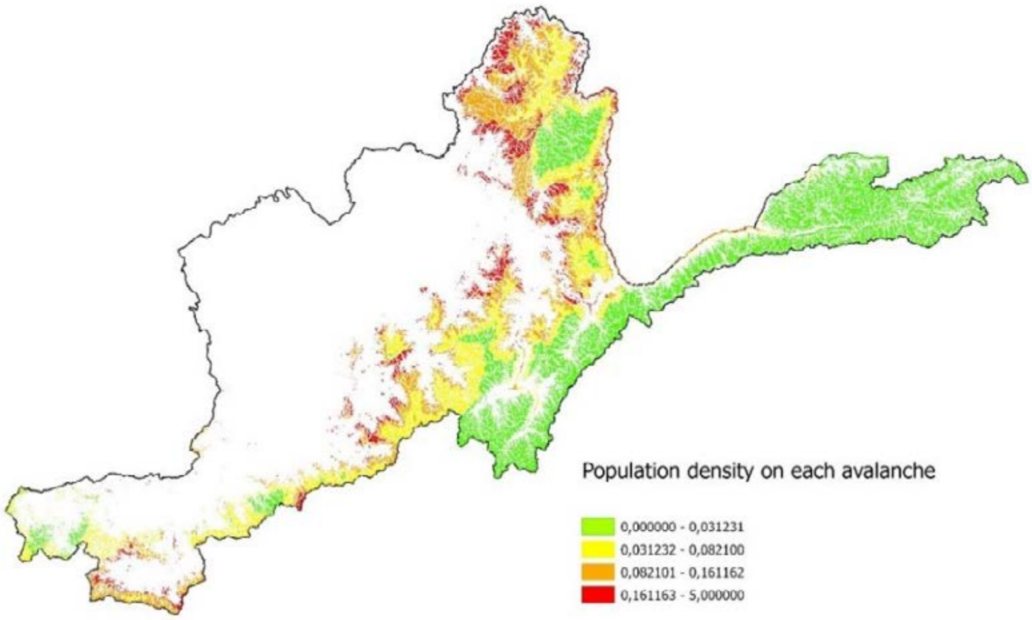

Figure 63. Population density (people/km^2) within regions of avalanches in the P-ARB (population density data from WorldPop, https://www.worldpop.org).

Results

In total, the P-ARB has been impacted by a total of 810,000 snow avalanches in the past 30 years (an example for 2021 is shown in Figure 59), covering an average area of 1.23% of the P-ARB every year. Avalanche events varied in size; some avalanches occupied larger areas than others, and there was considerable variability in their spatial distribution. Four avalanche size classes were detected in the past 30 years: small (< 1000 m^2), medium (1000-5000 m^2), large (5000-15,000 m^2), and very large (15,000-100,000 m^2) (Figure 64). The smaller avalanches are likely to have less impact than larger ones; however, small snow packages (<1000 m^2) can still block a road for several days or destroy settlements (e.g., Figure 65). Altogether, these avalanches occurred at an average elevation of 3820 m asl; the lowest occurred at 1755 m where villages and infrastructure are present.

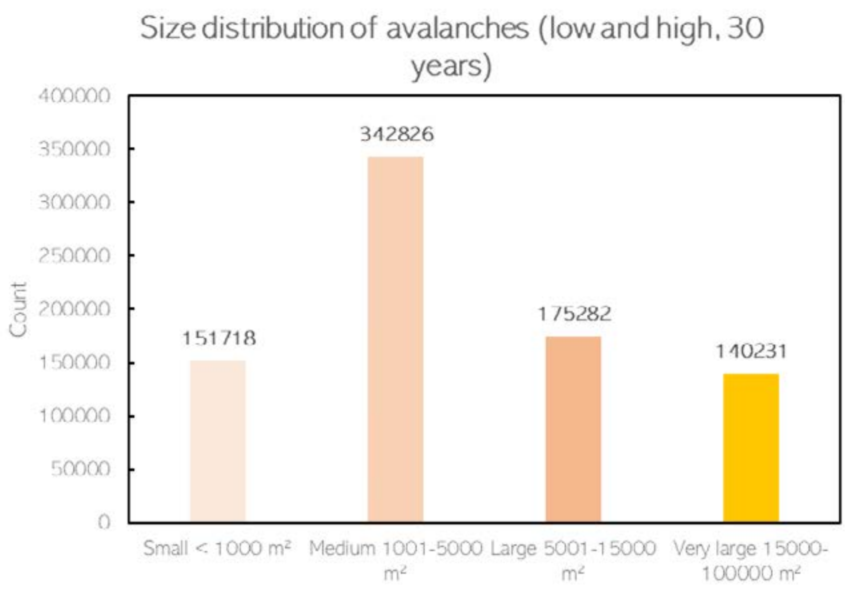

Figure 64. Size distribution of avalanches during the past 30 years in the P-ARB.

Figure 65. An excavator clearing the road after an avalanche in Badakhshan, April 2021.

There was no significant trend in the number of snow avalanches over time during the past 30 years (Figure 66). Every year, between 1-2% of the P-ARB is covered by avalanches. In 2003, the avalanche cover was much higher, almost 6%, and the average elevation of avalanche occurrence was much lower due to high snowfall.

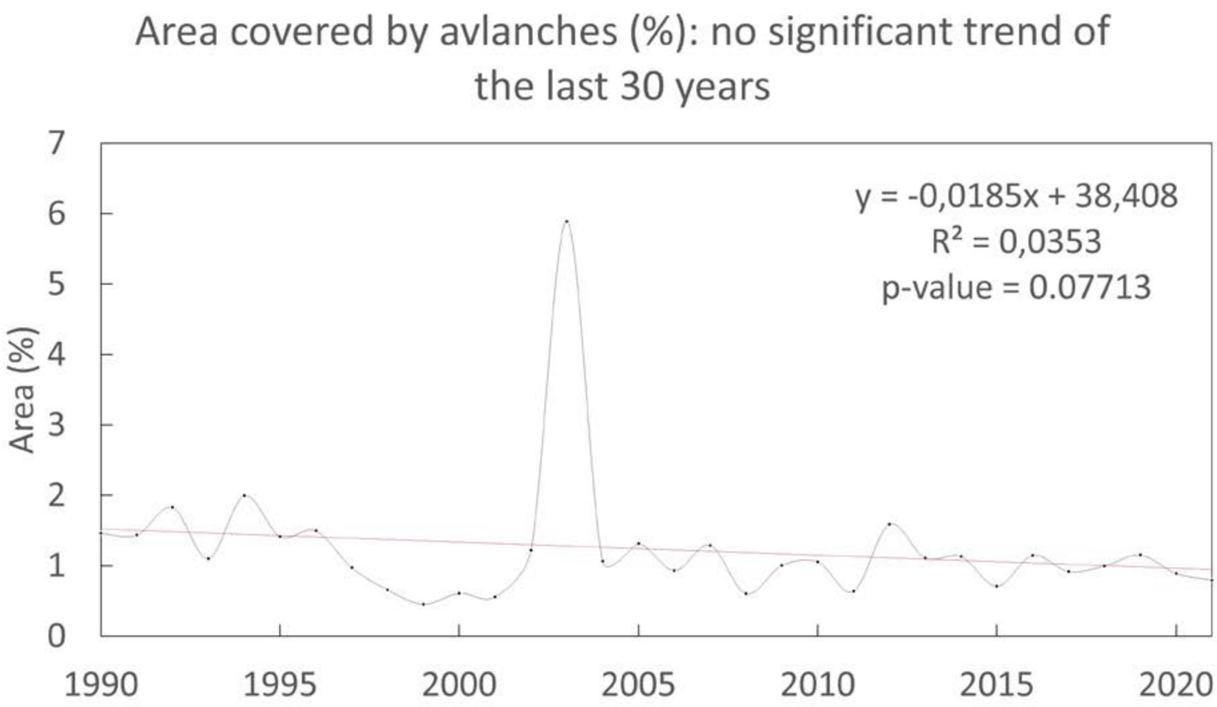

Figure 66. Time series of avalanche area as percent. There was no significant trend during the past 30 years.

Nevertheless, the absence of a trend in avalanche occurrence does not negate the impact of repeated avalanches nearly every year at the same locations. Annual frequency maps show cumulative avalanche events over the past 30 years at each pixel location. Throughout the P-ARB, at the pixel level, the mean frequency is 0.08 avalanches per year. However, some areas recorded higher frequencies, with a maximum value of one avalanche per year at the same location. The full information of village-level avalanches is given in Appendix 3 and each village has been individually mapped at 1:25000 scale as in Figure 67 (figures for all 604 villages available on request).

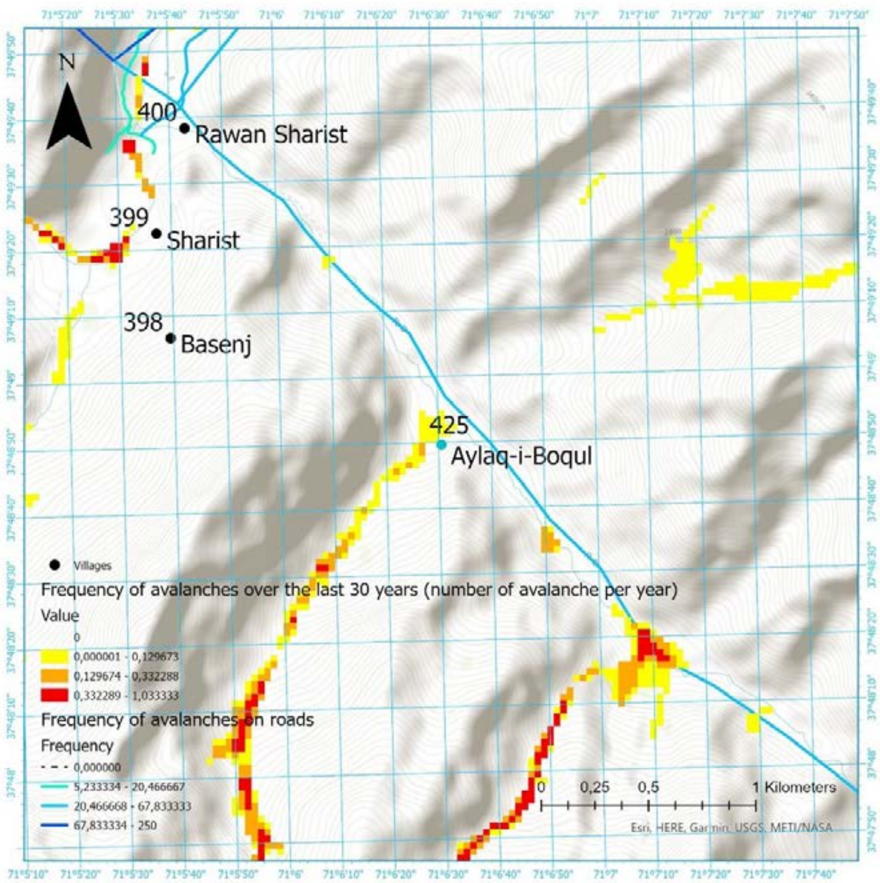

Figure 67. Example map of avalanche frequencies in Aylaq-i-Boqul, Shighnan district.

Data were also summarized and mapped by sub-catchment (Figure 60), for all villages (Figure 61), along the road network (Figure 62), and against population density (Figure 63) based on the size and the total number of avalanches.

Sub-catchments

The steep mountainous catchments are those most exposed to avalanches, especially at high elevations of Badakhshan in the north and in the Wakhan corridor in the east (Figure 60). Those locations are considerably more vulnerable than in the lowlands. Overall, 10 basins were impacted by more than one avalanche per square km every year and the mean frequency was 0.26 avalanches/km² in those sub-catchments. Most of those avalanches were category 1 and 2 (small and medium), but the highest sub-catchments in Wakhan and high Badakhshan were affected by category 4 (very large) avalanches, which represents a higher risk of destruction and casualties for local and remote communities that are far from rescue possibilities. Indeed, the results show that the most remote areas are often the most vulnerable in terms of avalanches.

Villages

In total, 604 out of 4154 villages have been impacted by at least one avalanche per year. As indicated above, villages in Wakhan and high Badakhshan are most vulnerable (Figure 61). Farmlands, households, roads, and other essential forms of infrastructure are exposed to these hazards. Villages in lower and flatter lands are less exposed, and many are not impacted by snow avalanches. The 10 most impacted villages during the past 30 years were Rabati, Yarkh, Gharan, Deh Chowid, Mina Do (2), Aylaq-i-Situn, Welo, Madud and Bughaz. Overall, 50 villages were impacted by more than 2 avalanches per year within a 1 km radius, mostly by category 2 avalanches. The mean snow avalanche frequency for all villages was 0.08 per year. Ninety-two villages, namely in remote mountainous areas, were affected by category 4 avalanches, with larger impacts on infrastructure. Full details of avalanche impacts on villages are given in Appendix 3.

Roads

More than 2000 roads, 5.47% of the total road network, were exposed to avalanches over the past 30 years. Once again, roads of Wakhan and high Badakhshan were most impacted by avalanches. The roads in dark blue on the maps in Figure 62 are the most vulnerable and particular attention is needed on those roads in winter and spring. Multiple avalanches could disconnect remote villages for several days on those roads shown in red. The road exposure map, combined with the avalanche frequency map, indicates target priority areas for protection measures against avalanches and is of high relevance to stakeholders. Based on these data, it is possible to determine which road sections are exposed to at least one avalanche per year. In areas of very high risk, almost 400 roads experienced more than 2 avalanches per year per kilometre (within a 1 km buffer) and the mean frequency was 0.86 per kilometre and per year. Most of the avalanches that occurred on those roads were category 2, though a few of them were category 4, which require extensive snow clearing to reconnect remote villages.

Population

Overall, despite a greater number of villages and roads affected by avalanches in the Wakhan corridor, the Wakhan region is the least vulnerable based on population density and avalanche occurrence because 70% of avalanches occur in very low population density areas (Figure 63). Indeed, Wakhan is a remote area with a very sparse population. However, this map should not minimize the complex situation of avalanches occurring in Wakhan. Despite the low population density, the remoteness of Wakhan communities present special concerns related to road clearing and rescue interventions when avalanches occur, which is relatively frequently. Nevertheless, at lower elevations (around 2000 m), where human population density is higher, the impact of avalanches is greater. In these lower areas, particular attention must be paid to roads, villages, infrastructure, and associated planning by community and government stakeholders. Still, avalanches in these regions are relatively rare; only 0.77% of the avalanches that occurred in the past 30 years were located in these areas with high population density. This implies that local communities may have already adapted their settlements and planning to the prevalence of avalanche hazards, at least to some extent.

Conclusions and Recommendations

Mapping the frequency of avalanches was possible using remote sensing archive products, namely Landsat 5, 7, and 8. Automation of snow extraction with using Google Earth Engine allows an assessment of avalanches across the entire P-ARB. This approach enables identifying the locations, size, and frequency of avalanches, which can be used to evaluate the vulnerability of local communities and infrastructure.

Based on the results of the avalanche mapping using the NDSI approach in Google Earth Engine, the following recommendations can be made to policy makers:

- The most remote villages are most vulnerable to avalanches: particular attention must be paid to those villages (cf list in Appendix 3). If these villages are not already equipped, one excavator should be available for each village (or shared between villages) to clear snow from the road in case of blocking.
- Data collected herein provides significant information about road exposure to avalanches. Based on avalanche frequency, location, and size, policymakers can target which roads are high priority for investment in avalanche protection and control. Information on the importance of each road for regular transportation could also help identify the most important roads for intervention. The map showing avalanche exposure along roads (Figure 62) provides support for such amelioration and prevention activities.

- The map of avalanches along roads can also be used as a winter itinerary advisor tool, by warning road users of the level of risk along the most vulnerable roads.
- The avalanche frequency map can be used to support village planning. Stakeholders must avoid construction in areas highly exposed to avalanches next to villages.
- It is strongly recommended that maps and results presented here are widely distributed to local stakeholders and, as far as possible, to local communities so that they can make better decisions related to snow avalanche occurrence and threats at a local level.
- Continuous collection and assessment of satellite images will enable uninterrupted monitoring of avalanches in the future using this NDSI approach. These models must be regularly validated against avalanche locations recorded from the ground using GPS. It is therefore recommended that policy makers ensure that both monitoring activities continue.

Community-led approaches to resilience-building can help Afghan people better prepare for and recover from natural hazards and other challenges, improving their overall well-being and quality of life.

Landslides

E

Indicator overview

Residents of the P-ARB region are exposed to many natural hazards, such as floods, earthquakes, landslides, snow avalanches, and extreme seasonal temperatures. Landslides represent 3.6% of all natural hazards, and 16.8% of the casualties triggered by natural hazards. Some landslides can evolve with time, impacting only infrastructure over months or years, but other landslides – rapid mass movements – can occur much more suddenly in response to individual rainfall or snowmelt events, resulting in massive destruction. This trend extends globally, but especially in developing countries, landslides pose the greatest risk due to a lack of research and development of mitigation efforts for such landslide (Sidle and Ochiai 2006).

Landslides have an important impact on regional agricultural production, food security, economic activity, and other socioeconomic aspects. Livelihoods and natural resources need to be addressed and reestablished as soon as possible after landslide occurrence, especially in remote mountainous areas. More importantly, landslides can inflict fatalities. Other impacts include damages to roads and blockages of streams (i.e., landslide dams) that can later fail and release huge floodwaters downstream. Landslides have a devastating effect on farmers' livelihoods as they can prevent access to land for years, alter productivity, destroy agricultural lands and food stocks, and result in the loss of livestock and crops. Also, where food scarcity exists, the health and stability of women and children are at special risk.

Therefore, a basic analysis of landslide risk is needed to assess the socioeconomic factors of villages at risk. Similarly, the development and testing of the methods for assessing the impact and influence of landslides on livelihoods in the region are extremely important tasks. Here, our objective was to map the areas at risk of landslides in the P-ARB to estimate the vulnerability of communities to this natural hazard.

Methods overview

In this assessment, we considered several approaches to identify landslides in this remote study region. After trying various methods, we focused on assessing the level of vulnerability of communities in a parsimonious manner by randomly selecting 105 representative villages in four ranges of slope gradient (0-14; 15-25; 25-34 and 35-100 degrees) (Figure 68). All of these villages are located in the category "Area at High Landslides Risk" based on the global Landslide Hazard Assessment for Situational Awareness (LHASA) (Kirschbaum et al. 2020). This susceptibility map has been developed to provide an indication of the time and location of potential landslides. The model combines near-real-time precipitation data with a global landslide susceptibility map as well as overlapping with Global Landslide Catalog (GLC) that was developed with the goal of identifying shallow rainfall-triggered landslide events around the world, regardless of size, impact, or location. The result of the LHASA is a raster with values ranging from 1 to 5, where the 1 is the minimum risk of landslides and 5 is the maximum risk. Therefore, villages were selected relevant to the value of 5. To determine the areas at risk proximate to the 105 villages, a 1 km buffer was applied around each village. This distance was defined as the maximum influence on settlement livelihoods due to landslides travelling short distances (i.e., 200-300 m). Accordingly, the vulnerability to landslides outside of this buffer area is low and is ignored in our assessment.

The buffers were converted to KML format to use in the Google Earth application (GE archived historical imagery), enabling users to access older imagery. Moreover, GE provides a series of other tools including an editor and a measure distance tool. Landslides were manually digitized within those buffers to determine the density of landslides within specific communities. Long shapes of debris and contrasting colors were used to visually detect the landslides.

The assessed landslides were classified as fast and slow. Gravity is a constant force on soils that move downhill as part of the erosion process. Depending on the type of soil, this movement can be fast or slow. Slow mass movements (slow landslide) can often be anticipated and managed to some extent or at least adapted to. If these slow landslides are deep, their effects can be devastating. This type of landslide usually appears as a wide mass movement with a rather smooth scarp and with minor damage to vegetation on GE satellite images. In contrast, rapid landslides result in most of the shallow soil mantle on the hillslope being stripped off and depositing the area at the bottom of the slope. Prevention of such translational landslides, including subsequent cleanup, can be significant. This type of landslide usually appears as a small mass movement with sharp scarps and with significant damage to vegetation on GE satellite images. Using QGIS software, slope gradients and aspects of the digitized landslides were calculated.

Spatial representation of indicator

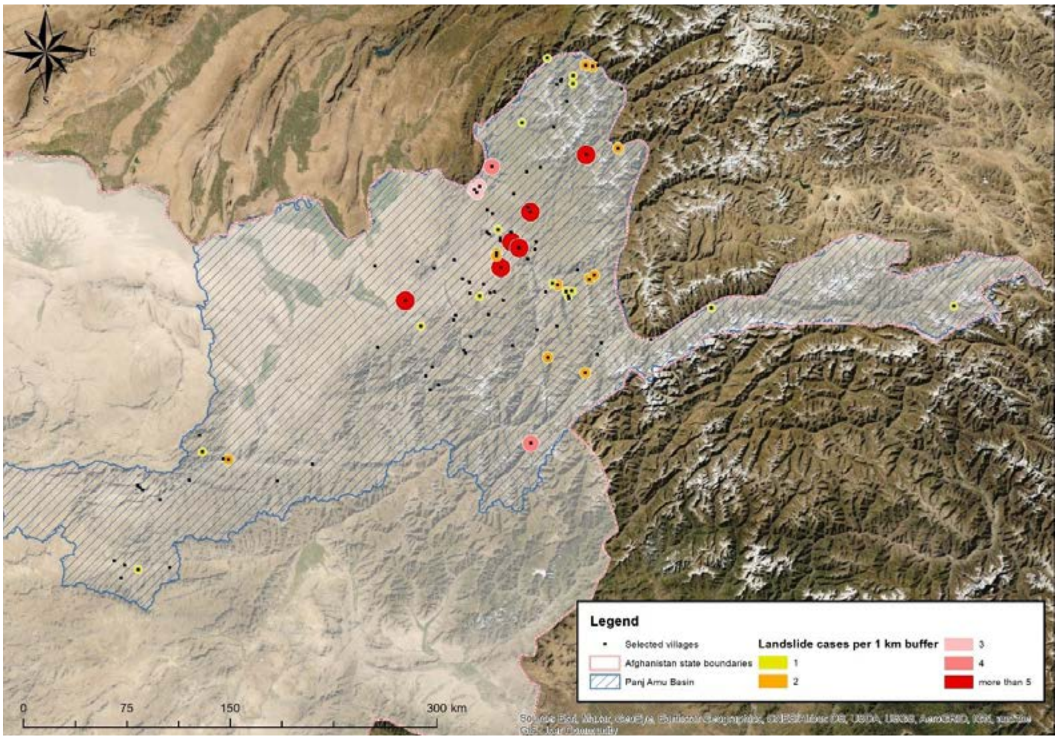

Figure 68. Villages at risk and affected by landslides in the study region.

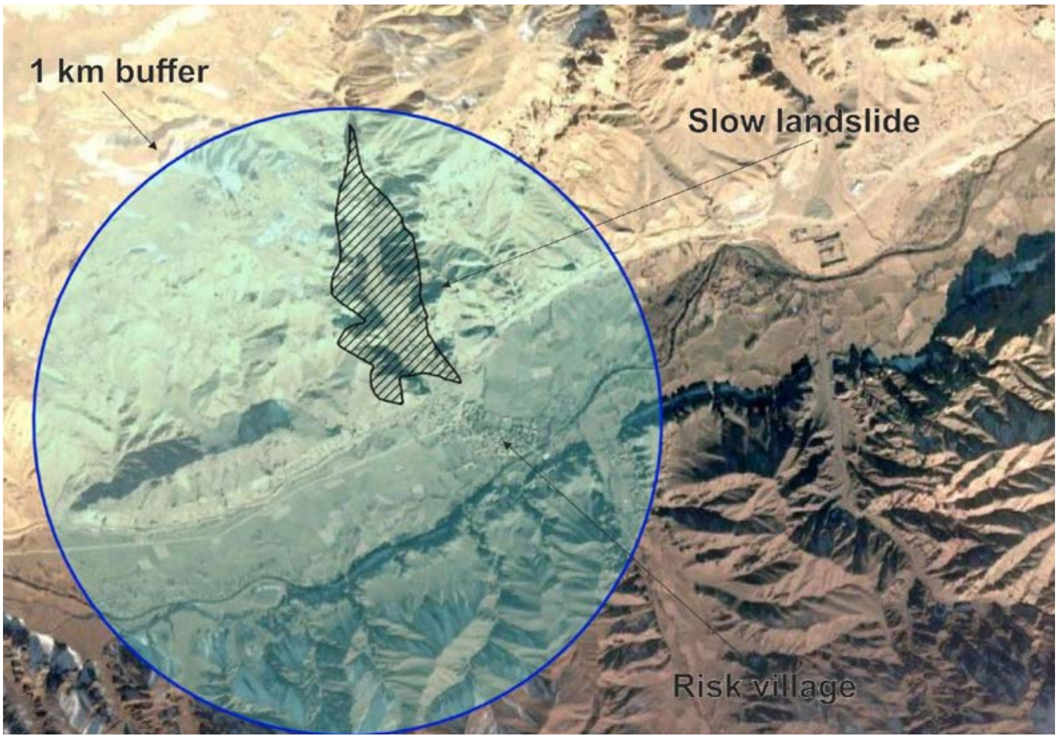

Figure 69. Slow landslide determination in one example village and showing the buffer distance considered.

Results

After a detailed visual assessment of the study area landscape within the buffers, 35% of the surveyed villages were assessed to be at high risk of landslides due to their proximity. Both single and multiple landslide events impacted these areas. A total of 122 landslides were detected in the selected study areas. It should be noted that all detected cases of landslides occurred at higher elevations (i.e., above settlements) and, thus, represent a real danger to these villages (Figure 69).

Slow landslides were three times more frequent than fast ones at the investigation sites. All landslide events occurred on hillslopes with gradients in the range from 12 to 43 degrees. In 33% of the cases, slow landslides occurred on slopes with a southern aspect. On slopes with eastern and western aspects, slow landslides occurred in 27% of cases; for northern aspects, slow landslides occurred in 13% of the cases. Rapid landslides showed a different pattern: 40% occurred in northern aspects, 32% in western aspects, and in 14% of the cases, these rapid landslides occurred on both eastern and southern aspects.

Conclusions and Recommendations

Landslides are frequent in the P-ARB. Almost one out of every three mountain settlements in the study area have been exposed to and have experienced landslides, both fast and slow, and every mountain village has the risk of facing this type of disaster (Figure 68). Landslides occur over a wide range of slope gradients, and to varying degrees in every aspect of the hillsides. Landslides are triggered either by individual rainfall or snowmelt events, which cause rapid and typically shallow landslides. Slow, deep-seated landslides typically are triggered by an accumulation of soil moisture during sequences of rainfall events or long-term snowmelt landslides (Sidle and Ochiai 2006, Sidle and Bogaard 2016).

Regular monitoring of landslides is an important task to understand the processes and occurrences that facilitate the prediction of landslides and debris flows. This can substantially reduce the threats to villages at risk. Unfortunately, none of the empirical approaches, hazard mapping practices, or even physical-based models for landslide/debris flow prediction are completely effective in all areas due to the complexity of interrelated factors that affect landslide initiation (Sidle and Bogaard 2016). This is particularly true in such remote areas with poor data. Nevertheless, conducting research on landslide hazards in specific vulnerable regions provides improved insights into their spatial and temporal occurrence, as well as the impact on the daily lives of people.

It should be noted that additional villages that were not selected for analysis could still have high risk to landslides, and these should be adequately assessed in future studies. Furthermore, it remains unclear whether historical risk to landslides is a useful predictor of future risks to landslides, though it is reasonable to assume that regions currently under high risk will remain that way in the feature.

The Panj-Amu River Basin's cryosphere is undergoing rapid changes that affect the livelihoods of millions of people. The melting of glaciers, snow and permafrost change the water distribution of water, as well as the geomorphology of the basin, with implications for water availability, food security, disaster risk and human health.

Rising temperatures are causing rapid ice melt in the Panj-Amu River Basin, leading to a range of environmental, economic, and social challenges.

Policy and Management Recommendations

Observations and projections of climate in the P-ARB can be linked to forecast natural hazards. Such forecasts show changes in areas currently experiencing permafrost, alterations to growing season length, increases in the number of extreme heat and extreme precipitation days, reductions in the snow water equivalent, and increases in the number of rare dry soil moisture drought events. These will have potentially significant consequences for ecosystems, biodiversity, and human well-being.

The results from the analysis of natural hazards vulnerability point to several key recommendations for policy and management to mitigate consequences for ecosystems, biodiversity, and local communities and increase their resilience under climate change. Many such recommendations parallel those needed to address overall climate vulnerability. These recommendations can be grouped into six domains:

1. Invest in nature-based solutions to joint climate mitigation-adaptation

- Maintain intact ecosystems to help buffer climate impacts
- Slow rates of degradation to bolster livelihood provisioning under ecosystem stress
- Recover areas identified as degraded to increase adaptation potential

2. Identify at-risk ecosystems and communities

- Determine where ecosystems and communities are most vulnerable, and to which natural hazard(s)
- Conduct spatial planning that considers climate impacts and forecasted natural hazard assessments

3. Build and strengthen infrastructure to proactively combat natural hazard impacts

- Identify where roads, bridges, and other infrastructure may be needed or strengthened to withstand future impacts
- Plant trees that combat soil erosion to limit landslides and debris flows
- Consider nature-based solutions to flood mitigation
- Anticipate risks to and opportunities for agriculture to adapt planted food crops accordingly

4. Educate the public about climate change and climate change impacts

- Develop community education programs suitable for all ages
- Target education campaigns to vulnerable communities and focus on anticipated risks
- Create courses and modules at the university level, including opportunities for research in natural hazard modeling and assessments
- Create jobs that utilize education and training for climate adaptation

5. Establish a system for long-term climate monitoring

- Ensure monitoring system uses both field-based and remote-sensing approaches
- Develop a glacier monitoring system
- Deploy weather stations across a representative sample of all terrestrial ecosystems at different elevations to monitor local climate changes and conditions
- Deploy Hydromet stations within a representative sample of rivers in all sub catchments
- Establish regular monitoring of all terrestrial ecosystems, including rangelands, forests, and riparian vegetation to link climate change to changes in ecosystems
- Develop a system to monitor carbon emissions from activities across sectors

6. Create a natural hazard warning system

- Conduct real-time/near real-time analyses of natural hazards, such as floods, droughts, landslides, and avalanches
- Develop a system to announce emergency warnings to local communities via mobile communications

Ecosystem Vulnerability

2.3 Ecosystem Vulnerability

Overview

Healthy ecosystems support biodiversity by providing habitat and food resources, and local communities by providing essential services such as water regulation, food production, pollination, carbon storage, natural resources, and livelihoods. Globally, rangelands—defined as the land on which potential native vegetation is predominantly grasses, grass-like plants, forbs, or shrubs (Kauffman and Pyke 2001)—support billions of people yet are being lost and degraded at alarming rates. Within global rangelands, nearly 50% of grasslands have been degraded to some extent, and this issue is particularly extensive throughout Central Asia and Afghanistan (Bardgett et al. 2021). Primary drivers of ecosystem loss and degradation in Afghanistan include conversion to rainfed agriculture, overgrazing by livestock, harvesting of shrubs, development of new road networks, and reduced rainfall and drought. Climate change is poised to exacerbate these latter drivers leading to reductions in the condition and extent of ecosystems, with consequences for people and biodiversity. The close links between ecosystem health and human well-being in Afghanistan necessitate a detailed assessment of historical trends in ecosystem condition, current ecosystem status, and projections of ecosystem persistence.

We evaluated several indicators related to ecosystem exposure, determining how indicators related to the size and condition of ecosystems have changed over time, as well as the stability of ecosystem distributions under climate change. We assessed ecosystem size using a 29-year time series of natural land cover extents to determine where natural land cover types are being lost and replaced by non-natural land cover types. Such losses represent reductions in habitat for wildlife species and potential livelihood sources for people. Our results show that while much of the P-ARB has retained natural land cover, large areas of the northwest and along river valleys have been converted to different forms of agriculture. The Afghan Mountains semi-desert, Badghyz and Karabil semi-desert, and Paropamisus xeric woodlands ecoregions had the highest decreases in natural land cover between 1992-2020, representing high vulnerability.

We assessed ecosystem condition by mapping ecosystem and rangeland degradation in multiple ways. First, by using a 36-year time series of vegetation dynamics inferred from changes in the normalized difference vegetation index (NDVI), and second using a 21-year time series of rangeland changes following three distinct pathways (green vegetation loss, dry vegetation loss, and desiccation, the drying of green plant matter) using spectral mixture analysis with field validation. Both the NDVI and spectral mixture analysis results showed large areas of degradation occurring in the northwestern portion of the P-ARB, with some evidence of greening or rehabilitation occurring in the southwest and eastern portions of the landscape. The Badghyz and Karabil semi-desert and Paropamisus xeric woodlands ecoregions both showed decreasing NDVI and rangeland condition trends; the Hindu Kush alpine meadow ecoregion showed a decreasing NDVI trend; and the Karakorum-West Tibetan Plateau alpine steppe ecoregion showed a decreasing rangeland condition trend, all of which represent high vulnerability.

We also assessed broad-scale ecosystem changes by assessing the degree to which the suitable climates supporting current ecosystem distributions would remain suitable by mid and end-century, and where such climates would shift within the P-ARB. Projections of future ecosystem distributions suggests that ecosystem shifts will be pervasive across much of the P-ARB, especially under a high-emissions scenario and by end-century. Such shifts will result in novel ecosystem types not currently found within the P-ARB, most notably in the northwestern and southeastern portions of the region. This may challenge both wildlife and local communities that may be poorly adapted to such novel conditions. In general, there is more projected ecosystem stability in the center of the P-ARB (western Badakhshan, Baghlan, and Samangan) and in northern and far northeastern Badakhshan. The Afghan Mountains semi-desert, Badghyz and Karabil semi-desert, and Ghorat-Hazarajat alpine meadow ecoregions had the largest projected ecoregion and biome shifts, representing high vulnerability.

We further evaluated several indicators related to ecosystem adaptive capacity, determining how indicators related to carbon storage, ecosystem protection, and thermal and topographic heterogeneity are distributed throughout the P-ARB. For carbon storage, we assessed above and belowground biomass carbon, soil carbon, and total carbon using multiple high-resolution remotely sensed datasets. The Gissaro-Alai open woodlands, Hindu Kush alpine meadow, and Ghorat-Hazarajat alpine meadow ecoregions had the highest average total carbon, representing high adaptive capacity.

For ecosystem protection, we evaluated the degree to which the current system of protected areas within the P-ARB represents the diversity of unique ecoregions. Several ecoregions are completely unprotected and represent unique ecosystem types within the P-ARB, Afghanistan, and even the entire world. For example, the Afghan Mountains semi-desert and Gissaro-Alai open woodlands ecoregions currently have no legally designated protected areas, but are rich in carbon and have relatively high ecosystem quality with an overall increasing trend in vegetation greenness. Enhanced protection and stricter ecosystem management are recommended for these regions to retain their quality, as these regions may be increasingly important refugia over the next several decades. The Pamir alpine desert and tundra, Karakorum-West Tibetan Plateau alpine steppe, and Ghorat-Hazarajat alpine meadow ecoregions had the highest ecoregion protection, representing high adaptive capacity.

Finally, we analyzed two metrics related to fine-scale spatial patterns of temperatures (thermal heterogeneity) and elevations (topographic heterogeneity), both of which provide potential micro (within 22,500 m^2) thermal refugia under extreme warm and cold conditions and thus represent adaptation potential. Adaptation potential represented by thermal and topographic heterogeneity is relatively high and uniform across most of the P-ARB, owing to the complex topographic and extreme elevational gradient, which could facilitate wildlife movements under climate change and provide critical climate refugia. The Gissaro-Alai open woodlands and Hindu Kush alpine meadow ecoregions both had high thermal and topographic heterogeneity; the Afghan Mountains semi-desert had high thermal heterogeneity; and the Karakorum-West Tibetan Plateau alpine steppe had high topographic heterogeneity, all of which represent high adaptive capacity.

Synthesizing our results across all indicators reveals ecoregions of higher relative ecosystem vulnerability (Figure 70). The Badghyz and Karabil semi-desert ecoregion has perhaps the highest ecosystem vulnerability, having high exposure to all four indicators considered (decreasing natural land cover, decreasing NDVI, decreasing rangeland condition, and high projected ecoregion shifts) and limited adaptive capacity. The Paropamisus xeric woodlands ecoregion is also characterized by high ecosystem vulnerability, having high exposure to three of the four indicators considered (decreasing natural land cover, decreasing NDVI, and decreasing rangeland condition), and again limited adaptive capacity. The Afghan Mountains semi-desert ecoregion also has high ecosystem vulnerability, having high exposure to two of the four indicators considered (decreasing natural land cover and high projected ecoregion shifts), but some adaptive capacity in terms of having high thermal heterogeneity. The policy and management recommendations, outlined at the end of this section of the report, would be particularly urgent and relevant in these highly vulnerable ecoregions.

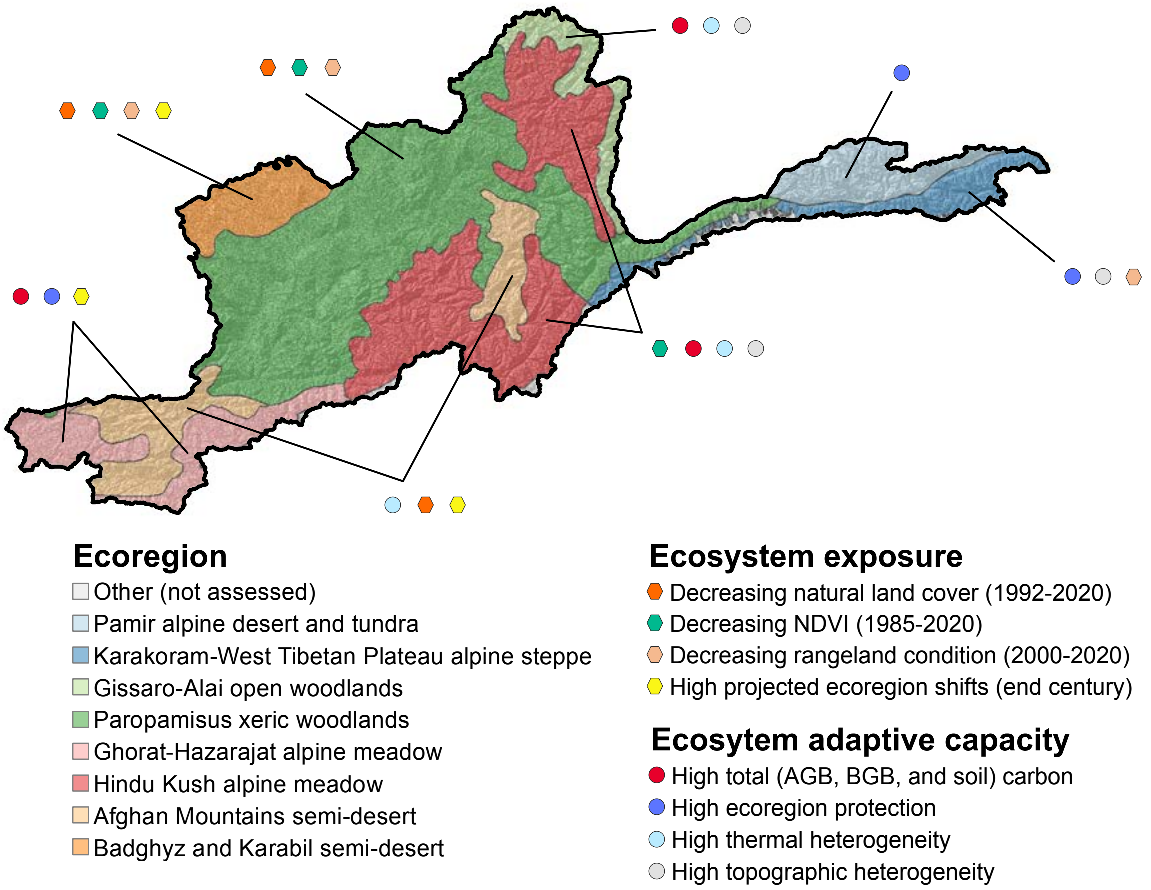

Figure 70. Overview of ecosystem exposure and adaptive capacity within ecoregions of the Panj-Amu River Basin.

Changes in Natural Land Cover Extents

E

Indicator overview

Natural ecosystems provide resources to people and support biodiversity. Ecosystem stability ensures the sustainability of these resources over time, while expansion of non-natural habitats through increases in the extents of cropland or the built environment can reduce resource availability and increase resource insecurity. While expanding croplands can increase food availability, many people in the P-ARB depend on natural ecosystems, such as grasslands, for multiple essential livelihoods. For example, grasslands are used extensively for fuelwood, fodder, and grazing. Tree cover from natural forests store carbon, provide wood, and can shelter communities from harsh climates. For biodiversity, the reduction of natural land cover typically equates to a direct loss of habitat, which can lead to diversity and population declines. Thus, reductions in natural land cover extents increase both wildlife and community vulnerability to climate change.

Methods overview

The European Space Agency has developed annual global land cover classifications at 300 m spatial resolution suitable for temporal change analysis (ESA 2017). The classifications have been validated for accuracy through assessment against independent data, including ground-truthed reference measurements and estimates from other satellite sensors and databases (e.g., the Landsat Global Land Survey Database, the TropForest dataset, SPOT imagery, GLC2000, and GlobCover). The validation of the ESA land cover classification was conducted for 2600 primary sampling units (PSUs), from which five secondary sampling units were also selected for each PSU. The dataset contains numerous natural vegetation classes with which to assess land cover changes. Annual land cover classifications from 1992 through 2020 were obtained and clipped to the boundaries of the P-ARB. Within this study area, the classes included three types of croplands (rainfed, irrigated, and mosaic), natural vegetation mosaic, two types of tree cover (broadleaved and needle-leaved), tree/shrub mosaic, herbaceous cover mosaic, shrubland, grassland, sparse vegetation, flooded shrub cover, urban, bare, water, and snow/ice. Natural land covers included all classes except for the three cropland classes and the urban class.

Data were extracted from each annual land cover map and stacked frequency distributions of each class were plotted to assess changes in natural land cover extents. The data were summarized by ecoregion and province.

Spatial representation of indicator

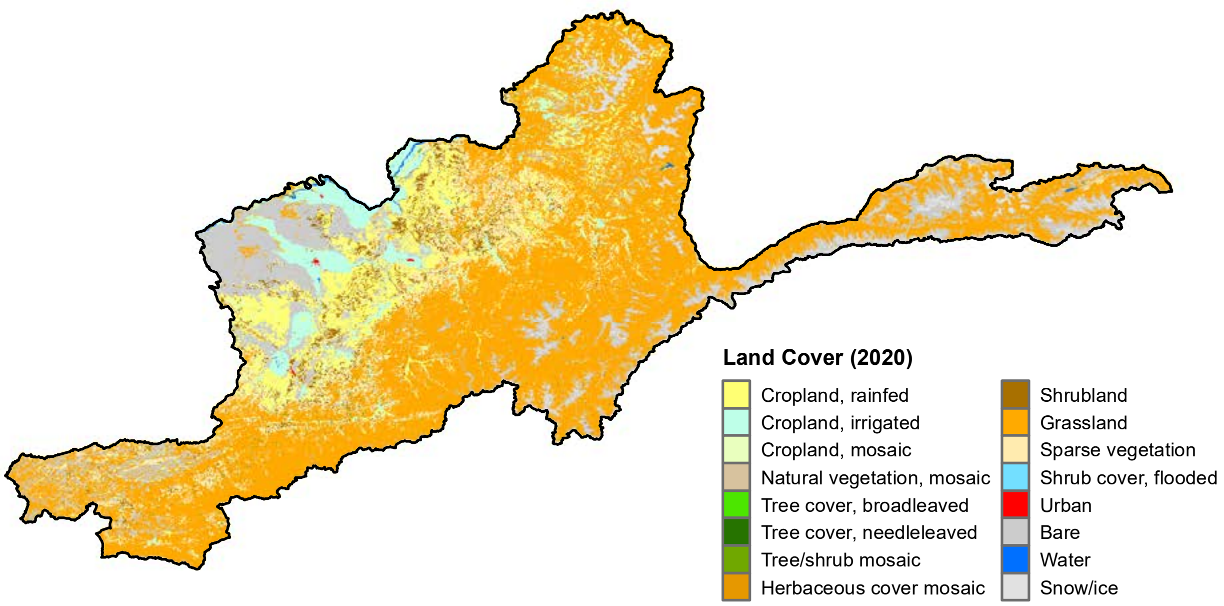

Figure 71. Land cover classification for 2020 (source: ESA 2017).

Summary plots of indicator by ecoregion and province

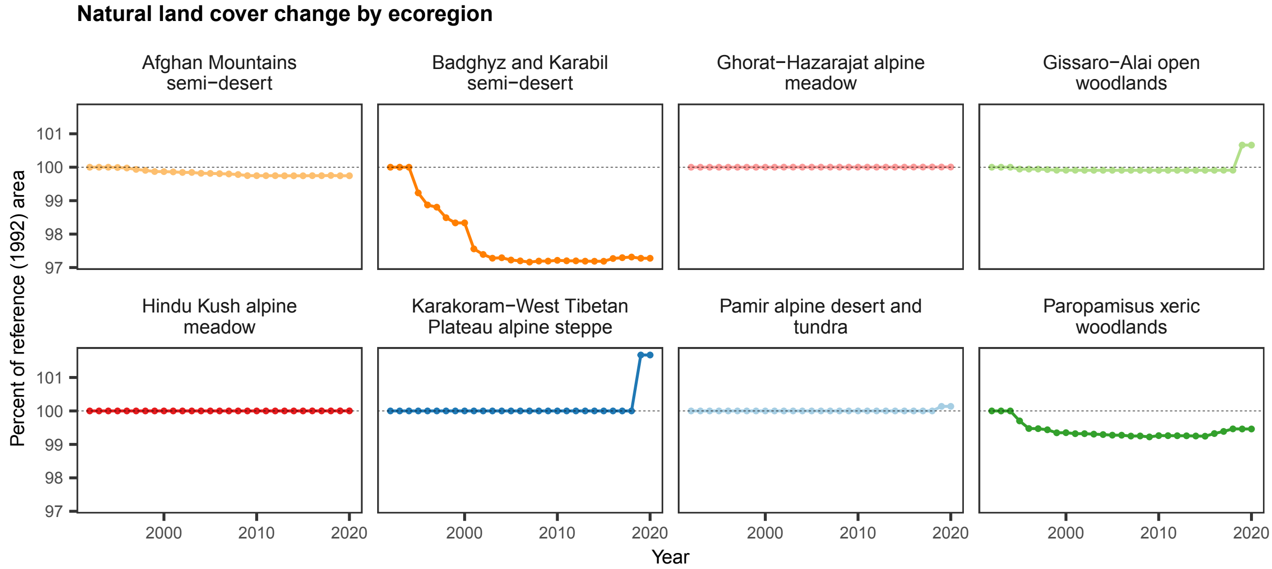

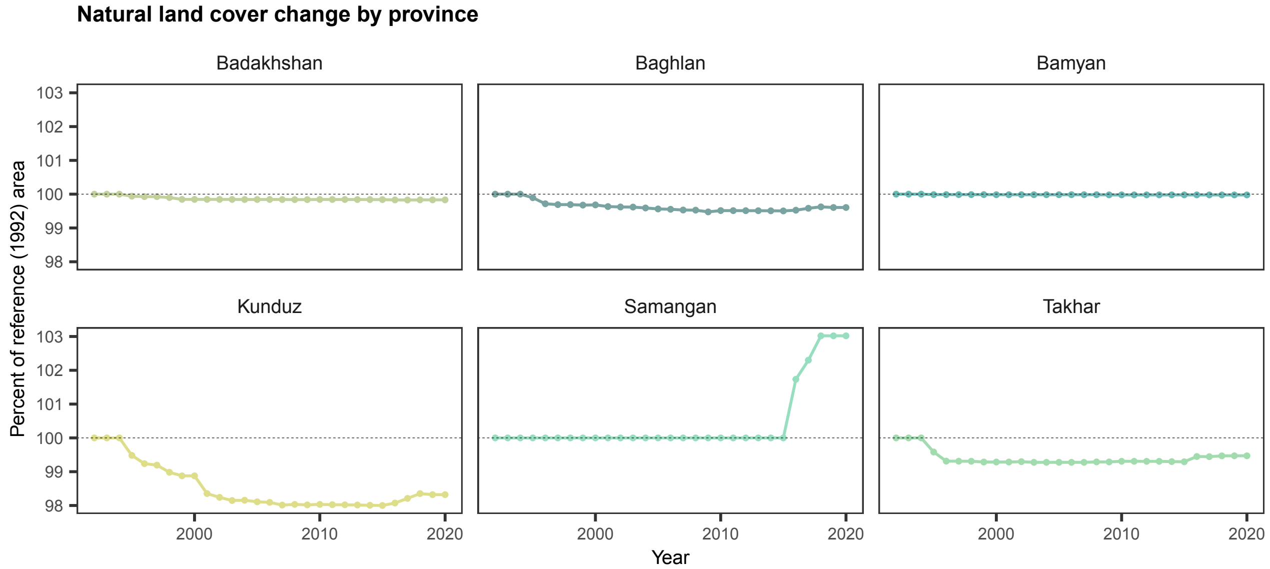

Figure 72. Natural land cover change in the P-ARB between 1992-2020 by ecoregion and province, as a percent of the reference area in 1992. Natural land cover includes all land cover classes from the ESA classification except croplands and urban. Horizontal dashed line indicates 100% of reference area, indicating no change in natural land cover area.

Results summary

Based on ESA land cover data, there has not been substantial conversion from natural land cover classes to non-natural (i.e., cropland or urban) land cover classes. The most extensive losses of natural land cover occurred in Paropamisus xeric woodlands (~1% loss), Badghyz and Karabil semi-desert (~3% loss), and Afghan Mountains semi-desert (~0.2% loss) ecoregions. Loss occurred gradually between 1992 and approximately 2010, 2003, and 2008 in these ecoregions, respectively, at which point natural land cover either increased (in the case of Paropamisus xeric woodlands) or mostly stopped. The Karakoram-West Tibetan Plateau alpine steppe and Gissaro-Alai open woodlands experienced natural land cover area gains of approximately 2% and 1%, respectively. By province, the largest losses of natural land cover occurred in Kunduz (~2% loss), Takhar (~1% loss), and Baghlan (~0.5% loss), with only very minor losses in Badakhshan (~0.1% loss) and Bamyan (<0.1% loss) and gains in Samangan (~3% gain). Most loss of natural land cover occurred by 2000, except in Baghlan, where loss continued until 2010. In Kunduz and Takhar, there have been minor upticks in natural land cover extents over the past five years.

Ecosystem carbon

AC

Indicator overview

Trees, rangelands, and other vegetation increase the carbon sequestration in a given area, while removal or degradation of trees, grasslands, and other vegetation decreases the carbon storage capacity. Regions with higher carbon are often associated with more vegetation that can support activities of the local communities while also providing food and shelter for wildlife. The carbon stored in vegetation and soils also provides climate mitigation benefits. Therefore, regions with greater carbon storage have greater resilience under climate change and are important areas to maintain to limit potential future emissions.

Methods overview

The challenge of calculating biomass carbon is obtaining spatial data for biomass distribution and density across the entire landscape. For this purpose, available datasets were reviewed, and it was determined that the recently released and globally available product by Spawn et al. (2020) is the best available product, because it contains both above- and belowground biomass carbon (AGB and BGB, respectively) for all vegetation types, and is particularly useful for grassland and agriculture types, which other datasets are not tuned for. The dataset provides separate "harmonized" measurements of above- and belowground carbon in t/ha circa 2010 at 300 m resolution. Other promising datasets, such as the ESA CCI biomass product (Santoro et al. 2021), while at a higher spatial resolution, lack information on belowground biomass carbon, which is the most important carbon pool in grassland ecosystems.

An additional important carbon pool is soil carbon, which is not readily available as an integrated product with any of the global biomass carbon datasets. To capture this source of carbon, data from the International Soil Reference and Information Centre (ISRIC), termed "Soil_Carbon_Stock", were used (Poggio et al. 2021). This dataset is produced globally in units of t/ha circa 2017 at a spatial resolution of 250 m for six different soil depths. The dataset is based on multiple soil profiles collected worldwide. To capture all soil carbon, the carbon stock values for all six depths were summed.

The datasets were compiled, projected to the same geographic projection, and the ISRIC soil carbon dataset was resampled to 300 m to match the resolution of the biomass carbon dataset. The soil carbon dataset contains no data values for regions that are covered by snow and ice. While there are data values for these areas in the biomass carbon dataset, these values are not likely accurate because they are based on land cover classifications rather than satellite images. To conservatively estimate the biomass carbon, biomass carbon pixels were removed by applying the soil carbon mask to both the above- and belowground datasets. Each dataset was analyzed separately to visualize each carbon component, and the AGB, BGB, and soil carbon datasets were summed, acknowledging that there is a slight (7 year) mismatch in the purported temporal window of the data.

Spatial representation of indicator

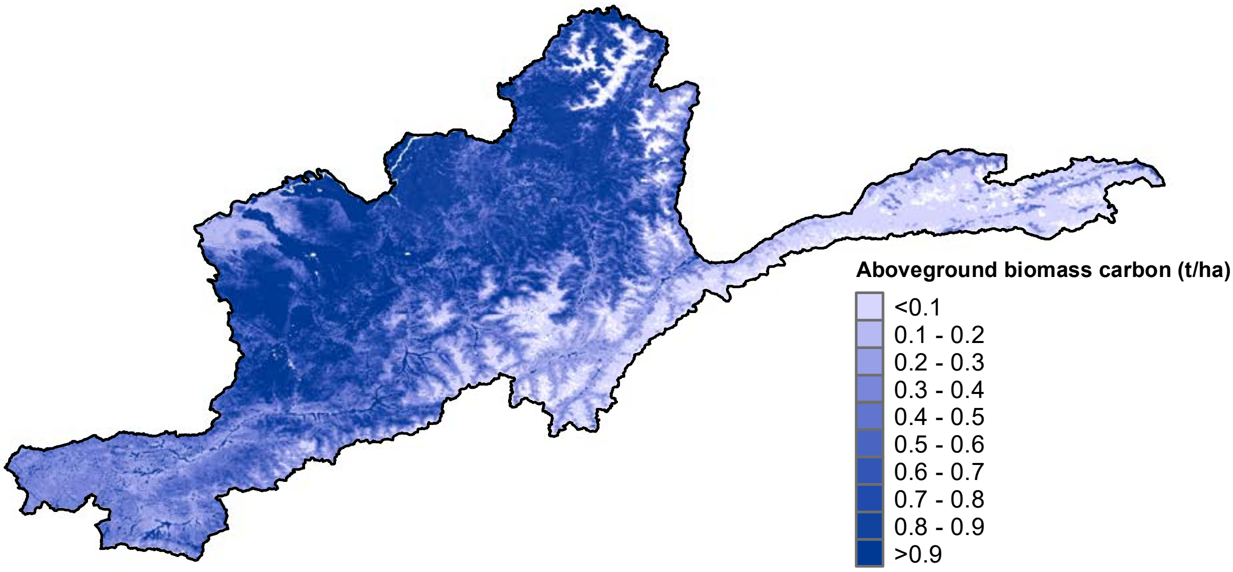

Figure 73. Aboveground biomass carbon (t/ha) (AGB) in the Panj-Amu River Basin.

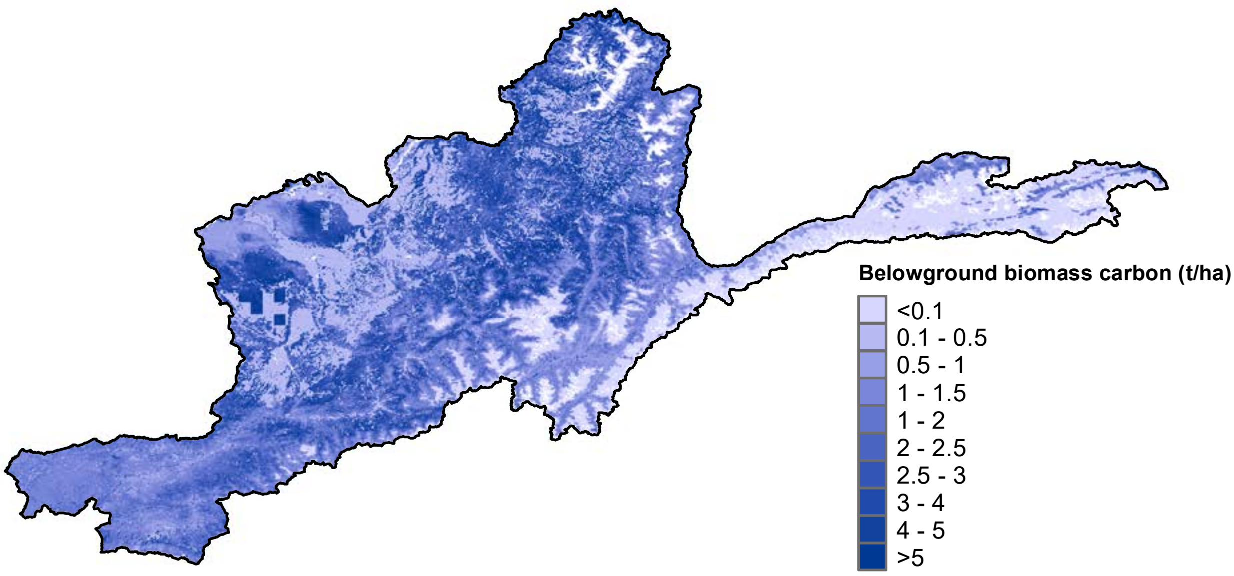

Figure 74. Belowground biomass carbon (t/ha) (BGB) in the Panj-Amu River Basin.

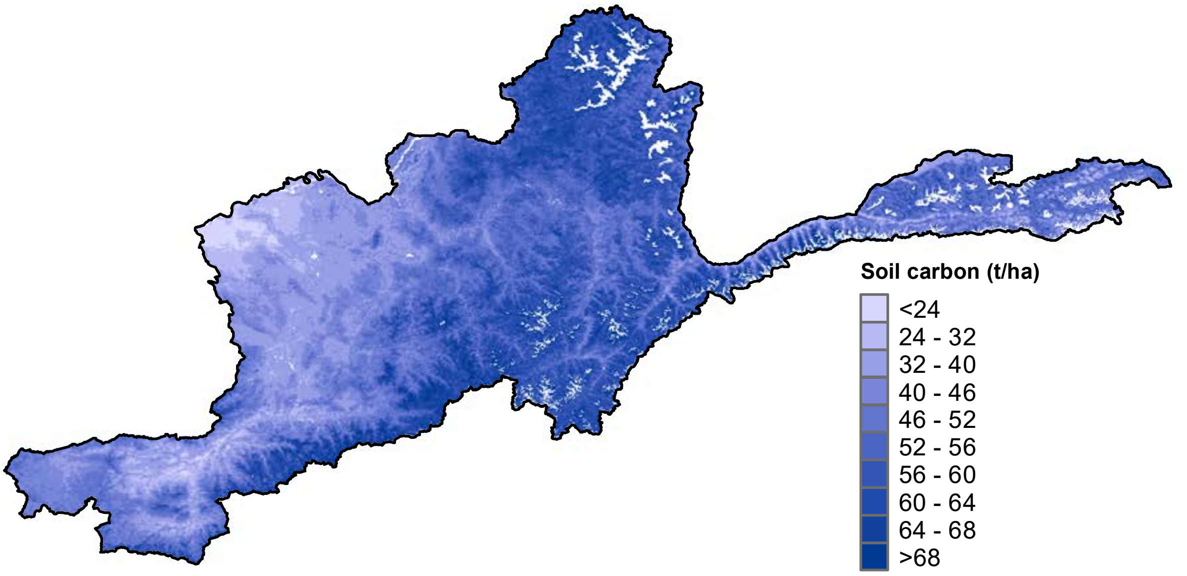

Figure 75. Soil carbon (t/ha) in the Panj-Amu River Basin.

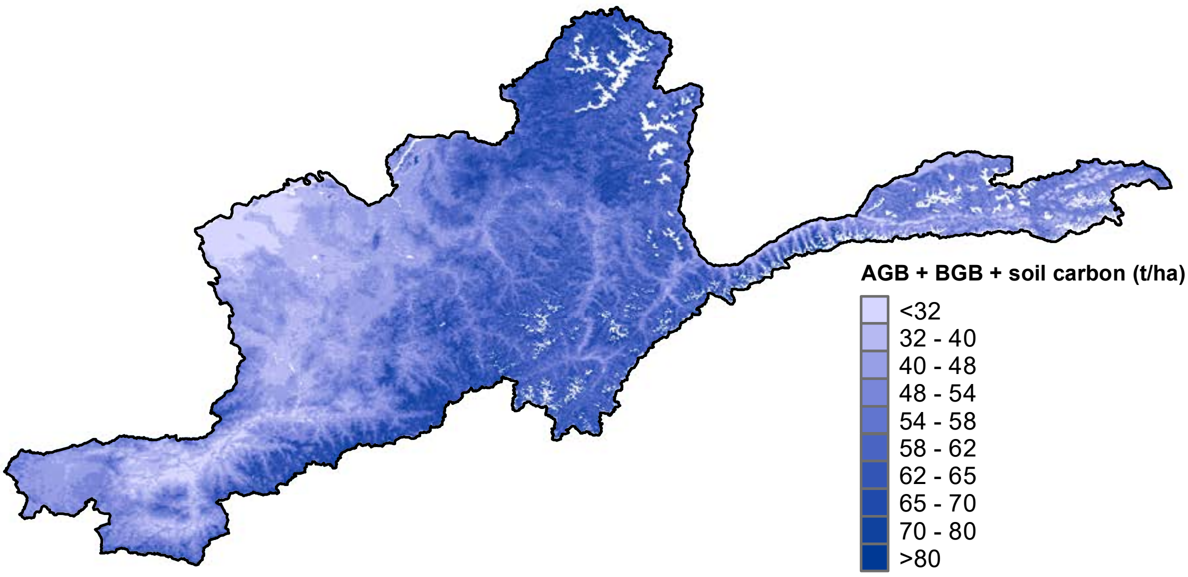

Figure 76. Combined AGB, BGB, and soil carbon (t/ha) in the Panj-Amu River Basin.

Summary plots of indicator by ecoregion and province

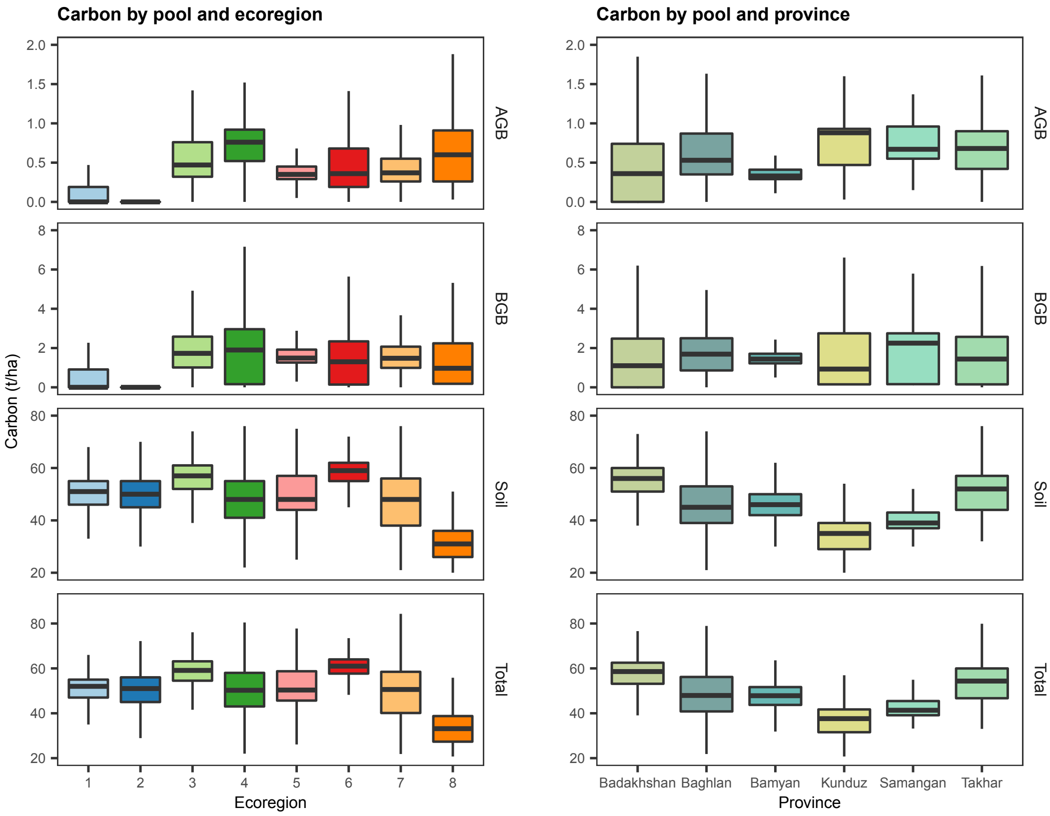

Figure 77. Boxplots of four carbon pools in the Panj-Amu River Basin by ecoregion and province. Note that outliers have been removed and the y axis has been rescaled per panel to enhance legibility. Ecoregion legend: 1 – Pamir alpine desert and tundra; 2 – Karakorum-West Tibetan Plateau alpine steppe; 3 – Gissaro-Alai open woodlands; 4 – Paropamisus xeric woodlands; 5 – Ghorat-Hazarajat alpine meadow; 6 – Hindu-Kush alpine meadow; 7 – Afghan Mountains semi-desert; 8 - Badghyz and Karabil semi-desert.

Results summary

The spatial patterns of the different carbon pools were similar, though there were some differences between patterns of biomass and soil carbon. Overall, high total carbon values (>60 t/ha) were mostly found on steep and bare slopes, especially in the north, northeastern, and southern parts of the P-ARB (Figure 76). These steeper slopes are less accessible to humans and tend to have lower human use in terms of agriculture, which could partly explain these patterns. The westernmost region also had some localized patches of high belowground biomass carbon (>5 t/ha) (Figure 74). While above and belowground biomass carbon were relatively lower in the northeast (<0.1 t/ha), that region was characterized by higher soil carbon (between 40-50 t/ha). The northwestern region and many of the valley bottom areas had the lowest combined carbon values (<32 t/ha). Variation in land cover of the landscape, from bare steep slopes to lowlands with denser vegetation, at least partially explains the variation in carbon values observed across the landscape. In general, the patterns of total carbon closely mirrored those of soil carbon, as soil carbon contributed far more to the total carbon pool than either AGB or BGB. Soil carbon was roughly 1-2 orders of magnitude greater than AGB, and roughly one order of magnitude greater than BGB across the region.

Overall, the highest carbon values were located in the Hindu Kush alpine meadow and the Gissaro-Alai open woodlands ecoregions (median total carbon ~60 t/ha each) and in Badakhshan, Takhar, Baghlan, and Bamyan provinces (median total carbon ~60 t/ha, 55 t/ha, 50 t/ha, and 50 t/ha, respectively). These ecoregions and provinces had high soil carbon and relatively high belowground biomass carbon, but not all of them had high aboveground biomass carbon. The Paropamisus xeric woodlands ecoregion, which contains more natural tree cover than many other ecoregions, contained the highest aboveground biomass carbon (median AGB ~1 t/ha). Kunduz was the province with the highest aboveground biomass carbon (median AGB ~1 t/ha), which could be influenced by agroforestry or aboveground biomass arising from agriculture.

However, while Kunduz had the highest aboveground biomass carbon, it had the lowest overall carbon of any province (median total carbon ~40 t/ha), underscoring the region's high climate vulnerability. The Badghyz and Karabil semi-desert, which is completely restricted to Kunduz province in Afghanistan, also is highly vulnerable with the lowest total carbon value (median total carbon ~30 t/ha).

Changes in the Normalized Difference Vegetation Index

E

Indicator overview

Vegetation serves as both an important component of habitat for wildlife and as a natural resource for local communities. For example, vegetation provides the main source of fodder for grazing livestock, which are prevalent throughout the P-ARB. Vegetation also absorbs and stores carbon, providing climate mitigation benefits. Regions exhibiting long-term negative trends in vegetation are associated with higher vulnerability because it signifies a reduction in habitat and natural resource availability, and increased land erosion risk, that are likely to be reflective of human-caused landscape degradation. Such degradation can be additional to vegetation losses that occur naturally through reductions in precipitation and snowfall that encourage vegetation growth.

Methods overview

For this indicator, we calculated a commonly used index of vegetation greenness known as the Normalized Difference Vegetation Index (NDVI) for annual composites of Landsat imagery from 1985-2020. We first compiled all Landsat 5 images from 1st January 1985 to 30th April 2012, all Landsat 7 images from 1st January 1999 to 31st December 2019, and all Landsat 8 images from 1st January 2014 to 31st December 2020 that overlapped the P-ARB. To each image, we applied a cloud mask that removed clouds, cirrus, and cloud shadows. We calculated NDVI for each image using the equation (NIR – Red) / (NIR + Red), where NIR and Red are the spectral reflectance measurements acquired in the near-infrared and red (visible) regions, respectively.

We then merged all images together into one set and calculated the maximum NDVI for each pixel for all images in each year. This resulted in annual maximum NDVI composites for 1985-2020 (35 composite images). To calculate trends in the annual NDVI composites, we calculated Kendall's Tau-b rank correlation, where a positive value indicates an increasing trend (lower vulnerability), and a negative value indicates a decreasing trend (higher vulnerability).

Spatial representation of indicator

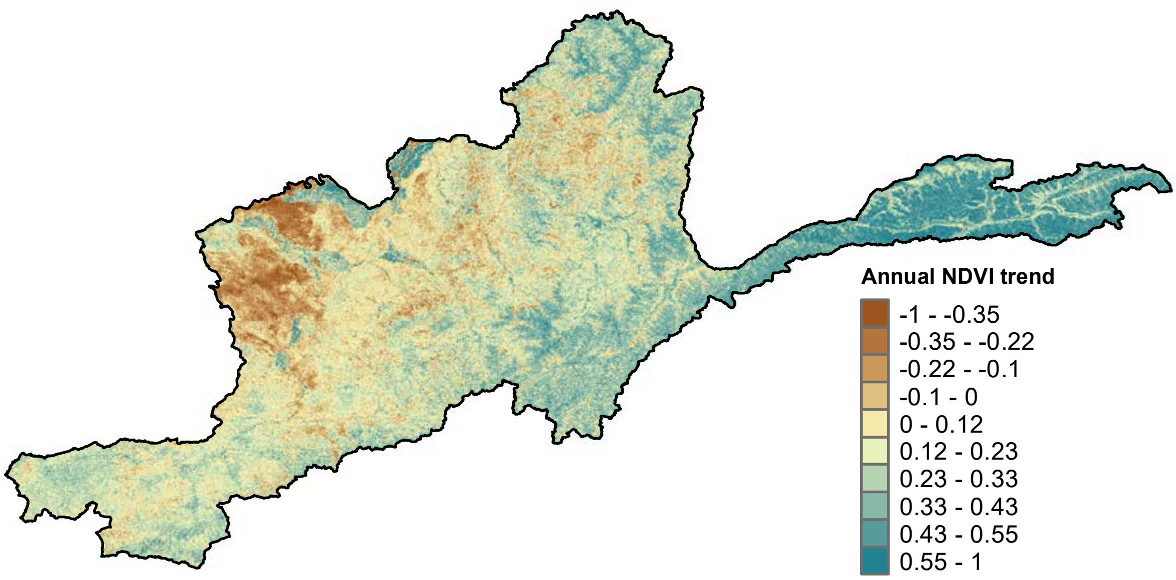

Figure 78. Annual trend in Normalized Difference Vegetation Index across the Panj-Amu River Basin from 1985-2020.

Summary plots of indicator by ecoregion and province

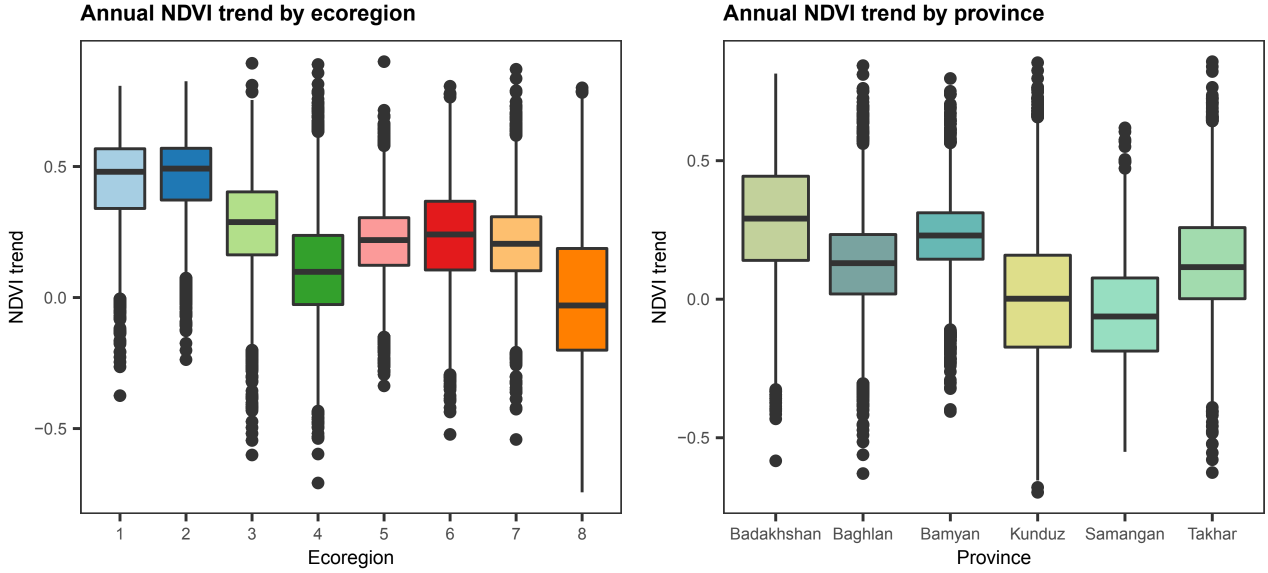

Figure 79. Boxplots of annual NDVI trends in the Panj-Amu River Basin by ecoregion and province, based on 5000 sample points. Ecoregion legend: 1 – Pamir alpine desert and tundra; 2 – Karakorum-West Tibetan Plateau alpine steppe; 3 – Gissaro-Alai open woodlands; 4 – Paropamisus xeric woodlands; 5 – Ghorat-Hazarajat alpine meadow; 6 – Hindu-Kush alpine meadow; 7 – Afghan Mountains semi-desert; 8 - Badghyz and Karabil semi-desert.

Results summary

Long-term (35 year) trends in maximum NDVI showed contrasting patterns across the P-ARB, with trends both substantially increasing and decreasing over time. The northeastern portion of the landscape showed the largest increases, while the western portion of the landscape showed the largest decreases (Figure 78). This means there has been the largest increase in green vegetation, as measured by NDVI, in the Karakorum-West Tibetan Plateau alpine steppe (99.3% of total area showed an increase over time) and Pamir alpine desert and tundra ecoregions (98.8% of area showed an increase), on average (Figure 79). By contrast, the Paropamisus xeric woodlands and Badghyz and Karabil semi-desert ecoregions had the largest decreases in NDVI, with 28.5% and 54.6% of their total areas showing decreases in NDVI over time. This is likely to increase vulnerability in these landscapes, as the availability of green, healthy vegetation for wildlife, communities, and livestock has been declining over the past 35 years. The areas with increasing NDVI trends are of relatively lower vulnerability, and it is interesting that the largest increases are found in areas with high mountains and many glaciers present. The greening in these regions could be the result of reduced glacier mass over time, which has led to increase in snow melt with the potential to increase greening in adjacent areas over time. Additional factors, such as changing precipitation trends over the past 35 years, could also have contributed to these patterns. Moreover, if the snowmelt arising from glacier mass loss is driving some of this greening, this may only provide a temporary input and once the glacier has receded further, the lack of the permanent snow and ice cover will likely reduce vegetation greenness in these regions at that point.

The provinces of Kunduz and Samangan have seen the largest decreases in NDVI over the 35-year period analyzed (51.5% and 61.5% of their total areas showed a decrease). Because these areas lack glaciers and have less annual snowfall, it is likely that these declines are due either to reductions in annual precipitation, grassland degradation, or habitat conversion. The land cover analysis did indicate a slight increase in the proportion of bare ground in Kunduz, but not an appreciable change in the proportion of cropland. This suggests that conversion of natural vegetation to cropland is not likely to be a major driver of the decreasing NDVI trend observed. The annual precipitation trend captured by the downscaled CHIRPS dataset indicated that these two provinces have largely had decreasing precipitation over the past two decades, which would be expected to limit NDVI potential over that period. However, there are some areas where the precipitation patterns alone cannot explain the declines in NDVI values observed, indicating that overutilization of grassland resources is likely partly responsible for the declines in NDVI trends in these regions. Human-caused grassland degradation resulting in reductions in NDVI values over time also appear to be occurring in the major valleys of Badakhshan and around heavily populated areas.

Changes in Rangeland Condition

E

Indicator overview

Dryland ecosystems, including grasslands and rangelands, support billions of people and important biodiversity by providing food, fuel, fodder, and habitat (Reynolds et al. 2007). However, their ability to function as natural support systems is hindered by both climate change and human activities, which have caused widespread degradation globally (Gang et al. 2014). Such degradation exacerbates threats to local livelihoods (Kwon et al. 2016), increases carbon emissions through vegetation loss (O'Mara 2012), and reduces human and wildlife adaptation potential under climate change (Smith et al. 2019). Climate change is expected to increase the frequency and magnitude of droughts and heatwaves in grasslands (Sheffield and Wood 2008, Brookshire and Weaver 2015, Frank et al. 2015), potentially increasing the rate and extent of degradation.

Rangeland degradation is of particular concern in Afghanistan, where political instability, overgrazing, and drought have reduced the extent and condition of natural vegetation (de Beurs and Henebry 2008), and where people extensively rely on rangeland resources with little access to alternative livelihoods (Pittroff 2015). Rangeland degradation in Afghanistan is also poised to be exacerbated by climate change (Aich et al. 2017), which has inspired the development of a national Climate Change Strategy and Action Plan and a National Adaptation Plan as part of Afghanistan's Intended Nationally Determined Contribution. Furthermore, several policies and plans aimed at bolstering sustainable development through environmental stewardship have been initiated, such as the National Environmental Action Plan, National Biodiversity Strategy and Action Plan, and Rangeland Management Plan. Because of the recognized concerns associated with rangeland degradation in the region (Saba 2009), a detailed assessment of rangeland degradation and its underlying drivers is essential for successfully implementing such plans.

Methods overview

For this indicator, dense timeseries satellite observations were used to identify and map three distinct rangeland degradation processes (Lewińska et al. 2020) over 21 years in the P-ARB. The approach incorporates several remote sensing techniques capable of detecting and characterizing land degradation in dryland ecosystems (Fensholt et al. 2013) including spectral unmixing (Adams et al. 1986) to distinguish sub-pixel fractional covers of soil, green vegetation, and non-photosynthetic (dry) vegetation, applying a Whittaker smoother (Whittaker 1922) to fill data gaps arising from clouds and cloud shadows, and using LandTrendr temporal segmentation (Kennedy et al. 2018) to evaluate piecewise trends in soil, green vegetation, and dry vegetation dynamics. Altogether, the procedure enables characterization of degradation patterns by determining the onset (the year when degradation begins), duration (the number of years over which degradation takes place), and magnitude (the amount of change in vegetation or soil fractional cover) for each distinct degradation event.

The procedure was applied to all rangelands, where the distribution of rangelands was determined through the development of a custom, high-resolution land cover map to match the resolution (30 m) of the rangeland condition change indicators (Figure 80). Land cover was modeled using random forest algorithms applied to Landsat 8 imagery and using over 2,500 primary observations of 14 land cover classes (riparian shrubs, riparian meadows, Leymus grass, forest, rangeland, alpine meadow, barren, irrigated agriculture, rainfed agriculture, snow/ice, water, sand, bright rock, dark rock). The random forest models used the following predictors: NDVI (normalized difference vegetation index) (including four seasonal NDVI components for winter, spring, summer, and fall), NDWI (normalized difference water index), NRVI (normalized ratio vegetation index), NDMI (normalized difference moisture index), GLI (green leaf index), EVI (enhanced vegetation index), SAVI (soil adjusted vegetation index), GOSAVI (green optimized soil adjusted vegetation index), MCTI (MERIS terrestrial chlorophyll index), elevation, slope, and aspect. In addition, Synthetic Aperture Radar (SAR) data from Sentinel 1 were used to facilitate agriculture mapping, including Vertical Transmit-Vertical Receive (VV) and Vertical Transmit-Horizontal Receive (VH) backscatter collected from pre-harvest (June-July) and post-harvest (September-October) periods. The land cover model was trained with 70% of the data points, reserving 30% for validation. The accuracy of the model was approximately 86%. To defined rangelands, we combined three classes: 'Leymus grass', 'alpine meadow', and 'rangeland'.

Rangeland model results were validated using field observations of green vegetation cover in two opposing and protected regions of the P-ARB, Wakhan and Bamyan National Parks. The focus of this indicator is on temporal trends in green vegetation, as this is the most important for wild herbivore and livestock grazing. Additional details describing the methodology can be found in Appendix 4.

Spatial representation of indicator

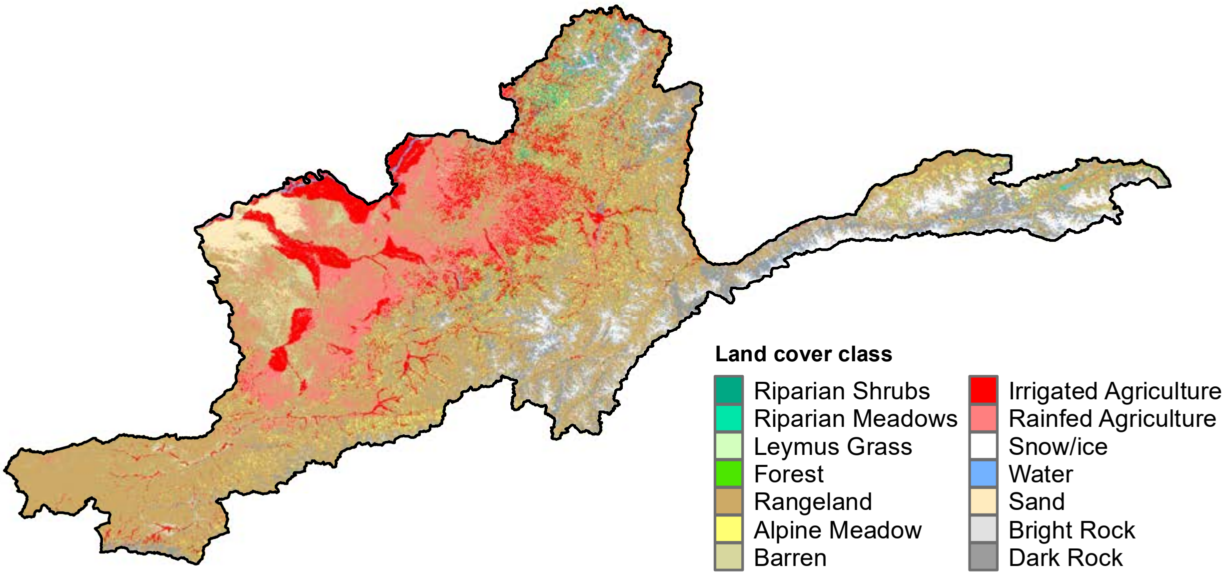

Figure 80. Custom land cover classification developed for the P-ARB used to delineate rangelands at 30 m spatial resolution. For the rangeland condition analysis, the ranglelands delineation cominbes Leymus, Alpine Meadow, and Rangelands classes from this classification.

Rangelands are the heart of Afghanistan's extensive livestock economy, providing grazing resources for millions of animals and vital livelihoods for people.

Dry pastures of Central Asia are critical to a range of valuable species. Pictured is a field of narrow-leaved foxtail lilies (Eremurus stenophyllus), a plant native to Central Asia where it grows in dry mountainous areas. Livestock grazing, coupled with climate change, fuel wood harvesting, and invasion of lower elevation plants, threaten rare plant communities of these areas.

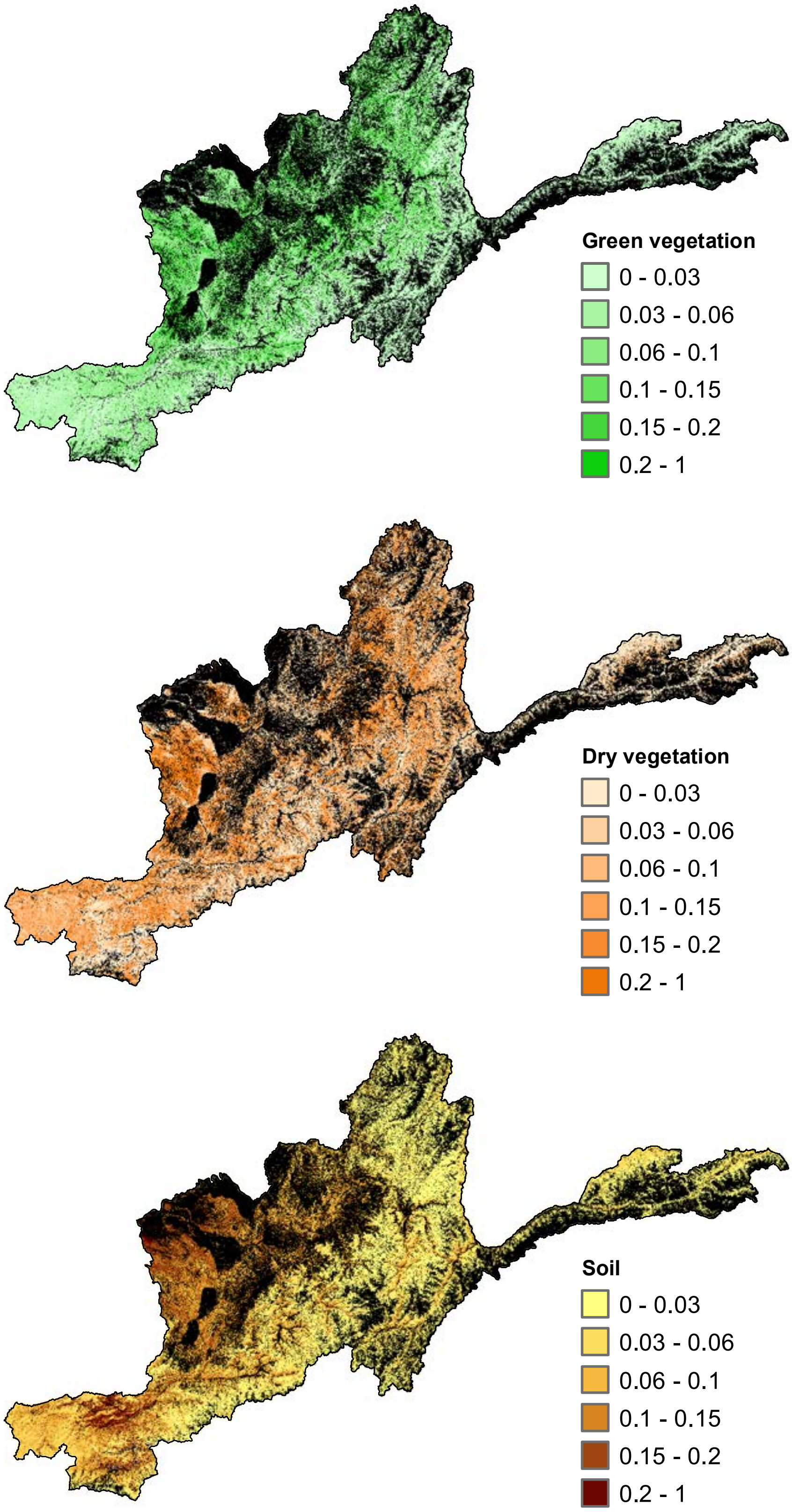

Figure 81. Maps of cumulative endmember fractions in 2020 for green vegetation (top row), dry vegetation (middle row), and soil (bottom row). Cumulative endmember fractions represent the proportion of each vegetation type/soil. Black regions represent non-rangeland and were excluded from analysis.

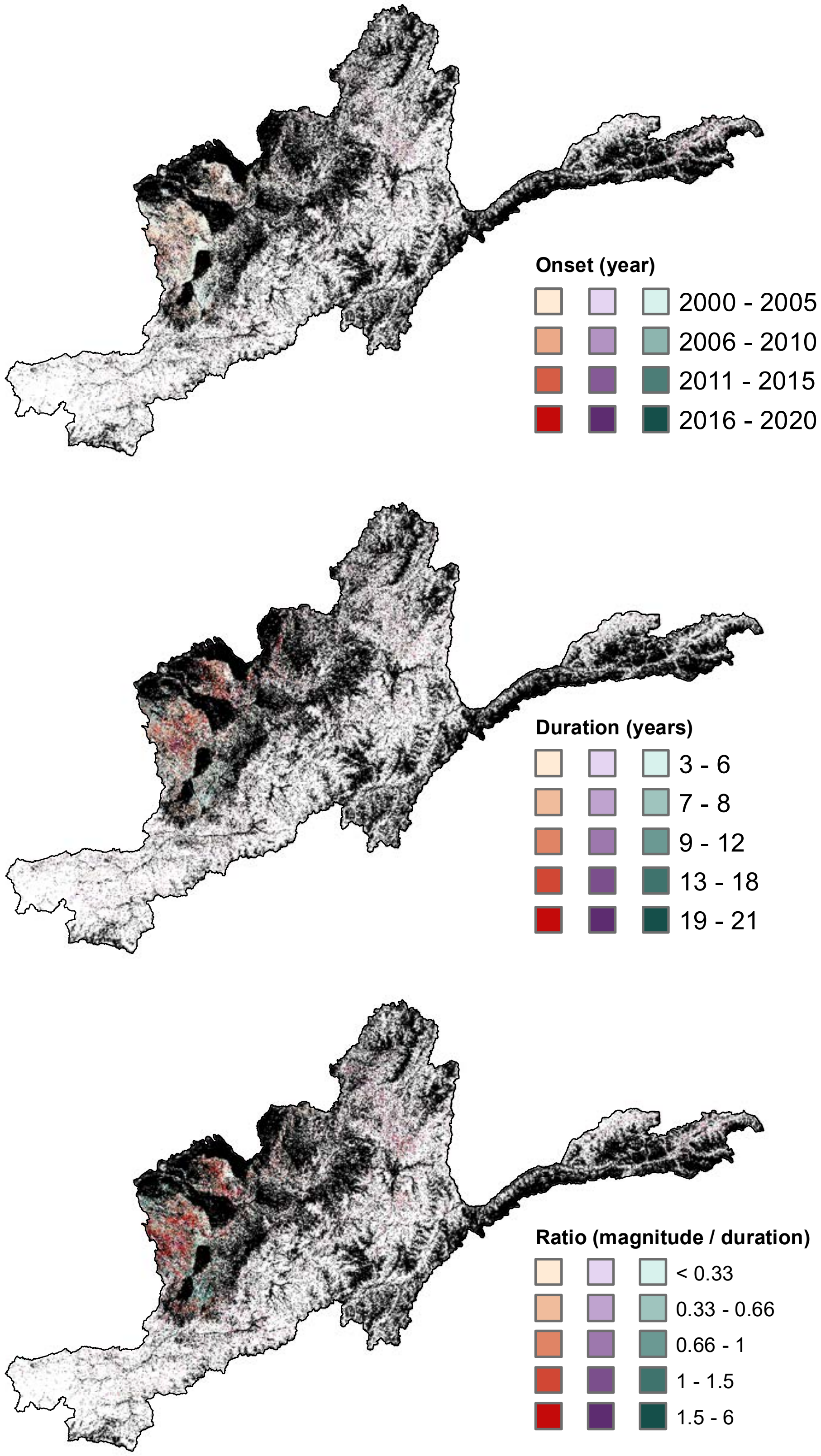

Figure 82. Maps of onset (top row), duration (middle row), and the ratio of magnitude to duration (bottom row) of rangeland degradation for three distinct degradation pathways: green vegetation loss (red color gradient), dry vegetation loss (purple color gradient), and desiccation (green color gradient). Black regions represent non-rangeland and were excluded from analysis.

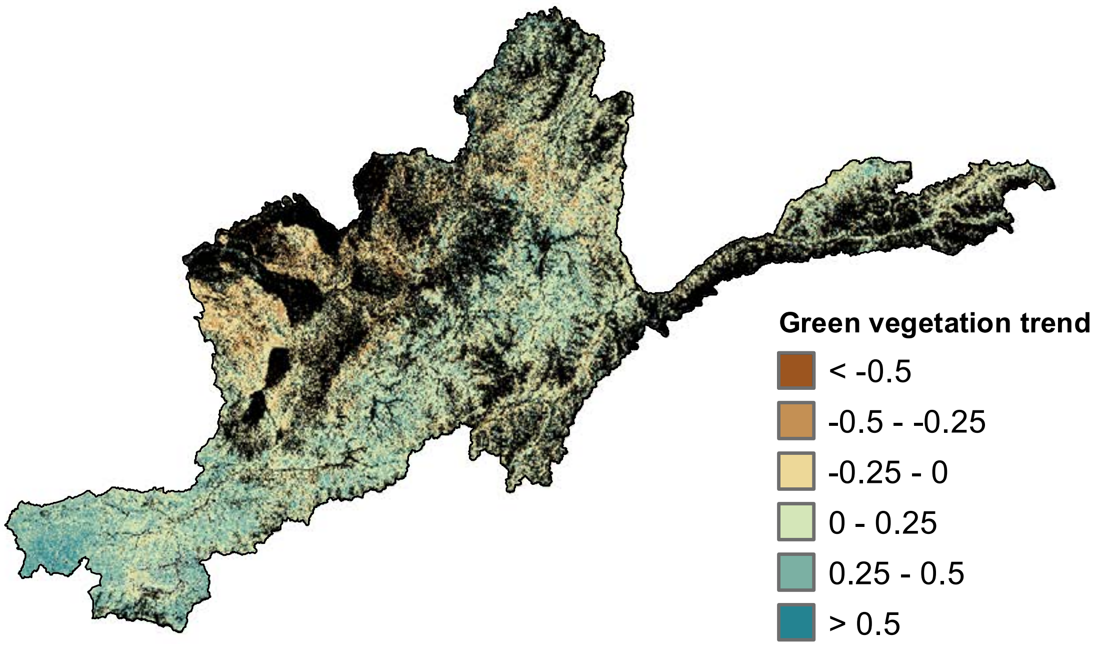

Figure 83. Map of trend in green vegetation between 2000-2020. Positive values reflect increases in green vegetation over the 20-year duration, while negative values reflect decreases. Black regions represent non-rangeland and were excluded from analysis.

Summary plots of indicator by ecoregion and province

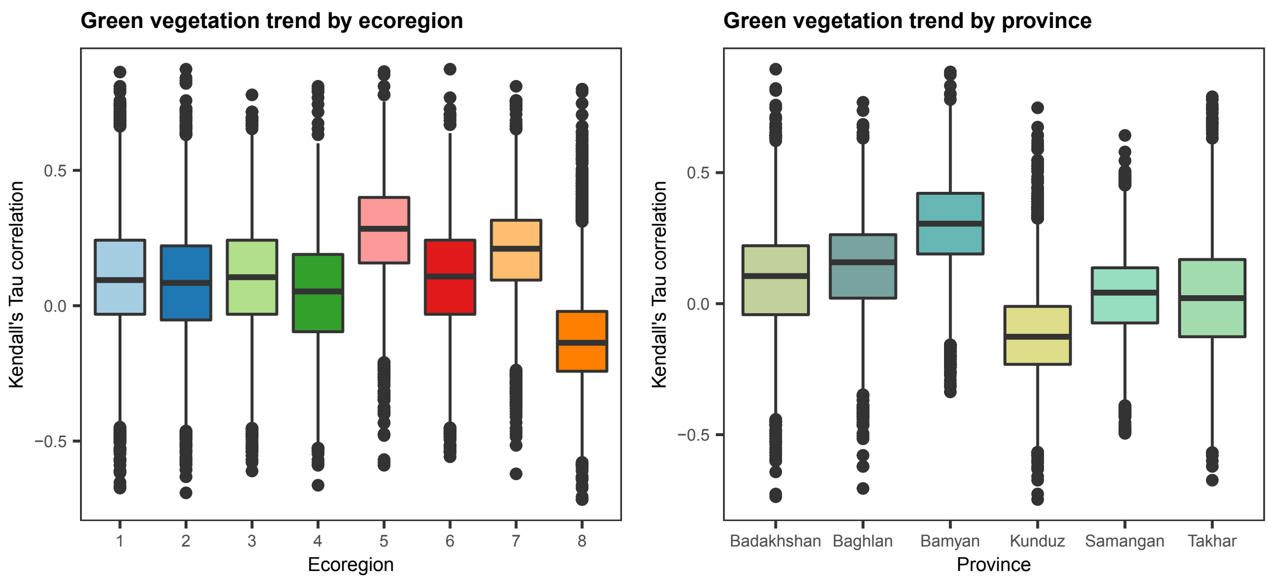

Figure 84. Green vegetation trend summary boxplots by ecoregion and province based on 5,000 stratified random samples. Positive values reflect positive trends, negative values reflect negative trends beween 2000-2020. Ecoregion legend: 1 – Pamir alpine desert and tundra; 2 – Karakorum-West Tibetan Plateau alpine steppe; 3 – Gissaro-Alai open woodlands; 4 – Paropamisus xeric woodlands; 5 – Ghorat-Hazarajat alpine meadow; 6 – Hindu-Kush alpine meadow; 7 – Afghan Mountains semi-desert; 8 - Badghyz and Karabil semi-desert.

Results summary

Location, onset, duration, and magnitude of rangeland degradation

Rangeland degradation was widespread throughout the P-ARB between 2000 and 2020 (Figure 82). Altogether, 8,142 km² (15.5% of total rangeland area) experienced degradation at some point during the 21-year period. The highest concentrations were in the northwestern portion of the landscape, in Kunduz and Baghlan provinces, with other significant regions of rangeland degradation in central Badakhshan and the northeastern reaches of the Wakhan corridor. Most of the rangeland degradation in the region was in the form of green vegetation loss (3,745 km², 7.1% of the study region), followed by desiccation (2,598 km², 4.9%) and dry vegetation loss (2,567 km², 4.9%). Green vegetation loss was widespread near Kunduz, two heavily populated regions in the western portion of the study region. Desiccation was most prominent on either side of the Kunduz River and at the junction of the Kunduz and Amy Darya Rivers. Dry vegetation loss was mainly located in higher mountains, both in the Hindu Kush and Pamir Mountains of Badakhshan.

In general, rangeland degradation events began early in the 21st century (median onset year = 2001 for green and dry vegetation loss and 2000 for desiccation; top row of Figure 82) and lasted approximately a decade on average for all degradation pathways (mean duration = 9.8 years for green vegetation loss, 10.3 years for dry vegetation loss, and 9.4 years for desiccation; middle row of Figure 82). Regions with high magnitudes of rangeland degradation tended to experience that degradation over many years; punctuated rangeland degradation events where green or dry vegetation were lost over just a few years were relatively rare (bottom row of Figure 82).

Validation of green vegetation and soil endmember fractions

Validation of modeled green vegetation and soil endmember fractions against field collected green vegetation and soil cover fractions showed high correlations for both soil cover (pooled $r^2 = 0.72$; range across sites/years = [0.53-0.82]; $p < 0.001$ for all correlations) and green vegetation cover (pooled $r^2 = 0.77$; range across sites/years = [0.55-0.79]; $p < 0.001$ for all correlations) (Table 6). Performance was slightly greater for field plots located in Wakhan than in Bamyan, for soil measurements compared to green vegetation.

Table 6. Performance measures of modeled cover fractions compared to field data collected from Wakhan (n = 178 plots) and Bamyan (n = 172 plots) between 2016-2019.

Site	Year	Variable	R²	RMSE	Rel. RMSE	MAE	Rel. MAE	Bias	Rel. Bias	Eff	Field mean (SD)
Wakhan	2016	Soil	0.82	13.57	19.64	9.63	13.93	4.97	7.20	0.60	69.10 (28.96)
Wakhan	2016	Green vegetation	0.67	17.26	63.36	11.54	42.36	-8.08	-29.65	0.46	27.23 (25.61)
Wakhan	2018	Soil	0.85	14.92	21.16	10.63	15.08	8.19	11.61	0.57	70.53 (29.97)
Wakhan	2018	Green vegetation	0.79	14.20	62.62	10.06	44.35	-7.96	-35.11	0.48	22.68 (23.74)
Bamyan	2019	Soil	0.53	10.15	12.55	7.89	9.76	-1.51	-1.87	0.15	80.86 (11.48)
Bamyan	2019	Green vegetation	0.55	9.63	60.65	7.82	49.22	-7.43	-46.81	-0.06	15.88 (9.00)
Pooled 2018-2019		Soil	0.72	12.80	16.93	9.29	12.28	3.42	4.53	0.47	75.61 (23.38)
Pooled 2018-2019		Green vegetation	0.77	12.17	62.95	8.96	46.32	-7.70	-39.83	0.33	19.34 (18.36)

Note: Pearson correlation between modeled fractional cover and measurements was statistically significant at $p < 0.001$ for all correlations. "Eff" refers to the coefficient of efficiency, a dimensionless measure ranging between -∞ and 1, where values <0 indicate that the observed mean value is a better predictor than the predicted value of the model.

Green vegetation trends

Between 2000 and 2020, green vegetation showed an increasing trend in the south and southwest and in small patches in the northwest, at the base of the Wakhan corridor, and just west of Big Pamir (Figure 83). Everywhere else, green vegetation showed a decreasing trend. Spatial patterns in green vegetation trends for 2000-2020 were similar to those represented by annual trends in NDVI from 1985-2020 (Figure 78), which provides further validation of these long-term trends.

The largest increase in green vegetation, as measured by cumulative endmember fractions, is in the Ghorat-Hazarajat alpine meadow and Afghan Mountains semi-desert ecoregions, on average. By contrast, the Paropamisus xeric woodlands and Badghyz and Karabil semi-desert ecoregions had the largest decreases in green vegetation, on average. As with NDVI trends in these ecoregions, it is important to note that some of both of these ecoregions had increasing green vegetation trends, but the general patterns were of green vegetation declines between 2000-2020. Reductions in green vegetation are likely associated with increased vulnerability, because it represents lower availability of resources for communities, livestock, and wildlife. Areas with increasing green vegetation trends are indicative of lower vulnerability, yet regions with the highest increasing green vegetation trends still have relatively low green vegetation cover in general (Figure 81). Unlike trends in NDVI, the largest increases in green vegetation were found in mid altitude mountains. High mountain areas with glaciers, such as those found in Badakhshan, tend to have slightly decreasing trends over the past 21 years. It is possible these areas could see increased greening as glaciers continue to retreat and there is increasing water availability.

The provinces of Kunduz, Takhar, and Samangan have seen the largest decreases in green vegetation over the 21-year period analyzed. This analysis does not look directly at the drivers of rangeland degradation, but it is likely that these declines are due by a combination in reduced precipitation and overgrazing, as this region has experienced declining rainfall and snow cover and has some of the highest livestock densities of the P-ARB. Even if rainfall and snow cover trends neutralized, the substantial impacts from high livestock densities could put additional pressure on rangeland ecosystems in this portion of the landscape. These findings are consistent with those from the NDVI analysis.

Bamyan has seen the largest increase in green vegetation, followed by Baghlan and Badakhshan (Figure 84). Based on precipitation data from CHIRPS and snow cover data from MODIS satellites, Bamyan has experienced increasing trends in precipitation and snow cover, and this could partially explain the increases in green vegetation over the 21-year period of analysis. Field surveys indicated that overgrazing is common in the region, so it is possible that in the absence of favorable climate conditions, rangeland conditions would be worse as a result. Moreover, while these regions showed the largest increases in green vegetation, they have relatively low green vegetation cover to begin with (Figure 81). Such greening could reflect slow recovery from previous overgrazing or climate-induced degradation. Indeed, the P-ARB, like much of Afghanistan, experienced severe and widespread drought during several years of the analysis period (2000-2001, 2007-2009, 2011-2013, and 2016-2018), and this likely contributes to degradation and desiccation processes. Still, the positive trends in green vegetation observed in these regions likely reflects lower vulnerability than those regions with declining trends.

Ecosystem Protection Status

AC

Indicator overview

Unique ecosystems are composed of different life forms, which provide different ecological functions and have different evolutionary histories. Ecosystem protection, through the establishment of protected areas, is a leading and effective conservation strategy (Watson et al. 2014). Protected areas act to reduce human pressure on landscapes, keeping ecosystems more intact, with greater species diversity and habitats of higher integrity. Ensuring that a minimum proportion of each unique ecosystem is under protection constitutes one of the global targets for biodiversity conservation in international agreements.

Conserving a representative sample of ecosystems is also an effective strategy for mitigating the negative impacts of climate change. For example, enhancing ecosystem representation under protection increases adaptive capacity by allowing ecosystems to restore naturally. It also allows organisms to shift their geographic ranges as the climate changes to find suitable habitats

Ecosystems that lack protection tend to be more vulnerable to climate change because there are no restrictions on development or extractive activities that lead to ecosystem degradation. Maintaining ecosystem integrity is a key defense mechanism against climate change (Martin and Watson 2016), so ecosystems with greater human pressure and without adequate protection measures often have reduced adaptive capacity.

Methods overview

For this indicator, we analyzed the degree to which unique ecosystems, known as ecoregions, are currently under legally designated protected areas. We used the definitive dataset on ecoregions produced by the World Wildlife Fund (Olson et al. 2001, Dinerstein et al. 2017) and maps of currently established protected areas provided by the Afghanistan government. We considered only PAs that were legally designated by December 2020 (up to when the analysis was conducted), which included Band-e Amir, Wakhan, Bamyan Plateau, Shah Foladi, and Kol-e-Hashmat Khan. In this case, 'designated' means by law that a justification process has been implemented and a justification document has been validated by the National Environmental Protection Agency (NEPA) of Afghanistan. The legally designated PAs are also deemed to be functional as they receive funding from the government and have either management plans or detailed justification documents. Using the set of legally designated PA delineations, we calculated both the total and protected land area of each ecoregion within the P-ARB and divided protected by total to calculate the proportion of each ecoregion under protection.

Spatial representation of indicator

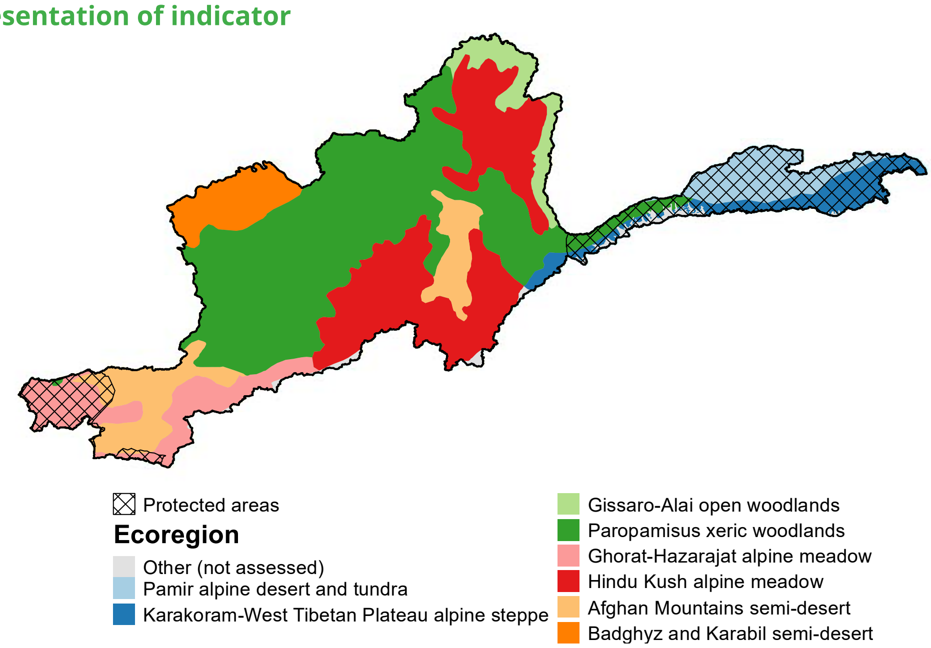

Figure 85. Representation of ecoregions by designated protected areas.

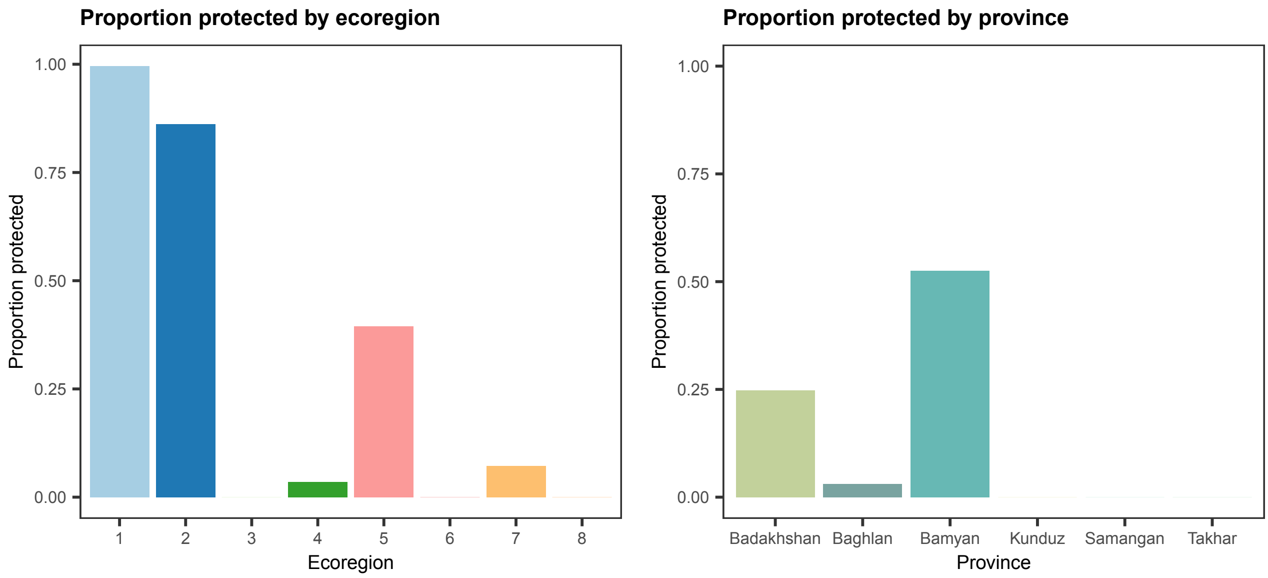

Figure 86. Proportion of ecoregions and provinces under protected areas. Ecoregion legend: 1 – Pamir alpine desert and tundra; 2 – Karakorum-West Tibetan Plateau alpine steppe; 3 – Gissaro-Alai open woodlands; 4 – Paropamisus xeric woodlands; 5 – Ghorat-Hazarajat alpine meadow; 6 – Hindu-Kush alpine meadow; 7 – Afghan Mountains semi-desert; 8 - Badghyz and Karabil semi-desert.

Results summary

Ecoregions varied widely in their representation under protection. The Pamir alpine desert and tundra and Karakorum-West Tibetan Plateau alpine steppe ecoregions have high levels of protection (99.6% and 86.2% protected, respectively) due to the presence of Wakhan National Park in the upper reaches of Badakhshan. The Ghorat-Hazarajat alpine meadow ecoregion in the southwest of the P-ARB also has relatively high levels of ecosystem protection (39.4% protected), above existing recommended global targets of 17% coverage, and also above the 30% targets currently under discussion. This coverage is due to the presence of Bamyan Plateau National Park.

All of the remaining ecoregions fall well short of even the current 17% recommended target for ecosystem protection, making them vulnerable to climate change. The Badghyz and Karabil semi-desert, Gissaro-Alai open woodlands, and Hindu Kush alpine meadow ecoregions lack protection altogether, which suggests they are the most vulnerable ecoregions from the perspective of protection. But other ecoregions of general concern include the Paropamisus xeric woodlands and the Afghan Mountains semi-desert ecoregions, which both have <10% of their areas protected. These ecoregions are generally found in Baghlan, Kunduz, Samangan, and Takhar provinces. Enhancing representation of these ecoregions would likely increase adaptive capacity by allowing ecosystem recovery and promoting ecosystem integrity.

Shifts in Spatial Distribution of Ecoregions

E

Indicator overview

Ensuring that ecoregions are proportionately represented in performance of protected area and other effective conservation measures (OECM) networks is crucial for ensuring the protection of biodiversity in the face of climate change. The WWF ecoregions dataset (Olson et al. 2001, Dinerstein et al. 2017) used in the previous analysis is the most widely used global classification in conservation and spatial planning contexts (Smith et al. 2018). However, most uses of this dataset assume that ecoregions will remain static in the future, which is ecologically unrealistic. While it is well known that individual species will shift their ranges as the climate changes around them (Parmesan and Yohe 2003) (see also section 2.4 for an analysis of this in the P-ARB), recently, more attention has been paid to understanding the ways in which ecoregions themselves may shift over time in response to climate change (Dobrowski et al. 2021).

Shifts in ecoregions pose threats to biodiversity in much the same way as shifts in species distributions do. As ecoregions are characterizations of combinations of unique habitat and climate types, changes in their position are likely force species inhabiting them to move or adapt. Here, we examine how and where the ecoregions contained within the P-ARB are projected to shift as an exposure indicator of ecosystem vulnerability.

Methods overview

The methods used in this analysis are similar to those used in Dobrowski et al. (2021). We performed a principal component analysis of the bioclimatic variables produced and described in section 2.1. Those variables were created for eight different general circulation model-regional circulation model (GCM-RCM) combinations, each for two emissions scenarios, a high-emissions scenario (RCP8.5) and a low-emissions scenario (RCP2.6), giving 16 total sets of climate data. The methods below were therefore repeated 16 times, once for each set of bioclimatic variables for each model set, and then averaged by emissions scenario for two time horizons (resulting in four total maps).

The bioclimatic variables were treated as 30-year averages for three periods–present, mid-century, and end-century. We retained the first five principal components (PCs), which collectively explained over 95% of the overall variation in the data. We then used the WWF ecoregions dataset to determine the ecoregions that exist within 150 kilometers of the P-ARB, which provided an adequate distance to encompass ecoregions that both currently occur within the boundaries of the P-ARB, and that could potentially shift to within its bounds by the two time horizons considered given the pace of climate change in the region. In addition to the eight focal ecoregions described in the introduction of this report, there are nine additional ecoregions found within that distance which we considered to have the potential to occur within the P-ARB in the future, giving a total of 17 candidate ecoregions. Using the five climate PCs for the present time period, we created a convex hull around the global distribution of each of these 17 ecoregions in climate space to understand the complete set of climate conditions under which each ecoregion currently occurs, as well as the center of mass for each convex hull. We also used a global dataset of soil types to create a list of soils that corresponded to each ecoregion.

At each location, we then examined the future climate PC values and the soil type to determine which ecoregion(s) could potentially occur there at mid-century and end-century. If the climate conditions fell within the convex hulls of multiple ecoregions, and the soil type was also suitable for them, then we chose the ecoregion whose hull center of mass was closest to the projected climate conditions. This process allowed us to generate maps of predicted ecoregions, which we could then compare to the current distribution of ecoregions to determine areas of stability and change. We were also able to map areas whose future climate conditions lie outside all 17 climate hulls–we describe such areas as having no-analog climates in the future, and therefore cannot predict their ecoregion status. As some of the differences between ecoregions in the P-ARB are subtle and may not carry much biological significance, we additionally grouped them into biomes using the classification given within the WWF dataset. Using this approach, the 17 ecoregions were represented by four biomes. We then created maps of stability and change at the biome level. Changes in biome type are more likely to be biologically significant and relevant for conservation purposes than changes at the ecoregion level, and we have therefore chosen to present those maps below.

Spatial representation of indicator

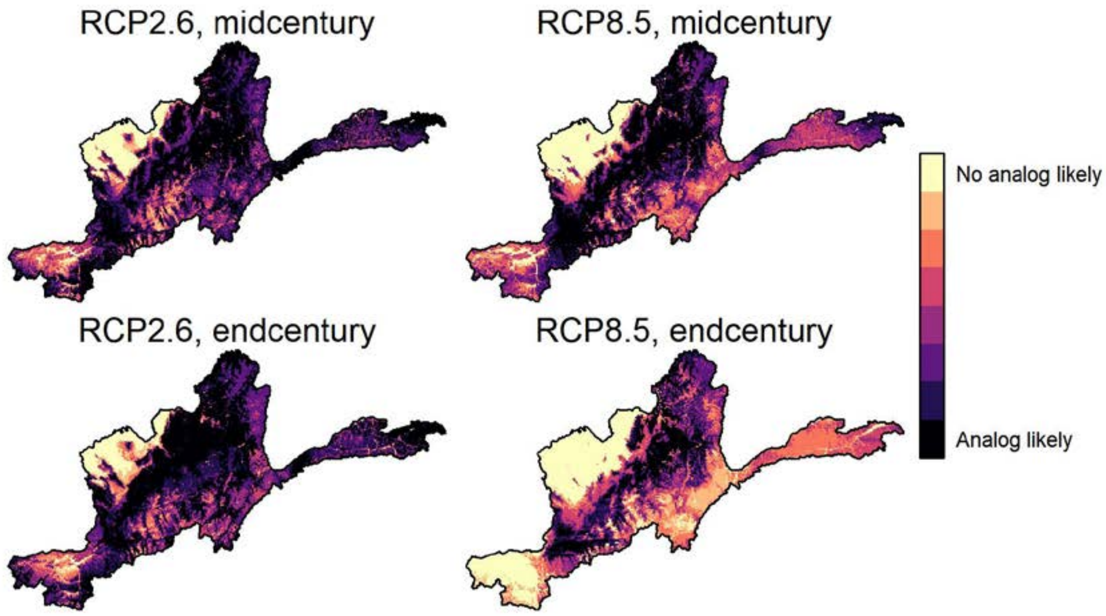

Figure 87. Likelihood of a location experiencing a climate outside the current climate envelop of all potential ecoregions. A high likelihood (hot colors) indicates a location that cannot be projected to any potential ecosystem.

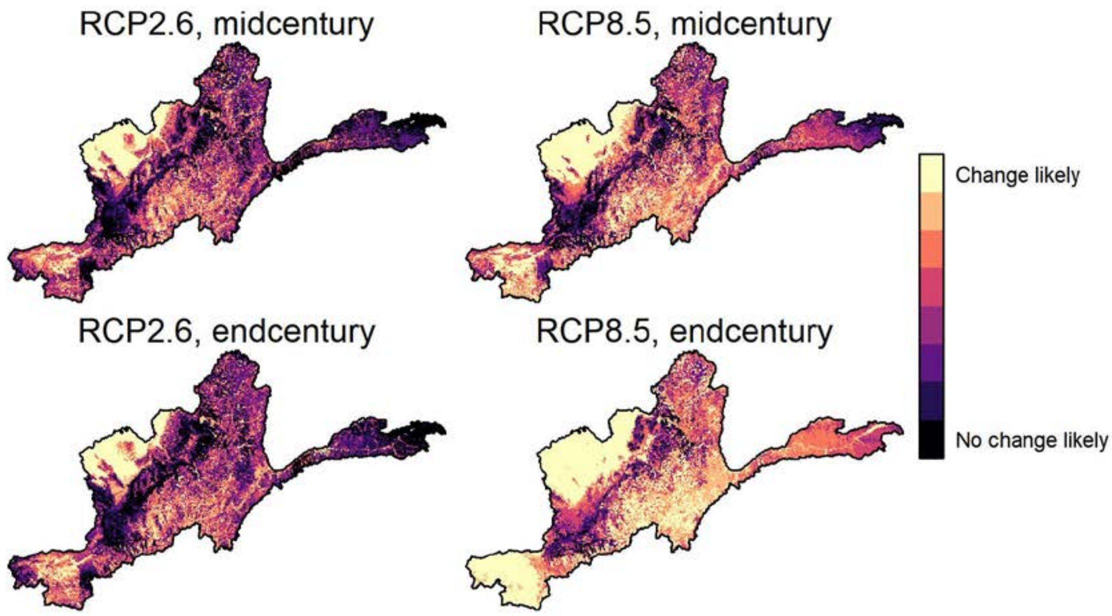

Figure 88. Likelihood of change in WWF biome type. Warmer colors (red to yellow) in the map indicate a greater likelihood of change and darker colors (purple to black) represent a lower likelihood of change (i.e., more stability).

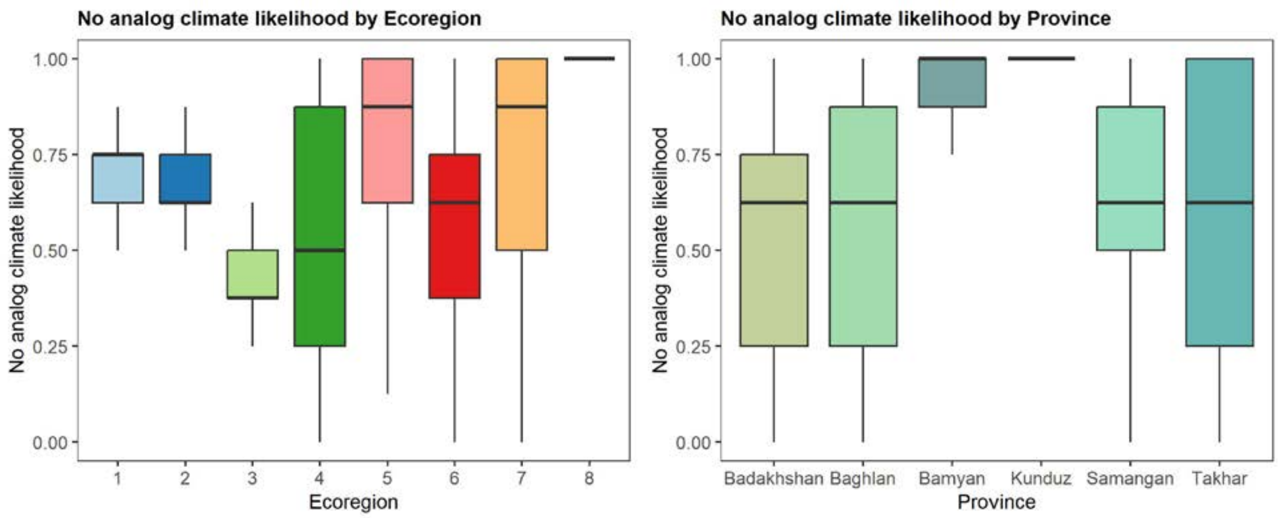

Figure 89. Summary by ecoregion and province of the likelihood of a location experiencing a no-analog climate at end-century under an RCP8.5 futures. Ecoregion legend: 1 – Pamir alpine desert and tundra; 2 – Karakorum-West Tibetan Plateau alpine steppe; 3 – Gissaro-Alai open woodlands; 4 – Paropamisus xeric woodlands; 5 – Ghorat-Hazarajat alpine meadow; 6 – Hindu-Kush alpine meadow; 7 – Afghan Mountains semi-desert; 8 - Badghyz and Karabil semi-desert.

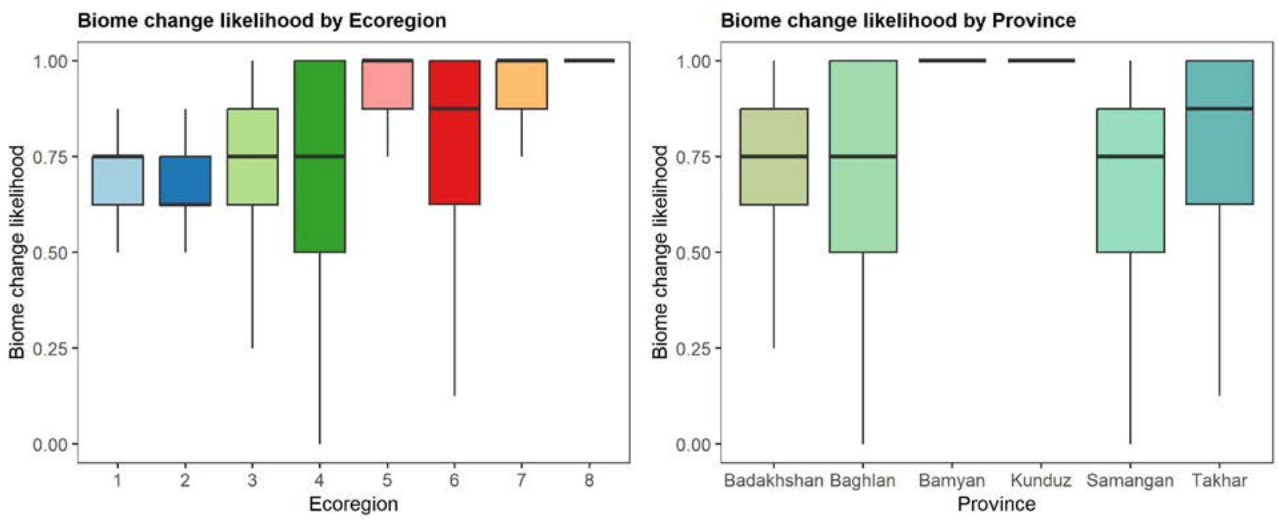

Figure 90. Summary by ecoregion and province of the likelihood of a location experiencing a projected change in WWF biome type at end-century under an RCP8.5 futures. Ecoregion legend: 1 – Pamir alpine desert and tundra; 2 – Karakorum-West Tibetan Plateau alpine steppe; 3 – Gissaro-Alai open woodlands; 4 – Paropamisus xeric woodlands; 5 – Ghorat-Hazarajat alpine meadow; 6 – Hindu-Kush alpine meadow; 7 – Afghan Mountains semi-desert; 8 - Badghyz and Karabil semi-desert.

Results summary

The results of this analysis show that no-analog climates (i.e., climates in the future that do not exist today in the region) are very likely to occur in Kunduz province even in a low-emissions (RCP2.6) scenario by mid-century (Figure 87, top left panel). Such conditions become more likely across the P-ARB by end-century and in a high-emissions (RCP8.5) future, particularly in the south and southwest (Figure 87, bottom right panel). These are also generally the areas where biome-level changes are likely to occur, with higher probabilities by end-century and under the high-emissions scenario. Under a high-emissions scenario and by end-century, no-analog climates are most likely to occur in Kunduz and Bamyan provinces, and in the Badghyz and Karabil semi-desert ecoregion (ecoregion 8) (Figure 89); the Gissaro-Alai open woodlands (ecoregion 3) are the least likely to encounter no-analog conditions. Biome-level changes are likewise predicted to be most extensive in Kunduz and Bamyan, and in the Badghyz and Karabil semi-desert ecoregion (Figure 88 and Figure 90); the Ghorat-Hazarajat alpine meadows (ecoregion 5) and Afghan Mountains semi-desert (ecoregion 7) are also projected to experience high levels of biome transitions. The Karakorum-West Tibetan Plateau alpine steppe (ecoregion 2) is projected to experience the lowest degree of biome transition, though it should be noted that the average likelihood of change is over 50% for every single ecoregion.

Thermal heterogeneity

AC

Indicator overview

Environmental heterogeneity has positive benefits for biodiversity by creating ecological niches and providing refugia (Stein et al. 2014, Carroll et al. 2017). Thermal heterogeneity—the spatial variation in temperature—provides a metric of thermal refugia for biodiversity under climate change (Elsen et al. 2020). Regions with high thermal heterogeneity have a more diverse set of microclimates that species can access to minimize extreme heat, buffer against cold winters, and track optimal thermal conditions without traveling far distances (Elsen et al. 2021). Consequently, regions with higher thermal heterogeneity provide adaptation benefits and reduce species and ecosystem vulnerability to climate change.

Methods overview

For this indicator, we analyzed spatial variability in temperature recorded from the Thermal Infrared Sensor (TIRS) onboard the Landsat 8 satellite. TIRS has collected thermal imagery since it launched in February 2013. While TIRS contains two bands (bands 10 and 11), we restricted our analysis to data from band 10 only to minimize bias introduced by out-of-field stray light that affects band 11 in particular (Barsi et al. 2014). The thermal data are collected at 100 m resolution and are then resampled by the USGS to a spatial resolution of 30 m using cubic convolution to produce the highest resolution remotely sensed thermal imagery available for the study region (Roy et al. 2014, Jimenez-Munoz et al. 2014).

We applied a cloud and water mask to all images collected between 1st January 2014 (the first full year of Landsat 8 imagery) and 31st December 2020 as our first preprocessing step. We then calculated thermal heterogeneity by assigning to the central pixel of a 5 x 5 pixel moving window the standard deviation of all pixels within the window for each thermal image, and subsequently calculating the median value for those standard deviation values across all images. Taking the median across all images minimizes differences between adjacent Landsat paths to produce a continuous and seamless map of representing the spatial variability of "average" thermal conditions across the study region.

Spatial representation of indicator

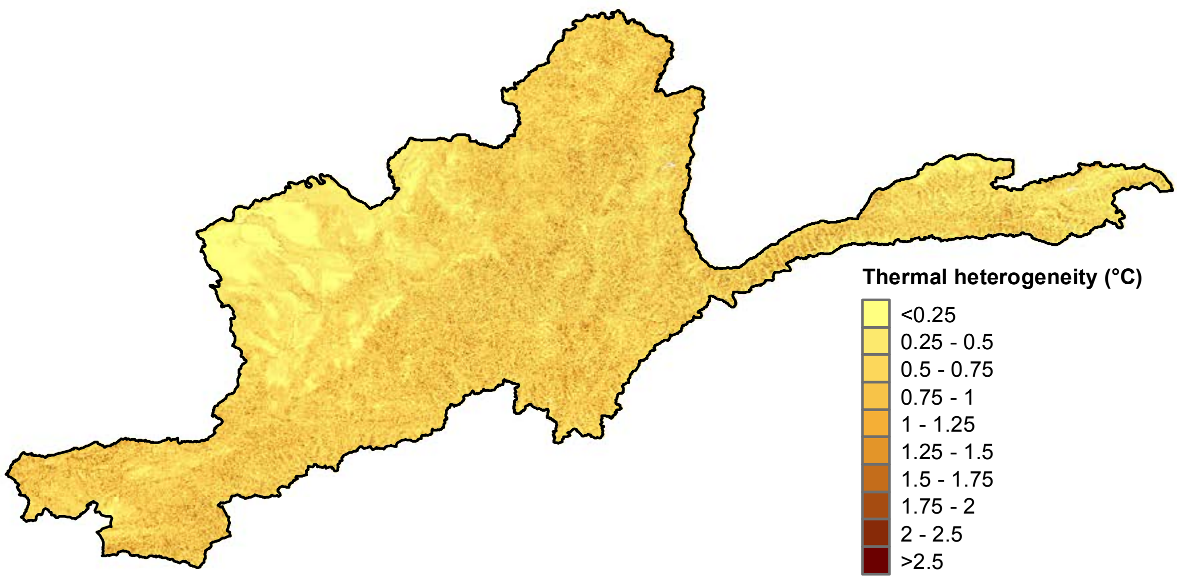

Figure 91. Thermal heterogeneity across the Panj-Amu River Basin.

Summary plots of indicator by ecoregion and province

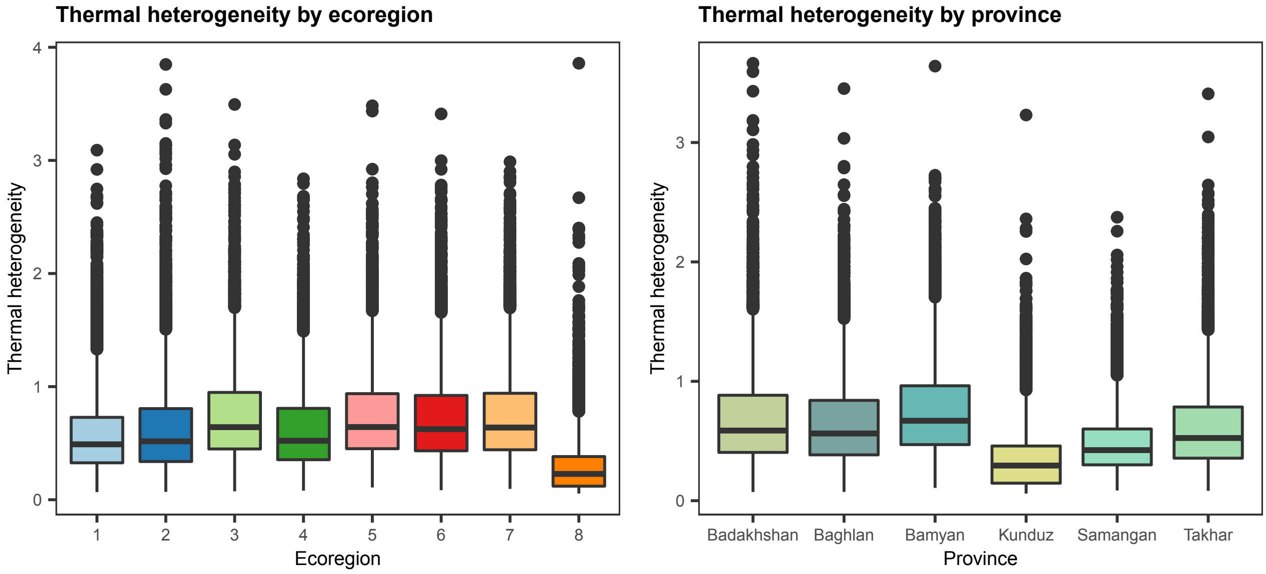

Figure 92. Thermal heterogeneity (°C) summary boxplots by ecoregion and province based on 5,000 stratified random samples. Ecoregion legend: 1 – Pamir alpine desert and tundra; 2 – Karakorum-West Tibetan Plateau alpine steppe; 3 – Gissaro-Alai open woodlands; 4 – Paropamisus xeric woodlands; 5 – Ghorat-Hazarajat alpine meadow; 6 – Hindu-Kush alpine meadow; 7 – Afghan Mountains semi-desert; 8 - Badghyz and Karabil semi-desert.

Results summary

Much of the Panj-Amu River Basin has complex topography, which drives thermal heterogeneity throughout the region. Thermal heterogeneity is generally highest in the north, northeast, and southwestern portions of the P-ARB (Figure 91). Ecoregions with the highest thermal heterogeneity include the Gissaro-Alai open woodlands (7.2% of total area has ≥1.5°C within the 22,500 m^2 [2.25 ha] analysis window), Hindu Kush alpine meadow (6.9%), Afghan Mountains semi-desert (6.5%), and Ghorat-Hazarajat alpine meadow (6.4%) (Figure 92). These regions are concentrated in Badakhshan (5.99%) and Bamyan (7.2%) provinces (Figure 92).

The western plains region of the Badghyz and Karabil semi-desert ecoregion has the lowest thermal heterogeneity (0.6%) and therefore the lowest adaptive capacity from this perspective. This is mainly in Kunduz (0.7%) and Samangan (0.7%) provinces, which contain a high proportion of agricultural area with little topographic complexity and thus less thermal heterogeneity (Figure 92).

Topographic heterogeneity

AC

Indicator overview

The spatial patterns of abiotic and ecological features are commonly used to inform conservation strategies because they are easy to measure and are often good indicators of biodiversity (Tuanmu and Jetz 2015, Farwell et al. 2020). Among environmental factors, topographic heterogeneity—the spatial variation in elevation—has a particularly strong positive relationship with species richness (Davies et al. 2007, Antonelli et al. 2018) because topographically heterogeneous landscapes contain a diversity of microclimates and habitat features that promote niche diversification, species, and species colonization (Price et al. 2014, Steinbauer et al. 2016), and provide refugia through climatic buffering (Scherrer and Körner 2010). As a result, topographically complex regions are often considered global conservation priorities (Brooks et al. 2006) and are recognized as facilitating species adaptation to climate change (Ackerly et al. 2010, Comer et al. 2015, Zarnetske et al. 2019).

Methods overview

For this indicator, we analyzed spatial variability in the continuous heat-insolation load index (CHILI) (Theobald et al. 2015) derived from the Shuttle Radar Topography Mission (SRTM) 1 arc-second (30 m) resolution digital elevation model data (Farr et al. 2007). CHILI is a modified version of the heat load index (HLI), which combined slope, aspect, and latitude to estimate potential annual direct incident radiation and thereby captures microclimatic diversity (McCune and Keon 2002). CHILI acts as a proxy for the effects of insolation and topographic shading on evapotranspiration.

We calculated topographic heterogeneity using a similar approach that we used for calculating our metric of thermal heterogeneity (see previous section) (Elsen et al. 2021). We assigned to the central pixel of a 5 x 5 pixel moving window the standard deviation of all pixels within the window of the CHILI dataset. The standard deviation of CHILI is highly correlated with a commonly-used terrain ruggedness index derived from the spatial variability in elevation values (Riley et al. 1999), but captures more components of topographic heterogeneity thought to promote adaptation potential.

Spatial representation of indicator

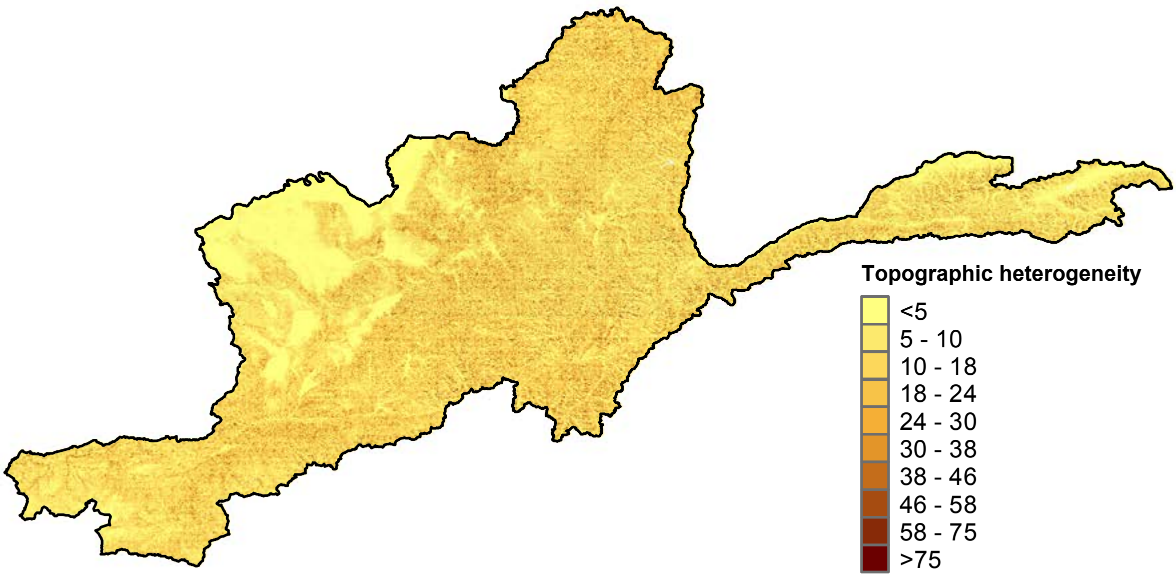

Figure 93. Topographic heterogeneity across the Panj-Amu River Basin based on spatial variation in the Continuous Heat-Insolation Load Index (CHILI).

Summary plots of indicator by ecoregion and province

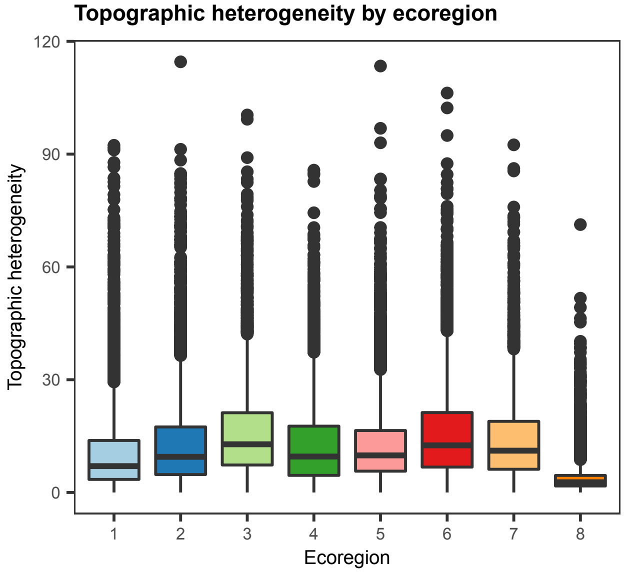

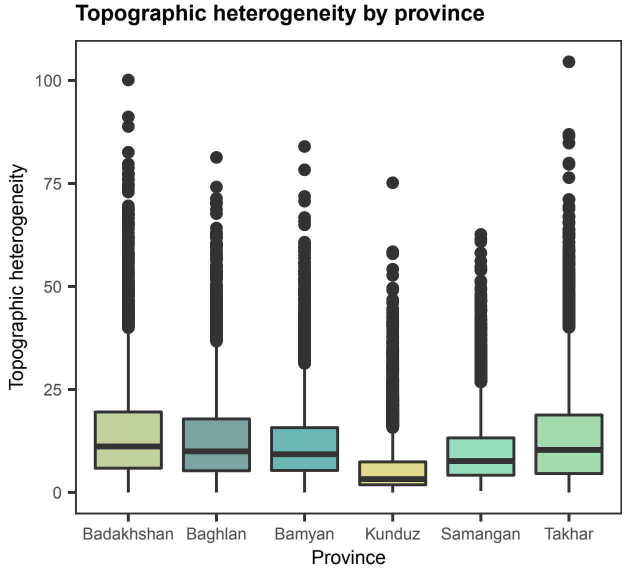

Figure 94. Topographic heterogeneity summary boxplots by ecoregion and province based on 5,000 stratified random samples.

Results summary

Much of the Panj-Amu River Basin has complex topography, which provides adaptation benefits throughout much of the region. Topographic heterogeneity shows similar patterns to thermal heterogeneity, and is generally highest in the north, northeast, and southern portions of the P-ARB (Figure 93). The Gissaro-Alai open woodlands, Hindu Kush alpine meadow, and Karakoram-West Tibetan Plateau alpine steppe ecoregions have the highest thermal heterogeneity (Figure 94). These regions are concentrated mostly in Badakhshan province, and to a lesser degree in Baghlan and Takhar provinces (Figure 94).

The western plains region of the Badghyz and Karabil semi-desert ecoregion has the lowest topographic heterogeneity and therefore the lowest adaptive capacity from this perspective. While Badakhshan has high topographic heterogeneity in general, the wide valleys of the Wakhan corridor in the Pamir alpine desert and tundra ecoregion have relatively lower topographic heterogeneity and are thus relatively more vulnerable. This is also the case for portions of Takhar and the Paropamisus xeric woodlands ecoregion.

Riparian meadow peat is a significant source of fuel for local communities and grazing for livestock in Wakhan National Park. Riparian high elevation meadows also provide other ecosystem services, such as water filtering, flood control, carbon sequestration, habitat for wildlife, and recreation.

The Bamyan Plateau in early spring after winter precipitation, showing lush green rangeland.

Policy and Management Recommendations

The analysis of ecosystem vulnerability aims to determine the current extent and condition of terrestrial ecosystems, how these have changed in the past, and how ecosystems might change in the future under climate change. The results point to several key recommendations for policy and management to retain or increase ecosystem health, which would increase the resilience of both biodiversity and local communities under climate change. These recommendations can be grouped into six domains, many of which reinforce recommendations described in other sections of this report. For each bulleted action, sub-bullets provide specific example actions that can be taken to support the overall goal, though these are not exhaustive. Some actions can meet multiple objectives and should be considered higher priorities.

1. Maintain ecosystem integrity through improved governance and better ecosystem management

- Maintain intact areas to help buffer climate impacts. Concentrations of intact rangelands located in Bamyan and Badakhshan provinces constitute priority areas.
  - Establish protected areas or other effective conservation measures
  - Create buffer zones
  - Apply more strict land-use regulations
- Slow rates of degradation. Concentrations of rangelands with degradation trends in Kunduz, Takhar, and Samangan provinces constitute priority areas.
  - Alter grazing patterns
  - Reduce dependence on livestock grazing and natural resource collection
  - Invest in alternative and sustainable sources of energy and heat
- Recover areas identified as degraded. Concentrations of degraded rangelands in Kunduz, Takhar, and Samangan provinces constitute priority areas.
  - Limit or restrict use and access for periods of the year
  - Alter grazing practices
  - Plant seeds of climate-adaptive species
  - Remove weeds and invasive species
  - Consider fire and hydrologic management as appropriate
- Establish and guide rangeland management institutions. Rangeland management institutions should be established across all provinces to ensure widespread sustainability and cohesive ecosystem management.
  - Prioritize institutions to retain high integrity rangelands and restore degraded rangelands
  - Publish and disseminate rangeland management plans
  - Update rangeland management practices following changes in local conditions.

2. Develop alternative strategies for energy generation and food production to reduce impacts on ecosystemss

- Utilize better technology, low energy savings, and alternatives. Alternative energy generation strategies should be investigated independently as such assessments were not included in this report.
  - Distribute solar cook stoves to resource-dependent communities
  - Increase hydropower capacity and distribution by building small and medium hydropower generators where water is available
  - Investigate wind power generation potential

- Invest in renewable energy sources. Alternative energy generation strategies should be investigated independently as such assessments were not included in this report.
  - Assess most effective opportunities at local scales, including solar, hydro, and wind power
  - Subsidize establishment of new energy sources
  - Create incentives for communities to use new alternative energy provided
- Distribute or subsidize efficient cook stoves and heaters. A national program to service all communities would be most effective.
  - Prioritize distribution and subsidies to most at-risk communities and in regions where dependence on natural resources is highest
- Embrace cultivation technologies and crop management techniques that maximize agricultural productivity and reduce agricultural footprints. Most agricultural recommendations apply particularly to Kunduz province given its agricultural focus.
  - Use improved irrigation systems
  - Increase pest and disease control measures
  - Embrace technical agricultural support
  - Construct and maintain food storage facilities
- Employ proper crop rotations to maximize yields. Most agricultural recommendations apply particularly to Kunduz province given its agricultural focus.
  - Determine which crops can grow in different seasons
  - Rotate crops to promote soil health, reduce soil erosion, and allow for longer growing seasons
- Plant crops that are drought tolerant with minimal need for additional water inputs. Most agricultural recommendations apply particularly to Kunduz province given its agricultural focus.Consult with plant and soil science scientists and relevant ministries to identify 'climate-smart' agriculture for the region
  - Consult with plant and soil science scientists and relevant ministries to identify 'climate-smart' agriculture for the region
  - Consult with communities to understand which crops are thriving under changing climate conditions
  - Subsidize drought-tolerant crops
- Control use of ground water. Applies to all provinces (see also recommendations in Hydrology section).
  - Create/improve water storage and capture facilities to improve irrigation systems and reduce runoff
- Understand where rainfed agriculture systems are at risk from future reductions in precipitation and use in agricultural planning and to prevent the conversion of natural ecosystems to rainfed agriculture systems with limited productivity potential. A more detailed assessment of rainfed agriculture distributions is needed to target recommendation to specific geographies.
  - Overlay climate model projections for precipitation with spatial maps of rangeland condition to identify where low-quality rangelands will remain potentially suitable for rainfed agriculture in the future

3. Perform large scale reforestation and restoration activities to increase extents of critical natural ecosystems

- Initiate tree planting campaigns to reforest communities and regions of high reforestation potential. A systematic reforestation potential analysis was not conducted, but these areas will be along rivers and valleys adjacent to communities in all provinces, especially at lower elevations.
  - Target and adapt plantings to serve multiple purposes and thrive in different contexts, e.g., plant trees to reduce soil erosion, provide shade, act as wind breaks, and provide habitat for wildlife
- Use native plant species that are climate resilient and provide wildlife habitat. Pistachio and juniper are important tree species for both people and wildlife, and may persist in extreme temperature conditions throughout much of the P-ARB.
  - Use species that are drought and frost tolerant
  - Plant trees creating a natural mixed community rather than monoculture plantations
  - Plant trees where wildlife would likely use them, such as along rivers, ridgelines, or other natural corridors
- Consider reforestation for biomass production. Willow and poplar could be considered for this purpose, and to provide other ecological services. They grow in a wide variety of climates so could be used in many parts of the P-ARB.
  - Establish fast-growing tree species that can support wood production for fuel
  - Balance biomass production reforestation with other reforestation objectives described above
- Focus reforestation on riparian areas to improve wildlife movement potential and restore healthy freshwater ecosystems. This should be a major aim across all river and stream networks, especially those spanning elevational gradients as in Badakhshan and Bamyan provinces.
  - Plant tree and shrub species known to be used by important wildlife
  - Maintain adequate buffers around riparian areas to reduce sedimentation and introduction of pollutants into water
- Propagate grassland restoration activities in heavily degraded grasslands. Kunduz, Takhar, and Samangan provinces have high rates of rangeland degradation that would be priorities for grassland restoration activities.
  - Plant native grasses and shrubs that are climate resilient
  - Actively remove invasive weeds and maintain invasive weed prevention initiatives
  - Employ sustainable livestock management practices
- Limit expansion of human habitation within and adjacent to protected areas. Protected areas in Bamyan province should be especially prioritized.
  - Create and enforce zoning restrictions for all protected areas

4. Expand the protected area network

- Increase the total amount of area under protection. Kunduz, Samangan, and Takhar are most underrepresented within the P-ARB and should be prioritized for new protected areas.
  - Create new protected areas and other effective conservation measures
  - Commit to meeting international targets set by the Convention on Biological Diversity and recommended in National Biodiversity Strategic Action Plans
- Ensure that protection is representative of the diverse ecoregions and biodiversity present in the P-ARB. Gissaro-Alai open woodlands, Hindu-Kush alpine meadow, and Badghyz and Karabil semi-desert ecoregions are unprotected and require most urgent attention to increase ecosystem representation.
  - Stratify ecosystem protection by ecoregion and ensure that each ecoregion has roughly the same amount of protection relative to its size

- Consider future climate change shifts in ecosystems and biodiversity in protected area planning. Shifts will mostly occur in Kunduz, Bamyan, and Badakhshan provinces, but conservation planning should be done across all regions to systematically allocate priorities.
  - When prioritizing additional protection, explicitly include climate change variables and ecosystem and biodiversity forecasts in assessments
- Ensure both habitat (structure) and climate (functional) connectivity between protected areas to help adapt to changes. Currently applies mostly to Bamyan and Badakhshan provinces given current protected areas, but as new protection is established it would apply throughout the P-ARB.
  - When prioritizing additional protection, consider the isolation of protected areas, both in terms of the surrounding matrix and human land uses that would impede wildlife movement, and in terms of how suitable the climate is projected to be in the future that could potentially facilitate wildlife movement
- Utilize other effective area-based conservation measures. This strategy can be employed equally in all provinces.
  - Develop locally governed and managed areas for conservation purposes that monitor and evaluate biodiversity and ecosystem outcomes
  - Consider adopting conservation easement model of recognized conservation of important habitat on private lands
- Establish buffer zones around protected and conservation areas. Currently applies mostly to Bamyan and Badakhshan provinces given current protected areas, but as new protection is established it would apply throughout the P-ARB.
  - Create buffer zones managed by local communities that limit human encroachment and resource extraction around protected and conservation efforts to strengthen conservation in the core protected area

5. Educate the public about the importance of ecosystem health

- Develop community education program on actions for sustaining ecosystem health suitable for all ages. Should be a national effort applying equally to all provinces, but material could be tailored to specific geographies.
  - Develop government, university, or non-profit led sets of educational programs that would be delivered at schools and other community centers and made available online
- Mainstream environmental education in the national education curriculum. Should be a national effort applying equally to all provinces, but material could be tailored to specific geographies.
  - Use textbooks and educational resources that include environmental education material
  - Make taking at least one course focused on environmental education mandatory
- Create courses and modules at the university level, including opportunities for research in forestry and ecosystem management. Should focus on top universities for all provinces, including Kunduz University, Badakhshan University, Bamyan University, Samangan University, and Takhar University. The modules should be systematically developed but tailored to specific needs in each province.
  - Expand university curricula within Afghanistan with departments, programs, and degrees specializing in sustainable ecosystem management and conservation science
  - Hire faculty to lecture and train students and conduct independent research in these fields
- Create jobs that utilize education and training in ecology and ecosystem management. Job creation should be focused on all universities as mentioned in the previous recommendation.
  - Create environmental monitoring and consulting positions, research and teaching positions, and technical/analytical positions with local and national institutions

6. Establish a system for long-term ecosystem monitoring

- Monitor ecosystem health and biodiversity within protected areas to ensure proper protection and functioning. Currently applies mostly to Bamyan and Badakhshan provinces given current protected areas, but as new protection is established it would apply throughout the P-ARB.
  - Focus on at-risk species described in this report
  - Follow monitoring protocols employed in this report and described in further detail in the Indicator Protocols document
  - Ensure monitoring is conducted at regular intervals and that records are analyzed in a timely fashion
  - Create action plans to respond to declines in ecosystem health based on observed threats
- Ensure ecosystem monitoring system uses both field-based and remote-sensing approaches. Field-based monitoring should cover all representative ecosystems; remote sensing monitoring facilitates wall-to-wall coverage.
  - Maintain active monitoring by park rangers or environmental NGO staff
  - Build capacity to analyze remote sensing datasets
  - Use cloud-computing platforms to analyze data that continuously provide up-to-date datasets
  - Validate remote sensing analysis results with field-based measurements and monitoring
- Understand where more inputs are needed as climate change will naturally stress rangelands and other ecosystems. Takhar, Samangan, and Bamyan provinces are priorities areas where natural hazards will pose increasing threats to communities; Kunduz also is at risk given high rangeland degradation currently.
  - Utilize active restoration guidance outlined in preceding sections
  - Employ adaptive management principles to adjust behaviors and actions in regions stressed by climate impacts (e.g., droughts, fires, floods)
- Create clear, enforceable criterion for sustainable ecosystem management within protected areas and other conservation areas. Currently applies mostly to Bamyan and Badakhshan provinces given current protected areas, but as new protection is established it would apply throughout the P-ARB.
  - Publish guidelines created by rangeland management associations
  - Create multi-use buffer zones
  - Maintain patrol and other enforcement officers to ensure policies are adhered to
- Develop a glacier monitoring system to understand on-the-ground changes in glacier size and extent as indicator of climate change and impacts. Applies mostly to Badakhshan province as it has the highest prevalence of glaciers in the P-ARB.
  - Combine remote sensing and field-based approaches
  - Conduct monitoring during regular intervals
  - Focus on most at-risk or influential glacier systems
  - Ensure that monitoring includes both upstream and downstream components
  - Develop emergency system for glacier dam bursts leading to mass flooding events
- Deploy weather stations across a representative sample of all terrestrial ecosystems at different elevations to monitor local climate changes and conditions. Applies to all provinces, but Badakhshan province is most underrepresented, especially high elevations.
  - Analyze existing distribution of weather station locations to identify gaps in ecosystem and elevation coverage
  - Use stations that are accurate, precise, and require minimal upkeep
  - Hire staff to maintain systems and retrieve data at regular intervals
  - Ensure systems continually operate and maintain systems in perpetuity
  - Analyze station data at regular intervals to develop appropriate management actions

- Deploy Hydromet stations within a representative sample of rivers in all sub-catchments. Applies to all provinces, but Badakhshan province is most underrepresented, especially high elevations.
  - Analyze existing distribution of Hydromet station locations to identify gaps in stream and elevation coverage
  - Ensure that monitoring extends to border regions, which will potentially require transboundary cooperation
  - Use stations that are accurate, precise, and require minimal upkeep
  - Hire staff to maintain systems and retrieve data at regular intervals
  - Ensure systems continually operate and maintain systems in perpetuity
  - Analyze station data at regular intervals to develop appropriate management actions
- Establish regular monitoring of all terrestrial ecosystems, including rangelands, forests, and riparian vegetation. Applies to all provinces and should be systematic across all ecoregions.
  - Employ monitoring protocols outlined in this document and detailed in the Indicator Protocols document
  - Ensure monitoring is systematic and conducted at regular intervals
  - Prioritize both measurements of ecosystem quantity and quality, including aspects of ecosystem structure, function, and composition
  - Prioritize monitoring of at-risk biodiversity within each ecosystem type
- Monitor human activities that disturb ecosystems such as urbanization, livestock grazing, and road network expansion. Applies to all provinces and should be systematic across all ecoregions.
  - Monitor using combination of remote sensing and field-based assessments
  - Employ Park Rangers and/or environmental NGO staff for monitoring and enforcement
  - Prioritize at-risk areas and areas with critical biodiversity and ecosystems
  - Create heavy penalties for violations in protected areas and other effective conservation measures
- Create a natural hazard warning system. Applies to all provinces, but will be most relevant for Takhar, Samangan, and Bamyan provinces that showed the highest natural hazard vulnerability across all metrics considered.
  - Develop near real-time analysis system that alerts to potential natural disaster events
  - Broadcast alerts using emergency services systems over mobile phones or through established siren warning systems

Hydrologic Vulnerability

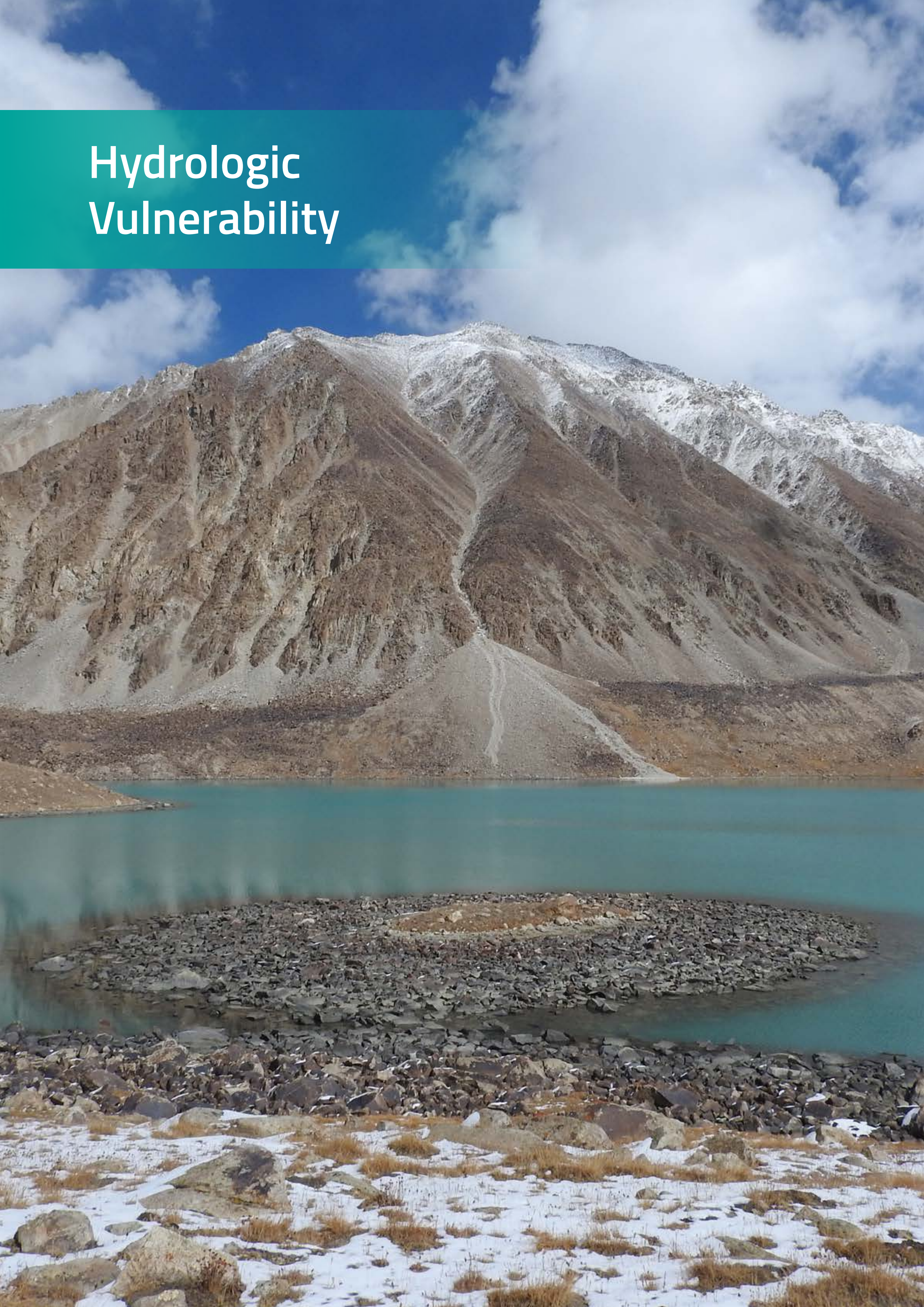

2.4 Hydrologic Vulnerability

Overview

The Panj-Amu River Basin (P-ARB) is a transboundary river basin shared among Afghanistan, Kyrgyzstan, Tajikistan, Turkmenistan, and Uzbekistan and is a primary water resource for human populations and ecosystems. It consists of four sub-basins, including Panj (28,490 km^2), Kokcha (22,450 km^2), Khanabad (12,018 km^2), and Kunduz (28,038 km^2). The P-ARB covers ~95% of the total glacier area in Afghanistan (2438 km^2), therefore, snow- and glacier-melting processes are important sources of the streamflow that contribute around 80% of the annual runoff in this basin. The P-ARB drains over half (57%) of Afghanistan's annual water flow, despite the fact that it only covers 14% of the country's land area and is the most productive region with the remarkable return capacity on additional investment in water resource development. However, the P-ARB's hydrological regime is vulnerable to the impact of climate change, which is expected to affect its snow and glacier cover and consequently poses a high risk of extreme hydrological events to both people and ecosystems. The change in runoff within the P-ARB is also expected to have large impacts on downstream water availability, especially for irrigated agriculture, which relies heavily on water withdrawal. Yet it is unclear as to what extent the basin is vulnerable to hydrological risks. Therefore, the current study was initiated using advanced modeling approaches to advance an understanding of current and future hydrological regimes within the P-ARB.

Hydrological modeling under current and potential future climate change scenarios

To model current and future hydrological conditions within the P-ARB, we setup and tested two hydrological modeling approaches (SWAT and J2000) based on data available in the existing hydro-meteorological stations in P-ARB. The J2000 model was selected as the preferred model to simulate hydrological conditions in the basin due to the dominant hydrological processes and accuracies of the results from both models. The J2000 model was first set up and evaluated based on historical datasets, then it was run for future climate projections using an ensemble of eight GCM/RCM downscaled and biased adjusted climate projections. The model outputs were further analyzed to extract hazard indicators (mean, minimum, maximum and standard deviation) of changes in river discharge in order to visualize the spatial and temporal distribution of current and future river discharges in each sub-basin.

Current hydrological regime of P-ARB

This study explored each sub-basins of the P-ARB separately due to their unique hydrological characteristics in terms of snow and glacier, soil, climate, and altitude. The mean annual runoff for the entire basin during the baseline period (1980-2009) was ~988 mm, while the contributions from each sub-basin amounted to 51, 273, 319, and 345 mm for Kunduz, Khanabad, Kokcha and Panj sub-basins, respectively. Moreover, for the baseline period (1980-2009) the runoff peak for Kunduz was simulated at ~8 mm in May and June with a minimum runoff of ~2.5 mm in September, whereas for Khanabad and Kokcha sub-basins, the peak runoff shifted to June and July, with values of 40-50 mm and 50-60 mm, respectively, and a minimum runoff of ~10 mm as baseflow from November to February. While the peak runoff for Panj sub-basin was almost constant at ~43 mm from May to August, the minimum runoff was simulated at ~12 mm from November to February.

Projected future changes in mean monthly runoff in comparison to baseline

When comparing future (2040-2069) with baseline (1980-2009) under RCP2.6 in Kunduz sub-basin, mean monthly runoff increased by 8-50 % from October to March, while it decreased by 2-10% in summer months (June-September). Noticeably, a new runoff peak of ~7.6 mm was generated in March, with an increase of ~8.7 mm in May. Under RCP8.5, there was a slightly smaller increase in runoff from October to March, whereas it decreased by 4-21% compared to baseline during the summer months.

In Khanabad sub-basin, the projected runoff peak under RCP2.6 remained similar as in the baseline period (June and July, it ranged 40-50 mm), but runoff was projected to increase from January to April by 13-32% (with the highest in March) and decline from August to November by 2-13% (with the maximum decreases in September). During the same months under RCP8.5, results projected a minor summer increase (1-21%) followed by a slightly greater fall/winter reduction (4-17%) in mean monthly runoff compared to baseline.

Under RCP2.6, the mean monthly runoff in Kokcha sub-basin was projected to increase from January to June by 10-50% (with a maximum increase in March and April) and the peak runoff was projected to shift from July to June and reduce by ~61 mm. In July to December, mean monthly runoff was projected to decline by 2-20% (with a maximum reduction in July and August). During the same months under RCP8.5, results projected a similar trend of summer runoff increase (5-50%) and fall/winter runoff reduction (8-28%) compared to baseline.

In Panj sub-basin, which has a greater proportion of glaciers than the other sub-basins (it covers 72% of all glacier area of Afghanistan), results projected an increase in mean monthly runoff under RCP2.6 of 4-60% from November to August (with a maximum increase of ~60% in February to April, and a rise of 17-34% in summer months) compared to baseline. Projections under RCP8.5 showed that the wettest conditions increased by 4-62% throughout the year compared to baseline, with the highest rise in spring months (~62%) and projected increases in the summer months ranging from 34-60%.

Overall, the P-ARB demonstrated pronounced spatiotemporal changes in river runoff. Projections for the western part of the basin (Kunduz and Khanabad sub-basins) under both scenarios indicated drier conditions in the summer months that could negatively impact summer irrigation (this trend was accelerated under RCP8.5). Projected early spring peaks, on the other hand, could result in flooding. In addition, due to earlier snowmelt, the central and southern parts of the basin (Kokcha sub-basin) are projected to experience an increase in both spring and early summer runoff. Furthermore, for the eastern part (Panj sub-basin) under RCP2.6, the results projected considerable increases in runoff throughout the year, mainly in spring and summer, whereas under RCP8.5 summer runoff was projected to increase further due to greater melting of glaciers. Both scenarios indicated a significant likelihood of flooding in this area of the Panj sub-basin during the spring and summer months.

Hydrological hazards (peak river discharge changes) in current and future

Considering the current and future periods, the Panj sub-basin had the highest projected change in discharge among all sub-basins. For instance, under RCP2.6, the discharge peak of 890 m^3/s would equate to flooding events that occur roughly 10 times more frequently, i.e., from floods having a return period of 29-31 years currently, to floods having a return period of just 1-3 years. Under RCP8.5, such floods are projected to be just as frequent (i.e., return periods of 1-3 years), but more intense (i.e., discharge peak of 985 m^3/s, a 10.7% increase). These results indicate that higher discharge peaks with increasing frequencies are expected under both RCP scenarios than previously experienced, although variation in magnitudes of discharge were observed across climate models for each sub-basin. In the Kokcha sub-basin, the discharge peak of 646 m^3/s was projected to have a return period of 29-31 years under RCP2.6 and 9-11 years under RCP8.5. As with the Panj sub-basin, these results show that higher discharge peaks are projected to occur more frequently under the higher emission scenario. However, such flood events were more common during the baseline period, with a return period of roughly 15-17 years. For Khanabad sub-basin, the discharge peak of 264 m^3/s had a return period of 5-7 years in the baseline period compared to a 1–3-year return period under RCP2.6 and a 3–5-year return period under RCP8.5, showing that higher discharge values are projected to occur more frequently in the future, and to a greater degree under RCP2.6 than under RCP8.5. The case was less severe for Kunduz sub-basin and while examining the return periods for maximum annual discharge, the 5–7-year flood discharge was 91.2 m^3/s under baseline; floods roughly of this magnitude would occur every 1-3 years on average under RCP2.6 and RCP8.5, respectively.

Background and Introduction

The Panj-Amu River Basin (P-ARB) is a transboundary river basin shared among Afghanistan, Kyrgyzstan, Tajikistan, Turkmenistan, and Uzbekistan and is a primary water resource for human populations and ecosystems (Figure 95). The total catchment area of the P-ARB is ~90,996 km^2 (Rakhmatullaev et al, 2010). The average mean annual precipitation is ~170 mm across the P-ARB, though annual precipitation varies widely from approximately 100 mm/year in the north-western steppes to 1000 mm/year in the south-eastern mountainous areas. Within this region, there is a high rate of evapotranspiration (ranging from 1,500– 2,000 mm/year) that results in a great volume of water going back into the atmosphere (Rakhmatullaev et al, 2010).

Melt from glaciers and high elevation snowpacks in the mountains of Tajikistan, Afghanistan, and Kyrgyzstan, generates a considerable amount of runoff. Hence, water runoff generation is the highest in the upstream countries while water consumption is highest in the downstream countries, i.e., Uzbekistan and Turkmenistan (Agaltseva 2005). According to Froebrich and Kayumov (2004), around 80% of the annual runoff is due to the melting of snow and glaciers in the Pamir mountains within the P-ARB. Over half (57%) of the annual water flow of all of Afghanistan is drained from the P-ARB, though it covers only 14% of the area of the country.

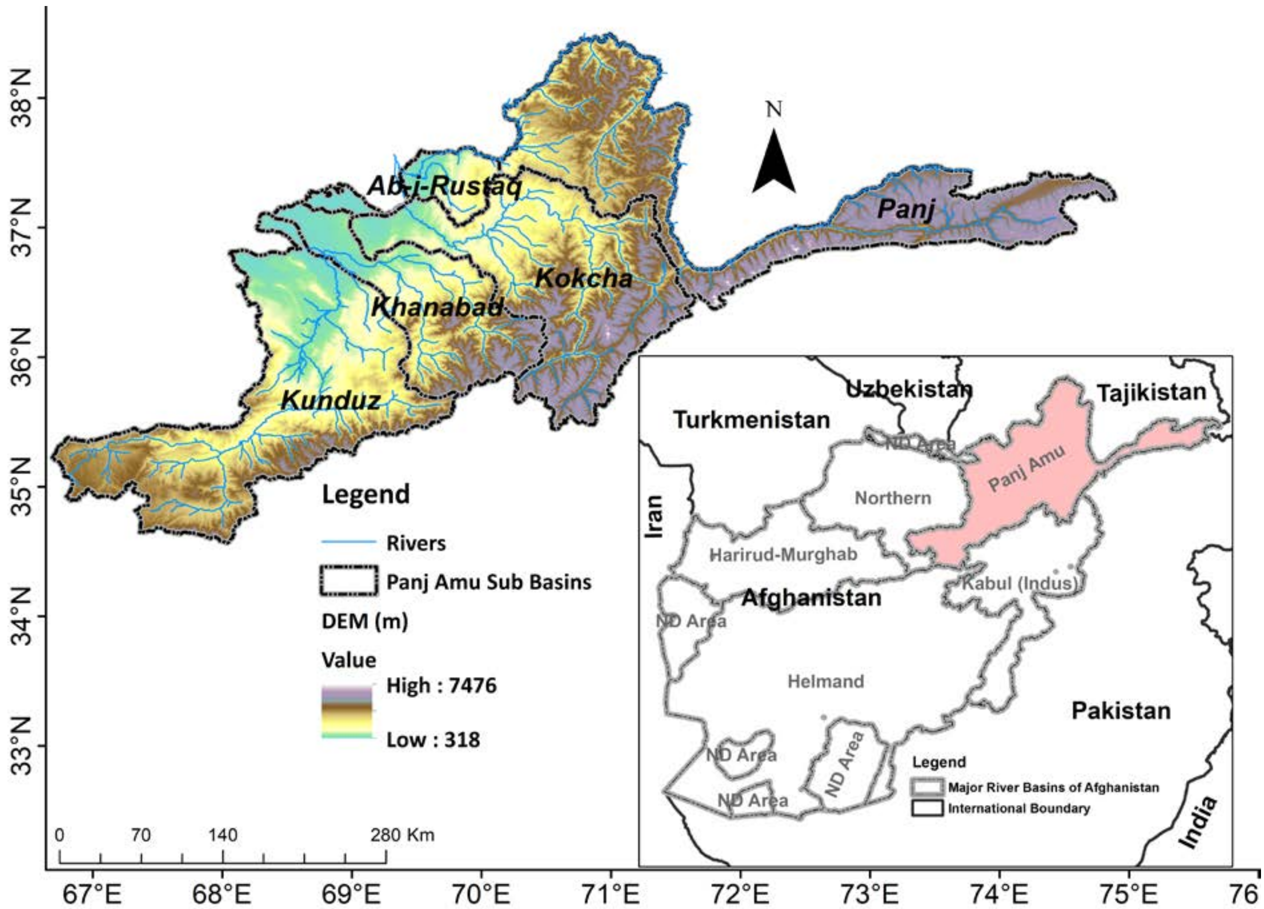

Figure 95. Location of the Panj-Amu River Basin in Afghanistan and neighboring countries.

Figure 95 also depicts the elevational distribution and river networks of the five sub-basins of the P-ARB, including Panj, Kokcha, Abi-Rustaq, Khanabad, and Kunduz.

Water availability in this region is of strategic importance for the agricultural economies; hence, agriculture is the primary sector (responsible for 90% of available water consumption) on the basis of which water management policies are governed in the region (Abdullaev et al. 2009). The hydrological network within the P-ARB is the most productive water source for Afghanistan and neighboring countries, which irrigates an estimated area of 6 million hectares. Its irrigation coverage area upstream encompasses 1.15 million hectares in Afghanistan, 0.5 million hectares in Tajikistan, and 0.1 million hectares in Kyrgyz Republic. Downstream, it irrigates 2.3 million hectares in Uzbekistan and 1.7 million hectares in Turkmenistan (Kamil, 2021). The P-ARB acts as a primary water source for ecosystems, supports potential opportunities for agriculture and hydropower, and provisions 30% of the Afghanistan's total water yield, benefitting nearly 25% of the total Afghan population (Sediqa Hassani, 2017).

According to Granit et al. (2012), there are clear indications that the melting of Central Asia's glaciers is accelerated by climate change. Approximately 20% of the ice cover in the glaciers of the Aral Sea Basin was lost from 1957–1980. Over the past five decades, there has been a notable reduction of 10% of glacier area in Tajikistan (Granit et al., 2012), while a reduction of 12.8% has been recorded in the past few decades in the Amu Darya (ICIMOD, 2021).

The Kunduz River Basin is a tributary of the Amu River. A recent study showed the implications of climate change on hydrology of the Kunduz River, where temperature fluctuations, precipitation patterns, river discharge, and changes in the land use and land cover were assessed. Since 1960, there has been a substantial decrease in river discharge due to extreme warming trends (slightly above 2°C) along with a reduction in precipitation of ~30%, an overall tendency towards drying conditions (Akhundzadah et al, 2020).

Despite the importance of the water resources in the P-ARB and the potential for changes in key hydrological processes under climate change, there is a lack of holistic investigations focusing on hydrology across the entire P-ARB. Such information is critical to go beyond narrow studies focusing only on select parameters or carried out in specific locations, such as a single river tributary. Furthermore, in order to adequately address the recent impacts of climate change, there is a need to incorporate the most recent climate data. The current study uses up-to-date climate projections that have undergone a rigorous bias-correction process to give greater confidence in results for this region (see Section 2.1 Climate Vulnerability). The results can support key stakeholders' decision-making to develop appropriate response plans for mitigation, prevention, and management.

The overall objective of this study is to develop baseline and future hydrological models for the P-ARB and evaluate regional climate vulnerability of hydrological resources that critically support ecosystems and people in the region.

The specific objectives of this study are as follows:

- To develop baseline hydrological models using in situ observations for the P-ARB
- To develop future hydrological models using a range of downscaled climate models specially developed for the P-ARB
- To understand projected spatiotemporal changes in key hydrological parameters, including runoff and discharge, across the P-ARB

Methodology

In this study, we aimed to setup and apply hydrological models for the P-ARB based on observed hydro-meteorological data available with Afghanistan entities. We considered two modeling frameworks, Soil Water Assessment Tools (SWAT) and J2000, that differ slightly in their parameterizations and outputs, but which have both been successfully applied within similar geographies. To determine the model with the best overall performance, both models were calibrated and validated using data from 42 hydro-met stations. The SWAT model was setup using a monthly timescale, while the J2000 model was setup using a daily timescale. After running the calibration and validation steps for both models, we assessed the accuracy of each to determine that the J2000 model outperformed the SWAT model, thus the J2000 model was selected for the full analysis of simulating future river discharge in the P-ARB (see Appendix 5 for a full comparison of the models and results related to the SWAT model). To simulate future river discharge, the input data from eight different global-regional downscaled climate model combinations were used. As a result of the modeling, hydrological risks were assessed using statistical indicators to show the spatial and temporal distribution of current and future river discharges in the P-ARB. An overview of the methodology is provided in Figure 96.

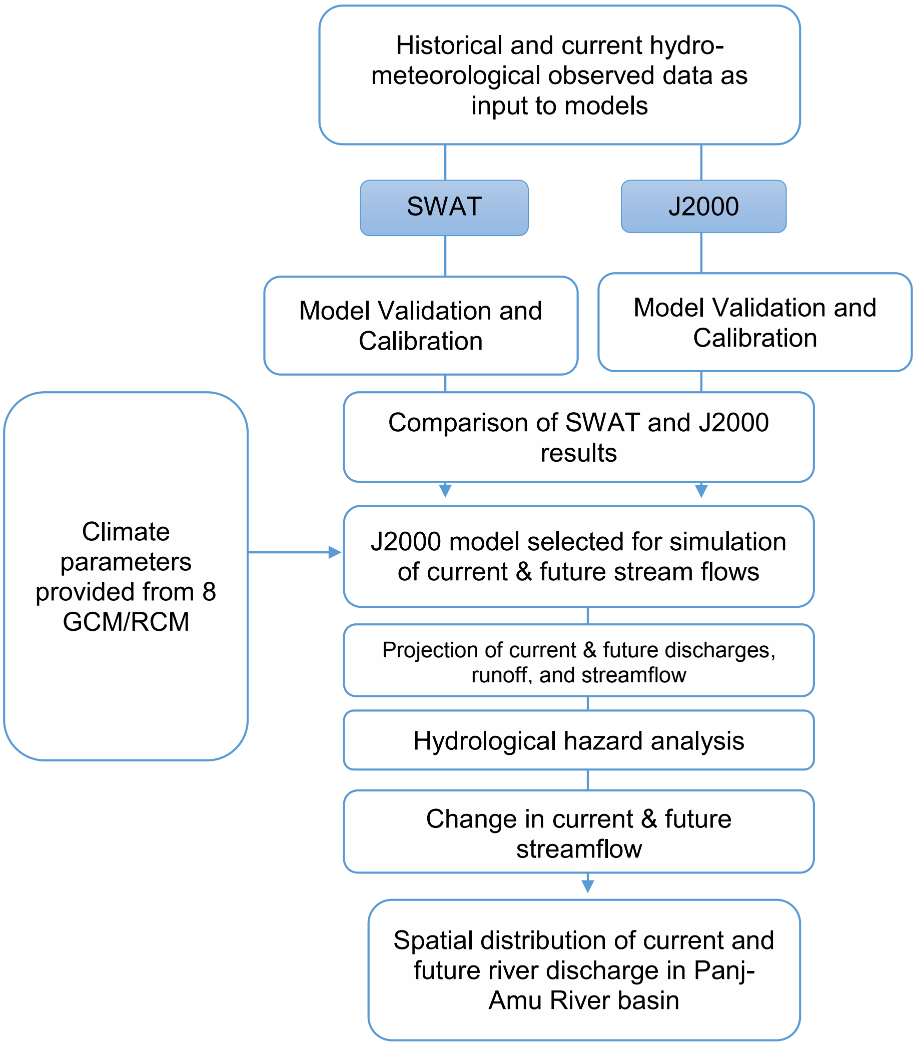

Figure 96. Flow chart of the study methodology (all information related to the SWAT model is provided in Appendix 5.

Data Collection and Preparation

In Afghanistan, different entities are responsible for collecting hydro-meteorological data, therefore, for better coordination, an orientation workshop was held on 30th December 2020. In the workshop, an introduction to the study framework, objectives, methodologies, and required datasets was presented by ROD experts to harmonize the ideas and attain the support from relevant stakeholders in providing the hydro-meteorological datasets available for the P-ARB. The stakeholders that participated in the workshop were from various relevant entities including the National Water Affairs Regulation Authority (NWARA), Ministry of Agriculture, Irrigation and Livestock (MAIL), Afghanistan Meteorological Department (AMD), Wildlife Conservation Society (WCS), and members of Afghan universities. At the workshop, officials from the mentioned organizations showed their interest and support towards the current study and presented their commitments to provide the required datasets. Following the meeting, the daily data for 42 meteorological stations were made available by NWARA and MAIL for the entire P-ARB. The datasets included precipitation, temperature, relative humidity, sunshine hours, and wind speed parameters. Figure 97 presents the river networks and locations of the hydro-meteorological stations in the P-ARB. The locations of the stations are not evenly distributed throughout the basin. Most of the stations are located in lowlands of the downstream and central parts of the basin, while only a few stations are located in the upstream part. Table 7 provides further information on all ground stations. The observed discharge data were specified as per the requirements for the hydrological model's calibration and validation. Such data were provided by NWARA for a limited number of stations presented in Figure 97 for the time period 1st January 2012 to 30th September 2019. J2000 models used four hydrological stations at the outlet of each sub-basin for model calibration and validation. Additional details on data preparation and input data for the J2000 model is provided in Appendix 5.

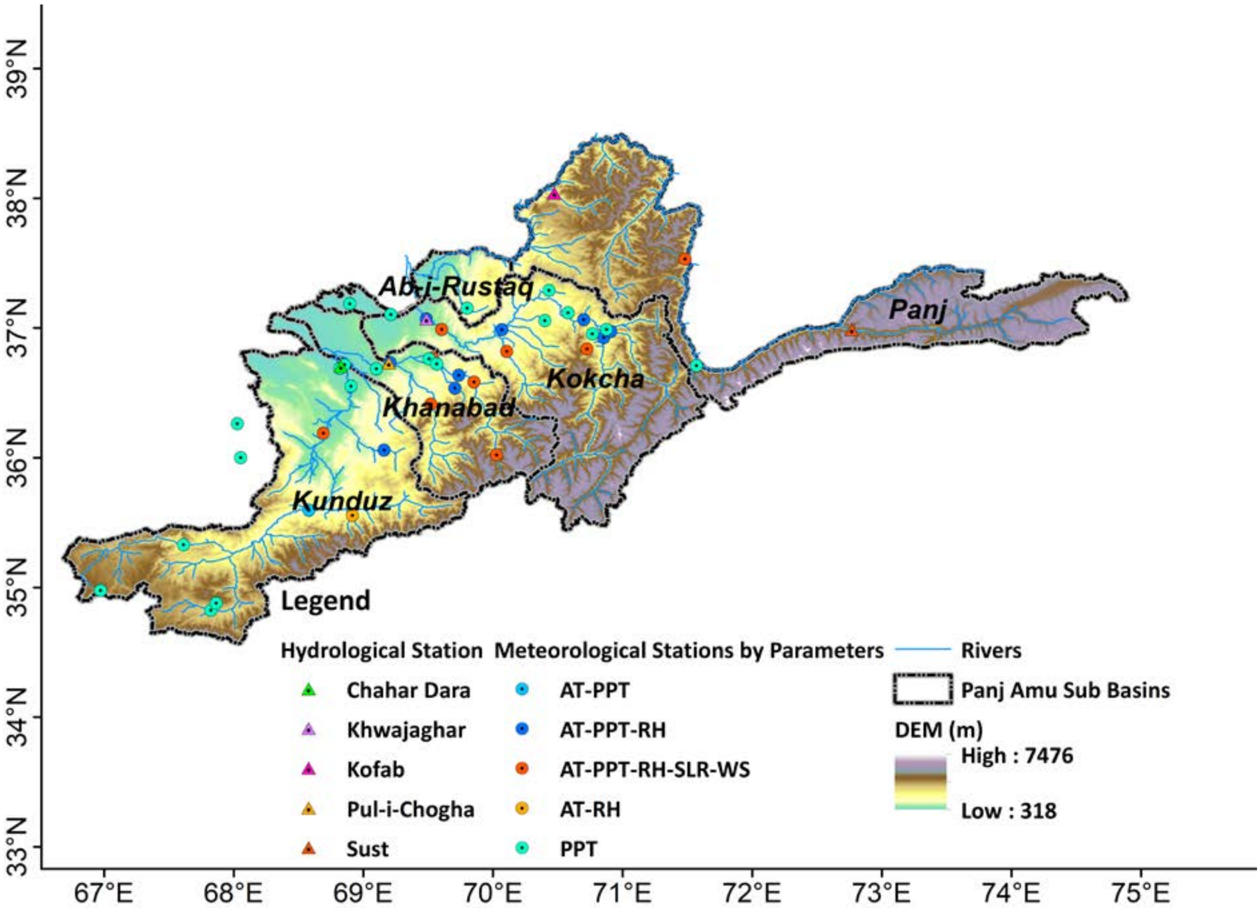

Figure 97. Location of hydro-meteorological stations in the P-ARB. Colors reflect the different climate parameters observed. AT = air temperature; PPT = precipitation; RH = relative humidity; SLR = solar radiation; WS = wind speed.

Table 7. Meteorological ground station locations and data availability periods within the P-ARB.

#	Station	Lat (°E)	Lon (°N)	Elev (m)	Parameters (Daily)	Duration	Source
1	Ali Abad	36.549	68.906	436	PPT	2008-2020	MAIL
2	Aybak	36.261	68.028	969	PPT	2008-2020	MAIL
3	Baharak	36.987	70.877	1434	PPT	2008-2020	MAIL
4	Balkh	36.766749	66.888672	342	PPT	2008-2020	MAIL
5	Bamyan	34.82178	67.82502	2531	PPT	1964-1973 & 2005-2015	AMD
6	Dara-e-Soof	35.868	67.269	1556	PPT	2008-2020	MAIL
7	Dawlat Abad	37.003743	66.841558	308	PPT	2008-2020	MAIL
8	Ishkashem	36.709	71.571	2677	PPT	2008-2020	MAIL
9	Farkhar-AWS	36.58234167	69.85538889	1137	PPT-AT-RH-SLR-WS	2012-2020	NWARA
10	Fayzabad	37.11489	70.58134	1209	PPT	1964-1973 & 2005-2015	AMD
11	Kalafgan-SSS	36.41161	69.522256	2243	PPT-AT-RH-SLR-WS	2012-2020	NWARA

#	Station	Lat (°E)	Lon (°N)	Elev (m)	Parameters (Daily)	Duration	Source
12	Keshem-AWS	36.81804444	70.10814167	987	PPT-AT-RH-SLR-WS	2012-2020	NWARA
13	Khash-SSS	36.953	70.768	2329	PPT-AT-RH-SLR-WS	2012-2020	NWARA
14	Khash	36.83643056	70.72684167	3076	PPT	2008-2020	MAIL
15	Khenjan	35.55271944	68.91745	1265	PPT-AT-RH	2009-2020	NWARA
16	Khwajaghar_AHS	37.06867222	69.48672222	488	PPT-AT-RH	2009-2020	NWARA
17	Khwa-jaghar-AWS	36.98818889	69.60495833	603	PPT-AT-RH-SLR-WS	2012-2020	NWARA
18	Kohmard	35.327	67.613	2069	PPT	2008-2020	MAIL
19	Kunduz	36.716	68.856	406	PPT	2008-2020	MAIL
20	Mazar	36.707001	67.112174	365	PPT	2008-2020	MAIL
21	Mula Ghulam	34.876	67.867	3096	PPT	2008-2020	MAIL
22	Nazdik-i- Ba-harak	36.972375	70.9108	1478	PPT-AT-RH	2009-2020	NWARA
23	Nazdik-i-Jurm	36.92581667	70.85761111	1438	PPT-AT-RH	2009-2020	NWARA
24	Nazdik Taluqan	36.63535833	69.73739444	1008	PPT-AT-RH	2009-2020	NWARA
25	Panjab	34.379	66.994	3171	PPT	2008-2020	MAIL
26	Pul-i-Bangi	36.730375	69.20813889	556	PPT-AT-RH	2009-2020	NWARA
27	Pul-i-Kun-dasang	35.59319722	68.58108056	893	PPT-AT	2009-2020	NWARA
28	Pul-i-Teshkan	36.98452222	70.07003333	818	PPT-AT-RH	2009-2020	NWARA
29	Rostaq	37.151	69.803	1230	PPT	2008-2020	MAIL
30	Sarbagh	35.999455	68.055028	1425	PPT	2008-2020	MAIL
31	Shebar	34.552461	66.799011	1985	PPT	2008-2020	MAIL
32	Sheghnan-AWS	37.53071944	71.48388333	2284	PPT-AT-RH-SLR-WS	2012-2020	NWARA
33	Sumdara	37.06352778	70.70118889	1316	PPT-AT-RH	2009-2020	NWARA
34	Takhtapul	36.663213	66.996225	396	PPT	2008-2020	MAIL
35	Taluqan_MAIL	36.722016	69.568917	825	PPT	2008-2020	MAIL
36	Tang-i-Nahrin	36.05786944	69.16081111	1190	PPT-AT-RH	2009-2020	NWARA
37	Tapa-i-Farhat-AWS	36.18820278	68.69178056	562	PPT-AT-RH-SLR-WS	2012-2020	NWARA
38	Urgo	37.056	70.403	1700	PPT	2008-2020	MAIL
39	Worsaj-SSS	36.01873889	70.028075	2666	PPT-AT-RH-SLR-WS	2012-2020	NWARA
40	Yaftal Sofla	37.289	70.435	1625	PPT	2008-2020	MAIL
41	Taluqan-AWS	36.76736667	69.53640556	847	PPT-AT-RH-SLR-WS	2012-2020	NWARA
42	Taqcha Kha-na_TMP	36.53367222	69.70823333	1472	AT-RH	2012-2020	NWARA

J2000 Model

The J2000 model is a physically-based hydrological model that is used for hydrological simulation of meso- and macro-scale catchments (Krause, 2001). This model is applied in the Jena Adaptable Modeling System (JAMS), which is a software framework for the development of component-based models and application of environmental simulations (Kralisch & Krause 2006; Kralisch et al., 2007). The model runs the hydrological processes together with different modules under the framework of JAMS described in Table 8.

Table 8. Descriptions of modules in the J2000 hydrological model (Krause, 2001; Ilmswiki, 2022).

Module	Brief description
Precipitation distribution module	Precipitation is first distributed between rain and snow, depending upon the air temperature through a certain threshold (global range: -5 to +5) (Nepal et al., 2020).
Regionalization of datasets	Based on a combination of linear regression and Inverse Distance Weighting (IDW), the model considers the horizontal and vertical variability of climate parameters and lapse rates (Ilmswiki, 2022).
Interception module	Given the Dickinson (1984) approach, the interception module uses a simple storage approach based on the Leaf Area Index (LAI) of the particular type of land cover to calculate a maximum interception storage capacity (Nepal et al., 2020; Ilmswiki, 2022).
Snow module	The snow module estimates snow depth, snow density, and snow water equivalent variables and describes the phases of accumulation, melting, and subsidence of snowpack (Nepal et al., 2020; Ilmswiki, 2022).
Glacier module	The glacier module uses an approach suggested by Hock (1999) and further adapted for ice melt estimation (Nepal 2012). Ice melt is further adapted using the slope and aspect of the particular Hydrological Response Unit (HRU) with glaciers present in the land-use type (Nepal et al., 2020; Ilmswiki, 2022).
Soil module	The soil module is the most complex part of the J2000 hydrological model, reflecting the soil zone as a regulation and distribution system. Middle pore storage (MPS) and large pore storage (LPS) represent the water-holding capacity of the soil (Nepal et al., 2020; Ilmswiki, 2022).
Groundwater module	Considering the storage and runoff behavior of the catchment geology, the model presents the groundwater runoff (Nepal et al., 2020; Ilmswiki, 2022).
Routing module	Using the commonly applied kinematic wave approach and the calculation of velocity according to Manning and Strickler (Krause, 2001), the routing inside the channel network is simulated by connecting each entity to the channel storage and receiving water from the stream channel.

The J2000 model output generates four different runoff components based on their runoff origin (Krause, 2001). The principal configuration of these model components is shown in Figure 98. Surface runoff or RD1 has the highest temporal dynamics and is fast direct runoff (Nepal, 2012). Specifically, this part includes runoff from sealed areas, saturation, or infiltration excess runoff (Ghulami 2017). On the other hand, Interflow 1 or RD2 is slow direct runoff similar to the lateral subsurface flow within the soil zone which reacts slightly more slowly (Nepal 2012; Ghulami 2017). Furthermore, there are two base flow runoff components, the relatively fast baseflow (called Interflow 2 or RG1), which contributes from the upper part of an aquifer that is more permeable due to weathering (Ghulami 2017), and the slow baseflow (called Baseflow or RG2) that flows within fractures of solid rocks or matrix flow in homogeneous loose rock aquifers (Nepal 2012).

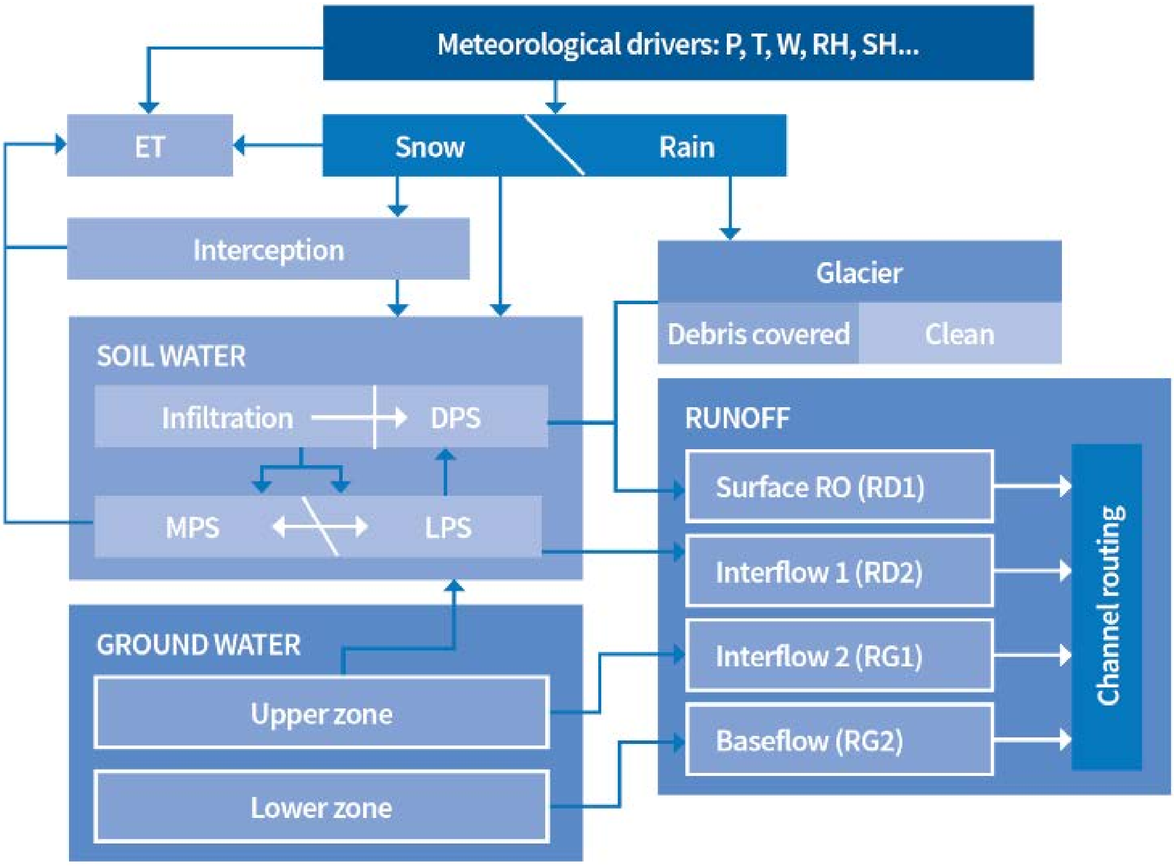

Figure 98. Principal flowchart of the J2000 model algorithm, adapted from Nepal et al. (2020). Meteorological drivers include precipitation (P), temperature (T), wind speed (W), relative humidity (RH), and sunshine (SH).

The model is applied based on five steps to simulate current and future hydrological parameters for the P-ARB (Figure 99).

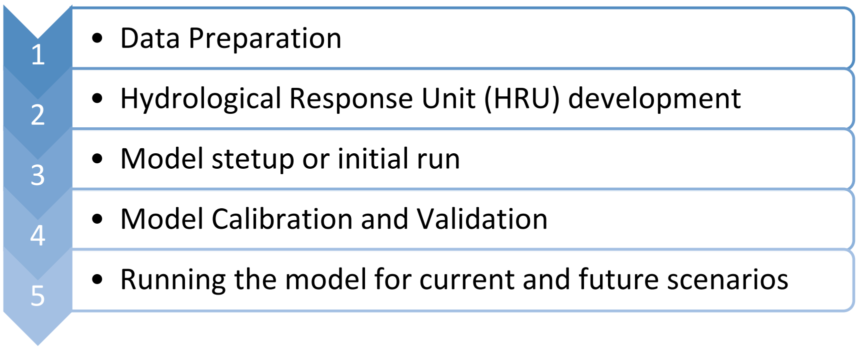

Figure 99. Application steps for modeling current and future hydrological parameters of the P-ARB.

Additional details on data preparation and input data for the J2000 model and the comparison of results between J2000 and SWAT models are provided in Appendix 5.

J2000 model setup (calibration and validation)

The J2000 model was calibrated and validated using 42 hydro-met stations data and was setup using a daily timescale. For calibration, the hydrological parameters were adjusted to obtain a better fit between observed and simulated variables until the desired model accuracy was achieved (Refsgaard and Storm 1996; Gupta and Beven 2005; Nepal 2012). To obtain optimal results, several model iterations with different parameterizations were run (parameter values used in these iterations are shown in Appendix 5). Model runs followed several steps for each iteration. First, the model was calibrated and validated from 2012 to 2019, because the observed data was available only for this period. Second, the model was run for each sub-basin separately, which helped to parameterize the model based on the characteristics of each sub-basin. This step increased the accuracy of each model compared to basin-wide model runs.

In mountainous regions, it is always challenging to regionalize precipitation data because smaller station networks tend to have spatial biases, being located at low elevations and in valleys, for example, which generally underestimates precipitation in some parts of the landscape (Nepal 2012). Therefore, the model used a regionalization approach to estimate the climate variables based on how precipitation changes with elevation (referred to as the precipitation lapse rate; details are provided in Appendix 5).

To regionalize the model, the J2000 model was calibrated and tested based on four sub-basins (Kunduz, Khanabad, Kokcha, and Panj) within the P-ARB (Figure 100). Within these sub-basins, discharge data at the outlets were used for model calibration and testing.

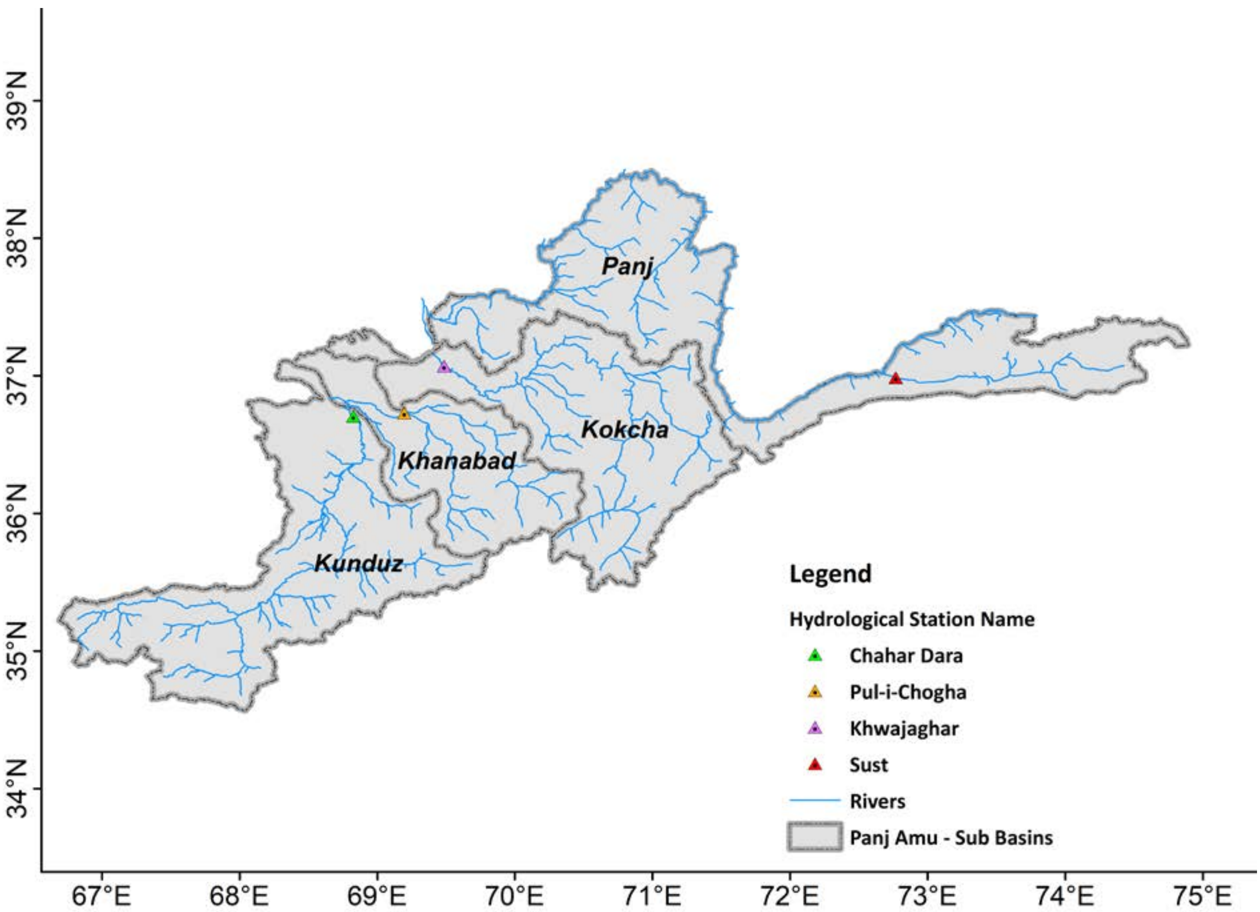

Figure 100. Location of the hydrological stations used for calibration and validation of the J2000 model for four sub-basins of the P-ARB.

Results

Current hydrological modeling for the P-ARB

Kunduz sub-basin

Daily discharge data from Chardara hydrological station were used to calibrate the model for Kunduz sub-basin (station location is shown in Figure 100). The calibration and validation periods with simulated and observed stream flows are depicted in Figure 101, while the accuracy assessment of the calibration and validation periods are presented in Table 9. For model calibration, the first four years of data from 2012-2015 were used on a daily scale and simulated results showed optimum fitting with observed data (Figure 101). The model's accuracy was evaluated based on two leading coefficients, the Nash–Sutcliffe (NS) model efficiency and coefficient of determination (r^2). The NS accuracy coefficient when considering a daily time scale was obtained as 0.65 and 0.64 for the calibration and validation periods, respectively. However, the model showed a better fit (r^2 of 0.70) when considering a monthly time scale (Table 9).

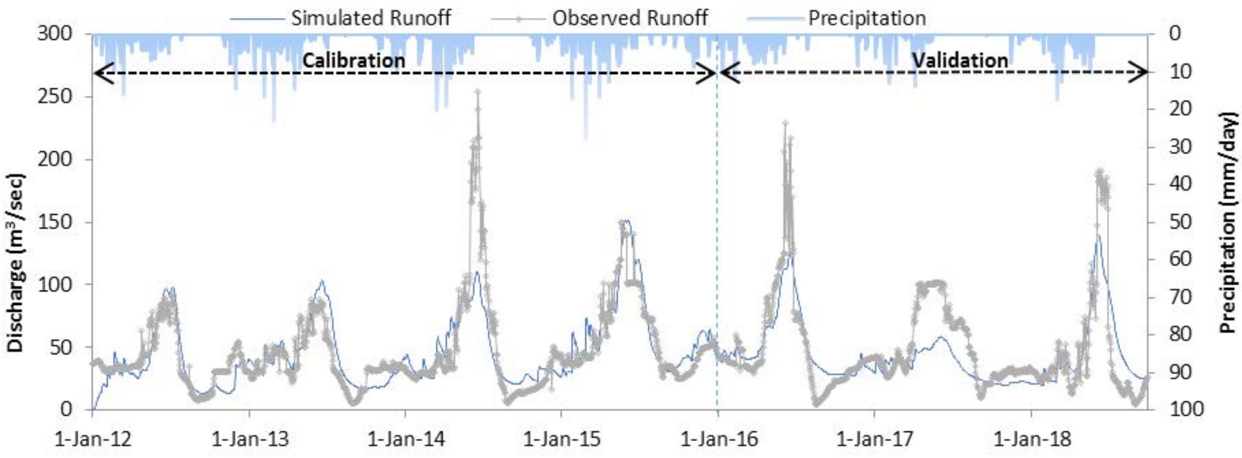

Figure 101. Simulated versus observed discharge (2012-2019) at Chardara station (Kunduz sub-basin).

Table 9. Accuracy coefficients for calibration (2012-2015) and validation (2016-2019) periods for Kunduz sub-basin.

Time scale	Accuracy coefficients	Calibration	Validation
Daily	Nash–Sutcliffe model efficiency coefficient	0.65	0.64
	Coefficient of determination (r^2)	0.66	0.68
Monthly	Nash–Sutcliffe model efficiency coefficient	0.70	0.69
	Coefficient of determination (r^2)	0.70	0.65

The results provided in Figure 102 show the contribution of different components to total runoff: surface runoff,18%, interflow 1, 39%, interflow 2, 7%, and baseflow 36% (Figure 102). The runoff peak was observed in June. Baseflow continuously contributed to the total runoff throughout the year at a rate of ~1.7 mm/month.

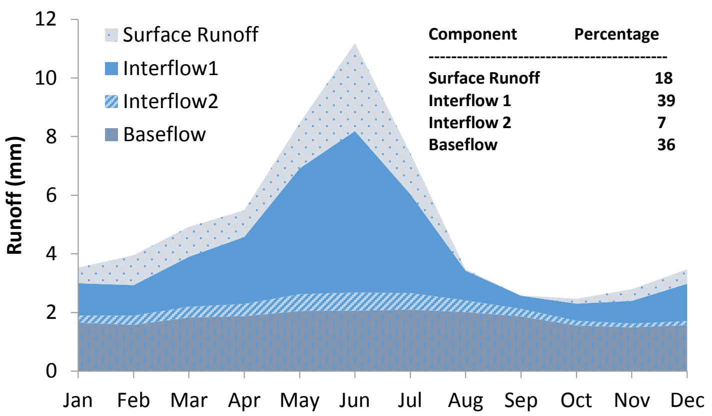

Figure 102. Simulated mean monthly runoff for Kunduz sub-basin at Chardara station (2012-2019).

Vulnerability Assessment

Khanabad sub-basin

The J2000 model performed well in Khanabad sub-basin compared to the Kunduz sub-basin, because the results showed higher accuracy for calibration and validation as depicted in Table 10. The comparison of the simulated and observed stream flows are provided in Figure 103. The daily input data for the calibration period resulted in 0.62 and 0.75 NS and r^2 coefficients, respectively, while the monthly input data led to an increase in coefficient values to 0.69 and 0.84 for NS and r^2, respectively (Table 10).

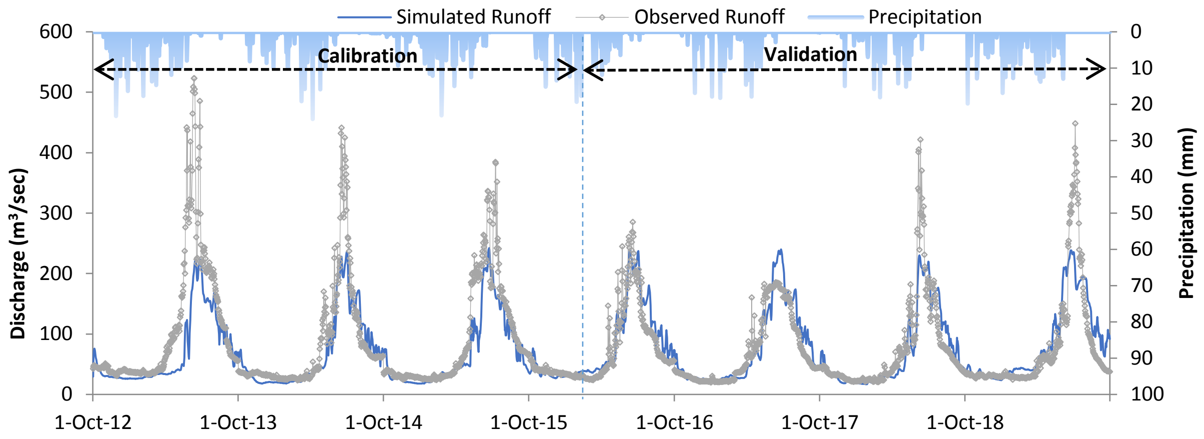

Figure 103. Simulated versus observed discharge (2012-2019) at Khanabad station (Khanabad sub-basin).

Table 10. Accuracy coefficients for calibration (2012-2015) and validation (2016-2019) periods for Khanabad sub-basin.

Time scale	Accuracy coefficients	Calibration	Validation
Daily	Nash–Sutcliffe model efficiency coefficient	0.62	0.76
	Coefficient of determination (r^2)	0.75	0.77
Monthly	Nash–Sutcliffe model efficiency coefficient	0.69	0.86
	Coefficient of determination (r^2)	0.84	0.86

The monthly total runoff components (Figure 104) showed that the surface runoff flows occurred from April until November, with a peak in June, while the baseflow feeds the river throughout the year. There were two large contributions to total runoff, the first from surface runoff (48%) and the second from the baseflow (45%). The remaining components contributed less (Interflow 1, 3%; Interflow 2, 7%).

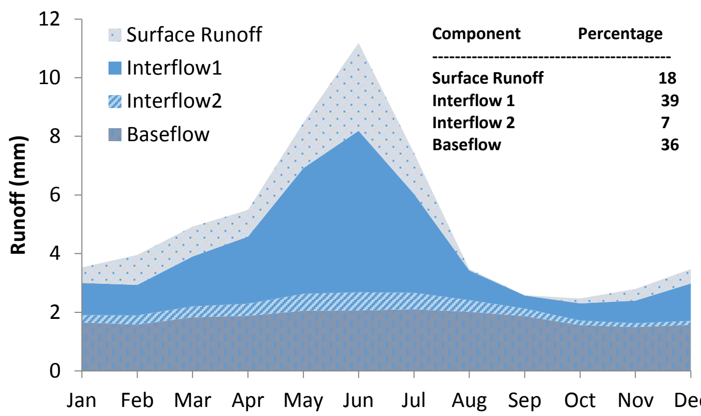

Figure 104. Simulated mean monthly runoff for Khanabad sub-basin at Khanabad station (2012-2019).

Kokcha sub-basin

In Kokcha sub-basin, glacier melting contributes to runoff. Therefore, the model had the best fit between observed and simulated data compared to other sub-basins (Figure 105). The calibration accuracy based on daily input data was 0.75 for both NS and r^2, while it increased when using monthly input data to 0.82 for NS and r^2 (Table 11). Similarly, daily data for the validation period resulted in accuracy coefficients of 0.78 and 0.79 for NS and r^2, respectively, while they increased to 0.87 for both NS and r^2 when using monthly data (Table 11).

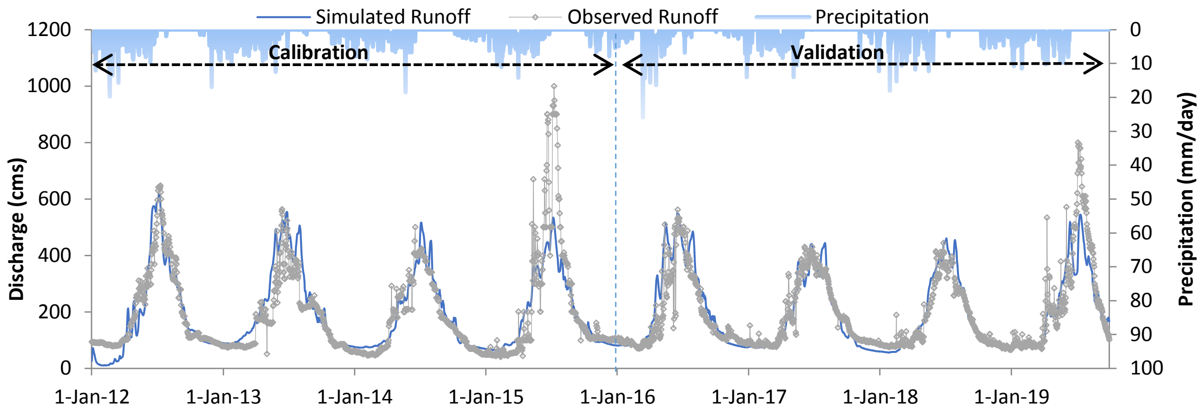

Figure 105. Simulated versus observed discharge (2012-2019) at Khwajaghar station (Kokcha sub-basin).

Table 11. Accuracy coefficients for calibration (2012-2015) and validation (2016-2019) periods for Kokcha sub-basin.

Time scale	Accuracy coefficients	Calibration	Validation
Daily	Nash–Sutcliffe model efficiency coefficient	0.75	0.78
	Coefficient of determination (r^2)	0.75	0.79
Monthly	Nash–Sutcliffe model efficiency coefficient	0.82	0.87
	Coefficient of determination (r^2)	0.82	0.88

Peak runoff in Kokcha sub-basin was observed in July and remained relatively high in August due to glacier melting. Overall, runoff in the Kokcha sub-basin consisted of 22% surface runoff, 11% interflow from upper soils (Interflow 1), 16% deeper interflow (Interflow 2), and 51% from baseflow (Figure 106).

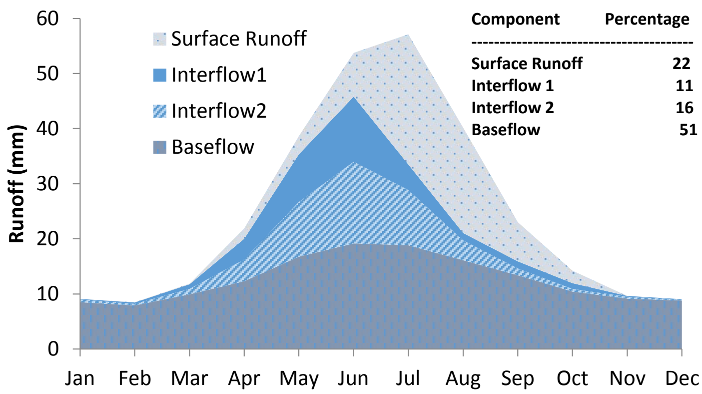

Figure 106. Simulated mean monthly runoff for Kokcha sub-basin at Khwajaghar station (2012-2019).

Panj sub-basin

Panj is a transboundary sub-basin fed by several tributaries in Afghanistan and some from neighboring countries downstream. Therefore, it was challenging to find an outlet with observed data from all tributaries of neighboring countries. For this reason, the model for the Panj sub-basin was calibrated at the Sust catchment located in the upper part of the sub-basin, within Wakhan National Park. The simulated and observed streamflow are presented in Figure 107. The model performance was evaluated based on NS and r^2 coefficients as 0.44 and 0.54, respectively, when considering daily input data for the calibration period. However, coefficient values increased to 0.56 and 0.70, respectively, when based on monthly data input (Table 12). Similarly, for the validation period, the model had NS and r^2 coefficients of 0.60 and 0.64, respectively, for daily data, and NS and r^2 coefficients of 0.71 and 0.76, respectively, for monthly data (Table 12).

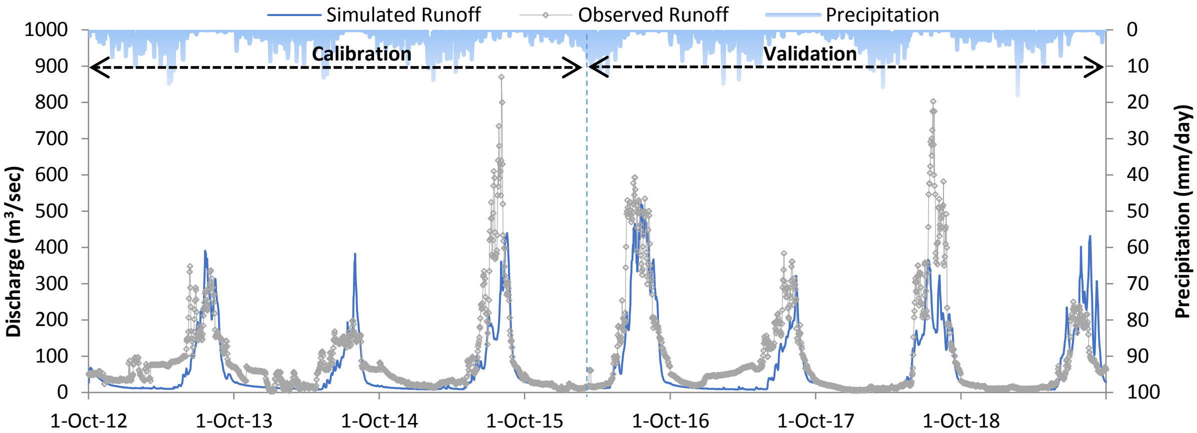

Figure 107. Simulated versus observed discharge (2012-2019) at Sust station (Panj sub-basin).

Table 12. Accuracy coefficients for calibration (2012-2015) and validation (2016-2019) periods for Panj sub-basin.

Time scale	Accuracy coefficients	Calibration	Validation
Daily	Nash–Sutcliffe model efficiency coefficient	0.44	0.60
	Coefficient of determination (r^2)	0.54	0.64
Monthly	Nash–Sutcliffe model efficiency coefficient	0.56	0.71
	Coefficient of determination (r^2)	0.70	0.76

The surface runoff at the Sust catchment is concentrated in the summer months (June to September), with peak runoff in July and August due to glacier melting contribution to runoff. Surface runoff accounts for 58% of the contribution to total runoff, while Interflow 1 contributed 11%, Interflow 2 contributed 9%, and Baseflow contributed 22% to the total runoff (Figure 108).

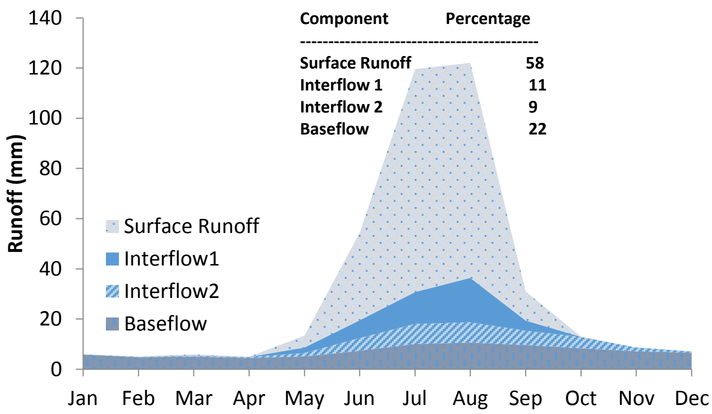

Figure 108. Simulated mean monthly runoff for Panj sub-basin at Sust station (2012-2019).

Projected changes in runoff from baseline (1980-2009 to future (2040-2069) time periods for the P-ARB

Approach to calculating projected changes in runoff under future scenarios

To simulate future runoff based on climate projections, eight downscaled climate models representing different combinations of global climate model-regional climate model (GCM-RCM) were used as described in section 2.1. The GCM-RCM combinations used are listed in Table 13. For each model, six individual meteorological variables were produced at daily timescales (precipitation, temperature, relative humidity, sunshine hours, wind speed, and solar radiation) and included as inputs to the J2000 model for 120 years (1980 to 2100).

Table 13. Global and regional climate model combinations used for future projections of climate parameters as inputs into J2000 models.

		Regional Climate Model (RCM)		
		RegCM4-7	REMO2015	COSMO-crCLIM
Global Climate Model (GCM)	MPI-ESM-LR		X	X
	MPI-ESM-MR	X		
	HadGEM2-ES		X	
	NorESM1-M	X	X	X
	MIROC5	X		

The results of simulated future runoff (2040-2069) simulated by the model for each sub-basin were compared with the baseline simulated runoff (1980-2009) under low emissions (RCP2.6) and high emissions (RCP8.5) scenarios for each GCM-RCM. To incorporate uncertainty across all eight GCM-RCM combinations, the results are presented as the mean of the eight GCM-RCMs for each sub-basin. Changes in mean monthly runoff for each GCM-RCM under two RCPs (RCP2.6 and RCP8.5) are provided in in Appendix 5 separately for each sub-basin.

Projected changes in runoff for Kunduz sub-basin

Long-term mean monthly runoff for the baseline period (1980-2009) in Kunduz sub-basin showed the highest total runoff peak (~8 mm) in May and June, while from September to January it remained steady at ~2 mm of the total runoff with ~1 mm contributed by baseflow (Figure 109). Figure 110 and Figure 111 illustrate the changes in long-term mean monthly runoff considering baseline (1980-2009) and future discharge (2040-2069) under RCP2.6 and RCP8.5, respectively. The runoff components increased in winter and spring months (November to May), but decreased in mid to late summer (June to September) under RCP2.6. Therefore, all runoff components contributing to annual runoff increased under future scenarios (under RCP2.6, increases of 0.08, 2.96, 1.89, and 2.76 mm for surface runoff, interflow 1, interflow 2 and baseflow, respectively). Under RCP8.5, there were slightly lower increases in all future runoff components compared to RCP2.6, while from May to September the runoff components declined more substantially compared to those under RCP2.6. Consequently, summer months (June to September) showed drier conditions under both scenarios compared to baseline.

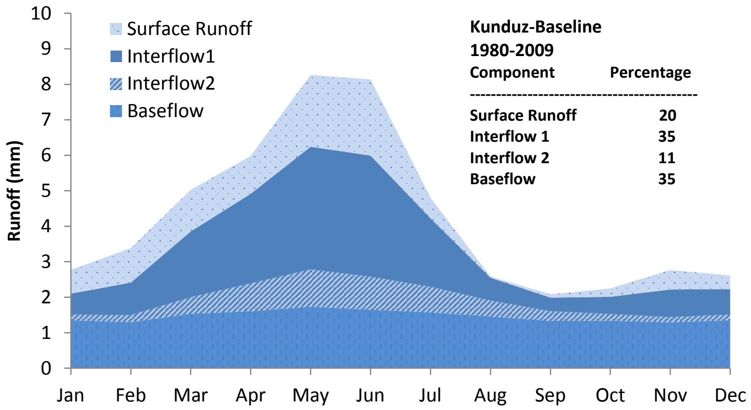

Figure 109. Long-term mean monthly runoff for Kunduz sub-basin for the baseline period (1980-2009).

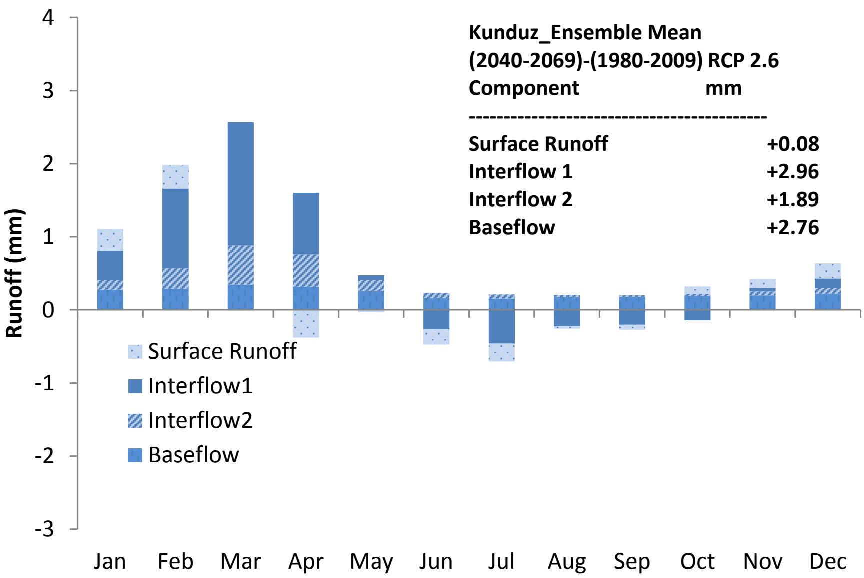

Figure 110. Projected changes in mean monthly runoff for Kunduz sub-basin under RCP2.6 using an ensemble mean of eight climate models.

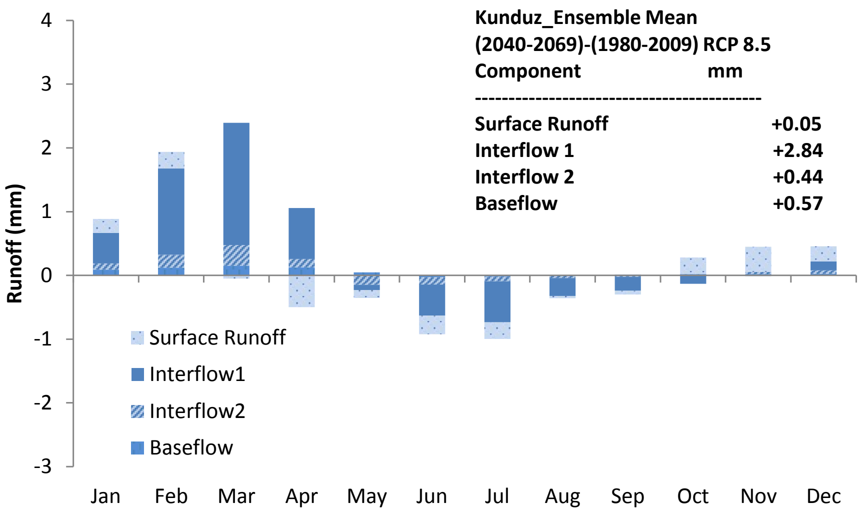

Figure 111. Projected changes in mean monthly runoff for Kunduz sub-basin under RCP8.5 using an ensemble mean of eight climate models.

Projected changes in runoff for Khanabad sub-basin

Long-term mean monthly runoff for the baseline period (1980-2009) in Khanabad sub-basin showed that peak runoff was in June, while surface runoff was concentrated in the summer months (June-August). In addition, the baseflow contribution to the total runoff was higher (60%) compared to surface runoff and other components (Figure 112). The future projection of total runoff under RCP2.6 showed an increase in the surface runoff component by ~14 mm, mainly during May to July (Figure 113), whereas under RCP8.5, the rate of increase in surface runoff almost doubled (up to ~25 mm) (Figure 114). However, under RCP8.5, projected runoff showed decreases in baseflow by ~22 mm and all other runoff components except for surface runoff (Figure 114).

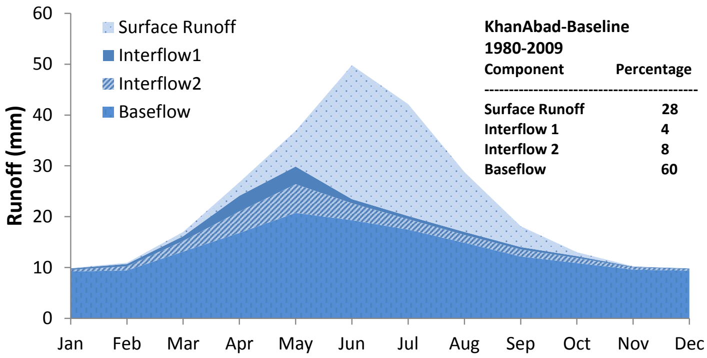

Figure 112. Long-term mean monthly runoff for Khanabad sub-basin for the baseline period (1980-2009).

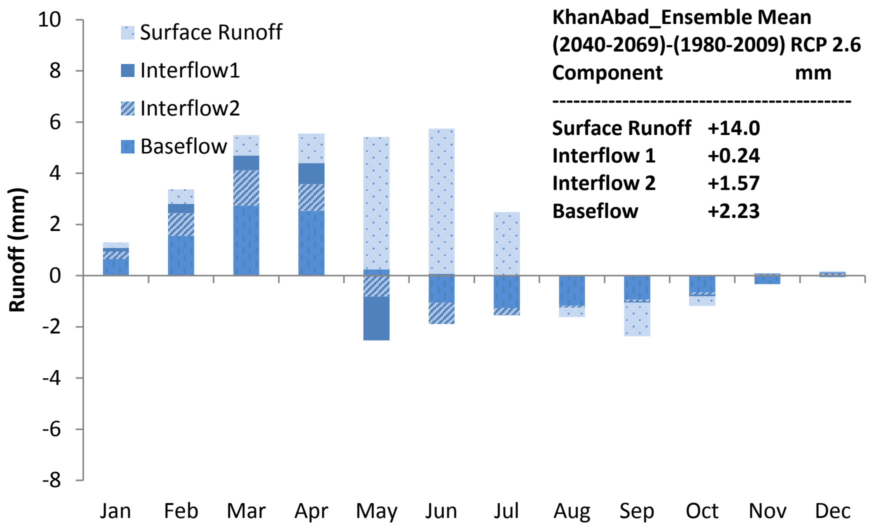

Figure 113. Projected changes in mean monthly runoff for Khanabad sub-basin under RCP2.6 using an ensemble mean of eight climate models.

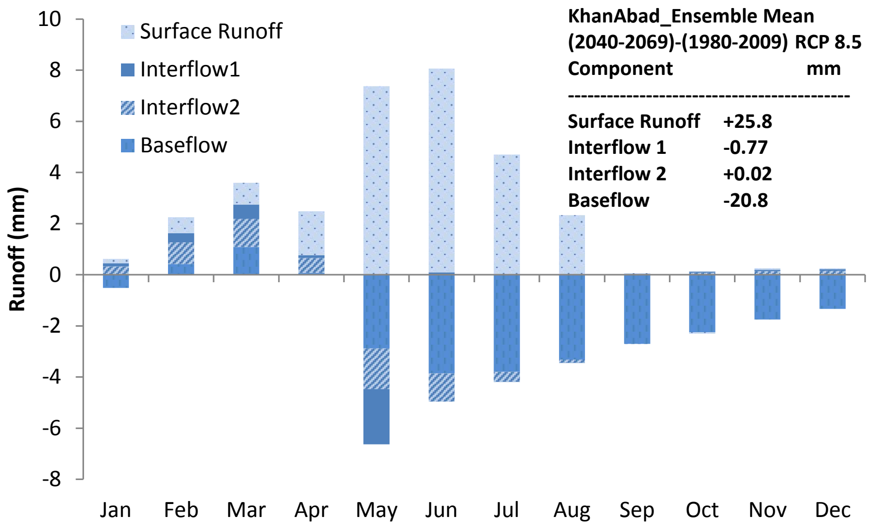

Figure 114. Projected changes in mean monthly runoff for Khanabad sub-basin under RCP8.5 using an ensemble mean of eight climate models.

Projected changes in runoff for Kokcha sub-basin

Long-term mean monthly runoff for the baseline period (1980-2009) in Kokcha sub-basin showed a 56% contribution of baseflow to total runoff with the lowest contribution from surface runoff (10%) (Figure 115). The future projection of the runoff changes under RCP2.6 showed an increase in all four components of total runoff: 9.8, 4.4, 5.5, and 5.7 mm for surface runoff, interflow 1, interflow 2, and baseflow, respectively. However, monthly runoff changes under RCP2.6 resulted in a decrease in all four runoff components from July to December (Figure 116). Under RCP8.5, the future projected runoff changes indicated a slight increase in surface runoff (17.4 mm) in spring and early summer months (April to June) compared with the results under RCP2.6 (9.8 mm). In addition, there was a decrease in baseflow of 5.8 mm under RCP8.5 (Figure 117). Overall, results for both scenarios indicated that there would be an earlier snow melt and less glacier contribution to the total runoff in July, August, and September in the future due to declines in the surface runoff component during these months.

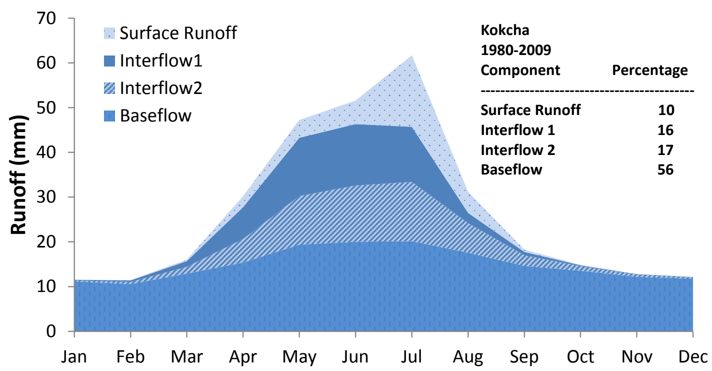

Figure 115. Long-term mean monthly runoff for Kokcha sub-basin for the baseline period (1980-2009).

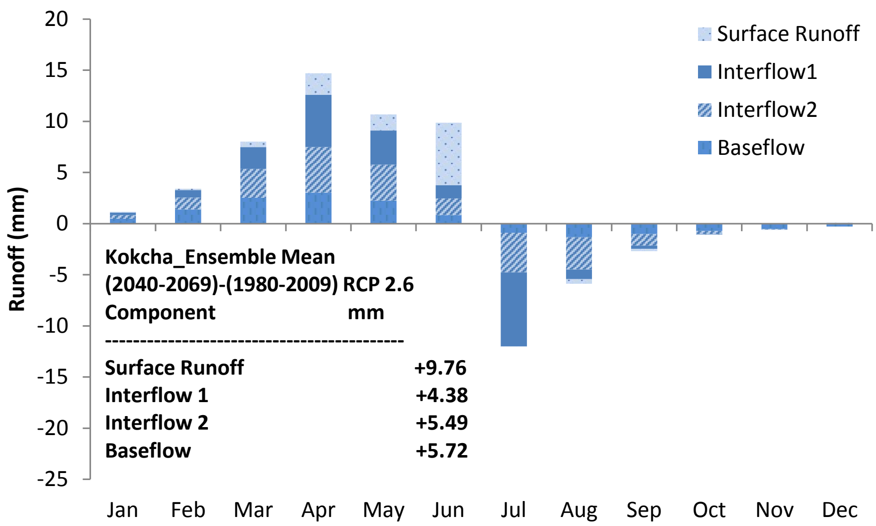

Figure 116. Projected changes in long-term mean monthly runoff for Kokcha sub-basin under RCP2.6 using an ensemble mean of eight climate models.

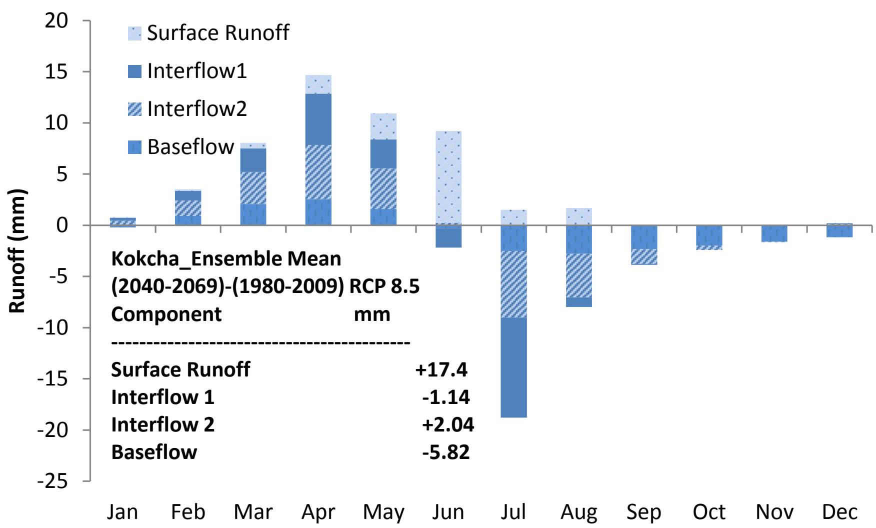

Figure 117. Projected changes in long-term mean monthly runoff for Kokcha sub-basin under RCP8.5 using an ensemble mean of eight climate models.

Projected changes in runoff for Panj sub-basin

Panj sub-basin has the highest proportion of glaciers in comparison to other sub-basins; therefore, consistent baseflow was noted throughout the year with 55% contribution to the total runoff in the baseline period (1980-2009) (Figure 118). The future projections of runoff changes under RCP2.6 showed an increase in surface runoff by 30 mm, mostly in the summer months (July and August), indicating the impact of climate warming on glacier retreat (Figure 119). Under RCP8.5, we observed a two-fold increase in surface runoff (up to 68 mm) along with an increase in all other components (30.2, 26.4, and 16.6 mm for interflow 1, interflow 2, and baseflow, respectively) (Figure 120).

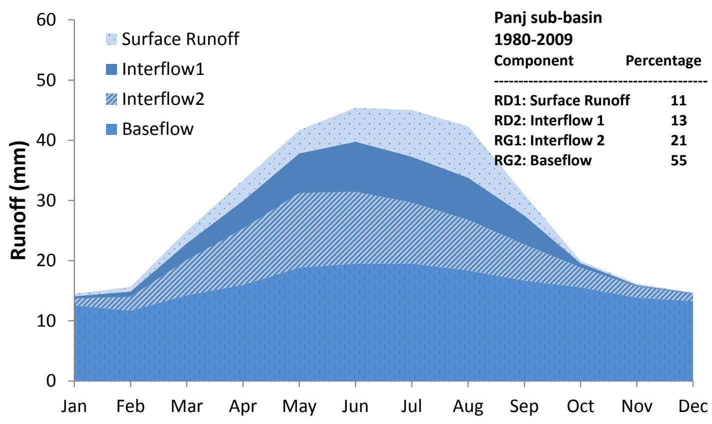

Figure 118. Long-term mean monthly runoff for Panj sub-basin for the baseline period (1980-2009).

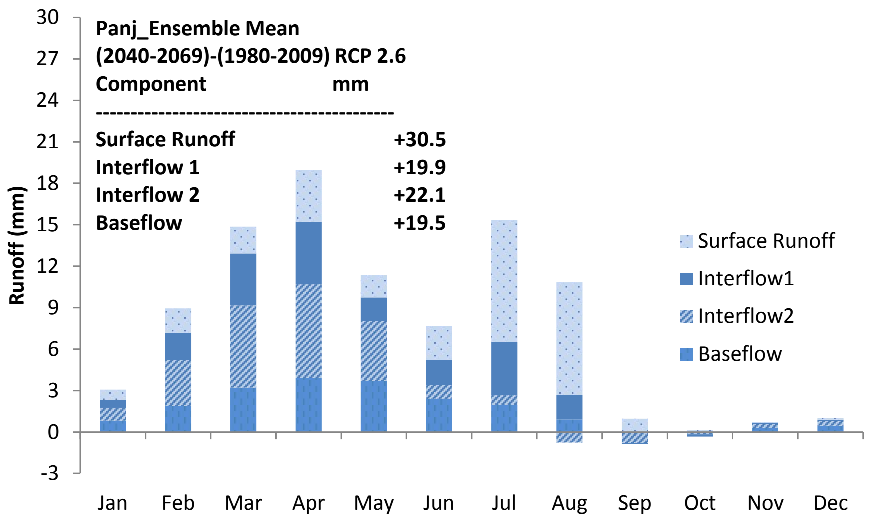

Figure 119. Projected changes in long-term mean monthly runoff for Panj sub-basin under RCP2.6 using an ensemble mean of eight climate models.

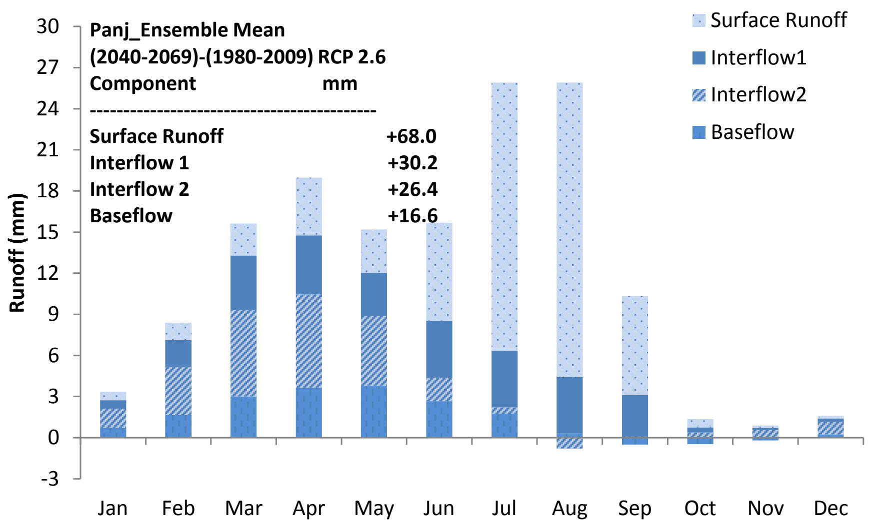

Figure 120. Projected changes in long-term mean monthly runoff for Panj sub-basin under RCP8.5 using an ensemble mean of eight climate models.

Hydrological hazard assessment

Approach to calculating projected changes in peak river discharge under future scenarios

Discharge (m^3/s) was derived from stations at outlets of each sub-basin and calculated in percentile intervals (10-90%, in 10% increments) for baseline (1980-2009) and future (2040-2069) periods under RCP2.6 and RCP8.5 using daily runoff. Next, percentage changes in discharge between future and baseline periods were calculated. The percentile approach was used to explore various peak river discharge values to provide indications of future extreme events, such as floods and droughts. In addition, the return periods of maximum yearly discharge for both periods, baseline and future (under both RCP2.6 and RCP8.5), were calculated to assess how the return period of flood peaks (an indicator of the frequency of extreme floods) is projected to change over time.

Projected changes in peak river discharge and return periods in Kunduz sub-basin

The highest increases (around 30%) in discharge occurred in Kunduz sub-basin between the 50th and 70th percentiles under both RCP scenarios in comparison to the baseline. Projected changes in discharge under RCP8.5 in the 20th to 50th percentile range had slightly higher increases of around 6% compared to RCP2.6, with the highest around 15% in the 60th percentile, while discharge decreased slightly (3%) in the 10th percentile (Figure 121). Examining the return periods for maximum annual discharge, the 5-7 year flood discharge was 91.2 m^3/s under baseline; floods roughly of this magnitude would occur every 1-3 years on average under RCP2.6 and RCP8.5, showing a future increase in peak river discharges in this basin (Table 14).

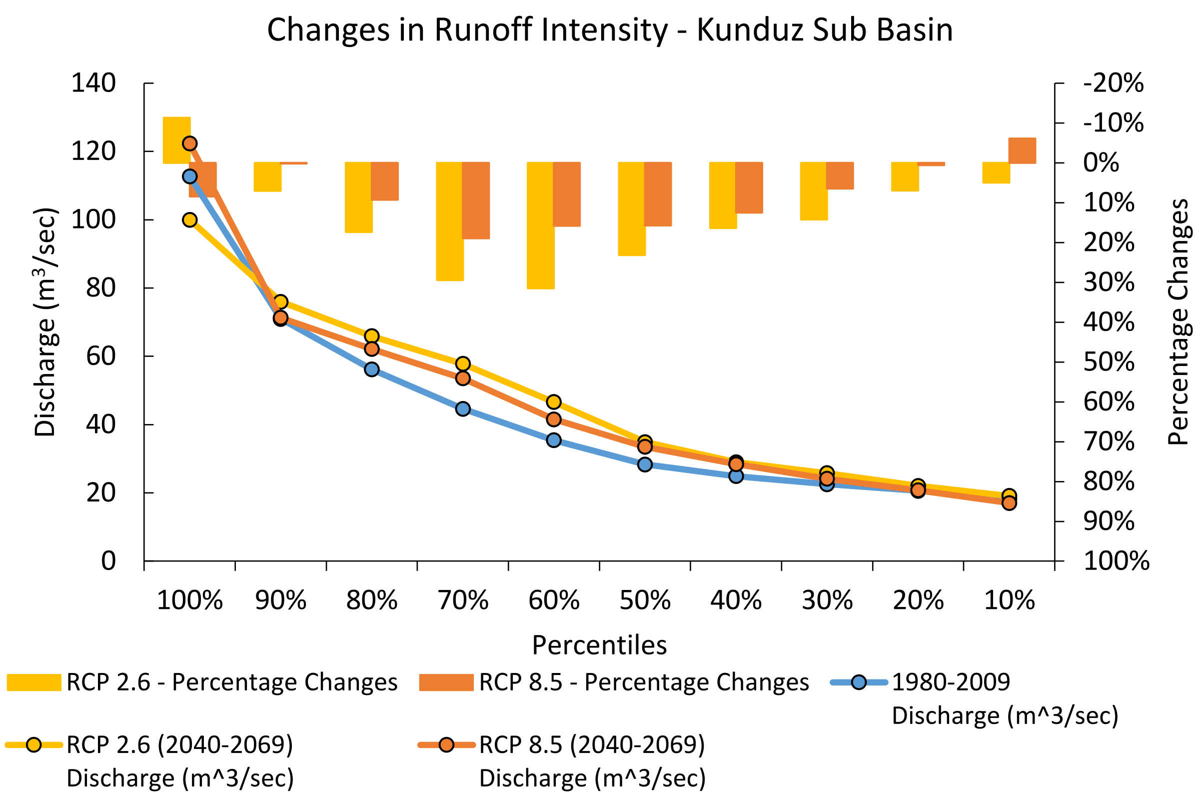

Figure 121. Projected changes in discharge for Kunduz sub-basin.

Table 14. Current and future return periods of maximum annual discharge (m^3/s) for Kunduz sub-basin.

Return Period (years)	1980-2009	2040-2069 (RCP2.6)	2040-2069 (RCP8.5)
1-3	82.9	91.6	84.3
3-5	88.5	94.5	89.9
5-7	91.2	97.8	95.1
7-9	95.1	98.3	96.4
9-11	96.4	98.8	97.0
15-17	103.6	99.3	103.6
29-31	112.7	100.0	112.8

Projected changes in peak river discharge and return periods in Khanabad sub-basin

The maximum discharge increase in Khanabad sub-basin was 10% under RCP2.6 for the 50th, 60th, 70th, and 100th percentiles compared to the baseline period; however, under RCP8.5, there was a decrease of 10% in discharge for the 10th to 40th percentiles (Figure 122). The highest change in peak discharge was 10% corresponding to the 100th percentile under RCP2.6; for the same percentile, the increase was around 3% under RCP8.5. The discharge peak of 264 m^3/s had a return period of 5-7 years in the baseline period compared to a 1-3 year return period under RCP2.6 and a 3-5 year return period under RCP8.5 (Table 15), showing that higher discharge values are projected to occur more frequently in the future, and to a greater degree under RCP2.6 than under RCP8.5.

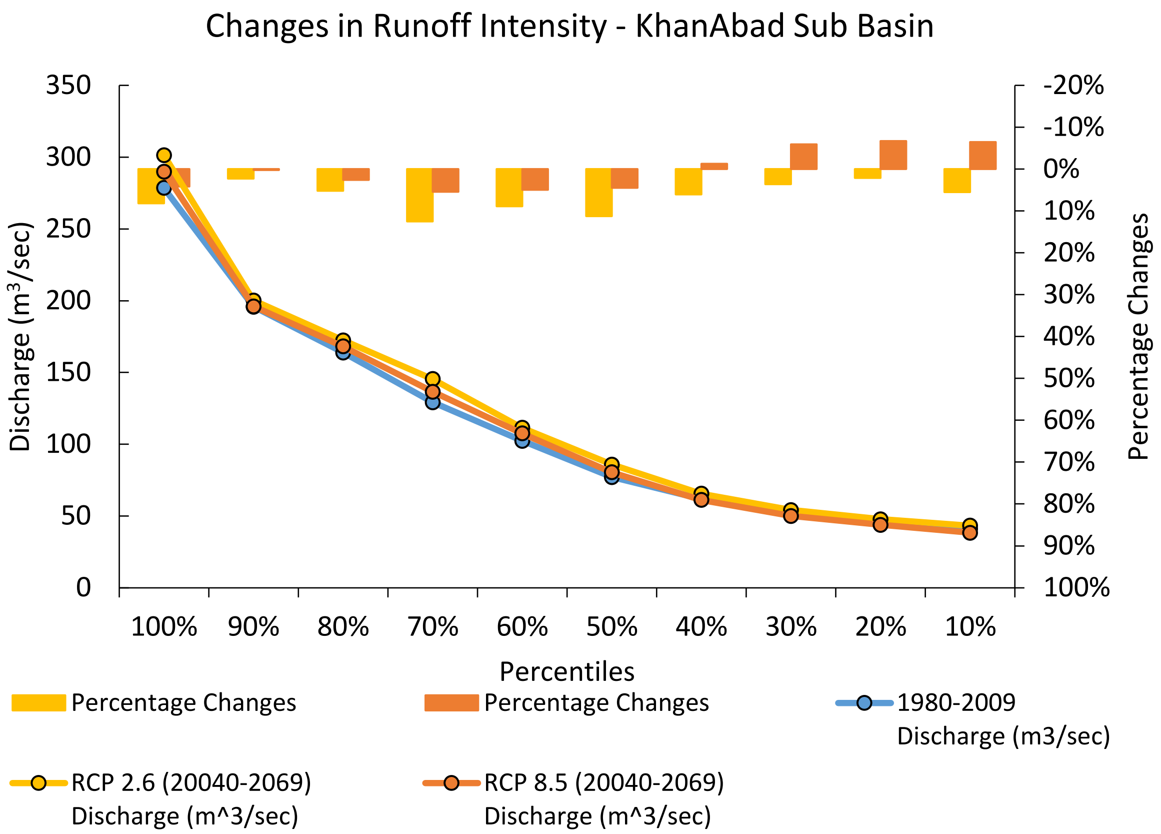

Figure 122. Projected changes in discharge for Khanabad sub-basin.

Table 15. Current and future return periods of maximum annual discharge (m^3/s) for Khanabad sub-basin.

Return Period (years)	1980-2009	2040-2069 (RCP2.6)	2040-2069 (RCP8.5)
1-3	252.7	268.0	252.1
3-5	259.5	271.9	261.0
5-7	263.9	272.6	270.0
7-9	270.1	273.3	271.9
9-11	273.0	278.1	272.9
15-17	277.8	286.4	277.8
29-31	278.6	301.4	278.5

Projected changes in peak river discharge and return periods in Kokcha sub-basin

In contrast to Kunduz and Khanabad sub-basins, projections of changes in peak river discharge in Kokcha sub-basin showed an increase of up to 20% in discharge at higher percentiles (70th to 90th percentiles) under RCP2.6 in comparison to the baseline period, while a decrease in discharge (3%) occurred in the percentile range of 10th to 30th under RCP8.5. Overall, discharge increases were lower under RCP8.5 compared to RCP2.6 across all percentiles except for the 100th percentile, where discharge was shown to increase more than for under RCP2.6 (by 12%) (Figure 123).

Under RCP2.6, the discharge peak of 646 m^3/s with a return period of 29-31 years had return period of 9-11 years under RCP8.5. This shows that higher discharge peaks are projected to occur more frequently under the higher emission scenario (Table 16). However, such flood events were more common during the baseline period, with a return period of roughly 15-17 years.

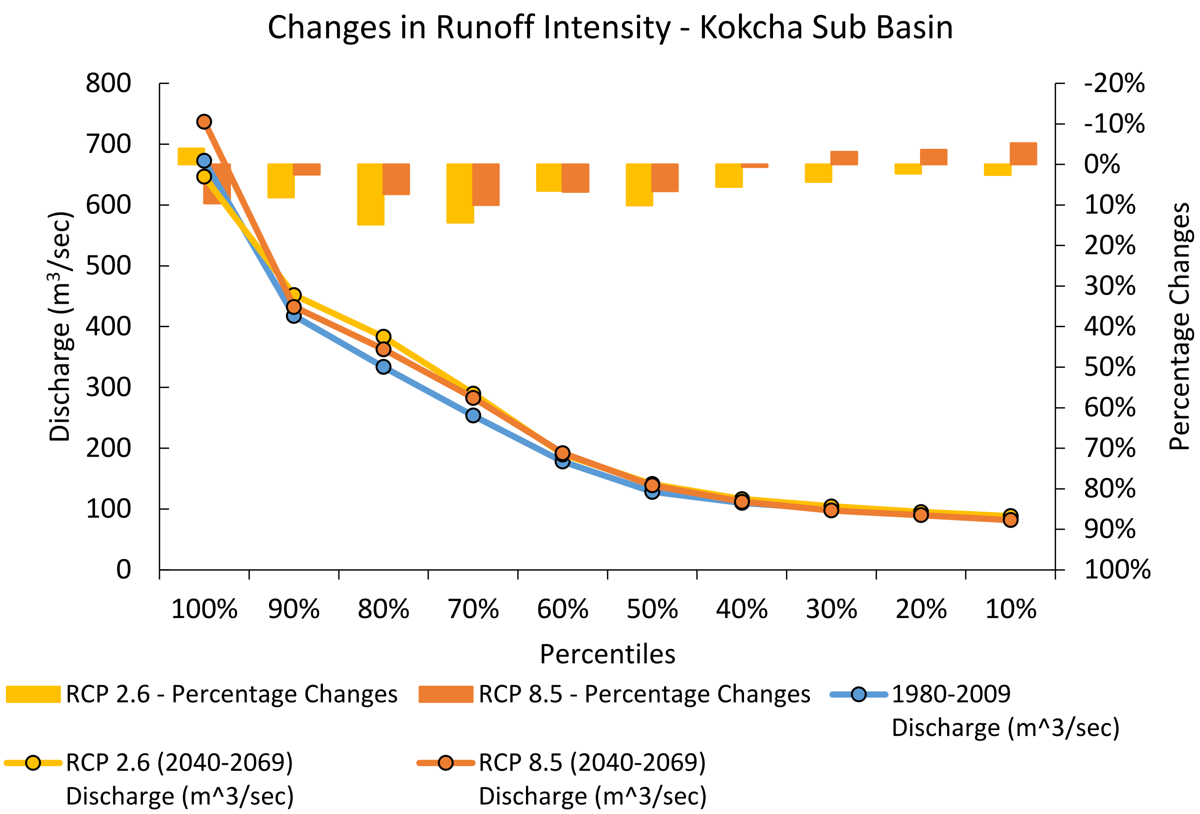

Figure 123. Projected changes in discharge for Kokcha sub-basin.

Table 16. Current and future return periods of maximum annual discharge (m³/s) for Kokcha sub-basin.

Return Period (years)	1980-2009	2040-2069 (RCP2.6)	2040-2069 (RCP8.5)
1-3	541.0	529.1	549.3
3-5	565.6	579.3	578.5
5-7	635.2	593.1	636.9
7-9	636.8	593.9	643.8
9-11	643.7	607.6	647.7
15-17	647.7	614.9	651.6
29-31	672.8	646.5	672.8

Projected changes in peak river discharge and return periods in Panj sub-basin

Panj sub-basin, with a higher percentage of glacier contribution to runoff than the other three sub-basins of the P-ARB, showed a projected increase in discharge peaks throughout all percentiles, especially between the 50th to 100th percentiles, where the increase was about 30% for RCP2.6 and 45% for RCP8.5 compared to the baseline period. Discharge peaks increased at the higher percentiles. There was a projected 70% increase in discharge in the 100th percentile under RCP2.6 compared to the baseline period, indicating that higher peaks are likely going to occur more frequently (Figure 124).

The discharge peak of 890 m³/sec with a return period of 29-31 years in the baseline period is projected to amount to a 'normal flood' (i.e., a return period of 1-3 years) under RCP2.6 and RCP8.5, with this latter scenario having even more discharge (985 m³/s). These results indicate that higher discharge peaks with increased frequencies are expected in the future under both emissions scenarios than have occurred during the baseline period (Table 17).

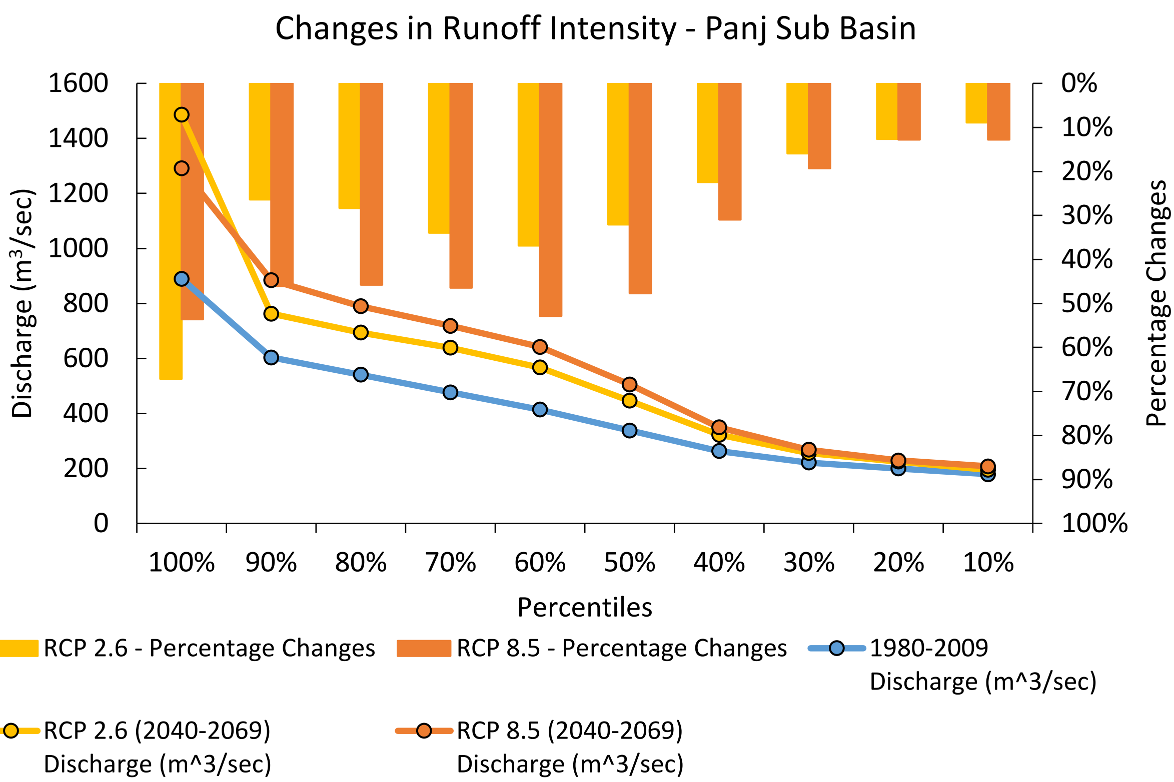

Figure 124. Projected changes in discharge for Panj sub-basin.

Table 17. Current and future return periods of maximum annual discharge (m3/s) for Panj sub-basin..

Return Period (years)	1980-2009	2040-2069 (RCP2.6)	2040-2069 (RCP8.5)
1-3	669.6	885.8	655.0
3-5	705.4	927.8	670.7
5-7	720.2	972.7	714.2
7-9	741.3	988.6	761.6
9-11	812.1	1007.1	785.6
15-17	858.9	1012.6	788.0
29-31	889.6	1486.9	841.2

Spatial distribution of river discharges in the P-ARB

Long-term mean, minimum, and maximum annual discharge values for baseline (1980-2009) and future (2040-2069) periods were obtained based on the outputs of the J2000 model considering both RCP2.6 and RCP8.5 for the eight GCM-RCM combinations for the entire P-ARB. The spatial distribution of statistical parameters of discharge over the stream network of the P-ARB were delineated along with calculations of the standard deviations of discharges across the full climate model set to illustrate variation in discharge accounting for uncertainty in climate model projections.

Considering baseline (1980-2009) long-term mean annual discharge across sub-basins, the lowest (0.02 m^3/s) mean annual discharge was obtained in Khanabad (Table 18; Figure 125). Discharge increased toward the Panj sub-basin due to high elevations and the presence of glaciers in the upper sub-basin. Therefore, the highest value (370 m^3/s) of mean annual discharge was simulated in the main rivers of the Kokcha and Panj sub-basins (Figure 125). Extreme changes in mean annual discharge across all streams of individual sub-basins are summarized in Table 18. Under the low emission pathway (RCP2.6), the projected mean annual discharge showed minimum decreases of up to 1 m^3/s in the sub tributaries of the Kunduz sub-basin. However, in the main tributary of Kunduz, Khanabad, Kokcha, and Panj sub-basins there were maximum increases in mean annual discharge of 4.8, 6.2, 15.70, and 68.90 m^3/s, respectively (Table 18; Figure 125).

The results for the high emission pathway (RCP8.5) revealed that the change in projected mean annual discharge further decreased in the sub tributaries by 2.73, 0.21, 0.45, and 0.14 m^3/s, while it increased in the main rivers by 8.69, 10.73, 3.35, and 126.97 m^3/s for Kunduz, Khanabad, Kokcha, and Panj sub-basins, respectively (Table 18; Figure 125). The standard deviation of mean annual discharge of the eight different future climate models under both RCPs showed deviations of 0 to 75 m^3/s across the P-ARB, with the highest variation simulated in the main rivers of the P-ARB (Figure 125).

Table 18. Summary of extreme changes (minimum and maximum values) in mean annual discharge (2040-2069)-(1980-2009) in m^3/s across all streams of individual sub-basins under RCPs 2.6 and 8.5.

Sub-basin	RCP2.6				RCP8.5			
	Max	Min	Mean	STD	Max	Min	Mean	STD
Kunduz	+4.85	-0.01	+0.68	1.20	+8.69	-2.73	+1.35	3.18
Khanabad	+6.29	+0.01	+1.51	2.29	+10.73	-0.21	+1.43	2.85
Kokcha	+15.70	+0.04	+2.30	3.98	+3.35	-0.45	+0.49	0.89
Panj	+68.90	+0.05	+15.10	23.30	+126.97	-0.14	+31.13	46.69

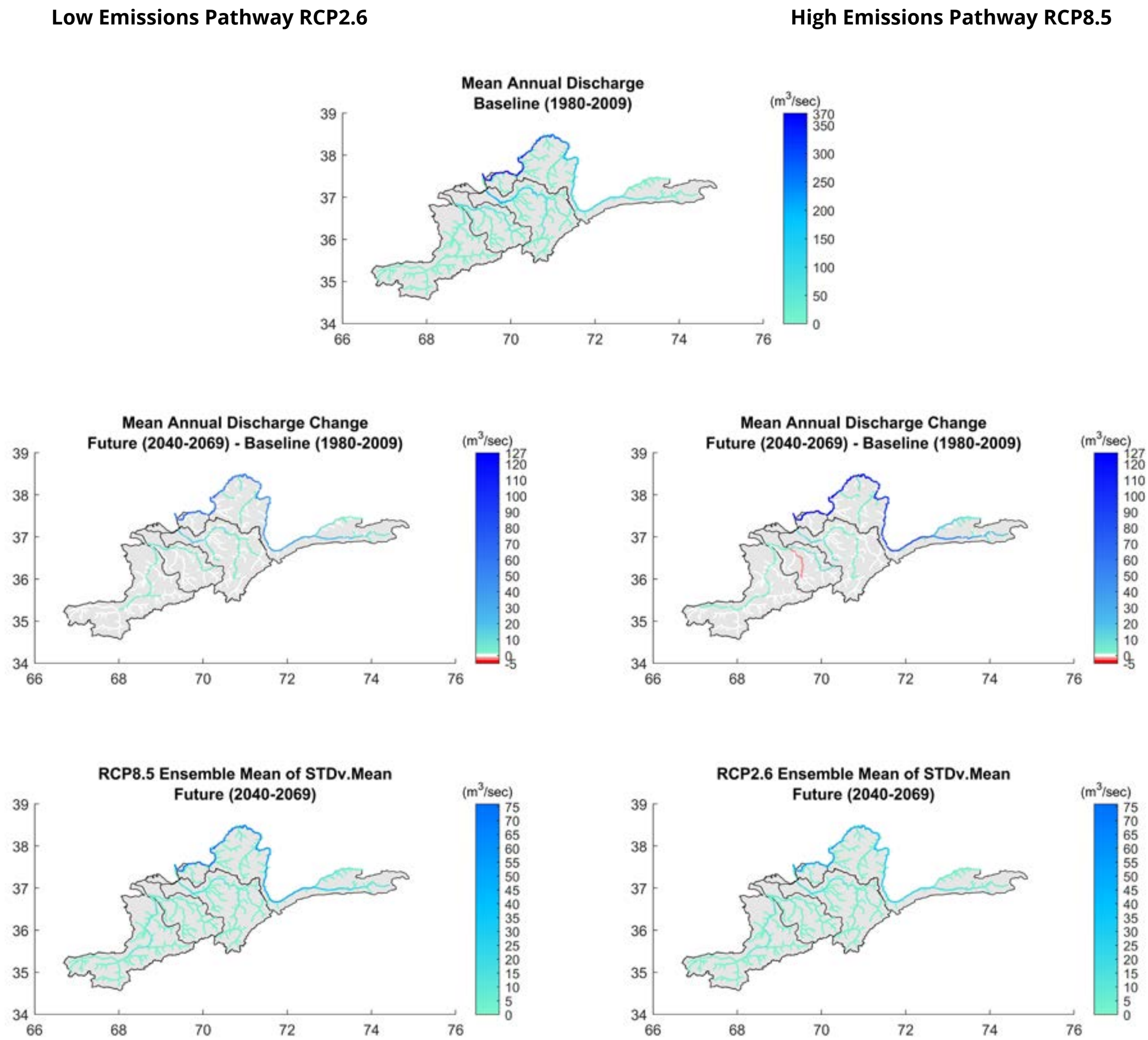

Figure 125. Spatial distribution of projected mean annual discharge changes across the P-ARB.

Similarly, the projected changes in minimum annual discharge under RCP2.6 compared to the baseline period revealed noticeable regions of reduced discharge in sub-tributaries of Kunduz, Kokcha, and Panj sub-basins (values ranging between -0.01 to -0.013 m^3/s), while no decrease was simulated in the sub-tributaries of Khanabad sub-basin. In comparison, a slight increase in minimum annual discharge was simulated in the main tributaries of the basin (Table 19; Figure 126). The results for RCP8.5 showed a higher impact of climate change that led to a decrease in minimum annual discharge in the main tributaries of Khanabad and Kokcha sub-basins that varied between -2.75 to -3.39 m^3/s, whereas under both emissions scenarios the discharge of the main rivers of Panj sub-basin increased, indicating contributions from glacier melting (Figure 126).

Table 19. Summary of extreme changes (minimum and maximum values) in minimum annual discharge (2040-2069)-(1980-2009) in m3/s across all streams of individual sub-basins under RCPs 2.6 and 8.5.

Sub-basin	RCP2.6				RCP8.5			
	Max	Min	Mean	STD	Max	Min	Mean	STD
Kunduz	+1.43	-0.04	+0.23	0.43	+0.20	-2.75	-0.38	0.63
Khanabad	+1.33	0.00	+0.23	0.31	+0.24	-3.39	-0.31	0.80
Kokcha	+1.11	-0.01	+0.17	0.28	+1.22	-0.77	+0.07	0.31
Panj	+4.40	-0.13	+0.90	1.32	+10.4	-0.20	+2.13	3.45

Low Emissions Pathway RCP2.6 **High Emissions Pathway RCP8.5**

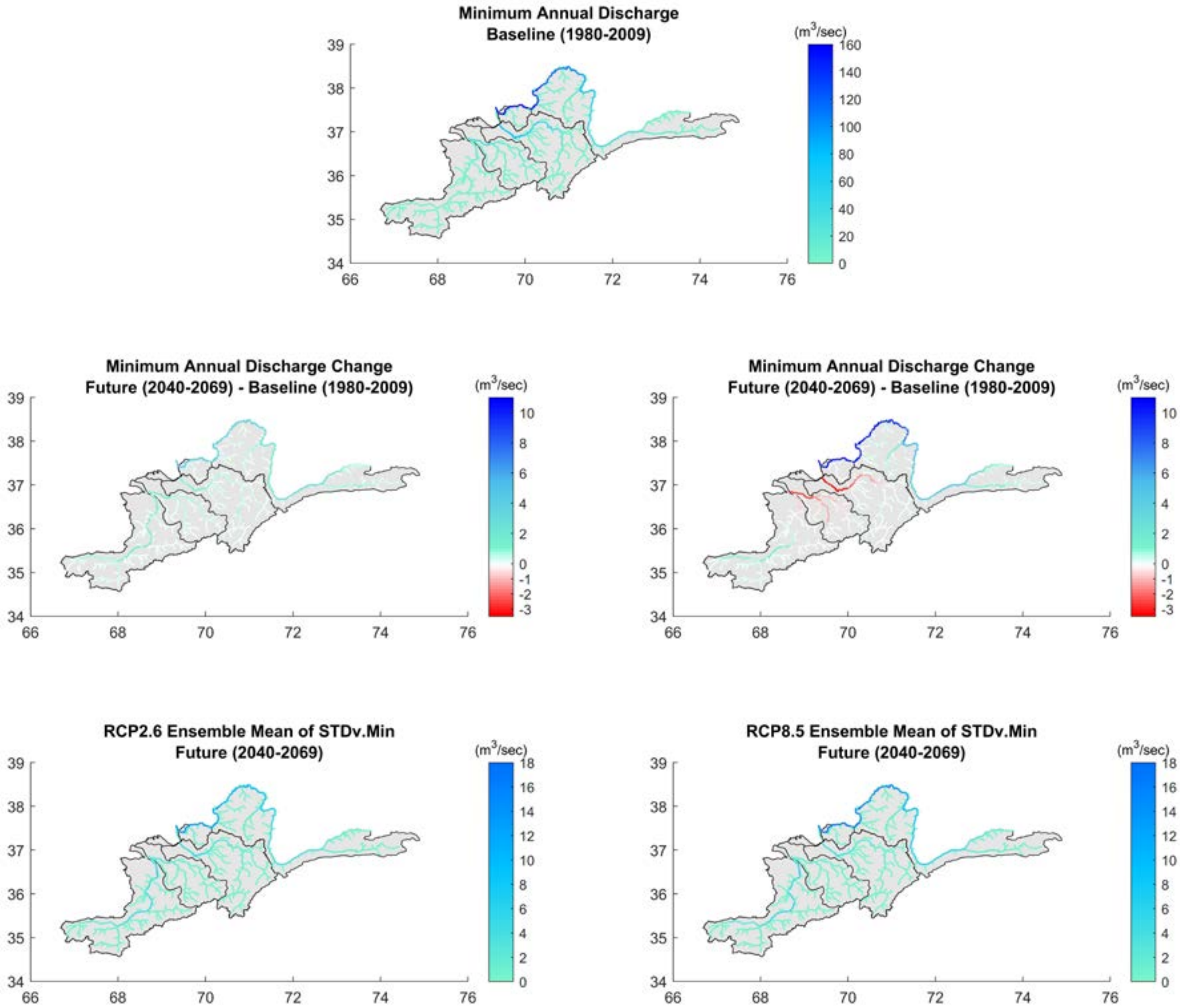

Figure 126. Spatial distribution of projected minimum annual discharge changes across the P-ARB.

The long-term maximum annual discharge showed the largest projected change in the main tributaries of the Kokcha (values ranging between 39.30 and 15.23 m^3/s) and Panj (values ranging between 186 and 365 m^3/s) sub-basins under RCPs 2.6 and 8.5, respectively, compared to the baseline period (1980-2009) (Table 20; Figure 127), while the changes in maximum annual discharge were lower in the main tributaries of the other two sub-basins. The change in maximum annual discharge showed the minimum values in the sub-tributaries of all four sub-basins between -0.98 to -7 m^3/s under RCP2.6 and between -1.87 to 8.02 m^3/s under RCP8.5 compared to the baseline values. Notably, there were larger variations (between 0 to 200 m^3/s) in maximum annual discharge simulated primarily in the main tributaries of the Panj and Kokcha sub-basins across the eight future climate models for both RCPs as represented by the standard deviation values (Figure 127).

Table 20. Summary of extreme changes (minimum and maximum values) in maximum annual discharge (2040-2069)-(1980-2009) in m^3/s across all streams of individual sub-basins under RCPs 2.6 and 8.5.

Sub-basin	RCP2.6				RCP8.5			
	Max	Min	Mean	STD	Max	Min	Mean	STD
Kunduz	+19.90	-7.00	+1.51	3.50	+24.60	-8.02	+3.80	7.99
Khanabad	+15.40	-0.98	+4.25	4.90	+29.87	-7.37	+4.90	10.15
Kokcha	+39.30	-4.10	+6.90	11.70	+15.23	-9.01	+0.63	3.69
Panj	+186.0	-1.86	+53.50	71.30	+365.0	-1.87	+105.5	142.2

Low Emissions Pathway RCP2.6

High Emissions Pathway RCP8.5

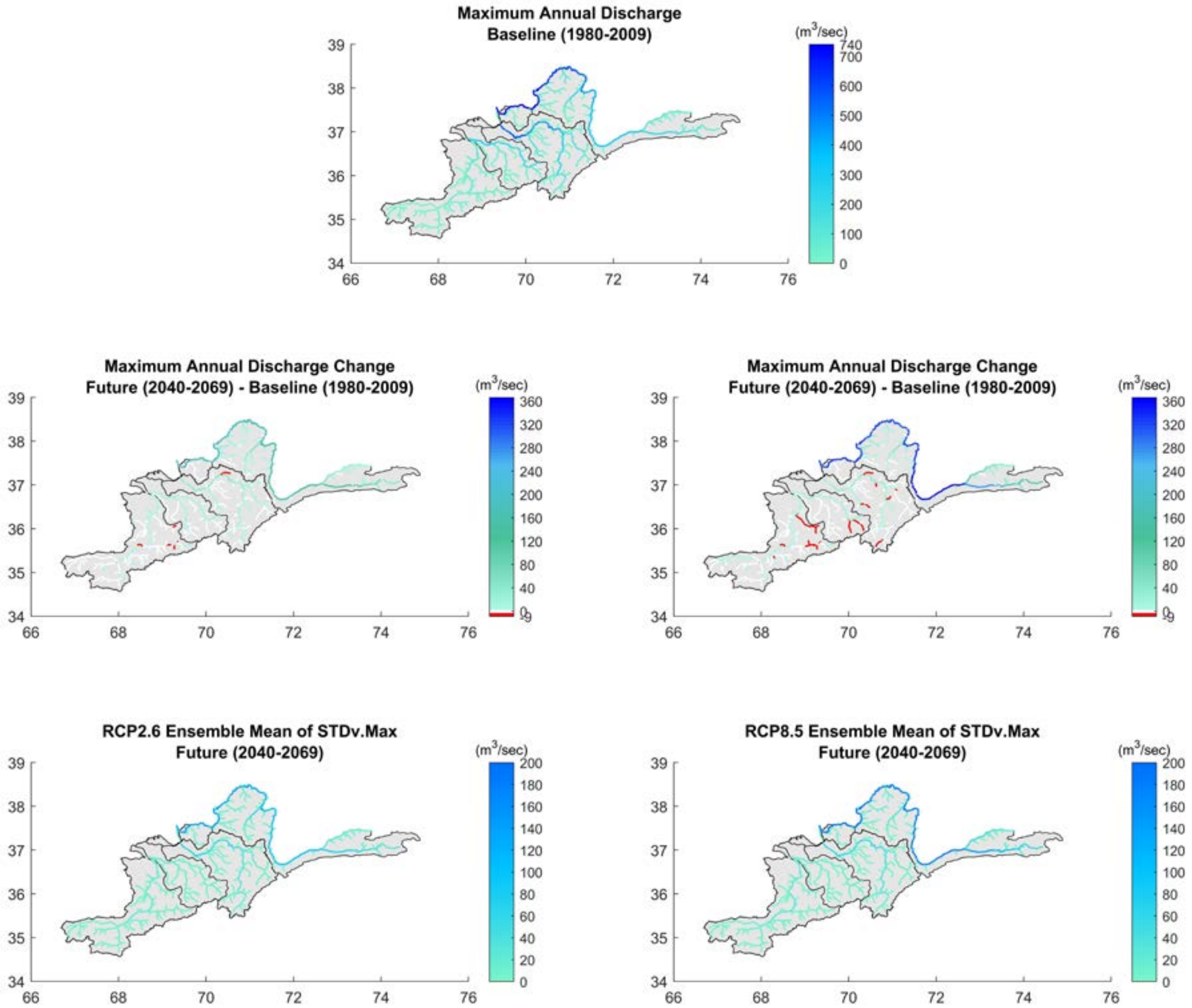

Figure 127. Spatial distribution of projected maximum annual discharge changes across the P-ARB.

Afghanistan›s Wakhan corridor, within the Panj-Amu River Basin, is a complex and dynamic hydrological system, spanning across multiple countries, and acts as a vital source of water, energy, food and livelihoods for the region.

Policy and Management Recommendations

The results of this analysis show wide-ranging and variable impacts of climate change on several hydrological parameters. In particular, projected changes in mean, minimum and maximum river discharges showed high- and low-flow conditions in the river stream network of the P-ARB, which could challenge water resource management and the adaptation of communities and ecosystems.

Designing particular hydrological risk management and adaptability measures requires the consideration of essential aspects of the results of this analysis, such as the relative uncertainties of the projected data and the hydrological model estimation processes, precipitation-elevation relationships at high altitudes due to lack of ground stations, dependencies of scenarios, and their temporal and spatial resolutions.

A better understanding of important hydrological processes and how they change over time can help policymakers and conservationists to better plan risk mitigation and capitalize on opportunities presented by river discharge-climate change interactions. The following key recommendations, clustered into three groups, are provided based on the results of this analysis to guide more sustainable water resource management under climate change.

1. Develop strategies to reduce the impact of floods and drought

- Plan readiness activities targeted at communities likely to be most affected based on the projected future magnitude and trend of flowing rivers in the P-ARB to ensure human and environmental sustainability
- Monitor and limit human activities such as deforestation and rangeland degradation that could erode soils and exacerbate flood effects
- Promote afforestation and restoration activities to mitigate flood consequences and prevent soil erosion
- Create a flood early warning system considering the high flow regime of the rivers in the future
- Understand potential low flow discharges of the river networks, especially in the sub-tributaries of the P-ARB, based on future trends of the flow to better plan agricultural activities
- Adapt cultivation practices to use high and low water-demanding, adaptable crops according to the projected change in the flow regime of the rivers
- Use a watershed management approach to mitigate the impact of drought and flood, including construction of dams at the upstream of high flow rivers for flood controls, and tracing and water harvesting activities, which could mitigate the potential effects of drought
- Construct storage dams in areas with potentially high future flows based on projected high potential for increasing river runoff under future climate change due to higher glacier melts

2. Establish a monitoring system for hydro-meteorological parameters

- Deploy hydrological stations to continuously monitor the discharge in major and minor rivers of the P-ARB, particularly in Panj sub-basin and at higher elevations where stations are currently limited
- Establish meteorological stations, especially at higher elevations in all sub-basins to monitor precipitation
- Develop a glacier monitoring system to record all relevant information, such as glacier mass balance, debris, and change over time

3. Improve public awareness of the current and future hydrological regime

- Increase awareness of vulnerable communities in regions of high and low flow discharges of promising mitigation and adaptation strategies to cope with flood and drought. The public awareness program should be conducted as a community-based workshop, and information could also be disseminated at community gatherings, such as local mosques
- Provide hydrological river discharge information as learning materials for schools and universities
- Facilitate and share results of further research on anticipated changes to the hydrological regime to advance current knowledge and support in community planning of hydrological risk adaptation and mitigation measures.

Wildlife Species Vulnerability

2.5 Wildlife Species Vulnerability

Overview

Biodiversity loss is one of the major issues faced by humanity over the coming century (Ceballos et al. 2015, 2017). Climate change is anticipated to exacerbate the ongoing decline, contributing to global extinction rates (Thomas et al. 2004, Malcolm et al. 2006, Pimm 2008, Bellard et al. 2012b). The effects of climate change on biodiversity are expected to be, and are currently observed as being, particularly important in montane landscapes such as those of the P-ARB (Sekercioglu et al. 2008, Gibson-Reinemer et al. 2015).

Wildlife species play critical roles in creating and maintaining ecosystems. As such, human livelihoods are closely connected to wildlife species, and this is as true in the P-ARB as it is anywhere else in the world. The connections between wildlife species and livelihoods are multifaceted and can be both positive and negative. Wild ungulates species may compete for forage with domestic livestock; however, they may also reduce the potential predation that might be suffered by livestock from carnivores such as snow leopards and wolves. Similarly, while predators may consume livestock and thereby threaten livelihoods, they may also help eliminate sick wild ungulates that may otherwise pose health threats to domestic flocks. Understanding the ways in which wildlife species may respond to climate change is integral to understanding the overall vulnerability of the region to climate change.

We examined the vulnerability of wildlife species in two ways. We used IUCN range data to create a list of bird and mammal species that could potentially occur in the P-ARB. There were 19 mammal and 60 bird species with a sufficiently large number of available georeferenced occurrence points (a list of species is given in Table 21). For these species, we created spatially explicit models of occurrence, both current and future for multiple emissions scenarios. Most of the occurrence data came from eastern Badakhshan (the Wakhan corridor) and Bamyan provinces, meaning that predicted species occurrence is likely to be most accurate for these highly sampled areas. Additionally, for all mammal and bird species whose ranges intersected with the P-ARB, we created an index of vulnerability based on known life history traits and used the IUCN range maps to create a predicted map of climate vulnerability.

Through these methods, we show that climate change poses a significant threat to wildlife in the region. The ranges of species are likely undergoing a net contraction, with the largest losses taking place in Bamyan and Kunduz provinces. Mammal species ranges are far more likely to contract than bird species. A few species, such as Long-legged Buzzard *Buteo rufinus* and Common Redshank *Tringa totanus*, are projected to expand their ranges, largely in Badakhshan. Overall mammal species vulnerability based on trait data was highest in Bamyan as well; however, bird vulnerability based on the same data was lowest in Bamyan, meaning that different conservation and management strategies will be required in different locations. These results highlight the need for cohesive and flexible conservation plans that ensure the ability of species to traverse the landscape and reduce potential conflicts with humans and their livelihoods.

Synthesizing our results across all indicators reveals ecoregions of higher relative wildlife species vulnerability (Figure 128). The Badghyz and Karabil semi-desert and Karakorum-West Tibetan Plateau ecoregions showed low projected range stability for both birds and mammals, illustrating potential high vulnerability. Similarly, the Gissaro-Alai open woodlands ecoregion showed high climate sensitivity for both taxonomic groups, representing potentially high vulnerability. For birds, the Paropamisus xeric woodlands ecoregion showed a combination of low projected range stability and high climate sensitivity, which underscores a high vulnerability for birds. However, the taxonomic differences in geographic patterns of exposure and sensitivity across ecoregions suggests different regional challenges and priorities for conserving birds and mammals under climate change. The policy and management recommendations, outlined at the end of this section, provide some guidance on best practices for successful biodiversity conservation under climate change in the P-ARB.

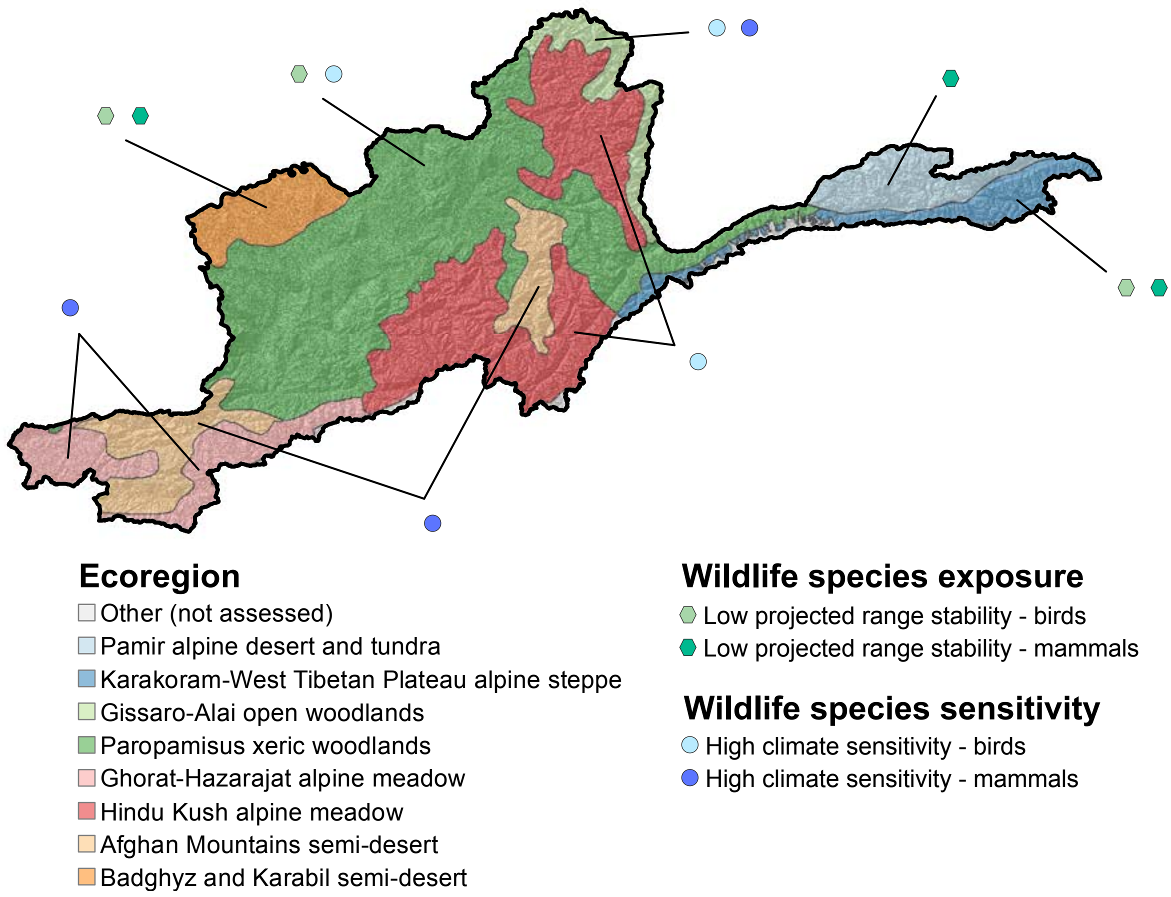

Figure 128. Overview of wildlife species exposure and sensitivity within ecoregions of the Panj-Amu River Basin.

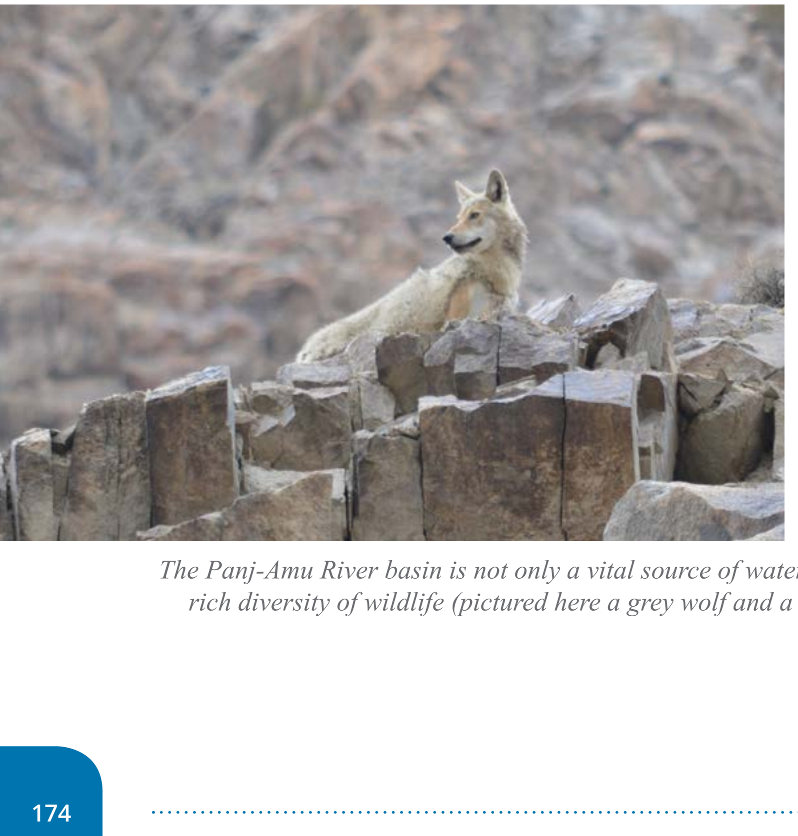

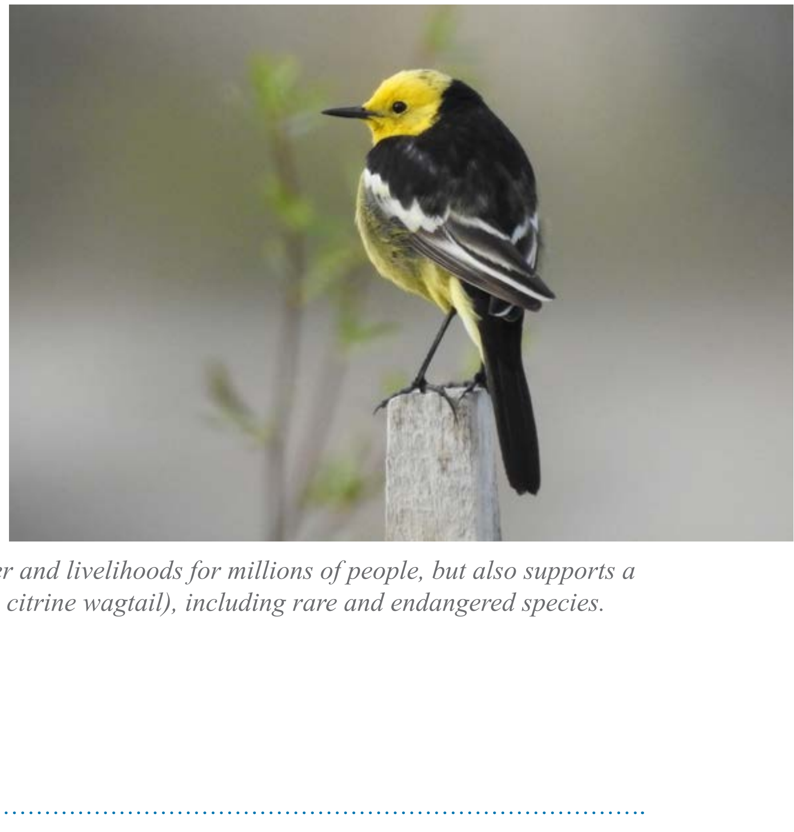

The Panj-Amu River basin is not only a vital source of water and livelihoods for millions of people, but also supports a rich diversity of wildlife (pictured here a grey wolf and a citrine wagtail), including rare and endangered species.

Changes in Mammal Range Size and Location

E

Indicator overview

Every species has a particular spatiotemporal distribution, otherwise known as a range, that is created by a combination of biotic and abiotic influences as well as by movement barriers (Hutchinson 1958, Soberón and Townsend Peterson 2005, Soberón 2007). The predominant way in which climate change is expected to influence individual species is by affecting their ranges, both in terms of their size as well as their location (Parmesan and Yohe 2003, Parmesan 2006). These changes to species have profound implications for their ecology and conservation (McClanahan et al. 2008, Sekercioglu et al. 2008, Bellard et al. 2012a). Because population size of a species is generally linked to its range size, species that undergo range contractions (i.e., reductions in their range size) are likely to undergo population contractions, thereby increasing their risk of extinction. A change in the location of a species' range, independent of any change in the size of that range, can also create risks for the long-term persistence of a species, including the potential for moving into areas where the risk of conflict with humans may be greater. For example, a species shifting its range may move into areas closer to human settlements, increasing its exposure to hunting.

While it is generally understood that climate change will affect species ranges, it is crucial to understand the specific ways that those changes to species' ranges will play out. A spatially explicit understanding of the ways in which a species' range may be impacted under climate change is essential to conserving them, as it allows for proactive management actions that can mitigate the negative effects of these changes (Jones et al. 2016, McGuire et al. 2016).

Methods overview

Species distribution models (SDMs) are a commonly used tool to understand the current and potential future distributions of species (Guisan and Zimmermann 2000, Elith and Leathwick 2009, Miller 2010). SDMs are a class of correlative model, where indices of a species' presence are used in conjunction with a set of predictor variables to create a spatially explicit prediction of a species occurrence across a landscape. Where information on the future values of predictor variables is available, those predictions may be projected onto expected future conditions to provide estimates of future species distributions, and thereby the expected changes in a species' range size and location (Elith et al. 2010, Anderson 2013). For the purposes of this indicator, we conceptualized the probability of the presence of species at a given location as being a hierarchical process occurring at two spatial scales. At a broad (regional) scale, the range of a species is determined by the climatic conditions it can tolerate, while at a fine (local) scale, occurrence is determined by variables such as human impacts, topography, and land cover. A schematic description is shown in Figure 129; precise methodological details are provided in Appendix 6.

For each mammal species, we collected confirmed georeferenced occurrence records across the entire spatial extent of the climate data generated and described in section 2.1 (see Figure 15 for a map depicting this extent). Occurrence records came from a variety of sources, included fieldwork and camera trap records, published literature, and biodiversity databases such as the Global Biodiversity Information Facility (GBIF). We used the SDM process described in Figure 129 to create models for the 19 mammal species for which at least five occurrence records were within the borders of the P-ARB (Table 21). These 19 mammal species represent 5 orders and 12 families.

Table 21. List of mammal species used in species distribution modelling analysis. Names and taxonomy follow the IUCN red list. The number of georeferenced presence points for each species overall and within the P-ARB is given in parentheses in the Common Name column.

Order	Family	Latin name	Common name	IUCN status
Carnivora	Canidae	*Canis lupus*	Grey Wolf (44; 10)	Least Concern
Carnivora	Canidae	*Vulpes vulpes*	Red Fox (192; 152)	Least Concern
Carnivora	Felidae	*Lynx lynx*	Eurasian Lynx (23; 18)	Least Concern
Carnivora	Felidae	*Otocolobus manul*	Pallas's Cat (21; 13)	Least Concern
Carnivora	Felidae	*Panthera uncia*	Snow Leopard (6519; 6401)	Vulnerable
Carnivora	Mustelidae	*Martes foina*	Beech Marten (100; 85)	Least Concern
Carnivora	Mustelidae	*Mustela altaica*	Altai Weasel (23; 9)	Near Threatened
Carnivora	Mustelidae	*Mustela erminea*	Stoat (13; 8)	Least Concern
Carnivora	Ursidae	*Ursus arctos*	Brown Bear (140; 75)	Least Concern
Cetartiodactyla	Bovidae	*Capra sibirica*	Siberian Ibex (3287; 3186)	Near Threatened
Cetartiodactyla	Bovidae	*Ovis ammon*	Argali (1255; 1225)	Near Threatened
Cetartiodactyla	Bovidae	*Ovis vignei*	Urial (741; 679)	Vulnerable
Eulipotyphla	Soricidae	*Crocidura suaveolens*	Lesser Shrew (19; 5)	Least Concern
Lagomorpha	Leporidae	*Lepus tibetanus*[1]	Desert Hare (106; 96)	Least Concern
Lagomorpha	Ochotonidae	*Ochotona rufescens*	Afghan Pika (94; 83)	Least Concern
Rodentia	Calomyscidae	*Calomyscus baluchi*	Baluchi Brush-tailed Mouse (47; 6)	Least Concern
Rodentia	Cricetidae	*Cricetulus migratorius*	Grey Dwarf Hamster (24; 5)	Least Concern
Rodentia	Muridae	*Rattus pyctoris*	Himalayan Rat (20; 5)	Least Concern
Rodentia	Sciuridae	*Marmota caudata*	Long-tailed Marmot (142; 101)	Least Concern

1. The taxonomic status of hares in the P-ARB, and in Central Asia in general, is unclear, with species limits constantly being revised. For the purposes of this analysis, we pooled all records within the region assigned to any of *Lepus capensis*, *Lepus tibetanus* and *Lepus tolai*, all of which have at various times been considered distinct or conspecific with each other and have been applied to hares from this region.

Efforts are being made to protect wild mammals (pictured here a stoat and a flock of Siberian ibex) in the Panj-Amu River Basin, including by establishing protected areas, community-based conservation programs, and efforts to reduce human-wildlife conflict.

The SDM process produced the following outputs for each species:

(1) Current distribution

(2) Projected distribution, mid-century (2040-2069), RCP2.6

(3) Projected distribution, end-century (2070-2099), RCP2.6

(4) Projected distribution, mid-century, RCP8.5

(5) Projected distribution, end-century, RCP8.5

Each output consisted of a raster with values ranging from 0 to 1, with 0 representing the least suitable habitat for the species and 1 representing the most suitable habitat. As continuous outputs are more difficult to interpret, these continuous rasters were converted into discrete output by applying two thresholds, a low and a high threshold (Liu et al. 2005, Freeman and Moisen 2008). The low threshold was calculated by sampling the value of the continuous raster at known presence points for the species and taking the lowest value (i.e., the minimum value known to correspond to a confirmed presence); raster cells below that value were considered unsuitable for the species. The high threshold was calculated by taking the 70th percentile value of all raster cells above the low threshold. Raster cells between the low and high thresholds were considered low-quality habitat, while raster cells above the high threshold were considered high-quality habitat. We then compared current and future extents of low-quality and high-quality habitat for each species (Figure 130 to Figure 148).

In addition to assessing individual species, we also summarized the total change in habitat (including both low and high-quality habitat) for all species by calculating the ratio of current to future habitat size (Figure 149). We also calculated a metric of community range stability at the pixel level (~1km), where pixel values were calculated as the proportion of species currently occupying the pixel and that are projected to remain there in the future (Figure 150). Similarly, we further calculated the number of species projected to occur in the future in each pixel that do not currently occur there as a metric of community range expansion (Figure 151). We also calculated the current and future centroids of each species' range and compared their distances and directions from one another, which provides a metric of the distance and direction the species is projected to move under climate change (summarized in Figure 152).

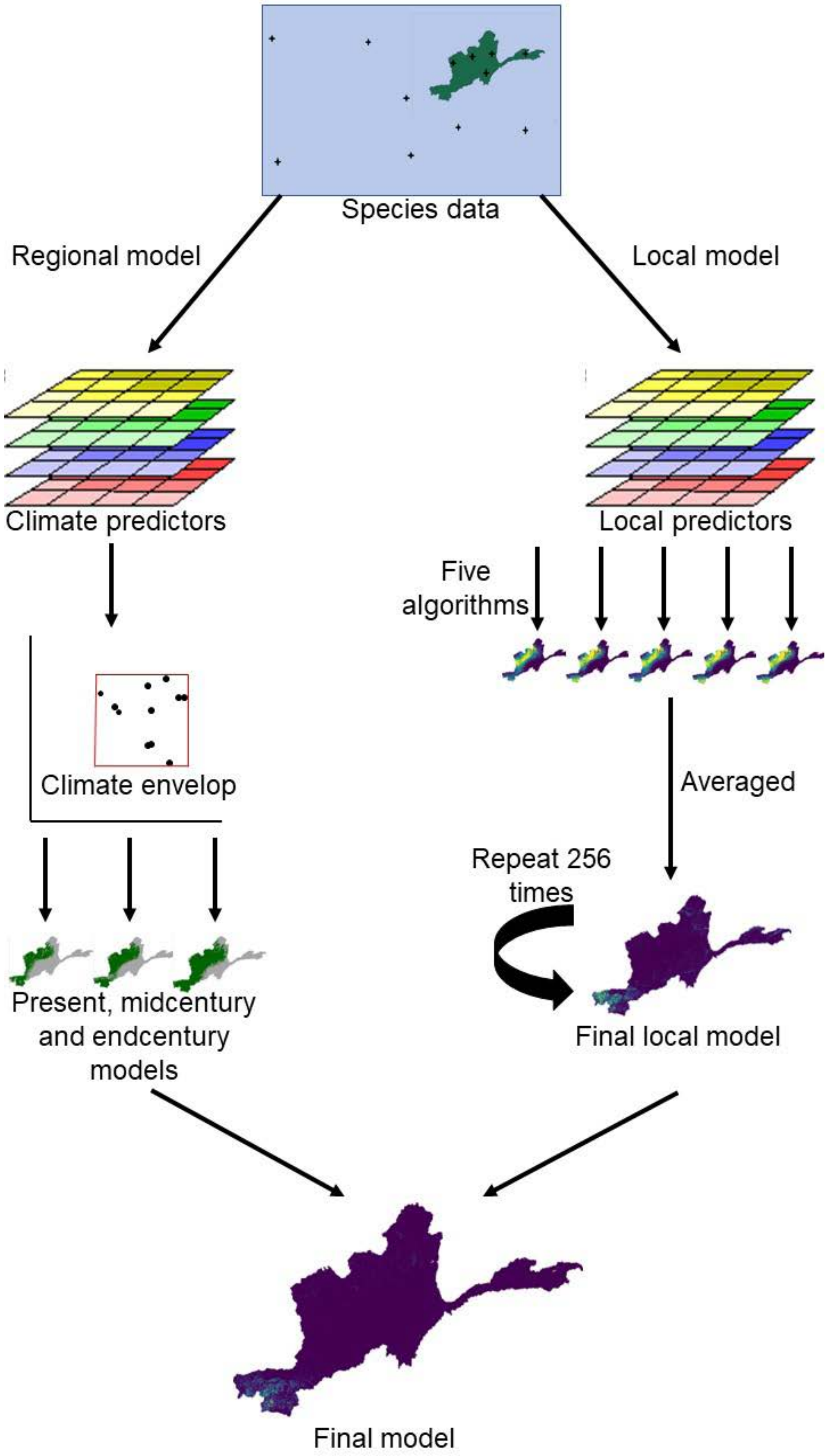

Figure 129. Schematic diagram of species distribution modelling process. Species points were obtained for the entire extent of the climate data described in section 2.1 and shown in Figure 15. All points, in conjunction with climate data, were used to generate climate envelopes as shown on the left; points within the P-ARB were used to create local occurrence models, as shown on the right.

Spatial representation of indicator

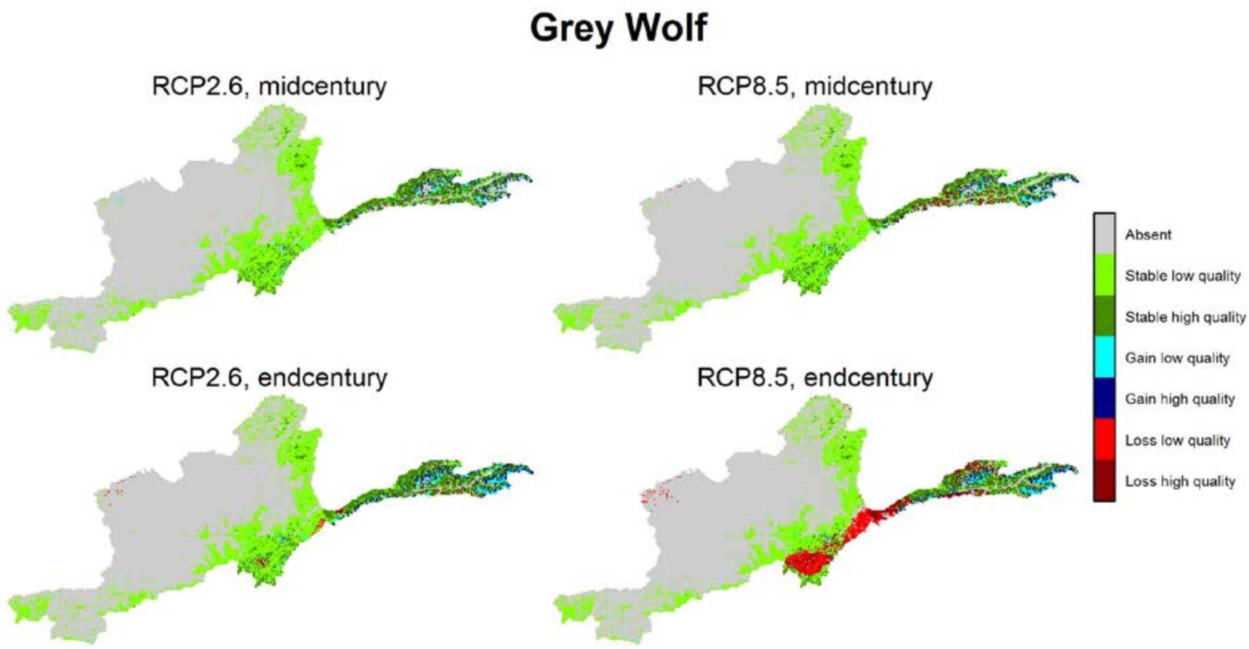

Figure 130. Changes in suitable habitat for Grey Wolf (*Canis lupus lupus*).

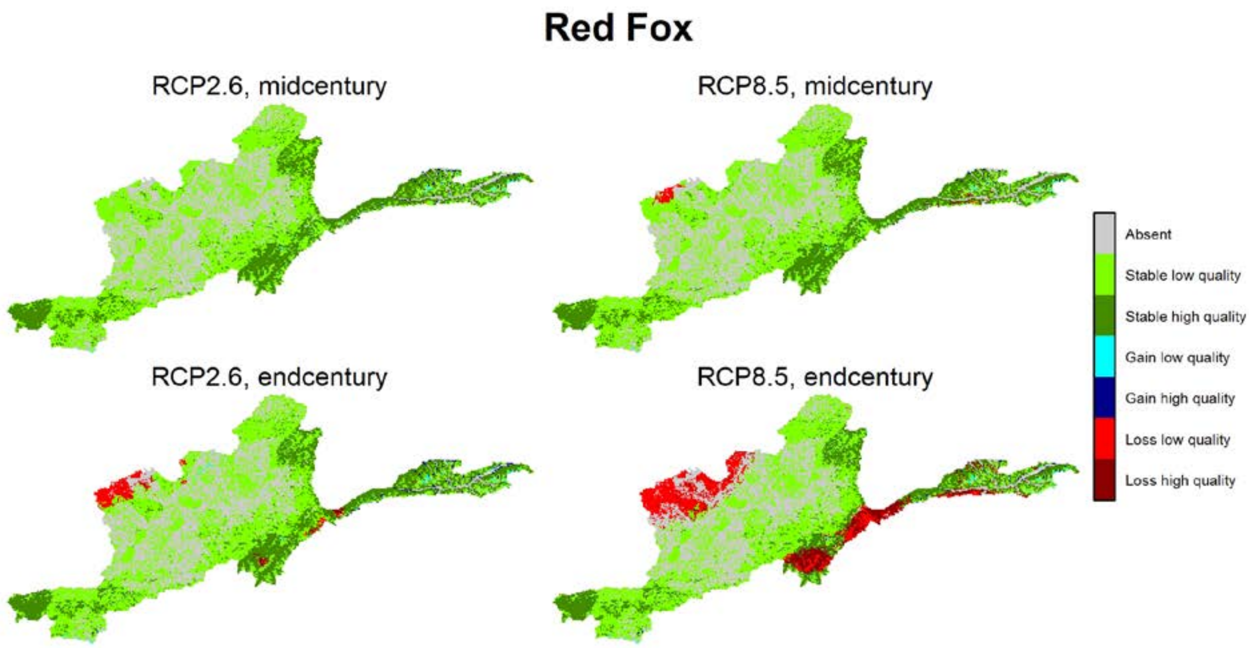

Figure 131. Changes in suitable habitat for Red Fox (*Vulpes vulpes griffithi*).

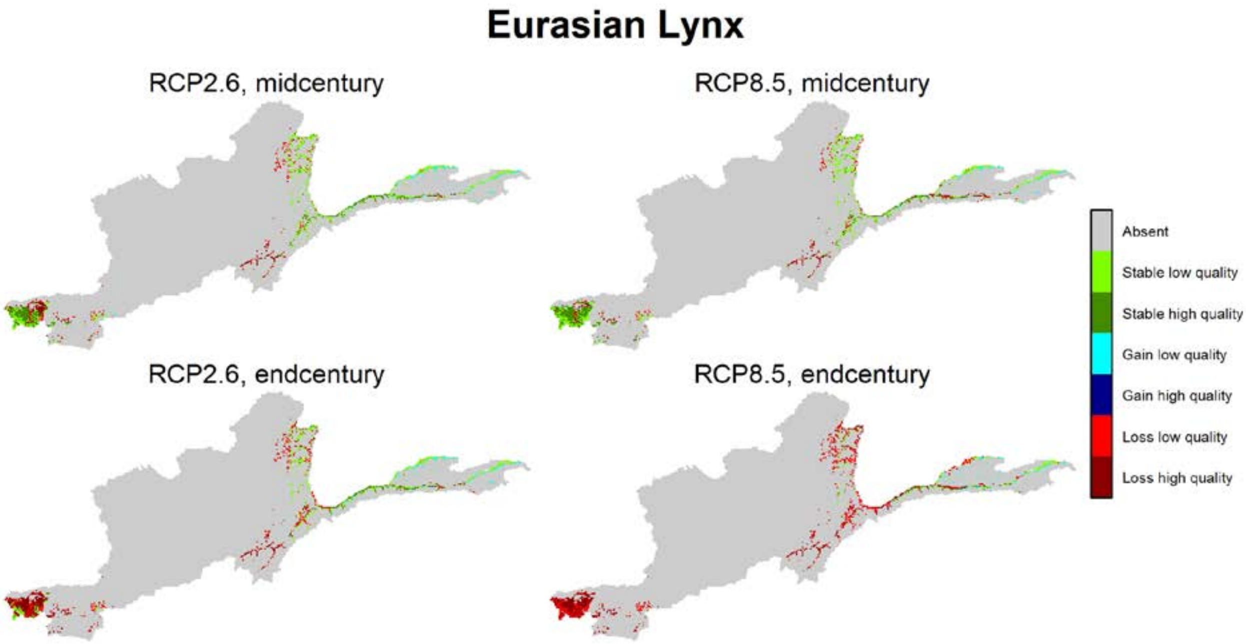

Figure 132. Changes in suitable habitat for Eurasian Lynx (*Lynx lynx isabellinus*).

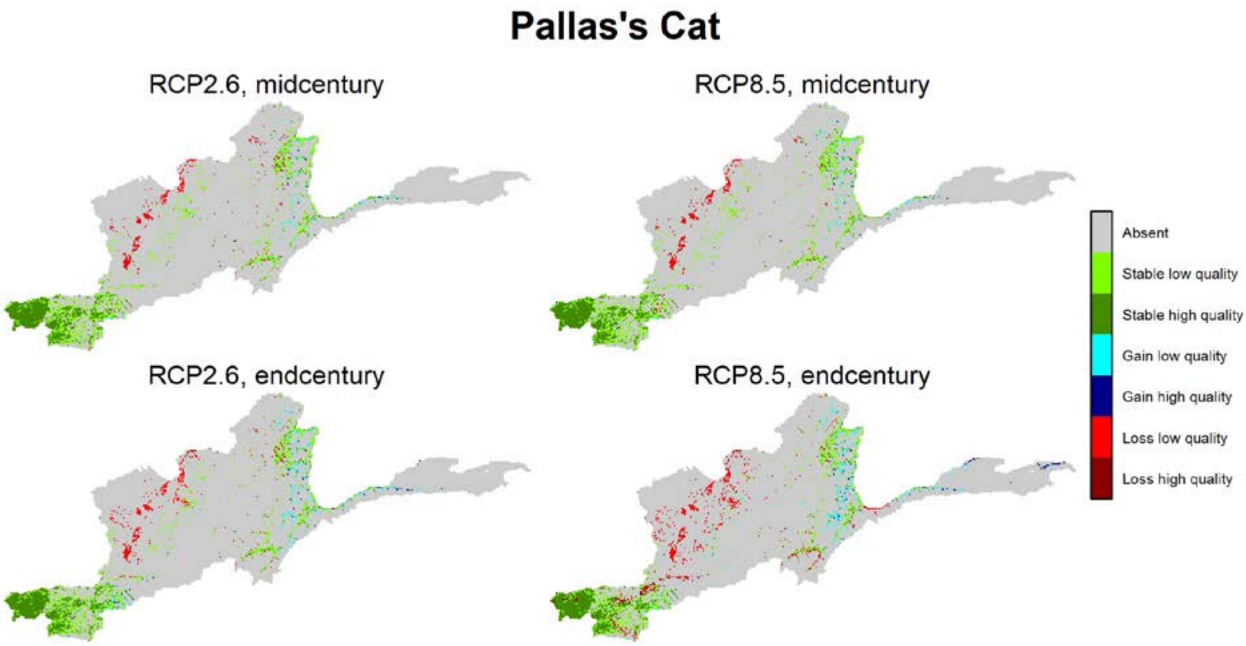

Figure 133. Changes in suitable habitat for Pallas's Cat (*Otocolobus manul manul*).

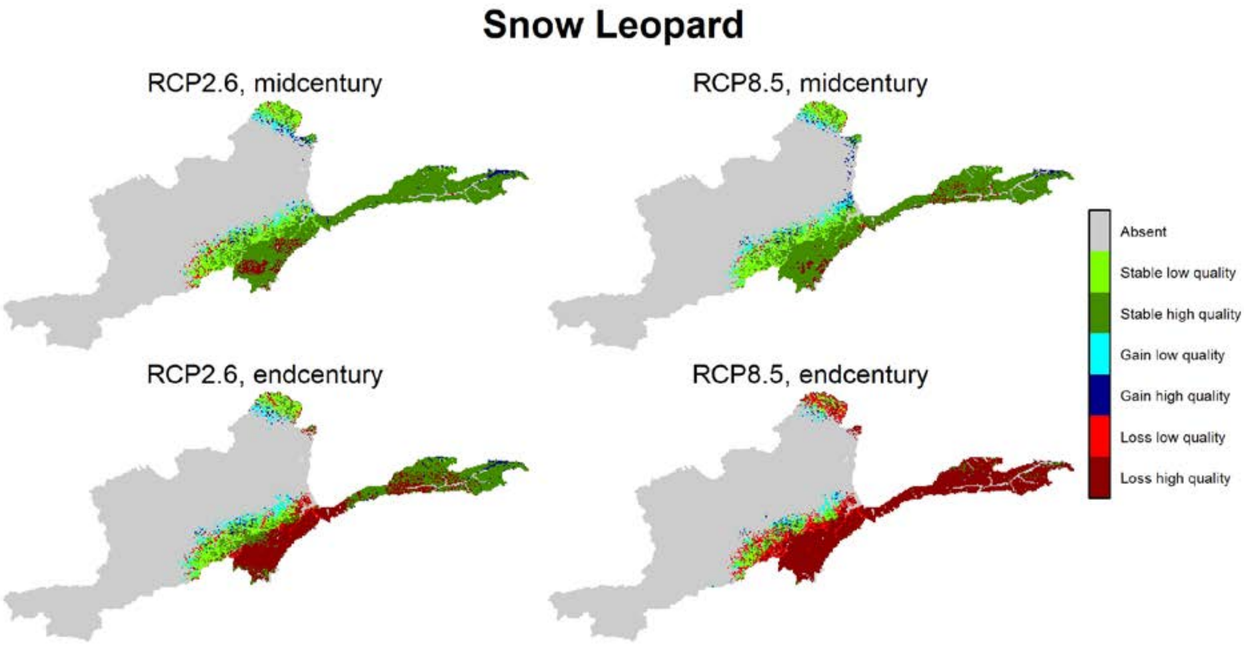

Figure 134. Changes in suitable habitat for Snow Leopard (*Panthera uncia*).

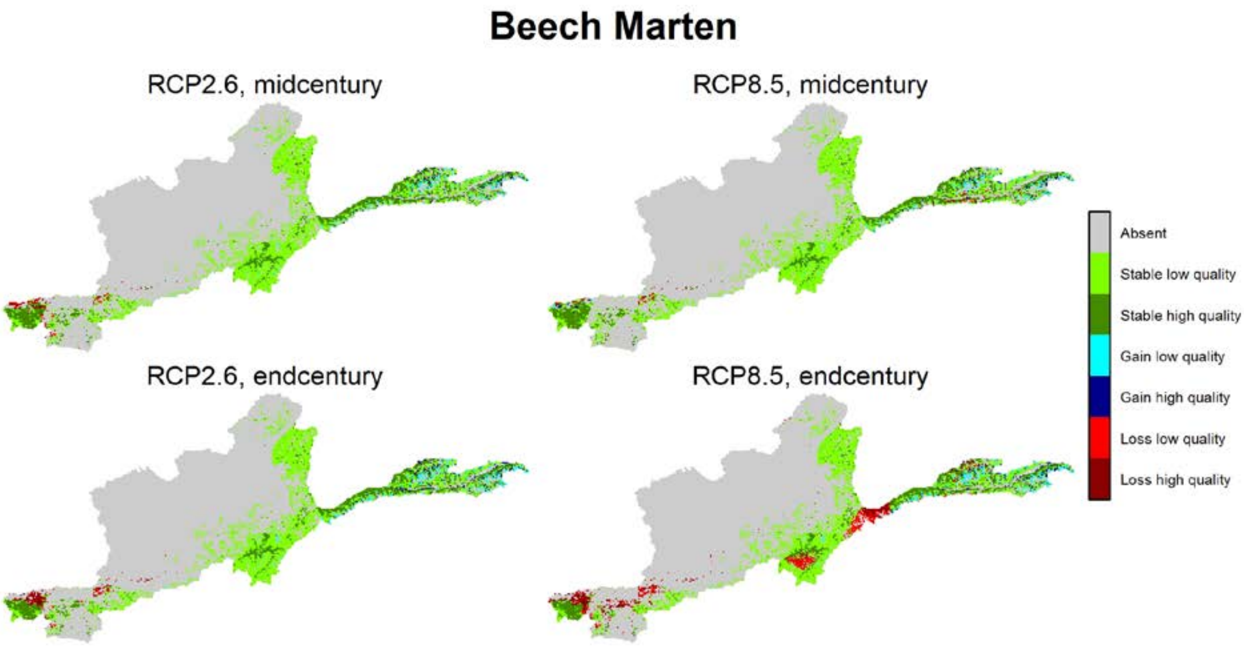

Figure 135. Changes in suitable habitat for Beech Marten (*Martes foina intermedia*).

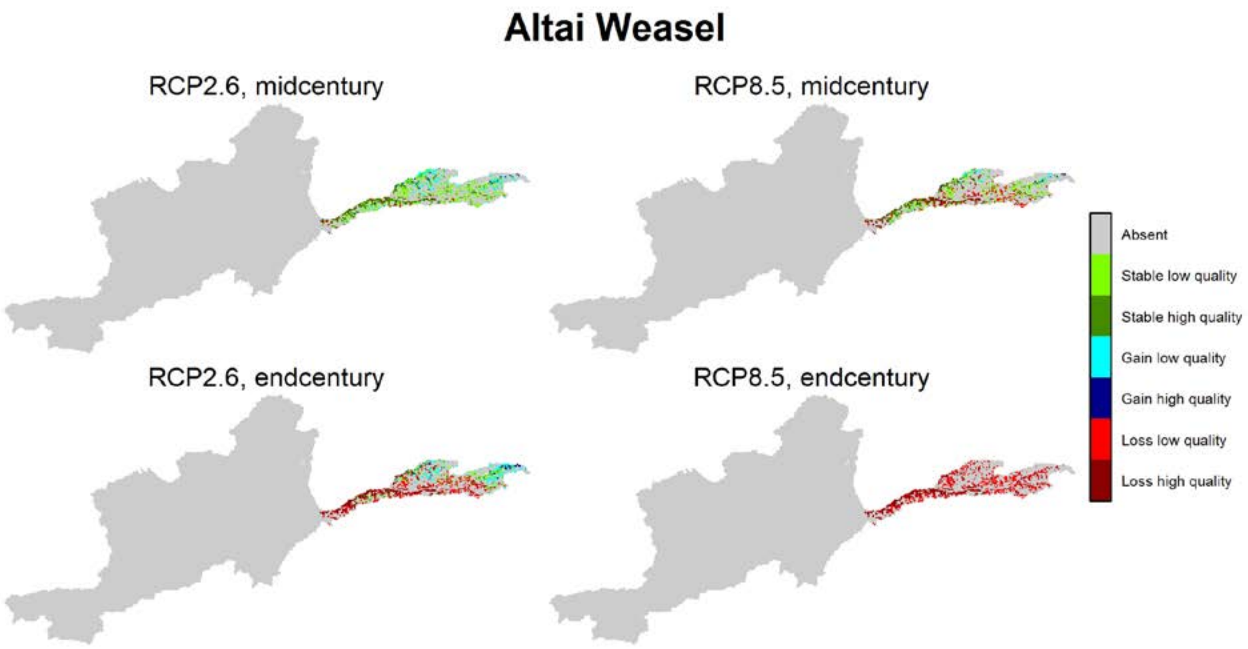

Figure 136. Changes in suitable habitat for Altai Weasel (*Mustela altaica*).

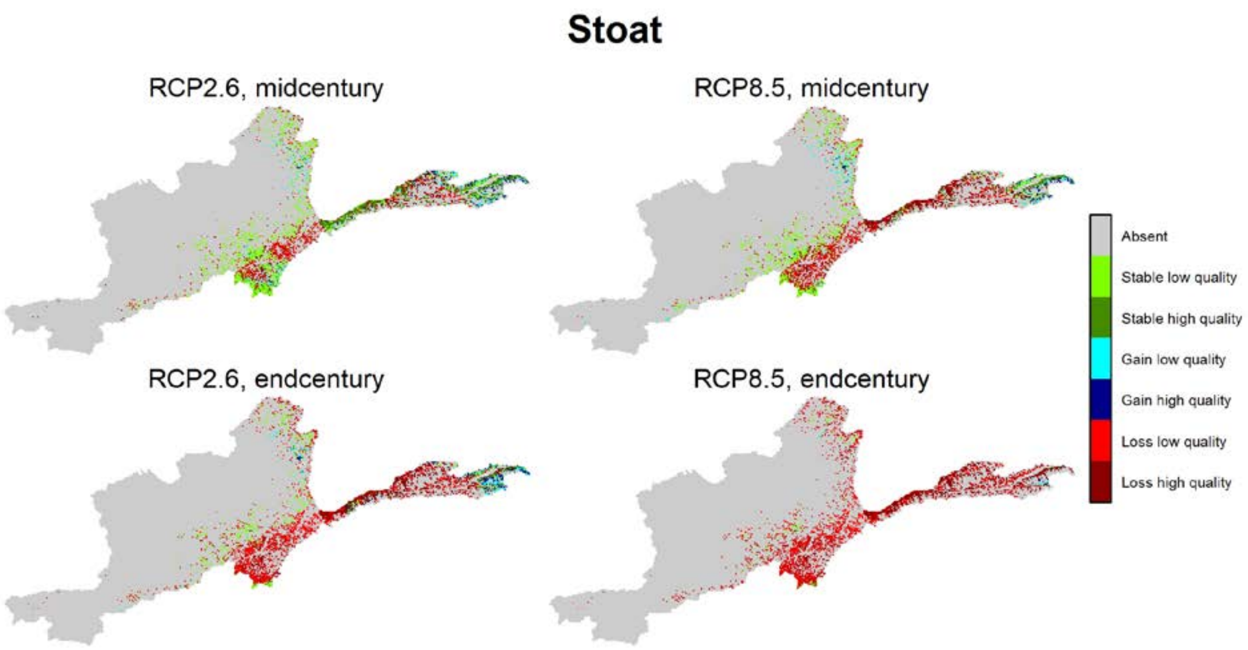

Figure 137. Changes in suitable habitat for Stoat (*Mustela erminea*).

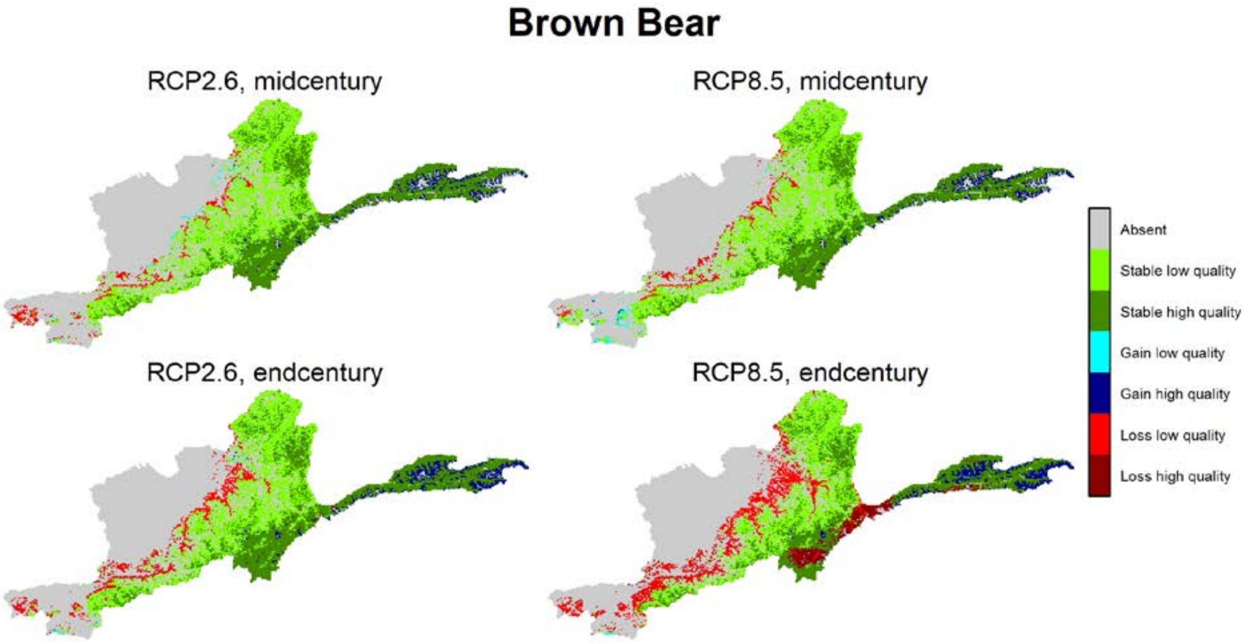

Figure 138. Changes in suitable habitat for Brown Bear (*Ursus arctos syriacus*).

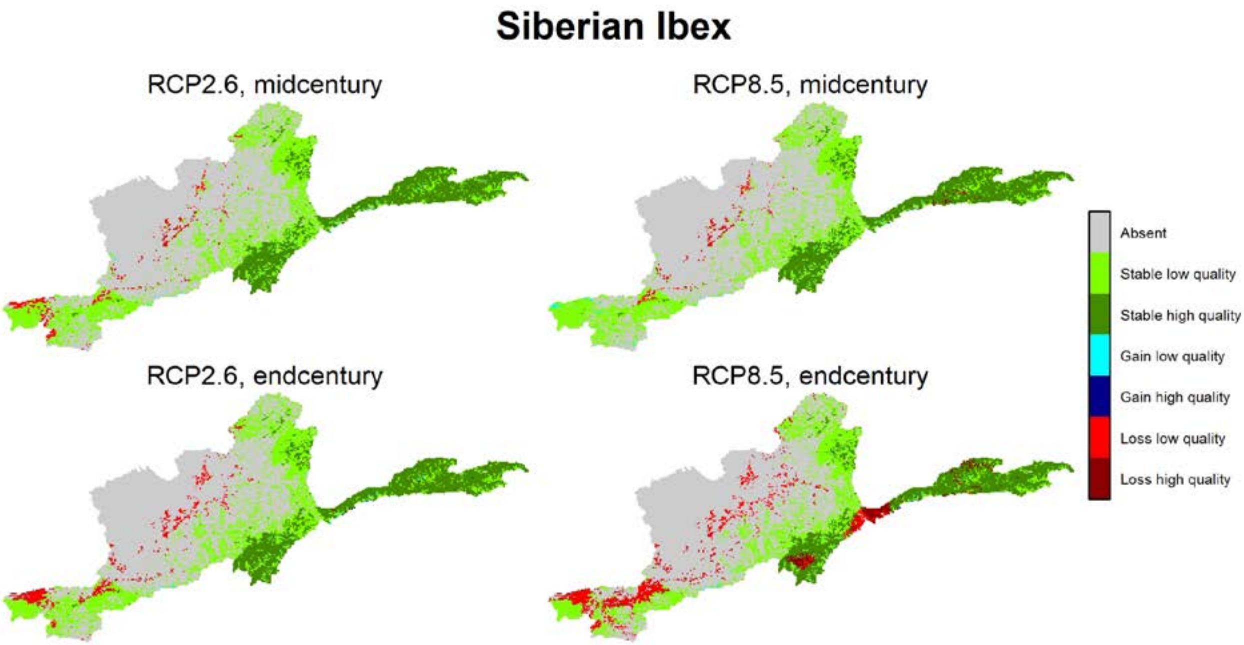

Figure 139. Changes in suitable habitat for Siberian Ibex (*Capra sibirica*).

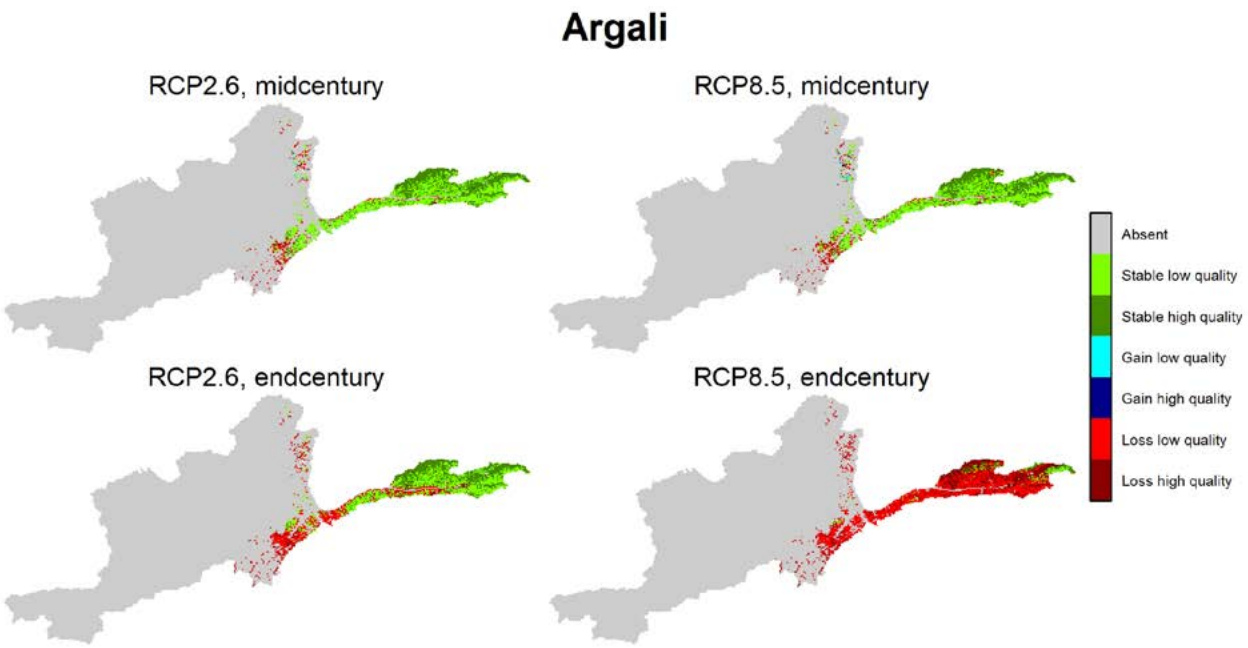

Figure 140. Changes in suitable habitat for Argali (*Ovis ammon*).

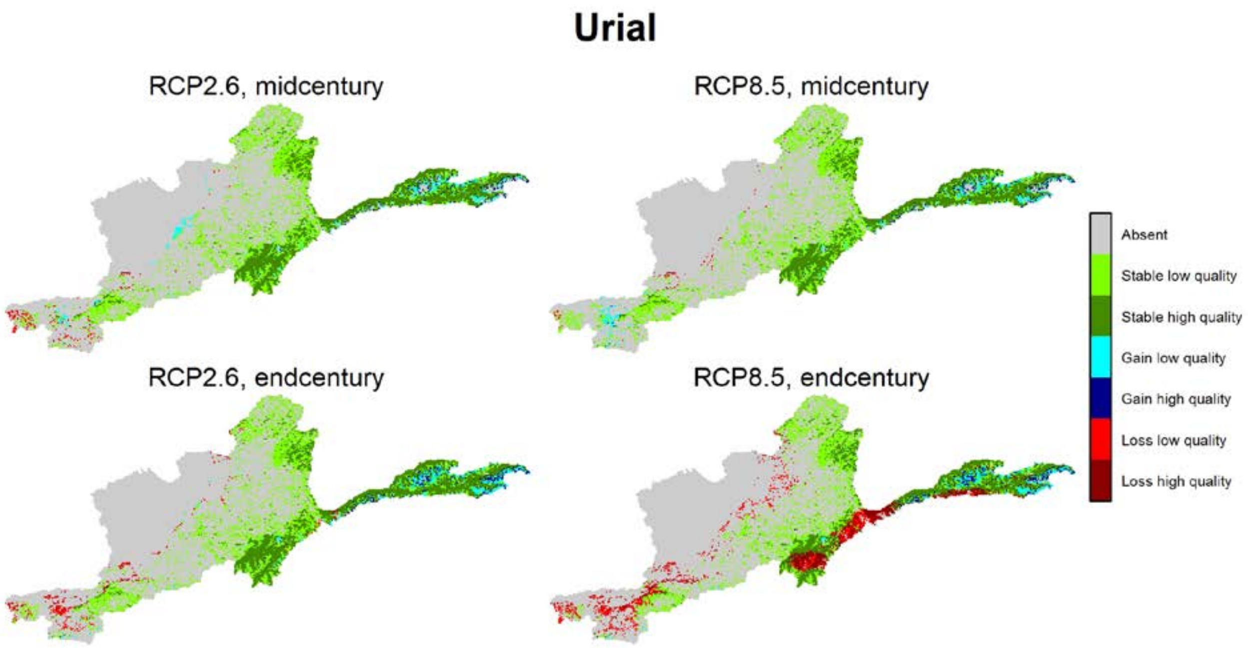

Figure 141. Changes in suitable habitat for Urial (*Ovis vignei*).

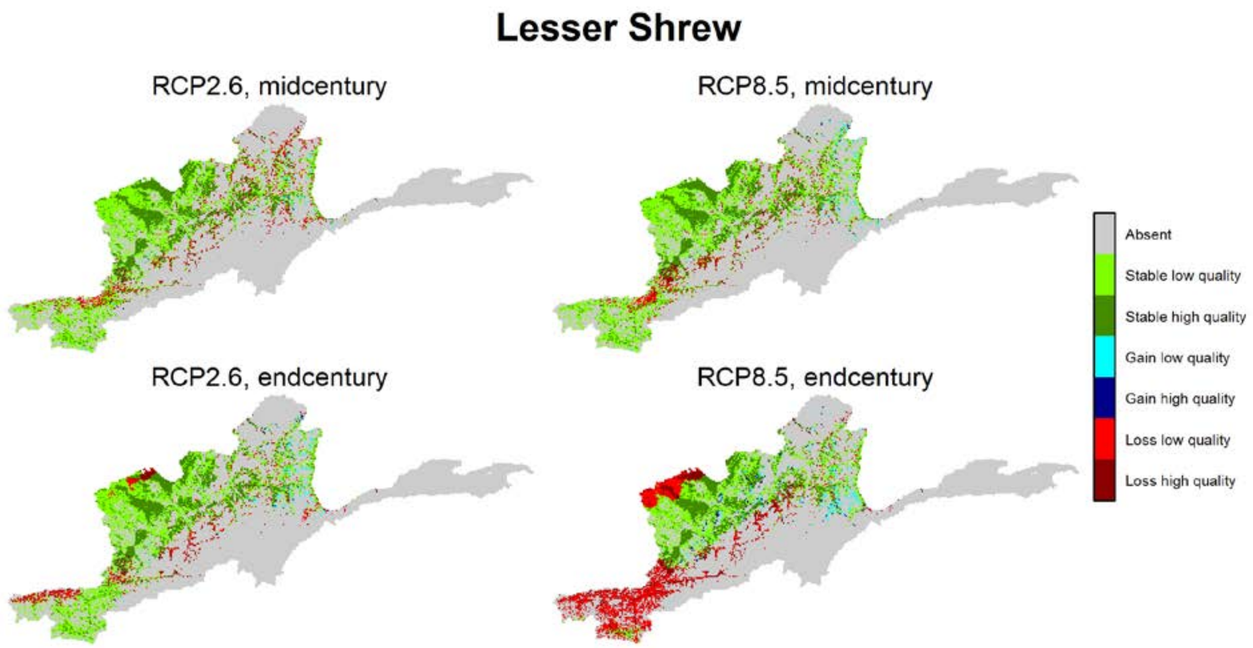

Figure 142. Changes in suitable habitat for Lesser Shrew (*Crocidura suaveolens*).

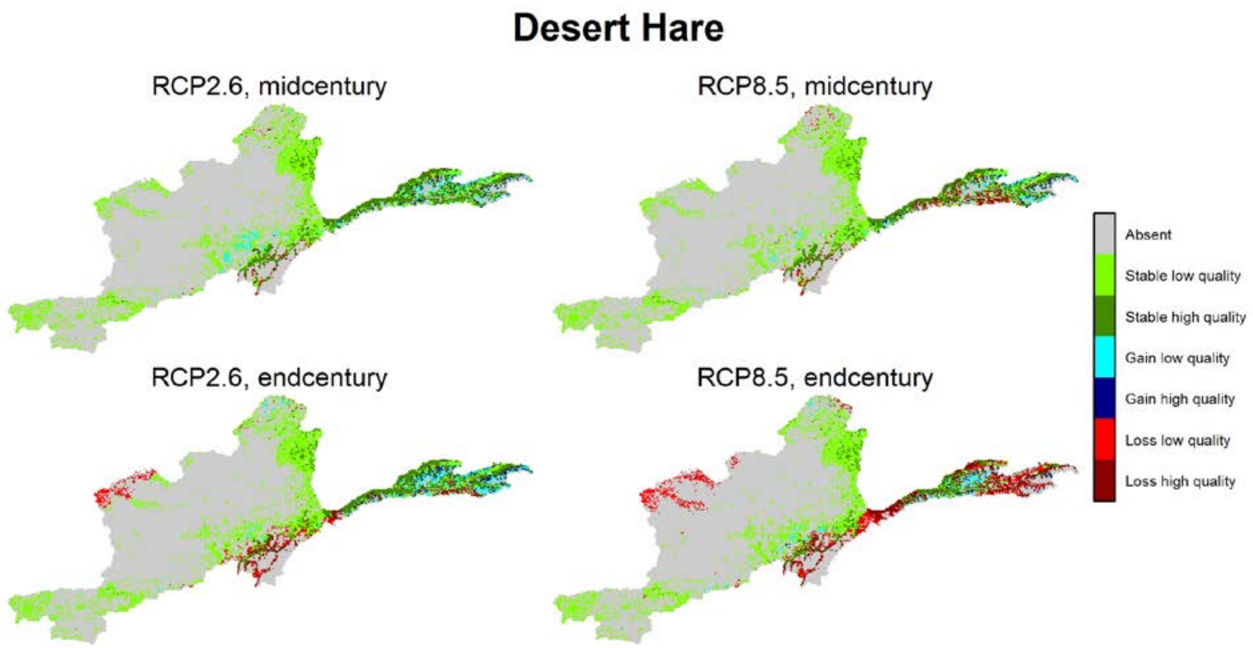

Figure 143. Changes in suitable habitat for Desert Hare (*Lepus tibetanus*).

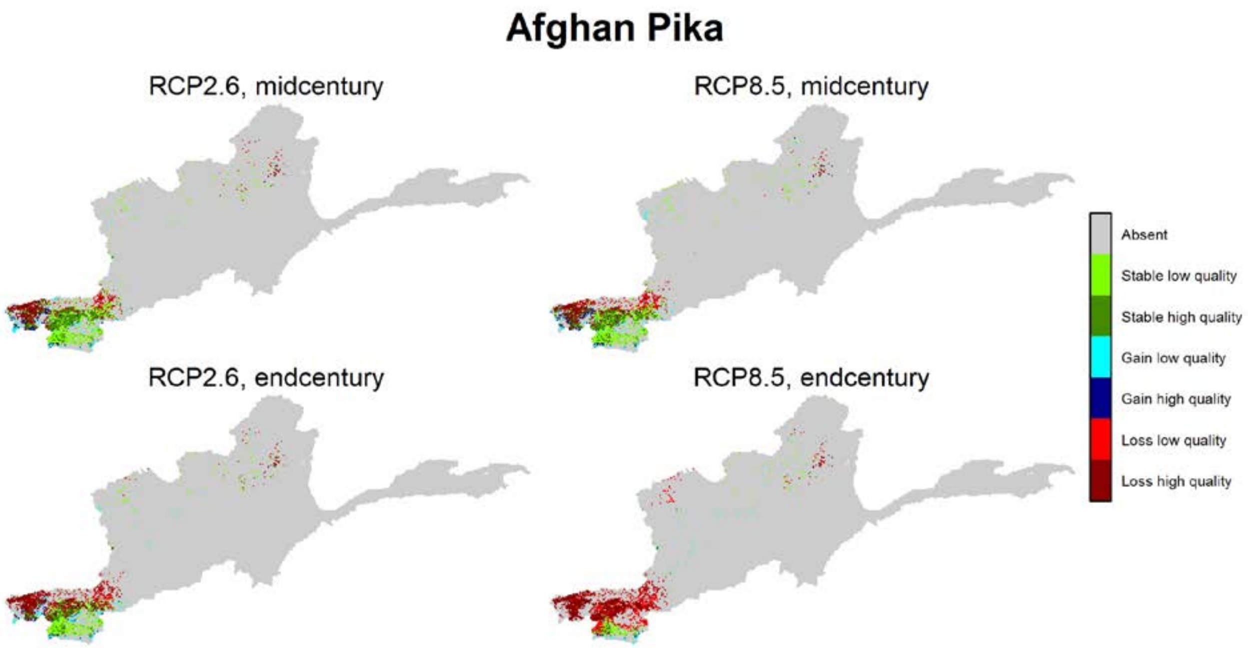

Figure 144. Changes in suitable habitat for Afghan Pika (*Ochotona rufescens*).

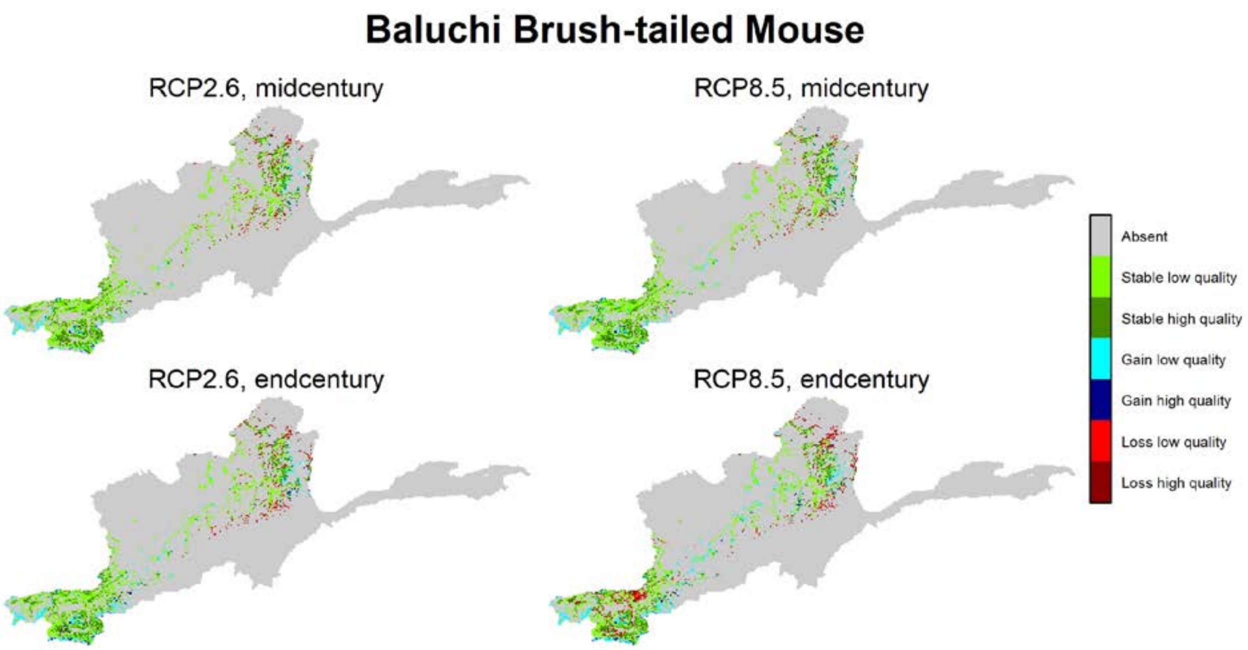

Figure 145. Changes in suitable habitat for Baluchi Brush-tailed Mouse (*Calomyscus baluchi*).

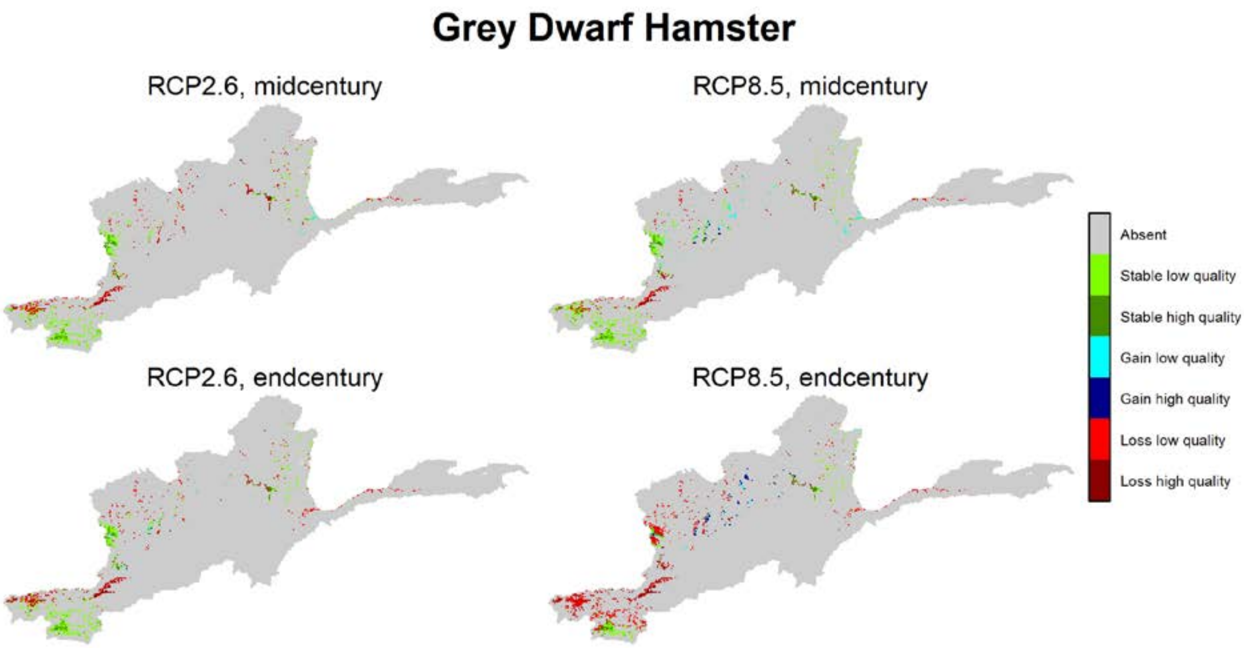

Figure 146. Changes in suitable habitat for Grey Dwarf Hamster (*Cricetulus migratorius*).

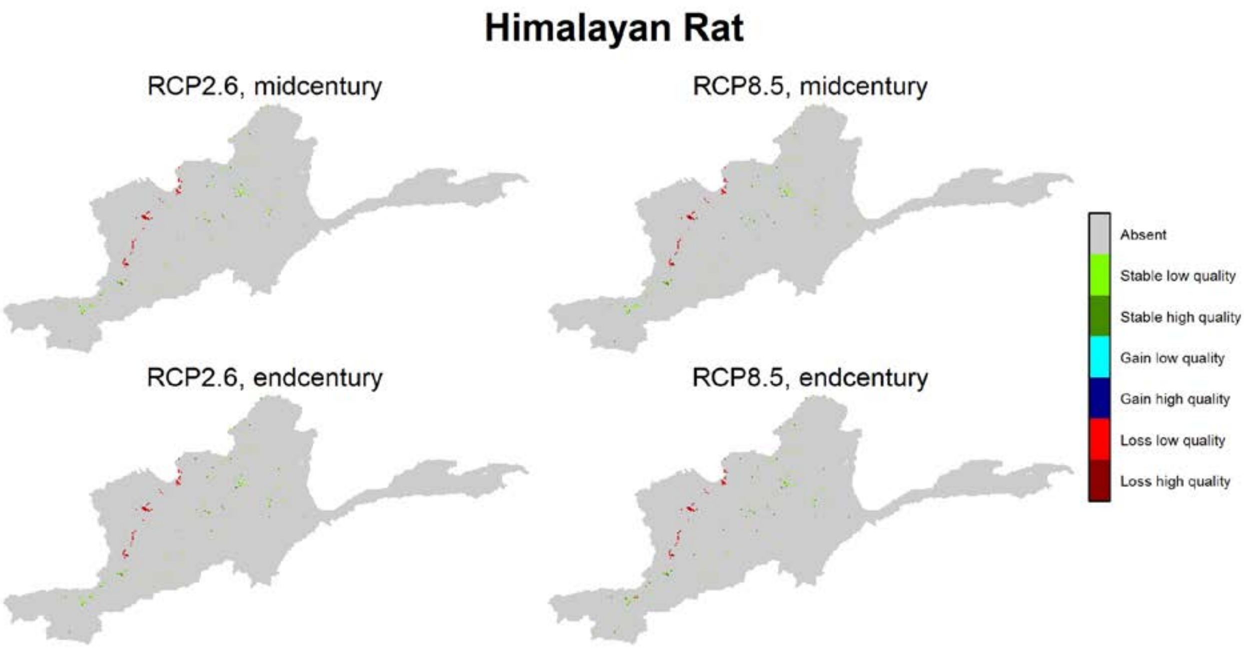

Figure 147. Changes in suitable habitat for Himalayan Rat (*Rattus pyctoris*).

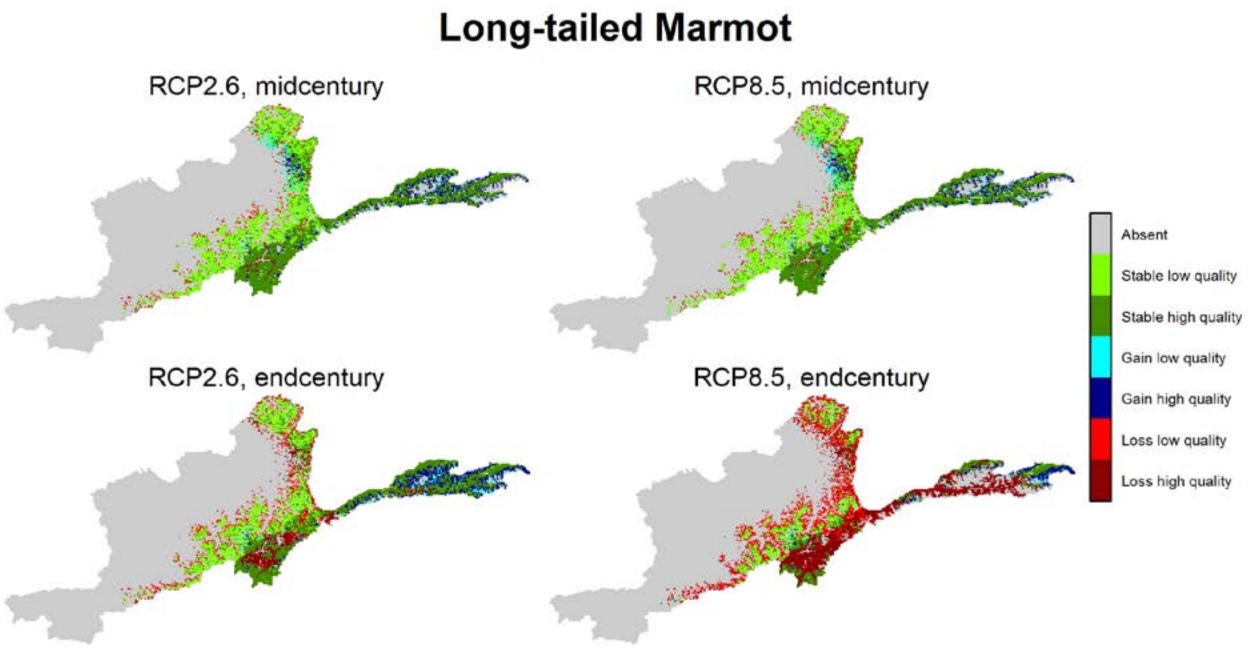

Figure 148. Changes in suitable habitat for Long-tailed Marmot (*Marmota caudata*).

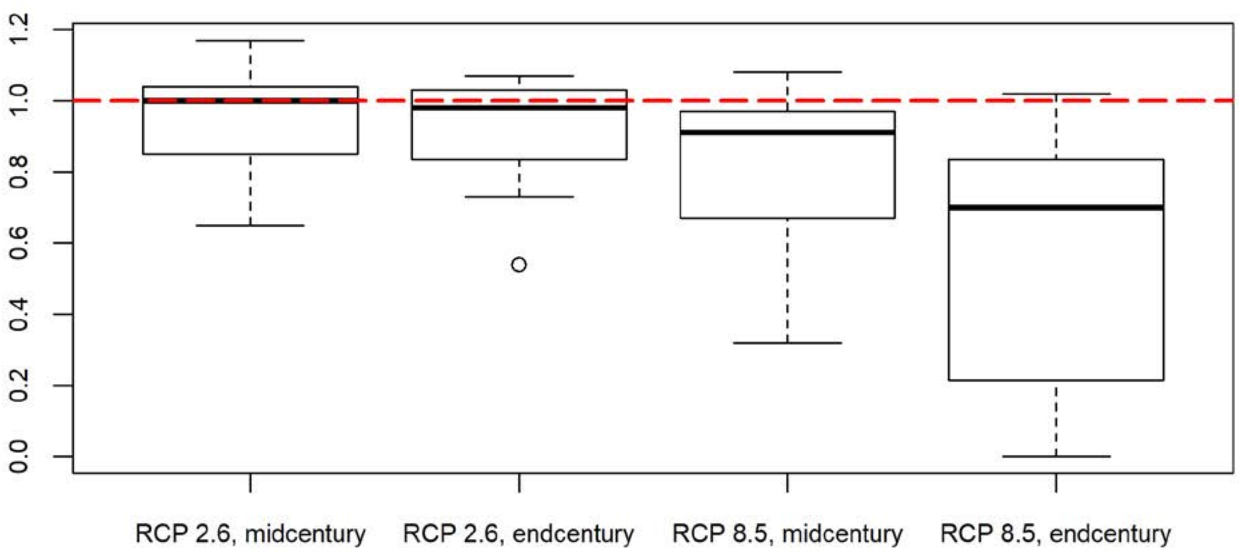

Figure 149. Ratio of current relative to future range size for 19 mammal species. A value of 1 (dashed red line) indicates no projected change in range size; values under one indicate range decreases, while values above one indicate range increases. Bold lines represent the median; the boxes extend from the 25th to 75th percentile values.

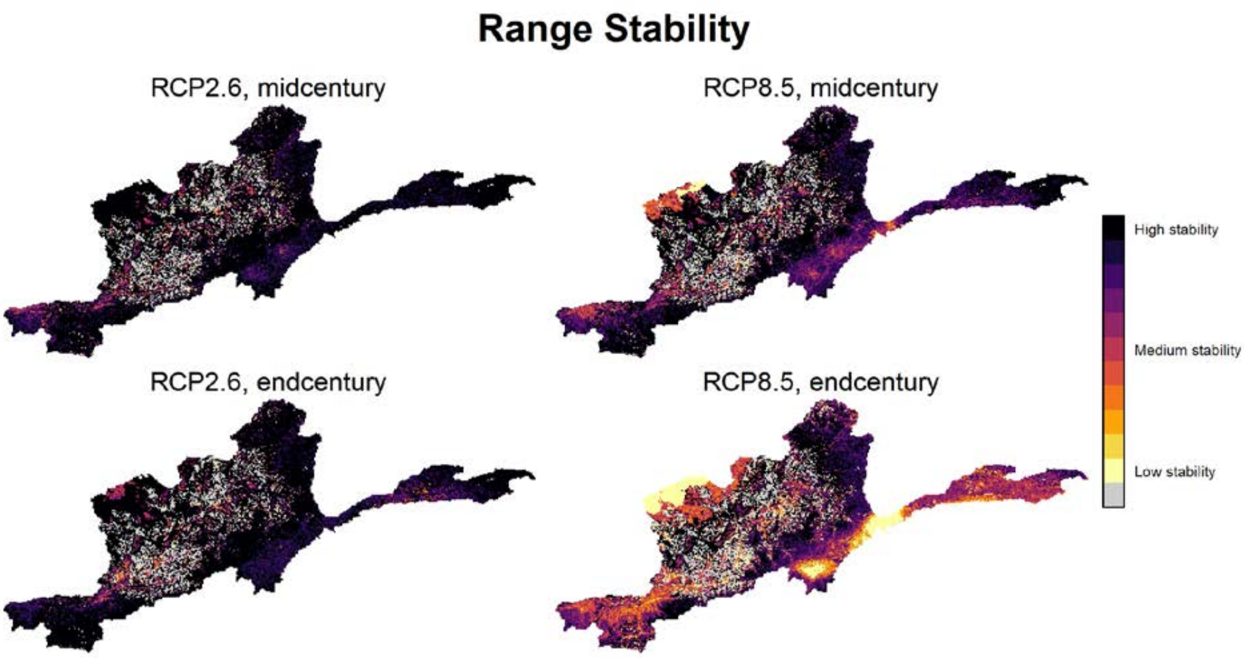

Figure 150. Spatial distribution of range stability, measured as the proportion of mammal species that will experience range losses relative to the number of species that currently occur at each location. Brighter colors indicate more range losses and hence more climate sensitivity (less stability); darker colors indicate fewer range losses and hence less sensitivity (more stability). Grey areas represent areas where all modelled species are currently absent.

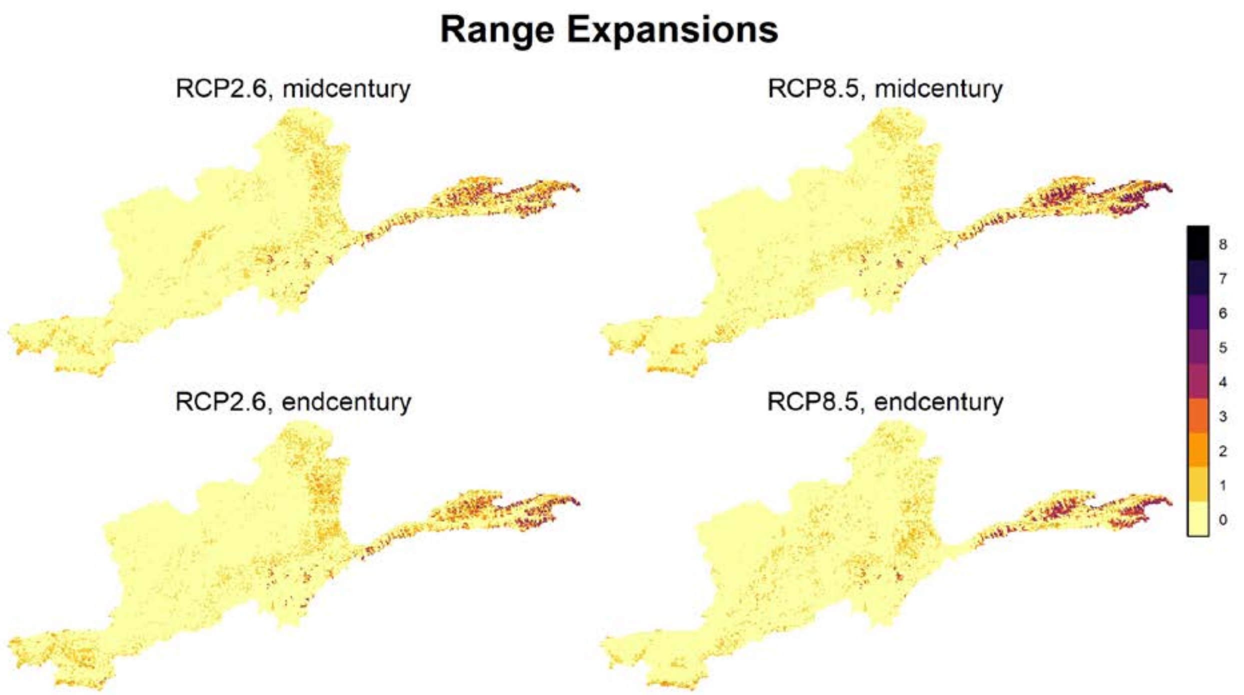

Figure 151. Spatial distribution of potential mammal species range expansions. Lighter colors indicate fewer new species are projected to occur in the future at a location. Darker colors indicate more potential new species moving into a given location.

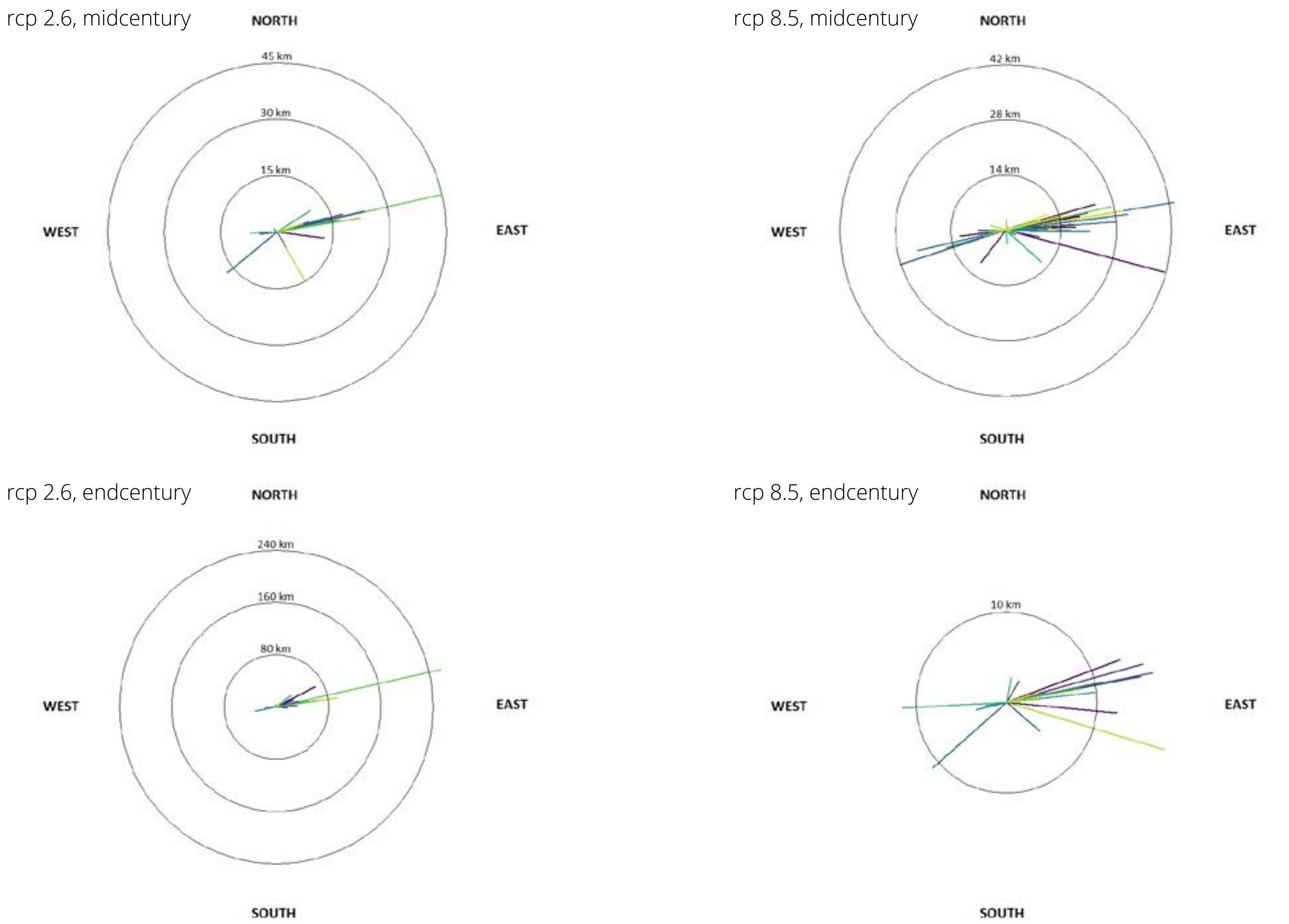

Figure 152. Plots showing the projected distance and direction of movement of the center of mass for each mammal species' distribution. Colored lines represent individual species. Note the scale of movement is far larger for RCP8.5 than for RCP2.6.

Summary plots of indicator by ecoregion and province

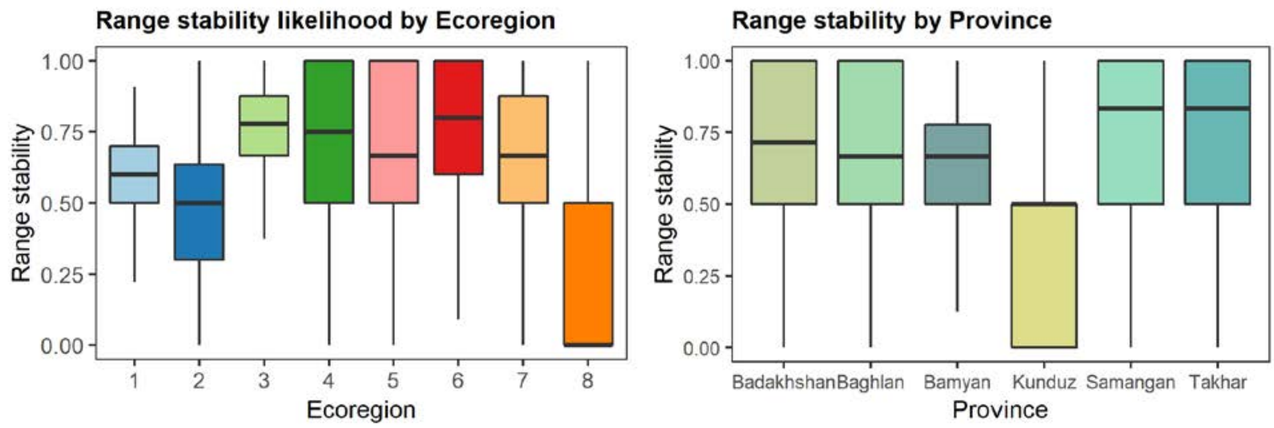

Figure 153. Range stability across all mammal species, summarized by ecoregion and province for RCP8.5, end-century. Higher values indicate a higher likelihood of stability. Ecoregion legend: 1 – Pamir alpine desert and tundra; 2 – Karakorum-West Tibetan Plateau alpine steppe; 3 – Gissaro-Alai open woodlands; 4 – Paropamisus xeric woodlands; 5 – Ghorat-Hazarajat alpine meadow; 6 – Hindu-Kush alpine meadow; 7 – Afghan Mountains semi-desert; 8 - Badghyz and Karabil semi-desert.

Results summary

The results show that species' range sizes are projected to decrease on average by end-century (Figure 149), with larger decreases under an RCP8.5 scenario compared to RCP2.6. Ranges are more likely to contract in the south, southwest and northwest parts of the region (Figure 150), with relative stability in the Wakhan corridor of the northeast. However, most areas will lose at least one currently present species by end-century in a high-emissions (RCP8.5) future. Range expansions are far sparser than range contractions and are projected to occur primarily in the Wakhan region of Badakhshan province, with other sparse expansions through the rest of Badakhshan province and in the southwest (Figure 151). More range expansions are projected to occur in an RCP8.5 future and by mid-century. These range expansions are most likely to occur in the Pamir Alpine Desert and Tundra and the Karakoram-West Tibetan Plateau Alpine Steppe ecoregions. The results in Figure 152 show that the center of mass of each species' distribution is projected to shift further when comparing end-century to mid-century projections, and when comparing RCP8.5 to RCP2.6. It is noteworthy that the direction of movement for all species, virtually without exception, is to the east/northeast. This is likely attributable to the temperature/elevation gradient of the P-ARB that runs roughly southwest-northeast (see Figure 5 and Figure 6) – movements to the northeast would generally be towards cooler, higher areas that would counteract the effects of climate change.

Eight species (Afghan Pika *Ochotona rufescens*, *Altai Weasel Mustela altaica*, *Argali Ovis ammon,* Eurasian Lynx *Lynx lynx,* Grey Dwarf Hamster *Cricetulus migratorius*, Long-tailed Marmot *Marmota caudate*, Snow Leopard *Panthera uncia* and Stoat *Mustela erminea*) are projected to lose over 50% of their range by end-century under a high-emissions scenario. No species is expected to lose over 50% of its range by mid-century or in a low-emissions future, highlighting the importance of climate mitigation efforts for wildlife in the P-ARB. A full table of estimated changes in range size is given in Table 61, in Appendix 6.

At the province level, mammal species ranges are projected to be most stable in Samangan and Takhar provinces (Figure 153). At the ecoregion level, mammal ranges are least likely to be stable in the Badghyz and Karabil Semi-Desert (Ecoregion 8) and most likely to be stable ecoregions in the Hindu Kush Alpine Meadow (Ecoregion 6).

It is important to note that these projections apply to the ranges of mammal species within the P-ARB only. That species may eventually be eliminated from the P-ARB does not necessarily imply anything about their future global status or their status within Afghanistan—it is entirely possible that range expansions could occur in other portions of the species' range outside of Afghanistan to offset losses occurring with Afghanistan. That said, these results are significant for conservation planning and policy purposes in the P-ARB, as they imply a great deal of biotic reorganization with poorly known consequences in the upcoming century.

Changes in Bird Range Size and Location

E

Indicator overview

In addition to the changes in mammal range sizes and locations discussed above, we also examined the same metrics for bird species. For a more complete discussion of this indicator, see the preceding section.

Methods overview

The methods used were the same as those used for mammal species (see the preceding section and particularly Figure 129 for further details). A notable difference is that birds, unlike the mammal species present in the region, undertake long-distance seasonal migrations. Therefore, we only considered records from May through September, which we consider indicative of the breeding range for a species rather than a migratory or non-breeding range. Table 22 gives the list of species used in the analysis. Occurrence models were created for 60 species in total, representing 9 orders and 26 families, for which at least 5 confirmed georeferenced presence records could be obtained within the P-ARB. All species are listed as Least Concern by the IUCN except for Bearded Vulture *Gypaetus barbatus* (Near Threatened) and Large-billed Reed Warbler *Acrocephalus orinus* (Data Deficient). It is also useful to note that Afghan Snowfinch *Pyrgilauda theresae*, while listed Least Concern, is Afghanistan's only endemic bird species and has a relatively small global range.

Table 22. List of bird species used in species distribution modelling analysis. Names and taxonomy follow International Ornithological Congress (IOC) v12.1 nomenclature. The number of confirmed occurrence records, and records within the PARB, is given after the common name of each species.

Order	Family	Latin name	Common Name
Accipitriformes	Accipitridae	*Buteo rufinus*	Long-legged Buzzard (166;8)
Accipitriformes	Accipitridae	*Gypaetus barbatus*	Bearded Vulture (392;7)
Apodiformes	Apodidae	*Apus apus*	Common Swift (334;11)
Bucerotiformes	Upupidae	*Upupa epops*	Eurasian Hoopoe (2001;17)
Charadriiformes	Charadriidae	*Charadrius mongolus*	Lesser Sand Plover (91;20)
Charadriiformes	Scolopacidae	*Actitis hypoleucos*	Common Sandpiper (539;10)
Charadriiformes	Scolopacidae	*Tringa totanus*	Common Redshank (293;16)
Columbiformes	Columbidae	*Columba livia*	Rock Pigeon (2984;14)
Coraciiformes	Coraciidae	*Coracias garrulus*	European Roller (529;6)
Coraciiformes	Meropidae	*Merops apiaster*	European Bee-eater (218;5)
Falconiformes	Falconidae	*Falco tinnunculus*	Common Kestrel (699;14)
Galliformes	Phasianidae	*Alectoris chukar*	Chukar Partridge (20;641)
Galliformes	Phasianidae	*Tetraogallus himalayensis*	Himalayan Snowcock (11;134)
Passeriformes	Acrocephalidae	*Acrocephalus orinus*	Large-billed Reed Warbler (15;11)
Passeriformes	Alaudidae	*Alauda gulgula*	Oriental Skylark (250;10)
Passeriformes	Alaudidae	*Calandrella acutirostris*	Hume's Short-toed Lark (137;23)
Passeriformes	Alaudidae	*Eremophila alpestris*	Horned Lark (617;215)
Passeriformes	Corvidae	*Corvus corax*	Northern Raven (334;5)
Passeriformes	Corvidae	*Corvus cornix*	Hooded Crow (88;7)
Passeriformes	Corvidae	*Corvus corone*	Carrion Crow (193;11)
Passeriformes	Corvidae	*Pica pica*	Eurasian Magpie (853;42)
Passeriformes	Corvidae	*Pyrrhocorax graculus*	Alpine Chough (495;23)
Passeriformes	Corvidae	*Pyrrhocorax pyrrhocorax*	Red-billed Chough (616;45)

Passeriformes	Emberizidae	*Emberiza bruniceps*	Red-headed Bunting (193;15)
Passeriformes	Emberizidae	*Emberiza buchanani*	Grey-necked Bunting (41;6)
Passeriformes	Emberizidae	*Emberiza cia*	Rock Bunting (698;6)
Passeriformes	Fringillidae	*Bucanetes mongolicus*	Mongolian Finch (81;37)
Passeriformes	Fringillidae	*Carpodacus erythrinus*	Common Rosefinch (19;830)
Passeriformes	Fringillidae	*Carpodacus grandis*	Blyth's Rosefinch (8;25)
Passeriformes	Fringillidae	*Carpodacus rubicilla*	Great Rosefinch (9;146)
Passeriformes	Fringillidae	*Carpodacus stoliczkae*	Pale Rosefinch (5;12)
Passeriformes	Fringillidae	*Leucosticte brandti*	Brandt's Mountain Finch (210;28)
Passeriformes	Fringillidae	*Linaria flavirostris*	Twite (116;246)
Passeriformes	Fringillidae	*Rhodopechys sanguineus*	Asian Crimson-winged Finch (41;23)
Passeriformes	Fringillidae	*Serinus pusillus*	Red-fronted Serin (14;423)
Passeriformes	Hirundinidae	*Delichon urbicum*	Common House Martin (202;15)
Passeriformes	Hirundinidae	*Ptyonoprogne rupestris*	Eurasian Crag Martin (276;36)
Passeriformes	Laniidae	*Lanius schach*	Long-tailed Shrike (1178;9)
Passeriformes	Motacillidae	*Motacilla alba*	White Wagtail (1041;16)
Passeriformes	Motacillidae	*Motacilla citreola*	Citrine Wagtail (854;77)
Passeriformes	Muscicapidae	*Monticola saxatilis*	Common Rock Thrush (59;8)
Passeriformes	Muscicapidae	*Monticola solitarius*	Blue Rock Thrush (286;13)
Passeriformes	Muscicapidae	*Oenanthe chrysopygia*	Red-tailed Wheatear (41;18)
Passeriformes	Muscicapidae	*Oenanthe deserti*	Desert Wheatear (232;24)
Passeriformes	Muscicapidae	*Oenanthe isabellina*	Isabelline Wheatear (60;191)
Passeriformes	Muscicapidae	*Oenanthe oenanthe*	Northern Wheatear (86;41)
Passeriformes	Muscicapidae	*Phoenicurus erythrogastrus*	Guldenstadt's Redstart (13;199)
Passeriformes	Muscicapidae	*Phoenicurus ochruros*	Black Redstart (1017;82)
Passeriformes	Muscicapidae	*Saxicola maurus*	Siberian Stonechat (587;15)
Passeriformes	Oriolidae	*Oriolus kundoo*	Indian Golden Oriole (921;14)
Passeriformes	Passeridae	*Montifringilla nivalis*	White-winged Snowfinch (46;77)
Passeriformes	Passeridae	*Passer domesticus*	House Sparrow (3287;21)
Passeriformes	Passeridae	*Passer montanus*	Eurasian Tree Sparrow (238;14)
Passeriformes	Passeridae	*Pyrgilauda theresae*	Afghan Snowfinch (54;63)
Passeriformes	Phylloscopidae	*Phylloscopus griseolus*	Sulphur-bellied Warbler (221;17)
Passeriformes	Prunellidae	*Prunella collaris*	Alpine Accentor (94;5)
Passeriformes	Prunellidae	*Prunella fulvescens*	Brown Accentor (84;18)
Passeriformes	Sittidae	*Sitta tephronota*	Eastern Rock Nuthatch (136;45)
Passeriformes	Sturnidae	*Pastor roseus*	Rosy Starling (322;5)
Passeriformes	Tichodromidae	*Tichodroma muraria*	Wallcreeper (9;78)

Spatial representation of indicator

As far more bird species (60 in total) were assessed than mammal species, a subset of the individual species results, including the three species (Bearded Vulture, Large-billed Reed Warbler and Afghan Snowfinch) of greatest conservation concern, are shown below. The summary figures (Figure 169 to Figure 173) are based on results for all 60 species. For individual maps for the other 45 species, see Appendix 6. For a table summarizing expected range size changes for each species, see Table 62 in Appendix 6.

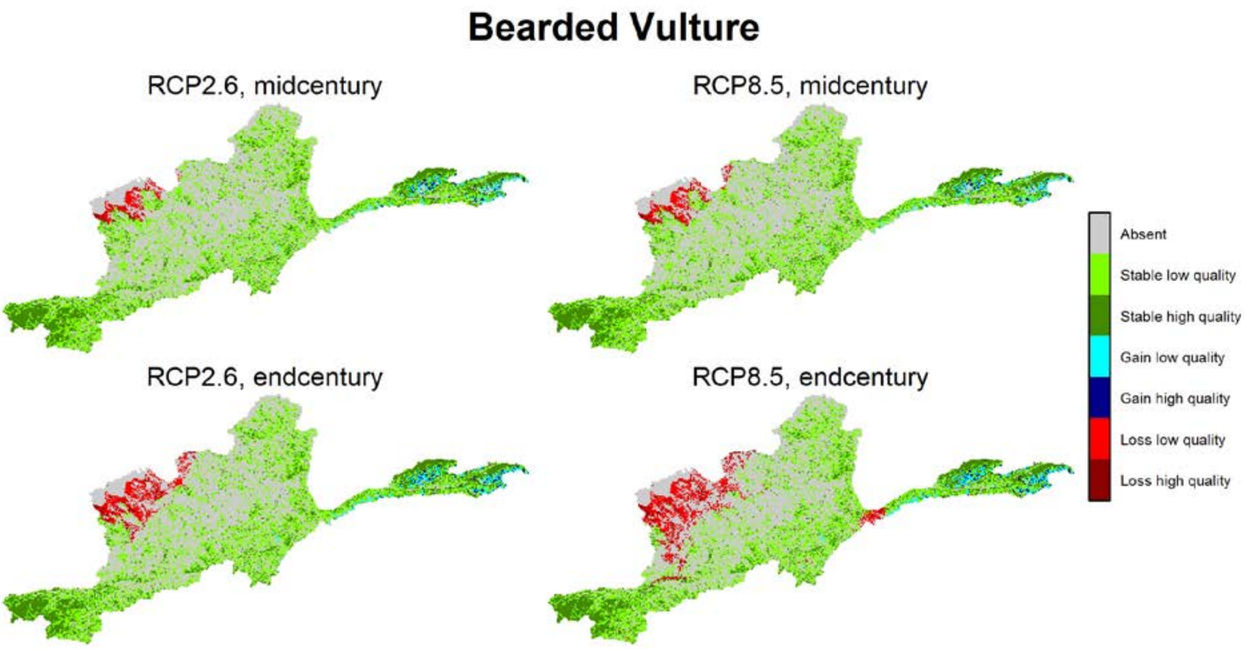

Figure 154. Changes in suitable habitat for Bearded Vulture (*Gypaetus barbatus*).

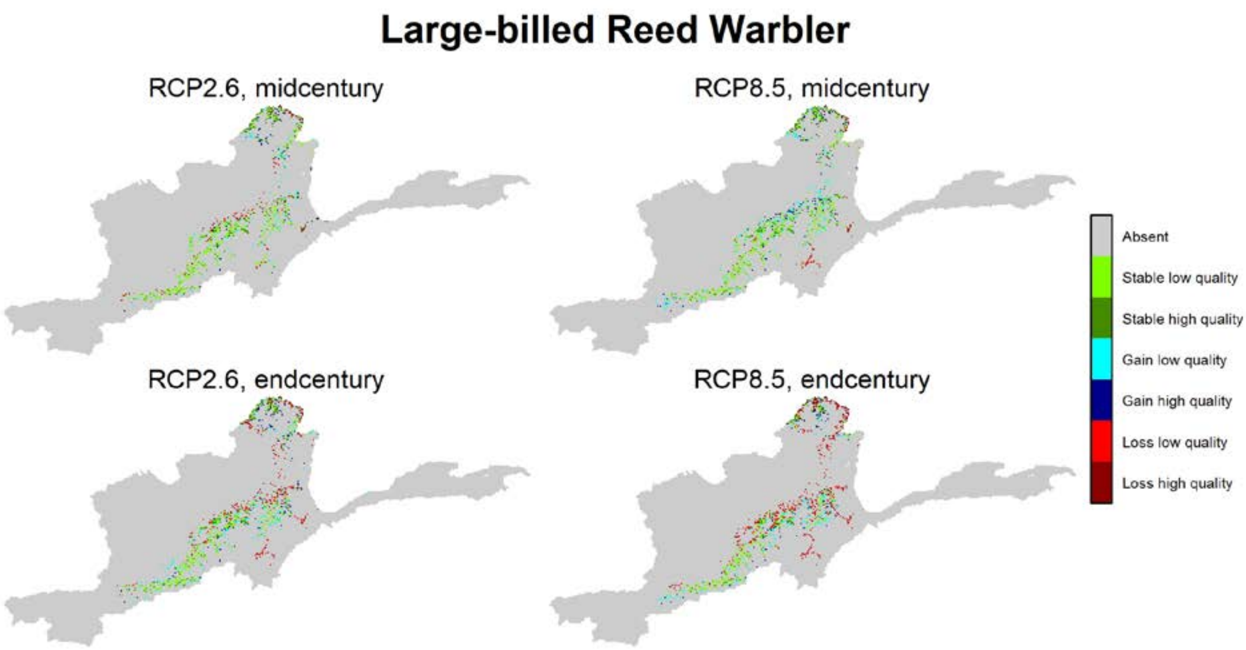

Figure 155. Changes in suitable habitat for Large-billed Reed Warbler (*Acrocephalus orinus*).

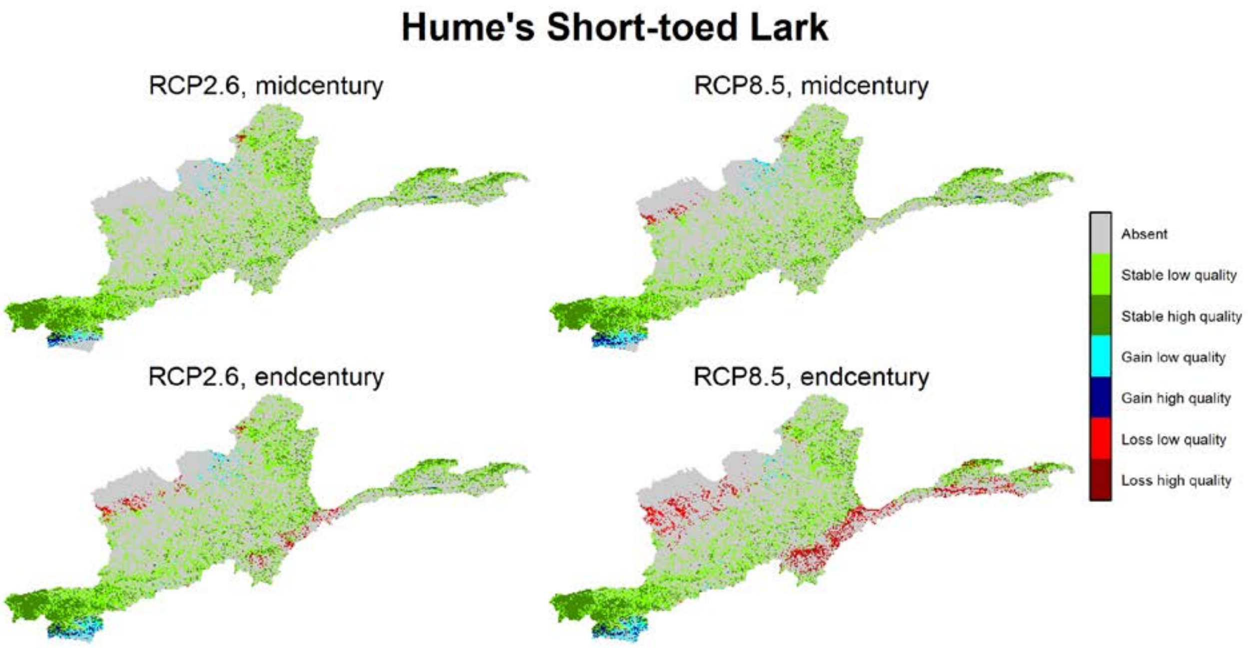

Figure 156. Changes in suitable habitat for Hume's Short-toed Lark (*Calandrella acutirostris*).

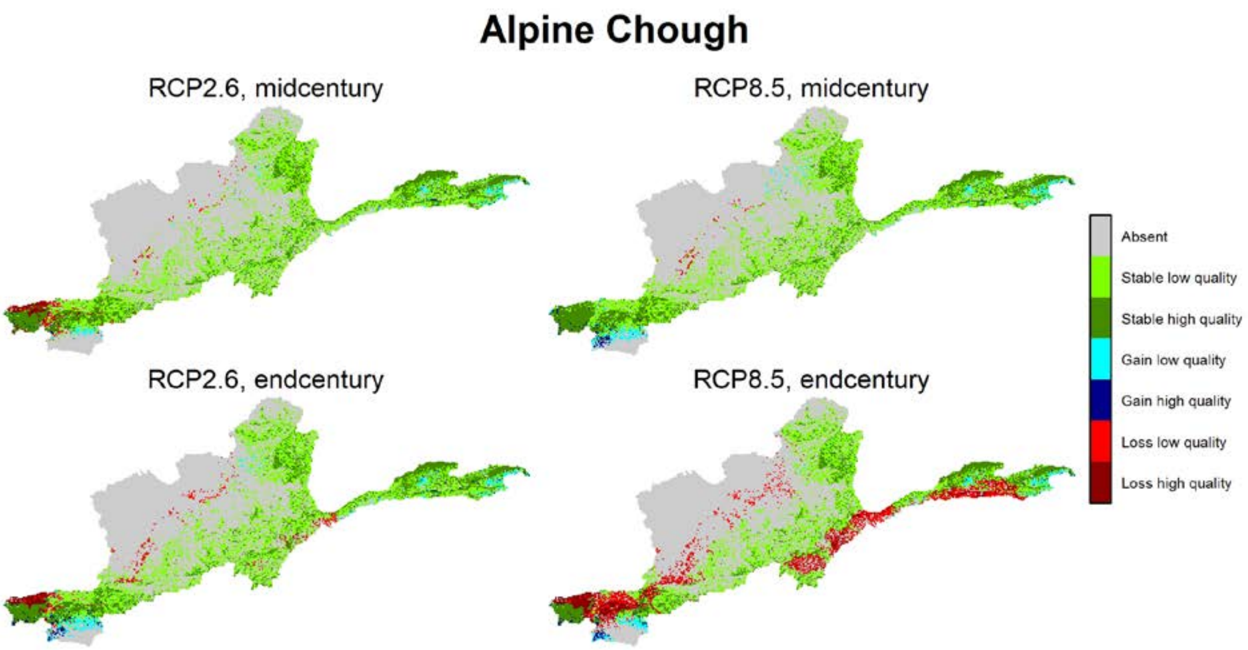

Figure 157. Changes in suitable habitat for Alpine Chough (*Pyrrhocorax graculus*).

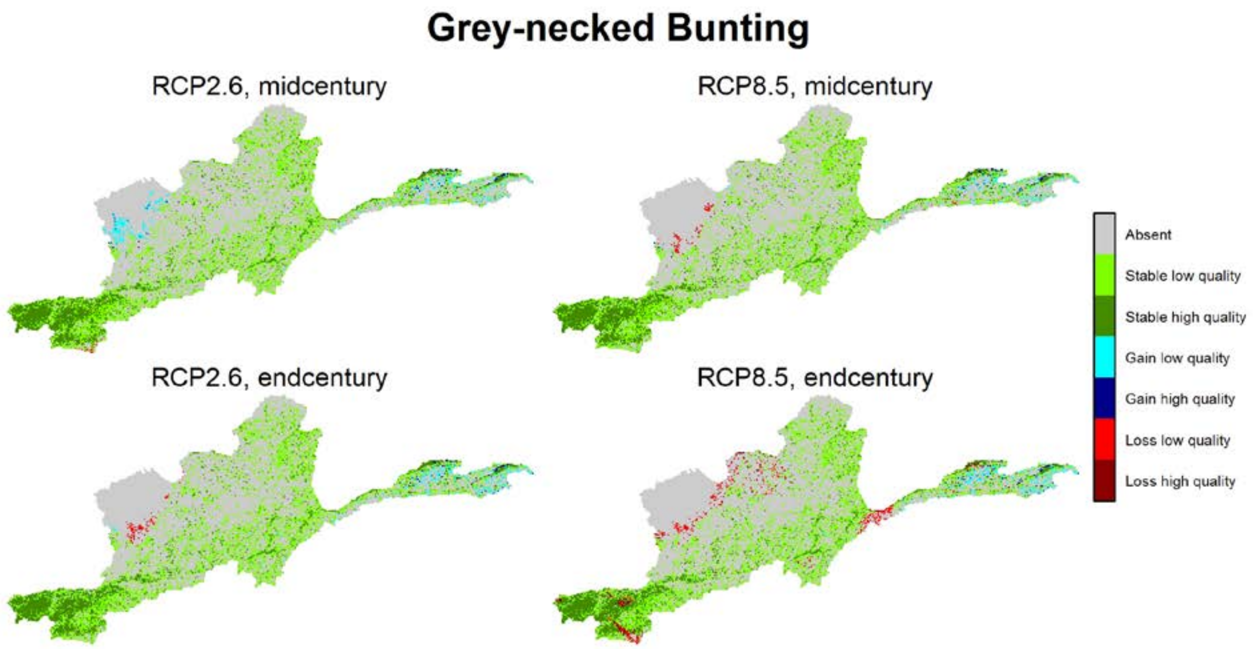

Figure 158. Changes in suitable habitat for Grey-necked Bunting (*Emberiza buchanani*).

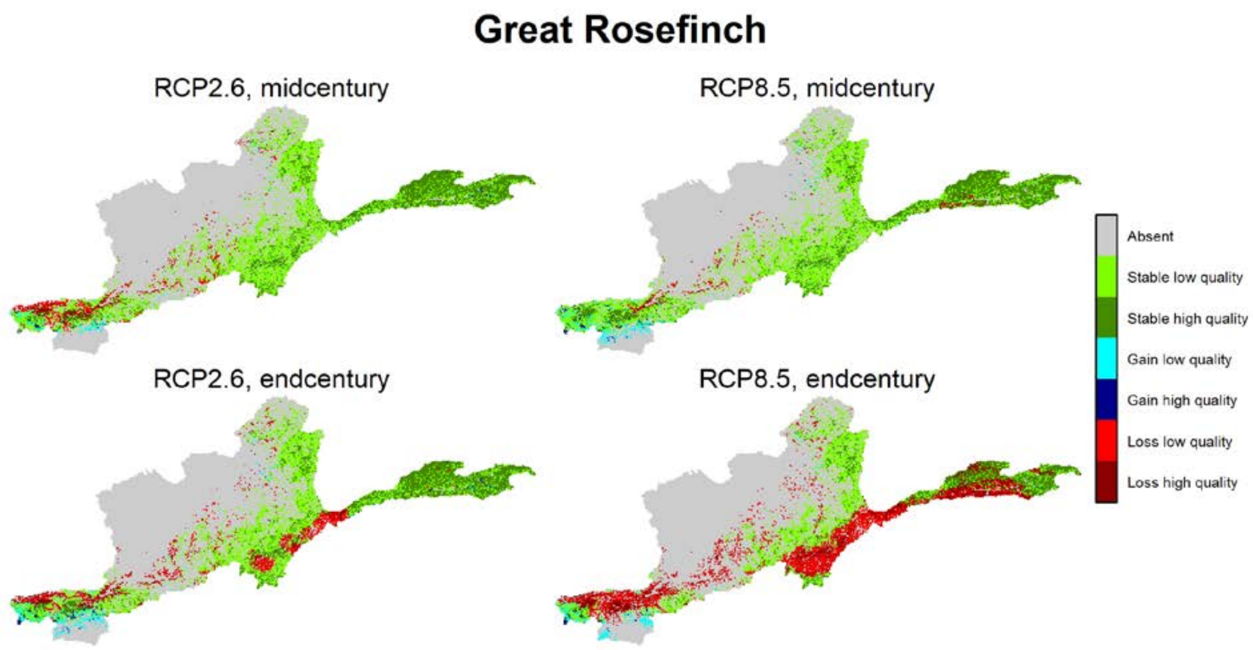

Figure 159. Changes in suitable habitat for Great Rosefinch (*Carpodacus rubicilla*).

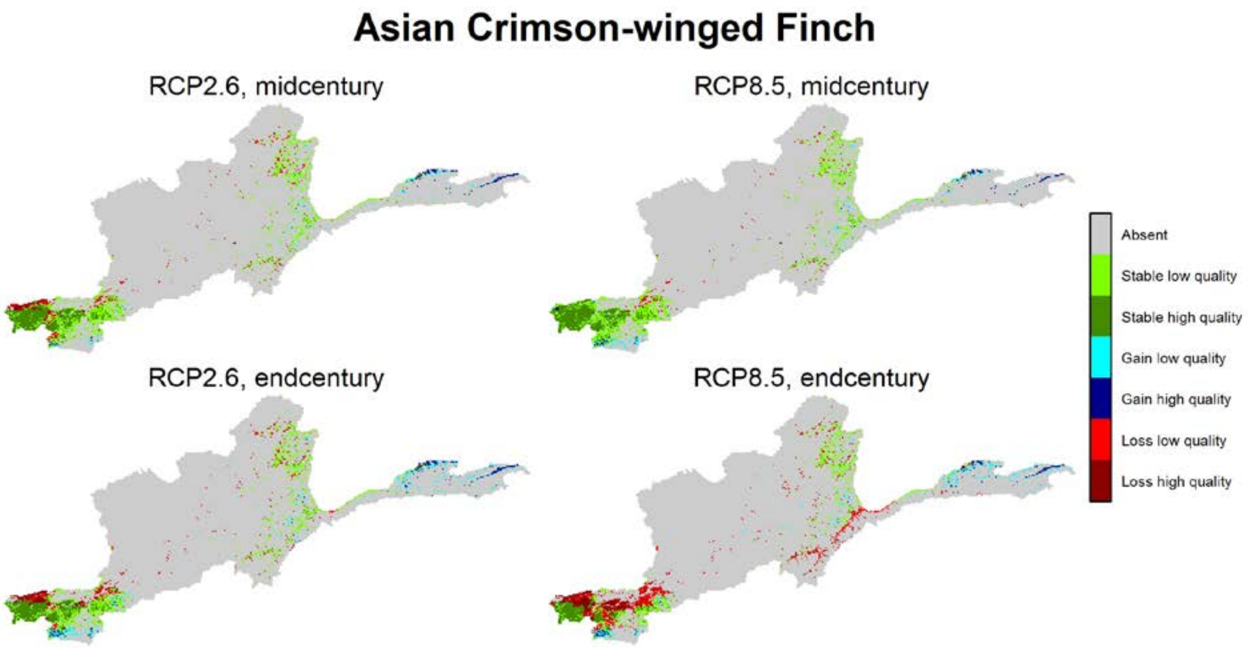

Figure 160. Changes in suitable habitat for Asian Crimson-winged Finch (*Rhodopechys sanguineus*).

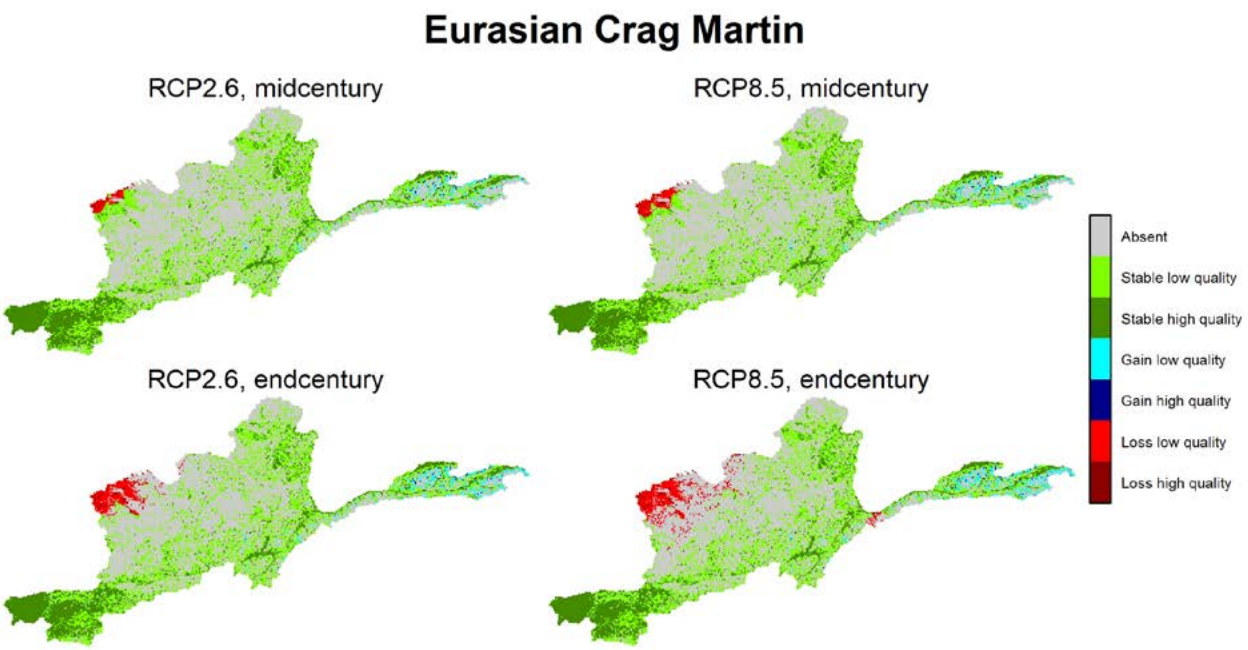

Figure 161. Changes in suitable habitat for Eurasian Crag Martin (*Ptyonoprogne rupestris*).

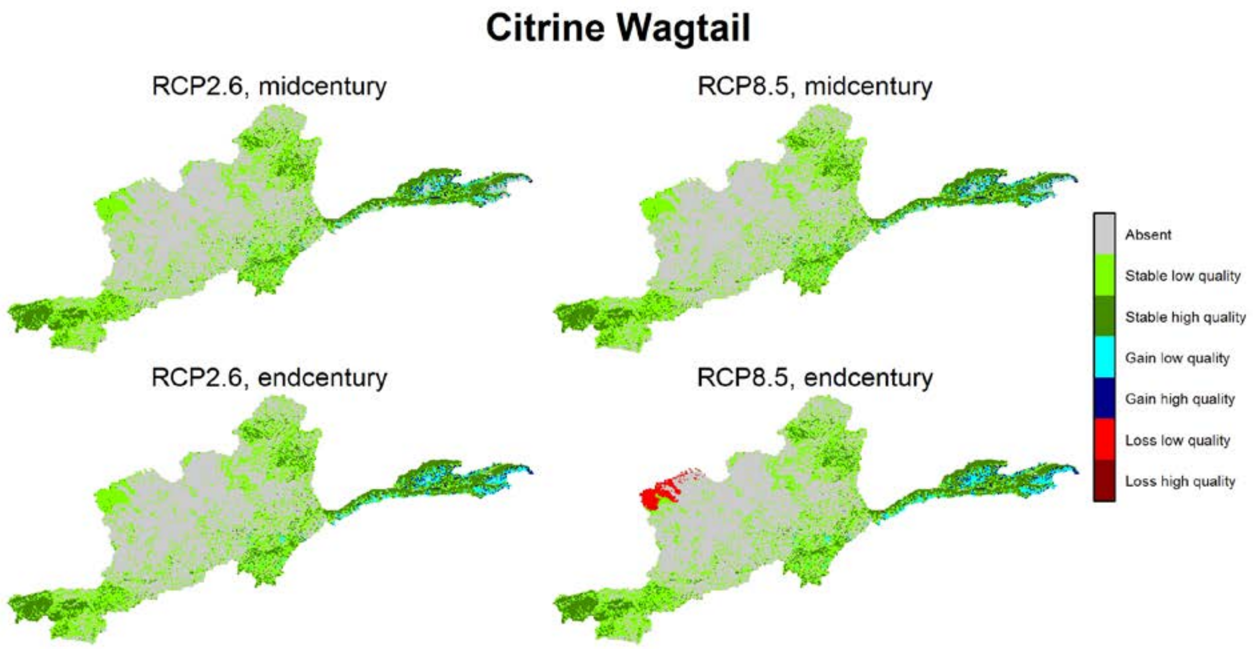

Figure 162. Changes in suitable habitat for Citrine Wagtail (*Motacilla citreola*).

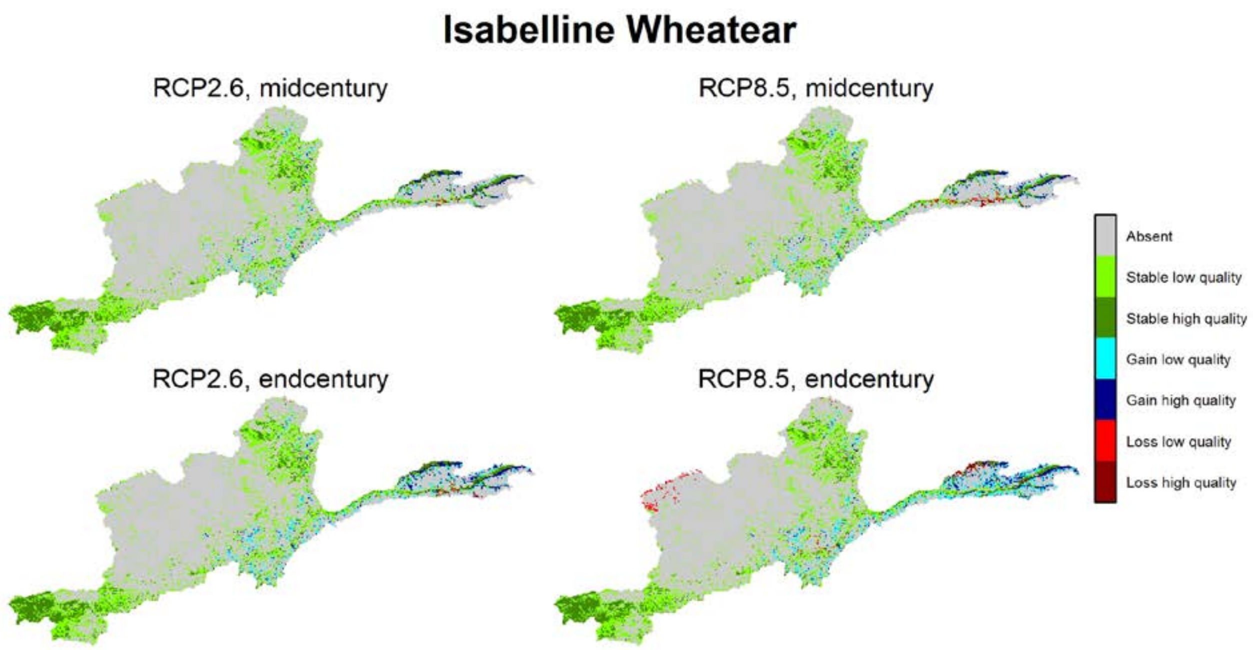

Figure 163. Changes in suitable habitat for Isabelline Wheatear (*Oenanthe isabellina*).

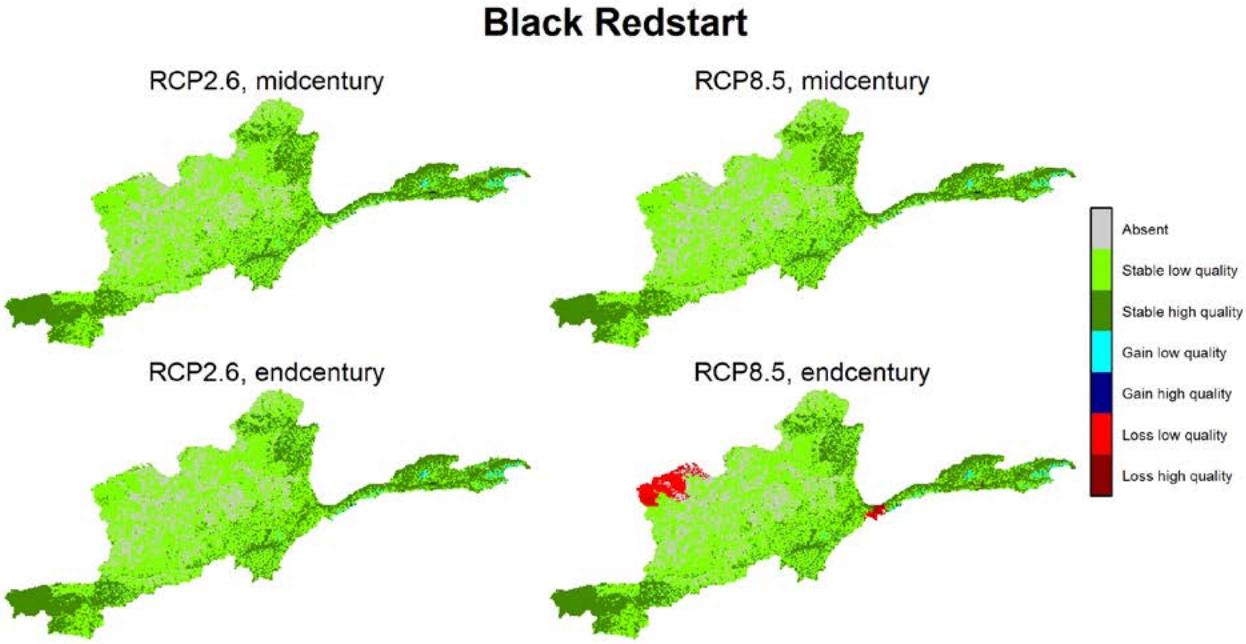

Figure 164. Changes in suitable habitat for Black Redstart (*Phoenicurus ochruros*).

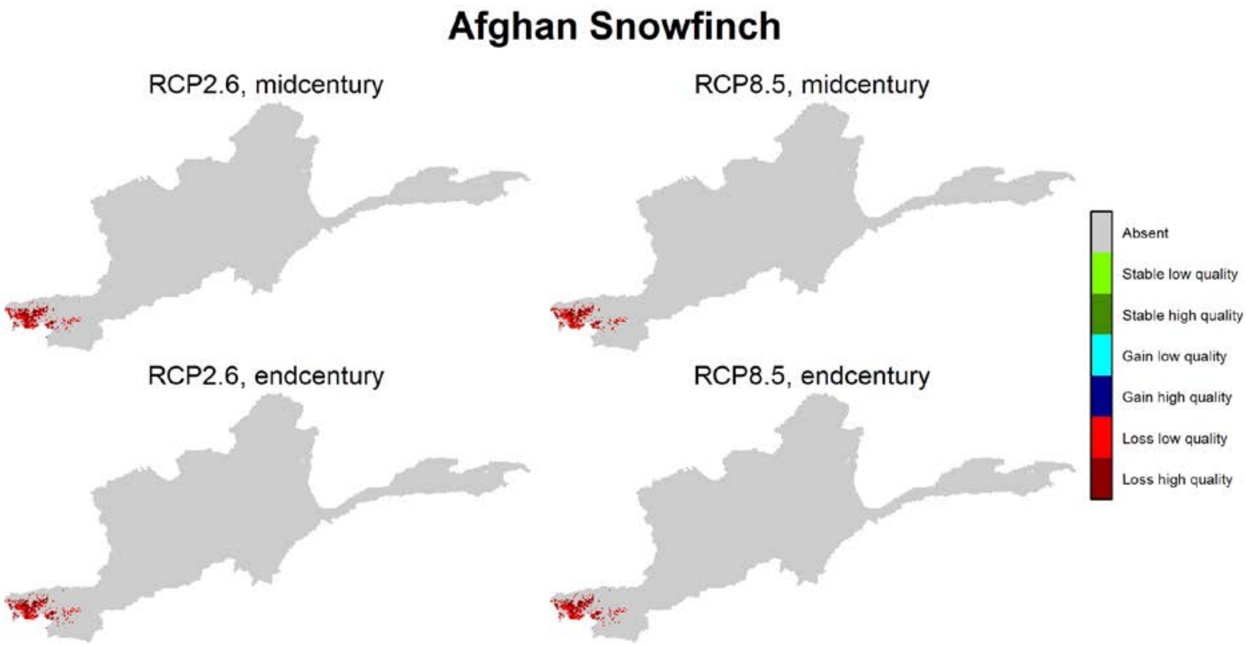

Figure 165. Changes in suitable habitat for Afghan Snowfinch (*Pyrgilauda theresae*).

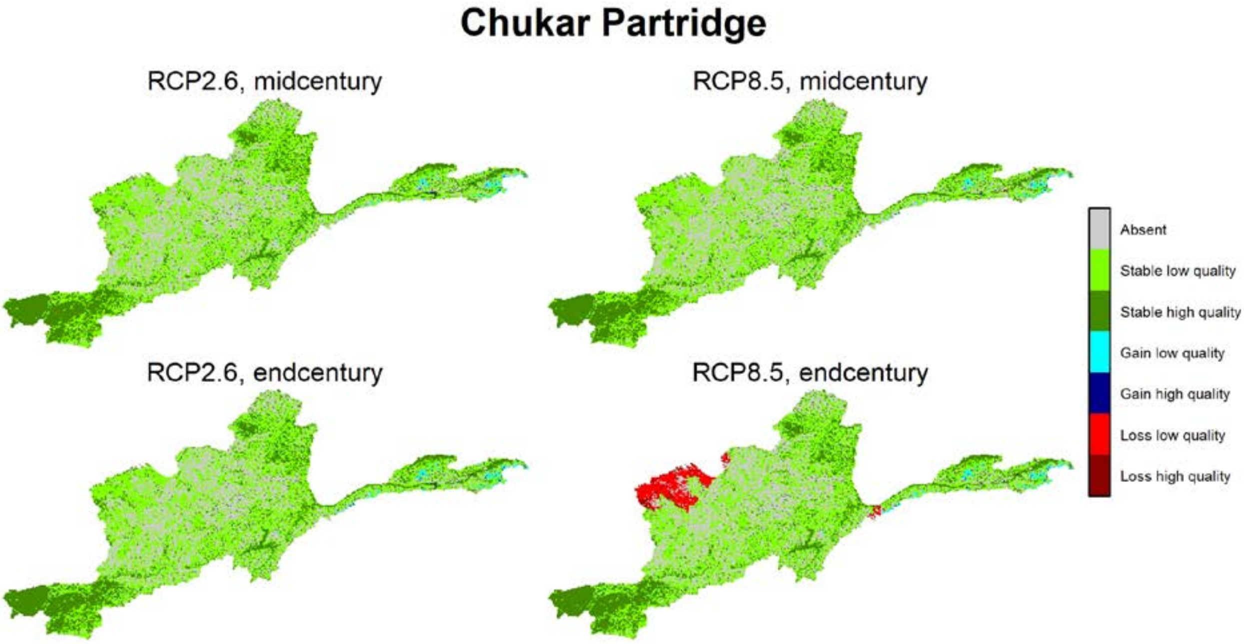

Figure 166. Changes in suitable habitat for Chukar Partridge (*Alectoris chukar*).

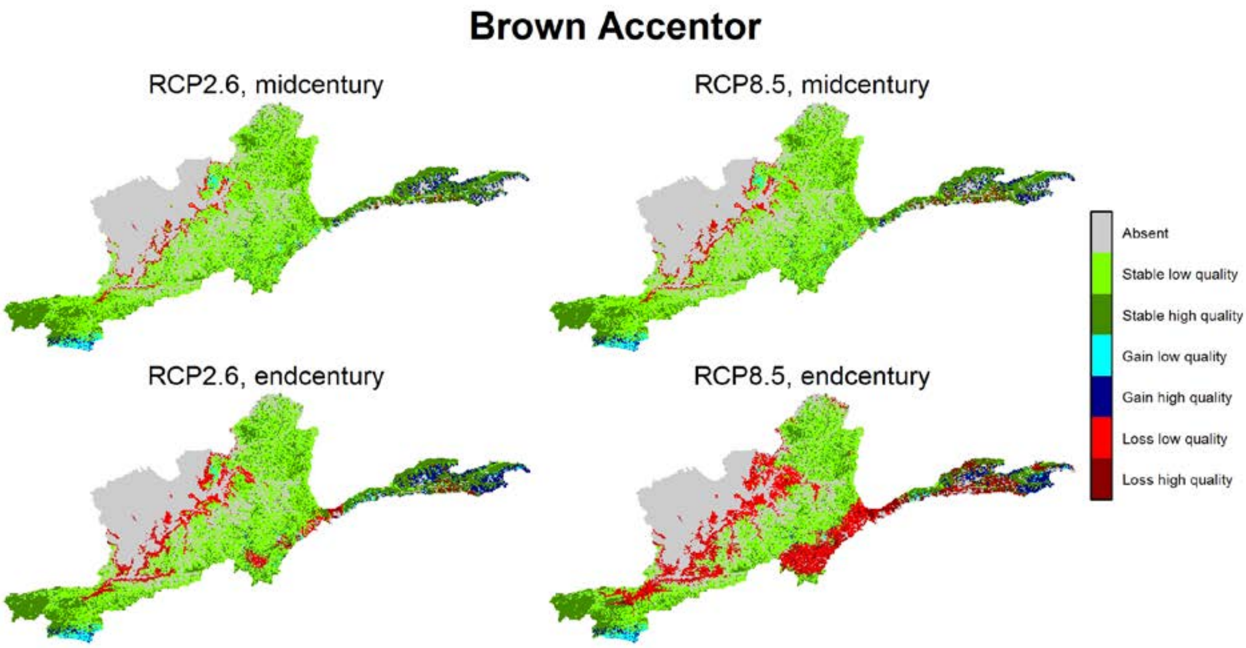

Figure 167. Changes in suitable habitat for Brown Accentor (*Prunella fulvescens*).

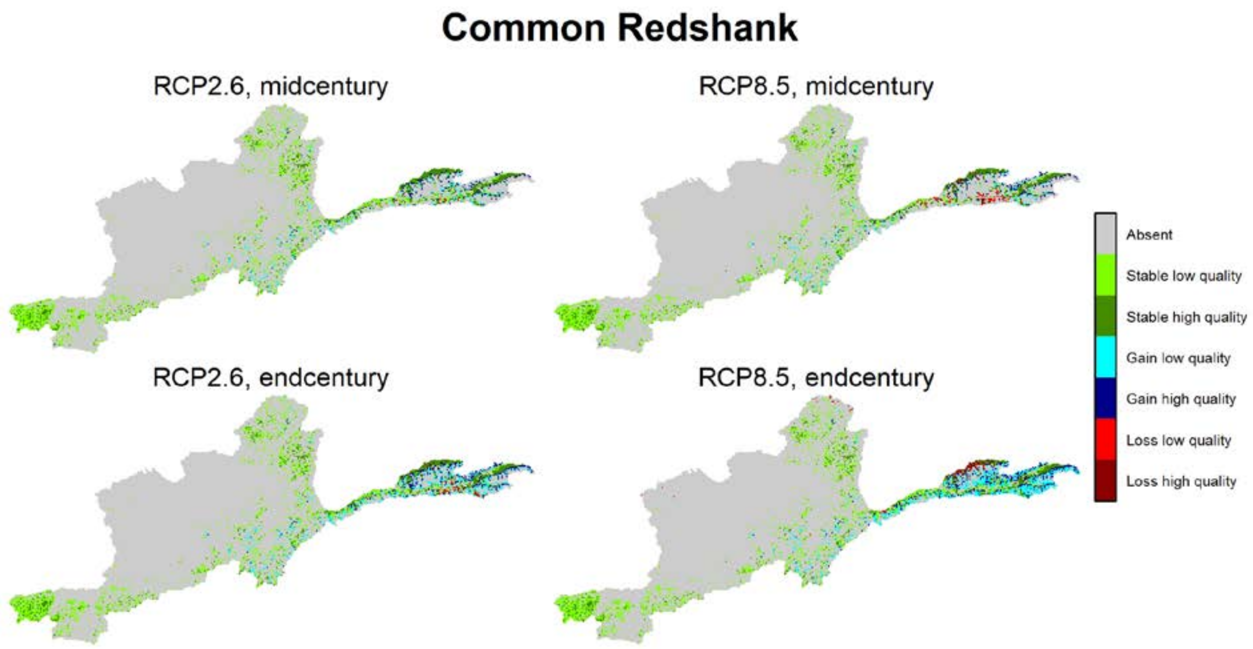

Figure 168. Changes in suitable habitat for Common Redshank (*Tringa totanus*).

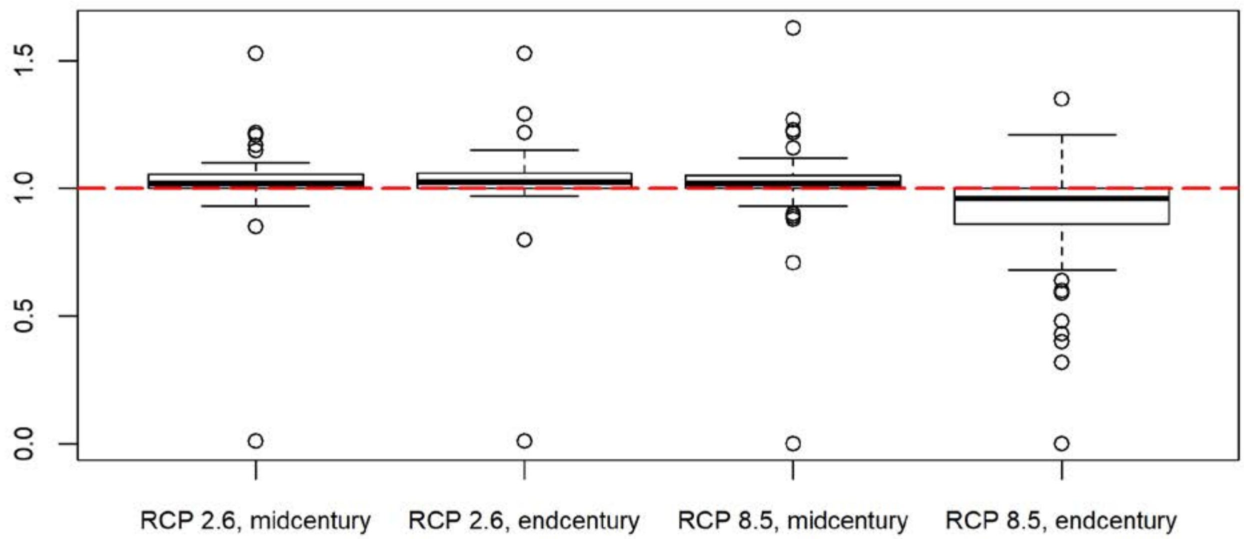

Figure 169. Ratio of current relative to future range size for all 60 focal bird species. A value of 1 (red dashed line) indicates no projected change in range size. Values less than one indicate range decreases, while values greater than one indicate range increases. Bold lines represent the median; the boxes extend from the 25th to 75th percentile values.

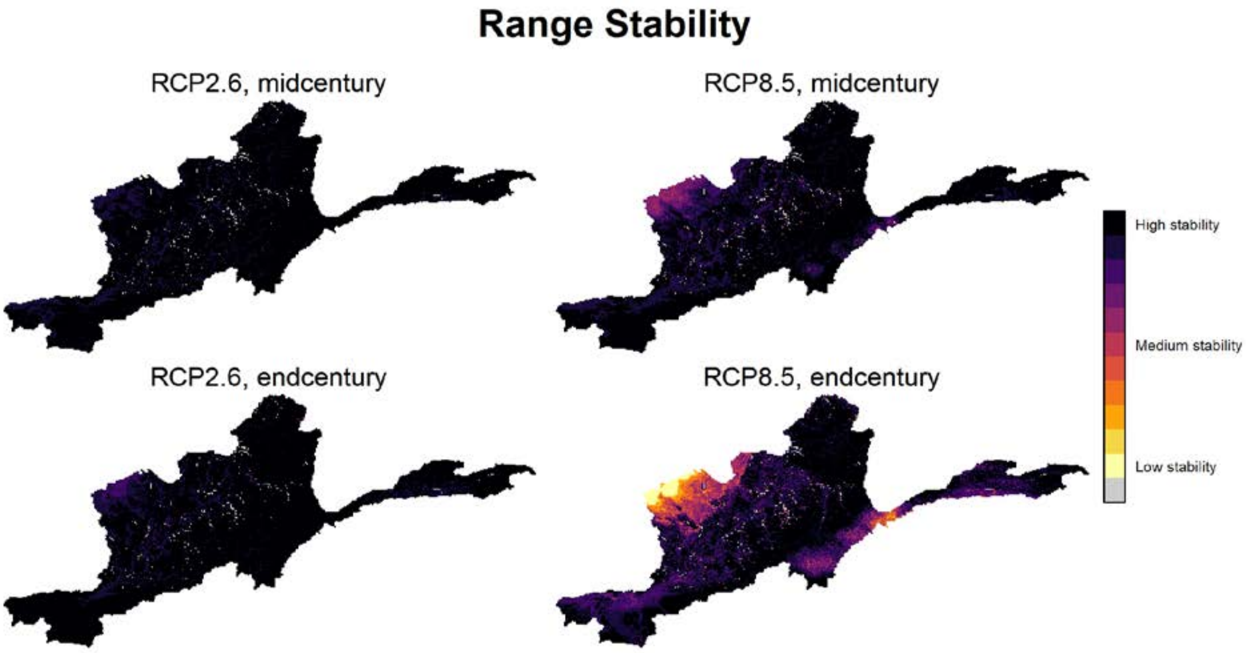

Figure 170. Spatial distribution of range stability calculated as the proportion of bird species that will experience range losses, relative to the number of species that currently occur at each location. Brighter colors indicate more range losses and hence more climate sensitivity (less stability); darker colors indicate fewer range losses and hence less sensitivity (more stability). Grey areas represent areas where all modelled species are currently absent.

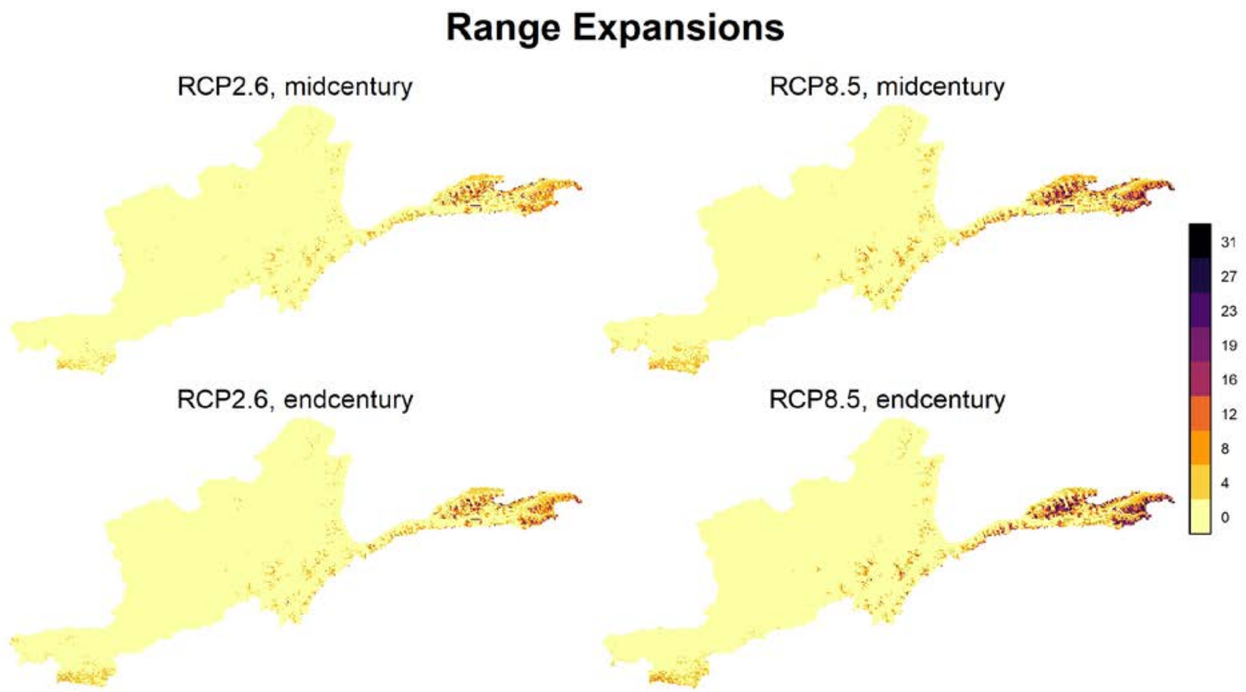

Figure 171. Spatial distribution of potential bird species range expansions. Lighter colors indicate fewer new species are projected to occur in the future at a location. Darker colors indicate more potential new species moving into a given location.

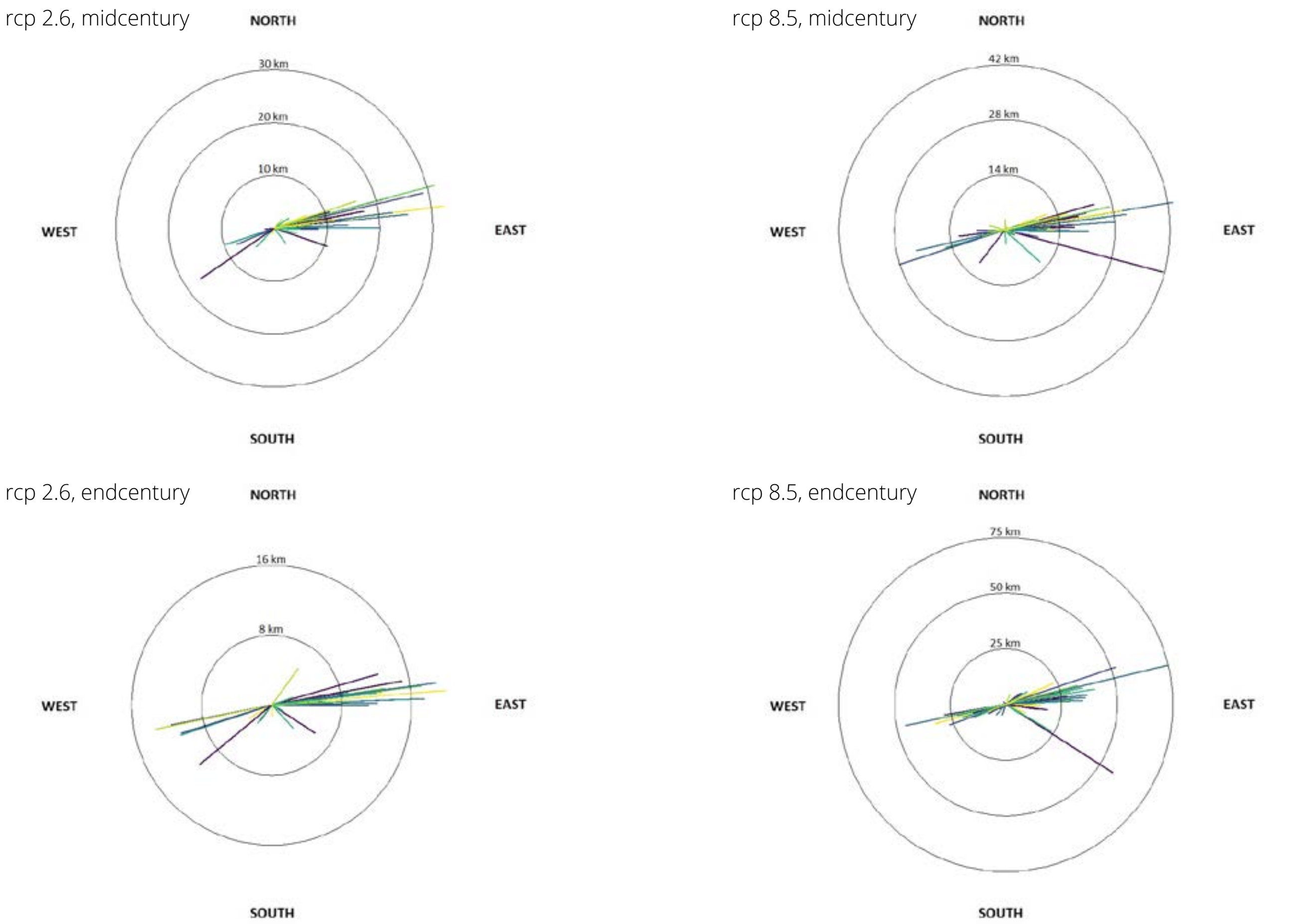

Figure 172. Plots showing the projected distance and direction of movement of the center of mass for each bird species' distribution. Colored lines represent individual species. Note the scale of movement is somewhat larger for RCP8.5 than for RCP2.6.

Summary plots of indicator by ecoregion and province

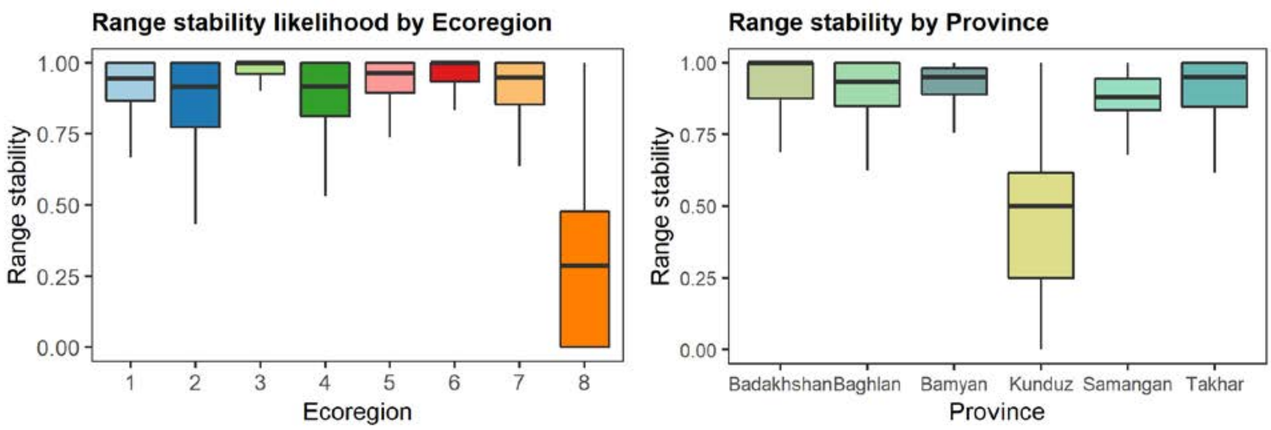

Figure 173. Range stability across all bird species, summarized by ecoregion and province for RCP8.5, end-century. Ecoregion legend: 1 – Pamir alpine desert and tundra; 2 – Karakorum-West Tibetan Plateau alpine steppe; 3 – Gissaro-Alai open woodlands; 4 – Paropamisus xeric woodlands; 5 – Ghorat-Hazarajat alpine meadow; 6 – Hindu-Kush alpine meadow; 7 – Afghan Mountains semi-desert; 8 - Badghyz and Karabil semi-desert.

The Bamyan plateau, located at the southern end of the Panj-Amu River Basin, is a dry and rugged habitat that supports the breeding of the Boreal Owl (Aegolius funereus). This owl species is very rare in Afghanistan and of national significant for conservation efforts, as it faces threats from habitat loss and climate change.

Wetlands in the Panj-Amu River Basin are critical stopovers for millions of birds using seasonally the Central Asian migratory flyway, including the two greater flamingos pictured here.

Results summary

Bird species ranges are overall projected to be generally stable on average, though with slight declines by end-century in a high-emissions future (Figure 169). Bird range sizes are projected to be far more stable than mammal range sizes (compare results to Figure 149). However, there is considerable variation between species, with some likely to experience gains while others projected to experience losses. Most notably, the endemic and range-restricted Afghan Snowfinch (*Pyrgilauda theresae*) is projected to lose virtually all of its suitable breeding range within the P-ARB by mid-century in both a high-emissions and a low-emissions future. Other species projected to lose over 50% of their range by end-century under a high-emissions future include Alpine Accentor (*Prunella collaris*), Hooded Crow (*Corvus cornix*), Güldenstädt's Redstart (*Phoenicurus erythrogastrus*) and Pale Rosefinch (*Carpodacus stoliczkae*). No species is projected to lose over 50% of its range in a low-emissions future, other than Afghan Snowfinch (Appendix 6, Table 62).

Bird range stability is overall lowest in the northwest portion of the P-ARB, though by end-century in a high-emissions future declines are also projected in the northern part of the Bamyan plateau in the southwest, as well as near the 'entrance' of the Wakhan corridor in the east (Figure 170). Range gains are sparser, and largely concentrated in the Wakhan corridor (Figure 171). This pattern is similar to that projected for mammal species. The direction of movement of the center of mass of species' distributions is eastward, with longer movements seen by end-century compared to mid-century and in a high-emissions future compared to a low-emissions future (Figure 172).

At the province level, bird ranges are projected to be the least stable in Kunduz province, with relatively similar stability in other provinces. At the ecoregion level, bird ranges in the Badghyz and Karabil Semi-Desert (Ecoregion 8) are projected to be the least stable, with other ecoregions having similar levels of stability (Figure 173).

A caveat to these results is that as mentioned above, the occurrence models described in this section are intended to describe the breeding range only, with exclusively presence records dated between May and September being used. It is possible, and indeed likely, that climate change will affect non-breeding and migratory stopover habitat. However, the combination of harsh winter climate and political instability means that virtually all fieldwork on birds has been conducted in the P-ARB during the nonbreeding season. As a result, we have chosen to only focus on breeding limitations – however, this does not allow us to detect potential climate-related threats that may occur during other seasons.

Mammal and Bird Species Sensitivity to Climate Change

S AC

Indicator overview

Certain intrinsic characteristics of wildlife species, often referred to as ecological traits, predispose them to being more sensitive to climate change or otherwise hinder their adaptive capacity, and thus more vulnerable to climate exposure (Pacifici et al. 2017). For instance, species with narrow geographic distributions (e.g., total range size, elevational range size), narrow physiological tolerances (e.g., narrow thermal or rainfall tolerances), or high habitat specificity (e.g., occur in few habitat types) are often more sensitive to climate change because they are adapted to a very specific set of biotic and abiotic conditions (Pearson et al. 2014). Such species are thought to be more vulnerable to climate change because they will likely face greater difficulties shifting their distributions to find suitable conditions under climate change (Sekercioglu et al. 2008).

Traits related to demography, including litter or clutch size, generation length, and sexual age of maturity, can also influence their adaptive capacity to cope with climate change (Pacifici et al. 2015). Species that have large litters, short generations, and reach sexual maturity at younger ages all tend to be more adaptable, and thus are less sensitive to changes in climate than those species that are long-lived, give birth to few offspring, and reproduce only after many years. Body mass also serves as an important indicator of species sensitivity, because small species are typically poorer thermoregulators than large-bodied species (Porter and Kearney 2009). Taken together, these ecological traits can provide useful information as they are proxies for vulnerability that can also inform conservation interventions and strategies (Foden et al. 2013).

Methods overview

For this indicator, we obtained information on 16 different ecological traits for mammals and 15 different ecological traits for birds with direct links to sensitivity and/or adaptive capacity from primary academic literature and published databases related to demography, reproduction, niche breadths, and reproduction for each mammal and bird species that occurs in the P-ARB. We translated individual traits into scores using quantiles and summed all scores across traits. We then obtained range maps depicting each species' geographic distribution and assigned to each range the summed sensitivity scores. We repeated this process for each species, then summed scores for all species within each taxonomic group at a given location (i.e., within a 1 km^2 pixel) and divided the summed scores by the total number of species of that taxonomic group found at that location to enable relative comparisons across regions (within taxonomic groups). Finally, for each taxonomic group, we rescaled resulting values from 0 to 1, where 0 indicates low relative sensitivity and 1 indicates high relative sensitivity.

Additional details related to this methodology can be found in Appendix 6.

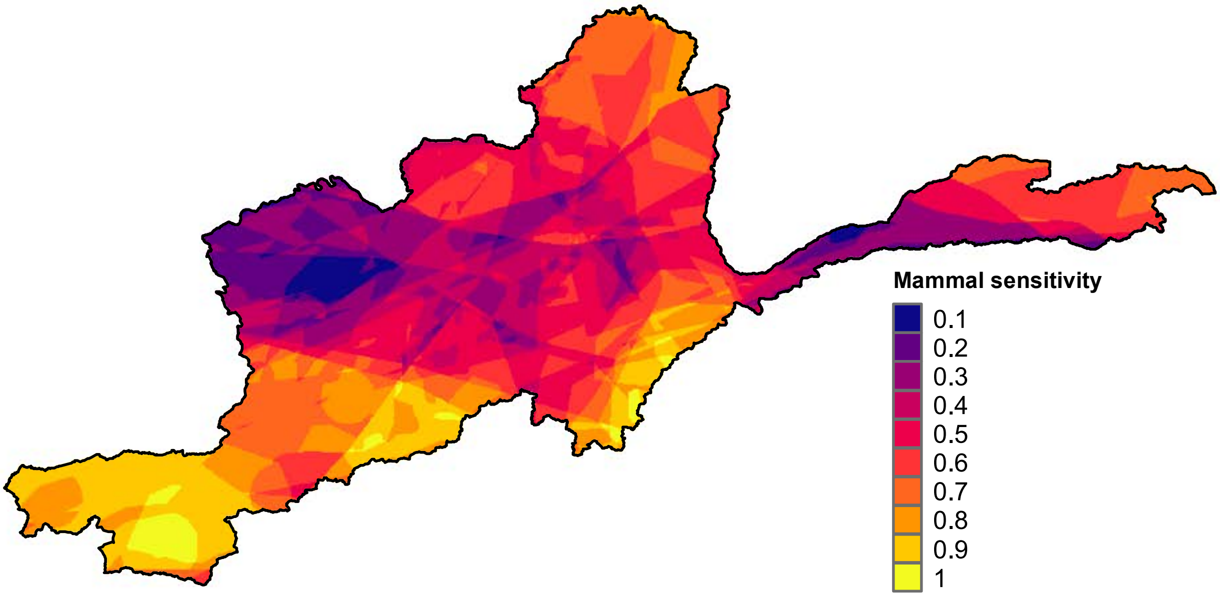

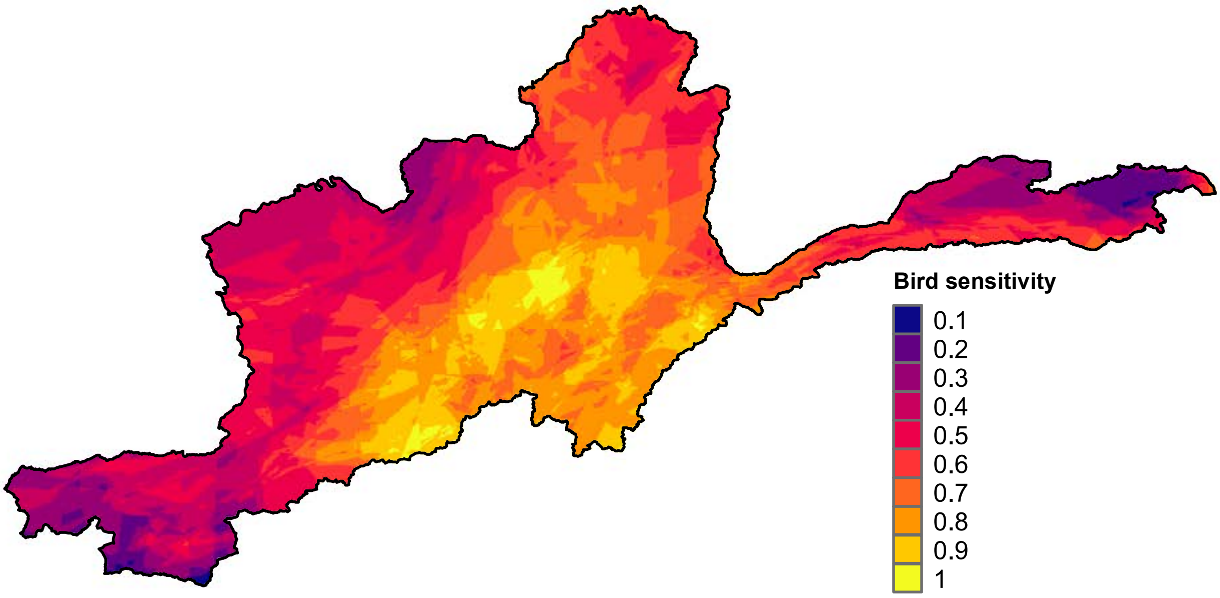

Figure 174. Mammal and bird species sensitivity to climate change based on ecological traits related to demography, niche breadths, diet, and reproduction. For each taxon, the scale is standardized by the number of species to produce a relative scale from least (0) to most (1) sensitive to climate change.

Summary plots of indicator by ecoregion and province

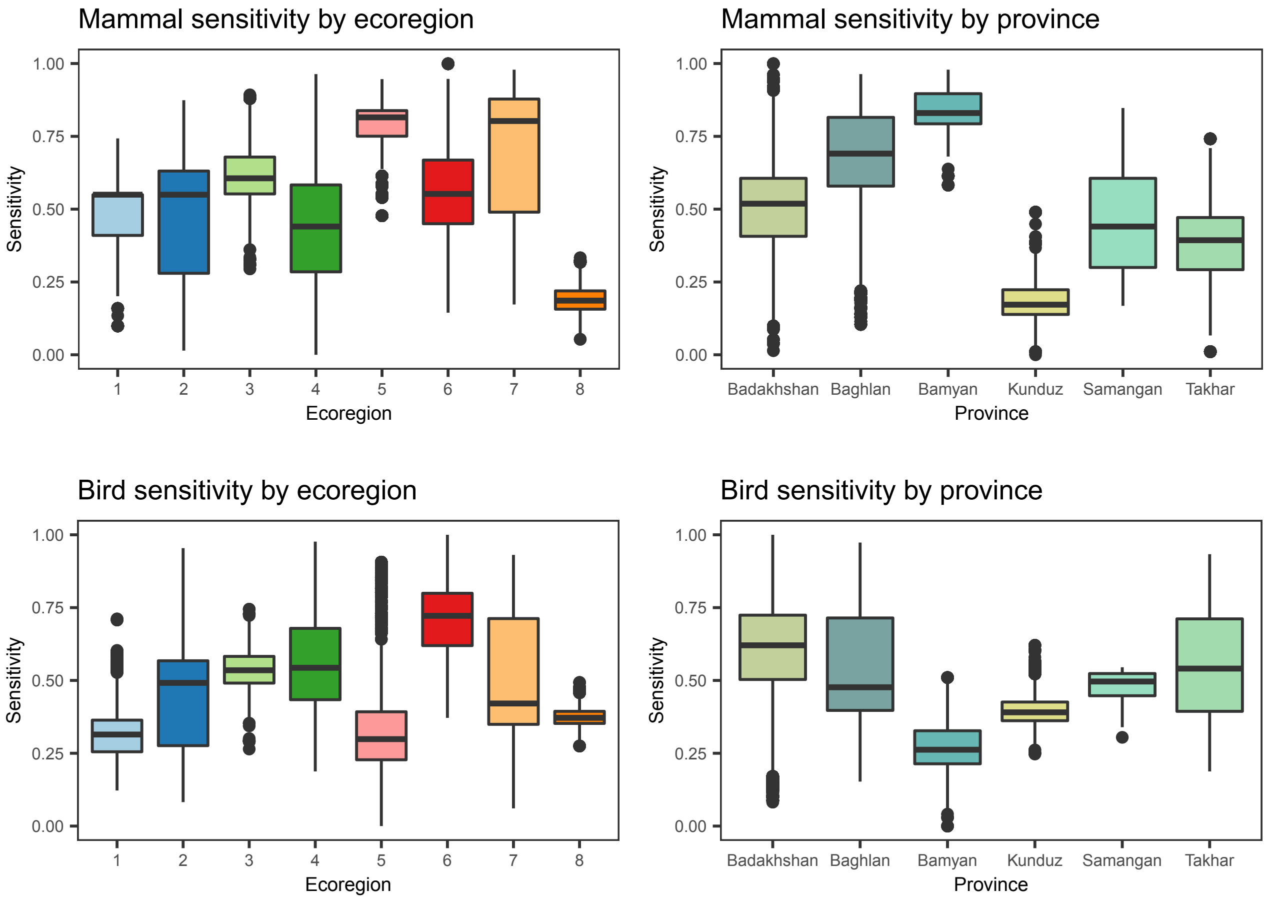

Figure 175. Boxplots of mammal and bird sensitivity by ecoregion and province. Ecoregion legend: 1 – Pamir alpine desert and tundra; 2 – Karakorum-West Tibetan Plateau alpine steppe; 3 – Gissaro-Alai open woodlands; 4 – Paropamisus xeric woodlands; 5 – Ghorat-Hazarajat alpine meadow; 6 – Hindu-Kush alpine meadow; 7 – Afghan Mountains semi-desert; 8 - Badghyz and Karabil semi-desert.

Results summary

Mammal and bird sensitivity spatial patterns show stark contrasts. Mammal species sensitivity to climate change is greatest in the southern and southwestern portions of the P-ARB, and lowest in the northwestern portion of the P-ARB and along the Wakhan corridor in the northeast. By contrast, bird species sensitivity to climate change is greatest in the center of the P-ARB and declines moving outward in any direction.

In terms of spatial patterns related to ecoregions, mammal sensitivity is highest in the Ghorat-Hazarajat alpine meadow (ecoregion 5) and Afghan Mountains semi-desert (ecoregion 7) ecoregions, and lowest in Badghyz and Karabil semi-desert (ecoregion 8). For birds, sensitivity is highest in the Hindu Kush alpine meadow ecoregion (ecoregion 6) and lowest in the Pamir alpine desert and tundra (ecoregion 1), Ghorat-Hazarajat alpine meadow (ecoregion 5), and Badghyz and Karabil semi-desert ecoregions (ecoregion 8). In terms of spatial patterns related to provinces, mammal sensitivity is highest in Baghlan and Bamyan provinces, and lowest in Kunduz province. For birds, sensitivity is highest in Badakhshan, Baghlan, and Takhar provinces, and lowest in Bamyan province.

Policy and Management Recommendations

The results shown in the preceding section have important implications for future policy and management. The broad patterns shown for mammals in Figure 174 are reasonably similar to those shown overall in Figure 150, with high vulnerability particularly in the southern parts of Badakhshan province. These results suggest that further monitoring of the fauna in this region will be critical, with species-specific management actions being implemented as appropriate. For the threatened ungulates such as argali and urial, it will likely be necessary to monitor livestock stocking rates and implement regulations to prevent overgrazing, thereby reducing competition for wild ungulates that may be stressed by climate change. Actions to mitigate the effects of climate change on prey species will also benefit carnivores such as snow leopards. Additionally, the Bamyan Plateau region, which has relatively high mammal sensitivity to climate change, has one of the few effective protected area complexes in the country, which may make implementation of such management actions in this area more feasible. The effectiveness of these protected areas should also be maintained and increased through policy actions taken at the central government level.

In the other major protected area in the P-ARB, the Wakhan National Park, mammal wildlife sensitivity is likely to be lower until midcentury, although this will increase by endcentury in a high-emissions future. Existing wildlife monitoring efforts for focal species should therefore receive funding, while new monitoring efforts should be considered, in order to continue to monitor the effects of climate change on wildlife. Specific attention should be devoted to areas that are projected to have species range extensions, as documenting these should they happen would increase the confidence in modelled projections. Likewise, surveys should also be conducted in areas where species are expected to disappear. By coming to a better understanding of the specific spatial effects of climate change, it will be possible to proactively address human-wildlife conflict issues that may arise. For example, in areas where snow leopards are expected to move in, local communities should be given training and resources to implement non-lethal predator controls such as fencing and livestock guardian dogs that would help secure their livelihoods while avoiding imperiling snow leopards. Likewise, in areas where wild ungulates are expected to come into increased contact with livestock, health monitoring programs and regular testing should be implemented in order to detect any livestock diseases that may spill over from wild populations and vice versa.

Bird sensitivity is more difficult to interpret, as the patterns shown in Figure 170 are quite different from those shown by birds in Figure 174. This is at least partially explainable by the difference in the two metrics – the range-based measure used in Figure 170 uses far fewer species than the trait-based measure, and relies on predictive modelling of occurrence rather than intrinsic biological traits. In both cases, there is also considerable uncertainty involved. As such, it is unsurprising that they differ. They can be seen as complementary approaches – areas showing high sensitivity under both metrics are likely to see the largest effects from climate change on bird species, areas with low sensitivity under both metrics the lowest impacts, with the remainder somewhere in between.

When considering individual bird species, the most vulnerable bird species (Afghan Snowfinch) is found primarily in the Bamyan Plateau region within the P-ARB, highlighting the importance of that specific protected area. Additionally, as the most vulnerable projected areas for bird species for both the range-based and trait-based metric lie outside current protected areas, it will be important to rely on other conservation measures such as enforcing poaching regulations, working with local communities to mitigate landuse conversion and rangeland degradation, and restoring habitat where possible (particularly for the Large-billed Reed Warbler, one of the world's least known bird species which breeds in riparian thickets) to help secure bird populations. Again, further fieldwork should be undertaken to monitor bird populations, elucidate their status and track any trends in population/range sizes.

In general, mammals appear more vulnerable overall as there is greater concordance between areas of high exposure and high sensitivity. For example, the Gissaro-Alai open woodlands ecoregion, and to a lesser degree the Ghorat-Hazarajat alpine meadow, both had reasonably low mammal range stability likelihoods and reasonably high mammal sensitivity to climate change. For birds, most ecoregions other than the Badghyz and Karabil semi-desert had relatively high range stability, so underlying sensitivity plays a more primary role in determining overall vulnerability. In this respect, in addition to the aforementioned Hindu-Kush alpine meadow, the Paropamisus xeric woods and to a lesser extent the Gissaro-Alai open woodlands should be characterized by high vulnerability.

The movement of species in a generally eastward direction, broadly following the southwest-northeast altitudinal/temperature gradient as shown in Figure 152 and Figure 172, poses some challenges but also some opportunities, particularly as they pertain to mammals. On the one hand, wild ungulate species may come into increased conflict with livestock as they move; predator species may likewise come into more conflict with people, especially if their movements fail to perfectly mirror their wild prey. Proactive measures may need to be taken to pre-empt conflict, including introducing non-lethal methods of predator avoidance to local communities. Moreover, protected areas and other effective conservation measures (OECMs) may need to be created to ensure that species have adequate protected habitat as they traverse the landscape. However, the fact that all species are expected to move congruently will assist in these efforts, as multiple species may be able to utilize the same corridors, particularly when there are ecological relationships connecting them (e.g. predators and prey species).

Overall, the results described above point to several key recommendations for policy and management to maintain viable wildlife populations, which would increase their resilience under climate change. These recommendations can be grouped into seven domains, many of which reinforce recommendations described in other sections of this report.

1. Maintain ecosystem integrity through improved governance and better ecosystem management

- Maintain intact areas to provide more suitable habitat and help buffer climate impacts. This is particularly important in Kunduz, Baghlan, and Bamyan provinces, where bird and mammal species are expected to be most affected by climate change.
  - Establish protected areas or other effective conservation measures
  - Create buffer zones
  - Apply more strict land-use regulations
- Slow rates of degradation to minimize reductions in habitat quality for wildlife species. This is particularly important in Kunduz, Baghlan, and Bamyan provinces, where bird and mammal species are expected to be most affected by climate change.
  - Alter grazing patterns
  - Reduce community dependence on livestock grazing and natural resource collection for livelihoods
  - Invest in alternative and sustainable sources of energy and heat
- Recover areas identified as degraded to increase potential species habitat. This is particularly important in Kunduz and Baghlan provinces, with projected high climate impacts to wildlife and observed high rates of degradation.
  - Prioritize institutions to retain high integrity rangelands and restore degraded rangelands
  - Publish and disseminate rangeland management plans
  - Update rangeland management practices following changes in local conditions.

2. Develop alternative strategies to increase food production (yields) while reducing overall agricultural footprint to reduce impacts on ecosystems

- Utilize better technology, low energy savings, and alternatives. Alternative energy generation strategies should be investigated independently as such assessments were not included in this report.
  - Distribute solar cook stoves to resource-dependent communities
  - Increase hydropower capacity and distribution by building small and medium hydropower generators where water is available
  - Investigate wind power generation potential
- Invest in renewable energy sources. Alternative energy generation strategies should be investigated independently as such assessments were not included in this report.
  - Assess most effective opportunities at local scales, including solar, hydro, and wind power
  - Subsidize establishment of new energy sources
  - Create incentives for communities to use new alternative energy provided
- Distribute or subsidize efficient cook stoves and heaters. A national program to service all communities would be most effective.
  - Prioritize distribution and subsidies to most at-risk communities and in regions where dependence on natural resources is highest
- Embrace cultivation technologies and crop management techniques that maximize agricultural productivity and reduce agricultural footprints. Most agricultural recommendations apply particularly to Kunduz province given its agricultural focus, as well as the high sensitivity of its wildlife.

  - Use improved irrigation systems
  - Increase pest and disease control measures
  - Embrace technical agricultural support
  - Construct and maintain food storage facilities
- Employ proper crop rotations to maximize yields. Most agricultural recommendations apply particularly to Kunduz province given its agricultural focus, as well as the high sensitivity of its wildlife.
  - Determine which crops can grow in different seasons
  - Rotate crops to promote soil health, reduce soil erosion, and allow for longer growing seasons

3. Perform large scale reforestation and restoration activities to increase extents of critical natural ecosystems

- Initiate tree planting campaigns to reforest communities and regions of high reforestation potential. A systematic reforestation potential analysis was not conducted, but these areas will be along rivers and valleys adjacent to communities in all provinces, especially at lower elevations.
  - Target and adapt plantings to maximize wildlife habitat for forest and/or riparian species
- Use native plant species that are climate resilient and provide wildlife habitat. Pistachio and juniper are important tree species for both people and wildlife, and may persist in extreme temperature conditions throughout much of the P-ARB.
  - Use species that are drought and frost tolerant
  - Plant trees creating a natural mixed community rather than monoculture plantations
  - Plant trees where wildlife would likely use them, such as along rivers, ridgelines, or other natural corridors
- Focus reforestation on riparian areas to improve wildlife movement potential and restore healthy freshwater ecosystems. This should be a major aim across all river and stream networks, especially those spanning elevational gradients as in Badakhshan and Bamyan provinces.
  - Plant tree and shrub species known to be used by important wildlife
- Propagate grassland restoration activities in heavily degraded grasslands. Kunduz and Baghlan provinces have high rates of rangeland degradation in addition to high wildlife sensitivity to climate change.
  - Plant native grasses and shrubs that are climate resilient
  - Actively remove invasive weeds and maintain invasive weed prevention initiatives
  - Employ sustainable livestock management practices
- Limit expansion of human habitation within and adjacent to protected areas. Protected areas in Bamyan province should be especially prioritized.
  - Create and enforce zoning restrictions for all protected areas

4. Expand the protected area network

- • Increase the total amount of area under protection. Kunduz, Samangan, and Takhar are most underrepresented within the P-ARB and should be prioritized for new protected areas.
  - Create new protected areas and other effective conservation measures
  - Commit to meeting international targets set by the Convention on Biological Diversity and recommended in the National Biodiversity Strategic Action Plan
- Ensure that protection is representative of the diverse ecoregions and biodiversity present in the P-ARB. The Badghyz and Karabil semi-desert ecoregion is unprotected and has high wildlife sensitivity to climate change.
  - Stratify ecosystem protection by ecoregion and ensure that each ecoregion has roughly the same amount of protection relative to its size
- Consider future climate change shifts in species' ranges in protected area planning.
  - Forecasts of shifts in species' ranges should be explicitly included in future protected area planning and prioritization

- Ensure both habitat (structure) and climate (functional) connectivity between protected areas to help adapt to changes. Currently applies mostly to Bamyan and Badakhshan provinces given current protected areas, but as new protection is established it would apply throughout the P-ARB.
    - When prioritizing additional protection, consider the isolation of protected areas, both in terms of the surrounding matrix and human land uses that would impede wildlife movement, and in terms of how suitable the climate is projected to be in the future that could potentially facilitate wildlife movement
- Utilize other effective area-based conservation measures. This strategy can be employed equally in all provinces.
- Develop locally governed and managed areas for conservation purposes that monitor and evaluate biodiversity and ecosystem outcomes
- Empower local communities as stewards for their environments
- Consider adopting conservation easement model of recognized conservation of important habitat on private lands
- Establish buffer zones around protected and conservation areas. Currently applies mostly to Bamyan and Badakhshan provinces given current protected areas, but as new protection is established it would apply throughout the P-ARB.
    - Create buffer zones managed by local communities that limit human encroachment and resource extraction around protected and conservation efforts to strengthen conservation in the core protected area
- Ensure proper functioning of protected areas through clear, enforceable criterion for species conservation within protected areas and other conservation areas. Currently applies mostly to Bamyan and Badakhshan provinces given current protected areas, but as new protection is established it would apply throughout the P-ARB.
    - Increase presence of rangers and other officials to deter poaching
    - Create rules specifying the legal limits on hunting/trapping activities, if any
- Monitor focal species within protected areas to ensure proper protection and functioning. Currently applies mostly to Bamyan and Badakhshan provinces given current protected areas, but as new protection is established it would apply throughout the P-ARB.
    - Conduct regular surveys of wildlife species, especially those of particular importance to a given protected area
    - Adjust management of protected areas based on observed trajectories of species' presence/populations

5. Educate the public about the importance of biodiversity

- Develop community education program on wildlife and conservation actions suitable for all ages. Should be a national effort applying equally to all provinces, but material could be tailored to specific geographies.
    - Develop government, university, or non-profit led sets of educational programs that would be delivered at schools and other community centers and made available online
    - Inculcate pride in the local wildlife/ecosystems amongst communities
- Mainstream environmental education in the national education curriculum. Should be a national effort applying equally to all provinces, but material could be tailored to specific geographies.
    - Use textbooks and educational resources that include environmental education material
    - Make taking at least one course focused on environmental education mandatory
- Create courses and modules at the university level, including opportunities for research in wildlife biology and conservation. Should focus on top universities for all provinces, including Kunduz University, Badakhshan University, Bamyan University, Samangan University, and Takhar University. The modules should be systematically developed but tailored to specific needs in each province.
    - Expand university curricula within Afghanistan with departments, programs, and degrees specializing in sustainable ecosystem management and conservation science
    - Hire faculty to lecture and train students and conduct independent research in these fields

- Create jobs that utilize education and training in ecology, wildlife biology, conservation biology and/or wildlife management. Job creation should be focused on all universities as mentioned in the previous recommendation.
  - Create environmental monitoring and consulting positions, research and teaching positions, and technical/analytical positions with local and national institutions
  - Expand the presence of district, provincial and/or national-level officials with training and understanding of conservation issues

6. Develop wildlife conflict mitigation strategies

- Proactively address wildlife conflicts that may increase under climate change. This will be particularly important in Badakhshan province, where most species' range expansions are projected to occur.
  - Educate local communities about potential conflicts that may occur
- Understand the nature of human-wildlife conflicts. This is particularly important for threatened predator species such as Snow Leopards, which primarily occur in Badakhshan province
  - Create a database of livestock predation events to track potential conflict
  - Create programs that transparently assess reports of conflict and deliver compensation (for e.g. predated livestock) in a timely manner
  - Monitor livestock diseases that may originate in wildlife
- Invest in nonlethal technologies for mitigating conflict
  - Assist with building livestock corrals that cannot be penetrated by predators
  - Facilitate communities in obtaining, training and maintaining livestock guardian dogs
  - Monitor wild herbivore herds to prevent conflict with livestock grazing practices

7. Establish a system for long-term biodiversity monitoring

- Establish regular monitoring of biodiversity, using both field-based and remote-sensing approaches. This is particularly important in Kunduz, Baghlan and Badakhshan provinces, where wildlife sensitivity to climate and changes to species' ranges are expected to be greatest.
  - Establish regular surveys of biodiversity, especially targeting species of conservation concern
  - Monitor the presence of species in areas where species are projected to disappear and/or areas where species are expected to colonize, in order to verify modelled projections of species' range shifts
  - Use remote-sensing data to assess habitat changes relevant to species of interest
- Continually update models of projected responses of species to climate change. This applies to the entire region..
  - Update species models using data derived from field-based and remotely-sensed monitoring of species and habitat, as well as updated climate model projections
- Monitor human activities that disturb ecosystems and species such as urbanization, livestock grazing, hunting, and road network expansion. This applies to the entire region.
  - Use remote-sensing data and regular monitoring/patrols to assess changes to infrastructure, particularly around protected and buffer areas
  - Require planned infrastructure projects to go through environmental review, specifically based on their potential impacts on threatened species
  - Create a mapped database of grazing activities that can be updated based on monitoring information

Local Communities Vulnerability

2.6 Local Communities Vulnerability

Overview

One of the main determinants of natural and human systems' vulnerability to climate change is adaptive capacity. Vulnerability is related both to the differential exposure and sensitivity of communities to stimuli such as climate change and also to the particular adaptive capacities of those communities to deal with the effects or risks associated with the exposures. While exposures, sensitivities and adaptive capacities are evident at community or local levels, they reflect broader forces, drivers or determinants that shape or influence local level vulnerabilities (Smit and Wandel 2006). Hence, the adaptive capacity is defined as the potential or ability of a system to adjust to climate change successfully through moderating potential damages, taking advantage of opportunities, and coping with the consequences. The ability of a system to adapt to climate change is crucially influenced by the socio-economic determinants as human actions can shape and influence adaptability both through biophysical and social elements of a system. The generic socio-economic determinants, such as education, income, and health, as well as determinants impacted by climate change, such as floods or droughts, are not independent of each other nor are they mutually exclusive as, for example, economic resources facilitate the implementation of new technologies and may ensure access to training opportunities. Moreover, the lower levels of adaptive capacity and, therefore, higher vulnerability to climate change in developing countries are often associated with the lower level in socio-economic determinants and poverty (Parry et al. 2007, Field et al. 2012).

To assess the level of vulnerability of the local communities of Afghanistan to climate change, this study uses estimation of such locally adapted socio-economic indicators as community use of and access to fuelwood, types and numbers of livestock owned, area of rainfed and irrigated land as well as percentage of households owning that land, household wealth distribution as well as income diversification and income sources, human and social capital, and rural population density and distribution.

One important determinant of the vulnerability to climate change by the local communities is the **use of and access to fuelwood**. The high dependency of the local communities on the availability of fuelwood contributes to their increased dependency on natural resources and, as a result, vulnerability to climate change. Nevertheless, fuelwood is the most important source for heating and cooking for the local communities in the P-ARB. On average, 95% of the population residing in the P-ARB rely on fuelwood rather than on more advanced and efficient electricity or coal. Hence, it is precedent that such a high dependency on such fuelwood is contributing significantly to depleting precious natural resources and endangering biodiversity. Furthermore, the excessive use of fuelwood is contributing to deforestation and soil degradation, reducing the adaptive capacity, and subsequently increasing the vulnerability to climate change.

Among all provinces within the P-ARB, households in Badakhshan and Bamyan provinces (98% of households) showed the highest dependence on fuelwood for heating and cooking purposes while households in Takhar province (90% of households) have the lowest. Furthermore, harvesting may become more difficult under climate change as forests and rangelands become stressed and degraded, leaving communities that depend on these resources with fewer alternatives for their survival.

Another determinant of vulnerability is **livestock ownership** by the local communities. Livestock are a significant contributor to the eradication of hunger and all forms of malnutrition and food insecurity. Livestock ownership is also an important indicator of rural household wellbeing, income and income diversification, and food and nutrition security. Households or communities that own fewer livestock likely have lower adaptive capacity and higher level of vulnerability to climate change. The sources of greenhouse gases (GHG) from livestock production systems were determined to be from land use and land change, feed production, animal production, managemenet, and processing and transportation (FAO 2006). Livestock breeding is dependent on healthy pasturelands, the degradation of which directly impact the availability of healthy habitat for livestock causing high vulnerability of households with income solely sourced from livestock.

According to the results of the analysis, households in Wakhan district of Badakhshan province reported the highest mean numbers of the livestock units per household, estimated at 8.1 LSU, including the highest mean numbers of 1.8 dairy cows,18 sheep, and 5.8 goats per household compared to the average of 2.6-3 LSU per household at the district level. At the province level, the highest mean number of dairy cows (1.32 per households) and goats (3.47 per household) was reported in Badakhshan, the highest mean number of sheep (6.05 per household) in Bamyan, and the highest mean number of poultry (5.14 per household) in Takhar. However, there is high variation and thus uneven distribution of the livestock ownership among households. Few households of one district/province own large numbers of animals, whereas most households own far fewer than the mean, reflecting their lower capacity for income opportunities and income diversification, and thus higher vulnerability.

A third determinant of adaptive capacity and vulnerability to climate change is **irrigated and rainfed land ownership.** Agricultural land is a prerequisite for agricultural production ensuring household food security, nutrition availability, and income diversification. Ownership and access to agricultural land thus increases farmers' adaptive capacity and resilience to climate change. Rainfed land is highly dependent on precipitation, which is substantially influenced by climate change. Consequently, access to irrigated land is expected to contribute to higher crop productivity and resilience of households under climate change, especially in regions with projected decreases in rainfall and long-term decreases in runoff and discharge owing to melting glaciers. According to the results of the analysis, households of Bamyan province have the highest level of land ownership (88% of households, of which 100% own irrigated land and 11.8% own rainfed land) and the largest mean area of irrigated land owned (0.76 ha per household). Conversely, households of Takhar province have the lowest level of land ownership (50% of households) and the highest reliance on rainfed land (74.1% of households own rainfed land versus 43.8% of households own irrigated land). Households in Bamyan province are thus more equipped with irrigation facilities and have better access to irrigated land, which increases their adaptive capacity compared to households in Takhar province, which are more reliant on natural water sources for agriculture and thus have lower adaptive capacity under climate change.

Another important socio-economic determinant of adaptive capacity is **household wealth and income.** Sustainable livelihoods at the household level are directly linked to household wealth conditions including adequate space in homes and access to sanitation, water, transportation, technologies, and vital services. The analysis shows that there is large variation across provinces in wealth and uneven distribution of population among wealth quantiles. The share of the population belonging to the two highest wealth quantiles comprises about 20% of the population in Baghlan, Takhar, and Kunduz provinces compared with only 7% in Badakhshan and Bamyan provinces. A substantial majority of the population belong to the two lowest wealth quintiles: 80.5% in Badakhshan, 84.1% in Bamyan, 68.1% in Baghlan, 62.1% in Takhar, and 56.6% in Kunduz. Poverty remains the main obstacle for the majority of households in the P-ARB. Inaccessibility and lack of purchase power for essential vital goods and services prevents them from improving their lives, livelihoods, and adaptive capacity.

Income sources is another crucial determinant of household adaptive capacity. Most of the households in Badakhshan and Baghlan provinces rely on cash income (98-99%), while a higher proportion of households in Bamyan province rely on in-kind income (97%). Reliance on in-kind income instead of monetary income can reduce household adaptive capacity, since in-kind income can limit a household's ability to afford other necessities and services, diversify livelihoods, and sustain shocks. Among most popular cash income sources, wages received from non-agricultural activities are the most widely received form of payment in the P-ARB (50-60% of households in some districts). Furthermore, income in the form of a salary is less common than cash and wages from agricultural activities. Additionally, more than half of the households tend to have diversified income sources, especially in Badakhshan province, but still many households rely on a single source for their cash income. Agriculture plays an important role of the income source both in terms of its products and employment. As a result, household income is dependent on agricultural yield and productivity, and thus, on favorable environmental and climate conditions, which may deteriorate under climate change.

Social and human capital are other important pillars of the region's sustainable development and resilience. They have a direct impact on individual and community wellbeing and livelihoods while also affecting the environment, as improved human capital can lead to the sustainable use and management of natural resources, improved sanitation, nutrition, and food security, helping also to mitigate climate change and natural hazards. The essential components of human capital are education and health, so that continuing education and accessible medical care can benefit society and improve human capital through building up a strong generation, qualified labor, diverse capabilities, and opportunities to improve wellbeing. The results of the analysis suggest that satisfaction with overall quality of life and health status of the population in the region are generally low, more so for females than for males. Among provinces, Badakhshan reported the highest scores of satisfactions for both genders and Takhar reported the lowest. Among the population there is a high unacceptability for females to be members of social institutions (51% of the respondents agreed that both genders are very acceptable to be members of community development centers). Literacy and schooling rates are very low in the region, and again are lower for females than males. On average, 85% of females and 53% of males cannot read at all, and 67.5% of females and 43.7% of males have not attained any education. Furthermore, there is high variation in the education indicators among provinces, districts within provinces, and population of districts/provinces. Among the five observed provinces, Kunduz had the lowest rates of all education and literacy determinants both for males and females (90% of females and 60% of males are illiterate). However, while the literacy rate is very low, the school enrollment rate has increased. On average, 76% of children attend primary school, and 47% attend secondary school, which signals improved access to education within the recent years. Gender inequality in school attendance is, however, still a concern.

Rural population density and distribution is another socio-economic indicator of population vulnerability to climate change. In Afghanistan, most of the total population is considered rural. The density and distribution of the rural population provides an indicator of access to land and production possibilities, and allows an assessment of land management, or how efficiently and adequately the land is consumed and developed. Higher rural population density implies higher competition for resources, which reduces the adaptive capacity of the population and increases their sensitivity to climate change-related natural hazards. At the same time, higher density stimulates the development of the rural infrastructure. In the P-ARB, the rural population has grown by 7% in the period of 2015-2018. While no significant changes in rural-urban proportions among the population have been observed, the share of the rural population is reported to be very high: 97% in Bamyan, 96% in Badakhshan, 87% in Takhar, 79% in Baghlan, and 74% in Kunduz provinces. Kunduz and Takhar provinces are the most rural-dense provinces, and Badakhshan is the least. At the same time, Kunduz and Takhar provinces are reported to be the most vulnerable as determined by their lower level of economic, social, and human development. As a result, high rural density combined with a low level of development increases competition for natural resources, including land and firewood, and, consequently, challenges the opportunities to mitigate shocks, improve livelihoods, and build resilience and living conditions of the population.

Additional indicators are described and assessed in Appendix 7.

Overview of the datasets

Quality of Life (QoL)

The Quality of Life (QoL) Survey was conducted by The Aga Khan Development Network (AKDN) in 2014 and carried out assessments in geographical areas where it undertakes multi-input area development (MIAD) programming. These assessments employ quantitative and qualitative research methods to examine indicators and topics across different domains (household economy, health, education, natural and built environment, social and cultural life, and voice and representation). The sample for the household survey was drawn using multi-stage, probability proportional to population size (PPS) random sampling (USAID and AKF 2015). The next set of QoL surveys is expected to be carried out in 2021, which will allow building panel data for more comprehensive and deeper research analysis with the long-term perspective and to observe dynamic changes in the society and determinants of wellbeing.

Within the observed region, QoL covers four (Badakhshan, Baghlan, Bamyan, and Takhar) of five (excluding Kunduz) provinces and 21 of 47 corresponding districts in the P-ARB. Table 23 and Table 24 present information on the sample size both for households and individuals at the district and province levels.

Table 23. Coverage and sample size of Quality of Life Survey 2014 by district.

Province	District	Code	Sample size	
			households	individuals
Badakhshan	Baharak	1108	175	1593
Badakhshan	Darwaz	1110	100	902
Badakhshan	Ishkashim	1107	25	265
Badakhshan	Jurm	1103	200	1575
Badakhshan	Kuran Wa Munjan	1117	100	1009
Badakhshan	Shighnan	1109	125	1123
Badakhshan	Wakhan	1106	50	535
Badakhshan	Zebak	1105	25	245
Baghlan	Andarab	1307	175	1487
Baghlan	Dahana-I-Ghori	1303	100	844
Baghlan	Doshi	1304	200	1605
Baghlan	Kahmard	2803	125	1114
Baghlan	Khinjan	1306	75	566
Baghlan	Tala Wa Barfak	1305	125	1132
Bamyan	Bamyan City	2801	200	1718
Bamyan	Shibar	2802	50	320
Takhar	Farkhar	1206	75	443
Takhar	Kalafgan	1207	50	329
Takhar	Rustaq	1208	350	2429
Takhar	Taluqan	1201	325	2140
Takhar	Warsaj	1205	50	311

Table 24. Coverage and sample size of Quality of Life Survey 2014 by province.

Province	Sample size	
	households	individuals
Badakhshan	800	7247
Baghlan	800	6748
Bamyan	250	2038
Takhar	850	5652

Demographic and Health Survey (DHS)

The Afghanistan Demographic and Health Survey (AfDHS) 2015 was implemented as part of the worldwide Demographic and Health Surveys (DHS) Program by the joint effort of the Central Statistical Organization (CSO) and the Ministry of Public Health (MoPH) (CSO et al. 2017). The primary objective of the 2015 AfDHS project was to provide up-to-date estimates of basic demographic and health indicators. Specifically, the AfDHS collected information on knowledge and practice of family planning, fertility levels, marriage, fertility preferences, child feeding practices, nutritional status of children and women, childhood mortality, maternal and child health, awareness and attitudes regarding HIV/AIDS, knowledge about other illnesses, and domestic violence. The target groups were women and men ages 15-49 in randomly selected households across Afghanistan (CSO et al. 2017).

Within the P-ARB, the AfDHS provides data at the province level in all five observed provinces, including Badakhshan, Baghlan, Bamyan, Takhar, and Kunduz. Table 25 presents information on the sample size both for households and individuals at the province level.

Table 25. Coverage and sample size of Demographic Health Survey 2015 by province.

Province	Sample size	
	households	individuals
Badakhshan	756	6329
Baghlan	756	5630
Bamyan	702	2370
Takhar	783	7664
Kunduz	756	8583

National Statistic and Information Authority (NSIA)

National Statistics and Information Authority, formerly known as the Central Statistics Organization, was established in 1972 as an independent authority within the government of Afghanistan in order to establish a coordination mechanism for managing statistical information within all sectors in the country. NSIA, as a prime national entity, is committed to providing timely and quality services to public and national and international organizations. NSIA is legally authorized and has the responsibility of collection, analysis, consolidation, and standardization of the official statistical data on socio-economic and environment conditions, including population, trade, financial issues, agriculture, social, health, environment and people living condition in national and subnational levels (NSIA 2018).

Within the P-ARB, the NSIA provides data at the province level in all five observed provinces, including Badakhshan, Baghlan, Bamyan, Takhar, and Kunduz. For the research, the most recent available data (2018) was used.

Community Use of and Access to Fuelwood

AC

Indicator overview

Communities that have high use of and low access to fuelwood likely have lower adaptive capacity and thus are likely more vulnerable. Furthermore, the emissions from traditional cookstoves and fuels also result in slow progress on environmental and climate-related goals.

Unsustainable wood harvesting can contribute to deforestation and soil degradation (SDG15) (UN 2018). These effects could become most sensitive at the community level. Fuelwood shortages can then have direct impacts on food and nutritional security, as fuelwood is extensively used for cooking purposes (FAO 2017). Furthermore, harvesting may become more difficult under climate change as forests and rangelands become stressed and degraded, such that communities that depend on these resources and have fewer alternatives will be more vulnerable.

Moreover, fuelwood remains one of the most polluting energy sources for heating and cooking. High reliance on wood burning in an inefficient cooking stove or heating system results in household air pollution that poses deadly health risks daily. Also, wood collection is time and energy consuming, so reduces household capability to spend time on other activities, such as education or forms of income generation (UN 2018).

Methods overview

Community use of and access to fuelwood is estimated from participants' responses about their use of fuelwood, and the plant species that typically constitute fuelwood. For assessing community use of fuelwood, the respondents/household heads who participated in the QoL 2014 Survey were asked about their main sources of heating in winter by answering the question, "What are the three main sources of heating for this household in winter?", and their main sources of cooking fuel by answering the question, "What are the three main sources of cooking fuel for your household?". Respondents provided three main sources for heating and cooking and ranked them according to the frequency and importance of the sources' use. The summary of responses is provided in Tables 26-28. The list of the proposed sources for heating and cooking included (i) animal dung, (ii) crop residues/saw dust/straw, (iii) twigs/branches/bushes, (iv) firewood, (v) charcoal, (vi) mountain coal, (vii) electricity (including solar), (viii) gas, and (ix) other. Tables 26-28 provide estimates on the percentage of households who identified the listed sources as at least one of the three main sources used for heating or cooking. To calculate fuelwood usage, two sources were combined and estimated: 'twigs/branches/bushes' and 'firewood'. In this way, if a household identified twigs/branches/ bushes or firewood as one of the main sources for heating or cooking, then this household was counted as a user of fuelwood. The available data have been disaggregated by province and district.

Summary tables of indicator by district and province

Table 26. Main sources of heating for households in winter by district.

Province	District	Code	Main sources of heating for household in winter (% of households)								
			Animal dung	Crop residues/ saw dust/ straw	Twigs/ branches /bushes	Firewood	Charcoal	Mountain coal	Electricity (incl. solar)	Gas	% of hh using fuelwood for heating
Badakhshan	Baharak	1108	89	2	76	96	2	1	0	7	99
Badakhshan	Darwaz	1110	74	0	79	74	0	0	0	0	99
Badakhshan	Ishkashim	1107	100	0	96	88	0	0	0	0	100
Badakhshan	Jurm	1103	91	1	76	86	1	1	0	8	98
Badakhshan	Kuran Wa Munjan	1117	39	1	70	83	0	0	9	0	100
Badakhshan	Shighnan	1109	89	4	65	66	0	1	10	1	97
Badakhshan	Wakhan	1106	100	16	90	64	0	0	0	0	94
Badakhshan	Zebak	1105	100	20	100	76	0	0	0	0	100
Baghlan	Andarab	1307	88	1	69	77	4	24	0	6	99
Baghlan	Dahana-I-Ghori	1303	97	46	70	36	3	5	0	0	81
Baghlan	Doshi	1304	70	10	45	71	14	51	0	4	95
Baghlan	Kahmard	2803	35	0	90	76	0	51	0	0	100
Baghlan	Khinjan	1306	79	7	37	91	3	45	0	3	99
Baghlan	Tala Wa Barfak	1305	64	2	44	88	1	81	0	0	100
Bamyan	Bamyan City	2801	93	1	78	33	1	44	0	1	99
Bamyan	Shibar	2802	62	0	92	52	0	6	0	4	100
Takhar	Farkhar	1206	96	15	97	65	0	1	0	0	100
Takhar	Kalafgan	1207	100	62	86	8	0	0	0	0	86
Takhar	Rustaq	1208	96	52	81	19	1	1	0	1	85
Takhar	Taluqan	1201	70	26	65	66	7	30	2	5	94
Takhar	Warsaj	1205	94	6	72	82	2	4	0	0	98

Table 27. Main sources of cooking fuel for households by district.

Province	District	Code	Main sources of cooking fuel for household (% of households)								
			Animal dung	Crop residues/ saw dust/ straw	Twigs/ branches /bushes	Firewood	Charcoal	Mountain coal	Electricity (incl. solar)	Gas	% of hh using fuelwood for heating
Badakhshan	Baharak	1108	99	1	74	97	1	0	0	17	100
Badakhshan	Darwaz	1110	91	0	79	74	0	0	0	0	99
Badakhshan	Ishkashim	1107	100	0	96	88	0	0	0	0	100
Badakhshan	Jurm	1103	92	1	72	82	0	0.5	0	24	98
Badakhshan	Kuran Wa Munjan	1117	47	0	67	83	0	0	18	0	99
Badakhshan	Shighnan	1109	90	3	66	65	0	0	0	1	97
Badakhshan	Wakhan	1106	100	22	88	60	0	0	0	4	94
Badakhshan	Zebak	1105	100	20	100	76	0	0	0	0	100
Baghlan	Andarab	1307	86	1	75	73	2	3	0	19	99
Baghlan	Dahana-I-Ghori	1303	90	48	67	30	0	1	0	21	78
Baghlan	Doshi	1304	64	17	74	44	0.5	2	0	42	93
Baghlan	Kahmard	2803	31	0	89	71	0	14	0	24	98
Baghlan	Khinjan	1306	72	9	68	69	0	0	0	32	99
Baghlan	Tala Wa Barfak	1305	63	10	80	72	0	22	0	4	100
Bamyan	Bamyan City	2801	86	1	75	32	0	7	0	54	98
Bamyan	Shibar	2802	54	0	96	56	0	0	0	18	100
Takhar	Farkhar	1206	96	17	97	59	0	0	0	1	99
Takhar	Kalafgan	1207	98	58	88	4	0	0	0	2	88
Takhar	Rustaq	1208	98	50	78	16	0.3	0	0	6	83
Takhar	Taluqan	1201	71	34	74	55	0.3	4	3	21	94
Takhar	Warsaj	1205	90	10	74	76	0	0	0	10	100

Source: QoL

Vulnerability Assessment


Women and children in Afghanistan play a vital role in collecting fuelwood for their families, often walking long distances to gather the wood they need for cooking and heating.

Table 28. Percent of households reporting fuelwood as primary energy source by province.

Province	% of hh reported fuelwood as one of the main sources	
	for heating	for cooking
Badakhshan	98.4	98.3
Baghlan	96.1	94.8
Bamyan	99.2	98
Takhar	90.8	89.6

Source: QoL

Results summary

The vast majority of households in the observed regions reported fuelwood use as one of the main sources for heating and cooking. This suggests they are dependent on the availability of and access to fuelwood. Wood is an easily and fast depleting resource that is only slowly renews. Households with higher reliance on fuelwood have lower adaptive capacity and thus higher vulnerability. Among all provinces, Badakhshan and Bamyan communities are the most dependent on fuelwood for their heating and cooking purposes (>98% of households), while Takhar is the least (90% of households).

Another source that respondents reported as an alternative, and one of the main sources both for heating and cooking, is animal dung. In some districts, crop residues/straw was also frequently used for heating and cooking. These sources are also related to vegetation, and have similar effects for human health and the environment; they will also be similarly affected by climate change. The use of more modern sources of energy—electricity and gas—is very small; in some parts of the P-ARB, gas is used for cooking.

According to this analysis, people in the study area heavily depend on fuelwood for heating and cooking with short- and long-term adverse implications for their health and local environmental sustainability.

Types and Numbers of Livestock Owned

AC

Indicator overview

Livestock ownership is an important indicator of rural household wellbeing, income, and income diversification. Societies, and especially the rural poor, remain critically reliant on animals for their livelihoods and food and nutrition security (FAO 2018a).

Animal husbandry is a significant contributor to hunger and all forms of malnutrition eradication in multiple ways. First, it provides direct food and nutrients consumption via animal-source foods. Second, it generates income revenue and employment. Third, it serves populations with sufficient and reliable meat, dairy products, eggs, and primary commodities for household items and clothing (FAO 2018a).

Households or communities that own fewer livestock likely have less income and lower income diversification, which equates to lower adaptive capacity. Thus, they are likely to be more vulnerable. Moreover, livestock breeding is highly dependent on the pastureland that is in turn highly dependent on climate conditions. Overgrazing and climate change have and will continue to impact and degrade pastureland, further causing high vulnerability of households with income solely sourced from livestock.

At the same time, a rise in livestock production leads to higher greenhouse gas emissions. Furthermore, animal breeding contributes to existing pressures on ecosystems and biodiversity and livestock owners face greater competition for labor, capital, land, water, and energy. This requires improved measures in animal husbandry practices, efficiency, and sustainable management in both production and consumption (FAO 2018a).

Methods overview

Types and numbers of livestock owned are estimated from households' responses about their livestock ownership. Households participated in the QoL 2014 Survey were asked to answer the question, "Does the household own any type of livestock?", and in case of positive answer, they were asked, "Please indicate the number of the following types of livestock that the household owns (list)". The proposed list of animals included: (i) dairy cows, (ii) sheep, (iii) chickens/other poultry, (iv) horses, (v) yaks, (vi) oxen, (vii) goats, (viii) donkeys/mules, and (ix) other. Tables 29 and 30 provide estimates on the mean numbers of dairy cows, sheep, poultry, and goats per household at the district and province levels. Although other types of livestock, such as horses, yaks, oxen, donkey/mules, and others are not largely represented in the household ownership both at the district and province levels, the mean numbers per household of which are low, they are included in the aggregate estimation of the Livestock Units (LSU). The LSU index was calculated as the total sum of the mean number of animals of each type per household, multiplied by the average internationally accepted coefficients for different animal types: dairy cow x 1.0; sheep, goats x 0.06; poultry x 0.025; horses, yaks, oxen, donkey x 0.66. The standard deviation of both the mean numbers and LSU were calculated to show the average variability of the household livestock ownership data at the district and province levels.

Data from the QoL survey was supplemented with spatially explicit data on livestock densities obtained from the Gridded Livestock of the World (GLW) dataset (version 3) (Gilbert et al. 2018). The GLW dataset provides gridded densities of cattle, sheep, goats, buffaloes, horses, pigs, chickens, and ducks circa 2010 at a spatial resolution of 5 arc minutes (~10 km). Densities were determined using random forest spatial models capable of accurate prediction, gap-filling, and data disaggregation. Livestock densities are disaggregated from census polygons using dasymetric weighting and random forest models fitted with high resolution spatial covariates. In this analysis, only data on cattle, chickens, ducks, goats, horses, and sheep were included to match the livestock types included in the QoL assessment.

Livestock play a vital role in the lives of Afghans living in rural areas. For centuries, livestock have been a crucial source of food, income, and social status for Afghan households.

Spatial representation of indicator

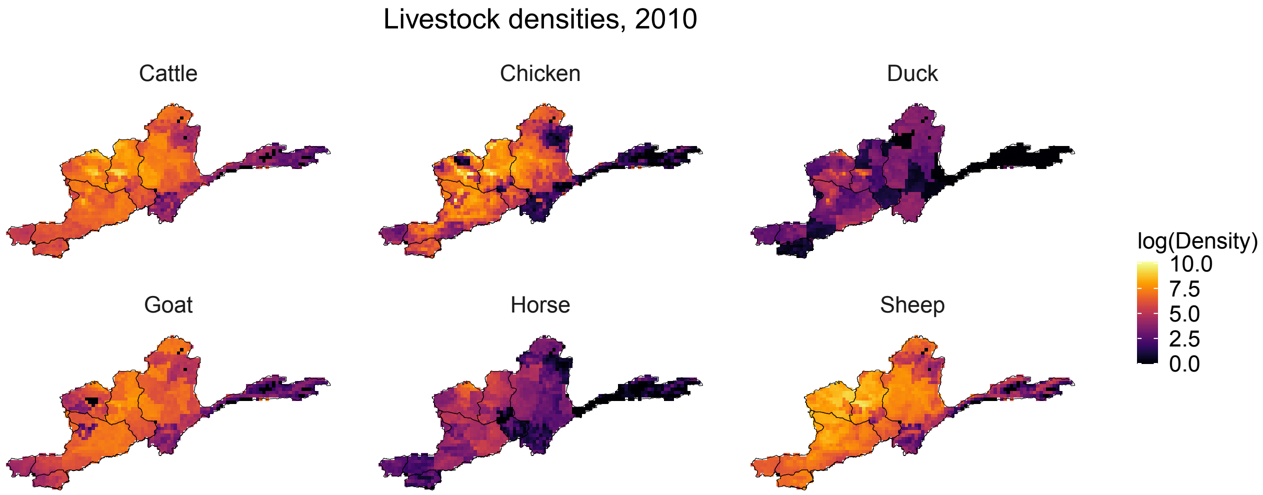

Figure 176. Modeled livestock densities (data from Gridded Livestock of the World, version 3).

Summary plots of indicator by ecoregion and province

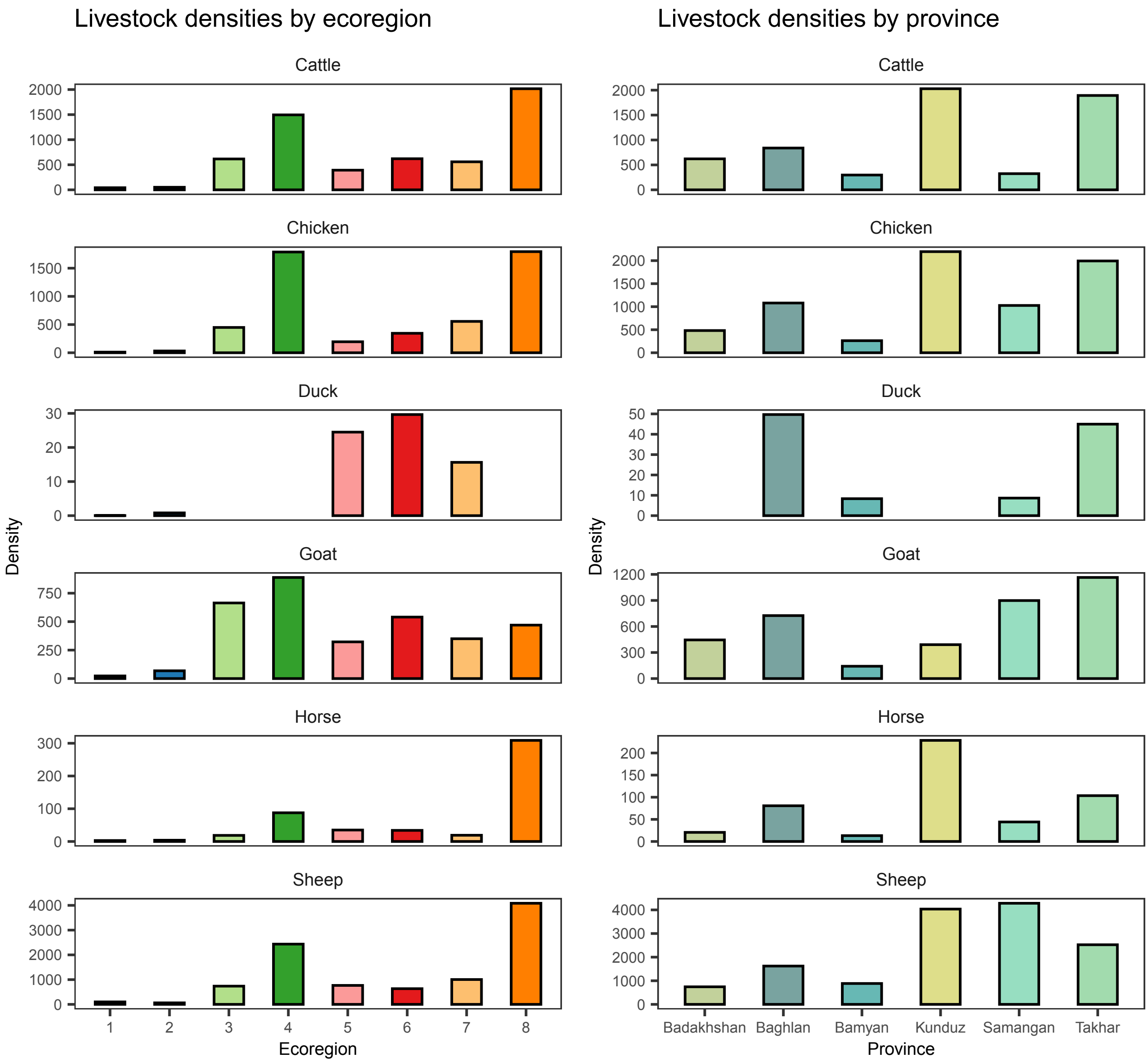

Figure 177. Modeled livestock densities by ecoregion and province (data from Gridded Livestock of the World, version 3).

Summary tables of indicator by district and province

Table 29. Numbers of animals per household by district.

Province	District	Code	Mean numbers of animals per household					Standard deviations (SDs)				
			Dairy cows	Sheep	Poultry	Goats	LSU (units)	Dairy cows_SD	Sheep_SD	Poultry_SD	Goats_SD	LSU_SD
Badakhshan	Baharak	1108	1.6	8.3	5.4	2.9	3.04	1.28	26.46	8.53	17.94	3.6
Badakhshan	Darwaz	1110	0.7	2.8	1.5	5.6	2.62	0.68	3.99	2.87	5.12	1.27
Badakhshan	Ishkashim	1107	1.7	6.5	1.5	4.7	4.81	1.27	7.6	2.72	7.07	5.34
Badakhshan	Jurm	1103	1.2	4	4.4	1.2	2.4	0.97	12.16	6.41	3.7	2.16
Badakhshan	Kuran Wa Munjan	1117	1.2	4	3.3	4.6	3.38	1.12	6.9	4.56	6.43	2.96
Badakhshan	Shighnan	1109	1.4	4.9	0.8	3.4	2.53	0.81	4.44	2.14	3.79	1.69
Badakhshan	Wakhan	1106	1.8	18	0.4	5.8	8.1	1.35	45.13	0.95	8.88	9.07
Badakhshan	Zebak	1105	1.5	8.3	1.9	4.7	3.9	0.88	6.36	1.9	5.23	2.11
Baghlan	Andarab	1307	1	5.5	8.7	2	2.73	0.83	12.25	10.48	4.71	0.16
Baghlan	Dahana-I-Ghori	1303	0.9	10.1	4.1	3	3.04	0.86	29.47	6.36	6.71	0.29
Baghlan	Doshi	1304	1.1	2.2	2.9	3.1	2.11	0.99	9.26	4.03	7.12	0.17
Baghlan	Kahmard	2803	1.1	7.3	3.7	1	3.17	1.07	15.89	4.59	2.61	0.21
Baghlan	Khinjan	1306	1	2.2	5.4	4.1	2.18	0.76	4.27	8.46	7.36	0.18
Baghlan	Tala Wa Barfak	1305	0.9	3.6	3.2	2.5	2.51	0.7	8.19	3.88	6.6	0.14
Bamyan	Bamyan City	2801	0.7	6	2.8	1.6	2.47	0.7	9.94	2.88	2.32	0.13
Bamyan	Shibar	2802	0.5	6.3	1	0.8	2.1	0.5	5.58	1.42	1.06	0.16
Takhar	Farkhar	1206	0.8	6.7	3.5	6.5	2.79	0.75	12.67	5.29	12.52	0.26
Takhar	Kalafgan	1207	0.4	3.7	5.6	3.6	2.25	0.55	5.68	4.67	3.72	0.24
Takhar	Rustaq	1208	0.7	3.1	5.9	3.5	2.58	0.83	8.49	6.54	6.26	0.11
Takhar	Taluqan	1201	1	2.4	4.9	1.1	2.22	0.85	9.56	5.07	4.94	0.14
Takhar	Warsaj	1205	1.1	2.8	2.5	2.9	2.08	0.93	3.56	3.06	3.11	0.21

Source: QoL

Table 30. Numbers of animals per household by province.

Province	Mean numbers of animals per household					Standard deviations (SDs)				
	Dairy cows	Sheep	Poultry	Goats	LSU (units)	Dairy cows_SD	Sheep_SD	Poultry_SD	Goats_SD	LSU_SD
Badakhshan	1.32	5.98	2.99	3.47	3.22	1.08	18.25	5.67	9.32	3.73
Baghlan	1.01	4.91	4.8	2.54	2.59	0.89	14.76	7.17	6.06	2.13
Bamyan	0.64	6.05	2.41	1.41	2.39	0.67	9.2	2.74	2.14	1.62
Takhar	0.78	3.29	5.14	3.11	2.45	0.84	9.02	5.81	6.77	1.93

Source: QoL

Results summary

Households of Badakhshan province reported the greatest mean number of LSUs per household. Wakhan district of Badakhshan province is reported to be significantly wealthier among all other analyzed districts in terms of the animals' ownership by households. The LSU estimation indicated 8.1 LSUs per household, including the highest mean numbers of 1.8 dairy cows,18 sheep, and 5.8 goats per household. At the same time, Wakhan district represented high values of standard deviation, which means that only few households own large numbers of the animals, resulting in the high mean values.

Furthermore, at the province level, households residing in Badakhshan province reported a higher mean number of dairy cows at 1.32 per household, and goats at 3.47 per household. Households in Bamyan province reported a higher mean number of sheep at 6.05 per household, and in Takhar province a significantly higher mean number of poultry at 5.14 per household. Analysis of the standard deviation values represents high variation in the numbers of animals among households, especially in the numbers of sheep, goats, and poultry. Thus, the number of animals owned is unevenly distributed among households. Few households own large numbers of livestock, whereas most households own far fewer than the mean number of livestock. This results in their low capacity for income opportunities and income diversification and constrains their food and nutrition security.

Based on the analysis of the GLW data, Kunduz had the highest densities of cattle, chickens, and horses; Baghlan had the highest densities of ducks; and Takhar had the highest densities of goats. These results are not consistent with those from the QoL, because the gridded data provide estimates for the entire province for each province, and thus densities in Badakhshan, which is a much larger province, become much smaller in this analysis. It should also be noted that data from Bamyan are not complete owing to incomplete coverage of the province within the P-ARB boundary.

Area and Ownership of Rainfed and Irrigated Crops

AC

Indicator overview

Agricultural land is a primary source of agricultural production that contributes to food security, income, and livelihoods. Access to land is an essential way to reduce a farmer's vulnerability, support better and long-term investment on their land, conserve natural resources, and promote more productive and sustainable practices (FAO 2018b).

The sustainable livelihoods and food security of the rural households of the P-ARB are highly dependent on agricultural production. Land is a primary source for the wellbeing and subsistence. Land ownership contributes to the households' sustainable livelihoods as it allows households to produce goods for consumption and to sell for income. Diversifying agricultural production can contribute to the nutrition of the population, income diversification, and sustainable and productive land usage practices. Availability of irrigated land provides farmers with more productive yields and resilience to the natural disasters and changing climate conditions. Households having only rainfed land for their agricultural activities are likely to rely on natural precipitations that vary both seasonally and annually. For most of the farmers, agricultural production tends to be the only source of subsistence and thus it is very important to have land and a sustainable harvest.

Additionally, access to land promotes biodiversity in the range of crops, plants, and animals. For households and communities, this is particularly important from the perspective of increasing food production, food, and nutrition diversification, and sustaining livelihoods, while also providing adaptability and resilience in the face of climate change and other pressures on food and water supplies (FAO 2018b).

While crop production and access to land are essential for many rural households' livelihoods, many smallholders operate on rainfed areas where infrastructure for irrigation is not needed, but where the water supply is inherently uncertain. This uncertainty is poised to increase under climate change, and many regions are projected to experience reductions in spring and annual rainfall, which will subsequently influence rainfed production. This is especially influential in the areas of drylands where rainfalls are sparse and highly variable, which results in frequent droughts and limited crop productivity. The resulting low yields can exacerbate poverty, and households relying more extensively on rainfed agriculture will be under more uncertain conditions and have lower adaptive capacity (FAO and WWC 2015).

Sustainable access to the essential source for food production and food security, land, is characterized not only by the area of the land, but also by the availability of land plots. The number of agricultural landholdings reflects the possibility to diversify food production and hence contribute and improve food security and nutrition as well as to secure household income and livelihood in the case of poor yields or natural disasters.

Consequently, households or communities that own less area of agricultural lands of various types are likely to have less income and lower income diversification and be more sensitive to climate change-related reductions in agricultural potential (particularly rainfed agriculture). And, as a result, they are likely to have lower adaptive capacity and be more vulnerable.

Methods overview

Area of rainfed and irrigated land, and percentage of households having agricultural landholdings were estimated from the householders' responses on the amount of agricultural land units they have in their ownership. The data were taken from the QoL 2014 survey where participants were asked the question, "How many Jeribs of agricultural land in total does your household own?". Responses were given separately for two types of the owned agricultural land: (i) rain-fed, and (ii) irrigated. QoL datasets contained responses on land area in two measure units: Jerib and Biswa. For estimation and presentation purposes, those units were converted into hectares (ha), where 1 ha is equal to 79.07 Biswa and to 5 Jerib. Tables 31-32 provide estimates on the mean ha of rainfed and irrigated lands per household at the district and province levels. The variability of the owned land among households is represented by the standard deviation. The total area was calculated by summing up the means of the rainfed and irrigated land areas to represent the overall households' land availability for their agricultural purposes. Additionally, the percentage of households who reported to have some land ownership was calculated from the total sample. Then, the percentages of rainfed and irrigated land reported by the landowners were estimated separately. The table presents data on the percentage of households that reported to have land in their ownership and on the percentage of landowners having either type of the agricultural land, rainfed and irrigated. The data is disaggregated at the district and province levels.

Additionally, recent available data were taken from the National Statistic and Information Authority (NSIA) of Afghanistan. The relevant datasets provided estimates on the area of both rainfed and irrigated land cultivated for wheat, barley, maize, rice, cotton, peach, almond, apple, grape, and pomegranate. To measure the average area of the cultivated land per capita, all cultivated area was summed and then divided by the total population of the province taken from NSIA. Further, to expend the analysis on the population's access to irrigated land within the available data, the share of wheat production on the irrigated land to the total wheat area was calculated. The data were then summarized following the same procedures described above for the QoL data.

Summary tables of indicator by district and province

Table 31. Rainfed and irrigated land per household by district.

Province	District	Code	Mean ha per household				
			Rainfed	Std. Dev.	Irrigated	Std. Dev.	Total area
Badakhshan	Baharak	1108	0.44	0.83	0.76	0.74	1.19
Badakhshan	Darwaz	1110	0.67	0.61	0.51	0.48	1.18
Badakhshan	Ishkashim	1107	0	0	0.78	0.77	0.78
Badakhshan	Jurm	1103	0.69	1.92	0.66	0.83	1.36
Badakhshan	Kuran Wa Munjan	1117	0.46	0.68	0.78	0.73	1.23
Badakhshan	Shighnan	1109	0.03	0.21	0.30	0.44	0.34
Badakhshan	Wakhan	1106	0	0	1.09	0.82	1.09
Badakhshan	Zebak	1105	0.03	0.09	0.77	1.08	0.80
Baghlan	Andarab	1307	0.72	1.17	0.66	0.74	1.38
Baghlan	Dahana-I-Ghori	1303	3.01	3.74	1.33	3.00	4.34
Baghlan	Doshi	1304	0.75	1.32	0.47	0.69	1.22
Baghlan	Kahmard	2803	0.30	0.70	0.78	0.76	1.08
Baghlan	Khinjan	1306	0.14	0.40	0.37	0.34	0.51
Baghlan	Tala Wa Barfak	1305	0.36	1.14	0.51	0.72	0.87
Bamyan	Bamyan City	2801	0.05	0.22	0.87	0.82	0.92
Bamyan	Shibar	2802	0.08	0.18	0.30	0.24	0.38
Takhar	Farkhar	1206	0.94	1.38	0.30	0.28	1.24
Takhar	Kalafgan	1207	3.19	3.65	0.01	0.08	3.20
Takhar	Rustaq	1208	3.30	6.58	0.06	0.24	3.36
Takhar	Taluqan	1201	1.34	3.53	0.70	1.16	2.04
Takhar	Warsaj	1205	0.40	0.91	0.25	0.20	0.65

Source: QoL

Table 32. Rainfed and irrigated land per household by province.

Province	Mean ha per household				
	Rainfed	Std. Dev.	Irrigated	Std. Dev.	Total area
Badakhshan	0.39	1.04	0.65	0.74	1.04
Baghlan	0.75	1.7	0.65	1.15	1.4
Bamyan	0.06	0.21	0.76	0.78	0.82
Takhar	2.3	5.15	0.28	0.72	2.58

Source: QoL

Table 33. Total and irrigated wheat area by province.

Province	cultivated area (ha per capita)	% irrigated wheat area to total wheat area
Badakhshan	0.1007	18.03
Baghlan	0.1054	79.75
Bamyan	0.0791	100
Takhar	0.1196	64.99
Kunduz	0.1788	88.64

Source: NSIA

Table 34. Percentage of households with agricultural land by district.

Province	District	Code	% households with agricultural land	% households-landowners reporting land type	
			Any land	Rainfed	Irrigated
Badakhshan	Baharak	1108	59	45	95
Badakhshan	Darwaz	1110	98	94	96
Badakhshan	Ishkashim	1107	92	0	100
Badakhshan	Jurm	1103	65	44	97
Badakhshan	Kuran Wa Munjan	1117	98	53	96
Badakhshan	Shighnan	1109	86	6	100
Badakhshan	Wakhan	1106	100	0	100
Badakhshan	Zebak	1105	96	8	100
Baghlan	Andarab	1307	82	53	98
Baghlan	Dahana-I-Ghori	1303	58	76	43
Baghlan	Doshi	1304	78	46	92
Baghlan	Kahmard	2803	87	27	100
Baghlan	Khinjan	1306	71	17	100
Baghlan	Tala Wa Barfak	1305	85	28	99
Bamyan	Bamyan City	2801	90	8	100
Bamyan	Shibar	2802	82	29	100
Takhar	Farkhar	1206	59	61	91
Takhar	Kalafgan	1207	56	1	4
Takhar	Rustaq	1208	58	98	8
Takhar	Taluqan	1201	39	42	83
Takhar	Warsaj	1205	48	38	96

Source: QoL

Table 35. Percentage of households with agricultural land by province.

Province	% households with agricultural land	% households-landowners reporting land type	
	Any land	Rainfed	Irrigated
Badakhshan	79.1	40.3	97.3
Baghlan	78.3	41.5	92.2
Bamyan	88	11.8	100
Takhar	50	74.1	43.8

Source: QoL

Results summary

According to the results of the QoL data analysis, households of Bamyan province had the highest mean ownership of irrigated land (0.76 ha per household) and Takhar province had the lowest mean irrigated area (0.28 ha per household). Conversely, households of Takhar province had the highest mean ownership of rainfed land among the four observed provinces (2.3 ha per household), while Bamyan had the lowest (0.06 ha per household). These results suggest that Bamyan province has more irrigation facilities, while households of Takhar province rely mostly on natural water sources for agriculture resulting in their high dependence on the variable and uneven climate conditions. The standard deviation measures are relatively high in Takhar and Baghlan provinces, which implies high variability and uneven land distribution among households of the provinces.

The two districts that reported the lowest ownership of irrigated land were Kalafgan and Rustaq, both in Takhar province, with means of 0.01 and 0.06 ha per household, respectively. Two districts of Badakhshan province (Ishkashim and Wakhan) reported no ownership of rainfed land, but the mean area of irrigated land was greater than the mean area at the province level.

NSIA data indicated that Kunduz province had the highest cultivated area per capita (0.18 ha per capita), followed by Takhar province (0.12 ha per capita) and Baghlan and Badakhshan provinces (0.1 ha per capita, for each). The lowest cultivated area per capita was reported in Bamyan province (0.08 ha per capita). Furthermore, while Bamyan province reported no usage of rainfed land for wheat production, it also recorded the second least (after Badakhshan) irrigated area under wheat production. The highest and most substantial usage of rainfed land for wheat production was reported in Badakhshan province.

Furthermore, households of Takhar province reported the lowest ownership of any agricultural land at 50% of households and just 43.8% of irrigated land from the total owned. Households in Bamyan, Badakhshan, and Baghlan provinces reported high availability of irrigated land from the total land they owned at 90-100%. About 79% of households of Badakhshan and Baghlan provinces and 88% of households of Bamyan province reported to have at least one type of agricultural land in their ownership. Rainfed land was the least presented in the ownership by the households of Bamyan province, while all households with land property reported to have irrigated land plots.

Household Wealth Distribution, Income Sources, and Income Diversification

S AC

Indicator overview

Household wealth is a multidimensional indicator constituting housing conditions, assets ownership, and access to basic vital services. Wealth is a primary indicator of household livelihoods and opportunities, and thus adaptive capacity.

Living in adequate homes promotes households with better health, better services, and higher chances to improve their human capital. Access to sanitation facilities, improved water services, safe drinking water, sufficient living areas, and durable housing are essential for household wellbeing and a decent and sustainable life.

Although households' access to water and sanitation facilities globally have progressed, access to safe drinking water is still a substantial challenge. Poorer people have limited access to clean water, especially in areas that lack improved water technologies and facilities. Moreover, climate change stresses water scarcity even more, with negative impacts on natural ecosystems such as forests, mountains, and freshwater rivers and streams[2].

Access to transportation, technologies, and innovation ensures household empowerment. Transportation improves household mobility, enabling access to education, employment opportunities, food, markets, and other services. Technology, innovation, and information promote equality, inclusive society, enhanced entrepreneurship, sustainable livelihoods, and better access to knowledge and services. Basic household goods can contribute to poverty reduction and improve wellbeing[2].

Poverty remains a significant threat to many households' livelihoods. A living income is an essential source for ensuring basic subsistence, food security, and the ability to afford decent life. Apart from unemployment and economic shocks, even those with work opportunities still fall short of sufficient incomes to secure decent lives for themselves and their families[4]. The factors that limit their abilities to afford vital needs also limit their abilities to mitigate environmental and economic shocks.

The diversification of income sources is an important aspect of population livelihoods as diversification helps to ensure that households maintain income in the event a particular revenue stream is lost and during shocks, the lean season, and extreme climate events. Furthermore, it advances income generation, creates jobs, and contributes to improved nutrition and health (FAO 2018b).

For instance, in agriculture, diversified cultivation contributes to household income stabilization, reduces vulnerability to shocks, and builds resilience to climate change and natural disasters. Production of multiple crops integrated with fishery and livestock provides significant benefits to help meet rural households' nourishment needs, contributing to food security and dietary diversity. Considering the seasonality of agricultural activities and yields, diverse productive activities help to avoid employment intervals often associated with food insecurity and nutrition gaps. Also, diversifying agricultural production improves soil and plant health, promotes biodiversity, and mitigates extreme-weather events and diseases (FAO 2018b).

Overall, income diversification can improve employment, productivity, production, nutrition, and income sustainability, further reducing the risks and shocks associated with market volatility, climate change, and natural disasters. At the same time, ensuring improved access to food and economic resources that have long-term positive effects on food security, incomes, and health (ICSU 2017).

Thus, households with lower wealth, lower income, and fewer income sources likely have fewer opportunities to obtain necessary livelihoods, which reduces their adaptive capacity and increases their vulnerability to climate change-related natural hazards.

2. https://unric.org/en/united-nations-sustainable-development-goals/
3. https://unric.org/en/united-nations-sustainable-development-goals/
4. https://www.living-income.com/sdg-s-and-living-income

Methods overview

Household wealth was estimated from the DHS data. According to the DHS, to measure the wealth index households were given scores based on the number and kinds of consumer goods they own, ranging from a television to a bicycle or car, in addition to housing characteristics such as the source of drinking water, toilet facilities, and flooring materials. These scores were derived using principal component analysis. National wealth quintiles were compiled by assigning the household score to each usual (de jure) household member, ranking each person in the household population by his or her score, and then dividing the distribution into five equal categories, each comprising 20% of the population (CSO et al. 2017). The break points in the wealth index that form the quintiles were calculated by obtaining a weighted frequency distribution of households, the weight being the product of the number of de jure members of the household and the sampling weight of the household. Thus, the distribution represents the national household population, where each member is given the wealth index score of his or her household. The persons were then ordered by the score, and the distribution was divided at the break points that formed the five 20% sections. Then, the household score was recoded into the quintile variable so that each member of a household also received that household's quintile category. The table below provides information on the share of the province population belonging to the five estimated wealth quintiles.

Household income was estimated from the households' responses on their income and the main sources of income. The data was taken from the QoL 2014 Survey. Although the question on the amount of income earned is sensitive and keeps confidential for most of the households, the survey asked about households' main sources of income and were asked the following questions: "Did any household members receive any cash income over the last 12 months?" and "Did household members receive any in kind income (e.g., products) over the last 12 months?". In case of a positive answer, households were asked to provide up to three main sources of cash and in-kind incomes. The list of cash income sources included: (i) cereal crops, (ii) horticulture (fruit and vegetables), (iii) livestock, (iv) collection of wild plants, (v) non-agricultural business (e.g., shop, trading), (vi) salary, (vii) wage: agriculture, (viii) wage: non-agriculture, (ix) rental income, (x) remittances (cash), (xi) cash loan/debt, (xii) aid from Govt./NGO, (xiii) charity, and (xiv) other. The list of kind income sources included: (i) wage: agricultural labor (products/goods), (ii) wage: non-agricultural labor (products/goods), (iii) barter, (iv) remittances (goods), (v) aid from Govt./NGOs, (vi) charity, and (vii) other. Tables 36-39 provide data on the percentages of households reported to receive cash income and in-kind income from the indicated main sources. Moreover, the additional measures were included to estimate percentages of households that reported receiving at least some cash income and in-kind income over the past 12 months. The data are disaggregated at the district and province levels.

Household diversification of income sources was estimated from households' responses on the income sources and employment. The data were taken from two data sources, QoL 2014 Survey and DHS 2015. The number of income sources reported by each household were derived from QoL 2014 Survey. Tables 40-41 present the mean number of income sources per household at the district and province levels. Also, the measures of standard deviation were calculated and added to assess variation in the number of sources among households. DHS datasets provide data on employment disaggregated by gender at the province level. The survey asked males and females on their employment status for the past 12 months. The data were divided into three categories: (i) if the person was employed within the past 12 months and employed at the moment of the survey – that is, employed, (ii) if the person was employed within the past 12 months, but not employed at the moment of the survey – that is, unemployed, and (iii) if the person was not employed within the past 12 months – that is, not in the labor force. Table 42 presents the shares of males and females that reported on their employment status based on the above three categories at the province level.

Summary tables on household wealth distribution by district and province

Table 36. Percentage of population belonging to wealth quintiles by province.

Province	% Population belonging to wealth quintiles				
	WQ1 – poorest	WQ2	WQ3	WQ4	WQ5 – richest
Badakhshan	54.3	26.2	13.3	3.8	2.4
Baghlan	44.8	23.3	12.2	7.1	12.6
Bamyan	68.7	15.4	8.6	6.3	1.1
Takhar	33.3	28.8	17.8	12.3	7.8
Kunduz	25.1	31.5	17.2	14.9	11.3

Source: DHS

Summary tables on household income sources by district and province

Table 37. Percentage of households receiving cash by district.

Province	District	Code	% Households received cash income from the reported sources													
			% hh having cash inc	Cereal crops	Horticulture (fruit and vegetables)	Livestock	Collection of wild plants	Non-agricultural business (e.g., shop, trading)	Salary	Wage: agriculture	Wage: non-agriculture	Rental income	Remittances (cash)	Cash loan/debt	Aid from Govt./ NGOs	Charity
Badakhshan	Baharak	1108	99	8	27	19	3	11	27	23	51	1	9	57	1	0
Badakhshan	Darwaz	1110	100	2	29	31	0	2	17	9	37	3	30	53	2	2
Badakhshan	Ishkashim	1107	100	4	4	36	4	0	28	36	44	4	16	68	0	0
Badakhshan	Jurm	1103	98	12	23	20	2	18	28	16	38	1	7	44	1	0
Badakhshan	Kuran Wa Munjan	1117	95	3	12	24	0	3	27	7	36	0	17	71	0	1
Badakhshan	Shighnan	1109	95	3	8	8	2	7	47	24	18	1	11	58	0	0
Badakhshan	Wakhan	1106	94	6	6	71	2	6	25	21	46	6	0	71	0	0
Badakhshan	Zebak	1105	100	0	0	52	0	8	20	20	64	0	12	84	0	0
Baghlan	Andarab	1307	99	24	29	20	0	8	42	34	33	0	6	5	1	1
Baghlan	Dahana-I-Ghori	1303	99	38	4	27	2	13	21	22	42	0	9	2	4	2
Baghlan	Doshi	1304	99	27	8	11	1	7	24	21	48	2	16	1	0	1
Baghlan	Kahmard	2803	98	18	66	20	1	2	27	15	32	1	5	29	0	0
Baghlan	Khinjan	1306	99	15	36	22	0	16	34	4	51	1	3	0	0	0
Baghlan	Tala Wa Barfak	1305	100	22	15	14	7	7	36	9	53	0	4	0	0	0
Bamyan	Bamyan City	2801	94	40	23	36	0	6	19	8	37	0	2	15	1	2
Bamyan	Shibar	2802	94	49	0	28	0	0	6	4	34	6	11	30	2	0
Takhar	Farkhar	1206	100	17	5	55	1	4	4	21	33	0	31	11	0	1
Takhar	Kalafgan	1207	98	26	0	42	0	6	18	18	44	0	18	8	0	2
Takhar	Rustaq	1208	95	23	3	27	2	8	8	24	50	1	14	19	0	1
Takhar	Taluqan	1201	100	29	6	14	0	13	15	17	52	2	16	14	0	1
Takhar	Warsaj	1205	92	17	19	17	2	2	15	21	45	0	23	30	0	0

Source: QoL

Table 38. Percent of households receiving in-kind income by district.

Province	District	Code	% Households received in kind income from the reported sources						
			% hh having in-kind inc	Wage: agricultural labour (products/ goods)	Wage: non-agricultural (products/ goods)	Barter	Remit-tances (goods)	Aid from Govt./ NGOs	Charity
Badakhshan	Baharak	1108	63	68	56	4	37	9	0
Badakhshan	Darwaz	1110	44	7	23	20	61	7	2
Badakhshan	Ishkashim	1107	100	76	28	12	32	28	12
Badakhshan	Jurm	1103	54	71	20	7	38	3	2
Badakhshan	Kuran Wa Munjan	1117	46	13	26	2	67	2	2
Badakhshan	Shighnan	1109	35	41	59	11	20	16	5
Badakhshan	Wakhan	1106	98	64	30	12	94	38	2
Badakhshan	Zebak	1105	96	38	38	8	79	33	13
Baghlan	Andarab	1307	86	30	5	0	13	0	0
Baghlan	Dahana-I-Ghori	1303	84	27	4	0	13	0	0
Baghlan	Doshi	1304	82	25	5	2	1	1	1
Baghlan	Kahmard	2803	98	100	1	2	2	2	0
Baghlan	Khinjan	1306	88	20	2	2	0	2	0
Baghlan	Tala Wa Barfak	1305	94	5	1	0	0	0	1
Bamyan	Bamyan City	2801	97	98	4	2	1	1	1
Bamyan	Shibar	2802	98	100	4	0	4	2	2
Takhar	Farkhar	1206	57	58	23	9	35	5	2
Takhar	Kalafgan	1207	76	59	31	3	54	3	5
Takhar	Rustaq	1208	54	62	38	5	19	3	4
Takhar	Taluqan	1201	55	70	29	2	29	7	1
Takhar	Warsaj	1205	56	50	36	21	21	11	4

Source: QoL

Table 39. Percentage of households receiving cash or in-kind income by province.

Province	% hh having cash income	% hh having in-kind income
Badakhshan	98	57
Baghlan	99	88
Bamyan	94	97
Takhar	97	56

Source: QoL

Summary tables on household diversification of income sources by district and province

Table 40. Number of income sources per household by district.

Province	District	Code	Average number of income sources per household	Std. Dev.
Badakhshan	Baharak	1108	2.41	0.7
Badakhshan	Darwaz	1110	2.18	0.7
Badakhshan	Ishkashim	1107	2.48	0.6
Badakhshan	Jurm	1103	2.11	0.8
Badakhshan	Kuran Wa Munjan	1117	2.03	0.7
Badakhshan	Shighnan	1109	1.9	0.7
Badakhshan	Wakhan	1106	2.6	0.6
Badakhshan	Zebak	1105	2.6	0.5
Baghlan	Andarab	1307	2.02	0.7
Baghlan	Dahana-I-Ghori	1303	1.89	0.8
Baghlan	Doshi	1304	1.72	0.7
Baghlan	Kahmard	2803	2.18	0.8
Baghlan	Khinjan	1306	1.86	0.8
Baghlan	Tala Wa Barfak	1305	1.71	0.7
Bamyan	Bamyan City	2801	1.91	0.8
Bamyan	Shibar	2802	1.77	0.8
Takhar	Farkhar	1206	1.84	0.8
Takhar	Kalafgan	1207	1.82	0.8
Takhar	Rustaq	1208	1.82	0.8
Takhar	Taluqan	1201	1.8	0.8
Takhar	Warsaj	1205	1.91	0.9

Source: QoL

Table 41. Number of income sources per household by province.

Province	Average number of income source groups per household	Std. Dev.
Badakhshan	2.2	0.7
Baghlan	1.89	0.8
Bamyan	1.89	0.8
Takhar	1.82	0.8

Source: QoL

Table 42. Employment status by sex by province.

Province	% Females employment status			% Males employment status		
	Employed in the 12 months preceding the survey		Not employed in the 12 months preceding the survey	Employed in the 12 months preceding the survey		Not employed in the 12 months preceding the survey
	Employed (Currently employed)	Unemployed (Not currently employed)	Not in the labour force	Employed (Currently employed)	Unemployed (Not currently employed)	Not in the labour force
Badakhshan	1.5	0.2	98.3	89.8	6.4	3.8
Baghlan	1	0.1	99	85.4	13.1	1.3
Bamyan	8.8	0.2	91	95	3.4	1.6
Takhar	4.3	0	95.6	94.5	4.6	0.9
Kunduz	11	0.2	88.4	95.8	3.2	1

Source: DHS

Results summary

In Afghanistan, the wealthiest households are concentrated in urban areas. Almost all of the urban population falls in the fourth and highest wealth quintiles, while most of the rural population is in the three lowest wealth quintiles. Also, it was reported that urban households are much more likely than rural households to own electronics such as televisions, mobile telephones, refrigerators, and computers (CSO et al. 2017).

There are large provincial variations in wealth. For instance, in Baghlan, Takhar, and Kunduz, 19.7%, 20.1%, and 26.2% of the population is concentrated in the two highest wealth quintiles, respectively. In Badakhshan and Bamyan, only 6.2% and 7.4% of the population, respectively, are concentrated in those quintiles.

However, the vast majority of the population among the observed provinces is concentrated in the lowest quintiles. Badakhshan and Bamyan provinces report more than half of the population live in the lowest wealth quintile. Overall, for all provinces, a substantial portion of the population is estimated to be poor and to live in the lowest two wealth quintiles: 80.5% in Badakhshan, 84.1% in Bamyan, 68.1% in Baghlan, 62.1% in Takhar, and 56.6% in Kunduz.

There is an evident, uneven distribution of population among wealth quintiles, especially apparent in Badakhshan and Bamyan provinces where much of the population is poor, with few very wealthy households. Kunduz reports the least variation in population among wealth quintiles.

Poverty remains a substantial obstacle for households of the P-ARB to access and afford essential vital goods and services, which prevents them from the opportunity to improve their wellbeing, livelihood, and adaptive capacity. As it is reported, the vast majority of population is likely to be vulnerable due to their wealth status. It affects their abilities to afford good housing conditions, sanitation facilities, clean water, assets, nutritious diversified food, good education, and health services—all factors necessary for a healthy lifestyle and an ability to withstand climate change impacts and shocks.

The majority of the households reported to receive cash income over the past 12 months within all districts and provinces. Badakhshan and Baghlan provinces reported the highest share of households having at least some cash income at 98% and 99%, respectively. While the share of households having cash income in Bamyan province is the lowest at 94%, at the same time Bamyan province reported the highest share of households (97%) that received in-kind income, that is, income received in the form of products and/or goods. All the households of Ishkashim district of Badakhshan province reported to receive both in-kind income and cash income over the past 12 months. The share of households receiving any in-kind income was the lowest in Takhar province (56% of households).

Furthermore, an analysis of the households' sources of cash income indicates that wages from non-agricultural activities was one of the most widely received cash income sources for households of all observed districts. On average, more than 40% of households rely on wages from non-agriculture as one of the main cash income sources. For some districts, the share of households receiving this income source reaches 50-60%. Cash income from cereal crops is most common among households in Bamyan province and over all cash income sources, and the least common in Badakhshan province. The cash income from horticulture is most prevalent among households of Baghlan province and some districts of Badakhshan province. Livestock is also one of the main sources of income among households of almost all observed districts, mainly in Wakhan district (Badakhshan) for 71% of households, in Farkhar district (Takhar) for 55% of households, in Zebak district (Badakhshan) for 52% of households, and lastly in Shighnan district (Badakhshan) for just 8% of households. Salary is another widely received main source of cash income, especially for households in Baghlan and Badakhshan provinces, but rarely for households in Takhar province. Wages from agricultural activities are on average earned by 20-30% of households in most of the observed districts of Badakhshan, Baghlan and Takhar provinces, but to a lesser degree by households in Bamyan province. Remittances are reported to be one of the main cash income sources by households of Takhar province.

Additional data show that cash from debt/loan is the most popular cash income source among households of all observed districts of Badakhshan province. On average, more than 60% of households of Badakhshan province reported debt/loan as one of the main cash income sources for their household. This reaches a maximum of 84% of households in Zebak district. Further, a lower but substantial share of households of Takhar and Bamyan provinces, reaching 30% in certain districts, also reported to rely on cash income from debts or loans. A use of debt/loan and this anomaly in Badakhshan can be viewed in two ways. First, it can be viewed from the perspective of availability and affordability of taking debts or loans by households to provide themselves with additional opportunities and the possibility to ensure a decent livelihood for their families. Second, it can be viewed from the perspective of a necessity to take debts or loans by households to obtain funds for their subsistence.

The least popular reported sources of cash income by households of the observed districts were non-agricultural business (e.g., shop, trading), collection of wild plants, rental income, aid from Govt/NGOs, and charity.

Most of the households of Badakhshan and Takhar provinces reported to receive an in-kind income in terms of goods and products as a wage from non-agricultural activities, remittances, or from agricultural activities. Also, about 30% of households in several districts of Badakhshan province, such as Wakhan, Zebak, and Ishkashim, reported receiving in-kind income as an aid from Government or NGOs. Charity provides one of the main in-kind income sources for 13 and 12% of households from Zebak and Ishkashim, respectively. Among households in Bamyan and Baghlan provinces who reported to receive in-kind income, wages from agricultural activities were indicated as a prevailing source with minor amounts of additional income reported from other sources.

To conclude, most of the households in the observed regions rely on cash income. Agriculture still plays an important role as an income source both in terms of its products and employment. As a result, household income is in many ways tightly linked to agricultural yield and productivity and thus to the environmental and climate conditions in the region. Still, most households in all observed provinces also reported to receive an in-kind income. However, products and goods are not a universal form of payment, so reliance on in-kind income could limit households from affording other necessities and services and inhibit diversifying their livelihood. This would decrease their adaptive capacity and increase their vulnerability.

According to the estimates of the QoL data, households of the Badakhshan province reported having more than two income sources, with an average of 2.2 sources. Wakhan and Zebak districts of Badakhshan province reported the largest mean number of income sources (2.6 per household). At the same time, standard deviation estimates are the lowest for Badakhshan, meaning that the variation in the average number of income sources among these households is lower than among households of other provinces. The lowest number of income sources was reported by the households of Takhar province (average of 1.82 per household). However, two districts of Baghlan province, Doshi and Tala Wa Barfak, reported an average of 1.7 income sources per household, the least among all observed districts.

According to the analysis of the DHS data, men are much more likely to be employed than women. There are large provincial variations in employment status, especially for women (CSO et al. 2017). In four observed provinces (all except Kunduz), more than 90% of women are not in the labor force, are not employed, and were not employed at least in the past 12 months. These numbers reached 99% of women of Baghlan province and 98.3% of women in Badakhshan province. About 11% of women in Kunduz province reported to be employed within the past 12 months, while 88.4% reported to not be in the labor force at least within the past year. Among the male population, about 90% on average reported to be currently employed, with the largest percentage of males at about 95% in Kunduz, Bamyan and Takhar provinces. About 13% of males of Baghlan province reported being unemployed, meaning that they had a job within the past 12 months, but are currently unemployed. Badakhshan province reported the largest share of males not in the labor force (not being employed within the past 12 months) at 3.8%, while the lowest share of males not in the labour force was reported in Takhar and Kunduz at 0.9 and 1%, respectively. To sum up, Bamyan and Kunduz provinces reported the largest shares of employed persons for both men and women, while Badakhshan and Baghlan reported the lowest shares for both genders. Moreover, women are largely underrepresented in the labor force.

The analysis shows that more than half of the households tend to have diversified income sources, especially in Badakhshan province, but still most of the households are limited with a maximum of one source for their cash income. At the same time, as previous analyses have shown, a majority of households rely on agriculture as a source for their earnings and subsistence. This suggests they may have higher vulnerability and a larger dependence on a suitable climate to sustain agricultural yield and productivity. Events such as natural disaster or general climate change can result in earning loss and cause these households to lose their primary and often only source of subsistence. Thus, the level of their food security is very low resulting in poor nutrition and health outcomes, and overall livelihoods.

The reported gender biases raise concerns about substantial limitations for households to increase income levels and ensure both genders have equal access to the labor market and employment opportunities. Females are considerably underrepresented in the labor force, which results in their limited possibilities to diversify household income sources, contribute to the household wellbeing, nutrition, and health.

Human and Social Capital

S AC

Indicator overview

Human and social capital are important pillars of sustainable development. They have a direct impact on individual and community well-being and livelihoods, and at the same time affect the environment. Social goods, such as trust, solidarity, helpfulness, friendliness, and hospitality, are non-material core assets to achieving sustainable development (Social Capital Assessment). Social capital is seen as "the networks and shared norms, values and understanding that facilitate cooperation within and among groups." Human capital is defined as "the knowledge, skills, competencies and attributes embodied in individuals that contribute to improved performance and wellbeing" (UNDP 2021).

Social capital involves relationships and networks in the community. It can be improved through developing social cohesion and community trust and cooperation to fulfill better economic and social outcomes[5]. Social and economic development require strong policy institutions and 7 responsive measures to economic opportunities and technology uptake. Social capital has a crucial effect on promoting sustainable policies, including those related to the economy, society, and environment. Simultaneously, social capital refers to the cooperation and collective decision-making in all aspects of human livelihoods, including management of natural resources, responses to shocks, and economic and social development.

The essential components of human capital are education and health. Thus, human capital can be improved through advancing skills, knowledge, competencies, and personal attributes, which can be gained through continuing education and training. This contributes to the development of capabilities and fulfillment of profitability as well as ensuring the availability of qualified labor. Education is seen as one of the most powerful and proven vehicles for sustainable development. At the same time, being a basic human right, education is a tool to empower people with knowledge, skills, and competencies to be able to build their better lives and to contribute to their societies[6]. Education provides better employment and entrepreneurship opportunities, better choices of decent work, and necessary skills for more efficient and productive lifestyles.

Affordable and accessible medical care, including basic and comprehensive, can benefit society through building a strong generation and improving human capital[3]. Eventually, improved human capital can lead to the sustainable usage and management of natural resources and improved sanitation, nutrition, and food security, which helps mitigate climate change and natural hazards.

Improved social and human capital can raise awareness of new technologies and practices and their adoption, provide society with skills and knowledge, open up opportunities and possibilities to improve their health, employment, and well-being.

Thus, households with lower education levels and literacy rates likely have fewer employment and income opportunities. Additionally, households with lower gender equality likely increase imbalances in resource and income distribution. These factors both likely reduce adaptive capacity and increase sensitivity to climate change-related natural hazards resulting in higher vulnerability.

5. https://ssir.org/articles/entry/using_six_conceptualizations_of_capital_to_help_achieve_the_sdgs

6. https://sdg4education2030.org/the-goal

Methods overview

Social and human capital were estimated from the information provided by respondents on their personal perception and satisfaction with the components of human and social capital. The data were taken from the QoL 2014 Survey. To determine human and social capital, several components were considered, which included education, health, gender equality, and quality of overall life. In the QoL survey, respondents were asked a set of the questions on the level of their satisfaction with those components of their livelihood. Specifically, respondents were asked the following questions: (i) How satisfied are you with the schools which your children attend? (ii) How would you rate your overall quality of life? (iii) In general, how would you say your health was in the last 12 months? and (iv) How acceptable is it to have both men and women as members of CDCs? Additionally, the questionnaire included the optional response "Don't know", meaning that the individual finds it difficult to assess his or her level of satisfaction with the component. These values were kept in the dataset and were not excluded from the sample since it indicates the level of awareness and involvement in the community. Men and women were separately asked these questions, which allows disaggregating the level of satisfaction with social and human capital by gender and comparing differences in perception. Furthermore, to assess the variability in the level of satisfaction among the population, the shares of both gender responses on each level of satisfaction with the components were estimated. Tables 43-46 present the percentage of males and females that responded at each level of satisfaction for four components and the mean estimates for assessing the average level of satisfaction with the four components at the district and province levels for both genders. Moreover, the sum of the mean values of all four components was calculated and presented to assess the overall level of human and social capital and life satisfaction, where lower values reflect higher levels of satisfaction.

Education of household members was estimated from the households' responses on the highest educational attainment, school enrollment, and literacy level of all members of the household aged 6 years old and above. Several data sources were used for corresponding estimations: QoL 2014 Survey, DHS 2015, and NSIA 2016-2018. An important assumption applied to the dataset and estimations of the school enrollment rate is the school age that is 6-19 years old taken as universal for Afghanistan school students, which was checked and confirmed with a more detailed QoL Survey.

NSIA provides data for 2016-2018 at the province level for all five observed provinces, including Kunduz that is omitted from QoL. The NSIA dataset includes data on the numbers of students enrolled in private and public schools. Table 47 presents estimates of the share of school students enrolled in private schools from the total population of enrolled school students. The gross school enrollment rate was calculated by taking the share of school aged children (6-19 years old) estimated from the nationally representative QoL Survey and applied to the total NSIA population. This allowed calculating the total number of school aged students and thus the gross school enrollment rate.

Within QoL 2014, households were asked to provide information about each household member: (i) whether they were currently enrolled in an educational institution, (ii) what was their highest level of education completed, and (iii) what is their adult literacy level. For estimating adult literacy levels, individuals aged 15 years and older were disaggregated into several categories: (i) cannot read and write, (ii) can read only, and (iii) can read and write. Tables 49-50 present the share of adults belonging to each category at the district and province levels. For estimating net school enrollment rate, the proportion of school students in district/province population was calculated and then divided by the school aged population of the district/province. The estimates were based on the assumption that the school age is between 6 and 19 years old. For estimating the highest level of educational attainment, individuals aged 6 years and older were assigned to several categories: (i) no education, (ii) school (1-12 school grade or madrassa), and (iii) above school (here including technical/vocational, tertiary, and university). Tables 49-50 present the share of individuals belonging to each category at the district and province levels. The standard deviation was calculated for each variable from the percentage estimates at the household level. This was included to integrate all variable estimations with their variability.

DHS 2015 datasets provide a range of data on education and different subsequent estimates, disaggregated by gender at the province level: (i) highest level of schooling, (ii) educational attainment, (iii) literacy level, and (iv) primary and secondary gross and net school attendance ratios. Tables 51-52 present the shares of individuals belonging to each variable category, separated by gender, and disaggregated at the province level.

Summary tables of indicator by district and province

Table 43. Male human and social capital by district.

Human and social capital for MALE																									
Province	District	% Satisfaction with school children attend (1-5)						% Overall quality of life (1-5)						% Health status in the last 12 months (1-5)						% Acceptability of both genders to be members of CDCs (1-4)					Mean sum (4-19)
		Mean	1	2	3	4	5	Mean	1	2	3	4	5	Mean	1	2	3	4	5	Mean	1	2	3	4	
Badakhshan	Baharak	1.8	49.1	28.7	8.2	8.2	1.8	2.39	8.8	55.6	24.6	10.5	0.6	2.1	27.5	50.3	8.2	12.9	1.2	1.6	63.2	23.4	2.3	10.5	7.89
Badakhshan	Darwaz	1.57	52.5	42.4	1	4	0	2.29	1	79.8	8.1	11.1	0	1.93	20.2	69.7	7.1	3	0	1.37	69.7	25.3	3	2	7.16
Badakhshan	Ishkashim	1.28	72	28	0	0	0	2.4	8	48	40	4	0	1.68	44	44	12	0	0	1.04	96	4	0	0	6.4
Badakhshan	Jurm	1.98	46.9	25.5	7.7	11.7	4.6	2.41	4.1	64.8	17.9	12.8	0.5	2.26	8.9	56.1	6.1	17.9	1	1.71	62.2	17.4	3.1	15.3	8.36
Badakhshan	Kuran Wa Munjan	1.73	45.7	41.5	2.1	8.5	0	2.15	5.3	79.8	9.6	5.3	0	2.01	22.3	62.8	6.4	8.5	0	1.27	77.7	14.9	4.3	1.1	7.16
Badakhshan	Shighnan	1.61	61.2	24.8	4.1	9.1	0	1.94	25.6	58.7	11.8	4.1	0	1.98	33.1	47.1	9.9	8.3	1.6	1.08	92.6	5	0	0.8	6.61
Badakhshan	Wakhan	1.69	40	52	0	2	2	2.3	6	64	26	2	2	2.1	20	58	16	4	2	1.08	92	8	0	0	7.17
Badakhshan	Zebak	1.28	72	28	0	0	0	2.4	4	64	20	12	0	1.92	24	68	0	8	0	1.52	60	32	4	4	7.12
Baghlan	Andarab	1.96	25.1	37.7	6.9	7.4	0	2.41	4.6	60	24.6	10.3	0	2.44	16	44	20	18.9	0.6	2.14	17.1	59.4	10.3	10.3	8.95
Baghlan	Dahana-I-Ghori	2.58	8.1	36.4	1	15.2	5.1	2.56	5.1	47.5	34.3	13.1	0	2.17	14.1	64.7	12.1	8.1	1	1.62	45.5	48.5	2	3	8.93
Baghlan	Doshi	2.03	24.5	32.5	4	10	1	2.5	7	55.5	21	13.5	3	2.27	14.5	59	12	14	0.5	1.83	51	25.5	5.5	14.5	8.63
Baghlan	Kahmard	2.33	28.2	28.2	6.5	13.7	7.3	2.13	11.3	66.1	21	1.6	0	2.19	16.9	58.1	14.5	10.5	0	2.45	39.5	16.1	4	40.3	9.1
Baghlan	Khinjan	2.07	22.7	38.7	0	8	4	2.6	1.3	52	32	14.7	0	2.17	12	72	4	10.7	1.3	1.95	52.2	20	5.3	21.3	8.79
Baghlan	Tala Wa Barfak	2.4	32.8	20	3.2	16.8	9.6	2.56	4	52.8	27.2	15.2	0.8	2.03	16	68.8	11.2	4	0	1.54	65.6	22.4	2.4	8.8	8.53
Bamyan	Bamyan City	1.91	27.8	43.8	5.2	6.7	0.5	2.47	3.6	56.2	29.4	10.8	0	2.38	14.4	54.6	10.8	19.1	1	1.56	69.6	14.4	6.2	9.8	8.32
Bamyan	Shibar	1.67	31.1	37.8	2.2	2.2	0	2.4	8.9	53.3	20	13.3	0	2.44	17.8	40	15.6	22.2	0	1.26	75.6	13.3	2.2	2.2	7.77
Takhar	Farkhar	2.04	16.7	18.3	5	6.7	0	2.7	3.3	40	40	16.7	0	2.27	8.3	61.7	25	5	0	2.03	21.7	55	15	5	9.04
Takhar	Kalafgan	1.56	26.1	32.6	0	0	0	2.59	0	47.8	45.7	6.5	0	2.3	2.2	71.7	19.6	6.5	0	2.04	19.6	58.7	19.6	2.2	8.49
Takhar	Rustaq	2.02	14	26.2	6.3	3	0.9	2.8	2.4	29.2	54.5	13.7	0.3	2.39	7.4	57.1	25.3	9.5	0.6	2.07	21.4	52.4	12.5	7.7	9.28
Takhar	Taluqan	2	19.1	33	3.8	6.6	0.7	2.78	0.35	38.5	46.2	12.9	2.1	2.17	12.5	65.6	15.3	5.6	1	1.99	24.7	54.2	15.3	4.2	8.94
Takhar	Warsaj	2.12	19	45.2	4.8	11.9	0	2.38	11.9	47.6	33.3	4.8	2.4	2.64	4.8	47.6	31	11.9	4.8	1.9	23.8	59.5	9.5	2.4	9.04

Source: QoL

Table 44. Male human and social capital by province.

Human and social capital for MALES																							
Province	% Satisfaction with school children attend (1-5)						% Overall quality of life (1-5)						% Health status in the last 12 months (1-5)						% Acceptability of both genders to be members of CDCs (1-4)					Mean sum (4-19)
	Mean	1	2	3	4	5	Mean	1	2	3	4	5	Mean	1	2	3	4	5	Mean	1	2	3	4	
Badakhshan	1.7	51.3	32	4.7	7.8	1.7	2.3	8.5	64.9	17.4	8.8	0.4	2.1	24.6	56.1	7.9	10.5	0.9	1.4	72.9	16.9	2.3	6.8	7.5
Baghlan	2.2	24.3	32.1	4.1	11.5	3.9	2.4	5.9	56.4	25.4	11.3	0.9	2.2	15.2	59	13.3	11.9	0.5	1.9	43.6	33.3	5.4	15.9	8.7
Bamyan	1.9	28.5	42.7	4.6	5.9	0.4	2.5	4.6	55.7	27.6	11.3	0	2.4	15.1	51.9	11.7	19.7	0.8	1.5	70.7	14.2	5.4	8.4	8.3
Takhar	2	17.1	29.5	4.8	4.9	0.7	2.8	2.1	35.6	48.6	12.7	1	2.3	8.9	61	21.5	7.6	0.9	2	22.7	54	14	5.6	9.1

Source: QoL

Table 45. Female human and social capital by district.

Human and social capital for FEMALES																									
Province	District	% Satisfaction with school children attend (1-5)						% Overall quality of life (1-5)						% Health status in the last 12 months (1-5)						% Acceptability of both genders to be members of CDCs (1-4)					Mean sum (4-19)
		Mean	1	2	3	4	5	Mean	1	2	3	4	5	Mean	1	2	3	4	5	Mean		2	3	4	
Badakhshan	Baharak	1.91	26.3	53.1	6.9	5.7	0	1.97	18.9	67.4	10.9	2.3	0	2.69	11.4	29.7	36.6	21.7	0	1.27	82.9	7.4	1.7	5.1	7.84
Badakhshan	Darwaz	1.39	62	25	4	1	0	2.07	17	63	14	5	0	2.77	6	36	33	23	1	1.36	70	18	2	4	7.59
Badakhshan	Ishkashim	1.7	40	48	0	0	4	2.48	4	56	28	12	0	2.8	4	32	44	20	0	1.32	76	16	8	0	8.3
Badakhshan	Jurm	1.95	25.3	51.5	3.5	7.1	1	1.97	27.3	53.5	13.1	5.6	0	2.79	11.6	27.3	32.3	26.8	1.5	1.49	65.7	19.7	4.6	6.1	8.2
Badakhshan	Kuran Wa Munjan	1.5	59	27	4	4	0	1.96	22	63	10	4	0	2.51	19	35	22	22	1	1.23	79	12	2	2	7.2
Badakhshan	Shighnan	1.39	66.4	24	2.4	0.8	1.6	2.06	17.6	62.4	16.8	0.8	1.6	2.38	16.9	42.7	25.8	12.1	1.6	1.38	62.4	15.2	2.4	4	7.21
Badakhshan	Wakhan	1.84	26	52	8	2	0	2.38	6	54	38	0	2	2.82	10	28	34	26	2	1.02	98	2	0	0	8.06
Badakhshan	Zebak	1.52	48	52	0	0	0	2.24	0	76	24	0	0	2.32	12	52	28	8	0	1	100	0	0	0	7.08
Baghlan	Andarab	1.84	32	31.4	8	5.1	0.6	2.77	3.4	33.7	46.3	13.1	2.3	2.81	6.3	27.4	45.1	18.9	1.1	2.29	15.4	20.6	11.4	10.3	9.71
Baghlan	Dahana-I-Ghori	1.92	31	21	5	6	3	2.69	0	43	45	12	0	2.88	5	31	35	29	0	1.63	32	36	5	0	9.12
Baghlan	Doshi	1.83	36	21	7	7	1	2.34	10	51.5	33	5.5	0	2.72	4.5	40.5	35	19	1	1.38	68.5	20.5	2.5	3.5	8.27
Baghlan	Kahmard	2.1	24	42.4	5.6	11.2	1.6	2.3	2.4	66.4	30.4	0.8	0	2.42	12	57.6	8	21.6	0.8	2.48	28.8	26.4	5.6	34.4	9.3
Baghlan	Khinjan	1.78	26.7	38.7	5.3	2.7	0	2.6	4	44	41.3	9.3	1.3	2.85	2.7	34.7	37.3	25.3	0	1.3	78.7	13.3	4	2.7	8.53
Baghlan	Tala Wa Barfak	1.84	32	40	4.8	5.6	0.8	2.7	3.2	44	33.6	18.4	0.8	2.88	1.6	41.6	24	32.8	0	1.47	62.4	28	1.6	4.8	8.89
Bamyan	Bamyan City	1.9	24.6	50.3	4.5	5	0.5	2.4	3	62.8	25.6	8.5	0	2.46	12.6	47.7	21.6	17.6	0.5	1.58	59.8	30.2	1.5	8	8.34
Bamyan	Shibar	1.82	30	38	0	8	0	2.24	0	76	24	0	0	2.16	18	56	20	4	2	1.68	42	48	10	0	7.9
Takhar	Farkhar	2.39	1.3	30.7	5.3	6.7	0	3.03	0	18.7	62.7	16	2.7	2.75	2.7	36	45.3	16	0	1.72	28	52	4	0	9.89
Takhar	Kalafgan	2.17	6	42	4	6	0	2.96	0	22	62	14	2	2.48	6	50	34	10	0	1.85	24	46	12	0	9.46
Takhar	Rustaq	2.39	5.1	27.7	7.7	5.4	1.7	2.95	0.6	25.4	54.6	17.1	2.3	2.72	5.4	32	48	14	0.6	1.89	20.9	38.6	8.6	2.3	9.95
Takhar	Taluqan	2.11	5.9	46.5	6.2	2.8	0.3	2.93	0.9	24.9	55.7	17.2	1.2	2.47	9.2	41.9	41.5	7.4	0	1.82	23.4	53.2	5.5	1.2	9.33
Takhar	Warsaj	2.24	8	44	18	4	0	2.8	2	30	56	10	2	2.86	2	28	54	14	2	1.73	28	38	8	0	9.63

Source: QoL

Table 46. Female human and social capital by province.

Human and social capital for FEMALES																								
Province	% Satisfaction with school children attend (1-5)						% Overall quality of life (1-5)						% Health status in the last 12 months (1-5)						% Acceptability of both genders to be members of CDCs (1-4)					Mean sum (4-19)
	Mean	1	2	3	4	5	Mean	1	2	3	4	5	Mean	1	2	3	4	5	Mean	1	2	3	4	
Badakhshan	1.7	42	41.1	4.3	3.9	0.6	2	19.1	61.2	15.3	3.5	0.4	2.7	12.3	33.3	31.4	21.5	1	1.3	74.6	13.3	2.6	4	7.7
Baghlan	1.9	31.1	31.3	6.3	6.5	1.1	2.6	4.5	47	37.9	9.6	0.8	2.7	5.5	38.8	31.5	23.4	0.6	1.7	46.1	23.9	5.3	9.5	8.9
Bamyan	1.9	25.7	47.8	3.6	5.6	0.4	2.4	2.4	65.5	25.3	6.8	0	2.4	13.6	49.4	21.3	14.9	0.8	1.6	56.2	33.7	3.2	6.4	8.3
Takhar	2.2	5.3	36.9	7.3	4.5	0.8	2.9	0.7	24.7	56.2	16.5	1.9	2.6	6.5	36.9	44.8	11.4	0.4	1.8	23.1	45.8	7.2	1.4	9.5

Source: QoL

Table 47. School enrollment by province.

Province	% Students in Private Schools			% Gross school enrollment rate		
	2016	2017	2018	2016	2017	2018
Badakhshan	0.28	0.36	0.58	83.71	81.64	84.50
Baghlan	1.29	1.48	1.72	79.02	80.45	77.76
Bamyan	0.48		1.18	73.28	70.45	70.82
Takhar	0.92	0.93	1.56	89.52	90.55	91.33
Kunduz	1.42	1.93	2.29	74.53	76.95	73.64

Source: NSIA

Table 48. Highest level of education completed by district.

Province	District	Code	% Highest level of education completed (>6 y.o.)					
			No education	Std.Dev. of % in hh	School	Std.Dev. of % in hh	Above school	Std.Dev. of % in hh
Badakhshan	Baharak	1108	37.7	19.9	57.36	20.6	4.93	9.6
Badakhshan	Darwaz	1110	48.79	21	48.51	19.1	2.7	5.8
Badakhshan	Ishkashim	1107	42.18	17.1	55.45	20.8	2.37	3.2
Badakhshan	Jurm	1103	43.35	25.7	53.04	22.1	3.6	18.3
Badakhshan	Kuran Wa Munjan	1117	53.23	20.7	43.67	18.5	3.1	10.9
Badakhshan	Shighnan	1109	25.95	16.9	52.34	20.1	11.71	13
Badakhshan	Wakhan	1106	57.52	18.1	40.81	19.8	1.67	7.2
Badakhshan	Zebak	1105	36.32	14.7	63.18	17.2	0.5	0
Baghlan	Andarab	1307	46.72	23.6	51.49	20.1	1.79	11.8
Baghlan	Dahana-I-Ghori	1303	57.58	23.7	41.36	18.6	1.06	15.2
Baghlan	Doshi	1304	48.15	25	50.39	20.9	1.47	5.5
Baghlan	Kahmard	2803	43.43	23.2	54.68	17	1.89	9.1
Baghlan	Khinjan	1306	43.07	24.4	54.58	20.4	2.34	6.7
Baghlan	Tala Wa Barfak	1305	47.81	21.2	50.22	21	1.97	6.8
Bamyan	Bamyan City	2801	46.92	21.9	51.74	18.6	1.34	6.9
Bamyan	Shibar	2802	47.74	28.4	52.26	22.2	0	0
Takhar	Farkhar	1206	71.73	23.7	27.05	19.8	1.21	8.5
Takhar	Kalafgan	1207	65.56	22.4	34.44	17.4	0	0
Takhar	Rustaq	1208	73.34	24.3	25.46	19.5	1.2	17.5
Takhar	Taluqan	1201	58.32	27.8	40.19	20.7	1.5	21
Takhar	Warsaj	1205	48.75	27.5	49.17	22	2.09	40.3

Source: QoL

Table 49. Adult literacy and enrollment in educational institutions by district.

Province	District	Code	% Adult (>15 y.o.) literacy level						Currently enrolled in educational institution			
			Cannot read and write	Std.Dev. of % in hh	Can read only	Std.Dev. of % in hh	Can read and write	Std.Dev. of % in hh	% School students	Std.Dev. of % in hh	% Net school enrollment rate	St.Dev. % Net sch enroll rate in hh
Badakhshan	Baharak	1108	50.23	14.2	4.64	7.3	45.13	18.6	32.14	15.9	78	27.4
Badakhshan	Darwaz	1110	61.49	16.3	4.81	9	33.7	14	34.37	14.8	88	32.8
Badakhshan	Ishkashim	1107	61.22	14.8	6.12	3.9	32.65	16.5	26.42	12.8	77	30.3
Badakhshan	Jurm	1103	56.26	23.4	3.36	8.5	40.38	18.1	31.56	16.9	82	32.8
Badakhshan	Kuran Wa Munjan	1117	67.16	17.7	4.22	5.8	28.62	12.6	27.95	13.4	75	23.3
Badakhshan	Shighnan	1109	35.93	12.7	8.98	7.3	55.09	19	36.06	15.8	88	21.8
Badakhshan	Wakhan	1106	71.57	15.3	6.07	9.3	22.36	12.6	17.76	13.3	52	26.8
Badakhshan	Zebak	1105	51.54	16.2	9.23	6.2	39.23	15.7	36.73	10.4	90	19.8
Baghlan	Andarab	1307	59.67	18.9	4.74	9.9	35.6	15	24.61	14.3	65	32.5
Baghlan	Dahana-I-Ghori	1303	72.45	18.9	4.4	6.2	23.15	11.8	17.77	11.8	45	32.8
Baghlan	Doshi	1304	55.33	19	5.67	8.1	39	18.2	24.17	15.6	61	29
Baghlan	Kahmard	2803	45.01	16.4	8.14	10.3	46.86	16.9	28.82	15.5	70	29.8
Baghlan	Khinjan	1306	57.49	22.8	2.75	5.6	39.76	19.6	25.62	17	65	26
Baghlan	Tala Wa Barfak	1305	59.54	15.7	2.94	8.9	37.52	15	28.98	14.5	72	28.6
Bamyan	Bamyan City	2801	50.97	17.9	10.16	9.3	38.87	17.7	28.87	14.3	76	29.5
Bamyan	Shibar	2802	43.37	20.3	7.23	8.1	49.4	20.2	31.88	17.5	78	23.5
Takhar	Farkhar	1206	86.83	21.4	3.41	6.7	9.76	12.5	16.48	12.8	46	26.2
Takhar	Kalafgan	1207	80.5	24.7	3.14	16.4	16.35	10.8	19.15	10.8	53	27.3
Takhar	Rustaq	1208	82.09	23.5	2.71	9.5	15.21	18.1	14.74	13.5	39	29.6
Takhar	Taluqan	1201	70.35	24.2	5.16	8	24.49	16.6	24.91	14.3	65	25.5
Takhar	Warsaj	1205	65.19	23	6.33	12.7	28.48	23.1	28.3	13	79	27.2

Source: QoL

Table 50. Adult literacy, enrollment in educational institutions, and highest level of education completed by province.

Province	% Adult (>15 y.o.) literacy level						Currently enrolled in educational institution				% Highest level of education completed (>6 y.o.)					
	Cannot read and write	Std.Dev. of % in hh	Can read only	Std.Dev. of % in hh	Can read and write	Std.Dev. of % in hh	% School	Std.Dev. of % in hh	% Net school enrollment rate	St.Dev. % Net sch enroll rate in hh	No education	Std.Dev. of % in hh	School	Std.Dev. of % in hh	Above school	Std. Dev. of % in hh
Badakhshan	54.9	18.3	5.33	7.6	39.77	17.8	31.2	15.8	80	29.1	42.04	22.1	53.23	21.3	4.73	12.9
Baghlan	56.81	18.5	5.18	8.9	38.02	17.2	25.16	15.1	64	30.5	47.71	23.9	50.57	20	1.72	8.8
Bamyan	49.74	18.4	9.69	9.2	40.57	18.8	29.34	15.1	77	28.5	47.06	23.4	51.83	19.4	1.12	6.9
Takhar	76.96	23.8	3.91	9.5	19.13	17.4	19.73	14	52	28.4	65.74	26.5	32.97	21	1.29	21.2

Source: QoL

Table 51. Literacy level by sex and school attendance ratios by province.

Province	% Literacy level for females					% Literacy level for males					% Primary school attendance ratio		% Secondary school attendance ratio	
	Secondary school or higher	Can read a whole sentence	Can read part of a sentence	Cannot read at all	Number of females	Secondary school or higher	Can read a whole sentence	Can read part of a sentence	Cannot read at all	Number of males	net attendance ratio	gross attendance ratio	net attendance ratio	gross attendance ratio
Badakhshan	13	1.2	5.3	80.6	1004	26	4.4	13.7	56	316	68.4	84.4	41.5	53.1
Baghlan	7.5	1.5	4.8	86.2	839	39.9	4.4	14.6	41.2	281	57.4	80.9	34	45
Bamyan	6.8	2.7	4.6	85.1	303	21.7	18.5	18	41.3	94	70.4	89.1	44	57.3
Takhar	9.1	1	4.4	85.5	1105	18.7	7.1	7.8	66.4	296	59.7	76.5	32.4	40.8
Kunduz	4.8	1	3.9	89.7	1232	28.2	2.9	8.6	60.2	479	39.1	50	29.3	40.3

Source: QoL

Table 52. Highest level of schooling and educational attainment by sex and province.

Province	% Highest level of schooling for females			% Highest level of schooling for males			% Educational attainment females			% Educational attainment males		
	No	School	Above school	No	School	Above school	No	School	Above school	No	School	Above school
Badakhshan	76.3	21.9	1.8	54.9	38.1	7	58.2	40.4	1.1	41.7	54.8	3.2
Baghlan	85.3	13.5	1.3	43.4	50.4	6.1	70.6	26.9	1.3	36.3	59.3	3.5
Bamyan	84.5	14.4	1	60.7	31	8.2	60.2	38.5	0.8	40.3	55.1	4
Takhar	84.9	12.7	2.4	58.9	34.7	6.4	68.1	29.9	1.8	47.4	48.8	3.4
Kunduz	90.2	8.4	1.5	56.3	38.7	4.9	80.3	17.7	1	53	44.9	1.5

Source: DHS

Results summary

Social and human capital were estimated through the combination of the components' assessment, including education, health, gender equality, and overall life satisfaction. Gender disaggregation allows an analysis of the differences in the perception of and satisfaction with important components of personal life, human and social capital.

Overall, for both genders, the indicators with the lowest values were related to the satisfaction with overall quality of life and the health status. Females of all provinces reported lower satisfaction with their health in the past 12 months than men. The indicator related to the acceptability of both genders to be members of CDCs had slightly higher values, but at the same time, males of all provinces (except Bamyan) reported a lower acceptability of both genders' representation in the community development councils.

Females of three out of four observed provinces (Badakhshan, Baghlan, and Takhar) reported lower cumulative scores on their satisfaction with life and social and human capital than males. In Bamyan province, both genders reported an equal cumulative satisfaction. Males and females of Badakhshan province reported higher satisfaction than in other provinces, with a score of 7.5 and 7.7 (ranging from 4 the highest to 19 the lowest) for males and females, respectively. The highest scores among males were reported in Ishkashim at 6.4 and Shighnan at 6.6, both districts of the Badakhshan province. The highest scores among females were reported in three districts of Badakhshan province (Zebak at 7.08 and Kuran Wa Munjan and Shighnan at 2.2). In general, districts of Badakhshan province reported the highest scores in all indicators. Males and females residing in Takhar province reported the lowest satisfaction among the four observed provinces with average scores of 9.1 for males and 9.5 for females. These lowest scores are consistent for females of all districts of Takhar province with the lowest in Rustaq at 9.95 and Farkhar at 9.89. The lowest scores were reported by males in Rustaq district of Takhar province at 9.28, Kahmard district of Baghlan province at 9.1, and Farkhar and Warsaj districts of Takhar province at 9.04.

Females residing in all observed districts of Takhar province reported lower satisfaction of education, health, and overall life than males. Moreover, males of all districts of Takhar province reported a lower acceptability of both genders being members of CDCs. The lowest scores of satisfaction with overall quality of life were reported by females of all districts of Takhar province, with a score of around 3 (1 being the highest and 5 being the lowest possible scores). Thus, the analysis shows that in Takhar province, the conditions for females are relatively worse than for males with respect to all four components, including education, health, gender equality, and overall life satisfaction.

Estimations of the level of satisfaction with social and human capital reveal gender biases with lower satisfaction by females than by males, on average. Also, Takhar province reported the lowest scores of satisfactions with social and human capital and overall life, while Badakhshan province reported the highest scores. Overall, the distribution of scores pointed to a poor assessment and dissatisfaction, especially with the health and overall quality of life, which indicates there are limited opportunities for households to improve their individual and community wellbeing and livelihood. These estimates further signal an urgent need for improvements in health and social sectors because society and future generations are predisposed to vulnerable and poor conditions.

NSIA data suggest that gross school enrollment rates between 2016 and 2018 years reduced largely for Bamyan, Baghlan and Kunduz provinces, but increased for Takhar and Badakhshan provinces. The share of students enrolled in private schools increased for all five provinces between 2016 and 2018.

The analysis of the QoL data on different determinants of education suggest that Takhar province has substantially lower rates of adult literacy, school enrollment and educational attainment among the observed provinces. Almost 77% of the adult population of Takhar province is illiterate, while only 19% can read and write. Also, the net school enrollment rate estimates are the lowest in Takhar province with only 52% of school aged children enrolled in school. At the same time, 66% of the population aged 6 years and above did not receive any education, and the lowest share of 33% of individuals received some form of school education. The lowest rates of adult illiteracy are reported from Bamyan province, where about half of adults are illiterate, and about 41% of adults can read and write. Schooling determinants are the highest in Badakhshan province, where the net school enrollment rate achieves 80% and the share of individuals having school education among the population aged 6 years and above and having higher school education are 53% and 5%, respectively. To conclude, QoL estimates show significant differences between provinces in the availability and affordability of education for the local population. Takhar province reported the highest rates of illiteracy in all determinants, while Badakhshan province reported the highest rates of schooling

WCS efforts in Afghanistan have played a significant role in building the capacity of local communities and local institutions to manage natural resources, sustainably, leading to greater conservation outcomes and positive socioeconomic impacts.

Environmental education programs in the Bamyan Plateau bring local school students together and explains ecosystems resilience to the impact of climate change and biodiversity loss.

and Bamyan province reported the highest rates of adult literacy. There is, however, high variation among different districts of the provinces and among households of the districts/provinces that is reflected in the values of the standard deviation.

The estimations from the DHS dataset reveal further details on gender disparity. According to the results, even though the observed region has very low education rates overall, literacy and schooling rates are much lower for the female population. More than 80% of female adults is illiterate among all provinces, reaching a maximum level of about 90% in Kunduz province. For males, there is high variation among provinces, with the lowest rate of illiteracy in Baghlan and Bamyan at 41% each and the highest in Takhar and Kunduz at 66% and 60% of the population, respectively. The school attendance ratio both for primary and secondary schools is the highest in Bamyan province and the lowest in Kunduz province. Moreover, schooling determinants show the highest rates in Badakhshan province for females and in Baghlan province for males, while the lowest rates for both genders are in Kunduz province. Summing up, among the five observed provinces, Kunduz province presented the lowest rates of all education and literacy determinants both for males and females, with figures reaching 90% illiterate females and 60% illiterate males. Takhar province is reported to be the next lowest in terms of the levels of education and literacy. While Badakhshan and Baghlan provinces reported slightly better rates comparatively, those provinces also reported very high illiteracy rates, especially for females.

Consequently, schooling and literacy are a major concern in the region. This limits the population in terms of employment opportunities and possibilities to improve their livelihood. Also, as majority of the population is employed in agriculture, has no education, and is without access to improving skills and knowledge, they are likely to be highly vulnerable to shocks. In poor regions, another important and significant limitation from schooling for children is that they need to work on their family farms for subsistence production, or elsewhere to help generate income to purchase food (ICSU 2017).

The rates are further aggravating for the female population. The surveys reveal existing and substantial gender disparity in access to education. The lowest rates of schooling and literacy were reported in Kunduz and Takhar provinces. Also, there is high variation in the rates between districts and households residing in the same territorial unit. This implies that sustainable wellbeing improvements are likely more restricted and that universal access to education is unavailable. However, it is important to note that while literacy rates and educational attainment of the adult population remains very low in the region, the school enrollment rate has increased, which signals improved access to education for the younger generation.

Rural Population Density and Distribution

S AC

Indicator overview

The rural population accounts for the predominant portion of the total population of Afghanistan. Thus, it is of high importance to invest into rural development for to boost economic and social wellbeing. Poor infrastructure, poverty, and a lack of technology and skills limit the economic growth to benefit the society. The major role of agriculture in terms of employment, production, and, in most cases, export highlight the importance of the development of the rural economy. At the same time, agriculture plays an important role in rural women empowerment and gender equality as it remains the primary source of employment for women. Moreover, agriculture is an essential source not only of staple foods, but also of dietary diversity that is important for adequate micronutrient intake, food security, nutrition, and health (UNCTAD 2015).

The vast majority of farmers are used to being disconnected from local, regional, and global markets due to limited access to infrastructure and good road networks, which constrains their agricultural production to a subsistence level rather than providing opportunities to develop businesses and enterprises and improve incomes and livelihoods (Purdie et al. 2016). Thus, rural development is critical for poverty eradication and improvements of livelihoods, including the quality of health and education, water and sanitation, and electricity that all are of vital importance for human wellbeing, but that are largely lacking in rural areas. Sustainable economic development requires technology and skills development that will allow improvements in productivity, increases primary incomes, and reductions in poverty levels (UNCTAD 2015).

Consideration of the rural population and its density is significant for land use and management. It determines land consumption and allows an assessment of how efficiently and adequately the land is consumed and developed. While high densities imply greater need for the land, high density neighborhoods have advantages in terms of infrastructure development, such as public transportation, roads and public spaces, larger local markets, and larger numbers of medical and educational facilities and professionals (UN-Habitat 2021).

As such, regions with greater rural population density have more competition for resources, which reduces their adaptive capacity and increases their sensitivity to climate change-related natural hazards. At the same time, higher densities should stimulate the development of rural infrastructure. Thus, rural population living in high densities and without good infrastructure, facilities, and road networks are likely to be more vulnerable.

Methods overview

Rural population density and distribution was estimated through the collected data on numbers of the total population and area. The data on the total province population and rural population was taken from the NSIA 2015 and 2018 datasets. First, the share of the rural population in the total population of the observed provinces was calculated. The two time periods of 2015 and 2018 were selected to observe the dynamics in data within the recent time. The rural density was then calculated as the number of rural residents divided by the total province area in km^2. The total province area was taken from the publicly available data sources (Badakhshan – 44,059 km^2, Baghlan – 21,118 km^2, Bamyan – 14,175 km^2, Kunduz – 8,040 km^2, Takhar – 12,333 km^2). The table presents estimates of rural population density in 2015 and 2018 as population per km^2 of the province area and the share of rural population in the total province population in 2015 and 2018.

Data from the NSIA survey was supplemented with spatially explicit data on human population densities obtained from the WorldPop dataset (www.worldpop.org). WorldPop provides gridded densities of people annually between 2001 and 2020 at a spatial resolution of 100 m. Densities were determined using recent census-based population counts that were matched to their associated administrative boundaries and disaggregated to 100 x 100 m grids. The disaggregation was done using daysmetric redistribution from Random Forest machine learning approaches that determine population density based on predictions from a large range of geospatial covariate layers. In this analysis, population data from 2020 are presented as the most up-to-date data on distributions of population densities. The data do not distinguish rural from urban populations directly, thus a land cover map from the European Space Agency depicting urban areas at 300 m spatial resolution circa 2020 was used to mask out urban pixels so that only pixels assumed to be rural remain.

Summary tables of indicator by district and province

Table 53. Rural population density by province.

Province	Rural density 2015	Rural density 2018	Rural population share 2015	Rural population share 2018
	Persons/km²		% of total	
Badakhshan	20.73	22.17	0.96	0.96
Baghlan	34.37	36.75	0.8	0.79
Bamyan	30.64	32.76	0.97	0.97
Kunduz	93.63	100.11	0.75	0.74
Takhar	69.17	73.96	0.87	0.87

Source: NSIA

Spatial representation of indicator

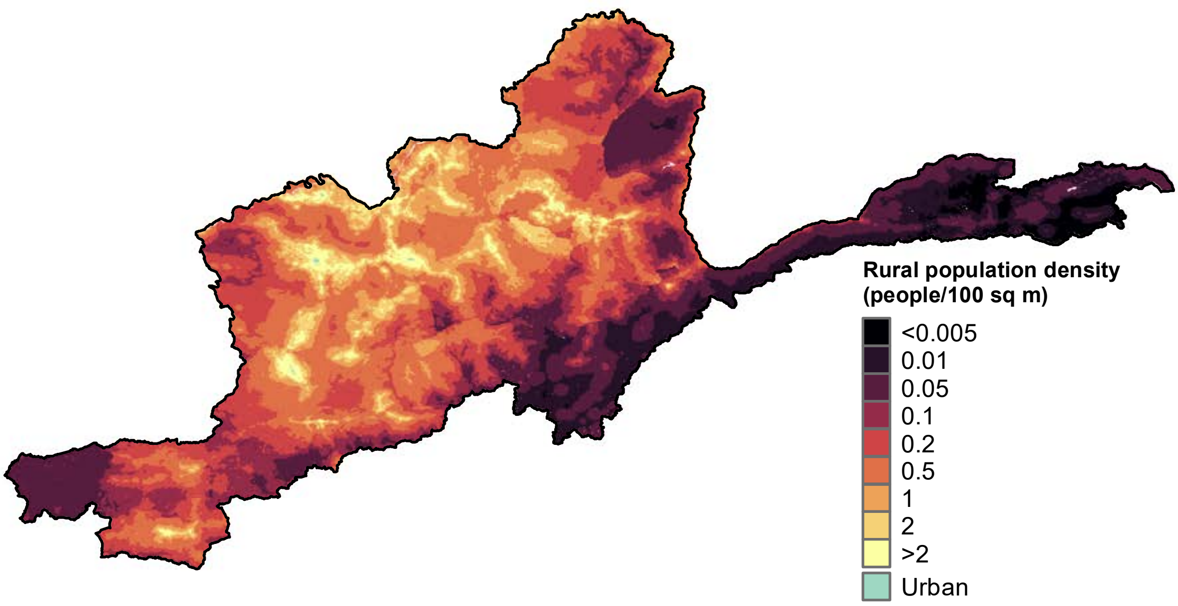

Figure 178. Rural population densities (data from WorldPop, 2020).

Summary plots of indicator by ecoregion and province

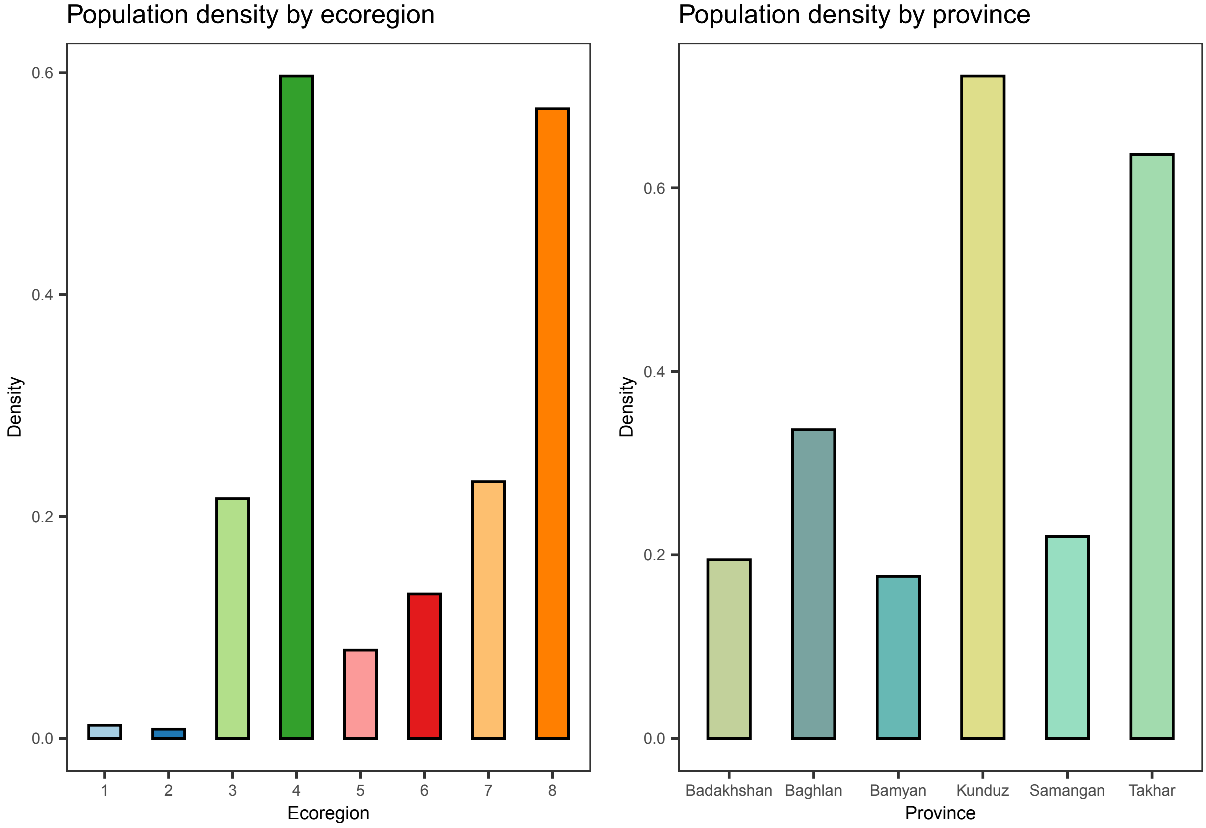

Figure 179. Rural population densities by ecoregion and province (data from WorldPop, 2020). Ecoregion legend: 1 – Pamir alpine desert and tundra; 2 – Karakorum-West Tibetan Plateau alpine steppe; 3 – Gissaro-Alai open woodlands; 4 – Paropamisus xeric woodlands; 5 – Ghorat-Hazarajat alpine meadow; 6 – Hindu-Kush alpine meadow; 7 – Afghan Mountains semi-desert; 8 - Badghyz and Karabil semi-desert

Results summary

The data analysis shows that the rural population grew by 7% between 2015 and 2018. There was no significant change between 2015 and 2018 in the rural-urban ratio for any of the five provinces observed. The share of the rural population is reported to be significantly higher in Bamyan province at 97% and Badakhshan province at 96% of the total population. The lowest share of rural population is reported in Kunduz province at 74% and Baghlan at 79% of the total population. The share of the rural population in Takhar province was 87% of the total population.

The highest density of the rural population among five observed provinces is reported in Kunduz province at 100 persons per 1 km^2 of the total province area in 2018 with a 7% increase from 2015 reported at 93-94 persons per 1 km^2 of the total province area. The next highest rural population density is in Takhar province at 74 persons per 1 km^2 of the total province area in 2018. The least dense rural population is in Badakhshan province with 22 rural persons per 1 km^2 of the total province area in 2018. In Baghlan and Bamyan, the rural population density accounts for 37 and 33 persons per 1 km^2 of the total province area in 2018, respectively.

The data from WorldPop representing gridded population density circa 2020 was consistent, showing Kunduz with the highest rural population density, followed by Takhar and Baghlan. The least dense rural population was in Bamyan, but again this could be due to the fact that the coverage in Bamyan (as well as Samangan) is incomplete owing to the location of the P-ARB boundary. Badakhshan also was among the lowest rural population densities.

The analysis suggests that the increasing rural population may increase the needs of the local population. Kunduz and Takhar provinces have the highest rural densities, yet they are reported to be the most vulnerable due to lower levels of economic, social, and human development based on the previous indicators of this report. As a result, high rural densities, in conjunction with low levels of development, will likely increase competition for natural resources, including land and firewood, and, consequently, challenge opportunities to mitigate shocks and improve the livelihoods, resilience, and living conditions of the population.

Policy and Management Recommendations

The above analysis forms the basis for the following recommendations. which aim to increase local communities' resilience and adaptability to climate change. These recommendations can be grouped into five domains. It should be noted that these policy and management recommendations should be considered in conjunction with those from the other sections of this assessment, especially related to ecosystems, species, and hydrology, to ensure that necessary improvements to development and livelihoods provide positive climate adaptation potential.

1. Household access to energy

The following recommendations are made to improve access to more efficient and less vulnerable forms of energy (such as electricity, coal, gas, and renewables) used by households:

- Ensure availability of sufficient electricity generation capacity; for that purpose, maintain mutually beneficial cooperation with existing energy generators, including supporting local and in-country solutions such as building small and medium hydropower dams
- Invest in power generators and the infrastructure necessary for broader electricity distribution
- Establish financially viable electricity tariffs and payment systems to ensure the electricity grid is properly maintained and has long-term sustainability
- Improve the supply and reduce the costs of coal in the area; for that purpose, invest in paved automobile roads and provide tax and other incentives for private companies supplying coal to the area
- Support the establishment and eventual roll-out of a network of liquified gas sale/recharging points
- Invest in renewable energy technologies to facilitate long-term sustainability, reduce reliance on extractive resources, and contribute to climate change mitigation
- Provide training to community representatives in efficient energy management at the household level and rules of safe management of the new energy sources; integrate basics of this energy-related knowledge into secondary school curricula
- Organize planting of trees to eventually replenish the stock of wood in the area and to prevent soil degradation
- Conduct research and choose tree varieties that will be the most resilient to expected climate conditions in the region 20-30 years from now
- Implement sustainable grazing and rangeland cultivation practices to keep rangeland ecosystems resilient

2. Livestock management

The following recommendations are made to ensure long-term sustainability of livestock breeding, rearing, and grazing in the region:

- Support/establish pasture management institutions (e.g., village committees, pasture sharing rules and enforcement mechanisms) that can prevent pasture over-grazing and pasture degradation; make sure that these institutions are consistent with current governance structures and practices in the region
- Conduct research and extension work to introduce/upgrade cattle, sheep, and other livestock breeds suitable for the local climate, taking into account its expected change trajectories; cooperate with relevant extension services and disseminate knowledge accumulated in the areas with similar climate conditions (e.g., GBAO, Tajikistan)
- Incentivize businesses providing access of livestock farmers to markets, e.g., collectors and processors of milk, meat, wool etc., and suppliers of veterinary services, medicines, and other key inputs
- Support education institutions in the region training livestock extension workers
- Establish systems to monitor livestock grazing patterns and rangeland condition to prevent overgrazing and rangeland degradation
- Support initiatives to provide feed for livestock to reduce reliance on rangeland grazing

3. Crop production

The following recommendations are made to support the region's crop production, which is strongly dependent on irrigation systems and, in the case of rain-fed agriculture, adequate and sustained rainfall:

- Strengthen the management of irrigation systems and attract investments into irrigation system expansion and maintenance
- Test and promote water-saving technologies among farmers in the region
- Develop and promote varieties of crops resilient to droughts and other climate shocks
- Determine where rain-fed agricultural areas are at greater risk from reductions in rainfall to target investments into irrigation systems

4. Income diversification

The following recommendations are made to reduce household reliance on agriculture (which is the most climate change-sensitive sector of the economy) as key/sole income source(s):

- Improve access of the local population to finance in order to facilitate establishing non-farm businesses (retail and other services, manufacturing from local raw materials, etc.)
- Develop electricity supply and other infrastructure (e.g., clean water supply or sewage) to enable manufacturing (e.g., food processing) and other non-arm activities)
- Develop money transfer infrastructure (e.g., by using fintech solutions) to facilitate labor migration and remittances of workers from urban/less remote parts of the country and/or from abroad
- Develop alternative markets (e.g., tourism) to generate additional revenue streams

5. Human and social capital

The following recommendations are made to increase the local population's capacity to adapt to climate change:

- Ensure peace and stability in the region
- Support the movement towards universal primary and secondary school enrollment for both girls and boys in the area
- Make primary and secondary education mandatory for the entire population
- Integrate climate change topics and basic knowledge on climate change and resilience to climate change into school curricula at all levels of education
- Mainstream climate change adaptation discourse in the local media
- Conduct awareness raising and advocacy campaigns on climate change challenges and adaptation approaches with local community and religious leaders

REFERENCES

Abbaspour, K. C. (2015). SWAT-CUP SWAT Calibration and Uncertainty Programs.

Abbaspour, K. C., Rouholahnejad, E., Vaghefi, S., Srinivasan, R., Yang, H., & Kløve, B. (2015). A continental-scale hydrology and water quality model for Europe: Calibration and uncertainty of a high-resolution large-scale SWAT model. Journal of Hydrology, 524, 733–752. https://doi.org/10.1016/j.jhydrol.2015.03.027

Abdullaev I, De Fraiture C, Giordano M, Yakubov M, Rasulov A (2009) Agricultural water use and trade in Uzbekistan: situation and potential impacts of market liberalization. Int J Water Resour Dev 25:47–63

Ackerly, D. D., S. R. Loarie, W. K. Cornwell, S. B. Weiss, H. Hamilton, R. Branciforte, and N. J. B. Kraft. 2010. The geography of climate change: implications for conservation biogeography. Diversity and Distributions 16:476–487.

Adams, J. B., M. O. Smith, and P. E. Johnson. 1986. Spectral mixture modeling: A new analysis of rock and soil types at the Viking Lander 1 Site. Journal of Geophysical Research: Solid Earth 91:8098–8112.

Adnan, M., Kang, S. C., Zhang, G. S., Anjum, M. N., Zaman, M., & Zhang, Y. Q. (2019). Evaluation of SWAT Model performance on glaciated and non-glaciated subbasins of Nam Co Lake, Southern Tibetan Plateau, China. Journal of Mountain Science, 16(5), 1075-1097.

Agaltseva N (2005) Climate changes impact to water resources within Amudarya River basin. Report for the NeWATER Amudarya Case Study, NIGMI, Tashkent, UzbekistanBates BC.

Agaltseva, N. (2005). Climate changes impact to water resources within Amudarya River basin. Report for the NEWATER Amudarya Case Study, NIGMI, Tashkent.

Aich, V., N. Akhundzadah, A. Knuerr, A. Khoshbeen, F. Hattermann, H. Paeth, A. Scanlon, and E. Paton. 2017. Climate Change in Afghanistan Deduced from Reanalysis and Coordinated Regional Climate Downscaling Experiment (CORDEX)—South Asia Simulations. Climate 5:38–25.

Akhundzadah, N. A., Soltani, S., & Aich, V. (2020). Impacts of Climate Change on the Water Resources of the Kunduz River Basin, Afghanistan. Climate, 8(10), 102.

Amate, J. I., and M. G. de Molina. 2013. 'Sustainable de-growth' in agriculture and food: an agro-ecological perspective on Spain's agri-food system (year 2000). Journal of Cleaner Production 38:27–35.

Anderson, R. P. 2013. A framework for using niche models to estimate impacts of climate change on species distributions. Annals of the New York Academy of Sciences 1297:8–28.

Antonelli, A., W. D. Kissling, S. G. A. Flantua, M. A. Bermúdez, A. Mulch, A. N. Muellner-Riehl, H. Kreft, H. P. Linder, C. Badgley, J. Fjeldså, S. A. Fritz, C. Rahbek, F. Herman, H. Hooghiemstra, and C. Hoorn. 2018. Geological and climatic influences on mountain biodiversity. Nature Geoscience 11:718–725.

Araújo, M. B., and M. New. 2007. Ensemble forecasting of species distributions. Trends in Ecology & Evolution 22:42–47.

Armitage, K. B. 2013. Climate change and the conservation of marmots. Natural Science 2013:36–43.

Arnold, J. G., Moriasi, D. N., Gassman, P. W., Abbaspour, K. C., White, M. J., Srinivasan, R., Santhi, C., Harmel, R. D., van Griensven, A., Liew, M. W. van, Kannan, N., Jha, M. K., Harmel, D., Member, A., Liew, M. W. van, & Arnold, J.-F. G. (n.d.). SWAT: MODEL USE, CALIBRATION, AND VALIDATION. Transactions of the ASABE, 55(4), 1491–1508. http://swatmodel.tamu.edu

Atkinson, P. M., C. Jeganathan, J. Dash, and C. Atzberger. 2012. Inter-comparison of four models for smoothing satellite sensor time-series data to estimate vegetation phenology. Remote Sensing of Environment 123:400–417.

Bagchi, S., and M. E. Ritchie. 2010. Herbivore effects on above- and belowground plant production and soil nitrogen availability in the Trans-Himalayan shrub-steppes. Oecologia 164:1075–1082.

Bardgett, R. D., J. M. Bullock, S. Lavorel, P. Manning, U. Schaffner, N. Ostle, M. Chomel, G. Durigan, E. L. Fry, D. Johnson, J. M. Lavallee, G. L. Provost, S. Luo, K. Png, M. Sankaran, X. Hou, H. Zhou, L. Ma, W. Ren, X. Li, Y. Ding, Y. Li, and H. Shi. 2021. Combatting global grassland degradation. Nature Reviews Earth & Environment:1–16.

Barsi, J., J. Schott, S. Hook, N. Raqueno, B. Markham, and R. Radocinski. 2014. Landsat-8 Thermal Infrared Sensor (TIRS) Vicarious Radiometric Calibration. Remote Sensing 6:11607–11626.

Beever, E. A., P. F. Brussard, and J. Berger. 2003. Patterns of apparent extirpation among isolated populations of pikas (Ochotona princeps) in the Great Basin. Journal of Mammalogy 95:37–54.

Bellard, C., C. Bertelsmeier, P. Leadley, W. Thuiller, and F. Courchamp. 2012. Impacts of climate change on the future of biodiversity. Ecology Letters 15:365–377.

Beurs, K. M. de, and G. M. Henebry. 2008. War, drought, and phenology: changes in the land surface phenology of Afghanistan since 1982. Journal of Land Use Science 3:95–111.

Boden, A.-A. 2005. Bodenkundliche Kartieranleitung, 5th edition. Hanover, Germany.

Brooks, T. M., R. Mittermeier, G. A. B. D. Fonseca, J. Gerlach, M. Hoffmann, J. Lamoreux, C. Mittermeier, J. Pilgrim, and A. Rodrigues. 2006. Global Biodiversity Conservation Priorities. Science 313:58–61.

Brookshire, E. N. J., and T. Weaver. 2015. Long-term decline in grassland productivity driven by increasing dryness. Nature Communications 6:7148.

Browne, E., and K. A. Millington. 2015. Social development and human development: Topic guide. GSDRC, University of Birmingham and HEART, Birmingham and Oxford, UK.

Bühler, Y. 2012. Remote sensing tools for snow and avalanche research. Pages 264–268 Proceedings, International Snow Science Workshop. Anchorage, Alaska.

Butt, N., and R. Gallagher. 2018. Using species traits to guide conservation actions under climate change. Climatic Change 151:317–332.

Caravaggi, A. 2018. Lagomorpha Life History. Page in J. Vonk and T. Shackelford, editors. Encyclopedia of Animal Cognition and Behavior, Living Edition.

Carroll, C., D. R. Roberts, J. L. Michalak, J. J. Lawler, S. E. Nielsen, D. Stralberg, A. Hamann, B. H. McCrae, and T. Wang. 2017. Scale-dependent complementarity of climatic velocity and environmental diversity for identifying priority areas for conservation under climate change. Global Change Biology 23:4508–4520.

Carroll, C., J. J. Lawler, D. R. Roberts, and A. Hamann. 2015. Biotic and Climatic Velocity Identify Contrasting Areas of Vulnerability to Climate Change. Plos One 10:e0140486-18.

Ceballos, G., P. R. Ehrlich, A. D. Barnosky, A. García, R. M. Pringle, and T. M. Palmer. 2015. Accelerated modern human–induced species losses: Entering the sixth mass extinction. Science Advances 1:e1400253.

Ceballos, G., P. R. Ehrlich, and R. Dirzo. 2017. Biological annihilation via the ongoing sixth mass extinction signaled by vertebrate population losses and declines. Proceedings Of The National Academy Of Sciences USA 47:201704949–206.

Chabot, D., and A. Kaba. 2016. Avalanche forecasting in the Central Asian countries of Afghanistan, Pakistan, and Tajikistan. Pages 480–483 Proceedings, International Snow Science Workshop, Breckenridge, Colorado, 2016. Breckenridge, Colorado.

Comer, P. J., R. L. Pressey, M. L. Hunter, C. A. Schloss, S. C. Buttrick, N. E. Heller, J. M. Tirpak, D. P. Faith, M. S. Cross, and M. L. Shaffer. 2015. Incorporating geodiversity into conservation decisions. Conservation Biology 29:692–701.

Council, U. E. and S. 2020. Progress towards the Sustainable Development Goals. Report of the Secretary-General. United Nations.

CSO, MoPH, and ICF. 2017. Afghanistan Demographic and Health Survey 2015. Central Statistics Organization, Kabul, Afghanistan.

Davies, R. G., C. D. L. Orme, D. Storch, V. A. Olson, G. H. Thomas, S. G. Ross, T.-S. Ding, P. C. Rasmussen, P. M. Bennett, I. P. F. Owens, T. M. Blackburn, and K. J. Gaston. 2007. Topography, energy and the global distribution of bird species richness. Proceedings Of The Royal Society B-Biological Sciences 274:1189–1197.

Davies-Colley, R. J., & Vant, W. N. (1988). ESTIMATION OF OPTICAL PROPERTIES OF WATER FROM SECCHI DISK DEPTHS 1. JAWRA Journal of the American Water Resources Association, 24(6), 1329-1335.

Dinerstein, E., D. Olson, A. Joshi, C. Vynne, N. D. Burgess, E. Wikramanayake, N. Hahn, S. Palminteri, P. Hedao, R. Noss, M. Hansen, H. Locke, E. C. Ellis, B. Jones, C. V. Barber, R. Hayes, C. Kormos, V. Martin, E. Crist, W. Sechrest, L. Price, J. E. M. Baillie, D. Weeden, K. Suckling, C. Davis, N. Sizer, R. Moore, D. Thau, T. Birch, P. Potapov, S. Turubanova, A. Tyukavina, N. de Souza, L. Pintea, J. C. Brito, O. A. Llewellyn, A. G. Miller, A. Patzelt, S. A. Ghazanfar, J. Timberlake, H. Klöser, Y. Shennan-Farpón, R. Kindt, J.-P. B. Lillesø, P. van Breugel, L. Graudal, M. Voge, K. F. Al-Shammari, and M. Saleem. 2017. An Ecoregion-Based Approach to Protecting Half the Terrestrial Realm. BioScience 67:534–545.

Diniz-Filho, J. A. F., L. M. Bini, T. F. Rangel, R. D. Loyola, C. Hof, D. Nogués-Bravo, and M. B. Araújo. 2009. Partitioning and mapping uncertainties in ensembles of forecasts of species turnover under climate change. Ecography 32:897–906.

Dobrowski, S. Z., and S. A. Parks. 2016. Climate change velocity underestimates climate change exposure in mountainous regions. Nature Communications 7:1–8.

Dobrowski, S. Z., C. E. Littlefield, D. S. Lyons, C. Hollenberg, C. Carroll, S. A. Parks, J. T. Abatzoglou, K. Hegewisch, and J. Gage. 2021. Protected-area targets could be undermined by climate change-driven shifts in ecoregions and biomes. Communications Earth & Environment 2:198.

Eckerstorfer, M., H. Vickers, E. Malnes, and J. Grahn. 2019. Near-Real Time Automatic Snow Avalanche Activity Monitoring System Using Sentinel-1 SAR Data in Norway. Remote Sensing 11:2863.

EDB & EB IFAS (2009) Impact of Climate Change to Water Resource in Central Asia 2009 (Almaty, Kazakhstan: Eurasian Development Bank).

Elith, J., and C. H. Graham. 2009. Do they? How do they? WHY do they differ? On finding reasons for differing performances of species distribution models. Ecography 32:66–77.

Elith, J., and J. R. Leathwick. 2009. Species Distribution Models: Ecological Explanation and Prediction Across Space and Time. Annual Review Of Ecology Evolution And Systematics 40:677–697.

Elith, J., M. Kearney, and S. Phillips. 2010. The art of modelling range-shifting species. Methods in Ecology and Evolution 1:330–342.

Elsen, P. R., L. S. Farwell, A. M. Pidgeon, and V. C. Radeloff. 2020. Landsat 8 TIRS-derived relative temperature and thermal heterogeneity predict winter bird species richness patterns across the conterminous United States. Remote Sensing of Environment 236:111514.

Elsen, P. R., L. S. Farwell, A. M. Pidgeon, and V. C. Radeloff. 2021. Contrasting seasonal patterns of relative temperature and thermal heterogeneity and their influence on breeding and winter bird richness patterns across the conterminous United States. Ecography.

ESA. 2017. Land Cover CCI Product User Guide Version 2. Tech. Rep.

Eyring, V., S. Bony, G. A. Meehl, C. A. Senior, B. Stevens, R. J. Stouffer, and K. E. Taylor. 2016. Overview of the Coupled Model Intercomparison Project Phase 6 (CMIP6) experimental design and organization. Geoscientific Model Development 9:1937–1958.

FAO, and WWC. 2015. Towards a water and food secure future: Critical perspectives for policy-makers. Food and Agriculture Organization and World Water Council, Rome, Italy and Marseille, France.

FAO. 2006. Livestock's Long Shadow. Food and Agriculture Organization, Rome.

FAO. 2017. Sustainable woodfuel for food security. Working Paper. Food and Agriculture Organization, Rome.

FAO. 2018a. World Livestock: Transforming the livestock sector through the Sustainable Development Goals. Food and Agriculture Organization, Rome.

FAO. 2018b. Transforming food and agriculture to achieve the SDGs. Food and Agriculture Organization, Rome.

FAO/UNESCO Soil Map of the World | FAO SOILS PORTAL | Food and Agriculture Organization of the United Nations. (n.d.). Retrieved February 25, 2022, from https://www.fao.org/soils-portal/data-hub/soil-maps-and-databases/faounesco-soil-map-of-the-world/en/

Farr, T. G., P. A. Rosen, E. Caro, R. Crippen, R. Duren, S. Hensley, M. Kobrick, M. Paller, E. Rodriguez, L. Roth, D. Seal, S. Shaffer, J. Shimada, J. Umland, M. Werner, M. Oskin, D. Burbank, and D. Alsdorf. 2007. The Shuttle Radar Topography Mission. Reviews of Geophysics 45:RG2004.

Farwell, L. S., P. R. Elsen, E. Razenkova, A. M. Pidgeon, and V. C. Radeloff. 2020. Habitat heterogeneity captured by 30-m resolution satellite image texture predicts bird richness across the United States. Ecological Applications:e02157.

Fensholt, R., K. Rasmussen, P. Kaspersen, S. Huber, S. Horion, and E. Swinnen. 2013. Assessing Land Degradation/Recovery in the African Sahel from Long-Term Earth Observation Based Primary Productivity and Precipitation Relationships. Remote Sensing 5:664–686.

Field, C. B., V. Barros, T. F. Stocker, D. Qin, D. J. Dokken, K. L. Ebi, M. D. Mastrandrea, K. J. Mach, G.-K. Plattner, S. K. Allen, M. Tignor, and P. M. Midgley, editors. 2012. Managing the Risks of Extreme Events and Disasters to Advance Climate Change Adaptation. Cambridge University Press, Cambridge, UK and New York, NY.

Foden, W. B., S. H. M. Butchart, S. N. Stuart, J.-C. Vié, H. R. Akçakaya, A. Angulo, L. M. Devantier, A. Gutsche, E. Turak, L. Cao, S. D. Donner, V. Katariya, R. Bernard, R. A. Holland, A. F. Hughes, S. E. O'hanlon, S. T. Garnett, Ç. H. Şekercioğlu, and G. M. Mace. 2013. Identifying the World's Most Climate Change Vulnerable Species: A Systematic Trait-Based Assessment of all Birds, Amphibians and Corals. Plos One 8:e65427.

Frank, D., M. Reichstein, M. Bahn, K. Thonicke, D. Frank, M. D. Mahecha, P. Smith, M. Velde, S. Vicca, F. Babst, C. Beer, N. Buchmann, J. G. Canadell, P. Ciais, W. Cramer, A. Ibrom, F. Miglietta, B. Poulter, A. Rammig, S. I. Seneviratne, A. Walz, M. Wattenbach, M. A. Zavala, and J. Zscheischler. 2015. Effects of climate extremes on the terrestrial carbon cycle: concepts, processes and potential future impacts. Global Change Biology 21:2861–2880.

Freeman, E. A., and G. G. Moisen. 2008. A comparison of the performance of threshold criteria for binary classification in terms of predicted prevalence and kappa. Ecological Modelling 217:48–58.

Frenierre, J. L., & Mark, B. G. (2014). A review of methods for estimating the contribution of glacial meltwater to total watershed discharge. Progress in Physical Geography, 38(2), 173-200.

Froebrich, J., & Kayumov, O. (2004). Water management aspects of Amu Darya. In Dying and Dead Seas Climatic Versus Anthropic Causes (pp. 49-76). Springer, Dordrecht.

Funk, C., P. Peterson, M. Landsfeld, D. Pedreros, J. Verdin, S. Shukla, G. Husak, J. Rowland, L. Harrison, A. Hoell, and J. Michaelsen. 2015. The climate hazards infrared precipitation with stations—a new environmental record for monitoring extremes. Scientific Data 2:150066.

Gang, C., W. Zhou, Y. Chen, Z. Wang, Z. Sun, J. Li, J. Qi, and I. Odeh. 2014. Quantitative assessment of the contributions of climate change and human activities on global grassland degradation. Environmental Earth Sciences 72:4273–4282.

Ghulami, M. (2017). Assessment of climate change impacts on water resources and agriculture in data-scarce Kabul basin, Afghanistan (Doctoral dissertation, Université Côte d'Azur; Asian institute of technology).

Gibson-Reinemer, D. K., K. S. Sheldon, and F. J. Rahel. 2015. Climate change creates rapid species turnover in montane communities. Ecology and Evolution 5:2340–2347.

Gilbert, M., G. Nicolas, G. Cinardi, T. P. V. Boeckel, S. O. Vanwambeke, G. R. W. Wint, and T. P. Robinson. 2018. Global distribution data for cattle, buffaloes, horses, sheep, goats, pigs, chickens and ducks in 2010. Scientific Data 5:180227.

Gleick, P. H. (1986). Methods for evaluating the regional hydrologic impacts of global climatic changes. Journal of hydrology, 88(1-2), 97-116.

Gorelick, N., M. Hancher, M. Dixon, S. Ilyushchenko, D. Thau, and R. Moore. 2017. Google Earth Engine: Planetary-scale geospatial analysis for everyone. Remote Sensing Of Environment 202:18–27.

Granit, J., Jägerskog, A., Lindström, A., Björklund, G., Bullock, A., Löfgren, R., ... & Pettigrew, S. (2012). Regional options for addressing the water, energy and food nexus in Central Asia and the Aral Sea Basin. International Journal of Water Resources Development, 28(3), 419-432.

Grenier, P., A.-C. Parent, D. Huard, F. Anctil, and D. Chaumont. 2013. An Assessment of Six Dissimilarity Metrics for Climate Analogs. Journal of Applied Meteorology and Climatology 52:733–752.

Grenouillet, G., L. Buisson, N. Casajus, and S. Lek. 2011. Ensemble modelling of species distribution: the effects of geographical and environmental ranges. Ecography 34:9–17.

Guisan, A., and N. E. Zimmermann. 2000. Predictive habitat distribution models in ecology. Ecological Modelling 135:147–186.

Gupta, H. V., Beven, K. J., & Wagener, T. (2006). Model calibration and uncertainty estimation. Encyclopedia of hydrological sciences.

Gutowski, W. J., F. Giorgi, B. Timbal, A. Frigon, D. Jacob, H.-S. Kang, K. Raghavan, B. Lee, C. Lennard, G. Nikulin, E. O'Rourke, M. Rixen, S. Solman, T. Stephenson, and F. Tangang. 2016. WCRP COordinated Regional Downscaling Experiment (CORDEX): a diagnostic MIP for CMIP6. Geoscientific Model Development 9:4087–4095.

Habibi, K. 2004. Mammals of Afghanistan. Zoo Outreach Organization with assistance from the US Fish and Wildlife Service.

Hamann, A., D. R. Roberts, Q. E. Barber, C. Carroll, and S. E. Nielsen. 2014. Velocity of climate change algorithms for guiding conservation and management. Global Change Biology 21:997–1004.

Henfrey, T. 2017. Permaculture education as ecology of mind: the head, hands, and heart of transformation. Pages 171–184 Mass intellectuality and democratic leadership in higher education. Bloomsbury, London, UK.

Henfrey, T., and G. Penha-Lopes. 2015. Permaculture and climate change adaptation: Inspiring ecological, social, economic, and cultural responses and resilience and transformation. Permanent Publications, East Meon, Hampshire.

Hijmans, R. J., S. E. Cameron, J. L. Parra, P. G. Jones, and A. Jarvis. 2005. Very high resolution interpolated climate surfaces for global land areas. International Journal of Climatology 25:1965–1978.

Hock, R. (1999). A distributed temperature-index ice-and snowmelt model including potential direct solar radiation. Journal of glaciology, 45(149), 101-111.

Hutchinson, G. E. 1957. Concluding remarks. Pages 415–427 Cold spring harbor symposium on quantitative biology.

Hutchinson, G. E. 1959. Homage to Santa Rosalia or Why Are There So Many Kinds of Animals? The American Naturalist 93:145–159.

ICLEI. 2015. The importance of all Sustainable Development Goals (SDGs) for cities and communities. Briefing Sheet, Urban Issues, No. 4. ICLEI.

ICSU. 2017. A guide to SDG interactions: from Science to Implementation. International Council for Science, Paris, France.

ILO. 2018. Decent Work and the Sustainable Development Goals: A Guidebook on SDG Labour Market Indicators. Department of Statistics, International Labour Organization, Geneva.

JAMS, Jena Adaptable Modelling System. Hydrological Model J2000 http://jams.uni-jena.de/ilmswiki/index.php/Hydrological_Model_J2000 (Last accessed 16.11.2021).

Jimenez-Munoz, J. C., J. A. Sobrino, D. Skokovic, C. Mattar, and J. Cristobal. 2014. Land Surface Temperature Retrieval Methods From Landsat-8 Thermal Infrared Sensor Data. IEEE Geoscience and Remote Sensing Letters 11:1840–1843.

Jones, K. E., J. Bielby, M. Cardillo, S. A. Fritz, J. O'Dell, C. D. L. Orme, K. Safi, W. Sechrest, E. H. Boakes, C. Carbone, C. Connolly, M. J. Cutts, J. K. Foster, R. Grenyer, M. Habib, C. A. Plaster, S. A. Price, E. A. Rigby, J. Rist, A. Teacher, O. R. P. Bininda-Emonds, J. L. Gittleman, G. M. Mace, and A. Purvis. 2009. PanTHERIA: a species-level database of life history, ecology, and geography of extant and recently extinct mammals. Ecology 90:2648–2648.

Jones, K. R., J. E. M. Watson, H. P. Possingham, and C. J. Klein. 2016. Incorporating climate change into spatial conservation prioritisation: A review. Biological Conservation 194:121–130.

Kamil, I. 2021. Afghanistan, the Amu Darya Basin and Regional Treaties. Chinese Journal of Environmental Law 5:37–62.

Karanth, K. U., J. D. Nichols, N. S. Kumar, W. A. Link, and J. E. Hines. 2004. Tigers and their prey: Predicting carnivore densities from prey abundance. Proceedings of the National Academy of Sciences of the United States of America 101:4854–4858.

Karger, D. N., O. Conrad, J. Böhner, T. Kawohl, H. Kreft, R. W. Soria-Auza, N. E. Zimmermann, H. P. Linder, and M. Kessler. 2017. Data Descriptor: Climatologies at high resolution for the earth's land surface areas. Scientific Data 4:1–20.

Kauffman, J. B., and D. A. Pyke. 2001. Range ecology, global livestock influences. Pages 330–344 in S. Levin, editor. Encyclopedia of biodiversity. Academic Press, San Diego, CA.

Kennedy, C. M., J. R. Oakleaf, D. M. Theobald, S. Baruch-Mordo, and J. Kiesecker. 2019. Managing the middle: A shift in conservation priorities based on the global human modification gradient. Global Change Biology 25:811–826.

Kennedy, R. E., Z. Yang, N. Gorelick, J. Braaten, L. Cavalcante, W. B. Cohen, and S. Healey. 2018. Implementation of the LandTrendr Algorithm on Google Earth Engine. Remote Sensing 10:691.

Khakisahne, S., A. Alizadeh, M. Kaboli, Z. Noori, and T. Ghadirian. 2013. Habitat modeling for the Afghan Pika (Ochotona rufescens) in Iran from a climatic perspective. Journal of Natural Environment 2:169–180.

Kirschbaum, D., T. Stanley, R. Emberson, P. Amatya, S. Khan, and H. Tanyas. 2020. Global Landslide Hazard Assessment for Situational Awareness (LHASA) Version 2: New Activities and Future Plans.

Kong, D., Y. Zhang, X. Gu, and D. Wang. 2019. A robust method for reconstructing global MODIS EVI time series on the Google Earth Engine. ISPRS Journal of Photogrammetry and Remote Sensing 155:13–24.

Kralisch, S., & Krause, P. (2006). JAMS–a framework for natural resource model development and application.

Kralisch, S., Krause, P., Fink, M., Fischer, C., & Flügel, W. A. (2007, December). Component based environmental modelling using the JAMS framework. In MODSIM 2007 international congress on modelling and simulation (Vol. 812, p. 818). Modelling and Simulation Society of Australia and New Zealand.

Krause, P. (2001). Das hydrologische Modellsystem J2000-Beschreibung und Anwendung in großen Flußgebieten (No. PreJuSER-37462). Programmgruppe Systemforschung und Technologische Entwicklung.

Kriegler, F. J., W. A. Malila, R. F. Nalepka, and W. Richardson. 1969. Preprocessing transformations and their effects on multispectral recognition. Remote Sensing of Environment, VI:97.

Krysanova, V., & Arnold, J. G. (2008). Advances in ecohydrological modelling with SWAT - A review. In Hydrological Sciences Journal (Vol. 53, Issue 5, pp. 939–947). https://doi.org/10.1623/hysj.53.5.939

Kwon, H.-Y., E. Nkonya, T. Johnson, V. Graw, E. Kato, and E. Kihiu. 2016. Global estimates of the impacts of grassland degradation on livestock productivity from 2001 to 2011 in Economics of Land Degradation and Improvement – A Global Assessment for Sustainable Development. Page (E. Nkonya, A. Mirzabaev, and J. von Braun, Eds.). Springer, Cham.

Lewińska, K. E., P. Hostert, J. Buchner, B. Bleyhl, and V. C. Radeloff. 2020. Short-term vegetation loss versus decadal degradation of grasslands in the Caucasus based on Cumulative Endmember Fractions. Remote Sensing Of Environment 248:111969.

Liu, C., M. White, and G. Newell. 2011. Measuring and comparing the accuracy of species distribution models with presence–absence data. Ecography 34:232–243.

Liu, C., P. M. Berry, T. P. Dawson, and R. G. Pearson. 2005. Selecting thresholds of occurrence in the prediction of species distributions. Ecography 28:385–393.

Loarie, S., P. Duffy, H. Hamilton, G. Asner, and C. Field. 2009. The velocity of climate change. Nature 462:1052–1055.

MacArthur, R. A., and L. C. H. Wang. 1974. Behavioral thermoregulation in the pika Ochotona princeps: a field study using radiotelemetry. Canadian Journal of Zoology 52:353–358.

Malcolm, J. R., C. Liu, R. P. Neilson, L. Hansen, and L. Hannah. 2006. Global Warming and Extinctions of Endemic Species from Biodiversity Hotspots. Conservation Biology 20:538–548.

Malekian, A., & Chitsaz, N. (2021). Concepts, procedures, and applications of artificial neural network models in streamflow forecasting. In Advances in Streamflow Forecasting (pp. 115-147). Elsevier.

Martin, T. G., and J. E. M. Watson. 2016. Intact ecosystems provide best defence against climate change. Nature Climate Change 6:122–124.

McClanahan, T. R., J. E. Cinner, J. Maina, N. A. J. Graham, T. M. Daw, S. M. Stead, A. Wamukota, K. Brown, M. Ateweberhan, V. Venus, and N. V. C. Polunin. 2008. Conservation action in a changing climate. Conservation Letters 1:53–59.

McCune, B., and D. Keon. 2002. Equations for potential annual direct incident radiation and heat load. Journal of Vegetation Science 13:603–606.

McGuire, J. L., J. J. Lawler, B. H. McCrae, T. A. Nuñez, and D. M. Theobald. 2016. Achieving climate connectivity in a fragmented landscape. Proceedings Of The National Academy Of Sciences USA 113:7195–7200.

McNaughton, S. J. 1979. Grazing as an Optimization Process: Grass-Ungulate Relationships in the Serengeti. The American Naturalist 113:691–703.

Meenal, R., & Selvakumar, A. I. (2016). Estimation of global solar radiation using sunshine duration and temperature in Chennai. Undefined. https://doi.org/10.1109/ICETETS.2016.7603089

Meer, F. D. V. der, and X. Jia. 2012. Collinearity and orthogonality of endmembers in linear spectral unmixing. International Journal of Applied Earth Observation and Geoinformation 18:491–503.

Melesse, A. M., Abtew, W., & Senay, G. (Eds.). (2019). Extreme Hydrology and Climate Variability: Monitoring, Modelling, Adaptation and Mitigation. Elsevier.

Miller, J. 2010. Species Distribution Modeling. Geography Compass 4:490–509.

Missoni, E. 2015. Degrowth and health: local action should be linked to global policies and governance for health. Sustainability Science 10:439–450.

Mohanty, A., M. Hussain, M. Mishra, D. B. Kattel, and I. Pal. 2019. Exploring community resilience and early warning solution for flash floods, debris flow and landslides in conflict prone villages of Badakhshan, Afghanistan. International Journal of Disaster Risk Reduction 33:5–15.

Moss, R. H., J. A. Edmonds, K. A. Hibbard, M. R. Manning, S. K. Rose, D. P. van Vuuren, T. R. Carter, S. Emori, M. Kainuma, T. Kram, G. A. Meehl, J. F. B. Mitchell, N. Nakicenovic, K. Riahi, S. J. Smith, R. J. Stouffer, A. M. Thomson, J. P. Weyant, and T. J. Wilbanks. 2010. The next generation of scenarios for climate change research and assessment. Nature 463:747–756.

Myhrvold, N. P., E. Baldridge, B. Chan, D. Sivam, D. L. Freeman, and S. K. M. Ernest. 2015. An amniote life-history database to perform comparative analyses with birds, mammals, and reptiles. Ecology 96:3109–3109.

NASA. 2020. IMERG: Integrated Multi-satellitE Retrievals for GPM. https://gpm.nasa.gov/data/imerg.

Nash, J. E., & Sutcliffe, J. v. (1970). River flow forecasting through conceptual models part I — A discussion of principles. Journal of Hydrology, 10(3), 282–290. https://doi.org/10.1016/0022-1694(70)90255-6

Neitsch, S. L., Arnold, J. G., Kiniry, J. R., & Williams, J. R. (2011). COLLEGE OF AGRICULTURE AND LIFE SCIENCES Soil and Water Assessment Tool Theoretical Documentation Version 2009.

Nenzén, H. K., and M. B. Araújo. 2011. Choice of threshold alters projections of species range shifts under climate change. Ecological Modelling 222:3346–3354.

Nepal, S. (2012). Evaluating upstream downstream linkages of Hydrological Dynamics in the Himalayan Region.

Nepal, S., Khatiwada, K. R., Pradhananga, S., & Kralisch, S. (2020). Application of the J2000 Hydrological Model in the Panjshir Catchment of the Hindu Kush Himalayan Region, Training Manual. ICIMOD, Kathmandu.

Network, A. 2018. Achieving the Global Goals through agroforestry. Agroforestry Network and Vi-skogen, Sweden.

NSIA. 2018. Afghanistan Provincial Profile. National Statistics and Information Authority, Kabul, Afghanistan.

O'Donnell, M. S., and D. A. Ignizio. 2012. Bioclimatic Predictors for Supporting Ecological Applications in the Conterminous United States. US Geological Survey Data Series 691:1–10.

O'Mara, F. P. 2012. The role of grasslands in food security and climate change. Annals of Botany 110:1263–1270.

Olson, D. M., E. Dinerstein, E. D. Wikramanayake, and 2001. 2001. Terrestrial Ecoregions of the World: A New Map of Life on Earth. BioScience 51:933–938.

Pacifici, M., L. Santini, M. D. Marco, D. Baisero, L. Francucci, G. G. Marasini, P. Visconti, and C. Rondinini. 2013. Generation length for mammals. Nature Conservation 5:87–94.

Pacifici, M., P. Visconti, S. H. M. Butchart, J. E. M. Watson, F. M. Cassola, and C. Rondinini. 2017. Species' traits influenced their response to recent climate change. Nature Climate Change 7:205–208.

Pacifici, M., W. B. Foden, P. Visconti, J. E. M. Watson, S. H. M. Butchart, K. M. Kovacs, B. R. Scheffers, D. G. Hole, T. G. Martin, H. R. Akçakaya, R. T. Corlett, B. Huntley, D. Bickford, J. A. Carr, A. A. Hoffmann, G. F. Midgley, P. Pearce-Kelly, R. G. Pearson, S. E. Williams, S. G. Willis, B. Young, and C. Rondinini. 2015. Assessing species vulnerability to climate change. Nature Climate Change 5:215–224.

Parmesan, C. 2006. Ecological and evolutionary responses to recent climate change. Annual Review Of Ecology Evolution And Systematics.

Parmesan, C., and G. Yohe. 2003. A globally coherent fingerprint of climate change impacts across natural systems. Nature.

Parry, M. L., O. Canziani, J. Palutikof, P. V. der Linden, and C. Hanson, editors. 2007. Climate change 2007-impacts, adaptation and vulnerability: Working group II contribution to the fourth assessment report of the IPCC. Cambridge University Press, Cambridge, UK.

Pearson, R. G., J. C. Stanton, K. T. Shoemaker, M. E. Aiello-Lammens, P. J. Ersts, N. Horning, D. A. Fordham, C. J. RAXWORTHY, H. Y. Ryu, J. McNees, and H. R. Akçakaya. 2014. Life history and spatial traits predict extinction risk due to climate change. Nature Climate Change 4:217–221.

Pimm, S. L. 2008. Biodiversity: Climate Change or Habitat Loss — Which Will Kill More Species? Current Biology 18:R117–R119.

Pittroff, W. 2015. Rangeland management and conservation in Afghanistan. International Journal of Environmental Studies 22:1–16.

Poggio, L., L. M. de Sousa, N. H. Batjes, G. B. M. Heuvelink, B. Kempen, E. Ribeiro, and D. Rossiter. 2021. SoilGrids 2.0: producing soil information for the globe with quantified spatial uncertainty. SOIL 7:217–240.

Porter, W., and M. Kearney. 2009. Size, shape, and the thermal niche of endotherms. Proceedings Of The National Academy Of Sciences USA 106:19666–19672.

Price, T. D., D. M. Hooper, C. D. Buchanan, U. S. Johansson, D. T. Tietze, P. Alström, U. Olsson, M. Ghosh-Harihar, F. Ishtiaq, S. K. Gupta, J. Martens, B. Harr, P. Singh, and D. Mohan. 2014. Niche filling slows the diversification of Himalayan songbirds. Nature:1–19.

Purdie, E., A. Diehl, and A. Iimi. 2016. On the road to sustainable growth: measuring access for rural populations.

Rakhmatullaev, S., Huneau, F., Kazbekov, J., Le Coustumer, P., Jumanov, J., El Oifi, B., ... & Hrkal, Z. (2010). Groundwater resources use and management in the Amu Darya river basin (Central Asia). Environmental Earth Sciences, 59(6), 1183-1193.

Refsgaard, J. C., & Storm, B. (1990). Construction, calibration and validation of hydrological models. In Distributed hydrological modelling (pp. 41-54). Springer, Dordrecht.

Reynolds, J. F., D. M. S. Smith, E. F. Lambin, B. L. Turner, M. Mortimore, S. P. J. Batterbury, T. E. Downing, H. Dowlatabadi, R. J. Fernández, J. E. Herrick, E. Huber-Sannwald, H. Jiang, R. Leemans, T. Lynam, F. T. Maestre, M. Ayarza, and B. Walker. 2007. Global Desertification: Building a Science for Dryland Development. Science 316:847–851.

Riley, S. J., S. D. DeGloria, and R. Elliot. 1999. A terrain ruggedness index that quantifies topographic heterogeneity. Intermountain Journal of Sciences 5:23–27.

Romanovsky, V., M. Burgess, S. Smith, K. Yoshikawa, and J. Brown. 2002. Permafrost temperature records: Indicators of climate change. Eos, Transactions American Geophysical Union 83:589–594.

ROD. 2022. Understanding current and future hydrological risk within the Panj-Amu River Basin. A project report for Wildlife Conservation Society. Research Organization for Development, Kabul, Afghanistan.

Roy, D. P., M. A. Wulder, T. R. Loveland, C. E. Woodcock, R. G. Allen, M. C. Anderson, D. Helder, J. R. Irons, D. M. Johnson, R. Kennedy, T. A. Scambos, C. B. Schaaf, J. R. Schott, Y. Sheng, E. F. Vermote, A. S. Belward, R. Bindschadler, W. B. Cohen, F. Gao, J. D. Hipple, P. Hostert, J. Huntington, C. O. Justice, A. Kilic, V. Kovalskyy, Z. P. Lee, L. Lymburner, J. G. Masek, J. McCorkel, Y. Shuai, R. Trezza, J. Vogelmann, R. H. Wynne, and Z. Zhu. 2014. Landsat-8: Science and product vision for terrestrial global change research. Remote Sensing Of Environment 145:154–172.

Roy, D. P., V. Kovalskyy, H. K. Zhang, E. F. Vermote, L. Yan, S. S. Kumar, and A. Egorov. 2016. Characterization of Landsat-7 to Landsat-8 reflective wavelength and normalized difference vegetation index continuity. Remote Sensing of Environment 185:57–70.

Saba, D. S. 2009. Afghanistan: Environmental degradation in a fragile ecological setting. International Journal of Sustainable Development & World Ecology 8:279–289.

Santoro, M., O. Cartus, N. Carvalhais, D. M. A. Rozendaal, V. Avitabile, A. Araza, S. de Bruin, M. Herold, S. Quegan, P. Rodríguez-Veiga, H. Balzter, J. Carreiras, D. Schepaschenko, M. Korets, M. Shimada, T. Itoh, Á. M. Martínez, J. Cavlovic, R. C. Gatti, P. da C. Bispo, N. Dewnath, N. Labrière, J. Liang, J. Lindsell, E. T. A. Mitchard, A. Morel, A. M. P. Pascagaza, C. M. Ryan, F. Slik, G. V. Laurin, H. Verbeeck, A. Wijaya, and S. Willcock. 2021. The global forest above-ground biomass pool for 2010 estimated from high-resolution satellite observations.

Earth System Science Data 13:3927–3950.

Sarwar, Q. A. 2002. Water resources management in Afghanistan: the issues and options. International Water Management Institute, Pakistan.

Sattar, S., A. B. uluu, and Y. Gulnazaryan. 2013. The Kyrgyz Republic: Poverty Update 2011. World Bank, Bishkek, Kyrgyzstan.

Scherrer, D., and C. Körner. 2010. Topographically controlled thermal-habitat differentiation buffers alpine plant diversity against climate warming. Journal Of Biogeography 38:406–416.

Sediqa Hassani, 2017. A Review of Current and Possible Future Relations in Amu River Basin, Duran Publication, Kabul – Afghanistan.

Sekercioglu, Ç., S. Schneider, J. P. Fay, and S. R. Loarie. 2008. Climate change, elevational range shifts, and bird extinctions. Conservation Biology 22:140–150.

Sheffield, J., and E. F. Wood. 2008. Projected changes in drought occurrence under future global warming from multi-model, multi-scenario, IPCC AR4 simulations. Climate Dynamics 31:79–105.

Sidle, R. C., and H. Ochiai. 2006. Landslides: Processes, Prediction, and Land Use. American Geophysical Union, Washington, DC.

Sidle, R. C., and T. A. Bogaard. 2016. Dynamic earth system and ecological controls of rainfall-initiated landslides. Earth-Science Reviews 159:275–291.

Singh, L., & Saravanan, S. (2020). Impact of climate change on hydrology components using CORDEX South Asia climate model in Wunna, Bharathpuzha, and Mahanadi, India. Environmental Monitoring and Assessment, 192(11). https://doi.org/10.1007/s10661-020-08637-z

Smit, B., and J. Wandel. 2006. Adaptation, adaptive capacity and vulnerability. Global Environmental Change 16:282–292.

Smith, A. T., and M. L. Weston. 1990. Ochotona princeps. Mammalian Species:1.

Smith, J. R., A. D. Letten, P.-J. Ke, C. B. Anderson, J. N. Hendershot, M. K. Dhami, G. A. Dlott, T. N. Grainger, M. E. Howard, B. M. L. Morrison, D. Routh, P. A. S. Juan, H. A. Mooney, E. A. Mordecai, T. W. Crowther, and G. C. Daily. 2018. A global test of ecoregions. Nature Ecology & Evolution 2:1889–1896.

Smith, P., K. Calvin, J. Nkem, D. Campbell, F. Cherubini, G. Grassi, V. Korotkov, A. L. Hoang, S. Lwasa, P. McElwee, E. Nkonya, N. Saigusa, J. Soussana, M. A. Taboada, F. C. Manning, D. Nampanzira, C. Arias-Navarro, M. Vizzarri, J. House, S. Roe, A. Cowie, M. Rounsevell, and A. Arneth. 2019. Which practices co-deliver food security, climate change mitigation and adaptation, and combat land degradation and desertification? Global Change Biology 26:1532–1575.

Soberón, J. 2007. Grinnellian and Eltonian niches and geographic distributions of species. Ecology Letters 10:1115–1123.

Soberón, J., and A. T. Peterson. 2005. Interpretation of Models of Fundamental Ecological Niches and Species' Distributional Areas. Biodiversity Informatics 2.

Sonnenschein, R., T. Kuemmerle, T. Udelhoven, M. Stellmes, and P. Hostert. 2011. Differences in Landsat-based trend analyses in drylands due to the choice of vegetation estimate. Remote Sensing Of Environment 115:1408–1420.

Spawn, S. A., C. C. Sullivan, T. J. Lark, and H. K. Gibbs. 2020. Harmonized global maps of above and belowground biomass carbon density in the year 2010. Scientific Data 7:112.

Stein, A., K. Gerstner, and H. Kreft. 2014. Environmental heterogeneity as a universal driver of species richness across taxa, biomes and spatial scales. Ecology Letters 17:866–880.

Steinbauer, M. J., R. Field, J.-A. Grytnes, P. Trigas, C. Ah-Peng, F. Attorre, H. J. B. Birks, P. A. V. Borges, P. Cardoso, C.-H. Chou, M. D. Sanctis, M. M. de Sequeira, M. C. Duarte, R. B. Elias, J. M. Fernández-Palacios, R. Gabriel, R. E. Gereau, R. G. Gillespie, J. Greimler, D. E. V. Harter, T.-J. Huang, S. D. H. Irl, D. Jeanmonod, A. Jentsch, A. S. Jump, C. Kueffer, S. Nogué, R. Otto, J. Price, M. M. Romeiras, D. Strasberg, T. Stuessy, J.-C. Svenning, O. R. Vetaas, and C. Beierkuhnlein. 2016. Topography-driven isolation, speciation and a global increase of endemism with elevation. Global Ecology and Biogeography 25:1097–1107.

Suess, S., S. van der Linden, A. Okujeni, P. Griffiths, P. J. Leitão, M. Schwieder, and P. Hostert. 2018. Characterizing 32 years of shrub cover dynamics in southern Portugal using annual Landsat composites and machine learning regression modeling. Remote Sensing Of Environment 219:353–364.

Taylor, K. E., R. J. Stouffer, and G. A. Meehl. 2012. An Overview of CMIP5 and the Experiment Design. Bulletin of the American Meteorological Society 93:485–498.

Teichmann, C., D. Jacob, A. R. Remedio, T. Remke, L. Buntemeyer, P. Hoffmann, A. Kriegsmann, L. Lierhammer, K. Bülow, T. Weber, K. Sieck, D. Rechid, G. S. Langendijk, E. Coppola, F. Giorgi, J. M. Ciarlo`, F. Raffaele, G. Giuliani, G. Xuejie, T. R. Sines, J. A. Torres-Alavez, S. Das, F. D. Sante, E. Pichelli, R. Glazer, M. Ashfaq, M. Bukovsky, and E.-S. Im. 2021. Assessing mean climate change signals in the global CORDEX-CORE ensemble. Climate Dynamics 57:1269–1292.

Theobald, D. M., D. Harrison-Atlas, W. B. Monahan, and C. M. Albano. 2015. Ecologically-Relevant Maps of Landforms and Physiographic Diversity for Climate Adaptation Planning. Plos One 10:e0143619-17.

Thomas, C., A. Cameron, R. Green, and M. Bakkenes. 2004. Extinction risk from climate change. Nature.

Tuanmu, M.-N., and W. Jetz. 2015. A global, remote sensing-based characterization of terrestrial habitat heterogeneity for biodiversity and ecosystem modelling. Global Ecology and Biogeography 24:1329–1339.

UN. 2018. Accelerating SDG7 achievement. Policy Brief.

UNCTAD. 2015. The Least Developed Countries Report 2015. Transforming Rural Economies. United Nations Conference on Trade and Development, New York and Geneva.

UNDP. 2021. SDG Impact Standards Glossary. United Nations Development Programme.

UN-Habitat. 2021. SDG indicator metadata. United Nations Human Settlements Programme.

USAID, and AKF. 2015. Quality of Life Study Report. Aga Khan Foundation, Badakhshan, Afghanistan.

Valentina Krysanova & Jeffrey G. Arnold (2008) Advances in ecohydrological modelling with SWAT—a review, Hydrological Sciences Journal, 53:5, 939-947, DOI: 10.1623/hysj.53.5.939.

Wahl, D. 2016. Designing regenerative cultures. Triarchy Press, Axminster.

Wanessa, C., & de Andrade, L. (2018). UNIVERSIDADE FEDERAL RURAL DE PERNAMBUCO DEPARTAMENTO DE ENGENHARIA AGRÍCOLA Hydrological modeling and scenarios of land use and climate changes in a representative basin, northeastern Brazil.

Watson, J. E. M., N. Dudley, D. B. Segan, and M. Hockings. 2014. The performance and potential of protected areas. Nature 515:67–73.

Whittaker, E. T. 1922. On a New Method of Graduation. Proceedings of the Edinburgh Mathematical Society 41:63–75.

Wilman, H., J. Belmaker, J. Simpson, C. de la Rosa, M. M. Rivadeneira, and W. Jetz. 2014. EltonTraits 1.0: Species-level foraging attributes of the world's birds and mammals. Ecology 95:2027–2027.

Wu, S., Bates, B., Zbigniew Kundzewicz, A. W., & Palutikof, J. (2008). Climate change and water. Technical Paper of the Intergovernmental Panel on Climate Change. Geneva.

Zandler, H. 2018. Wakhan Rangeland Assessment Report 2018. Unpublished Report. WCS, GEF, and UNDP.

Zarnetske, P. L., Q. D. Read, S. Record, K. D. Gaddis, S. Pau, M. L. Hobi, S. L. Malone, J. Costanza, K. M. Dahlin, A. M. Latimer, A. M. Wilson, J. M. Grady, S. V. Ollinger, and A. O. Finley. 2019. Towards connecting biodiversity and geodiversity across scales with satellite remote sensing. Global Ecology and Biogeography 28:548–556.

Zhu, Z., and C. E. Woodcock. 2012. Object-based cloud and cloud shadow detection in Landsat imagery. Remote Sensing of Environment 118:83–94.

APPENDICES

Appendix 1. Literature Review

To understand the scope of established science and research in the P-ARB and on topics related to indicators used in this vulnerability assessment, a literature review was conducted. Because the scope of the vulnerability assessment is quite broad, the literature review was not systematic, meaning it did not exhaustively cover all literature on each topic. Rather, significant papers, reports, and other documents were gathered using a combination of Google Scholar searches and by consulting referenced literature within the papers and reports obtained and reviewed. Terms from each main vulnerability category were included in searches, such as “climate change”, “downscaling”, “natural hazards” (including searches for individual hazards), “ecosystem change”, “land cover change”, “rangeland condition”, “biomass carbon”, “species sensitivity”, “species distribution models”, “socioeconomic vulnerability”, “climate adaptation”, “vulnerability assessments”, “hydrology”, and others. When possible, papers related to the P-ARB, Afghanistan, or Central Asia were prioritized in searches, though foundational literature from other study regions was also considered and included.

Over 200 scientific papers and reports were collated through initial searches (see selected examples in Table 54). Dozens of additional papers and reports were subsequently added to the database on more general topics related to climate change, ecosystems, hydrology, wildlife species, and local communities to support the introductory and methods sections of the indicators in this report. While not all of the references that were included in the literature review are cited in this document, many are.

Table 54. Sixty selected references obtained through a literature review on various topics related to the vulnerability assessment.

Topic	Author(s)	Year	Journal	Overview and findings
Adaptation	Brooks et al.	2005	Global Environmental Change	Develop a set of indicators of vulnerability and adaptive capacity at a national level on a decadal timescale. Look at climate hazards and social variables. Relevant to Afghanistan because it is ranked the most vulnerable country
Adaptation	Cross et al.	2012	Conservation Biology	Develop a model for collaborative planning for adaptive management and discuss its use with natural resource managers
Adaptation	Cross et al.	2012	Environmental Management	Develop the ACT tool and framework for addressing climate change in natural resource management
Adaptation	Ford et al.	2015	Regional Environmental Change	Document the current status of adaptation in 47 countries of Asia and Africa based on literature review. Large gaps of knowledge of policy and practice in North Africa and Central Asia
Adaptation	Groves et al.	2012	Biodiversity and Conservation	Propose five approaches to climate change adaptation that can be integrated into existing or new biodiversity conservation plans and discuss assumptions and trade-offs
Adaptation	Jawid & Khadjavi	2019	Economic Analysis and Policy	Collect data from farmers in Central Afghanistan to see how external support influence farmers' adaptation to climate change. Support influences behavior towards practices promoting adaptation (e.g., types of seeds planted, access to irrigation water). Also look at hazard risks and economic, financial, and institutional constraints
Adaptation	Lawler	2009	Annals of the NY Academy of Sciences	Reviews adaptation strategies for managing natural systems and offers recommendations
Adaptation	Oliver et al.	2012	Journal of Applied Ecology	Develop a decision framework for considering climate change adaptation in biodiversity conservation planning (primarily expert opinion based, with some quantitative models). Present 8 case studies and conclude that key interventions are local management and expansion of sites
Adaptation	Schloss et al.	2011	Plos One	Use two conservation planning approaches that compare strategies to protect current biodiversity versus a suite of abiotic factors thought to underlie future biodiversity and show that they yield different results
Adaptation	Sud et al.	2015	Regional Environmental Change	Review literature for three glacier-fed river systems of South Asia to understand governance mechanisms for climate adaptation, examining policy objectives, institutions, and practice. Afghanistan is highlighted as needing to improve legal, policy, and implementing frameworks by developing new legislation related to natural resource management. Several challenges and barriers to implementing adaptation measures are outlined in Table 6
Adaptation	Watson et al.	2011	Chapter in Climate Change: Research and Technology for Adaptation and Mitigation	Review concepts for biodiversity conservation under climate change with discussions of 1) continuing best practice; 2) extending best practice principles; and 3) integrating assessments on species vulnerability to climate change into a conservation planning framework

Topic	Author(s)	Year	Journal	Overview and findings
Adaptation	Xu & Grumbine	2014	Climatic Change	Review regional (Asian highland) literature to evaluate role of evolving hybrid forms of adaptive knowledge for coping with environmental and social change, focusing on the role of local knowledge. Local knowledge is necessary, but not sufficient: enfranchising people with decision-making and resource rights is also required. Minimal discussion of Afghanistan due to lack of literature in review
Climate Change	Aich et al.	2017	Climate	Analyze past and projected climate change in Afghanistan from downscaled climate models in terms of temperature, precipitation, and five indices: heavy precipitation, spring precipitation, growing season length, the heat wave magnitude index, and the standardized precipitation and evapotranspiration index. Discuss several climate risks posed by increased temperatures and decreased precipitation forecasts, with biggest consequences on water management and agriculture
Climate Change	de Sherbinin	2014	Climatic Change	Reviews maps of climate change hotspots (yet no actual maps in paper!), focusing more on strengths and weaknesses to actual mapping approaches while also discussing regions that will have high exposure and sensitivity and low adaptive capacity. Afghanistan is mentioned as a hotspot of the climate-demography vulnerability index (which shows areas that support high population densities, have high growth rates, and decline in climatic conditions) and the human vulnerability index (which combines indices of natural vulnerability, social vulnerability, financial vulnerability, and physical vulnerability), and is mentioned as being a resource-poor area with severe to moderate poverty that is more vulnerable to climate change
Communities	Krishnamurthy et al.	2014	Global Environmental Change	Develop a Hunger and Climate Vulnerability Index and apply it globally, using data from IMF, EM-DAT, World Bank, FAOSTAT, WRI, CIESIN, UNFPA, and UNDP. Provide descriptions and rationales for indicators in Appendix A and B. Afghanistan is ranked 2nd most vulnerable country behind Bangladesh
Communities	Mohibbi & Cochard	2014	Environmental Development	Conduct household surveys in 15 villages in Band-e-Amir, collecting data on occupation, population, livestock, grazing, fuelwood collection, agriculture, and resource use
Ecosystems	de Beurs & Henebry	2008	Journal of Land Use Science	Use remote sensing to quantify how war and drought have affected land surface phenology (NDVI) of Afghanistan
Ecosystems	Emadi	2011	International Journal of Environmental Studies	Discusses how poverty has inhibited adequate natural resources management in Afghanistan. Some useful background and discusses existing challenges
Ecosystems	Gardelle et al.	2013	The Cryosphere	Use remote sensing of DEMs to quantify changes in mass balance of Pamir-Karakorum-Himalaya glaciers from 2000-2010 and show reductions in glacier mass, but which are 2-3 times less negative than the global average
Ecosystems	Haritashya et al.	2009	Climatic Change	Use remote sensing of ASTER and Landsat MSS data and field data from 30 glaciers to evaluate glacier fluctuations in the Wakhan Pamir from 1976-2003 and show average glacial retreat rate of 36 m per year and disconnection of tributary glaciers from main trunks. They also observed formation of high-altitude lakes and increased frequency and size of proglacial lakes, all of which points to increased hazard potential

Topic	Author(s)	Year	Journal	Overview and findings
Ecosystems	Jacobs & Schloeder	2012	Journal of Arid Land Studies	Provide an overview of factors contributing to land degradation in Afghanistan and discuss the PEACE project aimed at helping to improve livestock production and rangeland management
Ecosystems	Khromova et al.	2006	Remote Sensing of Environment	Use historical surveys and remote sensing to map and assess glacier recession in the eastern Pamir over the past three decades and quantify changes in area of 5 glaciers and terminus positions of 44 glaciers. Show that glacier area has decreased 7.8% during 1978-1990 and 11.6% in 1990-2001, mainly as a response to increasing summer temperatures. Also find increase in debris-covered areas and new lakes
Ecosystems	Mohibbi et al.	2018	Japanese Journal of Farm Work Research	Evaluate the spatiotemporal changes in land cover in Bamyan from 1990-2015 through field questionnaire with 97 local people and farmers. Main changes reported were population increases, overuse of resources, overgrazing, shrub collection, drought, and mismanagement. Also use remote sensing of Landsat images to produce land cover maps for 1990, 1999, 2008, and 2015 and show rangeland decreased from 60.2% to 37.9% with rapid increases in bare soil and built-up classes
Ecosystems	Najmuddin et al.	2017	Physics and Chemistry of the Earth	Use a dynamic land system (DLS) model to simulate land use/land cover for the years of 2020 and 2030 for the Kabul River Basin. The DLS incorporates various socio-economic and bio-physical datasets and produces three scenarios: baseline, economic development, and environmental protection. Under all three scenarios, cultivated land, grassland, and built-up areas increase, while forest, water, and unused land decrease under the first two scenarios
Ecosystems	Pervez et al.	2014	Remote Sensing of Environment	Use 16-day composites of MODIS NDVI to create 23-point time series for each year from 2000-2013 and a thresholding algorithm to map irrigated areas in Afghanistan. Evaluated the maps with irrigated areas classified from multiple snapshots of landscape during growing season from Landsat 5 optical and thermal sensor images. Agriculture was highly dependent on surface water, especially snowmelt, and varied by as much as 30% between water surplus and water deficit years
Ecosystems	Ponce-Reyes et al.	2017	Biological Conservation	Perform a vulnerability assessment for 7 ecosystems across Africa's Albertine Rift. Use Maxent to estimate each ecosystem's extent using current climate data and potential distribution for 2050 and 2070. Only the Combretum-grasslands savannah ecosystem is expected to expand; all others face large contractions. Approach can be adapted for any other system
Ecosystems	Sarikaya et al.	2012	Remote Sensing Letters	Use Landsat and ASTER imagery to quantify terminus locations for 52 glaciers in the Hindu Kush Range of Afghanistan in 1976, 1992, 2001, and 2007. Show that 76% of the sampled glaciers retreated, 16% advanced, and 8% were relatively unchanged. Because glaciers in the Karakorum were previously shown to be expanding, the authors suggest there is a spatial gradient in glacier fluctuations in the Western Himalaya governed by precipitation
Ecosystems	Weißuhn et al.	2018	Environmental Management	Provide background on the concept of vulnerability and summarize existing ecosystem vulnerability research through a systematic literature review. Propose a framework for ecosystem assessments that connect concepts of vulnerability, resilience, and adaptability
Ecosystems	Xu et al.	2008	Conservation Biology	Review of regional (Himalayan) literature on the effects of climate change on water, biodiversity, and livelihoods. Provides good background in these key areas, especially related to hydrology and ecosystems, but not specifically targeted at Afghanistan

Topic	Author(s)	Year	Journal	Overview and findings
Rangelands	Bedunah et al.	2010	Rangelands	Describe rangelands of Band-e-Amir NP and Ajar Provisional Wildlife Reserve, with some data on climate, NPP, NDVI. Provide a description for each rangeland type and other habitat types in region. Also discuss conservation issues pertaining to shrub collection, livestock grazing, plowing of rangelands, and cultivation, and make management recommendations
Rangelands	Eddy et al.	2017	Ecological Indicators	Use MODIS imagery from 2000-2015 in Kyrgyzstan to characterize browning trends in rangeland vegetation and to distinguish between climate- and grazing-induced trends, but also compare with local ecological knowledge perceptions of rangeland degradation from participatory mapping (in absence of reliable historical livestock stocking rates). Found widespread browning across 24% of landscape and that perceptions better matched changes in NDVI rather than NDVI controlled for climate. Offer advice for linking local ecological knowledge with remote sensing
Rangelands	Hassanyar	1977	Environmental Conservation	Gives overview of major vegetation types in Afghanistan and discusses restoration and regeneration approaches, particularly of rangelands
Rangelands	Jacobs et al.	2015	Journal of Arid Land	Perform a rudimentary visual assessment of Google Earth Imagery to generate map of rangelands and combine with climate data to map dryland agriculture for nearly all of Afghanistan (though not Wakhan). Use these maps to discuss rangeland restoration priorities and create a spatial prioritization. Find the highest-ranking priorities throughout much of the north of the country (including areas in Badakhshan)
Rangelands	McArthur et al.	1979	Journal of Arid Environments	Collect data on livestock and pasture productivity, husbandry systems, and the size, major problems, and attitudes to change of livestock-owning groups in Heart, western Afghanistan. Found areas supported 370k sheep and 310k goats in winter, with an average stocking rate of 1.63 ha per ewe. Provide lots of statistics and some recommendations for integrated livestock and rural development
Rangelands	Mirzabaev et al.	2016	Journal of Arid Land	Review challenges and opportunities for rangelands in Central Asia. Discuss present status; extent, causes, and consequences of rangeland degradation; and technologies and methods controlling rangeland degradation
Rangelands	Petz et al.	2014	Global Environmental Change	Quantify and map grazing intensity and its effect on forage utilization by livestock, carbon sequestration, erosion prevention, and biodiversity using global datasets. Show that erosion prevention is 10% lower, carbon emissions >4 times higher, and biodiversity is lower overall in areas with higher grazing intensity. Provide good schematics for all processes (like theory of change) in Fig. 1. Mention Afghanistan as having high grazing intensity
Rangelands	Pitroff	2011	International Journal of Environmental Studies	Discusses general rangeland management in Afghanistan. Provides individual problem trees for water, crop production, livestock production, and rangeland management. Outlines a program approach for rangeland conservation in Afghanistan and policy needs, knowledge gaps, and intervention priorities
Rangelands	Robinett et al.	2008	Rangelands	Provide a history of tribal rule, grazing, war, and rebuilding in Central Afghanistan rangelands
Rangelands	Saba	2001	International Journal of Sustainable Development and World Ecology	Provides a broad overview of environmental degradation issues in Afghanistan, focusing on ecosystems, agriculture and forestry, pollution, wildlife, conservation/protection, and land management

Topic	Author(s)	Year	Journal	Overview and findings
Rangelands	Sharma et al.	2007	Mountain Research and Development	Describe ICIMOD's regional rangeland program (RRP) for HKH. Fig. 1 gives stages of the participatory action research strategy adopted by the RRP. Key concerns addressed by the RRP include sustainable pastoralism, ecosystem restoration, renewable energy, and co-management approach. Also focus on capacity building, knowledge generation, and policy advocacy
Hydrology	Basu & Shaw	2013	International Journal of Environmental Studies	Provide overview of water resources in South Asia (including Afghanistan) with particular reference to climate change and adaptation. Analyze water policies and formulate conceptual water policy framework that makes adaptation central. Provide data, statistics, and context for each country. Fig. 2 provides schematic of conceptual water policy issues; Table 1 outlines existing water policies/laws/plans by country, identifies gaps and challenges; Fig. 3 provides schematic for making adaptation central in National Water Policy
Hydrology	Granit et al.	2012	International Journal of Water Resources Development	Explore the water, energy, and food nexus in Central Asia. Discuss how unilateral action has been the norm, but outlines several opportunities for collaborative resource management. An integrated approach could include exploring existing regional frameworks with a focus on additional investment in hydropower generation, regional power market development, irrigation reforms, and addressing regional environmental public goods such as water flows and quality
Hydrology	Ibrahimzada & Sharma	2012	International Journal of Environmental Sciences	Conduct vulnerability assessment of water resources for Amu Darya River basin, which considers the availability of water resources, enhancement and usage of water resources, ecological health of water resources base on supply and demand relationship, and management of water resources
Hydrology	Krysanova et al.	2010	Water Resources Management	Compare climate change adaptation strategies for large river basins in Europe, Africa, and Asia (specifically Amu-Darya), based on opinions of policy makers and water management experts. Consider expected climate change, impacts, drivers for development of adaptation strategies, barriers for adaptation, state of water management measures, and status of adaptation strategy implementation. Decreasing water availability and increasing frequency and intensity of droughts is expected in all river basins. Good description of Amu-Darya, issues, plans, etc., see especially Figs. 3 and 4
Hydrology	Ososkova et al.	2000	Environmental Monitoring and Assessment	Provide a history of water regimes in the Aral Sea basin of Central Asia. Also estimate regional water resources and calculate changes of some components of the hydrological cycle due to climate change (broadly speaking - no quantitative analyses). Discuss adaptation measures in the southern part of the region
Hydrology	Rakhmatullaev et al.	2010	Environmental Earth Science	Analyze groundwater resources use and management in the Amu Darya River basin. Discuss present extent, reserves, quality, institutional management, and transboundary aspects of groundwater resources. Particular attention is paid to Afghanistan and to irrigated agriculture

Topic	Author(s)	Year	Journal	Overview and findings
Hydrology	Vick	2014	International Journal of Water Resources Development	Outlines steps towards an Afghanistan-Pakistan water-sharing agreement, with particular reference to the Kabul basin. Steps include creating common sets of data and information, identifying interests (not projects or treaty provisions), limiting talks to water, conducting talks within a legal framework, supporting capacity building and consolidating donor and organizational support, and creating institutional agreements for continuous communication
Species	Aryal et al.	2016	Ecology and Evolution	Use Maxent to model current and future distributions of snow leopards and blue sheep in the Nepal Himalaya. Predicted future habitat will decline for both species and is more pronounced for snow leopards when blue sheep are factored into models. Provide some recommendations for extensions of protected areas
Species	Busuttil et al.	2010	Sandgrouse	Describe two nests of Afghan Snowfinch in Afghan Pika burrows
Species	Escobar et al.	2015	Biological Conservation	Integrate ecological niche models with nighttime satellite imagery to identify areas suitable for Asiatic black bear after anthropogenic alteration. Found 10% of potential distribution not suitable owing to (sub)urban encroachment. Models overestimate suitable areas when only based on climate. Suggest approach is transferrable to other species
Species	Forrest et al.	2012	Biological Conservation	Map current snow leopard habitat in the Himalayas using a mechanistic approach that incorporates field data and combined it with a climate impact model using a correlative approach. The climate impact model considered how climate would influence treeline. Shifting treeline could reduce snow leopard habitat by 30%, but many areas will remain suitable and should be protected. Expect that threats from livestock grazing, retaliatory killing, and medicinal plant collecting will intensify
Species	Kanderian et al.	2011	International Journal of Environmental Studies	Give a detailed overview of current status of wildlife in Afghanistan, including descriptions of habitats, major threats, and conservation activities. Specific reference to Marco Polo Sheep, Markhor, Urial, Snow Leopard, Asiatic Black Bear, Saker Falcon, Large-billed Reed Warbler, Greater Flamingo, and Paghman Salamander. Includes 101 references
Species	Lewis & Songster	2016	BJHS: Themes	Provide a long descriptive article on snow leopard conservation across the China-India border. Not focused specifically on Afghanistan
Species	Li et al.	2016	Biological Conservation	Assess impacts of climate change on global snow leopard habitat from the last glacial maximum to present, using occurrence records from 1983-2015 through the species' range and Maxent models with LGM, mid-Holocene, and 2070 time periods. Identify areas that have acted as refugia from LGM and will likely continue to do so to 2070, including in Pamirs, which should be most valuable to protect
Species	Liu et al.	2009	Diversity and Distributions	Create a map of Asiatic Black Bear distribution in southwest China by interviewing villagers and verifying reports of bear presence in 494 15 x 15 km grid cells. Use regression to show that occurrence related to forest cover, negatively related to roads and agriculture

Topic	Author(s)	Year	Journal	Overview and findings
Species	Simms et al.	2011	International Journal of Environmental Studies	Provide overview of snow leopards in Afghanistan, with particular reference to Wakhan. Present camera trap data and discuss threats including fur trade, retaliatory killings, and the capture of animals as pets. Discuss WCS' integrated management approach, including local governance, protection efforts, education, construction of predator-proof livestock corrals, livestock insurance program, tourism, and research activities
Species	Timmins et al.	2009	BirdingASIA	Describe the discovery of Large-billed Reed Warbler in Wakhan
Vulnerability Assessments	Foden et al.	2018	WIREs Climate Change	Overview climate change vulnerability assessments for species, including describing key concepts, terms, steps, and considerations. Outline four CCVA approaches: trait-based, correlative, mechanistic, and combined approaches and discuss their use. Discuss finding, selecting, and applying input data. Also discuss how to best handle rare, small-range, and declining-range species
Vulnerability Assessments	Lee et al.	2018	Conservation Letters	Develop a new spatially explicit framework for assessing relative ecosystem vulnerability to climate change and apply it to Mozambican forest mangroves (though discuss a broader framework that can be applied elsewhere)
Vulnerability Assessments	Lioubimtseva & Henebry	2009	Journal of Arid Environments	Review climate and environmental change in arid Central Asia, with particular respect to vulnerability (food security, water stress, and human health), adaptation, and mitigation, and provide exposure, sensitivity, and adaptive capacity indicators for assessment

Appendix 2. Field work

Some indicators required field-based surveys to collect primary information. An overview of surveys conducted during the project period is presented in Table 55. The methodologies of these surveys are included below.

Table 55. Dates and locations of fieldwork conducted for wildlife and rangeland surveys during the project period.

Species/group	Location	Year	Start Date	End Date
Afghan Pika	Bamyan	2021	15 Jun	5 Aug
Afghan Pika	Bamyan	2020	05 Jul	15 Aug
Bird community	Bamyan	2021	27 Jun	11 Jul
Bird community	Bamyan	2020	10 Jul	22 Jul
Rangeland survey (biomass, transect survey, land cover/land use)	Bamyan	2021	15 Jun	8 Jul
Rangeland survey (biomass, transect survey, land cover/land use)	Bamyan	2020	23 Jun	23 Jul
Rangeland survey (biomass, transect survey, land cover/land use)	Bamyan	201 9	23 Jun	16 Jul
Camera trapping (large mammals)	Wakhan	2021	27 May-24 Jun	20-31 Oct
Camera trapping (large mammals)	Wakhan	2020	16 Jun-1 Jul	24 Sep-24 Oct
Camera trapping (large mammals)	Wakhan	2019	19 Jun-23 Jul	21 Oct-03 Nov
Marco Polo Sheep	Wakhan	2020	25 Sep	29 Sep
Marco Polo Sheep	Wakhan	2019	3 Oct	7 Oct
Marco Polo Sheep	Wakhan	2018	6 Oct	9 Oct
Long-tailed Marmot	Wakhan	2020	11 Jul	3 Aug
Rangeland survey (biomass, land cover/land use)	Wakhan	2020	11 Jul	3 Aug
Bird community	Wakhan	2020	10 Jul	22 Jul

Rangeland surveys

To support the ecosystem and biodiversity components of the vulnerability assessment, rangeland surveys were conducted in the Big Pamir and Little Pamir regions of the P-ARB. The objectives of the surveys were to:

1. Identify key indicators of rangeland condition
2. Assess the current vegetation extent and status of rangeland condition
3. Assess rangeland carbon storage through collecting vegetation biomass and soil samples
4. Collect geospatial data to support land cover mapping

Identification of indicators of rangeland condition

Rangeland condition indicators relate to structural and compositional features of plant communities and signify the quality of vegetation as habitat for biodiversity and forage for both wildlife and livestock. In this context, vegetation cover and productivity are among the most important variables and were considered the focal indicators for the rangeland assessment. Many ecosystem services are correlated with vegetation cover such as preventing soil erosion and retaining hydrological productivity (Zandler 2018). In addition, soil organic matter is an important factor for soil fertility, stability, water cycling, and sequestration of carbon. Specifically, this survey was focused on the following indicators:

- Soil organic matter
- Vegetation biomass
- Vegetation productivity

Soil organic matter

Soil samples were taken from Big Pamir and Little Pamir. The samples were taken from different types of vegetation communities and from the same biomass plots that were used to sample vegetation for biomass carbon measurements (see below). The samples were taken between 5-15 cm belowground. Each sample contained 200 g of soil.

To measure the soil organic matter, the most straightforward method is to calculate the organic carbon values derived from soil samples using a combustion method (Zandler 2018). However, this method requires a laboratory and laboratory analyses. Because access to such facilities was not possible, the approach of Zandler (2018) was followed. This approach uses Munsell Soil Color Charts and values derived from Boden (2005), which uses soil color variation as an indicator of soil organic matter.

Vegetation biomass

To assess vegetation biomass, the aboveground green biomass of plants (i.e., the fresh, green parts of plants) was clipped from 106 plots of 4x4 m (Figure 180; Figure 181). Of the 106 plots where biomass samples were collected, 84 plots were located in Little Pamir and 22 were located in Big Pamir. To determine the locations of these plots, GPS points were randomly chosen by an expert based on their NDVI values, and locations were identified in the field using a Garmin GPS 60 handheld unit. Immediately after cutting the green biomass from each plot, the sample was weighed. The samples were then air-dried and weighed again at different times until their weights were constant, at which point their weight was subtracted from their initial weight (which contained water content). The dry weight represents the amount of biomass in vegetation, which is a proxy for carbon storage.

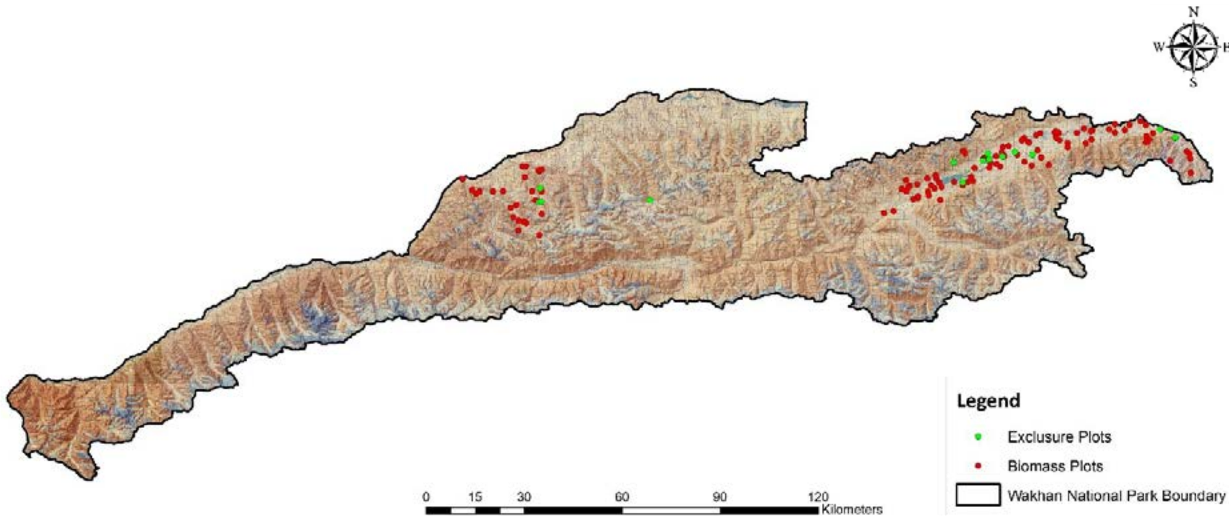

Figure 180. Locations of biomass and exclosure plots in Little Pamir (eastern cluster of points) and Big Pamir (western cluster).

APPENDICES

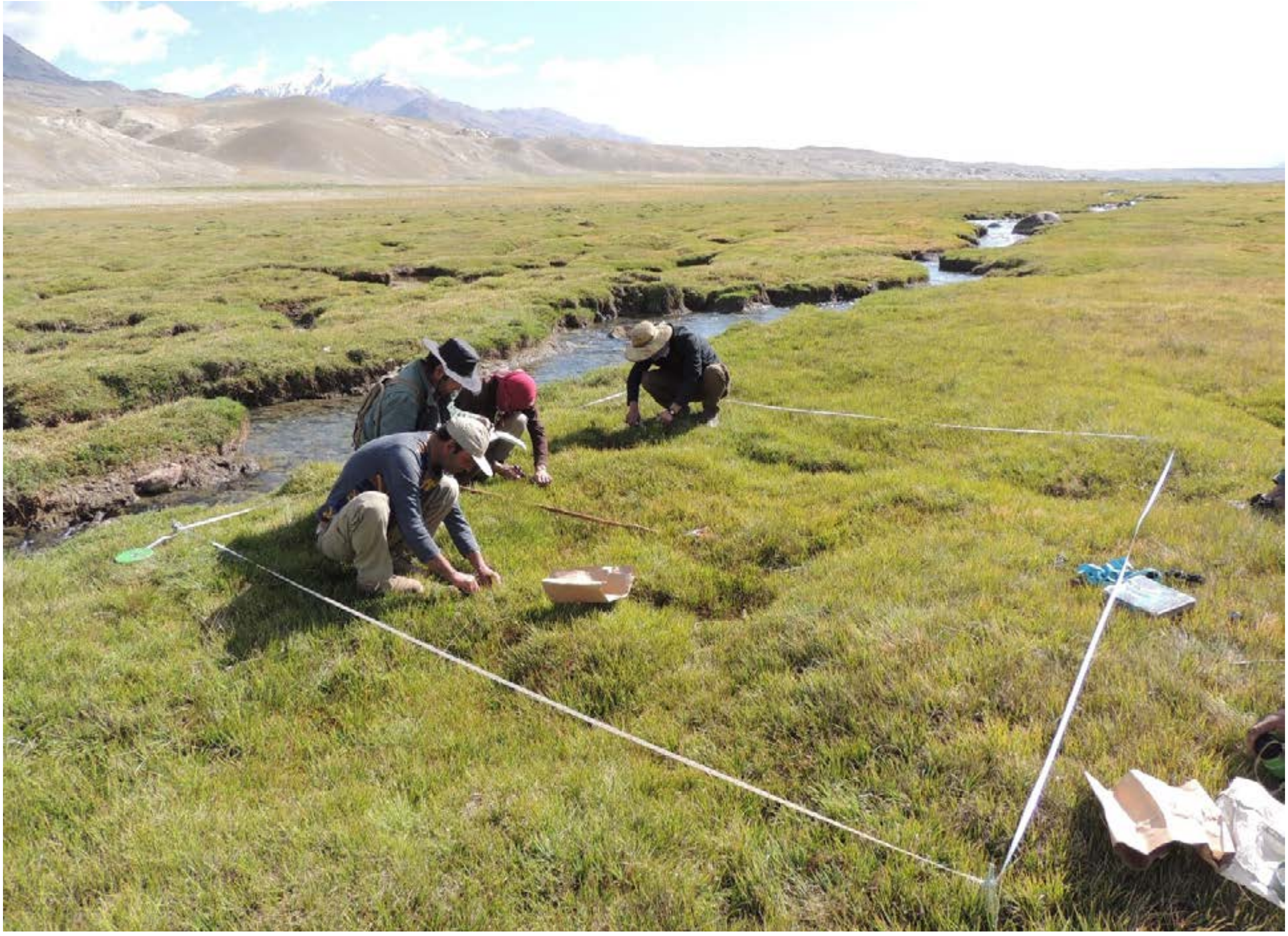

Figure 181. Clipping of standing biomass from within a 4x4 m plot in a riparian meadow grass community in the Achaqtash area of Little Pamir (photo © N. Jahed).

Vegetation productivity

Vegetation productivity is defined as aboveground net primary plant production. To measure productivity, exclosure plots were established and the annual green parts of vegetation were subsequently clipped. Vegetation biomass was also harvested from outside of the exclosure plots to generate matching (disturbed) values. The survey team established eight new exclosure plots in Little Pamir (Table 56). In Little Pamir, biomass of two existing exclosure plots (one 1x1 m, and one 4x4 m) was also harvested. In Big Pamir, biomass of four existing exclosure plots in the Abakhan Valley was harvested. Three previously established exclosure plots in Aliso were damaged by unknown causes, perhaps due to brown bears as their signs were present. All harvested vegetation was weighed immediately after cutting and was then air-dried and reweighed to measure the amount of biomass as above.

Table 56. Name, location, UTM coordinates, and the vegetation community of newly established exclosure plots in Little Pamir.

No.	Location	Easting	Northing	Elevation	Vegetation Community
1	Beginning of Tiger Mansu	442185	4128635	3985	Dwarf Shrub
2	Qaraqorom	429425	4119545	4123	Dwarf Shrub
3	Qaraqorom	446462	4127832	4147	Dwarf Shrub
4	Endemin	434407	4126144	4030	Dwarf Shrub
5	Endemin	435576	4128151	4073	Riparian Meadow
6	Endemin	435967	4126474	4037	Riparian Meadow
7	Close to Munara School	439148	4127351	4025	Riparian Meadow
8	Qaraqorom	427315	4125732	4115	Dwarf Shrub

Wildlife surveys

Large mammal surveys

Large mammals perform vital ecosystem functions yet are threatened by both human activities and climate change. Ungulates help maintain vegetation structure and composition and positively contribute to nutrient cycling (McNaughton 1979; Bagchi and Ritchie 2010). They also are an important prey base for large carnivores (Karanth et al. 2004). Efforts by WCS to document and monitor large mammals began in the early 2000s and have focused on about a dozen species, including Siberian Ibex (*Capra sibirica*), Urial (*Ovis vignei*), Marco Polo Sheep (*Ovis ammon polii*), Brown Bear (*Ursus arctos*), Turkestan Lynx (*Lynx lynx isabellinus*), and several small to medium size wild cat species.

Survey sites and methodology

WCS-Afghanistan conducted surveys for large mammals in Wakhan primarily using the double observer method, though some large mammal species were also recorded by camera traps targeted for snow leopards (see next section). The double-observer method is a variant of the line transect whereby two survey teams of two people each walk to a series of pre-determined vantage points that are selected based on their visibility. Observers spend an average of 10 minutes scanning for ungulates with binoculars and a spotting scope at each vantage point. Approximately 45 minutes to one hour after the first team has surveyed a particular vantage point, the second team follows a parallel route with vantage points slightly displaced, such that the range of observations of the first and second teams just overlap. Observers can also record sightings between vantage points. During the surveys, teams kept in constant communication by walkie talkie to report their observations to minimize double counting. Observers recorded the GPS location and bearing of all observations, along with the aspect, location, number of individuals, age and sex composition, behavior, prominent morphological features, escape behavior (if the second team noticed anything), and a second GPS point and bearing from the next vantage point.

Snow leopard surveys

The snow leopard (Panthera uncia) is found in mountain ranges across South and Central Asia. It is listed as Vulnerable by the IUCN. In Afghanistan, snow leopards occur in the northeastern part of the country, particularly in the Wakhan district of Badakhshan province which contains the Wakhan National Park.

Across its range, the species is threatened by poaching, illegal trade of its pelts, and hunting of its natural prey. Their prey includes Siberian ibex (*Capra sibirica*), urial (*Ovis vignei*), and Marco Polo sheep (*Ovis ammon polii*). Snow leopards are also threatened by retaliation killings due to livestock predation. WCS supports snow leopard conservation in Afghanistan through activities including research using camera trapping and satellite collars, as well as community awareness initiatives.

Survey sites and methodology

WCS-Afghanistan initiated a baseline camera trap survey from 2011 to 2013 in the Hindu Kush Mountain range between Wergund Payan and Qila-e Wust. During this period, 5000 pictures were collected and analyzed, resulting in an estimate of 36-40 snow leopards in the study area. Camera trapping was subsequently conducted in Big Pamir from May 2016 to May 2017, and again in the Hindu Kush range from October 2017 to May 2018. Most recently, WCS conducted camera trapping in the Hindu Kush mountains during from 19th June to 3rd November 2019, from 16th June to 24th October in 2020, and from 27th May to 31st October in 2021 (Figure 182).

Camera trapping is a passive survey method that automatically takes pictures of species that move in front of stationary cameras, making them ideal for cryptic, nocturnal, and difficult-to-observe wildlife such as snow leopards. Cameras were set out in a grid and in some instances were placed along trails and paths thought to be used for species movement and dispersal to maximize detection, though the placement of cameras also considered human activities and potential for theft or vandalism to avoid conflicts. Approximately 40 cameras were deployed in Wakhan at any given time. Camera traps ran continuously, and data were downloaded from cameras approximately twice per year to avoid data loss or damaged equipment.

Between 15th and 19th May 2019, the WCS representative Ali Madad Rajabi (AMR) met with agriculture managers, the head of district and CDCs, and local community members to discuss the camera trapping effort. AMR showed examples of camera trap photos and explained the mechanism and emphasized the fact that this project is solely for the purpose of documenting the presence and distribution of snow leopards, which are elusive and shy animals that cannot be surveyed during the day like their prey species. The camera trap locations were predefined based on earlier surveys. In each area before deployment of the camera, the team met with the head of CDC and informed them about the installation, and the head of CDC passed the information to the community, instructing them not to interfere with the units while collecting shrubs and grazing livestock. This was intended to forestall incidents of vandalism and other loss that have previously occurred on surveys.

The team for the installation and deployment consisted of Ayan Big, Aziz Big, and one local ranger. Before deployment, the team checked that all the camera traps were functioning as designed, practiced setting the date and time, and prepared all the SD cards and batteries for the camera trapping efforts.

Between 19th June and 21st July 2019, the team started camera trap installation from Wergund Payan and continued to the upper corridor in Qila-e Wust area on the southern slopes of the Hindu Kush mountains. During these 35 days, the team installed a total of 42 cameras in the mountains and valleys. To mitigate vandalism, the team collected all the SD cards and inserted new cards in the cameras from 4th to 21st September 2019. Finally, between 21st October and 3rd November 2019, all cameras were retrieved by the team of Karmal, Ayan Big, Aziz Big, and Shanbe (NRM assistant). All the data were transferred to permanent digital storage.

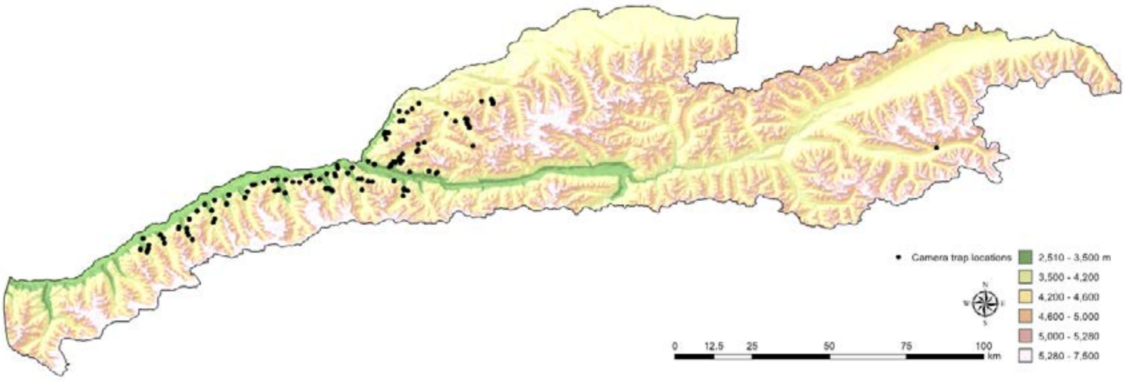

Figure 182. Geographic location of camera trapping efforts carried out by WCS between 2016 and 2020 in Wakhan National Park, Badakhshan province, Afghanistan.

Afghan Pika surveys

The Afghan Pika (*Ochotona rufescens*) is a small mammal belong to the family Ochotonidae, part of the order Lagomorpha along with hares and rabbits. It occurs in mountainous regions of Afghanistan, Pakistan, Iran, southwest Turkmenistan, Armenia, the trans-Caspian region of Russia, and southwest Turkey (Habibi 2004, Khakisahne et al. 2013). In Afghanistan the Afghan Pika's range extends from the Salang Pass to the Uruzgan and Sabzak pass in the north-west, encompassing the Paghman range, Kohe Baba, Firoz Koh, and Spinghar.

Climate change is expected to alter the range sizes and locations of species, which has critical implications for conservation. These changes generally take the form of movements towards higher latitudes and/or higher elevations. Pikas are cold-adapted species with high body temperatures (MacArthur and Wang 1974). They are very sensitive to ambient temperature and are not physiologically able to survive at temperatures above a certain threshold (Smith and Weston 1990). This sensitivity means that their distribution is directly associated with climate (Caravaggi 2018), thereby making them an excellent indicator species for climate change (Beever et al. 2003).

Survey sites and methodology

WCS-Afghanistan conducted surveys for pikas between 5th July to 15th August 2020 and between 15th June to 5th August 2021 in the Saighan and Yakawlang districts of Bamyan Province. Surveys were repeated at locations surveyed by Nasratullah Jahid and Mirza Hussain; pikas were present at all those locations. Additionally, surveys were carried out at new locations which seemed suitable for pikas.

At each survey point, the team created a 12-meter circular plot. Each point was surveyed over two days. On the first day, the team recorded data related to the number of pikas seen and heard (adults and juveniles), and whether there were any indirect signs of pikas (burrows, hay piles, and fecal pellets). Surveyors closed all active and inactive burrows with litter and light animal feces. Activity status of a burrow was judged by the presence of hay piles (fresh and old), fecal pellets (fresh and old), signs of recent burrowing, pika urine and/ or and pika pawprints, as well as the actual presence of a pika in or on the burrow. On the second day, the team evaluated whether closed burrows were reopened, and recorded the number and behavior of pikas.

As the GPS error of ~3 meters is a quarter of the plot radius, to fix the center for resurveying in future years, the team placed three to four colored rocks at the center of the plot. This will help reduce the rate of error in subsequent years.

Long-tailed Marmot surveys

WCS-Afghanistan monitored the status of Long-tailed Marmots (*Marmota caudate*) in Big and Little Pamir from 11th July to 3rd August 2020 as particularly suitable indicators of climate change. Because they live at high elevation, marmots are thought to be very sensitive to temperature changes, and therefore are expected to become increasingly impacted by climate change through global warming and extreme weather events (Armitage 2013).

Survey sites and methodology

WCS-Afghanistan conducted surveys for marmots in Little Pamir and Big Pamir in northeastern Afghanistan, the main portion of the Long-tailed Marmot's distribution in Afghanistan. Thirty-nine line transects were established in Little Pamir and 22 line transects in Big Pamir. Line transects were determined by experts through an analysis of suitable habitat conditions based on elevation and land cover derived from satellite imagery. Within locations that were deemed suitable based on this analysis, the survey sites contained different topography and different slopes with different vegetation communities. At a given survey site located in flat, plains areas, the direction of each line transect was determined randomly by throwing a pen. By contrast, in steppe areas and in valleys, line transect directions were oriented to align with the valley (i.e., straight up or down the valley). The length of the line transects varied according to the topography and was set between 200 to 500 meters. The survey was conducted between 7 am to 6 pm, when marmots are most active. Two observers were required for conducting the survey, with different responsibilities for the first and second observer.

The first observer had the responsibility to record direct observations of marmots with their distance to the transect line. The first observer established the transect line and recorded the number of marmots seen along with details of their sexes and ages. The first observer also recorded the distance and angle of marmots seen using a rangefinder and a compass. Temperature, clouds, and wind were also recorded during the survey. The second observer had the responsibility to record indirect signs of marmots within a 10-meter range on either side of the line transect. Burrows in each cluster within the range were also counted by the second observer.

Marmot monitoring was conducted from 11th July to 3rd August 2020 in Little Pamir and between 10th to 22nd August 2020 in Big Pamir. The locations of the line transects are given in Figure 183. The survey team established 61 line transects in both study regions combined. The overall length of all transects established was 3500 meters. All transects were between 3500 and 5000 meters in elevation.

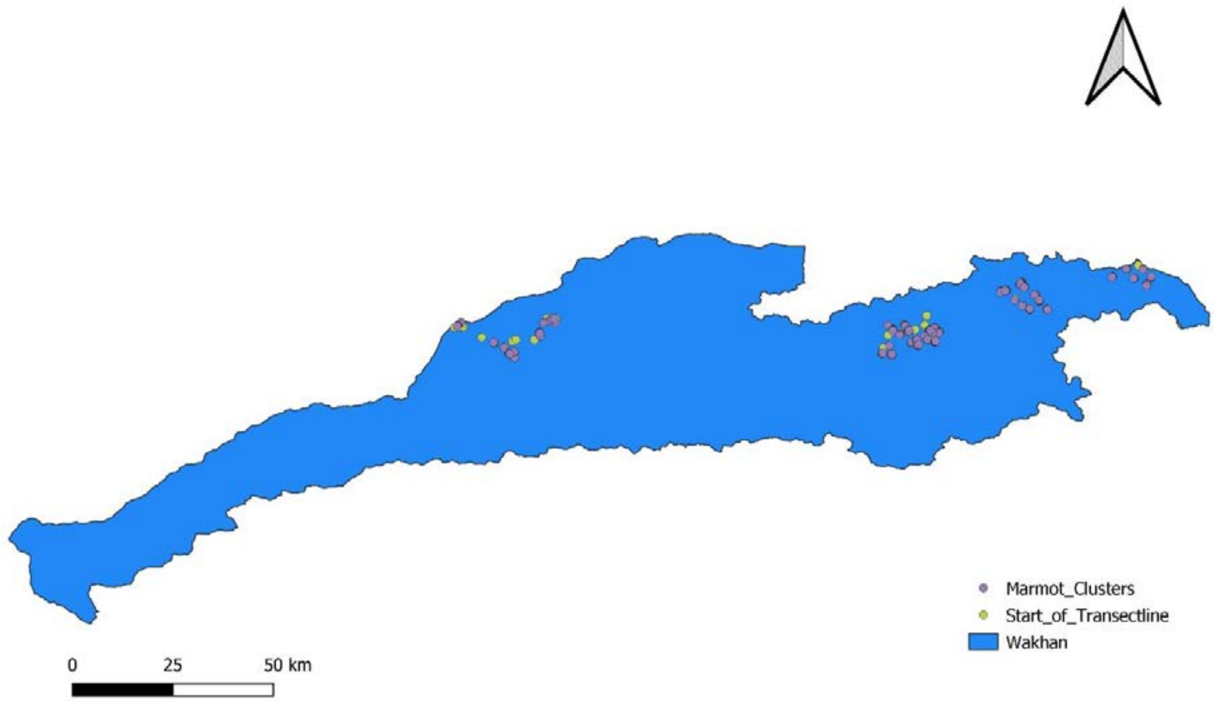

Figure 183. Map of Wakhan with positions of line transects and clusters of marmots within the line transects.

Bird community surveys

Birds contribute vital services to ecosystems and people through pollination, seed dispersal, scavenging, and pest control. They also help maintain vegetation and thus contribute to general ecosystem functioning. The diverse landscapes and ecosystems in Afghanistan host a wide variety of bird species, including several threatened species, one endemic species, and a few near-endemic species. Despite the large number of species found in Afghanistan, their current status and distribution is poorly known. WCS has conducted bird surveys in Wakhan and Bamyan since 2007 to document bird occurrences. Most recently, bird surveys were conducted in Wakhan and Bamyan by WCS-Afghanistan staff to add to the existing georeferenced database on bird occurrences and to continue regular monitoring of bird populations in these two study areas.

Survey sites and methodology

WCS-Afghanistan conducted point counts surveys in Bamyan from 10th July to 22nd July 2020 and 27th June to 11th July 2021, and in Wakhan from 10th July to 22nd July 2020 of all bird seen and heard in each location. A single point count consisted of a pair of observers standing at a predetermined fixed location and identifying all species seen and heard within a fixed amount of time. One observer was the primary observer, responsible for conducting the count. The second observer was responsible for taking notes, but would observe when possible.

Observers identified and counted the numbers of each species seen or heard from within 360 degrees of their position for a duration of 10 minutes. For each observation, the following data was recorded:

(1) The species of the bird

a. The bird was identified to the highest taxonomic level (e.g., species) whenever possible. If the exact species was unknown, a general description of the bird was recorded (e.g., “unknown rosefinch”).

(2) The number of individuals seen or heard

a. This was recorded exactly whenever possible, or was otherwise best estimated, for example, when the bird was heard only or when birds occurred in large groups. If multiple unique individuals or a species were seen throughout the count, but at different times, they were entered separately in the count.

b. Individuals detected during the survey were not counted more than once. For example, if a bird was seen flying over in the first minute, and another bird of the same species was seen flying over a few minutes later, it was up to the observer to determine whether the individual was unique or not. When in doubt, observers erred on the side of omitting the second observation. Having two observers helped to keep track of the movements of birds that had already been recorded in the survey, to ensure they were not counted twice.

(3) The mode of observation (sight or sound)

a. It was recorded whether the bird was seen or heard for each observation. If the bird was heard, and later that same individual was seen, the entry was updated to seen.

(4) Their distance from the bird (in meters)

a. This was accomplished by measuring the distance to a seen bird using a rangefinder, or when the bird was heard only, the distance was estimated to the nearest meter by using a rangefinder to identify the distance of an object believed to be close to the bird, such as a rock or tree. Birds of any distance were recorded (this is known as an 'unlimited radius count').

(5) The time of their observation

a. Next to each entry, the time of the observation was recorded to the nearest minute.

When a count was completed, additional general information about the count was recorded:

(1) The date of the count

(2) The start time of the count

(3) The end time of the count

(4) The GPS location of the count (coordinates and count station ID number)

(5) The names of the primary and secondary observers

(6) The sky conditions (clear, cloudy, partly cloudy, or rainy)

(7) The wind conditions (still, breezy, windy)

Once a count was complete and the information was recorded, the observers walked in the direction of the line transect for a distance of at least 250 m before establishing a new point count station (i.e., no two points were closer than 250 m together). The next count started immediately when getting to the point. This way, point count locations were situated along line transects, spaced apart approximately every 250 m. For example, a line transect that was 3 km long had 13 point count stations. These counts took 130 minutes to complete, not including transit time between stations. Counts were conducted starting just after dawn, when colors were just visible, and were concluded by 10 am.

Counts at a given location were repeated at least twice per field mission. That is, point counts were conducted in the same location at least twice during the field season, with at least a one-day gap in between surveys.

Appendix 3. Natural Hazards Supplementary Methods & Results

Modelling and Analysis

E

Avalanches

The following table (Table 57) shows villages ordered from most to least impacted by avalanches. Each ID number matches a page number with individual maps the specified village in a separate PDF file containing 604 individual maps depicting the frequency of avalanches around villages and avalanches proximate to roads (available upon request).

Table 57. Village level summary of avalanches by size category, ordered from most to least impacted.

Ref no.	Latitude	Longitude	Name	District	Total					Percent			
					Cat 1	Cat 2	Cat 3	Cat 4	All	Cat 1	Cat 2	Cat 3	Cat 4
1	37.86279	71.58170	Rabati	Shighnan	19.0	25.0	2.0	1.0	47.0	40.4	53.2	4.3	2.1
2	37.90480	71.31335	Yarkh	Shighnan	51.0	12.0	2.0	8.0	73.0	108.5	25.5	4.3	17.0
3	36.97641	71.40255	Gharan	Ishkashim	77.0	80.0	12.0	4.0	173.0	163.8	170.2	25.5	8.5
4	37.89770	71.37690	Deh Chowid	Shighnan	13.0	19.0	3.0	0.0	35.0	27.7	40.4	6.4	0.0
5	38.24059	70.62109	Mina Do (2)	Darwaz	46.0	48.0	3.0	0.0	97.0	97.9	102.1	6.4	0.0
6	37.54208	71.13023	Aylaq-i-Situn	Shighnan	38.0	93.0	2.0	2.0	135.0	80.9	197.9	4.3	4.3
7	35.92309	70.89669	Welo	Kuran Wa Munjan	27.0	50.0	0.0	0.0	77.0	57.4	106.4	0.0	0.0
8	38.10715	70.90554	Madud	Darwaz	37.0	32.0	5.0	0.0	74.0	78.7	68.1	10.6	0.0
9	38.14967	70.88994	Bughaz	Darwaz	6.0	37.0	2.0	2.0	47.0	12.8	78.7	4.3	4.3
10	38.19999	70.60609	Mayling-i-Bala	Darwaz	69.0	71.0	8.0	3.0	151.0	146.8	151.1	17.0	6.4
11	37.88341	71.34953	Suduj	Shighnan	1.0	7.0	0.0	2.0	10.0	2.1	14.9	0.0	4.3
12	36.89542	71.51231	Sar Shkh	Ishkashim	58.0	29.0	2.0	0.0	89.0	123.4	61.7	4.3	0.0
13	37.91925	70.51654	Naw Abad (1)	Khwahan	17.0	72.0	23.0	7.0	119.0	36.2	153.2	48.9	14.9
14	36.17434	70.77706	Lajawardshoy	Kuran Wa Munjan	85.0	65.0	0.0	0.0	150.0	180.9	138.3	0.0	0.0
15	38.06469	71.16443	Begav	Darwaz	12.0	39.0	3.0	1.0	55.0	25.5	83.0	6.4	2.1
16	37.89484	70.84728	Shil Khazar	Fayzabad	10.0	20.0	5.0	6.0	41.0	21.3	42.6	10.6	12.8
17	37.89774	71.38554	Pajward	Shighnan	3.0	4.0	0.0	0.0	7.0	6.4	8.5	0.0	0.0
18	37.41980	71.36538	Wrizon	Shighnan	16.0	29.0	5.0	2.0	52.0	34.0	61.7	10.6	4.3
19	37.89779	70.77270	Wyaj	Khwahan	69.0	78.0	4.0	1.0	152.0	146.8	166.0	8.5	2.1
20	37.87423	70.83660	Aylaqi Awistan	Khwahan	59.0	58.0	3.0	1.0	121.0	125.5	123.4	6.4	2.1
21	37.01724	72.68950	Gaz Khan	Wakhan	52.0	71.0	2.0	0.0	125.0	110.6	151.1	4.3	0.0
22	38.24399	70.62150	Wasku	Darwaz	37.0	41.0	2.0	0.0	80.0	78.7	87.2	4.3	0.0
23	37.11077	74.08583	Zimistani Qizil Atak	Wakhan	34.0	44.0	12.0	1.0	91.0	72.3	93.6	25.5	2.1
24	38.07859	70.55240	Kharaba-i-Pidjikh	Khwahan	60.0	73.0	4.0	3.0	140.0	127.7	155.3	8.5	6.4
25	38.32180	70.72469	Khadarrah	Darwaz	45.0	49.0	2.0	1.0	97.0	95.7	104.3	4.3	2.1
26	38.32929	70.70459	Pur Tel	Darwaz	45.0	30.0	1.0	0.0	76.0	95.7	63.8	2.1	0.0
27	36.86160	71.51910	Sar Shakh (1)	Ishkashim	19.0	23.0	2.0	0.0	44.0	40.4	48.9	4.3	0.0

Ref no.	Latitude	Longitude	Name	District	Total					Percent			
					Cat 1	Cat 2	Cat 3	Cat 4	All	Cat 1	Cat 2	Cat 3	Cat 4
28	37.89484	70.31625	Kishin Dara-I-Bala	Fayzabad	12.0	44.0	5.0	2.0	63.0	25.5	93.6	10.6	4.3
29	37.52696	71.48999	Shighnan	Shighnan	31.0	18.0	0.0	0.0	49.0	66.0	38.3	0.0	0.0
30	37.02000	72.67000	Pekot	Wakhan	48.0	60.0	3.0	0.0	111.0	102.1	127.7	6.4	0.0
31	37.33733	71.38840	Shikha	Shighnan	17.0	44.0	12.0	2.0	75.0	36.2	93.6	25.5	4.3
32	37.88808	71.14719	Moda Khers	Shighnan	139.0	133.0	2.0	1.0	275.0	295.7	283.0	4.3	2.1
33	38.28071	70.79116	Wesh Khoru (1)	Darwaz	11.0	27.0	0.0	1.0	39.0	23.4	57.4	0.0	2.1
34	37.00304	72.69638	Ab Gach	Wakhan	84.0	74.0	7.0	1.0	166.0	178.7	157.4	14.9	2.1
35	36.95762	71.45895	Yashtew	Ishkashim	44.0	24.0	0.0	0.0	68.0	93.6	51.1	0.0	0.0
36	37.96372	71.12482	Rulubj	Shighnan	29.0	55.0	0.0	2.0	86.0	61.7	117.0	0.0	4.3
37	38.29895	70.97584	Shajak	Darwaz	56.0	57.0	3.0	1.0	117.0	119.1	121.3	6.4	2.1
38	37.00324	73.29375	Neshkhawr	Wakhan	32.0	39.0	4.0	1.0	76.0	68.1	83.0	8.5	2.1
39	37.01202	72.69839	Qara Bar	Wakhan	74.0	71.0	6.0	1.0	152.0	157.4	151.1	12.8	2.1
40	37.88206	71.14417	Parabir	Shighnan	145.0	91.0	2.0	0.0	238.0	308.5	193.6	4.3	0.0
41	37.87054	70.81268	Sut Kham	Khwahan	26.0	62.0	5.0	2.0	95.0	55.3	131.9	10.6	4.3
42	37.70267	70.73542	Kajlar	Ragh	13.0	20.0	8.0	2.0	43.0	27.7	42.6	17.0	4.3
43	37.91489	70.76810	Shuhuch	Khwahan	38.0	32.0	7.0	1.0	78.0	80.9	68.1	14.9	2.1
44	38.23969	70.66610	Ulun	Darwaz	77.0	41.0	3.0	4.0	125.0	163.8	87.2	6.4	8.5
45	37.00051	72.59010	Qala-i-Panj	Wakhan	25.0	31.0	0.0	0.0	56.0	53.2	66.0	0.0	0.0
46	37.43314	71.39611	Puli Zarban	Shighnan	17.0	19.0	5.0	4.0	45.0	36.2	40.4	10.6	8.5
47	37.95532	71.20040	Darrah-i-Shir	Shighnan	51.0	50.0	0.0	0.0	101.0	108.5	106.4	0.0	0.0
48	36.91612	71.48553	Walij (1)	Ishkashim	55.0	38.0	2.0	0.0	95.0	117.0	80.9	4.3	0.0
49	37.70470	70.72171	Shap Dur	Ragh	18.0	26.0	9.0	0.0	53.0	38.3	55.3	19.1	0.0
50	38.17110	70.61480	Shalak	Darwaz	15.0	50.0	7.0	4.0	76.0	31.9	106.4	14.9	8.5
51	37.52516	71.02948	Aylaq-i-Khuda Rajak (1)	Shighnan	21.0	37.0	2.0	1.0	61.0	44.7	78.7	4.3	2.1
52	38.22140	70.66419	Kham-i-Kasku	Darwaz	8.0	16.0	3.0	2.0	29.0	17.0	34.0	6.4	4.3
53	38.32560	70.72820	Khundak	Darwaz	44.0	52.0	2.0	1.0	99.0	93.6	110.6	4.3	2.1
54	37.06101	74.14006	Gortik	Wakhan	22.0	38.0	11.0	9.0	80.0	46.8	80.9	23.4	19.1
55	36.35710	70.88745	Deh Payan	Jurm	10.0	11.0	5.0	0.0	26.0	21.3	23.4	10.6	0.0
56	38.19600	70.59599	Mayling-i-Pain	Darwaz	25.0	44.0	6.0	1.0	76.0	53.2	93.6	12.8	2.1
57	37.05454	74.18864	Zimistani Duldul	Wakhan	11.0	21.0	11.0	2.0	45.0	23.4	44.7	23.4	4.3

Ref no.	Latitude	Longitude	Name	District	Total					Percent			
					Cat 1	Cat 2	Cat 3	Cat 4	All	Cat 1	Cat 2	Cat 3	Cat 4
58	36.37883	70.85949	Qalata	Jurm	2.0	7.0	1.0	2.0	12.0	4.3	14.9	2.1	4.3
59	37.05555	74.15813	Chartash	Wakhan	14.0	40.0	13.0	3.0	70.0	29.8	85.1	27.7	6.4
60	38.12590	70.89861	Shilimad	Darwaz	21.0	37.0	6.0	3.0	67.0	44.7	78.7	12.8	6.4
61	36.48754	70.96025	Mushtaraw	Jurm	11.0	30.0	7.0	1.0	49.0	23.4	63.8	14.9	2.1
62	37.20732	71.41973	Darmadar	Ishkashim	16.0	20.0	4.0	1.0	41.0	34.0	42.6	8.5	2.1
63	38.16550	70.59019	Duspi	Darwaz	26.0	34.0	7.0	1.0	68.0	55.3	72.3	14.9	2.1
64	37.82732	71.09526	Rawan Sharist	Shighnan	93.0	93.0	3.0	0.0	189.0	197.9	197.9	6.4	0.0
65	36.07000	70.46120	Parwardah	Kuran Wa Munjan	17.0	26.0	10.0	5.0	58.0	36.2	55.3	21.3	10.6
66	36.45783	70.95759	Ocidar	Jurm	8.0	4.0	4.0	5.0	21.0	17.0	8.5	8.5	10.6
67	38.24520	70.63270	Hajdah Wun	Darwaz	7.0	17.0	4.0	1.0	29.0	14.9	36.2	8.5	2.1
68	37.84072	70.44856	Shakar Labi Bala	Fayzabad	4.0	30.0	6.0	4.0	44.0	8.5	63.8	12.8	8.5
69	38.04811	71.20035	Kushuj	Darwaz	14.0	44.0	4.0	2.0	64.0	29.8	93.6	8.5	4.3
70	36.24480	71.05625	Baghtah	Baharak	4.0	27.0	9.0	5.0	45.0	8.5	57.4	19.1	10.6
71	37.07000	74.42000	Zamestani Dawan Su	Wakhan	4.0	5.0	1.0	3.0	13.0	8.5	10.6	2.1	6.4
72	38.15160	71.23266	Barghed	Darwaz	5.0	23.0	5.0	1.0	34.0	10.6	48.9	10.6	2.1
73	38.25019	70.62409	Buni Bad	Darwaz	30.0	21.0	2.0	0.0	53.0	63.8	44.7	4.3	0.0
74	37.82292	71.09365	Sharist	Shighnan	72.0	72.0	0.0	1.0	145.0	153.2	153.2	0.0	2.1
75	37.86017	71.11961	Qarya-i-Ba Khersak	Shighnan	32.0	60.0	1.0	1.0	94.0	68.1	127.7	2.1	2.1
76	35.36037	67.48992	Yelgahe Ajar	Kahmard	7.0	13.0	0.0	0.0	20.0	14.9	27.7	0.0	0.0
77	38.17268	70.88242	Derch	Darwaz	12.0	20.0	3.0	3.0	38.0	25.5	42.6	6.4	6.4
78	37.00816	72.60668	Eshan	Wakhan	25.0	21.0	7.0	0.0	53.0	53.2	44.7	14.9	0.0
79	38.28313	70.80022	Waj Kon	Darwaz	5.0	9.0	0.0	0.0	14.0	10.6	19.1	0.0	0.0
80	37.91997	71.28851	Chasnud	Shighnan	12.0	3.0	1.0	0.0	16.0	25.5	6.4	2.1	0.0
81	36.88878	70.99725	Dara Bagh Sufla	Fayzabad	10.0	19.0	5.0	4.0	38.0	21.3	40.4	10.6	8.5
82	36.33945	70.91267	Kajaw	Jurm	7.0	12.0	6.0	2.0	27.0	14.9	25.5	12.8	4.3
83	35.90360	70.89169	Shahe Pari	Kuran Wa Munjan	32.0	57.0	2.0	0.0	91.0	68.1	121.3	4.3	0.0
84	34.80136	68.20641	Lalma	Shibar	8.0	24.0	8.0	0.0	40.0	17.0	51.1	17.0	0.0
85	37.47869	70.96300	Khetef	Shighnan	9.0	30.0	8.0	7.0	54.0	19.1	63.8	17.0	14.9

Ref no.	Latitude	Longitude	Name	District	Total					Percent			
					Cat 1	Cat 2	Cat 3	Cat 4	All	Cat 1	Cat 2	Cat 3	Cat 4
86	35.32333	69.02393	Salange Shamali	Khinjan	6.0	13.0	5.0	4.0	28.0	12.8	27.7	10.6	8.5
87	35.90869	70.88760	Ghaz	Kuran Wa Munjan	25.0	46.0	1.0	0.0	72.0	53.2	97.9	2.1	0.0
88	37.81852	71.09427	Basenj	Shighnan	63.0	64.0	0.0	1.0	128.0	134.0	136.2	0.0	2.1
89	37.75718	70.50000	Howz-e Shah-e Bala	Khwahan	16.0	29.0	14.0	6.0	65.0	34.0	61.7	29.8	12.8
90	37.06366	71.42646	Zic	Ishkashim	12.0	15.0	1.0	0.0	28.0	25.5	31.9	2.1	0.0
91	35.04910	68.02049	Dahane Mahmadkecha	Shibar	3.0	8.0	3.0	0.0	14.0	6.4	17.0	6.4	0.0
92	38.20676	71.01895	Khejwand	Darwaz	10.0	13.0	3.0	0.0	26.0	21.3	27.7	6.4	0.0
93	37.97529	70.80668	Ghezew	Khwahan	10.0	27.0	3.0	2.0	42.0	21.3	57.4	6.4	4.3
94	35.03818	68.02625	Pa’intoghay	Shibar	2.0	6.0	3.0	1.0	12.0	4.3	12.8	6.4	2.1
95	37.82808	70.46088	Sokhta Kohi Bala	Fayzabad	11.0	20.0	8.0	1.0	40.0	23.4	42.6	17.0	2.1
96	37.89045	70.78603	Roghud	Khwahan	21.0	46.0	1.0	0.0	68.0	44.7	97.9	2.1	0.0
97	34.77090	67.42159	Kuhnadeh	Bamyan	10.0	11.0	10.0	6.0	37.0	21.3	23.4	21.3	12.8
98	36.35102	70.88094	Faraz	Jurm	1.0	6.0	2.0	0.0	9.0	2.1	12.8	4.3	0.0
99	37.36907	70.74775	Qalat (2)	Ragh	6.0	21.0	6.0	2.0	35.0	12.8	44.7	12.8	4.3
100	38.07886	71.22685	Ghumai	Darwaz	22.0	39.0	2.0	0.0	63.0	46.8	83.0	4.3	0.0
101	37.87144	71.12601	Aylaq-i-Panja-i-Mard	Shighnan	46.0	50.0	0.0	1.0	97.0	97.9	106.4	0.0	2.1
102	36.02601	70.75547	Ewem	Kuran Wa Munjan	29.0	23.0	9.0	0.0	61.0	61.7	48.9	19.1	0.0
103	38.22945	70.77904	Darrah-i-Mazar	Darwaz	18.0	29.0	2.0	0.0	49.0	38.3	61.7	4.3	0.0
104	34.75069	67.39489	Charchashma	Bamyan	9.0	10.0	7.0	4.0	30.0	19.1	21.3	14.9	8.5
105	37.76262	70.48505	Howz-e Shah-e Pa’in	Khwahan	5.0	20.0	9.0	5.0	39.0	10.6	42.6	19.1	10.6
106	37.91873	71.20260	Khizaw	Shighnan	13.0	11.0	2.0	0.0	26.0	27.7	23.4	4.3	0.0
107	37.39511	70.86179	Kamar-i-Sayqan	Shighnan	6.0	16.0	6.0	5.0	33.0	12.8	34.0	12.8	10.6
108	36.99000	73.56000	Zemestani Pasa	Wakhan	41.0	33.0	3.0	0.0	77.0	87.2	70.2	6.4	0.0
109	38.21821	70.77534	Jawa Duk	Darwaz	2.0	23.0	0.0	0.0	25.0	4.3	48.9	0.0	0.0
110	36.99197	72.53439	Paghn	Wakhan	56.0	14.0	4.0	0.0	74.0	119.1	29.8	8.5	0.0
111	37.68249	70.50365	Naw Abad (3)	Ragh	7.0	8.0	4.0	3.0	22.0	14.9	17.0	8.5	6.4
112	37.37178	71.40011	Wishtachi	Shighnan	12.0	15.0	5.0	0.0	32.0	25.5	31.9	10.6	0.0
113	37.03000	73.25000	Shashom	Wakhan	7.0	9.0	2.0	2.0	20.0	14.9	19.1	4.3	4.3

Ref no.	Latitude	Longitude	Name	District	Total					Percent			
					Cat 1	Cat 2	Cat 3	Cat 4	All	Cat 1	Cat 2	Cat 3	Cat 4
114	36.41778	70.96042	Ambadewal	Jurm	1.0	3.0	3.0	3.0	10.0	2.1	6.4	6.4	6.4
115	38.37339	71.12475	Mirak	Darwaz	6.0	20.0	7.0	0.0	33.0	12.8	42.6	14.9	0.0
116	34.78289	67.41640	Top'ali	Bamyan	5.0	10.0	7.0	4.0	26.0	10.6	21.3	14.9	8.5
117	37.54263	71.43741	Behsar	Shighnan	11.0	16.0	3.0	2.0	32.0	23.4	34.0	6.4	4.3
118	38.07806	71.22552	Pur Goj	Darwaz	20.0	38.0	1.0	0.0	59.0	42.6	80.9	2.1	0.0
119	37.07199	71.14941	Rezwan	Baharak	9.0	18.0	2.0	0.0	29.0	19.1	38.3	4.3	0.0
120	38.19470	70.58849	Urchaw	Darwaz	16.0	19.0	4.0	1.0	40.0	34.0	40.4	8.5	2.1
121	36.02731	70.76576	Kuran Wa Munjan	Kuran Wa Munjan	24.0	21.0	5.0	0.0	50.0	51.1	44.7	10.6	0.0
122	37.36582	71.42715	Arakht	Shighnan	0.0	10.0	1.0	0.0	11.0	0.0	21.3	2.1	0.0
123	37.80198	70.43097	Sabz Dasht	Khwahan	2.0	21.0	6.0	4.0	33.0	4.3	44.7	12.8	8.5
124	36.98520	72.40190	Ishmurg	Wakhan	3.0	11.0	0.0	0.0	14.0	6.4	23.4	0.0	0.0
125	38.27998	70.80397	Wesh Khoru (2)	Darwaz	2.0	6.0	0.0	0.0	8.0	4.3	12.8	0.0	0.0
126	37.96476	70.50243	Pedew	Khwahan	9.0	24.0	3.0	2.0	38.0	19.1	51.1	6.4	4.3
127	38.22098	71.00853	Khevaj	Darwaz	10.0	6.0	0.0	1.0	17.0	21.3	12.8	0.0	2.1
128	38.17400	70.88869	Kay	Darwaz	14.0	15.0	7.0	4.0	40.0	29.8	31.9	14.9	8.5
129	37.81380	71.10847	Aylaq-i-Boqul	Shighnan	10.0	10.0	1.0	1.0	22.0	21.3	21.3	2.1	2.1
130	37.07150	71.14565	Sarkhan	Baharak	7.0	14.0	2.0	0.0	23.0	14.9	29.8	4.3	0.0
131	38.22534	70.97625	Khorodun	Darwaz	5.0	9.0	4.0	0.0	18.0	10.6	19.1	8.5	0.0
132	38.31364	70.79718	Delwakh (1)	Darwaz	9.0	22.0	2.0	1.0	34.0	19.1	46.8	4.3	2.1
133	38.23870	70.78682	Sar Jaway	Darwaz	21.0	17.0	1.0	1.0	40.0	44.7	36.2	2.1	2.1
134	37.49014	71.43460	Ghar Jowan	Shighnan	12.0	19.0	5.0	0.0	36.0	25.5	40.4	10.6	0.0
135	36.55384	71.32893	Gul Khana	Baharak	37.0	46.0	4.0	0.0	87.0	78.7	97.9	8.5	0.0
136	36.72776	71.58161	Zargaran	Ishkashim	63.0	17.0	0.0	0.0	80.0	134.0	36.2	0.0	0.0
137	37.07440	71.14864	Deh Khalla	Baharak	7.0	14.0	1.0	0.0	22.0	14.9	29.8	2.1	0.0
138	37.53627	70.98132	Khinj	Shighnan	6.0	16.0	1.0	1.0	24.0	12.8	34.0	2.1	2.1
139	37.06975	71.14108	Dasht M Raziq	Baharak	6.0	13.0	1.0	0.0	20.0	12.8	27.7	2.1	0.0
140	37.12598	73.98408	Sawab Khana	Wakhan	13.0	26.0	8.0	2.0	49.0	27.7	55.3	17.0	4.3
141	37.81487	70.44815	Jerwu Bala	Khwahan	12.0	26.0	4.0	3.0	45.0	25.5	55.3	8.5	6.4
142	37.77670	70.36456	Kamar	Khwahan	0.0	9.0	2.0	1.0	12.0	0.0	19.1	4.3	2.1

Ref no.	Latitude	Longitude	Name	District	Total					Percent			
					Cat 1	Cat 2	Cat 3	Cat 4	All	Cat 1	Cat 2	Cat 3	Cat 4
143	37.07452	71.15065	Shakh Yarak	Baharak	7.0	11.0	1.0	0.0	19.0	14.9	23.4	2.1	0.0
144	37.92638	70.77067	Wudar Khuft	Khwahan	5.0	11.0	1.0	0.0	17.0	10.6	23.4	2.1	0.0
145	37.04508	73.83481	Zimistani Walma	Wakhan	1.0	2.0	5.0	3.0	11.0	2.1	4.3	10.6	6.4
146	37.83306	70.42491	Ruyanzar	Khwahan	5.0	20.0	1.0	2.0	28.0	10.6	42.6	2.1	4.3
147	36.00928	70.72591	Razer	Kuran Wa Munjan	8.0	13.0	1.0	0.0	22.0	17.0	27.7	2.1	0.0
148	37.07474	71.14602	Deh Dara	Baharak	4.0	11.0	1.0	0.0	16.0	8.5	23.4	2.1	0.0
149	38.23709	70.64529	Lech	Darwaz	20.0	18.0	7.0	1.0	46.0	42.6	38.3	14.9	2.1
150	37.94965	70.54619	Guzari Khirqa	Fayzabad	6.0	10.0	1.0	0.0	17.0	12.8	21.3	2.1	0.0
151	34.80939	67.43069	Sharah	Bamyan	4.0	8.0	3.0	3.0	18.0	8.5	17.0	6.4	6.4
152	38.37444	70.80605	Worashan	Darwaz	7.0	12.0	0.0	0.0	19.0	14.9	25.5	0.0	0.0
153	37.39000	74.48000	Zemestani Qara Tash	Wakhan	2.0	0.0	1.0	3.0	6.0	4.3	0.0	2.1	6.4
154	34.78749	67.40589	Qal'a-i-Gaday	Bamyan	0.0	7.0	8.0	2.0	17.0	0.0	14.9	17.0	4.3
155	36.47321	70.95791	Pasilak	Jurm	0.0	5.0	0.0	0.0	5.0	0.0	10.6	0.0	0.0
156	34.75089	67.52659	Darrahi Darvazeh	Bamyan	4.0	8.0	4.0	4.0	20.0	8.5	17.0	8.5	8.5
157	38.21089	70.78152	Ghonvar	Darwaz	2.0	17.0	2.0	0.0	21.0	4.3	36.2	4.3	0.0
158	36.38543	70.74517	Farghamu	Jurm	42.0	41.0	1.0	0.0	84.0	89.4	87.2	2.1	0.0
159	37.34023	71.44448	Wishtayn	Shighnan	3.0	4.0	2.0	1.0	10.0	6.4	8.5	4.3	2.1
160	37.01259	73.41219	Chehel Kand	Wakhan	6.0	8.0	2.0	2.0	18.0	12.8	17.0	4.3	4.3
161	36.02097	70.77409	Pas Koran	Kuran Wa Munjan	17.0	17.0	2.0	0.0	36.0	36.2	36.2	4.3	0.0
162	37.76826	70.47488	Drel	Khwahan	5.0	17.0	3.0	4.0	29.0	10.6	36.2	6.4	8.5
163	35.02348	67.68592	Regnaw	Kahmard	3.0	6.0	2.0	4.0	15.0	6.4	12.8	4.3	8.5
164	37.93450	70.75935	Rewud	Khwahan	9.0	11.0	0.0	0.0	20.0	19.1	23.4	0.0	0.0
165	37.70870	70.71106	Safed Chut	Ragh	10.0	16.0	8.0	1.0	35.0	21.3	34.0	17.0	2.1
166	37.34305	71.48147	Darmarakht	Shighnan	11.0	23.0	1.0	0.0	35.0	23.4	48.9	2.1	0.0
167	37.27038	71.47685	Pastiw	Shighnan	1.0	4.0	0.0	1.0	6.0	2.1	8.5	0.0	2.1
168	37.93816	70.76144	Rawinj	Khwahan	9.0	10.0	0.0	0.0	19.0	19.1	21.3	0.0	0.0
169	35.09919	68.19995	Bashal	Tala Wa Barfak	1.0	5.0	3.0	3.0	12.0	2.1	10.6	6.4	6.4
170	36.44238	70.97003	Khajan	Jurm	0.0	3.0	4.0	2.0	9.0	0.0	6.4	8.5	4.3

Ref no.	Latitude	Longitude	Name	District	Total					Percent			
					Cat 1	Cat 2	Cat 3	Cat 4	All	Cat 1	Cat 2	Cat 3	Cat 4
171	37.68324	70.42525	Chegrin	Ragh	2.0	5.0	5.0	1.0	13.0	4.3	10.6	10.6	2.1
172	37.05812	71.15518	Ghuzew	Baharak	6.0	12.0	2.0	1.0	21.0	12.8	25.5	4.3	2.1
173	38.23249	70.90722	Badmag	Darwaz	2.0	14.0	4.0	0.0	20.0	4.3	29.8	8.5	0.0
174	37.02000	73.28000	Malang Zan	Wakhan	7.0	14.0	7.0	3.0	31.0	14.9	29.8	14.9	6.4
175	34.79780	67.42809	Sawzi	Bamyan	3.0	0.0	0.0	3.0	6.0	6.4	0.0	0.0	6.4
176	37.83986	70.40653	Jerwu Pa'in	Khwahan	4.0	14.0	3.0	2.0	23.0	8.5	29.8	6.4	4.3
177	37.95958	70.78793	Mandiz	Khwahan	7.0	22.0	2.0	0.0	31.0	14.9	46.8	4.3	0.0
178	37.10282	73.94662	Khana-i-Khash Kor	Wakhan	10.0	16.0	2.0	2.0	30.0	21.3	34.0	4.3	4.3
179	37.02359	73.89950	Gustaw	Wakhan	9.0	10.0	4.0	3.0	26.0	19.1	21.3	8.5	6.4
180	38.22519	70.77903	Wurachak	Darwaz	4.0	17.0	2.0	0.0	23.0	8.5	36.2	4.3	0.0
181	38.19030	70.58399	Shinazm	Darwaz	5.0	22.0	1.0	0.0	28.0	10.6	46.8	2.1	0.0
182	38.06928	71.18340	Rakhunwij	Darwaz	2.0	14.0	2.0	2.0	20.0	4.3	29.8	4.3	4.3
183	37.02987	73.79006	Langar (1)	Wakhan	9.0	14.0	1.0	2.0	26.0	19.1	29.8	2.1	4.3
184	37.90177	71.18275	Aylaq-i-Khuda Rajak (2)	Shighnan	0.0	3.0	3.0	2.0	8.0	0.0	6.4	6.4	4.3
185	36.27701	70.79735	Robate Payan	Jurm	34.0	33.0	2.0	0.0	69.0	72.3	70.2	4.3	0.0
186	36.42524	69.61431	Deh Sayad	Chal	0.0	0.0	0.0	3.0	3.0	0.0	0.0	0.0	6.4
187	38.17623	71.31769	Jamarji Payan	Darwaz	3.0	6.0	0.0	0.0	9.0	6.4	12.8	0.0	0.0
188	37.71422	70.45071	Mushuk March	Khwahan	0.0	6.0	4.0	3.0	13.0	0.0	12.8	8.5	6.4
189	37.69883	70.45348	Rawanjuk	Ragh	1.0	3.0	3.0	3.0	10.0	2.1	6.4	6.4	6.4
190	36.49670	70.88898	Charambada	Jurm	8.0	17.0	2.0	0.0	27.0	17.0	36.2	4.3	0.0
191	37.35239	74.35258	Tash Seri (2)	Wakhan	1.0	3.0	4.0	2.0	10.0	2.1	6.4	8.5	4.3
192	36.57346	71.02232	Layrak (1)	Jurm	3.0	11.0	6.0	1.0	21.0	6.4	23.4	12.8	2.1
193	36.55250	71.01602	Darawan	Jurm	3.0	9.0	0.0	1.0	13.0	6.4	19.1	0.0	2.1
194	37.97580	70.62722	Bakharow	Khwahan	14.0	20.0	2.0	0.0	36.0	29.8	42.6	4.3	0.0
195	37.06000	73.88000	Kadan Khana	Wakhan	2.0	7.0	5.0	0.0	14.0	4.3	14.9	10.6	0.0
196	37.94862	70.57287	Sar-i-Pul (1)	Khwahan	7.0	5.0	5.0	2.0	19.0	14.9	10.6	10.6	4.3
197	38.12439	70.61719	Mushtiw	Darwaz	8.0	4.0	2.0	0.0	14.0	17.0	8.5	4.3	0.0
198	35.01336	66.89637	Sur Lugh	Yakawlang	0.0	0.0	0.0	2.0	2.0	0.0	0.0	0.0	4.3
199	36.83464	70.44658	Yamchian	Fayzabad	2.0	1.0	1.0	3.0	7.0	4.3	2.1	2.1	6.4
200	36.66880	71.73019	Qazi Deh (2)	Wakhan	4.0	5.0	0.0	0.0	9.0	8.5	10.6	0.0	0.0

Ref no.	Latitude	Longitude	Name	District	Total					Percent			
					Cat 1	Cat 2	Cat 3	Cat 4	All	Cat 1	Cat 2	Cat 3	Cat 4
201	37.94710	70.74097	Zaghar	Khwahan	3.0	13.0	3.0	1.0	20.0	6.4	27.7	6.4	2.1
202	36.20744	70.79186	Sar Sang	Kuran Wa Munjan	16.0	23.0	2.0	0.0	41.0	34.0	48.9	4.3	0.0
203	35.09994	67.46437	Khwajakesht	Kahmard	2.0	4.0	0.0	0.0	6.0	4.3	8.5	0.0	0.0
204	36.76236	71.07497	Sufian	Baharak	8.0	13.0	6.0	0.0	27.0	17.0	27.7	12.8	0.0
205	35.01954	67.71841	Ghoraw	Kahmard	1.0	4.0	1.0	3.0	9.0	2.1	8.5	2.1	6.4
206	36.68240	71.86169	Keshnikhan	Wakhan	4.0	5.0	1.0	0.0	10.0	8.5	10.6	2.1	0.0
207	36.03051	70.77554	Qal'eh	Kuran Wa Munjan	12.0	10.0	2.0	0.0	24.0	25.5	21.3	4.3	0.0
208	38.31848	70.80771	Jaway	Darwaz	5.0	6.0	1.0	0.0	12.0	10.6	12.8	2.1	0.0
209	35.36555	67.48045	Dehqanqal'a	Kahmard	3.0	3.0	0.0	0.0	6.0	6.4	6.4	0.0	0.0
210	35.03092	67.63994	Kohgaday	Kahmard	3.0	7.0	4.0	2.0	16.0	6.4	14.9	8.5	4.3
211	38.27605	70.90928	Bahshar	Darwaz	3.0	7.0	0.0	3.0	13.0	6.4	14.9	0.0	6.4
212	38.02419	70.54420	Delwakh (1)	Khwahan	7.0	10.0	3.0	1.0	21.0	14.9	21.3	6.4	2.1
213	35.98049	70.89649	Shahran	Kuran Wa Munjan	6.0	11.0	1.0	0.0	18.0	12.8	23.4	2.1	0.0
214	37.94222	70.73396	Pay Mazar	Khwahan	17.0	6.0	3.0	0.0	26.0	36.2	12.8	6.4	0.0
215	37.59058	70.64948	Seh Abshar	Ragh	0.0	1.0	1.0	2.0	4.0	0.0	2.1	2.1	4.3
216	37.91114	70.70104	Delwakh (2)	Khwahan	3.0	4.0	3.0	1.0	11.0	6.4	8.5	6.4	2.1
217	37.05927	71.16710	Ghazaw Bala	Baharak	1.0	10.0	2.0	1.0	14.0	2.1	21.3	4.3	2.1
218	35.01762	67.73660	Ghorawe Shamadbeg	Kahmard	4.0	6.0	3.0	1.0	14.0	8.5	12.8	6.4	2.1
219	37.69778	70.69478	Dahana-i-Shala Darrah	Ragh	3.0	13.0	8.0	0.0	24.0	6.4	27.7	17.0	0.0
220	35.10824	67.92816	Sare Kundi	Kahmard	1.0	0.0	1.0	2.0	4.0	2.1	0.0	2.1	4.3
221	35.17382	68.24448	Zarsange Pa'in	Tala Wa Barfak	0.0	0.0	0.0	1.0	1.0	0.0	0.0	0.0	2.1
222	37.74860	70.45891	Shalil	Khwahan	3.0	11.0	1.0	0.0	15.0	6.4	23.4	2.1	0.0
223	37.70717	70.70702	Safed Ab	Ragh	3.0	8.0	7.0	1.0	19.0	6.4	17.0	14.9	2.1
224	35.01942	67.70944	Baluch	Kahmard	5.0	3.0	2.0	1.0	11.0	10.6	6.4	4.3	2.1
225	38.24743	70.79374	Darrah Jaway	Darwaz	7.0	15.0	4.0	1.0	27.0	14.9	31.9	8.5	2.1
226	37.69424	70.69147	Gala Dur	Ragh	4.0	11.0	5.0	0.0	20.0	8.5	23.4	10.6	0.0
227	37.37019	74.38550	Tash Seri (1)	Wakhan	1.0	5.0	3.0	2.0	11.0	2.1	10.6	6.4	4.3
228	38.24761	70.79743	Dur Khakh	Darwaz	7.0	15.0	4.0	1.0	27.0	14.9	31.9	8.5	2.1

Ref no.	Latitude	Longitude	Name	District	Total					Percent			
					Cat 1	Cat 2	Cat 3	Cat 4	All	Cat 1	Cat 2	Cat 3	Cat 4
229	37.64795	70.48414	Kushlar (2)	Ragh	0.0	0.0	1.0	2.0	3.0	0.0	0.0	2.1	4.3
230	35.03098	68.01489	Toghay (2)	Shibar	1.0	5.0	2.0	1.0	9.0	2.1	10.6	4.3	2.1
231	35.98140	70.88409	Ghomand	Kuran Wa Munjan	6.0	9.0	1.0	0.0	16.0	12.8	19.1	2.1	0.0
232	38.00132	71.16682	Aylaq-i-Khodun	Shighnan	1.0	3.0	3.0	0.0	7.0	2.1	6.4	6.4	0.0
233	36.72542	71.11375	Nulan	Baharak	6.0	20.0	1.0	1.0	28.0	12.8	42.6	2.1	2.1
234	37.43526	70.89336	Taqarcha	Shighnan	3.0	10.0	1.0	0.0	14.0	6.4	21.3	2.1	0.0
235	37.93372	70.62669	Chatniw	Khwahan	3.0	3.0	0.0	1.0	7.0	6.4	6.4	0.0	2.1
236	37.94711	70.74991	Saydan	Khwahan	0.0	12.0	0.0	1.0	13.0	0.0	25.5	0.0	2.1
237	35.05230	67.43102	Darrahe Bacha	Kahmard	1.0	3.0	0.0	3.0	7.0	2.1	6.4	0.0	6.4
238	35.02613	67.62354	Khawal	Kahmard	0.0	0.0	0.0	1.0	1.0	0.0	0.0	0.0	2.1
239	36.26321	70.80534	Robate Bala	Kuran Wa Munjan	3.0	18.0	1.0	0.0	22.0	6.4	38.3	2.1	0.0
240	36.98417	72.48157	Powkowy	Wakhan	3.0	3.0	2.0	0.0	8.0	6.4	6.4	4.3	0.0
241	34.63820	68.02410	Qole Beda	Hisa-I- Awali Bihsud	5.0	14.0	0.0	0.0	19.0	10.6	29.8	0.0	0.0
242	35.85289	70.85379	Myandeh	Kuran Wa Munjan	10.0	10.0	0.0	0.0	20.0	21.3	21.3	0.0	0.0
243	38.06488	71.20646	Radij	Darwaz	7.0	10.0	1.0	1.0	19.0	14.9	21.3	2.1	2.1
244	37.36713	70.89359	Qal'eh-ye Mirza Shah (2)	Shighnan	4.0	24.0	1.0	0.0	29.0	8.5	51.1	2.1	0.0
245	38.25472	70.80678	Durman	Darwaz	7.0	14.0	0.0	0.0	21.0	14.9	29.8	0.0	0.0
246	37.97892	70.58237	Karniw (2)	Khwahan	5.0	8.0	1.0	1.0	15.0	10.6	17.0	2.1	2.1
247	37.30250	74.27380	Qara Jelga	Wakhan	9.0	12.0	2.0	1.0	24.0	19.1	25.5	4.3	2.1
248	38.33699	70.68980	Nirsad	Darwaz	4.0	3.0	1.0	0.0	8.0	8.5	6.4	2.1	0.0
249	34.77740	67.48459	Sebartu	Bamyan	4.0	3.0	1.0	0.0	8.0	8.5	6.4	2.1	0.0
250	34.94559	67.06190	Kochkak	Yakawlang	0.0	0.0	0.0	1.0	1.0	0.0	0.0	0.0	2.1
251	38.30646	70.80692	Arkhod	Darwaz	5.0	13.0	1.0	0.0	19.0	10.6	27.7	2.1	0.0
252	38.30708	70.80455	Mina Do (1)	Darwaz	5.0	13.0	1.0	0.0	19.0	10.6	27.7	2.1	0.0
253	35.87634	69.53101	Khamkhafi	Khost Wa Firing	0.0	6.0	2.0	1.0	9.0	0.0	12.8	4.3	2.1
254	37.34506	70.69379	Khamkok	Ragh	1.0	2.0	3.0	2.0	8.0	2.1	4.3	6.4	4.3
255	34.75768	68.04260	Jandargale Ulya	Shibar	1.0	0.0	0.0	2.0	3.0	2.1	0.0	0.0	4.3

Ref no.	Latitude	Longitude	Name	District	Total					Percent			
					Cat 1	Cat 2	Cat 3	Cat 4	All	Cat 1	Cat 2	Cat 3	Cat 4
256	37.70342	70.46738	Ray Darrah	Ragh	2.0	4.0	2.0	2.0	10.0	4.3	8.5	4.3	4.3
257	34.99843	67.67289	Qatarsum	Kahmard	4.0	7.0	5.0	1.0	17.0	8.5	14.9	10.6	2.1
258	34.77027	68.10045	Berana	Shibar	3.0	3.0	0.0	1.0	7.0	6.4	6.4	0.0	2.1
259	38.33952	70.91164	Arward	Darwaz	0.0	4.0	1.0	0.0	5.0	0.0	8.5	2.1	0.0
260	37.90932	70.64208	Chashm Darrah	Khwahan	10.0	13.0	1.0	0.0	24.0	21.3	27.7	2.1	0.0
261	37.92733	70.68124	Shkharow Wari	Khwahan	5.0	19.0	1.0	0.0	25.0	10.6	40.4	2.1	0.0
262	34.90619	67.50839	Jow Palal	Bamyan	0.0	3.0	0.0	2.0	5.0	0.0	6.4	0.0	4.3
263	35.99695	69.66893	Myandeh	Khost Wa Firing	6.0	21.0	1.0	0.0	28.0	12.8	44.7	2.1	0.0
264	38.23647	70.91421	Magay	Darwaz	1.0	8.0	3.0	0.0	12.0	2.1	17.0	6.4	0.0
265	35.59910	69.27129	Tangi Arzo	Andarab	0.0	1.0	0.0	1.0	2.0	0.0	2.1	0.0	2.1
266	34.67139	67.96997	Syah Sangak	Shibar	5.0	8.0	3.0	1.0	17.0	10.6	17.0	6.4	2.1
267	38.07310	71.22766	Pitab	Darwaz	1.0	3.0	0.0	0.0	4.0	2.1	6.4	0.0	0.0
268	38.18048	71.26916	Begaw (1)	Darwaz	3.0	10.0	0.0	0.0	13.0	6.4	21.3	0.0	0.0
269	37.78389	70.38358	Safed Sangan	Khwahan	2.0	1.0	2.0	1.0	6.0	4.3	2.1	4.3	2.1
270	37.32825	70.75371	Sin Shal	Ragh	0.0	9.0	5.0	0.0	14.0	0.0	19.1	10.6	0.0
271	35.96629	70.90899	Dasht	Kuran Wa Munjan	5.0	8.0	3.0	0.0	16.0	10.6	17.0	6.4	0.0
272	38.31828	70.91933	Qarya-i-Ba Dard	Darwaz	3.0	12.0	1.0	0.0	16.0	6.4	25.5	2.1	0.0
273	34.90771	67.57353	Qowlahli-ye Bala	Bamyan	0.0	1.0	0.0	1.0	2.0	0.0	2.1	0.0	2.1
274	37.75580	70.44778	Zarich	Khwahan	15.0	14.0	1.0	0.0	30.0	31.9	29.8	2.1	0.0
275	36.74350	71.93970	Langar (2)	Wakhan	0.0	2.0	0.0	0.0	2.0	0.0	4.3	0.0	0.0
276	36.52202	71.34042	Zebak	Zebak	6.0	12.0	1.0	1.0	20.0	12.8	25.5	2.1	2.1
277	37.32850	73.10099	Khaneh-ye-Garmatak	Wakhan	2.0	3.0	1.0	0.0	6.0	4.3	6.4	2.1	0.0
278	37.58855	70.62967	Rabat-i-Seh Ab	Ragh	1.0	2.0	0.0	1.0	4.0	2.1	4.3	0.0	2.1
279	35.83350	69.57297	Khalyan	Khost Wa Firing	3.0	6.0	0.0	1.0	10.0	6.4	12.8	0.0	2.1
280	34.70732	67.58649	Kamati	Bamyan	0.0	4.0	0.0	1.0	5.0	0.0	8.5	0.0	2.1
281	37.42954	70.34657	Hasan-i-Diwana	Fayzabad	0.0	0.0	0.0	2.0	2.0	0.0	0.0	0.0	4.3
282	36.15219	69.94352	Bala Mokhow-ye (1)	Warsaj	1.0	3.0	1.0	0.0	5.0	2.1	6.4	2.1	0.0
283	37.58839	70.65431	Wedin Dur	Ragh	0.0	2.0	0.0	1.0	3.0	0.0	4.3	0.0	2.1
284	37.05687	71.17477	Dargaw	Baharak	0.0	5.0	2.0	0.0	7.0	0.0	10.6	4.3	0.0

Ref no.	Latitude	Longitude	Name	District	Total					Percent			
					Cat 1	Cat 2	Cat 3	Cat 4	All	Cat 1	Cat 2	Cat 3	Cat 4
285	36.01610	70.68639	Poruch	Kuran Wa Munjan	3.0	17.0	1.0	0.0	21.0	6.4	36.2	2.1	0.0
286	37.96584	70.57503	Karniw (1)	Khwahan	2.0	1.0	1.0	2.0	6.0	4.3	2.1	2.1	4.3
287	37.37822	70.89334	Qal'eh-ye Mirza Shah (1)	Shighnan	2.0	16.0	2.0	0.0	20.0	4.3	34.0	4.3	0.0
288	35.73624	69.42168	Ghorisang	Andarab	1.0	8.0	3.0	0.0	12.0	2.1	17.0	6.4	0.0
289	38.17950	70.58699	Feryam Bab	Darwaz	1.0	12.0	0.0	0.0	13.0	2.1	25.5	0.0	0.0
290	37.00883	73.38013	Patukh	Wakhan	0.0	0.0	0.0	0.0	0.0	0.0	0.0	0.0	0.0
291	36.07593	70.06752	Khujo	Warsaj	1.0	7.0	3.0	0.0	11.0	2.1	14.9	6.4	0.0
292	35.54578	69.51188	Pase Kandeh	Andarab	2.0	3.0	3.0	0.0	8.0	4.3	6.4	6.4	0.0
293	37.97799	70.61137	Wajud	Khwahan	4.0	11.0	0.0	0.0	15.0	8.5	23.4	0.0	0.0
294	37.69701	70.67744	Dashti Lakhsh	Ragh	5.0	13.0	0.0	0.0	18.0	10.6	27.7	0.0	0.0
295	37.45079	70.54853	Qalat (1)	Ragh	2.0	8.0	3.0	0.0	13.0	4.3	17.0	6.4	0.0
296	38.05413	71.22050	Barchud	Darwaz	1.0	4.0	1.0	0.0	6.0	2.1	8.5	2.1	0.0
297	36.80700	72.04059	Urgunt-i-Payan	Wakhan	2.0	1.0	1.0	0.0	4.0	4.3	2.1	2.1	0.0
298	37.69082	70.67309	Ledur	Ragh	2.0	10.0	3.0	0.0	15.0	4.3	21.3	6.4	0.0
299	36.42947	69.60840	Alemi	Chal	0.0	0.0	0.0	1.0	1.0	0.0	0.0	0.0	2.1
300	37.60220	71.49006	Baved (Deh Shar Sarcheshma)	Shighnan	2.0	6.0	2.0	0.0	10.0	4.3	12.8	4.3	0.0
301	37.35237	70.65981	Glek-i-Elga	Ragh	2.0	4.0	0.0	0.0	6.0	4.3	8.5	0.0	0.0
302	37.57605	70.68671	Deh Qadyan	Ragh	1.0	5.0	1.0	0.0	7.0	2.1	10.6	2.1	0.0
303	36.68566	71.64199	Fotur	Wakhan	37.0	8.0	0.0	0.0	45.0	78.7	17.0	0.0	0.0
304	34.71390	67.82589	Jowzari	Bamyan	0.0	0.0	0.0	0.0	0.0	0.0	0.0	0.0	0.0
305	36.01672	70.67685	Askazir	Kuran Wa Munjan	4.0	10.0	1.0	0.0	15.0	8.5	21.3	2.1	0.0
306	34.95793	67.69366	Dara-i-Gulestan	Kahmard	0.0	0.0	0.0	2.0	2.0	0.0	0.0	0.0	4.3
307	36.40314	70.95071	Tazaknawa	Jurm	0.0	0.0	0.0	1.0	1.0	0.0	0.0	0.0	2.1
308	37.69328	70.67587	Duzd Darrah	Ragh	5.0	13.0	1.0	0.0	19.0	10.6	27.7	2.1	0.0
309	37.78815	71.31526	Mazar Bay Khwaja	Shighnan	3.0	8.0	2.0	0.0	13.0	6.4	17.0	4.3	0.0
310	37.34050	70.67426	Kelklew	Ragh	0.0	3.0	5.0	0.0	8.0	0.0	6.4	10.6	0.0
311	35.98689	70.05999	Aylaqe Ab-anich	Warsaj	2.0	9.0	1.0	0.0	12.0	4.3	19.1	2.1	0.0
312	34.72389	67.66570	Burghasun	Bamyan	0.0	0.0	0.0	1.0	1.0	0.0	0.0	0.0	2.1

Ref no.	Latitude	Longitude	Name	District	Total					Percent			
					Cat 1	Cat 2	Cat 3	Cat 4	All	Cat 1	Cat 2	Cat 3	Cat 4
313	36.49726	70.26506	Darya Mir (1)	Kishim	0.0	3.0	1.0	1.0	5.0	0.0	6.4	2.1	2.1
314	35.72567	69.39726	Gali	Andarab	5.0	8.0	2.0	0.0	15.0	10.6	17.0	4.3	0.0
315	35.05458	67.41322	Taq	Kahmard	0.0	2.0	0.0	1.0	3.0	0.0	4.3	0.0	2.1
316	37.05447	71.17372	Mazar (1)	Baharak	0.0	5.0	2.0	0.0	7.0	0.0	10.6	4.3	0.0
317	36.84599	71.52309	Yakh Daru	Ishkashim	7.0	11.0	1.0	0.0	19.0	14.9	23.4	2.1	0.0
318	34.69649	67.83960	Molla Naw	Bamyan	4.0	8.0	0.0	0.0	12.0	8.5	17.0	0.0	0.0
319	37.00430	73.24249	Rowchun	Wakhan	4.0	4.0	0.0	0.0	8.0	8.5	8.5	0.0	0.0
320	35.72635	69.41261	Kasterash	Andarab	1.0	10.0	0.0	0.0	11.0	2.1	21.3	0.0	0.0
321	34.75509	68.08087	Sokhta	Shibar	0.0	4.0	2.0	0.0	6.0	0.0	8.5	4.3	0.0
322	38.26098	70.81060	Zinjaren	Darwaz	1.0	8.0	1.0	0.0	10.0	2.1	17.0	2.1	0.0
323	37.35301	70.69979	Beduk	Ragh	0.0	3.0	1.0	1.0	5.0	0.0	6.4	2.1	2.1
324	37.35064	70.70023	Worsuk	Ragh	0.0	3.0	1.0	1.0	5.0	0.0	6.4	2.1	2.1
325	37.35676	70.69468	Khwaja Mashtu	Ragh	0.0	3.0	1.0	1.0	5.0	0.0	6.4	2.1	2.1
326	37.97075	70.60528	Pur Zarg	Khwahan	3.0	5.0	0.0	0.0	8.0	6.4	10.6	0.0	0.0
327	36.60064	71.24287	Robat-i-Cheheltan	Baharak	9.0	4.0	0.0	0.0	13.0	19.1	8.5	0.0	0.0
328	38.06135	71.21272	Winwij	Darwaz	7.0	6.0	0.0	0.0	13.0	14.9	12.8	0.0	0.0
329	36.28903	70.61132	Neshi	Jurm	0.0	0.0	0.0	0.0	0.0	0.0	0.0	0.0	0.0
330	37.06000	74.20000	Zamestani Doldol	Wakhan	1.0	7.0	0.0	0.0	8.0	2.1	14.9	0.0	0.0
331	34.65588	68.06873	Pay Kotal	Shibar	1.0	12.0	1.0	0.0	14.0	2.1	25.5	2.1	0.0
332	35.81950	70.83129	Qal`a-i-Shah	Kuran Wa Munjan	0.0	11.0	0.0	0.0	11.0	0.0	23.4	0.0	0.0
333	38.05165	71.23184	Zicharw	Darwaz	4.0	6.0	0.0	0.0	10.0	8.5	12.8	0.0	0.0
334	35.80439	70.82219	Tili	Kuran Wa Munjan	1.0	9.0	0.0	0.0	10.0	2.1	19.1	0.0	0.0
335	36.67470	71.82410	Ork	Wakhan	7.0	5.0	0.0	0.0	12.0	14.9	10.6	0.0	0.0
336	36.51109	71.32854	Keda	Zebak	5.0	5.0	2.0	0.0	12.0	10.6	10.6	4.3	0.0
337	38.38073	71.13263	Mahnaw	Darwaz	0.0	5.0	0.0	0.0	5.0	0.0	10.6	0.0	0.0
338	38.17079	70.53629	Watkhich	Darwaz	2.0	5.0	1.0	0.0	8.0	4.3	10.6	2.1	0.0
339	36.66590	71.70800	Uch Drag	Wakhan	4.0	9.0	0.0	0.0	13.0	8.5	19.1	0.0	0.0
340	35.99611	69.65319	Hazarabay	Khost Wa Firing	2.0	10.0	0.0	0.0	12.0	4.3	21.3	0.0	0.0

Ref no.	Latitude	Longitude	Name	District	Total					Percent			
					Cat 1	Cat 2	Cat 3	Cat 4	All	Cat 1	Cat 2	Cat 3	Cat 4
341	35.81372	68.32880	Khwajabed	Dahana-I- Ghori	0.0	0.0	0.0	1.0	1.0	0.0	0.0	0.0	2.1
342	37.64529	70.50177	Darrah-i-Char	Ragh	1.0	2.0	0.0	0.0	3.0	2.1	4.3	0.0	0.0
343	35.13309	68.19408	Nayak	Tala Wa Barfak	0.0	1.0	0.0	1.0	2.0	0.0	2.1	0.0	2.1
344	38.09198	71.31344	Chiwich	Darwaz	0.0	3.0	2.0	0.0	5.0	0.0	6.4	4.3	0.0
345	37.40508	70.87010	Chaka Khwa	Shahri Buzurg	0.0	4.0	2.0	0.0	6.0	0.0	8.5	4.3	0.0
346	38.33989	70.68999	Bur Ghur	Darwaz	1.0	2.0	1.0	0.0	4.0	2.1	4.3	2.1	0.0
347	37.92307	70.66713	Parkhich	Khwahan	5.0	8.0	0.0	0.0	13.0	10.6	17.0	0.0	0.0
348	37.92490	70.71014	Ghuwiz	Khwahan	1.0	2.0	1.0	0.0	4.0	2.1	4.3	2.1	0.0
349	37.47238	70.34126	Mazek Dasht	Ragh	0.0	0.0	0.0	1.0	1.0	0.0	0.0	0.0	2.1
350	37.92853	70.71624	Zang Zard	Khwahan	3.0	2.0	1.0	0.0	6.0	6.4	4.3	2.1	0.0
351	38.28600	70.80621	Munikharw	Darwaz	1.0	3.0	0.0	0.0	4.0	2.1	6.4	0.0	0.0
352	35.73419	69.43330	Pasha'i	Andarab	0.0	1.0	3.0	0.0	4.0	0.0	2.1	6.4	0.0
353	37.32756	70.73762	Taq Neshash	Ragh	0.0	2.0	2.0	0.0	4.0	0.0	4.3	4.3	0.0
354	36.19640	70.11416	Sare Dehgaz	Warsaj	0.0	4.0	1.0	0.0	5.0	0.0	8.5	2.1	0.0
355	38.38852	70.80457	Ghumay (2)	Darwaz	4.0	5.0	1.0	0.0	10.0	8.5	10.6	2.1	0.0
356	38.38082	71.12137	Wuruf	Darwaz	2.0	6.0	2.0	0.0	10.0	4.3	12.8	4.3	0.0
357	36.45640	70.72875	Dara-I-Kalafazan Deh Bala	Jurm	0.0	1.0	0.0	1.0	2.0	0.0	2.1	0.0	2.1
358	35.36374	67.99583	Ferozak	Kahmard	0.0	1.0	1.0	1.0	3.0	0.0	2.1	2.1	2.1
359	36.02192	70.66901	Warwarzu	Kuran Wa Munjan	3.0	2.0	1.0	0.0	6.0	6.4	4.3	2.1	0.0
360	35.64156	69.56269	Shamaluk	Andarab	0.0	0.0	0.0	1.0	1.0	0.0	0.0	0.0	2.1
361	36.79180	72.01599	Dogor Gunt	Wakhan	3.0	6.0	1.0	1.0	11.0	6.4	12.8	2.1	2.1
362	36.13293	69.69054	Espyan	Khost Wa Firing	1.0	0.0	1.0	0.0	2.0	2.1	0.0	2.1	0.0
363	38.02109	70.53740	Khufak	Khwahan	1.0	1.0	2.0	0.0	4.0	2.1	2.1	4.3	0.0
364	38.43158	70.89146	Paryad	Darwaz	1.0	4.0	1.0	0.0	6.0	2.1	8.5	2.1	0.0
365	37.05169	71.28369	Yasich	Baharak	1.0	1.0	2.0	0.0	4.0	2.1	2.1	4.3	0.0
366	37.34084	70.73784	Zazanwurs	Ragh	0.0	4.0	1.0	0.0	5.0	0.0	8.5	2.1	0.0
367	37.04822	71.27747	Zarghaw	Baharak	1.0	1.0	2.0	0.0	4.0	2.1	2.1	4.3	0.0
368	34.73528	67.62882	Chehel Tan	Bamyan	0.0	0.0	0.0	1.0	1.0	0.0	0.0	0.0	2.1
369	37.45140	70.56038	Zarnud (2)	Ragh	2.0	4.0	1.0	0.0	7.0	4.3	8.5	2.1	0.0

Ref no.	Latitude	Longitude	Name	District	Total					Percent			
					Cat 1	Cat 2	Cat 3	Cat 4	All	Cat 1	Cat 2	Cat 3	Cat 4
370	36.61576	71.18225	Koyak	Baharak	2.0	5.0	0.0	0.0	7.0	4.3	10.6	0.0	0.0
371	37.98914	71.16753	Top	Shighnan	0.0	1.0	2.0	0.0	3.0	0.0	2.1	4.3	0.0
372	37.04257	74.25955	Zimistani Qara Tash	Wakhan	2.0	7.0	1.0	0.0	10.0	4.3	14.9	2.1	0.0
373	37.04912	71.23203	Sela	Baharak	2.0	3.0	2.0	0.0	7.0	4.3	6.4	4.3	0.0
374	37.04586	71.23534	Iwinak	Baharak	2.0	3.0	2.0	0.0	7.0	4.3	6.4	4.3	0.0
375	36.02780	70.78330	Sekwa	Kuran Wa Munjan	3.0	5.0	0.0	0.0	8.0	6.4	10.6	0.0	0.0
376	34.68349	67.97202	Nawjoy	Shibar	4.0	7.0	1.0	0.0	12.0	8.5	14.9	2.1	0.0
377	35.80738	68.38332	Nilan	Dahana-I- Ghori	0.0	0.0	0.0	1.0	1.0	0.0	0.0	0.0	2.1
378	38.34150	70.68489	Fark	Darwaz	0.0	2.0	0.0	0.0	2.0	0.0	4.3	0.0	0.0
379	36.56981	71.39265	Dand	Ishkashim	1.0	6.0	1.0	0.0	8.0	2.1	12.8	2.1	0.0
380	36.42060	70.76115	Gawhar	Jurm	0.0	2.0	0.0	0.0	2.0	0.0	4.3	0.0	0.0
381	36.41600	70.76660	Jaw	Jurm	0.0	2.0	0.0	0.0	2.0	0.0	4.3	0.0	0.0
382	34.71434	67.76152	Jawkar	Bamyan	0.0	3.0	1.0	0.0	4.0	0.0	6.4	2.1	0.0
383	36.01125	70.53354	Yamak	Kuran Wa Munjan	0.0	1.0	0.0	0.0	1.0	0.0	2.1	0.0	0.0
384	37.37034	70.72397	Kushka Darrah	Ragh	1.0	3.0	0.0	0.0	4.0	2.1	6.4	0.0	0.0
385	37.92235	70.70926	Qary-i-Sar	Khwahan	1.0	2.0	0.0	0.0	3.0	2.1	4.3	0.0	0.0
386	36.00673	70.89047	Dasht Parghish	Kuran Wa Munjan	0.0	6.0	0.0	0.0	6.0	0.0	12.8	0.0	0.0
387	37.57270	70.68024	Raghchyan Darrah	Ragh	2.0	5.0	0.0	0.0	7.0	4.3	10.6	0.0	0.0
388	37.98529	70.47992	Kham-i-Ish Darah	Khwahan	1.0	3.0	1.0	0.0	5.0	2.1	6.4	2.1	0.0
389	34.72405	67.78617	Sar Qowl	Bamyan	1.0	1.0	1.0	0.0	3.0	2.1	2.1	2.1	0.0
390	35.47240	69.09940	Chaharmaghzzar	Khinjan	3.0	4.0	0.0	0.0	7.0	6.4	8.5	0.0	0.0
391	37.25375	70.54961	Kaji-i-Kham-i-Pa'in	Fayzabad	0.0	0.0	1.0	0.0	1.0	0.0	0.0	2.1	0.0
392	37.26595	70.55121	Deh-i-Murghan	Fayzabad	0.0	0.0	1.0	0.0	1.0	0.0	0.0	2.1	0.0
393	37.40041	70.73971	Gerd Bad	Ragh	0.0	3.0	1.0	0.0	4.0	0.0	6.4	2.1	0.0
394	37.00500	73.44949	Sarhad	Wakhan	0.0	6.0	1.0	0.0	7.0	0.0	12.8	2.1	0.0
395	35.78920	69.27630	Gelasdara	Andarab	0.0	0.0	1.0	0.0	1.0	0.0	0.0	2.1	0.0
396	36.19422	70.10457	Petaw	Warsaj	0.0	0.0	1.0	0.0	1.0	0.0	0.0	2.1	0.0
397	36.59180	71.44469	Uspu	Ishkashim	0.0	0.0	0.0	0.0	0.0	0.0	0.0	0.0	0.0

Ref no.	Latitude	Longitude	Name	District	Total					Percent			
					Cat 1	Cat 2	Cat 3	Cat 4	All	Cat 1	Cat 2	Cat 3	Cat 4
398	37.93118	70.71967	Duraj	Khwahan	1.0	1.0	1.0	0.0	3.0	2.1	2.1	2.1	0.0
399	36.63723	71.14480	Deh Qalat	Baharak	3.0	5.0	0.0	0.0	8.0	6.4	10.6	0.0	0.0
400	38.28548	70.82793	Zir-e Pol-e Juy	Darwaz	0.0	1.0	0.0	0.0	1.0	0.0	2.1	0.0	0.0
401	38.28038	70.82593	Band	Darwaz	0.0	1.0	0.0	0.0	1.0	0.0	2.1	0.0	0.0
402	37.99649	70.49219	Nasher	Khwahan	0.0	2.0	1.0	0.0	3.0	0.0	4.3	2.1	0.0
403	37.66888	70.46012	Waji Kil	Fayzabad	0.0	3.0	0.0	0.0	3.0	0.0	6.4	0.0	0.0
404	38.38238	71.10125	Iwdan	Darwaz	0.0	3.0	0.0	0.0	3.0	0.0	6.4	0.0	0.0
405	36.55813	71.35065	Dag Khana	Baharak	0.0	6.0	0.0	0.0	6.0	0.0	12.8	0.0	0.0
406	37.05150	71.10014	Arghand	Baharak	6.0	5.0	0.0	0.0	11.0	12.8	10.6	0.0	0.0
407	37.05619	71.09345	Pijangiw	Baharak	6.0	5.0	0.0	0.0	11.0	12.8	10.6	0.0	0.0
408	37.05853	71.10015	Shuhada	Baharak	6.0	5.0	0.0	0.0	11.0	12.8	10.6	0.0	0.0
409	37.05505	71.09440	Ybaba Kakan	Baharak	6.0	5.0	0.0	0.0	11.0	12.8	10.6	0.0	0.0
410	35.00840	67.08419	Kochokak	Yakawlang	1.0	3.0	1.0	0.0	5.0	2.1	6.4	2.1	0.0
411	37.98746	70.45745	Wargh	Khwahan	1.0	1.0	1.0	0.0	3.0	2.1	2.1	2.1	0.0
412	37.03299	71.42774	Andoj	Ishkashim	1.0	2.0	1.0	0.0	4.0	2.1	4.3	2.1	0.0
413	37.49514	70.57036	Shepu-i-Pa’in	Ragh	0.0	0.0	1.0	0.0	1.0	0.0	0.0	2.1	0.0
414	37.84425	71.33275	Rundan Darrah	Shighnan	4.0	5.0	0.0	0.0	9.0	8.5	10.6	0.0	0.0
415	38.39050	70.70589	Zamin-i-Zawasf	Darwaz	0.0	3.0	0.0	0.0	3.0	0.0	6.4	0.0	0.0
416	36.12507	69.67341	Dehe Naw	Khost Wa Firing	1.0	4.0	0.0	0.0	5.0	2.1	8.5	0.0	0.0
417	37.33110	70.72741	Deh-i-Beland (1)	Ragh	2.0	2.0	1.0	0.0	5.0	4.3	4.3	2.1	0.0
418	38.14195	71.28107	Ghumay (3)	Darwaz	2.0	3.0	0.0	0.0	5.0	4.3	6.4	0.0	0.0
419	36.60083	71.38586	Zar Khan	Ishkashim	2.0	1.0	1.0	0.0	4.0	4.3	2.1	2.1	0.0
420	36.68824	71.14297	Orchi Targnan	Baharak	1.0	5.0	0.0	0.0	6.0	2.1	10.6	0.0	0.0
421	36.83268	70.43536	Deh Miyana	Fayzabad	0.0	0.0	0.0	0.0	0.0	0.0	0.0	0.0	0.0
422	37.25044	70.70876	Khmi Sarbana	Fayzabad	1.0	4.0	0.0	0.0	5.0	2.1	8.5	0.0	0.0
423	37.93210	70.29023	Guzun	Khwahan	2.0	4.0	0.0	0.0	6.0	4.3	8.5	0.0	0.0
424	35.36156	67.51589	Dehe Tajek	Kahmard	0.0	4.0	0.0	0.0	4.0	0.0	8.5	0.0	0.0
425	37.05170	71.08451	Yabab	Baharak	4.0	4.0	0.0	0.0	8.0	8.5	8.5	0.0	0.0
426	36.68088	71.12501	Alezhgerew	Baharak	1.0	4.0	0.0	0.0	5.0	2.1	8.5	0.0	0.0
427	36.66982	71.76736	Qazi Deh (1)	Wakhan	5.0	9.0	0.0	0.0	14.0	10.6	19.1	0.0	0.0

Ref no.	Latitude	Longitude	Name	District	Total					Percent			
					Cat 1	Cat 2	Cat 3	Cat 4	All	Cat 1	Cat 2	Cat 3	Cat 4
428	37.68180	70.64326	Khalichot	Ragh	0.0	3.0	0.0	0.0	3.0	0.0	6.4	0.0	0.0
429	34.75607	67.58043	Ladu	Bamyan	0.0	0.0	1.0	0.0	1.0	0.0	0.0	2.1	0.0
430	35.74100	69.31079	Kharpushta	Andarab	0.0	0.0	0.0	0.0	0.0	0.0	0.0	0.0	0.0
431	38.23194	70.97623	Mizak	Darwaz	0.0	1.0	1.0	0.0	2.0	0.0	2.1	2.1	0.0
432	37.46767	70.54877	Wakhirdew	Ragh	0.0	0.0	1.0	0.0	1.0	0.0	0.0	2.1	0.0
433	36.48539	70.27161	Hasrat	Kishim	2.0	1.0	1.0	0.0	4.0	4.3	2.1	2.1	0.0
434	37.28544	71.47897	Tibinak	Shighnan	0.0	0.0	0.0	0.0	0.0	0.0	0.0	0.0	0.0
435	37.05296	71.18194	Wala	Baharak	1.0	2.0	1.0	0.0	4.0	2.1	4.3	2.1	0.0
436	36.82283	72.08276	Kashkandyow	Wakhan	0.0	2.0	1.0	0.0	3.0	0.0	4.3	2.1	0.0
437	38.26915	70.81593	Deh-i-Mad	Darwaz	1.0	1.0	1.0	0.0	3.0	2.1	2.1	2.1	0.0
438	36.64560	71.13782	Sarask (2)	Baharak	1.0	3.0	0.0	0.0	4.0	2.1	6.4	0.0	0.0
439	37.58578	70.67950	Chedek Dur	Ragh	2.0	4.0	0.0	0.0	6.0	4.3	8.5	0.0	0.0
440	37.25524	70.71167	Kara Sakh	Fayzabad	1.0	4.0	0.0	0.0	5.0	2.1	8.5	0.0	0.0
441	34.85168	67.66752	Khawale Eslam	Bamyan	0.0	0.0	0.0	0.0	0.0	0.0	0.0	0.0	0.0
442	35.98878	69.68057	Jaladan	Khost Wa Firing	3.0	2.0	0.0	0.0	5.0	6.4	4.3	0.0	0.0
443	35.79095	69.34318	Shashan	Andarab	0.0	4.0	0.0	0.0	4.0	0.0	8.5	0.0	0.0
444	37.54568	70.58920	Rabat	Ragh	1.0	1.0	1.0	0.0	3.0	2.1	2.1	2.1	0.0
445	38.28800	70.81781	Ab Band Matkat	Darwaz	0.0	0.0	0.0	0.0	0.0	0.0	0.0	0.0	0.0
446	35.36381	67.50854	Dehe Myana	Kahmard	0.0	3.0	0.0	0.0	3.0	0.0	6.4	0.0	0.0
447	37.12541	70.84871	Gawayla	Baharak	1.0	0.0	1.0	0.0	2.0	2.1	0.0	2.1	0.0
448	38.25861	71.31901	Delwakh (2)	Darwaz	1.0	1.0	1.0	0.0	3.0	2.1	2.1	2.1	0.0
449	37.55081	70.39086	Yustan	Ragh	0.0	0.0	1.0	0.0	1.0	0.0	0.0	2.1	0.0
450	37.47581	70.54627	Chika Kham	Ragh	0.0	0.0	1.0	0.0	1.0	0.0	0.0	2.1	0.0
451	37.04541	71.09402	Ab Cheshma	Baharak	4.0	3.0	0.0	0.0	7.0	8.5	6.4	0.0	0.0
452	35.02771	68.13212	Qarnala	Shibar	0.0	0.0	1.0	0.0	1.0	0.0	0.0	2.1	0.0
453	37.24232	71.47070	Androb	Ishkashim	0.0	2.0	0.0	0.0	2.0	0.0	4.3	0.0	0.0
454	36.85130	71.51619	Sher	Ishkashim	4.0	0.0	0.0	0.0	4.0	8.5	0.0	0.0	0.0
455	37.34017	70.72373	Khambew-i-Bala	Ragh	0.0	3.0	0.0	0.0	3.0	0.0	6.4	0.0	0.0
456	35.71952	69.38454	Gadalak	Andarab	1.0	5.0	0.0	0.0	6.0	2.1	10.6	0.0	0.0
457	37.34710	70.71205	Khambew-i-Pa'in	Ragh	0.0	3.0	0.0	0.0	3.0	0.0	6.4	0.0	0.0

Ref no.	Latitude	Longitude	Name	District	Total					Percent			
					Cat 1	Cat 2	Cat 3	Cat 4	All	Cat 1	Cat 2	Cat 3	Cat 4
458	35.26764	68.39951	Shakh Mazar	Tala Wa Barfak	0.0	0.0	1.0	0.0	1.0	0.0	0.0	2.1	0.0
459	36.19834	70.22856	Poshostan	Warsaj	0.0	0.0	1.0	0.0	1.0	0.0	0.0	2.1	0.0
460	37.91970	70.70264	Raj	Khwahan	0.0	3.0	0.0	0.0	3.0	0.0	6.4	0.0	0.0
461	36.64149	71.15268	Safid Darreh	Baharak	2.0	3.0	0.0	0.0	5.0	4.3	6.4	0.0	0.0
462	37.58228	70.66830	Manjin Dur	Ragh	2.0	3.0	0.0	0.0	5.0	4.3	6.4	0.0	0.0
463	37.04936	71.17994	Unar	Baharak	1.0	1.0	1.0	0.0	3.0	2.1	2.1	2.1	0.0
464	37.65872	70.61681	Walek	Ragh	0.0	2.0	0.0	0.0	2.0	0.0	4.3	0.0	0.0
465	37.66406	70.61855	Wor Sendur	Ragh	0.0	2.0	0.0	0.0	2.0	0.0	4.3	0.0	0.0
466	34.99640	67.15859	Zardigah	Yakawlang	0.0	0.0	0.0	0.0	0.0	0.0	0.0	0.0	0.0
467	37.00359	73.33035	Issik	Wakhan	0.0	0.0	2.0	0.0	2.0	0.0	0.0	4.3	0.0
468	37.04046	74.32930	Zimistani Dawan Su	Wakhan	1.0	1.0	1.0	0.0	3.0	2.1	2.1	2.1	0.0
469	35.47950	69.13429	Kuhnadeh	Khinjan	0.0	0.0	1.0	0.0	1.0	0.0	0.0	2.1	0.0
470	37.24884	70.70650	Sar Band	Fayzabad	1.0	3.0	0.0	0.0	4.0	2.1	6.4	0.0	0.0
471	37.04499	71.20834	Yababuk	Baharak	1.0	3.0	0.0	0.0	4.0	2.1	6.4	0.0	0.0
472	36.18740	70.14870	Pazek	Warsaj	1.0	3.0	0.0	0.0	4.0	2.1	6.4	0.0	0.0
473	38.06302	71.23923	Wusan	Darwaz	1.0	2.0	0.0	0.0	3.0	2.1	4.3	0.0	0.0
474	37.44643	70.55966	Selat	Ragh	0.0	1.0	0.0	0.0	1.0	0.0	2.1	0.0	0.0
475	37.58134	70.64433	Kham-i-Shahan	Ragh	0.0	0.0	0.0	0.0	0.0	0.0	0.0	0.0	0.0
476	37.01000	73.57000	Zemestani Baharak	Wakhan	0.0	0.0	1.0	0.0	1.0	0.0	0.0	2.1	0.0
477	37.81549	70.31790	Bariki	Khwahan	6.0	1.0	0.0	0.0	7.0	12.8	2.1	0.0	0.0
478	37.37801	70.70979	Shekh-i-Mast	Ragh	0.0	0.0	1.0	0.0	1.0	0.0	0.0	2.1	0.0
479	36.53778	70.28721	Kawari	Kishim	1.0	0.0	1.0	0.0	2.0	2.1	0.0	2.1	0.0
480	38.00610	70.54220	Pashar	Khwahan	0.0	2.0	0.0	0.0	2.0	0.0	4.3	0.0	0.0
481	34.63362	68.02911	Syahsangak	Hisa-I- Awali Bihsud	0.0	2.0	0.0	0.0	2.0	0.0	4.3	0.0	0.0
482	37.05088	71.21786	Sarasak	Baharak	0.0	3.0	0.0	0.0	3.0	0.0	6.4	0.0	0.0
483	37.48397	70.58801	Shepu-i-Bala	Ragh	0.0	2.0	0.0	0.0	2.0	0.0	4.3	0.0	0.0
484	36.95750	72.33659	Yozuk	Wakhan	1.0	1.0	0.0	0.0	2.0	2.1	2.1	0.0	0.0
485	36.12467	69.65500	Mirangana	Khost Wa Firing	0.0	2.0	0.0	0.0	2.0	0.0	4.3	0.0	0.0
486	37.04908	71.26221	Dasht	Baharak	0.0	2.0	0.0	0.0	2.0	0.0	4.3	0.0	0.0

Ref no.	Latitude	Longitude	Name	District	Total					Percent			
					Cat 1	Cat 2	Cat 3	Cat 4	All	Cat 1	Cat 2	Cat 3	Cat 4
487	37.04250	71.25087	Tarwaza	Baharak	0.0	2.0	0.0	0.0	2.0	0.0	4.3	0.0	0.0
488	37.57918	70.67862	Sar-i-Buqi	Ragh	2.0	3.0	0.0	0.0	5.0	4.3	6.4	0.0	0.0
489	36.11787	69.65386	Mulwar	Khost Wa Firing	0.0	2.0	0.0	0.0	2.0	0.0	4.3	0.0	0.0
490	36.62155	71.19029	Abdaw	Baharak	0.0	1.0	0.0	0.0	1.0	0.0	2.1	0.0	0.0
491	37.01000	73.38000	Karkat	Wakhan	0.0	0.0	0.0	0.0	0.0	0.0	0.0	0.0	0.0
492	35.55004	69.48498	Darrahe Shu	Andarab	0.0	0.0	1.0	0.0	1.0	0.0	0.0	2.1	0.0
493	35.77350	69.31633	Qajghari	Andarab	0.0	2.0	0.0	0.0	2.0	0.0	4.3	0.0	0.0
494	37.61998	70.59809	Kalar-i-Pain	Ragh	0.0	2.0	0.0	0.0	2.0	0.0	4.3	0.0	0.0
495	37.58559	70.61801	Nawabad-i-Seh Ab	Ragh	0.0	1.0	0.0	0.0	1.0	0.0	2.1	0.0	0.0
496	36.55318	71.37589	Naw Abad	Zebak	0.0	1.0	0.0	0.0	1.0	0.0	2.1	0.0	0.0
497	35.83790	70.84419	Panam	Kuran Wa Munjan	1.0	2.0	0.0	0.0	3.0	2.1	4.3	0.0	0.0
498	35.09940	68.01353	Dahane Reshqaw	Kahmard	0.0	0.0	1.0	0.0	1.0	0.0	0.0	2.1	0.0
499	35.19448	68.33958	Dahan Lakhshanak	Tala Wa Barfak	0.0	1.0	0.0	0.0	1.0	0.0	2.1	0.0	0.0
500	37.58448	70.62305	Darrah-i-Sabahi	Ragh	0.0	1.0	0.0	0.0	1.0	0.0	2.1	0.0	0.0
501	38.38954	70.84057	Zahghar	Darwaz	0.0	1.0	0.0	0.0	1.0	0.0	2.1	0.0	0.0
502	38.29709	70.82434	Kerawar	Darwaz	0.0	1.0	0.0	0.0	1.0	0.0	2.1	0.0	0.0
503	35.84250	70.84579	Yeghdak	Kuran Wa Munjan	1.0	2.0	0.0	0.0	3.0	2.1	4.3	0.0	0.0
504	38.28261	70.81679	Ur Gaz	Darwaz	1.0	1.0	0.0	0.0	2.0	2.1	2.1	0.0	0.0
505	37.58711	70.66863	Jerin Dur	Ragh	2.0	1.0	0.0	0.0	3.0	4.3	2.1	0.0	0.0
506	38.28131	70.81732	Kul	Darwaz	1.0	1.0	0.0	0.0	2.0	2.1	2.1	0.0	0.0
507	36.62776	71.36887	Gharib	Ishkashim	0.0	0.0	1.0	0.0	1.0	0.0	0.0	2.1	0.0
508	35.09398	68.01115	Dahane Bisrak	Kahmard	0.0	0.0	1.0	0.0	1.0	0.0	0.0	2.1	0.0
509	36.63037	71.14955	Kazdeh	Baharak	2.0	2.0	0.0	0.0	4.0	4.3	4.3	0.0	0.0
510	38.01601	71.28503	Sadwad	Darwaz	0.0	1.0	0.0	0.0	1.0	0.0	2.1	0.0	0.0
511	36.99355	70.66811	Pata Guzar	Jurm	0.0	0.0	0.0	0.0	0.0	0.0	0.0	0.0	0.0
512	36.25563	70.19153	Emend	Warsaj	0.0	0.0	1.0	0.0	1.0	0.0	0.0	2.1	0.0
513	37.04373	71.20351	Suchu	Baharak	1.0	2.0	0.0	0.0	3.0	2.1	4.3	0.0	0.0
514	36.45645	70.25591	Robat (2)	Kishim	0.0	2.0	0.0	0.0	2.0	0.0	4.3	0.0	0.0

Ref no.	Latitude	Longitude	Name	District	Total					Percent			
					Cat 1	Cat 2	Cat 3	Cat 4	All	Cat 1	Cat 2	Cat 3	Cat 4
515	35.61797	69.54688	Dahane Qaza	Andarab	0.0	1.0	0.0	0.0	1.0	0.0	2.1	0.0	0.0
516	36.03362	69.73060	Chaharqeshlaq	Khost Wa Firing	0.0	2.0	0.0	0.0	2.0	0.0	4.3	0.0	0.0
517	34.71976	67.60818	Zard Khaval	Bamyan	0.0	0.0	1.0	0.0	1.0	0.0	0.0	2.1	0.0
518	35.62486	69.54846	Tajekan	Andarab	0.0	1.0	0.0	0.0	1.0	0.0	2.1	0.0	0.0
519	35.40035	67.81151	Madr	Kahmard	0.0	1.0	0.0	0.0	1.0	0.0	2.1	0.0	0.0
520	38.25362	70.91582	Vod Ab	Darwaz	0.0	2.0	0.0	0.0	2.0	0.0	4.3	0.0	0.0
521	38.04609	71.28149	Rawand	Darwaz	0.0	1.0	0.0	0.0	1.0	0.0	2.1	0.0	0.0
522	36.48645	70.76974	Sarsabil	Jurm	0.0	1.0	0.0	0.0	1.0	0.0	2.1	0.0	0.0
523	34.99318	67.93523	Dahane Shakhe Taka	Shibar	0.0	1.0	0.0	0.0	1.0	0.0	2.1	0.0	0.0
524	37.36124	70.69484	Sar-i-Sang (2)	Ragh	0.0	2.0	0.0	0.0	2.0	0.0	4.3	0.0	0.0
525	34.99079	67.94663	Anvah-ye Kalan	Shibar	0.0	1.0	0.0	0.0	1.0	0.0	2.1	0.0	0.0
526	36.90319	71.48770	Walij (2)	Ishkashim	0.0	1.0	0.0	0.0	1.0	0.0	2.1	0.0	0.0
527	36.69284	71.14083	Pan Deh Targnan	Baharak	1.0	2.0	0.0	0.0	3.0	2.1	4.3	0.0	0.0
528	36.54015	70.66802	Khash	Jurm	0.0	1.0	0.0	0.0	1.0	0.0	2.1	0.0	0.0
529	37.05706	71.20068	Yakhchew	Baharak	1.0	1.0	0.0	0.0	2.0	2.1	2.1	0.0	0.0
530	35.05432	67.96787	Mahmadkecha	Shibar	0.0	1.0	0.0	0.0	1.0	0.0	2.1	0.0	0.0
531	36.62480	71.42699	Surkh Dara	Ishkashim	1.0	2.0	1.0	0.0	4.0	2.1	4.3	2.1	0.0
532	35.76607	69.31971	Mirbaya	Andarab	0.0	1.0	0.0	0.0	1.0	0.0	2.1	0.0	0.0
533	37.39131	70.68066	Sheblan Jel	Ragh	0.0	1.0	0.0	0.0	1.0	0.0	2.1	0.0	0.0
534	37.82919	70.30846	Bostanak	Khwahan	0.0	1.0	0.0	0.0	1.0	0.0	2.1	0.0	0.0
535	38.06849	70.50509	Shipun	Khwahan	1.0	1.0	0.0	0.0	2.0	2.1	2.1	0.0	0.0
536	37.54100	70.56370	Bashidew	Ragh	0.0	2.0	0.0	0.0	2.0	0.0	4.3	0.0	0.0
537	34.94298	67.96726	Dehradza	Shibar	0.0	0.0	0.0	0.0	0.0	0.0	0.0	0.0	0.0
538	37.55972	70.61602	Dega	Ragh	1.0	1.0	0.0	0.0	2.0	2.1	2.1	0.0	0.0
539	37.57473	70.61429	Kalarek	Ragh	1.0	1.0	0.0	0.0	2.0	2.1	2.1	0.0	0.0
540	38.31216	70.84345	Arun	Darwaz	0.0	1.0	0.0	0.0	1.0	0.0	2.1	0.0	0.0
541	36.50249	70.26242	Darya Mir (2)	Kishim	0.0	1.0	0.0	0.0	1.0	0.0	2.1	0.0	0.0
542	34.82500	67.82719	Shekh Rezah	Bamyan	0.0	1.0	0.0	0.0	1.0	0.0	2.1	0.0	0.0
543	35.40389	68.99709	Doshakh	Khinjan	0.0	1.0	0.0	0.0	1.0	0.0	2.1	0.0	0.0
544	37.36641	70.46366	Ujikel	Fayzabad	1.0	1.0	0.0	0.0	2.0	2.1	2.1	0.0	0.0

Ref no.	Latitude	Longitude	Name	District	Total					Percent			
					Cat 1	Cat 2	Cat 3	Cat 4	All	Cat 1	Cat 2	Cat 3	Cat 4
545	34.99877	67.82051	Kandeh Sang	Shibar	1.0	1.0	0.0	0.0	2.0	2.1	2.1	0.0	0.0
546	37.04351	71.26187	Yawach	Baharak	0.0	1.0	0.0	0.0	1.0	0.0	2.1	0.0	0.0
547	36.72127	70.44957	Nawaran	Kishim	0.0	1.0	0.0	0.0	1.0	0.0	2.1	0.0	0.0
548	36.72276	70.44427	Ghuri Sang	Kishim	0.0	1.0	0.0	0.0	1.0	0.0	2.1	0.0	0.0
549	37.35862	70.46587	Shael	Fayzabad	1.0	1.0	0.0	0.0	2.0	2.1	2.1	0.0	0.0
550	34.82178	67.82502	Bamyan	Bamyan	0.0	1.0	0.0	0.0	1.0	0.0	2.1	0.0	0.0
551	34.70719	67.84219	Mulgar	Bamyan	0.0	1.0	0.0	0.0	1.0	0.0	2.1	0.0	0.0
552	38.30772	70.89477	Daraw	Darwaz	0.0	0.0	0.0	0.0	0.0	0.0	0.0	0.0	0.0
553	36.71665	70.45259	Khush Dam	Kishim	0.0	1.0	0.0	0.0	1.0	0.0	2.1	0.0	0.0
554	36.56303	71.38730	Hazrati Dawud	Baharak	2.0	1.0	0.0	0.0	3.0	4.3	2.1	0.0	0.0
555	34.82707	67.82511	Shikh Reza	Bamyan	0.0	1.0	0.0	0.0	1.0	0.0	2.1	0.0	0.0
556	34.82976	67.83492	Dawoodi	Bamyan	0.0	1.0	0.0	0.0	1.0	0.0	2.1	0.0	0.0
557	34.83292	67.83316	Bute Shamame	Bamyan	0.0	1.0	0.0	0.0	1.0	0.0	2.1	0.0	0.0
558	36.61488	71.37451	Razrak	Ishkashim	0.0	0.0	1.0	0.0	1.0	0.0	0.0	2.1	0.0
559	38.12788	71.29169	Ablun	Darwaz	0.0	1.0	0.0	0.0	1.0	0.0	2.1	0.0	0.0
560	34.65382	68.01217	Sare Gharghara	Shibar	1.0	1.0	0.0	0.0	2.0	2.1	2.1	0.0	0.0
561	34.83019	67.82669	Bute Salsal	Bamyan	0.0	1.0	0.0	0.0	1.0	0.0	2.1	0.0	0.0
562	37.05010	71.22237	Azrew	Baharak	0.0	1.0	0.0	0.0	1.0	0.0	2.1	0.0	0.0
563	37.06012	71.10261	Dani Deh	Baharak	2.0	1.0	0.0	0.0	3.0	4.3	2.1	0.0	0.0
564	37.66623	70.62634	Tajel Darrah	Ragh	0.0	1.0	0.0	0.0	1.0	0.0	2.1	0.0	0.0
565	37.47094	70.61433	Pas Pul	Ragh	0.0	2.0	0.0	0.0	2.0	0.0	4.3	0.0	0.0
566	34.65791	68.00748	Saryak	Shibar	1.0	1.0	0.0	0.0	2.0	2.1	2.1	0.0	0.0
567	36.14994	70.34812	Piw	Warsaj	0.0	1.0	0.0	0.0	1.0	0.0	2.1	0.0	0.0
568	36.43304	69.60719	Mandakan	Chal	0.0	0.0	0.0	0.0	0.0	0.0	0.0	0.0	0.0
569	35.62559	69.44961	Dehyak	Andarab	1.0	1.0	0.0	0.0	2.0	2.1	2.1	0.0	0.0
570	36.45453	70.78475	Langar	Jurm	1.0	1.0	0.0	0.0	2.0	2.1	2.1	0.0	0.0
571	35.98219	70.90409	Malesheja	Kuran Wa Munjan	0.0	2.0	0.0	0.0	2.0	0.0	4.3	0.0	0.0
572	36.45734	70.77911	Raagh	Jurm	1.0	1.0	0.0	0.0	2.0	2.1	2.1	0.0	0.0
573	36.13750	70.28531	Royandara	Warsaj	0.0	1.0	0.0	0.0	1.0	0.0	2.1	0.0	0.0
574	36.49134	70.47743	Arghenchkha	Kishim	1.0	2.0	0.0	0.0	3.0	2.1	4.3	0.0	0.0

Ref no.	Latitude	Longitude	Name	District	Total					Percent			
					Cat 1	Cat 2	Cat 3	Cat 4	All	Cat 1	Cat 2	Cat 3	Cat 4
575	37.64595	70.57789	Gor Dur	Ragh	1.0	1.0	0.0	0.0	2.0	2.1	2.1	0.0	0.0
576	37.55739	70.37012	Tyael	Ragh	0.0	0.0	0.0	0.0	0.0	0.0	0.0	0.0	0.0
577	37.22352	70.76721	Kulan	Fayzabad	1.0	1.0	0.0	0.0	2.0	2.1	2.1	0.0	0.0
578	35.02069	67.09209	Syahkhaki	Yakawlang	0.0	1.0	0.0	0.0	1.0	0.0	2.1	0.0	0.0
579	34.99610	67.82909	Seh Dewar	Shibar	1.0	1.0	0.0	0.0	2.0	2.1	2.1	0.0	0.0
580	36.48396	70.26453	Ajel	Kishim	2.0	0.0	0.0	0.0	2.0	4.3	0.0	0.0	0.0
581	36.46224	70.77977	Markaz Hazrat Sayed	Jurm	1.0	1.0	0.0	0.0	2.0	2.1	2.1	0.0	0.0
582	37.64825	70.60255	Tenilar	Ragh	0.0	1.0	0.0	0.0	1.0	0.0	2.1	0.0	0.0
583	37.04338	71.22784	Syahi	Baharak	0.0	0.0	0.0	0.0	0.0	0.0	0.0	0.0	0.0
584	38.41418	70.81670	Darwaz (Nusay)	Darwaz	0.0	1.0	0.0	0.0	1.0	0.0	2.1	0.0	0.0
585	37.05611	71.19891	Doha	Baharak	1.0	0.0	0.0	0.0	1.0	2.1	0.0	0.0	0.0
586	35.61615	69.46996	Puli Hisar	Andarab	0.0	1.0	0.0	0.0	1.0	0.0	2.1	0.0	0.0
587	37.08225	70.42717	Hazar Mishi	Fayzabad	0.0	1.0	0.0	0.0	1.0	0.0	2.1	0.0	0.0
588	36.45995	70.77908	Hazrat-e Sa'id	Jurm	1.0	1.0	0.0	0.0	2.0	2.1	2.1	0.0	0.0
589	38.16713	71.26143	Supaj	Darwaz	0.0	1.0	0.0	0.0	1.0	0.0	2.1	0.0	0.0
590	37.76870	70.45629	Lal Margh	Khwahan	0.0	1.0	0.0	0.0	1.0	0.0	2.1	0.0	0.0
591	37.46271	70.67154	Safed Jeraw	Ragh	0.0	1.0	0.0	0.0	1.0	0.0	2.1	0.0	0.0
592	34.63844	68.04082	Jemati	Hisa-I- Awali Bihsud	0.0	0.0	0.0	0.0	0.0	0.0	0.0	0.0	0.0
593	35.62485	69.46495	Piransamya	Andarab	1.0	1.0	0.0	0.0	2.0	2.1	2.1	0.0	0.0
594	36.81524	72.05821	Urgand	Wakhan	0.0	1.0	0.0	0.0	1.0	0.0	2.1	0.0	0.0
595	38.31309	70.82391	Waryak	Darwaz	0.0	0.0	0.0	0.0	0.0	0.0	0.0	0.0	0.0
596	34.90499	68.03347	Shekari	Bamyan	1.0	0.0	0.0	0.0	1.0	2.1	0.0	0.0	0.0
597	35.36068	67.47255	Sare Shahr	Kahmard	0.0	1.0	0.0	0.0	1.0	0.0	2.1	0.0	0.0
598	35.08741	67.44972	Dame Jangal	Kahmard	1.0	0.0	0.0	0.0	1.0	2.1	0.0	0.0	0.0
599	37.76408	70.38061	Bed Khah (2)	Khwahan	0.0	0.0	0.0	0.0	0.0	0.0	0.0	0.0	0.0
600	37.05752	71.19891	Doha Bala	Baharak	1.0	0.0	0.0	0.0	1.0	2.1	0.0	0.0	0.0
601	36.69400	71.14552	Bini Jar	Baharak	0.0	1.0	0.0	0.0	1.0	0.0	2.1	0.0	0.0
602	37.06352	71.10759	Madrasah	Baharak	2.0	0.0	0.0	0.0	2.0	4.3	0.0	0.0	0.0
603	37.06544	71.10732	Sherkan	Baharak	1.0	0.0	0.0	0.0	1.0	2.1	0.0	0.0	0.0
604	38.38743	71.12253	Pun Shahr	Darwaz	0.0	1.0	0.0	0.0	1.0	0.0	2.1	0.0	0.0

Appendix 4. Ecosystem Supplementary Methods & Results

Changes in rangeland condition

S AC

Satellite observations and grassland classification

The analysis was conducted using all atmospherically corrected surface reflectance images from Landsat 7 ETM+ and 8 OLI Collection 1 Tier 1 products (30 m spatial resolution) between 2000-2020 in Google Earth Engine (GEE) (Gorelick et al. 2017). The Quality Assessment band was used to remove pixels flagged as containing clouds, cloud shadows, or snow (Zhu and Woodcock 2012), and followed established approaches to appropriately combine ETM+ and OLI scenes for further analysis (Roy et al. 2016).

A custom land cover classification was developed to identify grasslands in the P-ARB using a random forest classification of Landsat 8 imagery from June to September 2018, which was trained and validated for accuracy using primary field observations of land cover types. All areas that were not identified as grasslands were masked out and excluded from analysis.

Spectral mixture analysis, cumulative endmember fractions, and vegetation loss

Spectral mixture analysis (SMA) (Adams et al. 1986) was used to calculate cumulative endmember fractions to determine vegetation loss within three distinct pathways (green vegetation loss, non-photosynthetic (dry) vegetation loss, and desiccation) following existing approaches (Lewińska et al. 2020). For the SMA, spectra were used to distinguish four endmembers (green vegetation, dry vegetation, soil, and shade), which were derived from multiple sources, and which have been used to document grassland changes in dryland ecosystems (Sonnenschein et al. 2011, Suess et al. 2018). For green vegetation, 'pure' green pixels were identified by calculating the Pixel Purity Index for each Landsat scene during the period of peak greenness (June through September), targeting regions of known complete green vegetation based on field surveys. For dry vegetation, spectra from the Ecological Spectral Information System (EcoSIS) Spectral Library (https://www.ecosis.org) were used. For soil, spectra from the ICRAF-ISRIC Soil VNIR Spectral Library (https://data.worldagroforestry.org/dataset.xhtml?persistentId=doi:10.34725/DVN/MFHA9C) were used. For shade, a value of 0.0001 was used to approximate zero reflectance while facilitating unmixing computations in GEE that cannot accommodate true zeros. The selection of endmembers was finalized by choosing candidate spectra from each endmember that had minimal correlations with each other (Van der Meer and Jia 2012).

Once spectra were finalized, constrained and non-negative SMA was applied to all Landsat scenes available during the peak of greenness as defined above and aggregated to monthly values, using the set of endmember fractions with the highest green vegetation value when there were multiple observations within a month. For months with missing values, a weighted Whittaker smoother (Whittaker 1922) was applied to fill these values following a three-pass process with slight modifications to previous applications to improve the weighting procedure (Kong et al. 2019). The process allows missing values to be filled in using observations from broader temporal extents and weights them according to observational quality, while preserving the general form of the monthly time series (Atkinson et al. 2012). In the first pass, data are filled by calculating the median value of a given month using a five-year moving window and applying a weight of 0.6. In the second pass, data are filled by calculating the median value of a given month over the whole time period (2000-2020) and applying a weight of 0.4. In the third and final pass, any remaining missing data are filled with the last observed value preceding the given month and applied a weight of 0.3.

The resulting monthly endmember fraction timeseries was aggregated to annual values by summing each monthly endmember fraction within a year to produce cumulative endmember fractions (CEFs). Values were then rescaled from 0 to 1 to aid interpretation (dry vegetation and shade endmembers were combined at this stage following Lewińska et al. (2020) (Figure 81). To determine vegetation dynamics over the 20-year time period, LandTrendr (Kennedy et al. 2018) was run using the green vegetation CEFs and used the following definitions for detecting trends: temporal trends were set to a minimum of three years and with a minimum of one year gap, and trends were only considered when green vegetation CEFs declined by a minimum of 20% of the maximum value at the pixel level. Thus, over the 21-year time period of the analysis, a maximum of five trend periods was possible. To account for co-registration errors, a minimum mapping unit of 11 pixels (~1 ha) was applied. Finally, negative trends, which signify vegetation degradation or loss episodes, were assessed for three distinct degradation pathways by analyzing shifts in starting and ending endmember fractions for a given degradation episode. Three degradation pathways were assessed: (*i*) green vegetation loss by analyzing shifts from green vegetation fractions to soil fractions; (*ii*) dry vegetation loss by analyzing shifts from dry vegetation fractions to soil fractions; and (*iii*) vegetation desiccation by analyzing shifts from green vegetation fractions to dry vegetation fractions.

For each of the three degradation pathways, a suite of metrics was calculated to characterize each degradation episode in terms of its location, onset, duration, and magnitude. The onset was defined as the first year of a detected trend. The duration was defined as the number of years between onset and the last year of the trend (inclusive). The magnitude was defined as the absolute difference in CEF values between onset and the last year of the trend, but used data from the SMA rather than the LandTrendr model fits to represent degradation more accurately. Degradation episodes were also characterized using a derived metric equal to the magnitude divided by the duration of a given episode, which is referred to as "ratio".

Validation of green vegetation and soil endmember fractions

Models of green vegetation and soil endmember fractions were validated using data collected during field surveys in two regions of the P-ARB: Bamyan National Park in June and July 2018, and Wakhan National Park in July and August 2018 and August and September in 2019 (see also 'Field work' above). During surveys, the proportion of green vegetation and bare ground cover were recorded every meter along a 50-m line transect from 172 plots in Bamyan and 178 plots in Wakhan. The values were averaged to produce plot-level estimates of green vegetation and bare ground cover. It was not possible to accurately estimate dry vegetation cover in the field owing to phenological differences across sites and transects, so a validation of dry vegetation endmember fractions was also not possible. To ensure fair comparisons, all line transects were located within one vegetation type and multiple transects did not intersect a given Landsat pixel. Pearson correlation coefficients were calculated between modeled monthly green vegetation and soil endmember fractions at the pixel level and plot-level estimates of these two variables, using the monthly values (prior to applying the Whittaker smoother) that aligned with the month and year of the field data collection.

Appendix 5. Hydrology Supplementary Methods & Results

SWAT model

All processes related to SWAT hydrology model including input data, methodology, calibration, validation, and results are described below:

Conceptualization of SWAT model

SWAT is the acronym for Soil and Water Assessment Tool, a river basin or watershed scale model developed by Jeff Arnold (Neitsch et al., 2011) for the United States Department of Agriculture and Agriculture Research Services (USDA-ARS). This model is used to predict the impact of land management practices on water, sediment, and agricultural chemical yields in large and complex watersheds with varying soil, land-use, and management conditions over long periods (Neitsch et al., 2011). The SWAT model is a comprehensive, semi-distributed, continuous-time, processed-based river basin model (Krysanova & Arnold, 2008), which was developed to evaluate the effects of alternative management decisions on water resources and diffuse pollution in mesoscale and large river basins. The model has been widely applied for modeling watershed hydrology and impact of climate change analysis in different part of the world (Abbaspour et al., 2015; Singh & Saravanan, 2020). Hydrological processes in SWAT are divided into two phases: (i) the land phase, which controls the amount of water, sediment, and nutrient loading in the main channel in each sub-basin; and (ii) the water routing phase, which simulates water movement through the channel network. The model delineates watersheds into sub-basins interconnected by a stream network, and each sub-basin is divided further into Hydrologic Response Units (HRUs) based on unique soils, land use, and topography characteristics in the sub-basin (Neitsch et al., 2011).

The hydrological cycle simulated by SWAT is based on the water balance equation, which considers the shallow aquifer and unsaturated zone above the impermeable layer as a unit. The calculation of the hydrological cycle by SWAT model is shown in the following equation (Eqn 1) (Neitsch et al., 2011).

$$SW_t = SW_0 + \sum_{i=1}^{n} (R_{day} - Q_{surf} - E_a - W_{seep} - Q_{gw} \qquad (1)$$

Where, SW_t is the final soil water content(mm_{H20}) SW_0 is the Initial soil water content (mm_{H20}), R_{day} is the amount of precipitation on day I (mm_{H20}), Q_{surf} is the amount of surface runoff on day i (mm_{H20}), E_a is the amount of evapotranspiration on day i (mm_{H20}), W_{seep} is the amount of water percolation or amount of water entering the vadose zone from soil profile on day I (mm_{H20}), Q_{gw} is the amount of return flow on day i (mm_{H20}), and t is time in days.

The conceptual framework of the SWAT model and its setup is described in Figure 229. The SWAT model requires four main data types, including a digital elevation model (DEM), soil type, land use and landcover type, and weather data. The model setup involves six major steps that must be carried out for hydrology simulations including, project setup, discretizing the sub-basins (watershed delineation), defining the HRUs, writing input tables, editing SWAT inputs (parameterization), and running the model. For simulation of rainfall-runoff in the P-ARB on a monthly time step, SWAT version 2012 with Geographic Information Systems (GIS) was used. The first step included data collection and processing. All data used for the purposes mentioned above were obtained from different sources as described in the Input Data section below. In step 2, all the collected data were prepared based on the SWAT model requirements and entered into the SWAT model. The DEM was obtained from the Shuttle Radar Topography Mission (SRTM) (available at https://earthexplorer.usgs.gov/) at 30 m resolution and was used to delineate the drainage network and the watershed sub-basins. The SWAT model must first be configured to delineate sub-basins within defined areas to generate the HRUs. The subdivision of HRUs is based on the similarity of characteristics of land use, soil type, and slope found in an area; in this way, HRUs have homogeneous properties. For HRU delineation, the land cover map developed in this Report was used and reclassified into eight classes based on SWAT requirements. A map of soil types was obtained from the Food and Agriculture Organization (FAO) (https://www.fao.org/soils-portal/data-hub/soil-maps-and-databases/faounesco-soil-map-of-the-world/en/) at the scale of 1:5.000.000. The slope map was derived from the DEM. The calculations of the variables were done separately for each HRU, and then summed to represent each sub-basin (Wanessa & de Andrade, 2018). With the generation of the HRUs, the series of daily meteorological data were obtained from the National Water Affairs Regulation Authority (NWARA), Ministry of Agriculture, Irrigation and Livestock (MAIL), and Afghanistan Meteorological Department (AMD) in Afghanistan and entered into the SWAT model. After this phase, the input data were edited to improve the characterization of the study area. Finally, the simulation with the model was performed.

The SWAT model outputs include surface runoff, evapotranspiration, percolation, interception, and water storage, which should be calibrated and validated. The calibration and validation procedures for the discharge in five stations of the P-ARB were performed using sequential uncertainty fitting 2 (SUFI-2) algorithms in SWATCUP (Abbaspour et al., 2015). SWATCUP is an independent software developed for uncertainty and sensitivity analyses, calibration, and validation processes, based on SWAT simulations (Abbaspour, 2015). Therefore, the results related to the performance of the model and its statistical indices can also be verified in Figure 229.

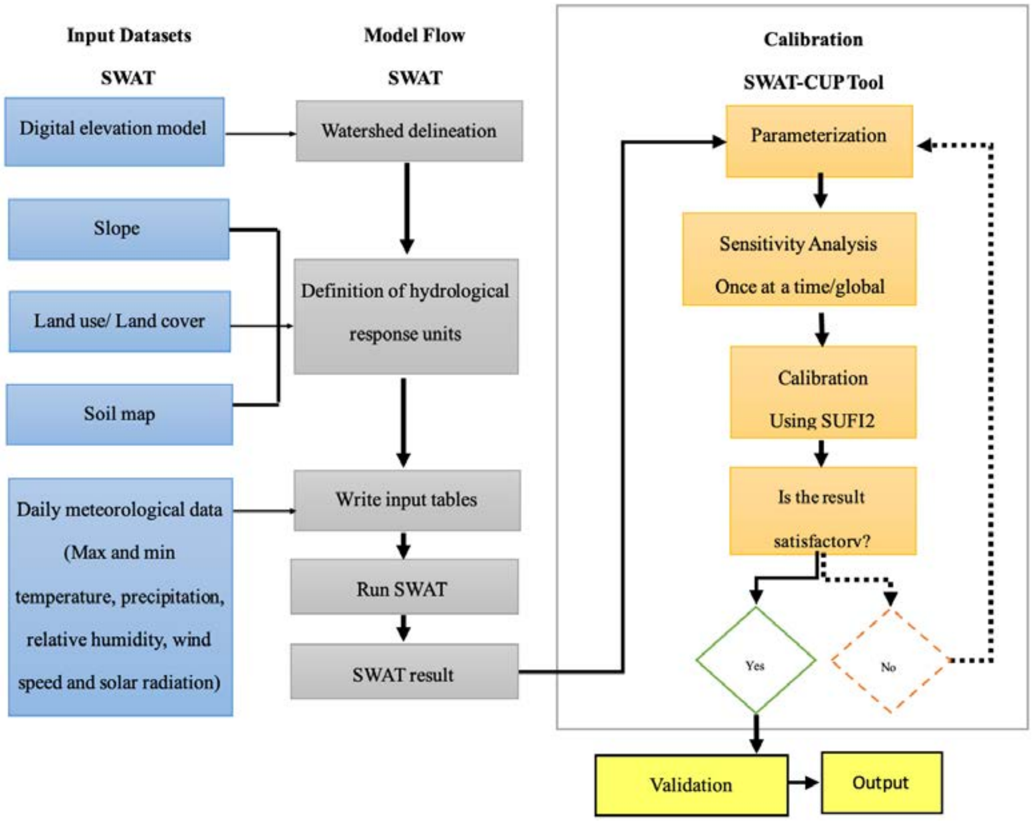

Figure 184. Flowchart for SWAT model setup, calibration, and validation.

SWAT input data

Input data such as land use, topography, weather, and soil data features are required to undertake watershed simulation using the SWAT model. In addition, observational hydrology data are required for model calibration and validation. In this analysis, the data were collected from different entities and prepared according to the model requirements. The source and types of data used in the P-ARB are indicated in Table 66 and more details are illustrated in the following section.

Digital Elevation Model (DEM)

Description: The Shuttle Radar Topographic Mission Digital Elevation Model (SRTM-DEM) at 30 m resolution was obtained from the United States National Aeronautics and Space Administration (NASA) at https://earthexplorer.usgs.gov/ (Figure 230). The data were distributed in 27 tiles in geographic projection GCS_WGS_1984. Each tile was converted to Universal Transverse Mercator (WGS 1984_UTM_Zone 42N) and then converted to a mosaic map using GIS software. The DEM was then used as an input to the SWAT model to delineate the sub-basin boundaries of the P-ARB.

(NWARA), Ministry of Agriculture, Irrigation and Livestock (MAIL), and Afghanistan Meteorological Department (AMD) in Afghanistan and entered into the SWAT model. After this phase, the input data were edited to improve the characterization of the study area. Finally, the simulation with the model was performed.

The SWAT model outputs include surface runoff, evapotranspiration, percolation, interception, and water storage, which should be calibrated and validated. The calibration and validation procedures for the discharge in five stations of the P-ARB were performed using sequential uncertainty fitting 2 (SUFI-2) algorithms in SWATCUP (Abbaspour et al., 2015). SWATCUP is an independent software developed for uncertainty and sensitivity analyses, calibration, and validation processes, based on SWAT simulations (Abbaspour, 2015). Therefore, the results related to the performance of the model and its statistical indices can also be verified in Figure 229.

Table 58. Detailed description of the input data into the SWAT hydrological model for the P-ARB.

Data type	Variable(s)	Source
Meteorological data	Daily precipitation (mm), maximum and minimum air temperature (°C), wind speed (m/sec), relative humidity (fraction), and solar radiation (MJ/m^2)	NWARA, AMD, MAIL
Digital elevation model (DEM)	SRTM (30m resolution), Shuttle Radar Topographic Mission	NASA's Earth Observing System Data and Information System
Land use/ land cover	The Land use map (2018)	Wildlife Conservation Society (WCS)
Soil type	Digital Soil Map of the World ver. 3.6	FAO/UNESCO
Hydrological data	Daily river discharge (m^3 S^{-1})	NWARA

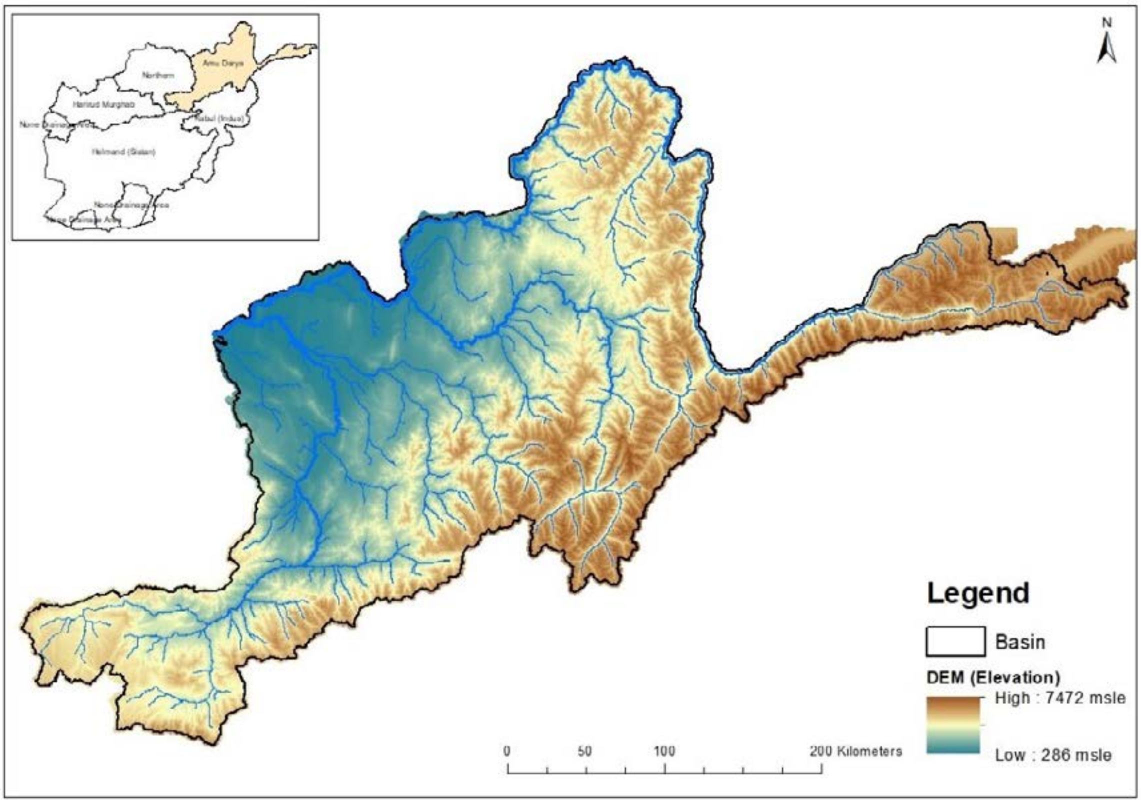

Figure 185. Digital Elevation Model (DEM) of the P-ARB.

Land-use/land cover Map

The land use and land cover (2018) data developed for this Report was further processed to meet SWAT model requirements. First, the land use map was buffered by 2 km beyond the P-ARB to accommodate the boundary river between Afghanistan and neighbouring countries. Next, the land use map was reclassified into eight classes for P-ARB (Figure 231). The primary land cover in the study area is "Rangelands-Grasses", which covers 56.56% of the total area; the second major land cover is "Barren land", which covers 21.97%; the third and fourth are "Agriculture land", with 8.06%, and "Spring wheat" with 7.71% of the total area.

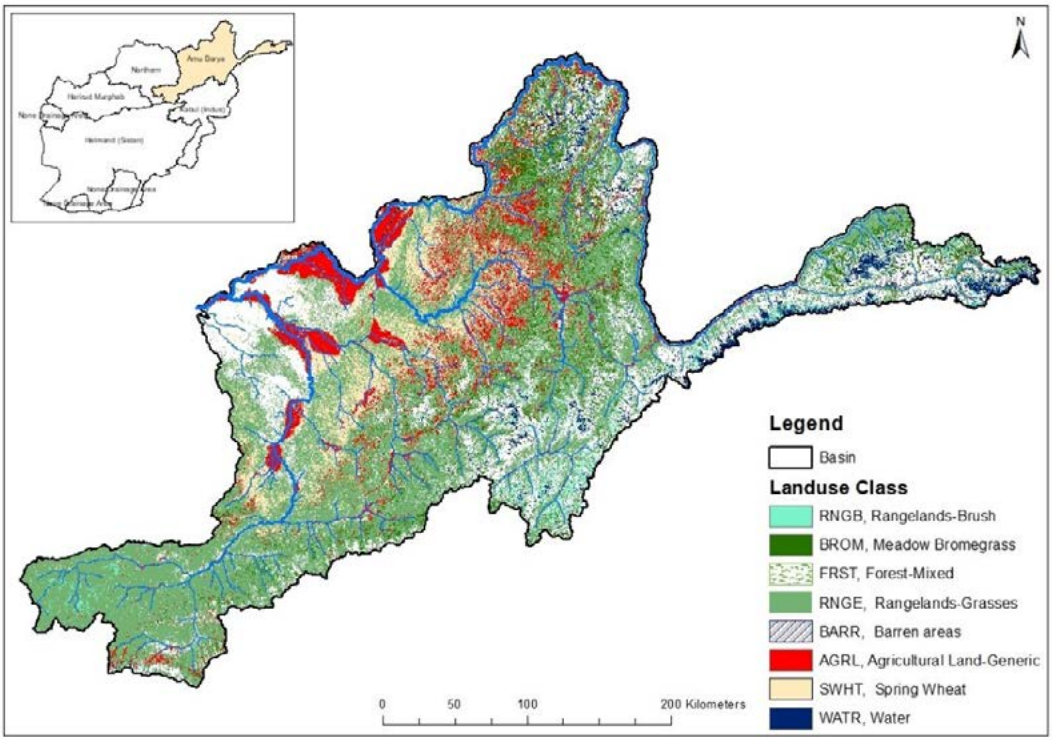

Figure 186. Land use/land cover map of the P-ARB.

Soil Map

The Digitized Soil Map of the World, at 1:5,000,000 scale and in geographic projection was intersected with a layer containing water related features (coastlines, lakes, glaciers, and rivers) and a layer of country boundaries from the World Data Bank II (with country boundaries updated to January 1994 at 1:3,000,000 scale), obtained from the FAO at https://www.fao.org/soils-portal/data-hub/soil-maps-and-databases/faounesco-soil-map-of-the-world/en/ (FAO/UNESCO Soil Map of the World, Food and Agriculture Organization of the United Nations). There are 10 major soil types in P-ARB (Figure 232). The soil shapefile map was prepared and used as input into the SWAT model. Loam is the main soil texture in the study area (Table 67).

Table 59. Soil Characteristics in P-ARB, including Hydrologic Soil Group (HYDGRP), and number of soil layers (NLAYER).

SOIL Type	NLAYERS	HYDGRP	TEXTURE	Area %	CLAY	SILT	SAND	ROCK
GLACIER-6998	1	D	UWB	4.6	5	25	70	98
I-X-c-3512	2	D	LOAM	44.0	22	33	45	0
I-Bh-U-c-3717	2	C	LOAM	1.4	26	33	41	0
I-B-U-2c-3503	2	C	LOAM	27.9	26	30	44	0
I-X-2c-3731	2	D	LOAM	4.5	22	33	45	0
I-Y-2c-3733	2	D	LOAM	3.4	23	39	38	0
Xk4-2b-3303	2	D	LOAM	3.9	27	45	29	0
Jc53-2a-3984	2	D	LOAM	0.7	18	48	34	0
Yh23-2ab-3581	2	D	LOAM	9.6	21	35	44	0

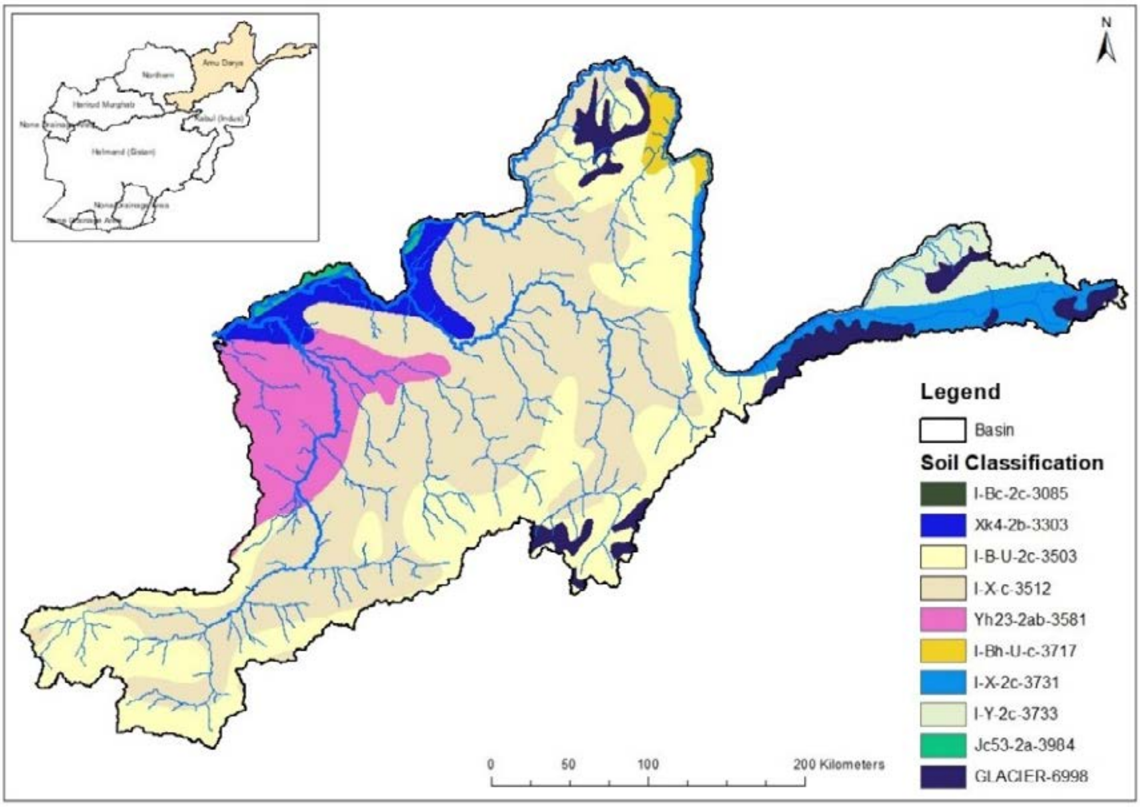

Figure 187. Soil types in the P-ARB.

A2.4. Slope map

The P-ARB was classified into five slope classes to model high and low elevations and calculate the elevational range within each HRU during the SWAT setup. Most of the upper sub-basins in the P-ARB had slopes over 57%, and the lower sub-basins had slope ranges between 0-16% (Figure 233).

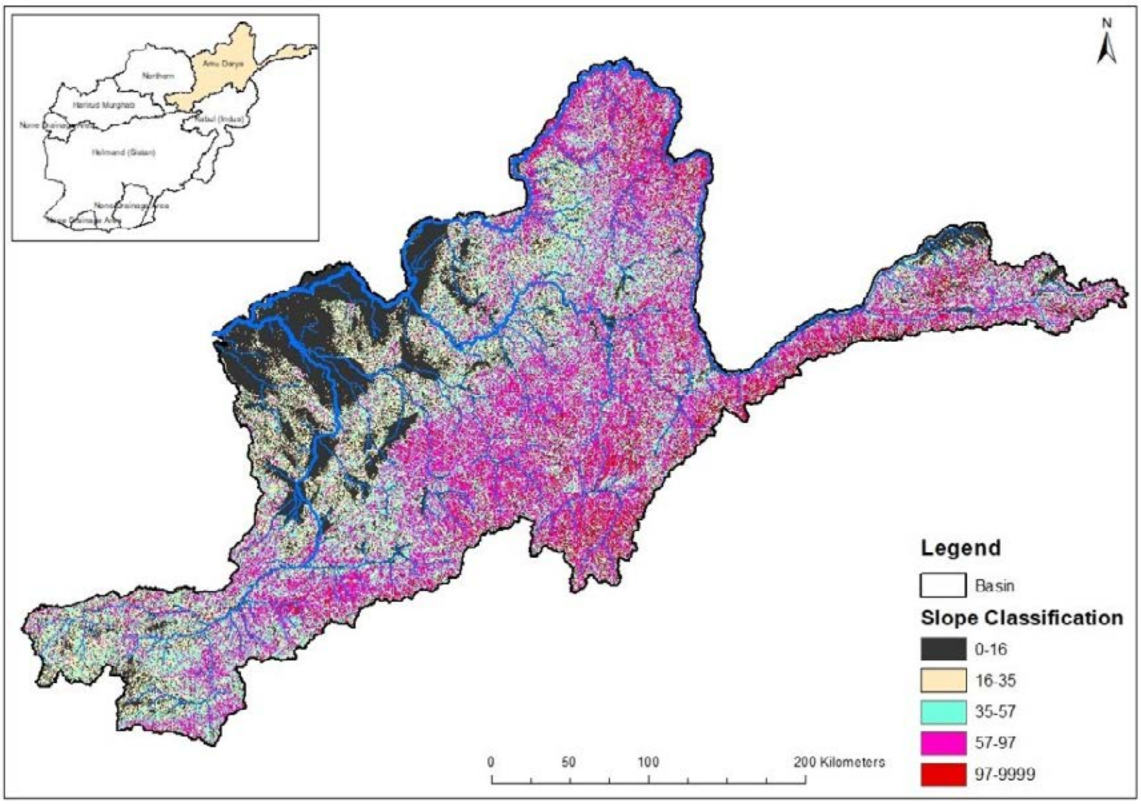

Figure 188. Slope Classes in the P-ARB.

Estimation of solar radiation (Rs)

Sunshine hours are measured by NWARA weather stations, but no long-term observations of solar radiation were recorded in the P-ARB. So, sunshine hours were used to estimate long-term solar radiation. Specifically, the Angstrom formula was used, parameterized with sunshine hours measured, to calculate solar radiation. The parameters were adjusted by minimization of average relative error. The Angstrom formula (Meenal & Selvakumar, 2016) is shown in Eqn 2:

$$R_S = \left(a_s + b_s \frac{n}{N}\right) R_a \qquad (2)$$

where R_s is solar radiation [MJ/m^2/day], R_a is extra-terrestrial radiation [MJ/m^2/day], n is actual duration of sunshine [hours], N is maximum possible sunshine or daylight hours [hours], a_s is a regression constant expressing the fraction of extra-terrestrial radiation reaching the earth on overcast days (n=0), and a_s+b_s is the fraction of extra-terrestrial radiation reaching the earth on clear days (n = N).

Calibration and Validation of the SWAT model

The model was calibrated using observed data from January 2013 to December 2016 and the validation was performed from January 2017 to September 2019 in five hydrological stations of the P-ARB, except the Kufab station. For Kufab station, the calibration was carried out from January 2013 to December 2015 and due to the lack of observed discharge for other years, no validation was performed for this station. The graphical representation of simulated versus observed discharge at five ground stations and a statistical indicator (Nash-Sutcliffe Efficiency, NSE) for each station are depicted in Figure 234.

The NSE was used to statistically evaluate the model performance. The NSE value indicates how well the plot of the observed values versus the simulated values fits the unit slope line. The NSE values range from –∞ to 1, with values less than or close to zero indicating unacceptable or poor model performance, and a value of one representing a perfect match. The NSE value is calculated using Eqn 3 (Nash & Sutcliffe, 1970):

$$NSE = 1.0 - \left(\frac{\sum_{i=1}^{n}\left(Y_{obs,i} - Y_{cal,i}\right)^2}{\sum_{i=1}^{n}\left(Y_{obs,i} - Y_{obs_{mean}}\right)^2}\right) \qquad (3)$$

Where n is the number of registered data, $Y_{obs,i}$ is the observed data at time i, $Y_{cal,i}$ is the simulated data, and Y_{obs_mean} is the mean value of the observed data.

SWAT Model Results for the P-ARB

The calibrated and validated results of the model exhibited better performance in simulating monthly river discharge compared to monthly observed discharge. Figure 234 shows the monthly observed versus simulated discharge in Sust, Khwajaghar, Chardara, Pul-i-Kundasang, and Kufab stations in the P-ARB. The vertical red line in these graphs separates the calibration period from the validation period. The NSE statistical results are shown for each figure for both calibration and validation periods.

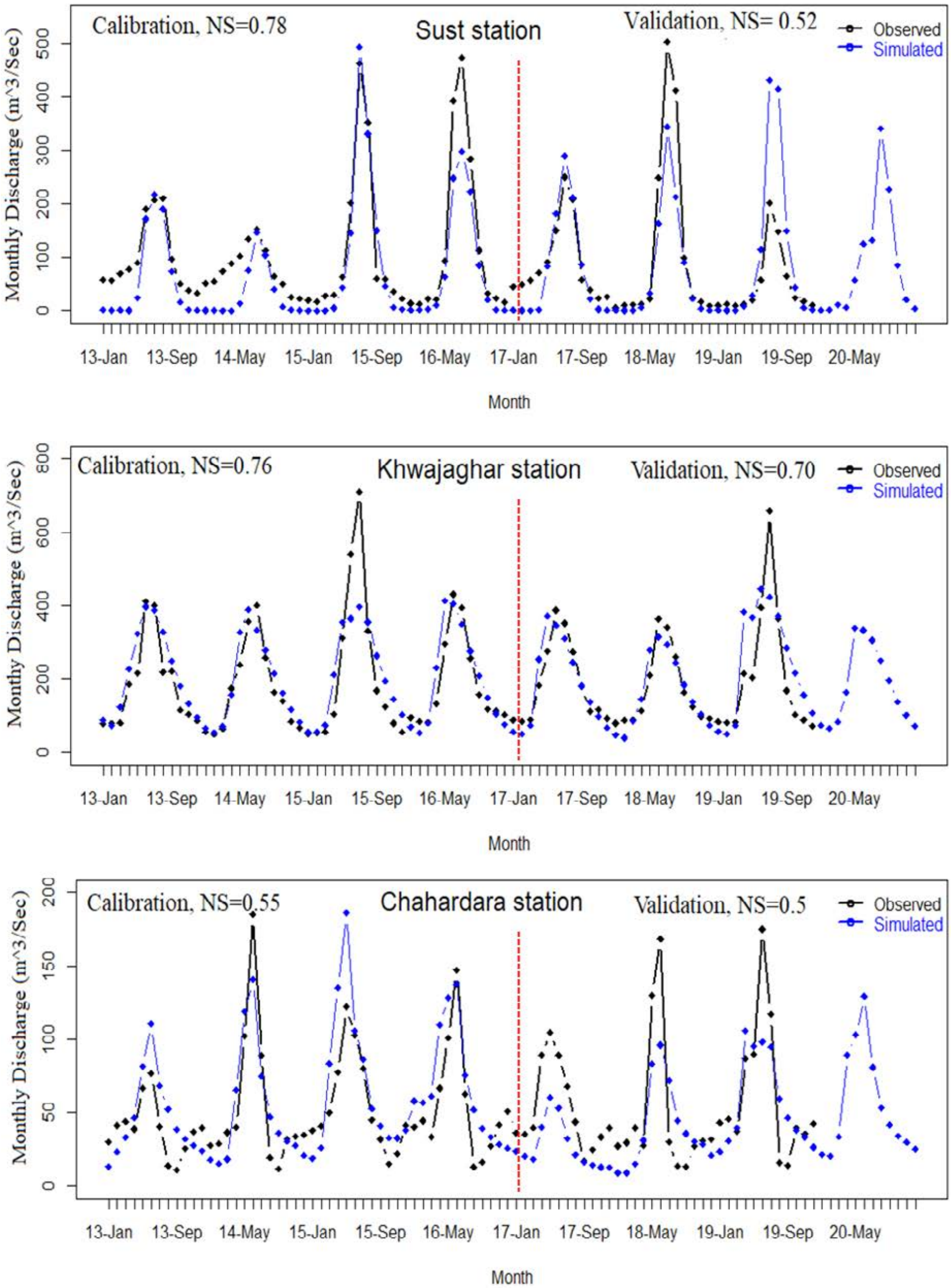
Sust station
Calibration, NS=0.78
Validation, NS= 0.52
Observed
Simulated
Monthly Discharge (m^3/Sec)
0
100
200
300
400
500
13-Jan
13-Sep
14-May
15-Jan
15-Sep
16-May
17-Jan
17-Sep
18-May
19-Jan
19-Sep
20-May
Month
Khwajaghar station
Calibration, NS=0.76
Validation, NS=0.70
Observed
Simulated
Monthly Discharge (m^3/Sec)
0
200
400
600
800
Month
Chahardara station
Calibration, NS=0.55
Validation, NS=0.5
Observed
Simulated
Monthly Discharge (m^3/Sec)
0
50
100
150
200
Month

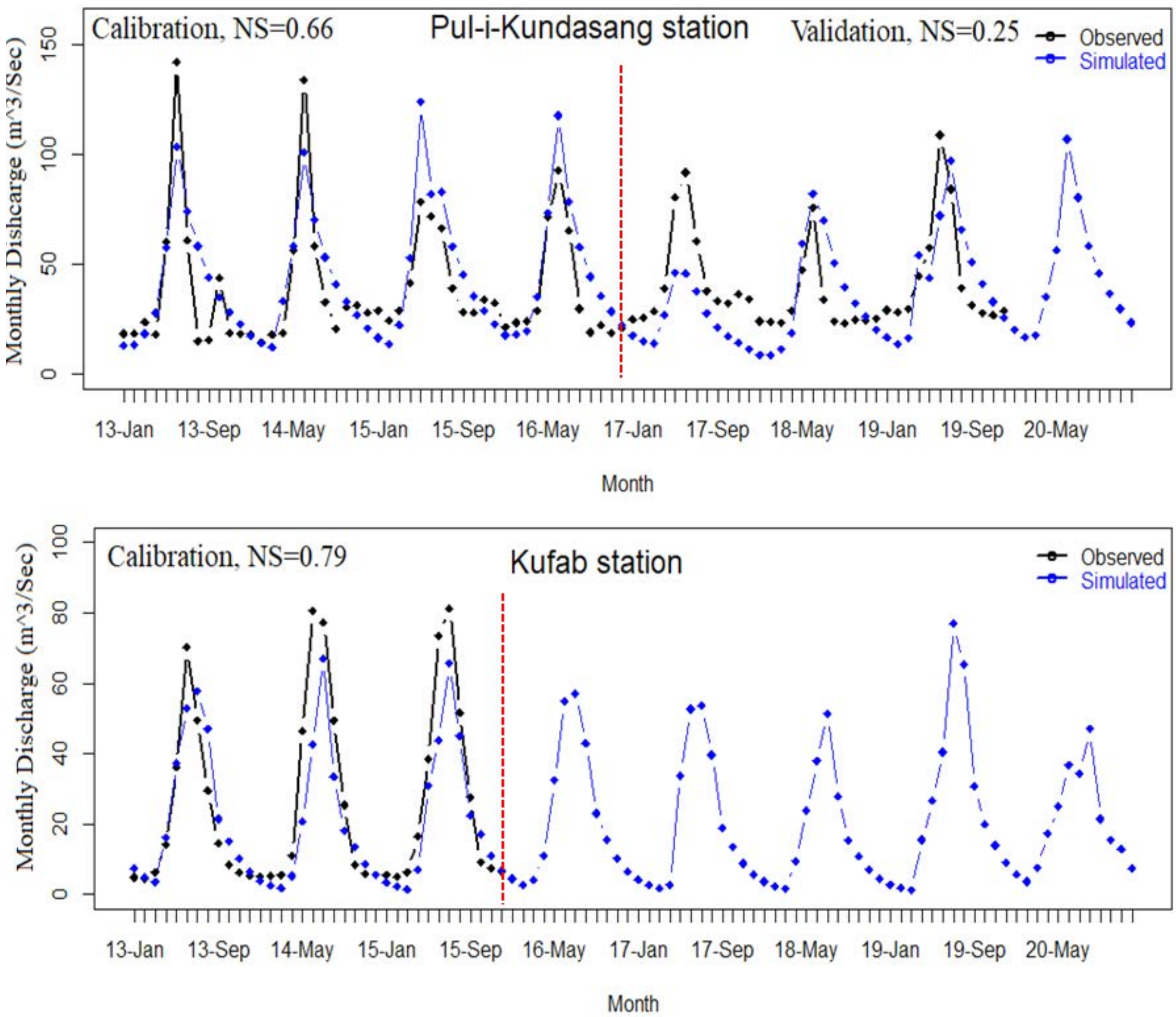

Figure 189: Comparison of monthly simulated and monthly observed discharge during calibration and validation period in Sust, Khwajaghar, Chardara, Pul-i-Kundasang, and Kufab Stations of the P-ARB. The vertical red line separates the calibration and validation periods.

After calibration and testing, the model generated the results for the mean monthly (2013 to 2020) hydrological processes in the P-ARB. The output variables include monthly surface runoff, lateral flow (flow from root zone), water yield, actual evapotranspiration, and potential evapotranspiration. Details of the mean monthly outputs are provided in Table 68 and Table 69.

Table 60. Mean monthly hydrological parameters based on SWAT models for the P-ARB from January 2013 to December 2020. The units are in mm for all variables. ET: Actual evapotranspiration, PET: Potential evapotranspiration.

Month	Rainfall	Snowfall	Surface Q	Lateral flow	Water yield	ET	PET
JAN	43.55	31.11	1.33	0.54	4.53	7.86	20.55
FEB	42.82	27.03	2.67	1.2	5.85	12.31	28.31
MAR	56.97	24.75	7.79	3.01	12.79	23.83	55.56
APR	86.22	33.23	10.61	3.3	18.65	35.34	82.3
MAY	66.82	25.38	8.44	3.48	21.59	44.68	120.88
JUN	20.84	6.92	4.83	3.13	21.48	35.84	146.13
JUL	5.98	0.82	4.21	2.85	21.99	23.19	158.61
AUG	2.83	0.45	1.38	1.73	17.77	12.85	139.31
SEP	1.69	0.56	0.11	0.36	10.91	6.74	105.2
OCT	16.77	8.62	0.23	0.38	7.63	7.65	64.79
NOV	26.72	13.58	0.42	0.61	5.64	8.64	31.16
DEC	28.02	18.92	0.56	0.49	4.46	7.13	21.03

Table 61. Mean annual hydrological parameter results based on SWAT models for the P-ARB from January 2013 to December 2020. All values are in mm.

Variable	Value
Precipitation	398.1
Snow fall	190.82
Snow melt	120.44
Sublimation	47.45
Surface runoff Q	42.5
Lateral soil Q	21.3
Groundwater (shallow Aq) Q	84.43
Groundwater (deep Aq) Q	5.03
Revap (shallow Aq to soil/plants)	18.59
Deep Aq recharge	5.01
Total Aq recharge	100.15
Total water yield	153.27
Percolation out of soil	99.81
Evapotranspiration	225.6
Potential evapotranspiration	972.5

Average monthly total water yields (combined surface flow, lateral flow, and groundwater flow) supply the river flow with peaks starting in April and continuing to August. In March, April, and May, the surface flow contributed about 30 mm to total water yield, more than other components (lateral and groundwater flow). This is due to inputs of rainfall, snowmelt, and glacier melt mostly in winter and spring months (December to May). River flow was mainly supplied by groundwater (baseflow) from August to December because in these months the occurrence of rain and snowfall was minimal, and it may be partly attributed to melt of snow and glaciers in the P-ARB (Figure 235).

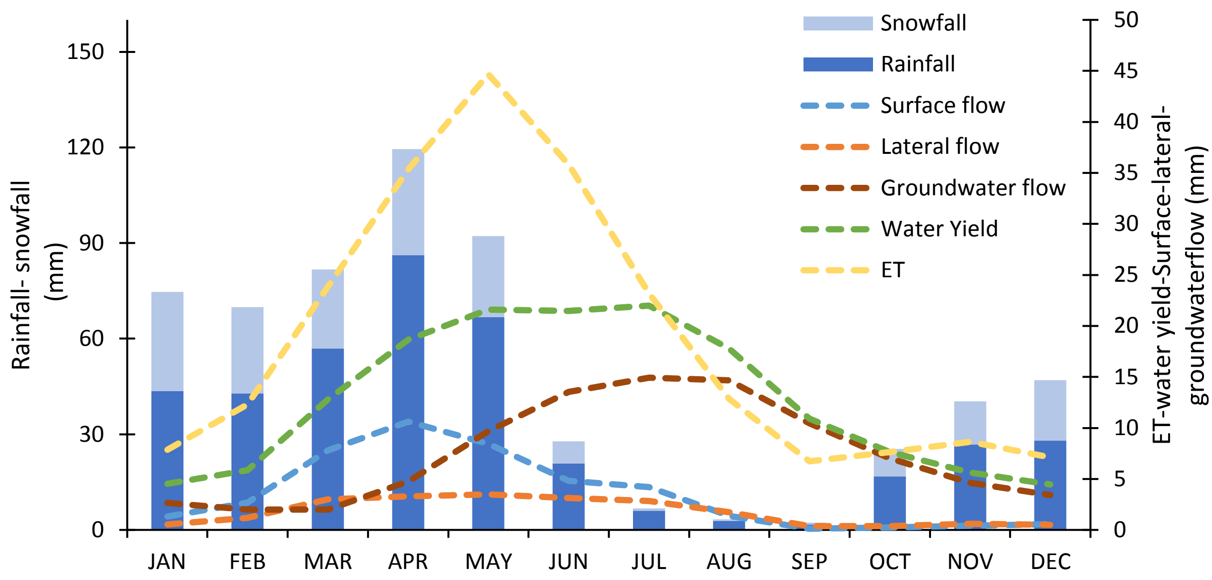

Figure 190. Mean monthly hydrological parameters for the PARB based on SWAT models from January 2013 to December 2020.

The mean annual water balance components (2013-2020) over the entire P-ARB are presented in Figure 236. By inserting an input of 398 mm average precipitation, the model simulation showed the output as 153 mm total water yield (combination of surface, lateral and groundwater flows) that accounts for 24% of the basin-wide water balance components. While due to larger potential evapotranspiration of 972 mm, the average ET obtained was greater than the total water yield as 226 mm, or 35% of the total hydrological parameters that goes back to the atmosphere. Moreover, the soil characteristics of the P-ARB allow percolation of 100 mm (Figure 236).

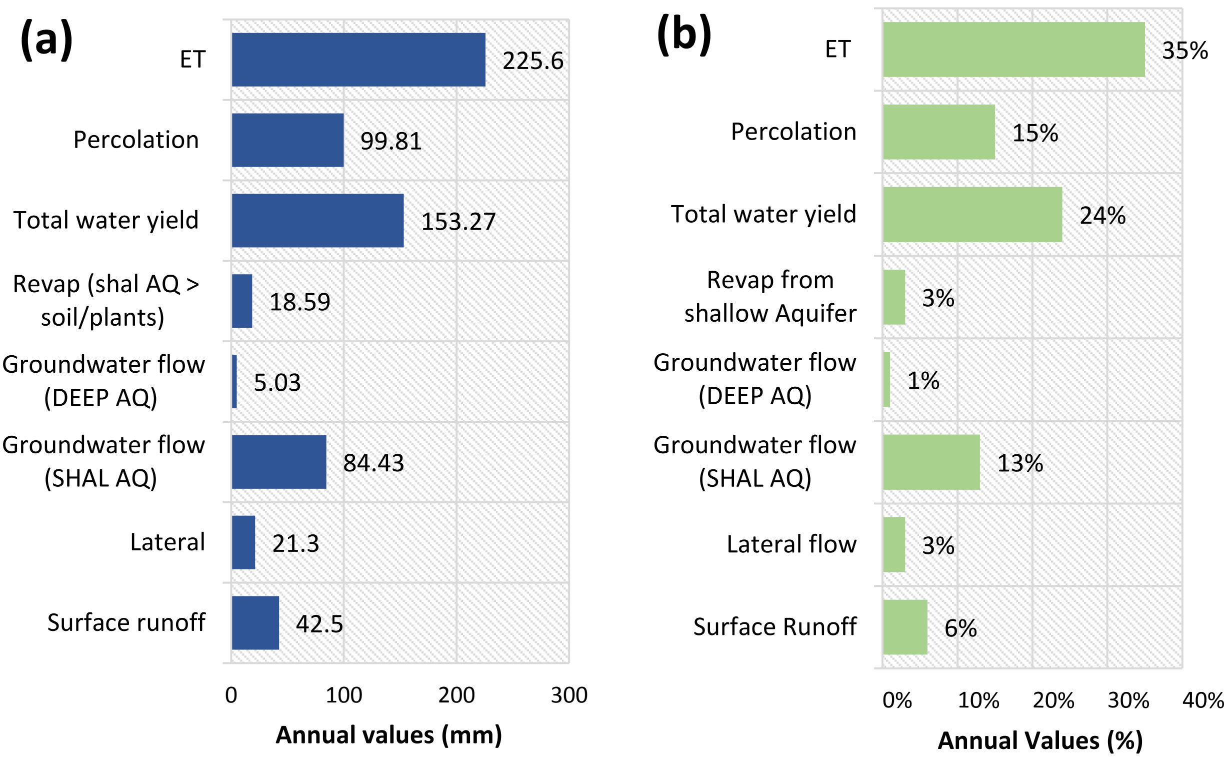

Figure 191. Average annual hydrological parameter contribution over the P-ARB based on SWAT models (a, values shown in mm; b, values shown as percentages).

Sensitivity analysis

The SWAT model has several hydrological variables to parameterize during calibration, therefore, sensitivity analysis is essential to perform during this process. The once-at-a-time and global sensitivity analysis techniques (Abbaspour et al., 2015) were carried out to determine the sensitive parameters related to hydrology for five hydrological stations of the P-ARB. Identifying sensitive parameters enables the module to focus only on those parameters that most affect the model output during the calibration process. The number of sensitive parameters was 15, 12, 11, 11, and 9 for Pul-i-Kundasang, Chahar Dara, Khwajaghar, Sust, and Kufab stations, respectively. More details are given in Table 70 and Table 71.

Table 62. Result of parameter sensitivity analysis in the P-ARB based on SWAT models. The numbers show the sensitivity of the parameters in a range (1 shows the most sensitive and 15 shows the least sensitive parameter). Note that v_ means the existing parameter value is to be replaced by a given value, r_ means an existing parameter value is multiplied by (1+ a given value) during the model calibration process.

No	Pul Kundasang	Chahar Dara	Khwajaghar	Sust	Kofab
1	V__PLAPS.sub	V__PLAPS.sub	V__PLAPS.sub	V__PLAPS.sub	V__PLAPS.sub
2	V__TLAPS.sub	V__TLAPS.sub	V__TLAPS.sub	V__TLAPS.sub	V__TLAPS.sub
3	v__SFTMP.bsn	v__SFTMP.bsn	v__SFTMP.bsn	v__SFTMP.bsn	v__SFTMP.bsn
4	v__SMTMP.bsn	v__SMTMP.bsn	v__SMTMP.bsn	v__SMTMP.bsn	v__SMTMP.bsn
5	v__SMFMX.bsn	v__SMFMX.bsn	v__SMFMX.bsn	v__SMFMX.bsn	v__SMFMX.bsn
6	v__SMFMN.bsn	v__SMFMN.bsn	v__SMFMN.bsn	v__SMFMN.bsn	v__SMFMN.bsn
7	v__TIMP.bsn	v__TIMP.bsn	v__TIMP.bsn	v__TIMP.bsn	v__TIMP.bsn
8	v__GW_DELAY.gw	r__CN2.mgt	r__HRU_SLP.hru	v__GW_DELAY.gw	v__GW_DELAY.gw
9	r__SOL_AWC().sol	v__GW_DELAY.gw	v__OV_N.hru	v__ESCO.hru	r__HRU_SLP.hru
10	v__ESCO.hru	r__HRU_SLP.hru	v__SLSUBBSN.hru	r__SOL_AWC().sol	-
11	r__CN2.mgt	v__SLSUBBSN.hru	v__GW_DELAY.gw	r__CN2.mgt	-
12	r__HRU_SLP.hru	v__OV_N.hru	-	-	-
13	v__OV_N.hru	-	-	-	-
14	v__SLSUBBSN.hru	-	-	-	-
15	v__SURLAG.bsn	-	-	-	-

Table 63. Description of sensitive parameters related to Table 62 in P-ARB.

No	Parameters	Details
1	PLAPS.sub	Precipitation lapse rate (mm H2O/km)
2	TLAPS.sub	Temperature lapse rate (°C/km)
3	SFTMP.bsn	Snowfall temperature (°C)
4	SMTMP.bsn	Snow melt base temperature (°C)
5	SMFMX.bsn	Maximum melt rate for snow during year (mm H2O/°C-day)
6	SMFMN.bsn	Minimum melt rate for snow during the year (mm H2O/°C-day)
7	TIMP.bsn	Snowpack temperature lag factor
8	GW_DELAY.gw	Groundwater delay (days)
9	ESCO.hru	Soil evaporation compensation factor
10	SOL_AWC ().sol	Available water capacity of the soil layer (mm H2O/mm soil)
11	CN2.mgt	SCS runoff curve number for moisture condition II
12	HRU_SLP.hru	Average slope steepness (m/m)
13	OV_N.hru	Manning's "n" value for overland flow
14	SLSUBBSN.hru	Average slope length
15	SURLAG.bsn	Surface runoff lag time

J2000 model

J2000 Data Preparation

Hydro-meteorological data

The J2000 model requires both climate and geospatial data. The climatic data is collected as a secondary source of data available with NWARA and MAIL at a daily time scale. There were 42 stations that covered the whole basin, 42 stations with precipitation records, 20 stations with temperature and relative humidity records, and 9 stations with solar radiation and wind speed data. The period of the climate data varied from station to station; some recorded from 2001, 2007, 2012, and 2013 to 2020. The model requires a consistent period; therefore, considering the minimum gap in the stations' data, we used 2012-2019 to run the model.

Geospatial Data

The model requires information about the streams and the topographic characteristics of the catchment and sub-catchments such as basin size, boundary, slope, aspect, channel network and contributing sub-catchments driven by the DEM. For our analysis, a 90-m resolution DEM data from NASA SRTM was obtained through the CGAIR-CSI Geoportal3.

Similarly, the land cover data is incorporated into the model that gives the properties of land cover including albedo and leaf area index, which helps the model to produce information about the storage capacity. The land cover dataset developed for this report at 30-m resolution circa 2018 was used for this analysis.

Soil data is another essential input to the model to simulate the infiltration rate. For this analysis, a soil map with 250-m resolution was obtained from ISRIC World Soil Information hub (Figure 237).

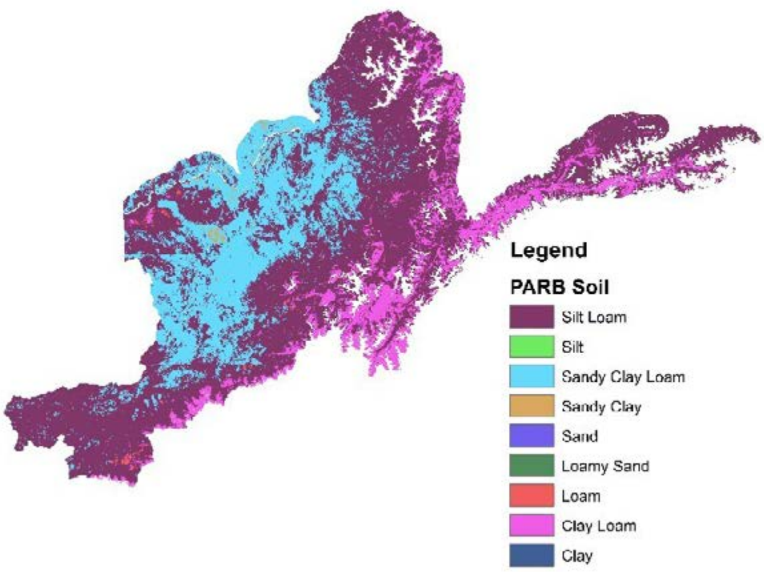

Figure 192. Soil map of the P-ARB obtained from the ISRIC data hub (source: SoilGrids250m 2017-03 - Texture class (USDA system).

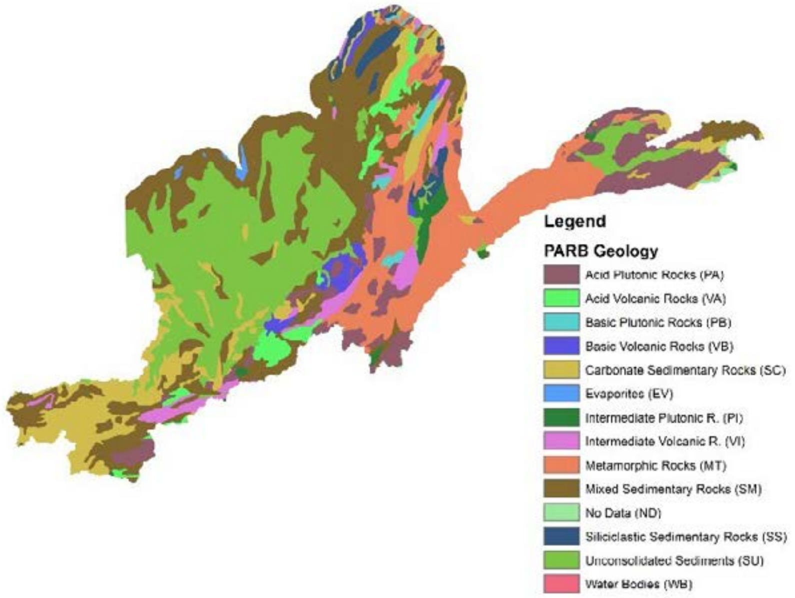

Figure 193. Geological map of the P-ARB (source: https://www.geo.uni-hamburg.de/en/geologie/forschung/geochemie/glim.html).

Hydrological Response Unit

In the J2000 modelling system, hydrological behaviour is calculated based on each HRU. HRUs have been derived from spatially distributed information about the topography, land use, soil type, and geology. In this process, individual HRUs are shaped based on similar properties such as topography (slope, aspects), land use, soil, and geology i.e., characteristics that behave similarly in their hydrological response. For this purpose, the HRUs of the study area were developed using an online platform (http://intecral.uni-jena.de/hruweb-qs/) with the input data for delineating HRUs including the DEM, soil map, geological map, LULC map, and the station points.

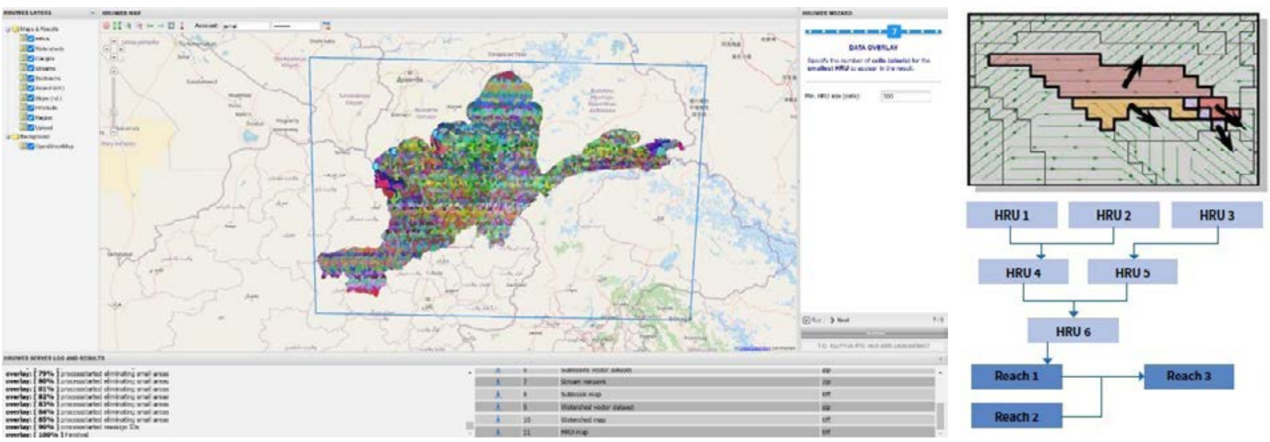

Figure 194. Window of the HRUWEB MAP online platform.

It is important to mention that one limitation of the J2000 model is that it is recommended to use at a coarse resolution and for larger catchments. If the catchment is small (e.g., 1,000 km^2), a resolution between 30-90 m is suitable depending on the resolution of the available dataset. Similarly, for a mesoscale catchment (e.g., 4,000 km^2), a resolution between 250-500 m is suitable (JAMS 2021). However, for this analysis, the resolution was set to 120 m. In addition, the model requires one outlet to validate and calibrate the results, but the P-ARB has several outlets from different sub-watersheds. Therefore, the model was separately setup and applied to each of the four sub-basins (Kunduz, Khanabad, Kokcha, and Panj).

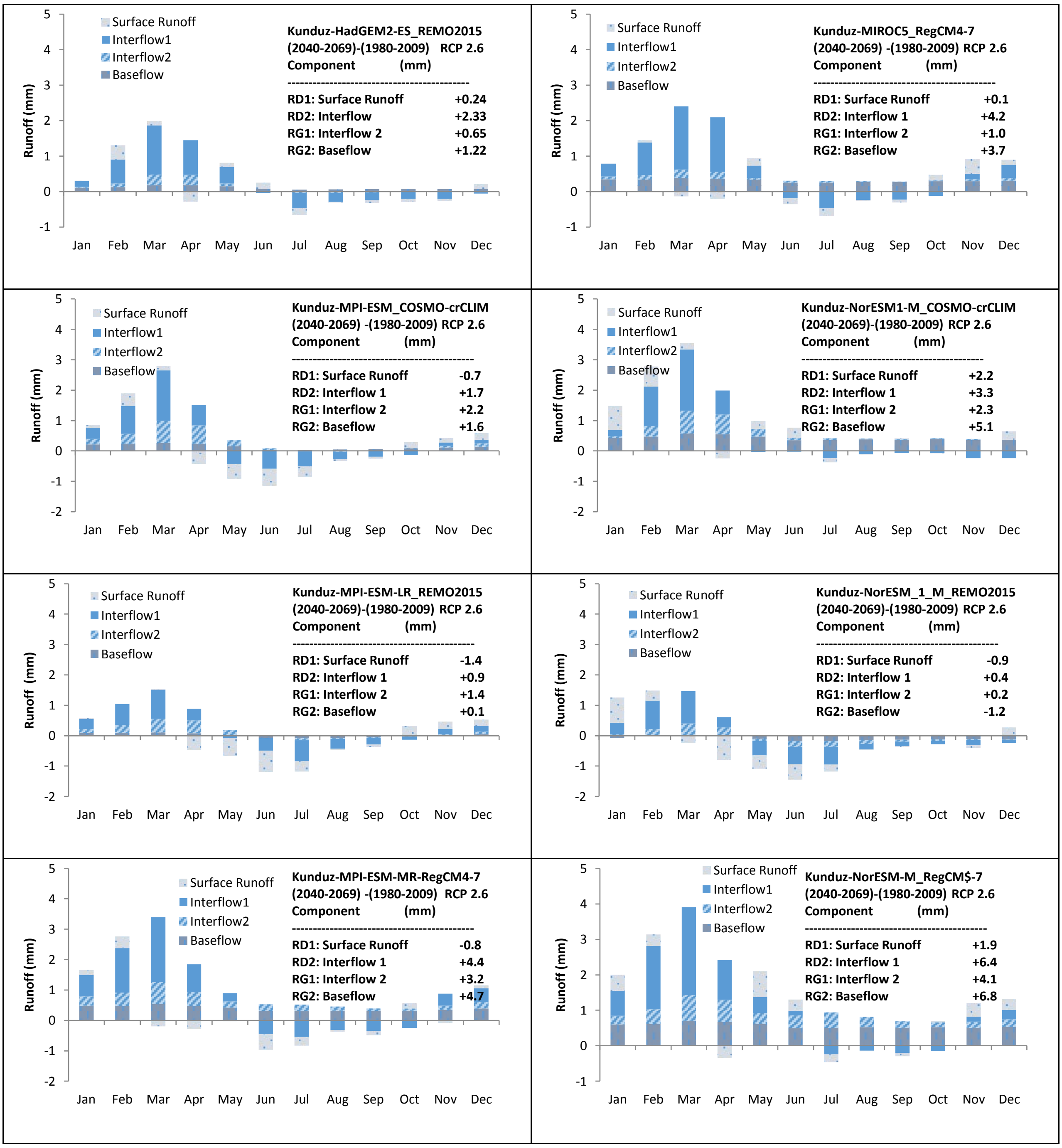

Figure 195. Change in monthly mean runoff future (2040-2069) – baseline (1980-2009) for Kunduz sub-basin, RCP2.6.

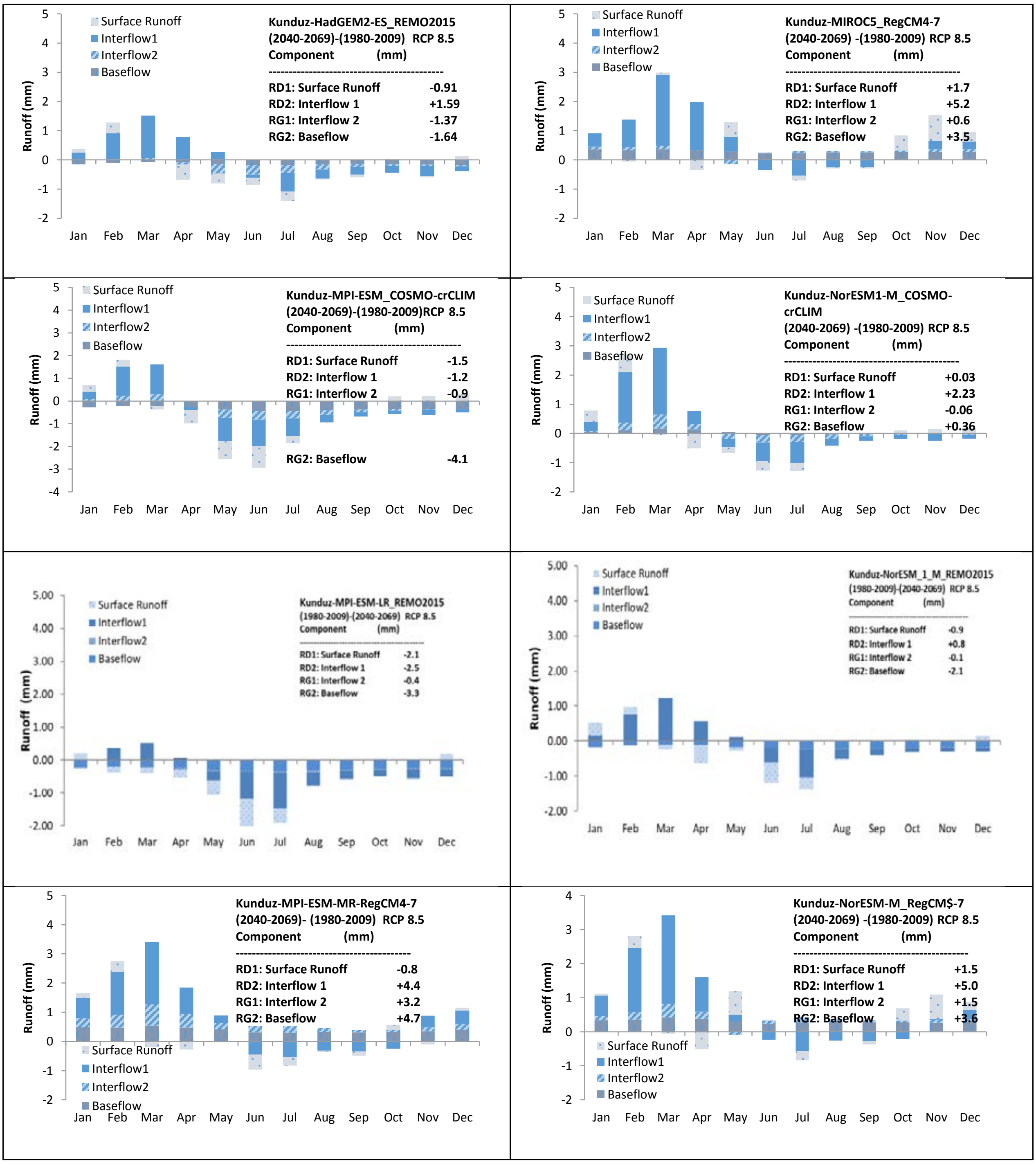

Figure 196. Change in monthly mean runoff future (2040-2069) – baseline (1980-2009) for Kunduz sub-basin, RCP8.5.

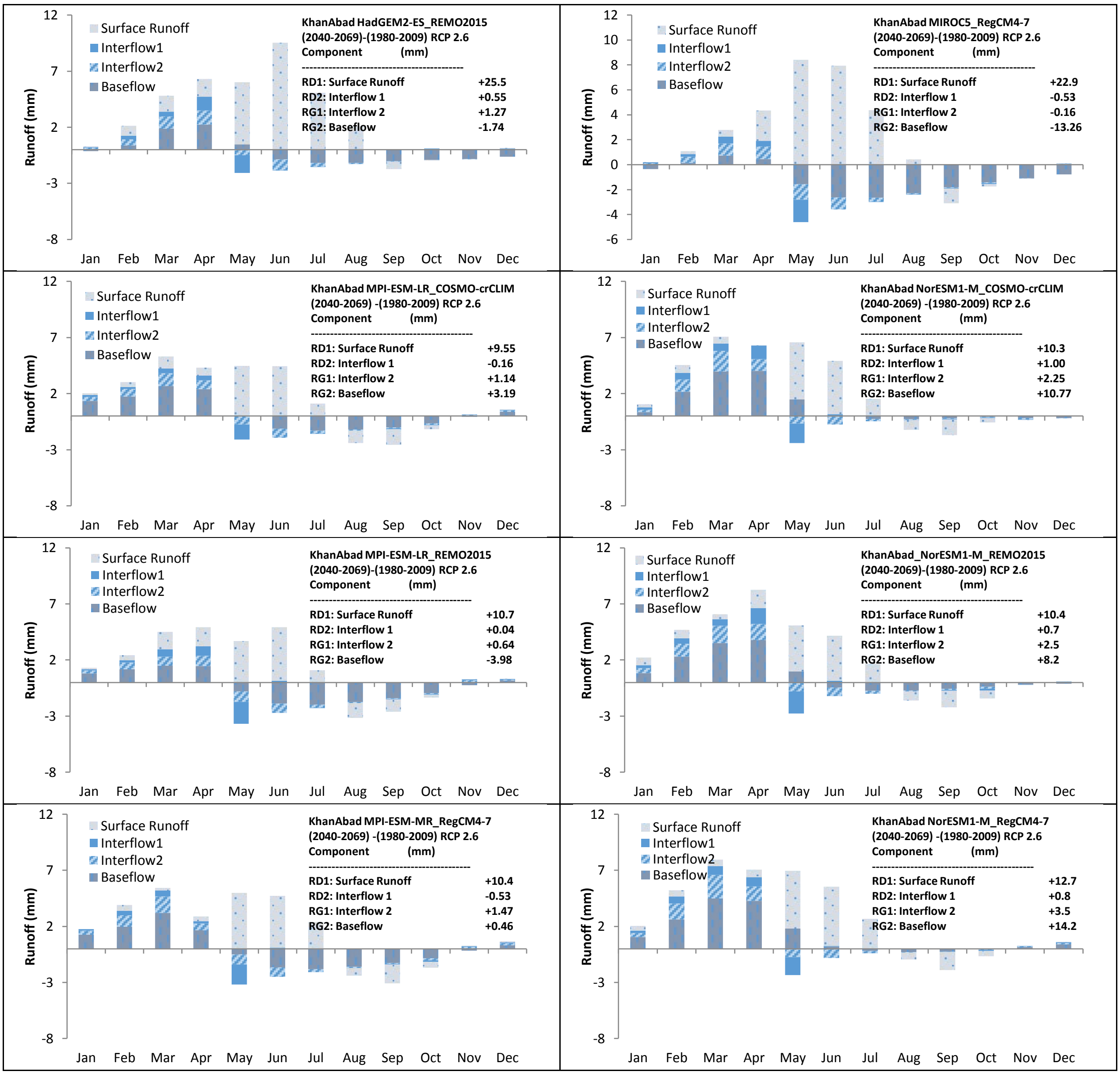

Figure 197. Change in monthly mean runoff future (2040-2069) – baseline (1980-2009) for Khanabad sub-basin, RCP2.6.

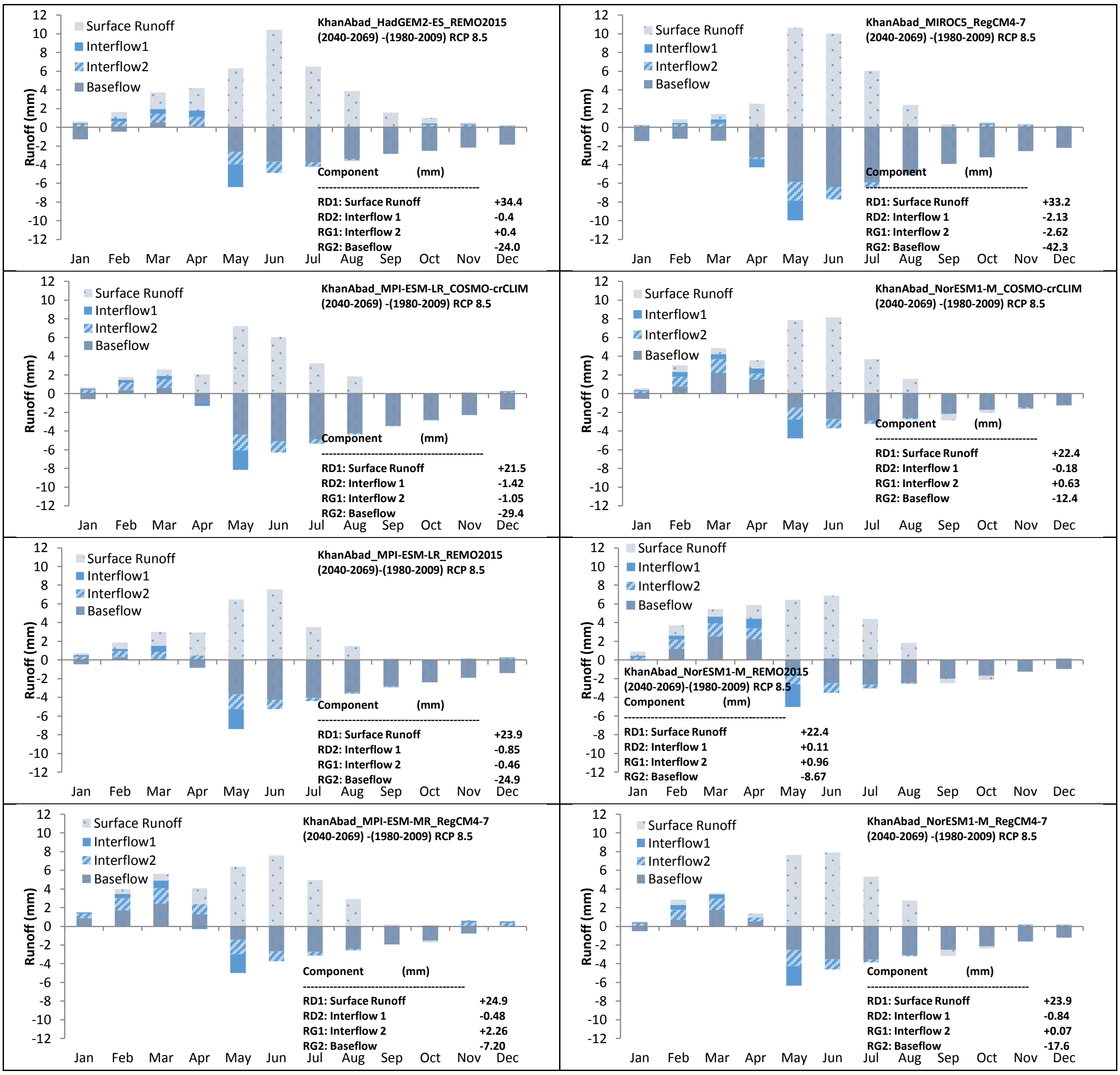

Figure 198. Change in monthly mean runoff future (2040-2069) – baseline (1980-2009) for Khanabad sub-basin, RCP8.5.

APPENDICES

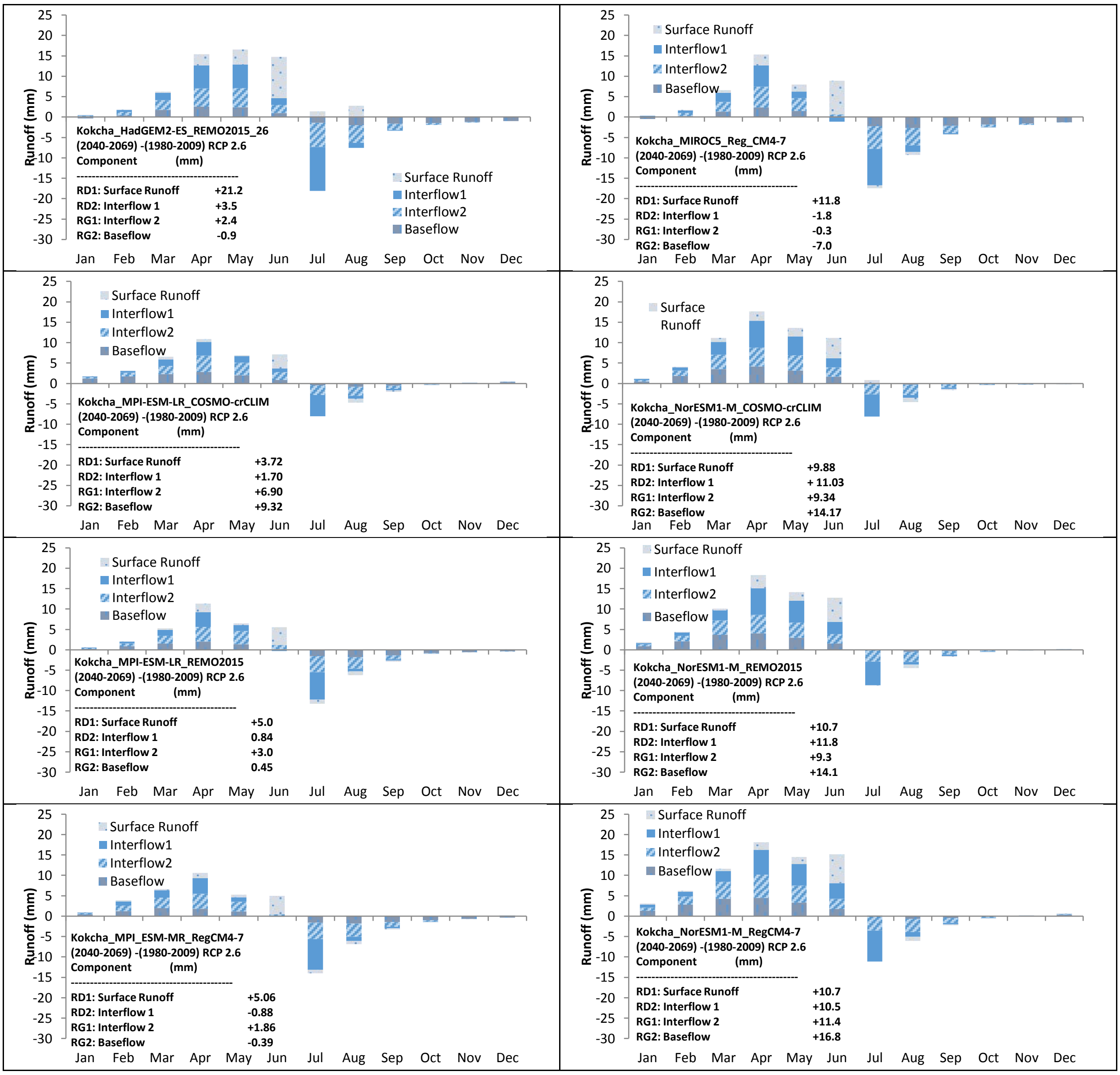

Figure 199. Change in monthly mean runoff future (2040-2069) – baseline (1980-2009) for Kokcha sub-basin, RCP2.6.

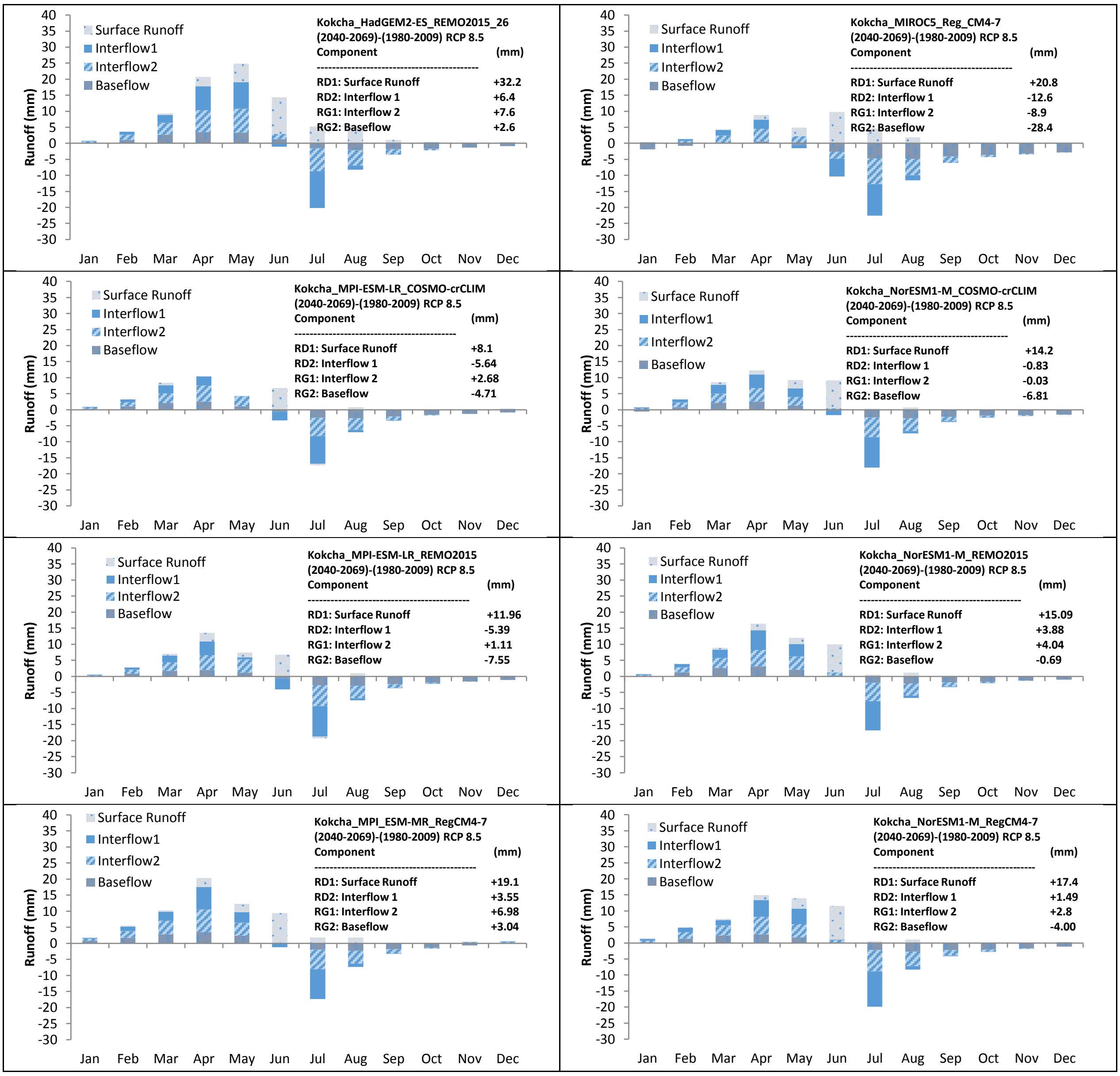

Figure 200. Change in monthly mean runoff future (2040-2069) – baseline (1980-2009) for Kokcha sub-basin, RCP8.5.

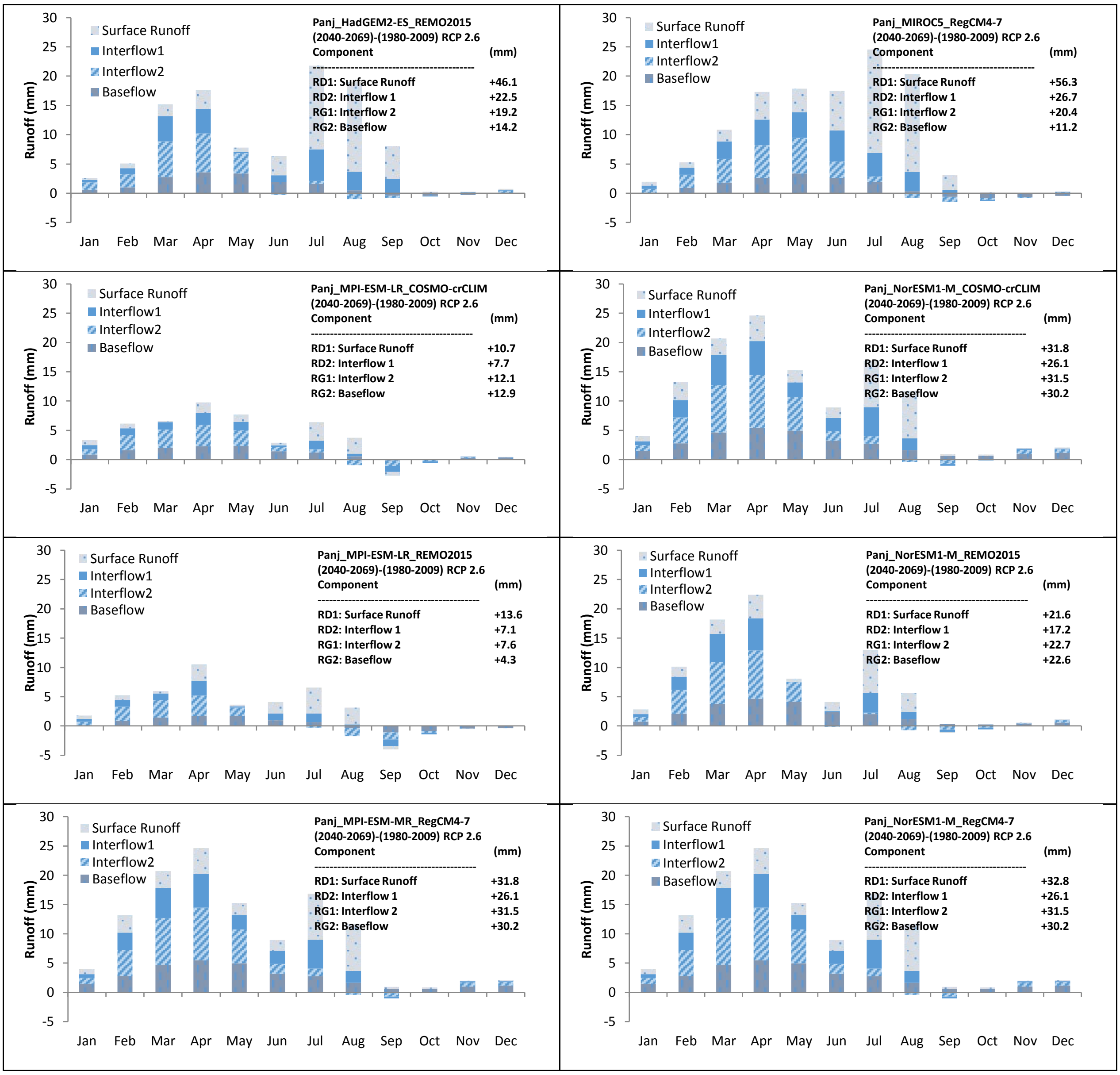

Figure 201. Change in monthly mean runoff future (2040-2069) – baseline (1980-2009) for Panj sub-basin, RCP2.6.

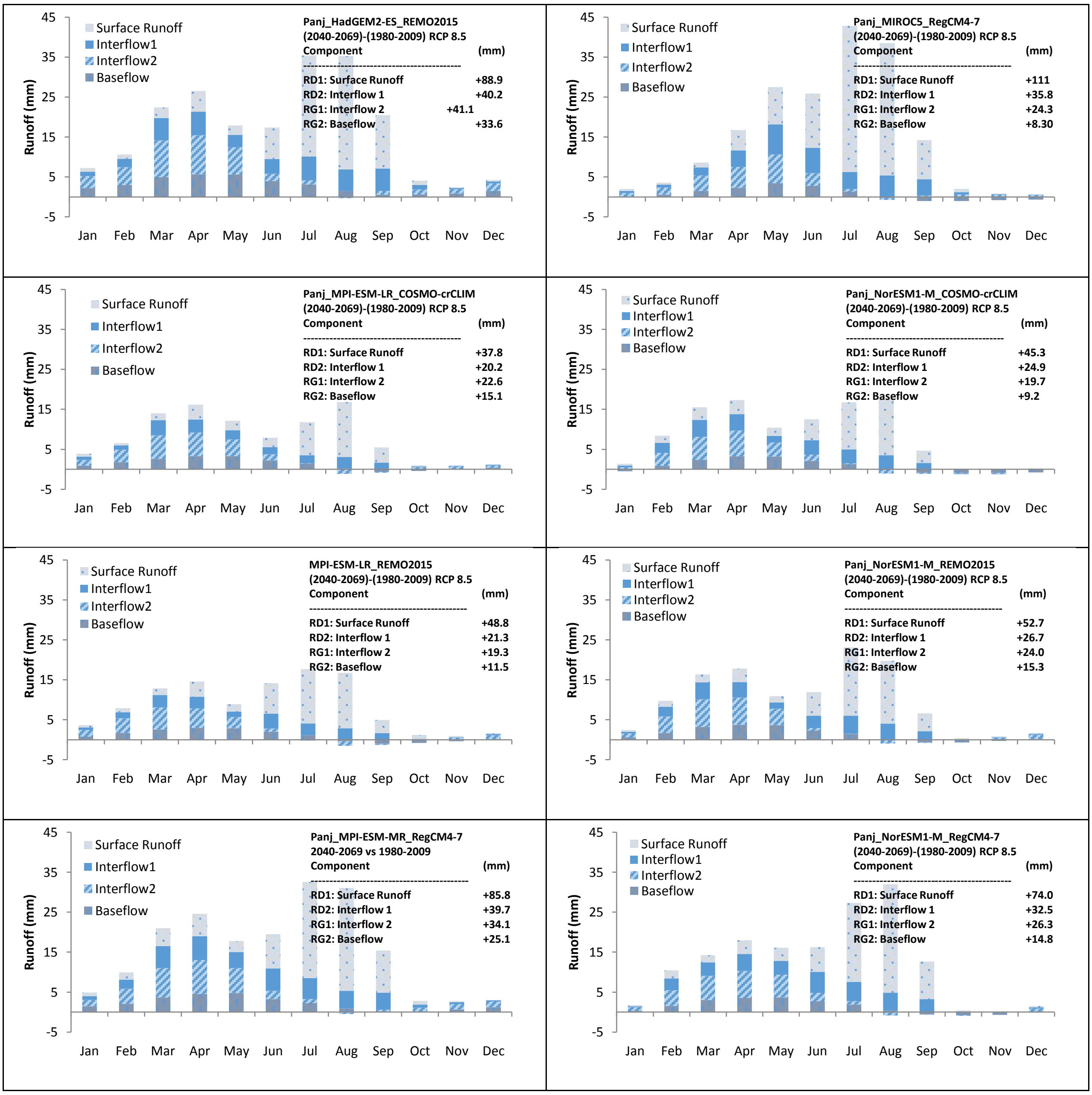

Figure 202. Change in monthly mean runoff future (2040-2069) – baseline (1980-2009) for Panj sub-basin, RCP8.5.

J2000 hydrological model sensitivity analysis

To understand the degree to which model outputs were influenced by the specific parameterizations in the model, two different sensitivity analyses were performed:

1. The model-sensitive parameters: these are the parameters that affect the shape of the hydrograph (Table 72). Thirty-six parameters were evaluated and grouped into three categories: a) initial condition parameters, b) soil parameters, and c) snow and glacier parameters. Individual models for each sub-basin were calibrated using different values of the parameters as shown in Table 72.

Table 64. J2000 hydrological model parameters used for model calibration of individual sub-basins (Kunduz-Ku, Khanahad-Kh, Kokcha-Ko, Panj-P).

Module	Parameter	Description	Actual Values	Range
Precipitation distribution	Trs	Base temperature	Kh, Ko 0.5 Ku 0.2 P 1	-1 to +1
Interception module	a_rain	Interception storage for rain	Kh, Ko, P 1.0 Ku 3.5	0-5
	a_snow	Interception storage for snow	Kh, Ko, P 1.28 Ku 3.0	0-5
Snow module	snowCritDens	Critical density of snowpack	Kh, Ko, P 0.38 Ku 0.1	0-1
	snowColdContent	Cold content of snowpack	Kh 0.0001 Ko, P 0.02	0-1
	baseTemp	Threshold temperature for snowmelt	Kh -3.5 Ko -2.5 Ku -1.4 P 2	-5 to +5
	t_factor	Melt factor by sensible heat	4.1 P 5	0-5
	r_factor	Melt factor by liquid precipitation	0.5	0-5
	g_factor	Melt factor by soil heat flow	Kh, Ko, P 1.73 Ku 0.01	0-5
Glacier module	meltFactorIce	Melt factor for ice melt	5 P 1	0-5
	al phaIce	Radiation melt factor for ice	0.9	0-5
	kIce	Routing coefficient for ice melt	0.5 P 4	0-50
	kSnow	Routing coefficient for snowmelt	5	0-50
	kRain	Routing coefficient for rain runoff	26.1	0-50
	debrisFactor	Debris factor for ice melt	3	0-10
	Tbase	Threshold temperature for melt	-3.7 P 3	-5 to +5

Module	Parameter	Description	Actual Values	Range
Soil module	soilMaxDPS	Maximum depression storage	Kh, Ko, P 0.5 Ku 6.2	0-10
	soilLinRed	Linear reduction coefficient for actual evapotranspiration	Kh, Ko, P 4.6 Ku 8	0-10
	soilMaxInfSummer	Maximum infiltration in summer	60	0-200
	soilMaxInfWinter	Maximum infiltration in winter	75	0-200
	soilMaxInfSnow	Maximum infiltration in snow cover areas	40	0-200
	soilImpLT80	Infiltration for areas lesser than 80% sealing	Kh, Ko, P 0.5 Ku 0.1	0-1
	SoilDistMPSLPS	MPS–LPS distribution coefficient	Kh, Ko, P 0.27 Ku 9.6	0-10
	SoilDiffMPSLPS	MPS–LPS diffusion coefficient	Kh, Ko, P 0.1 Ku 8.9	0-10
	soilOutLPS	Outflow coefficient for LPS	Kh, Ko, P 2.3 Ku 2.5	0-10
	soilLatVertLPS	Lateral vertical distribution coefficient	Kh, Ko, P 0.3 Ku 2.9	0-10
	soilMaxPerc	Maximum percolation rate to	Kh, Ko, P 20 Ku 60.1	0-100
	soilConcRD1Flood	Recession coefficient for flood event	Kh, Ko, P 1.3 Ku 0.2	0-10
	soilConcRD1Flood threshold	Threshold value for soilConcRD1Flood	300	0-500
	soilConcRD1	Recession coefficient for overland flow	Kh, Ko, P 2.8 Ku 4.0	0-10
	soilConcRD2	Recession coefficient for interflow	Kh, Ko, P 3 Ku 9.5	0-10
Groundwater module	gwRG1RG2dist	RG1–RG2 distribution coefficient	Kh, Ko, P 2.1 Ku 2.4	0-5
	gwRG1Fact	Adaptation for RG1 flow	Kh, Ko, P 0.3 Ku 2.8	0-10
	gwRG2Fact	Adaptation for RG2 flow	Kh, Ko, P 0.4 Ku 4.1	0-10
	gwCapRise	Capillary rise coefficient	Kh, Ko, P 0.01 Ku 0.4	0-10
Reach routing	flowRouteTA	Flood routing coefficient	Kh 30.3 Ko 20.1 Ku 8.3 P 18.3	0-100

a. Individual condition parameters: the results suggest that initRG2 or Initial groundwater is the most sensitive parameter in the model, this usually affects the baseflow in the model (Figure 248).

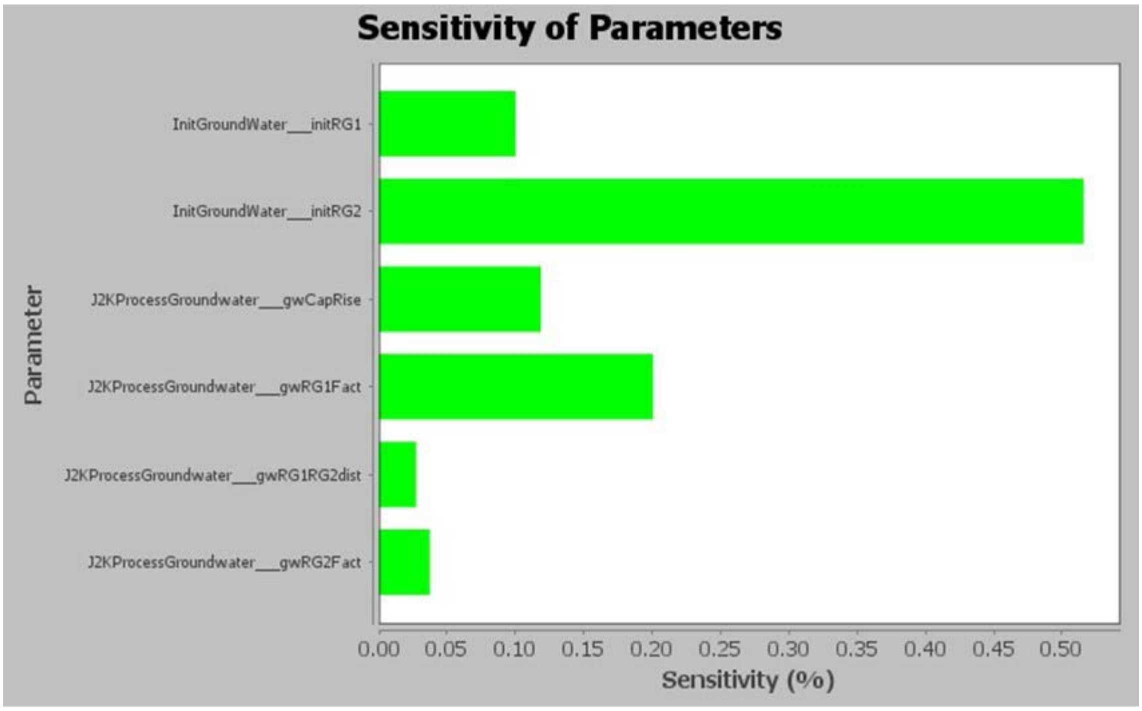

Figure 203. Sensitive parameters for initial conditions in the J2000 model (see Table 72 for descriptions of the parameters).

b. Soil parameters: the results suggest that soilLinRed, which is the linear reduction coefficient for actual evapotranspiration, is the most sensitive soil parameter in the model (Figure 249).

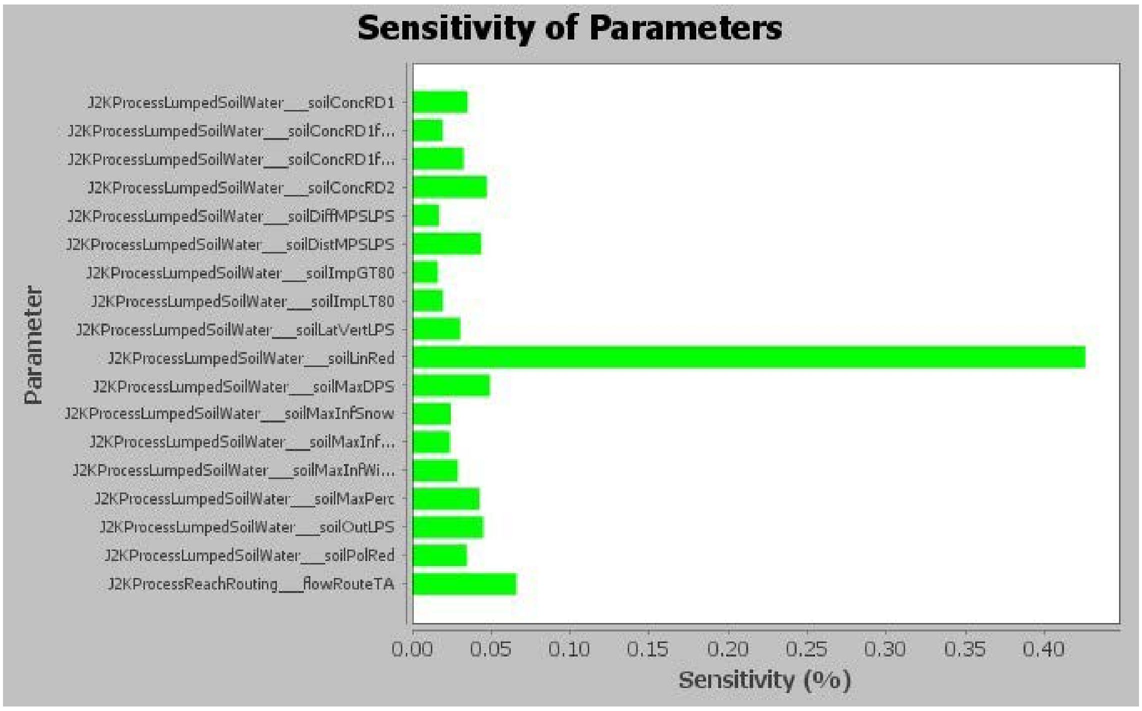

Figure 204. Sensitive parameters for soil parameters in the J2000 model (see Table 72 for descriptions of the parameters).

APPENDICES

c) Snow and glacier parameters: these parameters usually adjust the summer peaks, ccf_factor and t_factor, which are the cold content of snowpack and melt factor by sensible heat, were suggested to be the most sensitive snow and glacier parameter in the model (Figure 248).

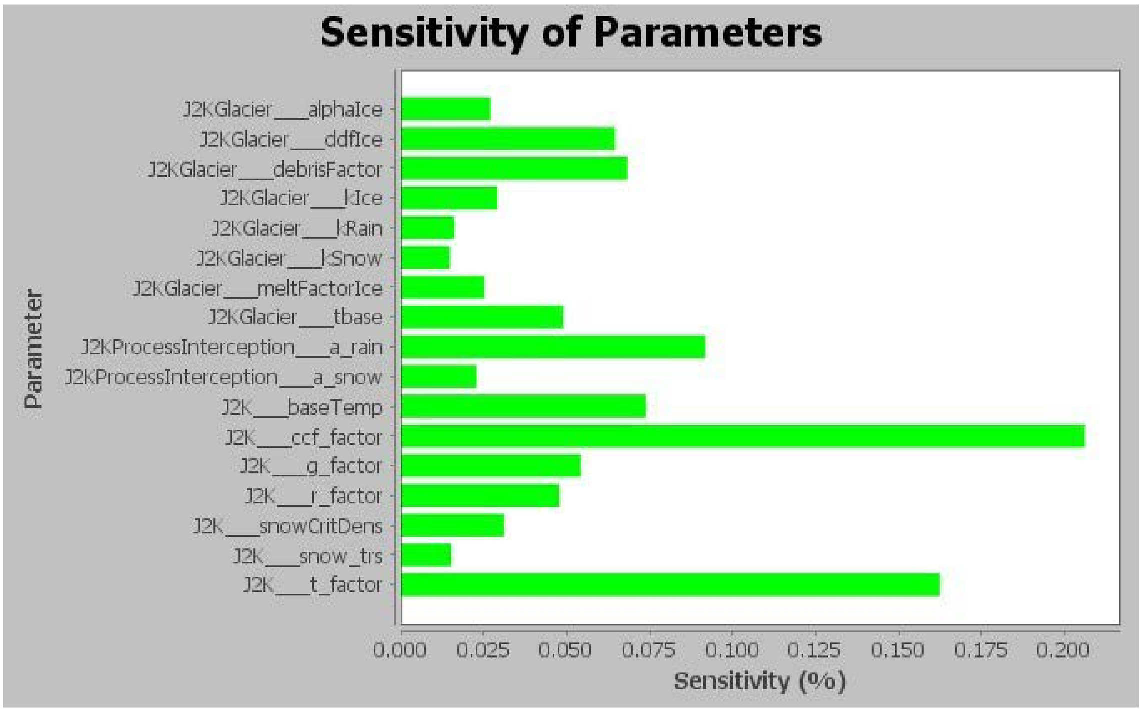

Figure 205. Sensitive parameters for snow and glacier parameters in the J2000 model (see Table 72 for descriptions of the parameters).

2. Sensitivity analysis of regionalization parameters: for transformation of point data into a spatially distributed dataset, the model adopted a regionalization approach (Krause, 2001). This sensitivity analysis is performed for three parameters that affect the regional distribution of climate conditions when modeling each sub-basin. The three main parameters are as follows:

a. Number of closest stations for regionalization: this parameter adjusts the number of closest stations to be considered in the calculations of hydrological outputs for each HRU. The closest stations are more likely to have homogeneous climate characteristics.

b. Power of the inverse distance-weighted (IDW) function used for regionalization: the model uses (IDW) interpolation method for interpolation of climate variables; adjusting this parameter adjusts the exponent of the function to weight closer stations more or less heavily in the model.

c. Elevation correction (on/off): this parameter enables consideration of elevation effects on climate parameters. This is the vertical variability quantified by a linear regression between station elevation and the parameter value, which provides a daily gradient and the coefficient of determination. If this coefficient is greater than a user defined threshold, the parameter values are adapted to the elevations of the discrete subareas by the gradient of the regression line (Krause, 2001). If this correction is set to off, not such adjustment is made.

To optimize performance of the models, we examined a range of values for IDW (1, 3, 5, 7, 10, and 20), the number of closest stations (1, 3, 5, and 7), and different threshold values for the coefficient of determination to elevation correction (0, 0.3, 0.5, 0.7, and off).

For Kunduz, the results indicated higher NS values with no elevation correction coefficient, and with higher IDW values. However, while the parameterization with the number of stations set to 3 had the highest NS among other results, using a higher number of stations in the model utilizes more data, which can reduce the uncertainty in the results. Evaluating the results with IDW = 7, number of stations = 7, and elevation correction coefficient = off, the results show minimal differences in terms of NS values as compared to when number of stations = 3. Therefore, we accepted IDW = 7, number of stations = 7, and elevation correction coefficient = off for this sub-basin (Figure 251).

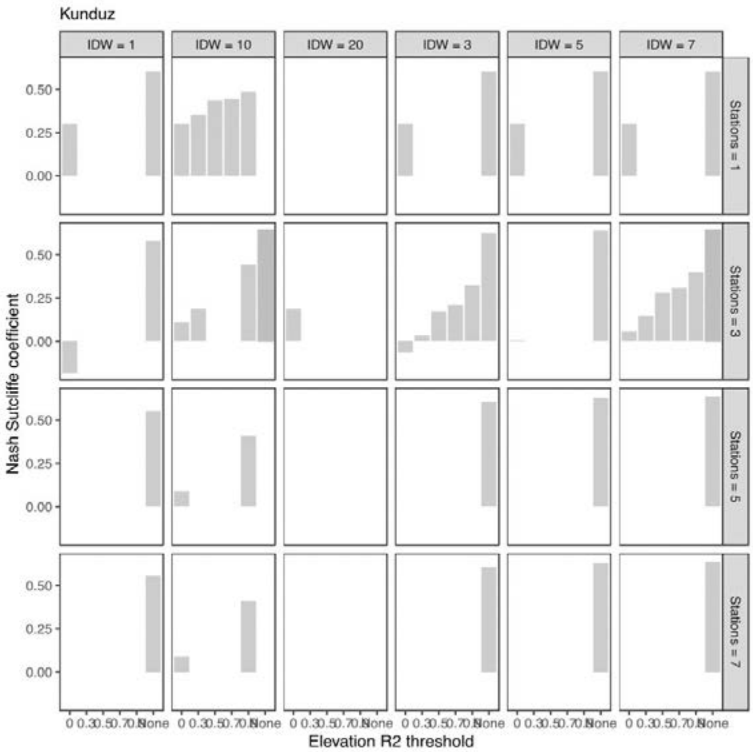

Figure 206. Results of sensitivity analysis based on comparative NS values for Kunduz sub-basin.

Similarly, for Khanabad, the parameterization with IDW = 1, number of stations = 7, and elevation correction coefficient = 0.7 was selected ().

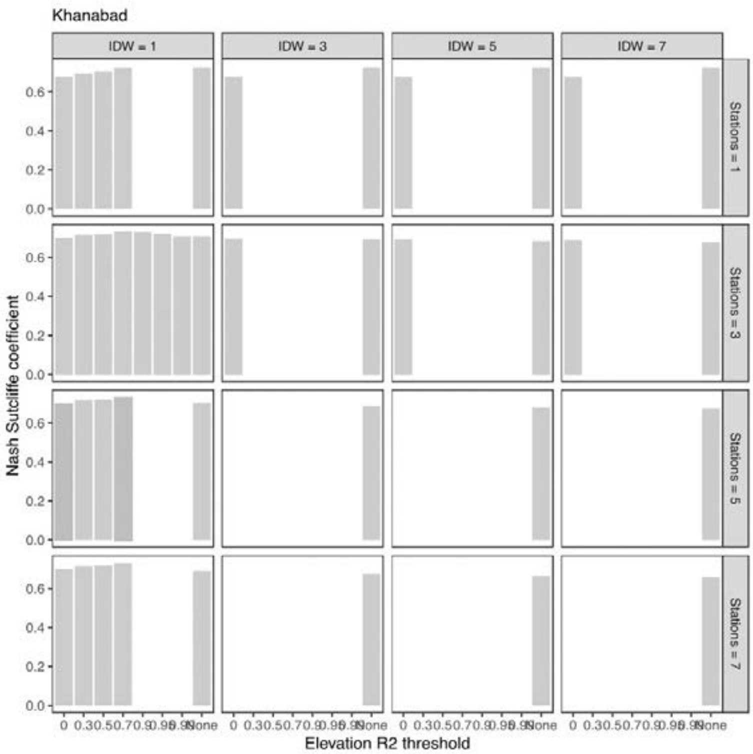

Figure 207. Results of sensitivity analysis based on comparative NS values for Khanabad sub-basin.

Kokcha had a higher NS value with number of stations = 5, IDW = 1, and elevation correction coefficient = off (Figure 253). However, following the previous approach of preferring a greater number of stations all else being equal, the result with number of stations = 7 had a very similar NS value and so was selected.

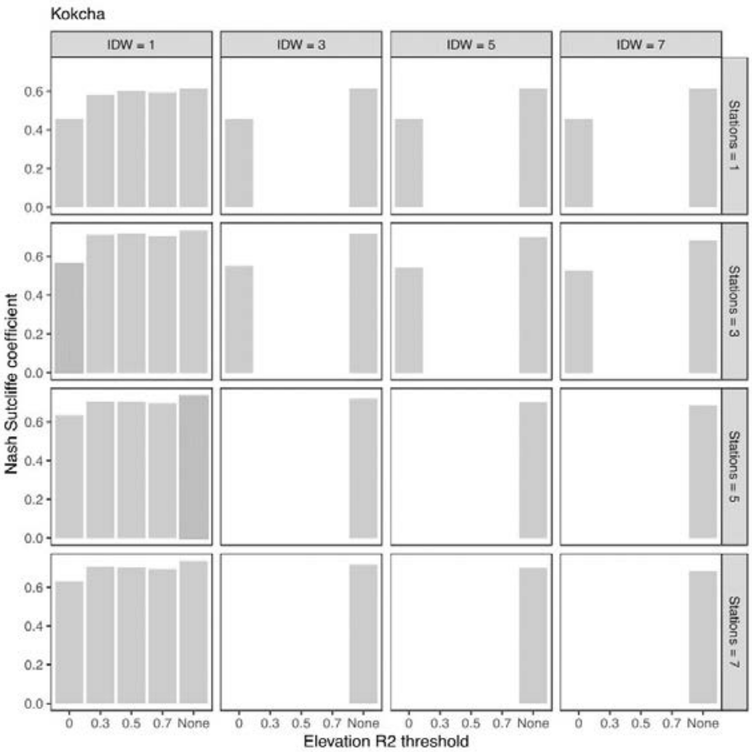

Figure 208. Results of sensitivity analysis based on comparative NS values for Kokcha sub-basin.

The Panj sub-basin outlet is along the northern Afghanistan border, which lacks hydrological data to evaluate, therefore the Sust catchment was used for this sub-basin instead. Sust is also different from the other catchments in having higher NS values with increasing numbers of stations and IDW values. The sensitivity analysis showed that there were minimal differences in NS values across different parameterizations of numbers of stations and IDW values, and the Sust catchment has only one closest station. Thus, we considered all Panj stations for the Sust catchment and selected the number of stations = 5, IDW = 5, and elevation correction coefficient = off following the results of the sensitivity analysis (Figure 254).

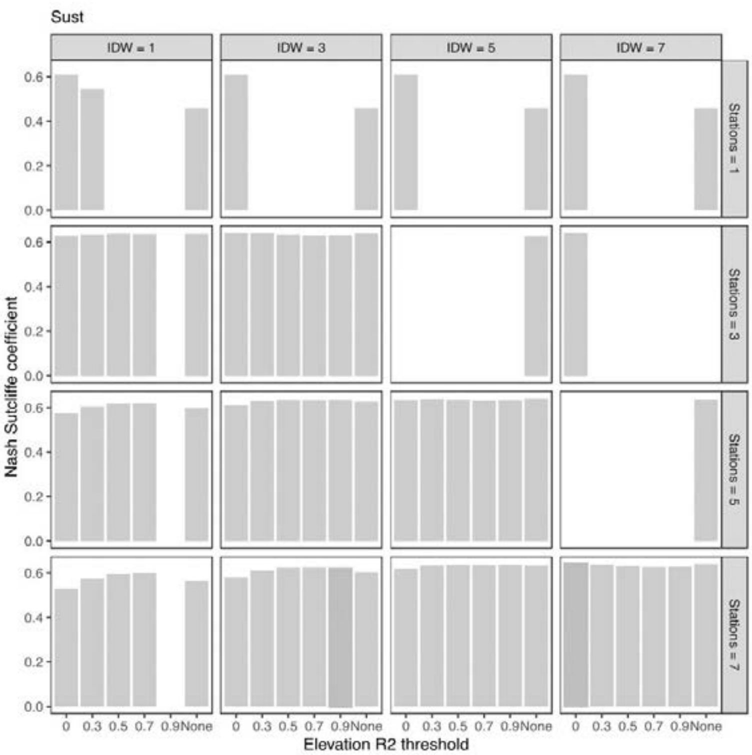

Figure 209. Results of sensitivity analysis based on comparative NS values for Sust sub-basin.

APPENDICES

Comparison of J2000 and SWAT Hydrological Model Results

Selecting a model for a particular case study is challenging and depends on many factors, i.e., purpose of the study, model algorithm, data availability, and model response considering actual characteristic of the basin (Gleick, 1986). Physically based models are more likely to consider glaciers and snow contributions to runoff as a collection or separate components. However, a conceptual model developed for a specific time and location cannot be transferable in space or time (Frenierre and Mark, 2014; Ghulami 2017). We applied two hydrological models (J2000 and SWAT) to evaluate the performance of the models considering the actual observed data and the characteristics of the P-ARB. In addition, a comparative analysis was also carried out that improves the scientific viability of the modeling results. We compared the outputs from the two models for the period (2013-2019) at the outlet of three sub-basins: Kunduz sub-basin, which is mainly rain and snow fed basin, and Kokcha and Panj sub-basins, which have glacier contributions as well.

SWAT and J2000 model comparison at Chardara station for the Kunduz sub-basin

The models outputs at Chardara station for Kunduz sub-basin revealed good fit to the observed data (Figure 255). However, when examining mean monthly discharge trends (Figure 256), the SWAT model overestimated runoff in spring (April and May), but better simulated the observed peak in June; however, SWAT continued to overestimate discharge peaks from July to October. In contrast, the J2000 model provided a better estimation of runoff in winter and spring months with a slight underestimation in June and better estimation in later summer months compared to SWAT. The main overestimation of runoff in the SWAT model was baseflow that led to high estimates of total runoff (Figure 256).

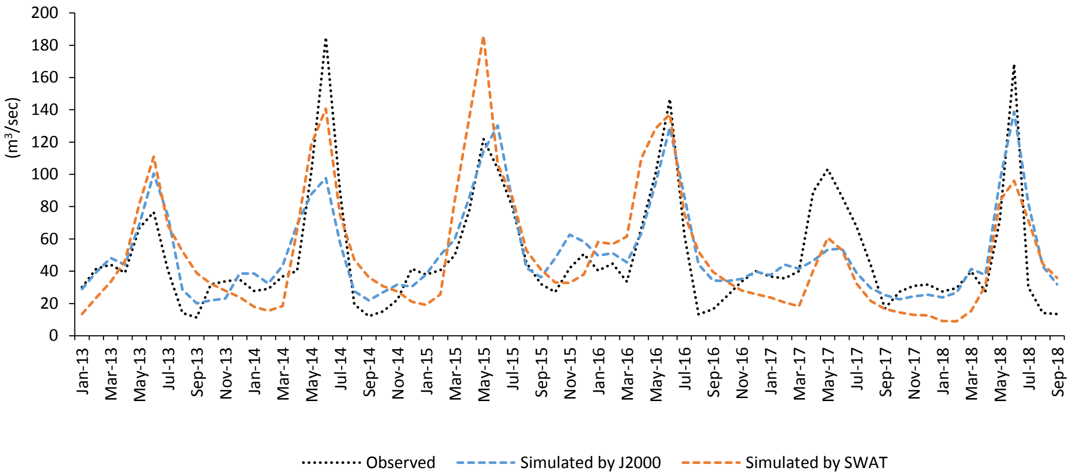

Figure 210. Observed monthly mean discharge at Chardara station and the simulated discharge with J2000 and SWAT models.

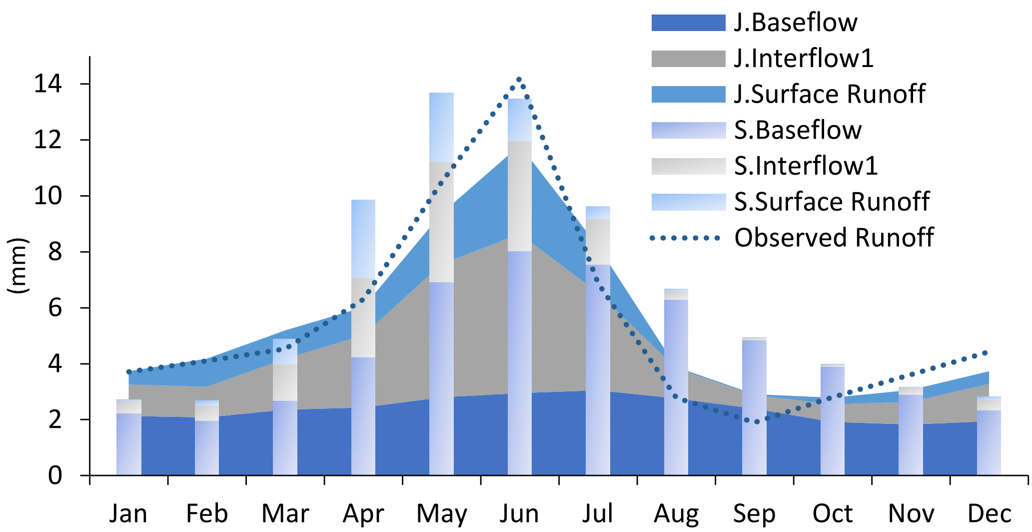

Figure 211. Mean monthly runoff components at Chardara station simulated by J2000 model abbreviated with J. and simulation by SWAT model abbreviated with S.

APPENDICES

The water balance components of both models were examined (Figure 257), and the SWAT model overestimated precipitation with potential and actual evapotranspiration over the sub-basin in comparison to the J2000 model results. Therefore, there are no significant differences in total runoff and snowmelt between the results of these models.

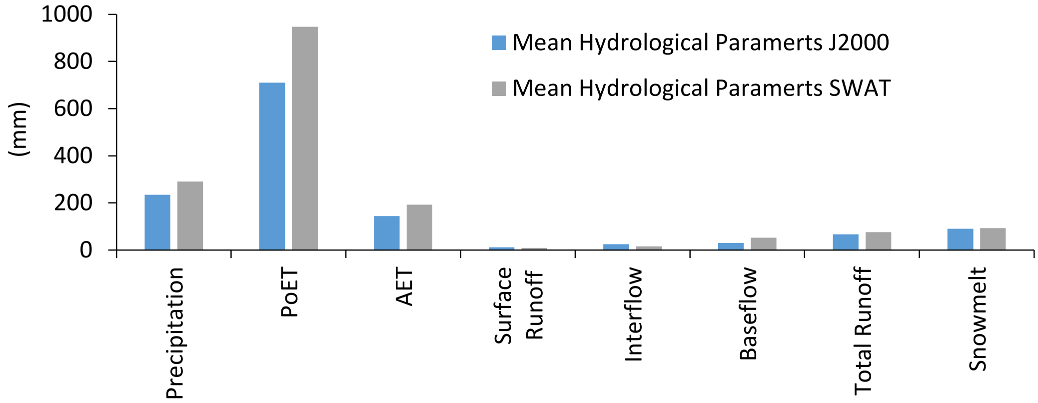

Figure 212. Water balance component estimation by J2000 and SWAT models at Chardara station.

While comparing the accuracy coefficients of both models for periods of calibration and validation, the J2000 model showed higher Nash-Sutcliffe model efficiency and r^2 than the SWAT model (Table 73).

Table 65. Comparison of J2000 and SWAT model accuracy at Chardara station.

Accuracy coefficients	Calibration	Validation
J2000 results accuracy		
Nash–Sutcliffe model efficiency	0.70	0.69
Coefficient of determination (r^2)	0.70	0.65
SWAT results accuracy		
Nash–Sutcliffe model efficiency coefficient	0.55	0.50
Coefficient of determination (r^2)	0.69	0.56

Model comparison at Khwajaghar station for the Kokcha sub-basin

Kokcha is partially a glacier fed sub-basin and both models performed very well in providing the outputs that matched observed monthly discharge data (Figure 258). In contrast to Chardara station, SWAT underestimated runoff in summer months (June, July, and August) and the simulated runoff in spring (April and May) was slightly overestimated (Figure 259). The J2000 model achieved better simulation results year-round. The underestimation of the SWAT model could be due to the contribution of glacier melting as a main variable in total runoff because SWAT is a rainfall-runoff model. Such uncertainty with SWAT was also observed in other studies (Adnan et al., 2019). Higher values of precipitation, potential evapotranspiration, and actual evapotranspiration were obtained by the SWAT model, while the J2000 model attained similar annual baseflow and snow melt with a slight decrease in total runoff in comparison to the SWAT model results (Figure 260). Examining the model simulation efficiencies, J2000 had higher Nash-Sutcliffe model efficiency for both calibration and validation periods (0.82, 0.87) compared to the SWAT model (0.76, 0.70) (Table 74).

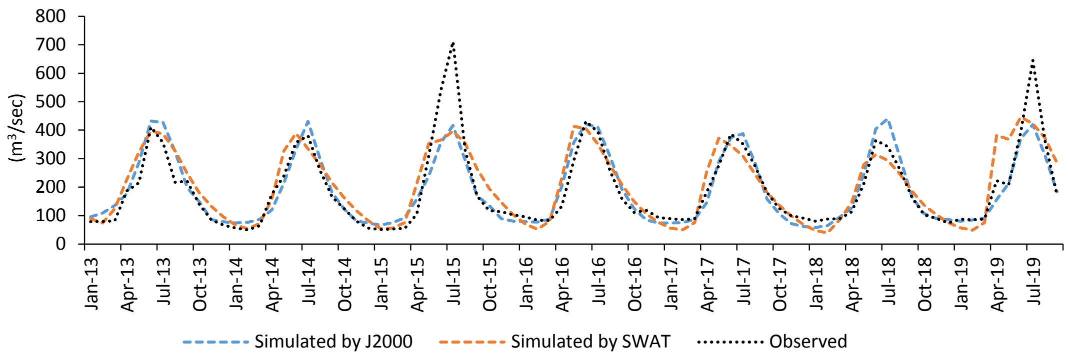

Figure 213. Observed monthly mean discharge at Khwajaghar station and the simulated discharge with both J2000 and SWAT models.

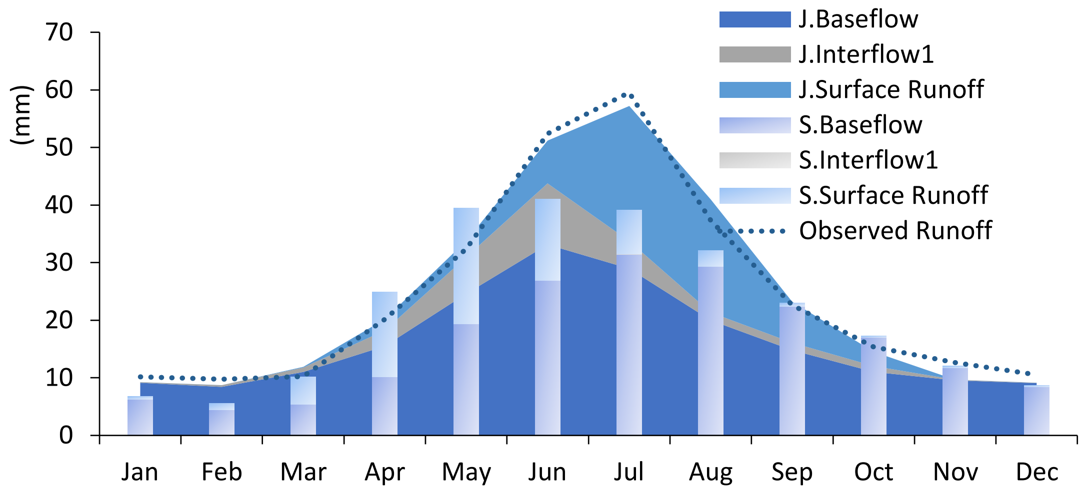

Figure 214. Mean monthly runoff component at Khwajaghar station simulated by J2000 model abbreviated with J. and simulation by SWAT model abbreviated with S.

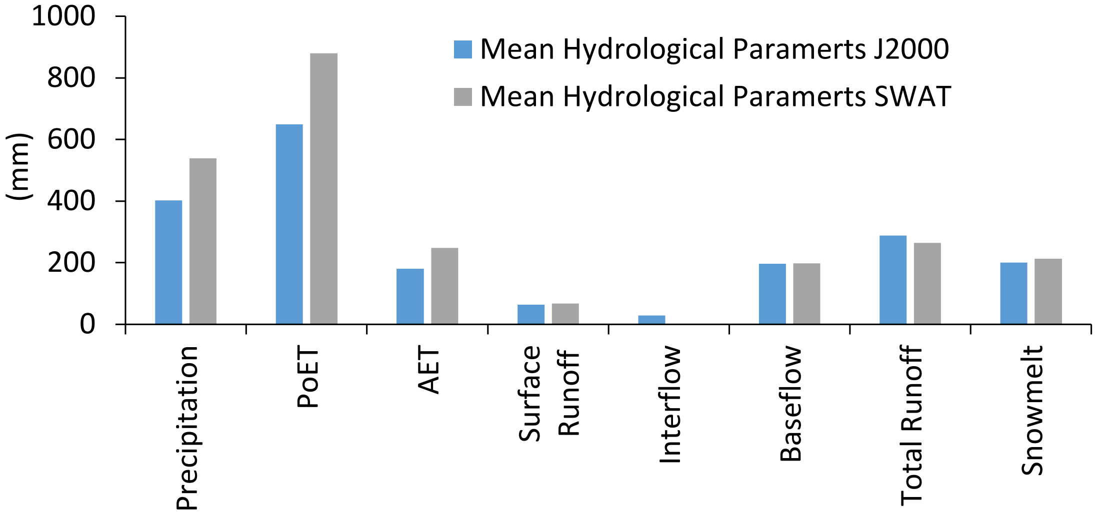

Figure 215. Water balance components estimated by J2000 and SWAT models at Khwajaghar station.

Table 66. Comparison of J2000 and SWAT model accuracy at Khwajaghar station.

Accuracy coefficients	Calibration	Validation
J2000 results accuracy		
Nash–Sutcliffe model efficiency	0.82	0.87
Coefficient of determination (r^2)	0.82	0.88
SWAT results accuracy		
Nash–Sutcliffe model efficiency coefficient	0.76	0.70
Coefficient of determination (r^2)	0.77	0.71

Model comparisons at Sust station for the Panj sub-basin

The Sust catchment has relatively more glaciers compared to the other catchments. As with Kokcha, the time series plots of observed and simulated discharge with both models fit well (Figure 261). The SWAT model adequately simulated summer peaks (July, August, and September) with higher contributions of baseflow, but it underestimated winter and spring peaks (from November to June). In contrast, the J2000 model simulated all peaks reasonably well except for early summer months (June and July) (Figure 262). Moreover, the J2000 model slightly overestimated total runoff in this sub-basin, possibly due to melting of glaciers (Figure 263). Therefore, the J2000 model obtained slightly better accuracy for the calibration and validation periods (Table 75).

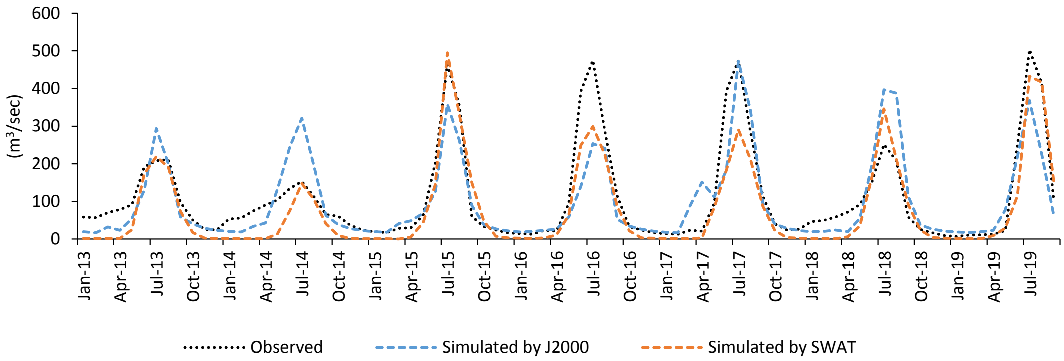

Figure 216. Observed monthly mean discharge at Sust station and the simulated discharge with both J2000 and SWAT models.

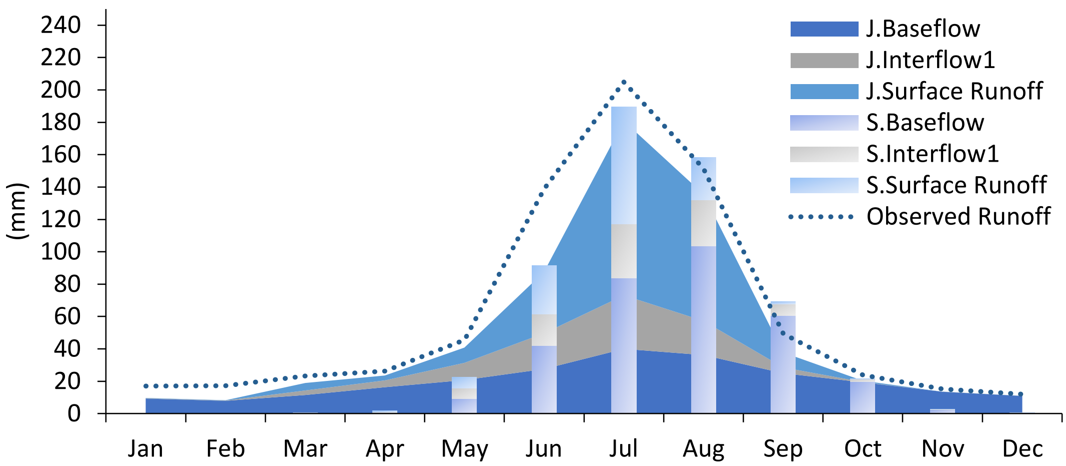

Figure 217. Observed monthly mean discharge at Sust station and the simulated discharge with both J2000 and SWAT models.

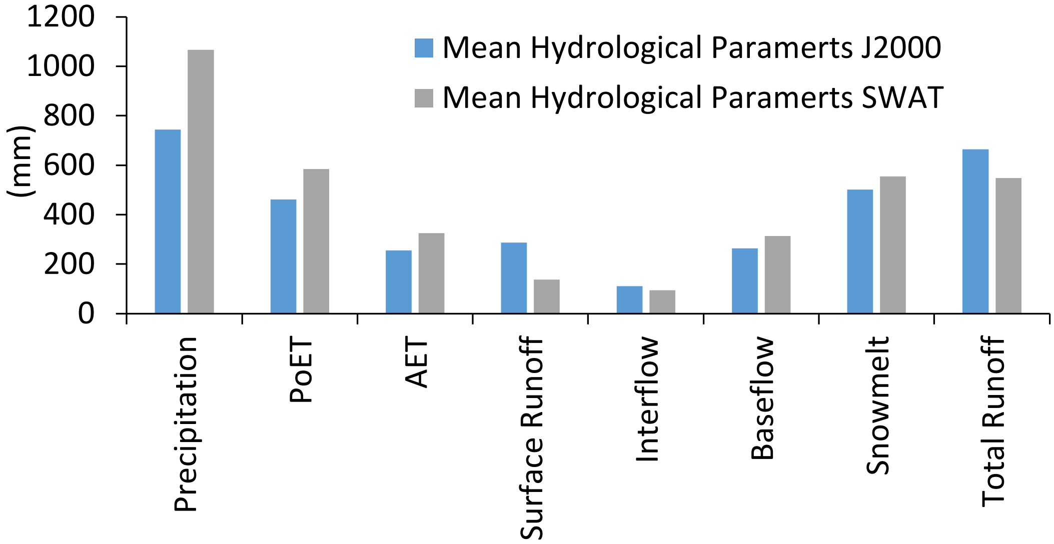

Figure 218. Water balance components estimated by J2000 and SWAT models at Sust station.

Table 67. Comparison of J2000 and SWAT model accuracy at Sust station.

Accuracy coefficients	Calibration	Validation
J2000 results accuracy		
Nash–Sutcliffe model efficiency	0.56	0.71
Coefficient of determination (r^2)	0.70	0.76
SWAT results accuracy		
Nash–Sutcliffe model efficiency coefficient	0.43	0.52
Coefficient of determination (r^2)	0.88	0.78

A comparative summary of the model performance of SWAT and J2000 shows that the J2000 model provided better statistical fit between simulated and observed data considering the characteristics of the sub-basins and performed better in estimating the peak runoff due to glacier contribution than the SWAT model (Table 76). Therefore, the J2000 model was selected for making future runoff estimations in the basin.

Table 68. Summary table of J2000 and SWAT model results comparison. Cal: calibration. Val: validation. NS: Nash–Sutcliffe model efficiency coefficient. R^2: coefficient of determination.

	Hydrological components	J2000 model	SWAT model
Khwajaghar Station	Monthly mean discharge	Cal-NS = 0.82 Cal-R2 = 0.82 Val-NS = 0.87 Val-R2 = 0.88	Cal-NS = 0.76 Cal-R2 = 0.77 Val-NS = 0.70 Val-R2 = 0.71
	Runoff Components	Captured summer peaks (June & July)	Underestimated the summer peaks and backward shifted (April & May)
	Water Balance component	Increased in total runoff due to glacier contribution	SWAT is more rainfall-runoff based and peaked in April and May
Chardara Station	Monthly mean discharge	Cal-NS = 0.70 Cal-R2 = 0.70 Val-NS = 0.69 Val-R2 = 0.65	Cal-NS = 0.55 Cal-R2 = 0.69 Val-NS = 0.50 Val-R2 = 0.56
	Runoff components	Well aligned with observed runoff peaks	SWAT well captured June peak, however overestimated April and May peaks
	Water Balance component	Both models were well aligned with total runoff and snowmelt simulation	Both models were well aligned with total runoff and snowmelt simulation
Sust Station	Monthly mean discharge	Cal-NS = 0.56 Cal-R2 = 0.70 Val-NS = 0.71 Val-R2 = 0.76	Cal-NS = 0.43 Cal-R2 = 0.88 Val-NS = 0.52 Val-R2 = 0.78
	Runoff components	Underestimated peaks in summer, however, well simulated baseflow	Well captured summer peaks, however, simulation of baseflow was poor
	Water Balance component	Surface flow component was simulated with higher values	Underestimated total runoff due to no consideration of runoff from glaciers

Long-term river discharge analysis

We examined measured mean monthly discharge data (2007 to 2019) versus observed historical mean monthly data (1965 to 1980) at Chardara and Khwajaghar stations based on availability of the historical data depicted (Figure 219 and Figure 220, respectively). The aim was to assess whether the observed data corresponds to a normal yearly dry or wet period. Such comparisons helped to realize that the observed data used for the model was distributed on both sides of the historical mean data.

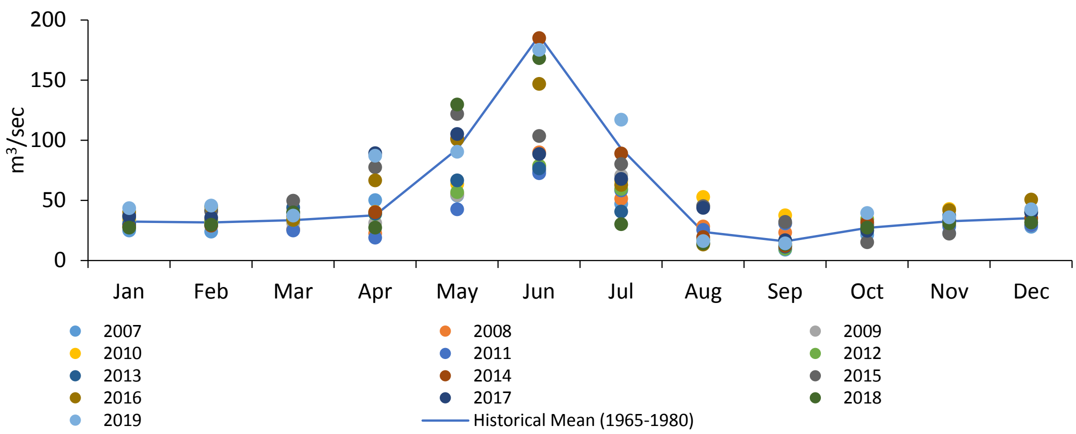

Figure 219. Historical long-term mean monthly discharge (1965-1980) versus current mean monthly discharge (2007-2019) at Chardara station in Kunduz sub-basin.

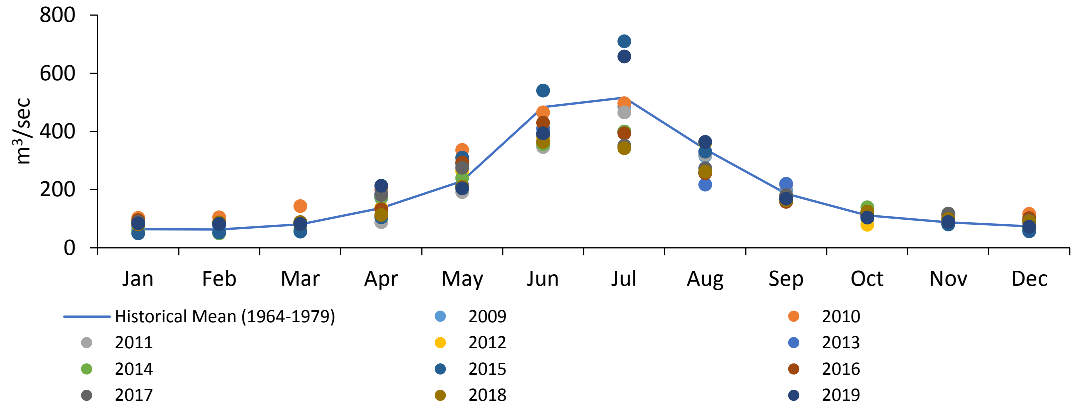

Figure 220. Historical long-term mean monthly discharge (1964-1979) versus current mean monthly discharge (2007- 2019) at Khwajaghar station in Kokcha sub-basin

Main hydrological variables

For long-term hydro-climatic change assessment, streamflow is a very useful indicator; its trend and variability assessment are critical for water resources planning purposes. Understanding dynamics and behaviours of hydrological variables over a long-term period (e.g., 30 years) is essential for adaptation and mitigation of climate change impacts (Melesse et al., 2019). There are some hydrological variables, which are also assessed in this study, for example, streamflow is one of the most important components of water cycle and its forecasting is of utmost importance for the planning and management of water resources at watershed, catchment, basin, regional, and continental spatial scales (Malekian and Chitsaz 2021). The different indicators assessed in this study are given in Table 69.

Table 69. Hydrological vulnerability indicator and Impact.

Hydrological vulnerability indicator	Definition
Change in Mean Stream flow	Streamflow is defined as "a measure of the rate at which water is carried by rivers and streams" (United States Environmental Protection Agency, 2021). It is important water resource for people and critical for environment. It has a direct influence on drinking water supply, irrigating crops, and generation of electricity. It is measured in *cubic meters per second*.
Change in Maximum Stream flow	Excess change in maximum stream flow cause severe floods, sediment, and pollutants transport. Communities and infrastructures are highly vulnerable to increases in maximum stream flow.
Change in Minimum Stream flow	The minimum stream flow is the amount of flow necessary to preserve desired stream values, including fish and wildlife habitat, aquatic life, navigation and transportation, recreation, water quality, and aesthetic beauty according to IDAHO (IDAHO Department of Water Resources, 2021). Reduces in minimum stream flow will negatively impact those inhabitants.

Appendix 6. Wildlife Species Supplementary Methods & Results

Change in Species Range Size and Location

E

As is the case with any model, the results obtained from an SDM modelling performance are a function of the inputs; in the case of an SDM, the major inputs are (a) the species data utilized, (b) the predictor variables utilized, and (c) the choice of mathematical algorithm used to relate (a) and (b) (Diniz-Filho et al. 2009, Elith and Graham 2009). Below, we briefly describe each of these three inputs and the rationale behind our decision-making process regarding each one.

Species data: We created a list of vertebrate species of interest for the P-ARB. Broadly, species that are of global conservation concern, that have a large proportion of their global range within the P-ARB, and/or that are have particularly large impacts on human livelihoods were considered for exclusion. We included mammal, reptile, and bird species to ensure taxonomic diversity.

For each species, we obtained presence data from multiple sources. We searched for occurrence records through the Global Biodiversity Information Facility (GBIF), an online portal that collates records from a variety of sources including museum specimens and citizen science efforts. Additionally, we relied on field data collected by WCS and other partner organizations. Finally, we conducted a literature search for each species and obtained publicly accessible datasets that included occurrence records. Only species with at least 5 occurrence records in the P-ARB were considered. A full list of species is given in

Table 21; a list of data sources in addition to GBIF and field data is given in Table 70.

Table 70. List of references for species occurrence data, in addition to fieldwork sources and GBIF data.

Species	Citation
Snow leopard	Watts, S. M., T. M. McCarthy, and T. Namgail. 2019. Modelling potential habitat for snow leopards (*Panthera uncia*) in Ladakh, India. *Plos One* 14:e0211509.
Urial	Siraj-Ud-Din, M., R. A. Minhas, M. Khan, U. Ali, S. Ali, B. Ahmad, and M. Awan. 2016. Conservation Status of Ladakh Urial (*Ovis vignei vignei Blyth*, 1841) in Gilgit Baltistan, *Pakistan. Pakistan Journal of Zoology* 48:1353–1365.
Large-billed Reed Warbler	Timmins, R. J., S. Ostrowski, N. Mostafawi, H. Noori, A. M. Rajabi, L. Svensson, U. Olsson, and C. M. Poole. 2016. New information on the Large-billed Reed Warbler *Acrocephalus orinus*, including its song and breeding habitat in north-eastern Afghanistan. *Forktail* 26: 9–23.

Predictor variables: In an SDM process, predictor variables are those variables which are thought to have some influence on a given species' range. The bioclimatic variables produced by Columbia University and described thoroughly in section 2.1 were the main set of predictor variables utilized, which are widely utilized in SDM studies. These variables were available for 8 Global Circulation Model-Regional Circulation Model (GCM-RCM) combinations, each of which was further available for two representative concentration pathways (RCPs)–RCP2.6 represents a low-emissions future while RCP8.5 represents a high-emissions future. These variables were utilized as multidecadal averages for three time horizons–present (1980-2009), mid-century (2040-2069) and end-century (2070-2099).

In addition to the climate variables, we also considered a modified version landcover classification developed in section 2.3, as well as the Normalized Difference Vegetation Index (NDVI). To address the potential effects of human activities on the landscape, we utilized the Global Human Modification (GHM) layer (Kennedy et al. 2019). Finally, we utilized three topographical variables—elevation, slope, and aspect. A full list and description of all predictor variables is given in Table 71.

Table 71. List of predictor variables for species distribution models.

Variable	Description	Source
Bioclimatic variables	A set of 19 variables derived from 4 major climate parameters at monthly timescales – mean temperature, minimum temperature, maximum temperature, and precipitation. These variables were utilized as multidecadal averages. 6 of the 19 variables were used – see Table 58 below for list and description	Produced for this project – see section 2.1
Topography – elevation, slope, and aspect	Elevation is self-explanatory. Slope and aspect are variables derived directly from gridded elevation data and refer to the steepness of the terrain and the direction it faces respectively	NASA SRTM dataset (Farr et al. 2007)
Global Human Modification	The GHM is a global dataset that quantifies the effect from a set of 13 anthropogenic stressors.	Kennedy et al. (2019)
Normalized Difference Vegetation Index	NDVI is an index based on remote sensing data, and specifically the red and near infrared spectral bands. NDVI is widely used as an index of vegetation density and has been shown to relate closely to on-the-ground conditions	The original derivation of NDVI comes from Kriegler et al. (1969). The NDVI maps used here were produced for this project – see section 2.3.
Landcover	Landcover denotes the present state of the area under consideration. Note that this is not identical to NDVI – for example, croplands may have similar NDVI to certain natural landcover types.	Produced for this project – see section 2.3

Table 72: List of bioclimatic variables used in species distribution models

Bioclimatic variable	Description
Bio2	Mean diurnal temperature range
Bio7	Mean annual temperature range
Bio10	Mean temperature of warmest quarter
Bio11	Mean temperature of coldest quarter
Bio16	Precipitation of wettest quarter
Bio17	Precipitation of driest quarter

Modelling algorithm: For the purposes of this indicator, we conceptualized the probability of the presence of species at a given location as being a hierarchical process occurring at two spatial scales. At a broad (regional) scale, the range of a species is determined by the climatic conditions it can tolerate, while at a fine (local) scale occurrence is determined by variables such as human impacts, topography, and land cover.

Regional climate model: A common pitfall of creating SDMs based on climate for a relatively small landscape like the P-ARB is underestimating the total range of climate conditions that are suitable for a given species (Elith et al. 2010). When projecting models forward to future climate conditions, this can cause underpredictions of future species' ranges, which can have serious implications for conservation planning and policy. Fortunately, the climate data produced by Columbia University covers a far larger area than the P-ARB alone. We were therefore able to use species occurrence points outside the P-ARB to gain a holistic picture of the suitable climate conditions for each species. Moreover, we elected to use a relatively simple and conservative envelop algorithm. For each bioclimatic input variable, the algorithm determined the minimum and maximum value that had at least one occurrence for a given species, thus creating a multidimensional hypercuboid of permissible values paralleling the concept of the ecological niche (Hutchinson 1957, 1959). For simplicity, the output from the regional model was taken to be binary –climate values within the hypercuboid were assigned values of 1 (indicating suitability), while locations with climate values outside the hypervolume were assigned values of 0 (indicating unsuitability). This hypercuboid then spatially projected onto each time horizon (present, mid-century, and end-century) for each GCM-RCM combination and averaged by RCP.

Local 'ecological' model: To create a fine-scale map of species' occurrences within the P-ARB, we fit a second model to species presence data within the P-ARB only (i.e., excluding the datapoints used above that were outside the P-ARB but within the geographical scope of the Columbia climate data). For this purpose, we used ecological predictors like topography, NDVI, GHM and landcover, excluding climate information. The choice of SDM modelling algorithm is a critical part of the SDM process, and different algorithms operating on the same dataset can produce very different results. To reduce this source of uncertainty, we created an averaged prediction of five different algorithms (Random Forest, Boosted Regression Trees, Classification and Regression Trees, Support Vector Machines and Generalized Linear Models) that are each known to perform well in an SDM context in isolation (Araújo and New 2007, Grenouillet et al. 2011, Liu et al. 2011). For each algorithm, we created a common set of pseudoabsence points drawn at random across the P-ARB, as the input species datasets were generally unreliable for inferring true absences due to, among other factors, a lack of consistent survey effort information. The input data (presences, pseudoabsences and predictors) for each algorithm was then split 70-30 into training and testing data. The outputs from each algorithm were then weighted based on their performance on testing data before being averaged. This process was repeated 256 times to eliminate any randomness produced by the pseudoabsence selection; these 256 models were then averaged to produce the final local model.

An additional consideration in the SDM process is the selection of a threshold allowing for the conversion of continuous model output to discrete output. Discrete output is generally easier to interpret, particularly for policymaking purposes. However, the selection of a threshold itself can alter the results of the modelling process significantly (Liu et al. 2005, Nenzén and Araújo 2011). As mentioned above, the envelop model was fitted for each of 8 GCM-RCM combinations for both RCP scenarios at mid-century and end-century and was natively created as discrete (0-1) output. We combined these 8 outputs using a simple majority rule – any location where at least 4 of the 8 models agreed was climatically suitable was held to be suitable overall; areas determined by three or fewer models to be unsuitable were deemed unsuitable overall.

For the local model, we used two thresholds, a low and a high threshold, to create three categories of habitat suitability. For the low threshold, we used a relatively liberal criterion to discretize the local model, based on the lowest predicted value for known presence points – anything above that value was deemed ecologically suitable, while anything below that was deemed unsuitable. We then calculated the 70th percentile value of all ecologically suitable cells and took that to be the high threshold. Cells between the low and high threshold (definitionally, 70% of the areas deemed suitable) were treated as low-quality habitat; cells above the high threshold (the top 30% of all suitable cells) were deemed high-quality habitat.

The discretized local model was then multiplied by the discretized consensus envelop model to produce the final output for each timepoint and emissions scenario. These models were then overlaid to determine areas of range stability, range expansions and range contractions for each species. We also determined the total area occupied by each species in the P-ARB (using the low threshold, i.e., combining low-quality and high-quality habitat as the total range), and compared that to model output for the present – the change in relative range size for each species is given in Table 73 for mammals and Table 74 for birds.

Table 73. Estimated changes in range size for mammal species modelled, for RCP2.6 and RCP8.5 at mid-century and end-century. Changes are expressed as area of future range divided by area of current range; values above 1 indicate range expansions, while values below 1 indicate range contractions. Range contractions of over 50% are colored in red text.

Species	RCP2.6, mid-century	RCP2.6, end-century	RCP8.5, mid-century	RCP8.5, end-century
Afghan Pika	0.83	0.78	0.63	0.20
Altai Weasel	1.17	0.73	0.54	0.00
Argali	0.91	0.90	0.70	0.09
Baluchi Brush-tailed Mouse	1.03	1.07	1.08	1.02
Beech Marten	1.03	1.03	1.04	0.92
Brown Bear	1.00	1.01	0.97	0.80
Desert Hare	1.07	0.98	0.97	0.76
Eurasian Lynx	0.80	0.83	0.52	0.23
Grey Dwarf Hamster	0.65	0.84	0.66	0.37
Grey Wolf	1.06	1.04	1.08	0.90
Himalayan Rat	0.75	0.74	0.74	0.70
Lesser Shrew	0.87	0.91	0.90	0.68
Long-tailed Marmot	1.08	1.07	0.91	0.39
Pallas's Cat	0.94	0.95	0.97	0.91
Red Fox	1.01	0.99	0.97	0.83
Siberian Ibex	0.96	0.98	0.93	0.81
Snow Leopard	1.01	1.03	0.68	0.18
Stoat	0.78	0.54	0.32	0.07
Urial	1.05	1.07	1.04	0.84

Table 74. Estimated changes in range size for bird species modelled, for RCP2.6 and RCP8.5 at mid-century and end-century. Changes are expressed as area of future range divided by area of current range; values above 1 indicate range expansions, while values below 1 indicate range contractions. Range contractions of over 50% are colored in red text.

Species	RCP2.6, mid-century	RCP2.6, end-century	RCP8.5, mid-century	RCP8.5, end-century
Afghan Snowfinch	0.01	0.01	0.00	0.00
Alpine Accentor	1.21	1.08	1.05	0.40
Alpine Chough	0.99	1.05	1.00	0.77
Asian Crimson-winged Finch	0.95	1.05	0.99	0.70
Bearded Vulture	1.00	0.99	0.97	0.91
Black Redstart	1.01	1.01	1.01	0.97
Blue Rock Thrush	1.03	1.03	1.01	0.94
Blyth's Rosefinch	1.10	1.10	1.12	0.95
Brandt's Mountain Finch	1.03	1.07	1.05	0.93
Brown Accentor	1.01	0.99	0.94	0.72
Carrion Crow	1.06	1.07	1.04	1.00
Chukar Partridge	1.01	1.01	1.01	0.95
Citrine Wagtail	1.05	1.06	1.07	1.04
Common House Martin	1.03	1.02	1.02	1.01
Common Kestrel	1.02	1.02	1.03	0.97
Common Redshank	1.15	1.11	1.27	1.35

Species	RCP2.6, mid-century	RCP2.6, end-century	RCP8.5, mid-century	RCP8.5, end-century
Common Rock Thrush	0.98	1.00	1.00	0.95
Common Rosefinch	1.04	1.04	1.02	0.97
Common Sandpiper	1.06	1.07	1.10	1.10
Common Swift	1.03	1.04	1.01	0.95
Desert Wheatear	1.00	1.00	1.00	0.97
Eastern Rock Nuthatch	1.03	1.05	1.09	1.14
Eurasian Crag Martin	1.02	1.01	0.99	0.96
Eurasian Hoopoe	1.01	1.02	1.02	0.97
Eurasian Magpie	1.01	1.01	0.99	0.93
Eurasian Tree Sparrow	1.04	1.04	1.05	1.02
European Bee-eater	1.03	1.00	0.93	0.81
European Roller	1.05	1.06	1.09	1.08
Great Rosefinch	0.93	1.01	0.89	0.59
Grey-necked Bunting	1.06	1.03	1.03	0.98
Guldenstadt’s Redstart	1.22	1.22	1.23	0.48
Himalayan Snowcock	1.02	1.05	1.02	0.88
Hooded Crow	0.85	0.80	0.71	0.32
Horned Lark	1.00	0.99	0.97	0.84
House Sparrow	1.00	1.00	1.01	0.97
Hume’s Short-toed Lark	1.03	1.04	1.01	0.89
Indian Golden Oriole	1.09	1.04	1.01	0.96
Isabelline Wheatear	1.09	1.09	1.16	1.18
Large-billed Reed Warbler	1.10	1.29	1.05	0.85
Lesser Sand Plover	1.53	1.53	1.63	0.60
Long-legged Buzzard	1.17	1.15	1.22	1.21
Long-tailed Shrike	1.01	1.01	1.01	0.97
Mongolian Finch	1.02	0.99	1.04	1.00
Northern Raven	1.00	1.00	1.01	0.96
Northern Wheatear	1.00	1.00	1.03	1.06
Oriental Skylark	1.06	1.07	1.09	1.05
Pale Rosefinch	0.97	0.97	0.93	0.43
Red-billed Chough	1.00	1.00	0.99	0.96
Red-fronted Serin	1.01	1.01	1.01	0.97
Red-headed Bunting	1.02	1.02	1.03	0.98
Red-tailed Wheatear	0.96	0.99	0.88	0.68
Rock Bunting	1.04	1.03	1.03	0.96
Rock Pigeon	1.03	1.03	1.04	1.01
Rosy Starling	1.08	1.08	1.12	1.13
Siberian Stonechat	1.01	1.01	1.01	1.01
Sulphur-bellied Warbler	1.06	1.05	1.07	0.98
Twite	0.99	1.02	1.02	0.98
Wallcreeper	1.02	1.07	1.06	0.87
White Wagtail	0.95	1.00	0.90	0.64
White-winged Snowfinch	1.00	1.00	1.00	0.95

The expected changes in range for 15 of the 60 modelled bird species, including those of greatest conservation concern, can be found in the main text of the report (Figure 153 to Figure 167). Below are the maps depicting projected range changes for the other 45 species.

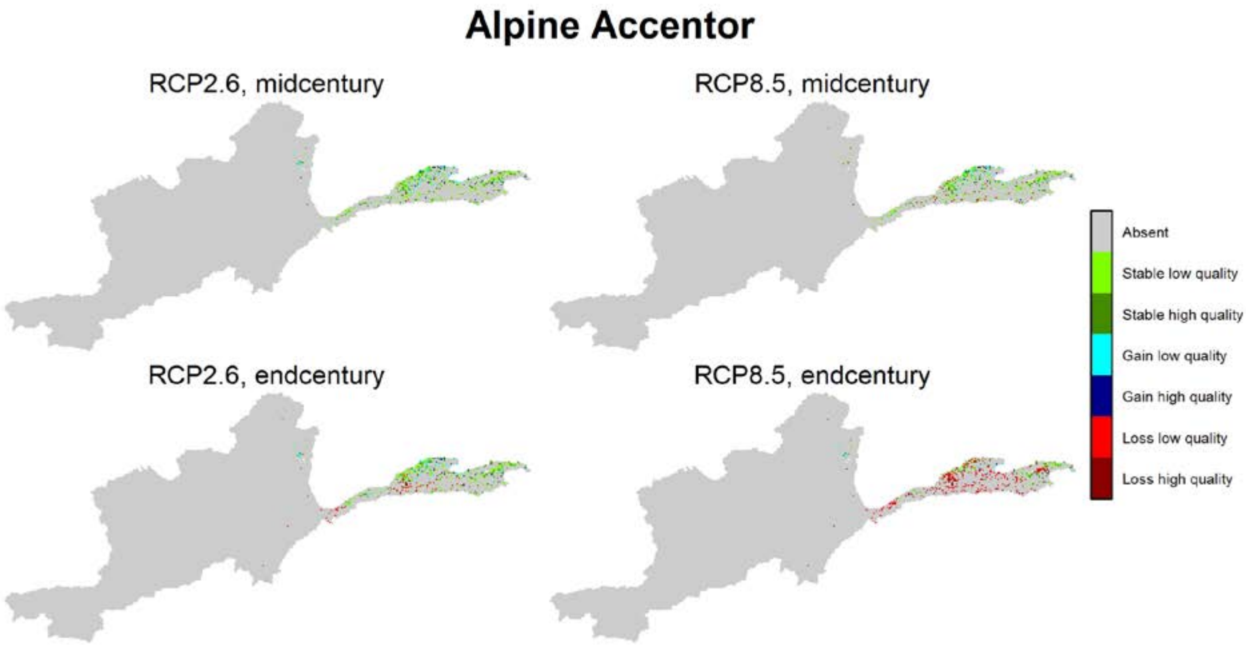

Figure 221. Changes in suitable habitat for Alpine Accentor (*Prunella collaris*).

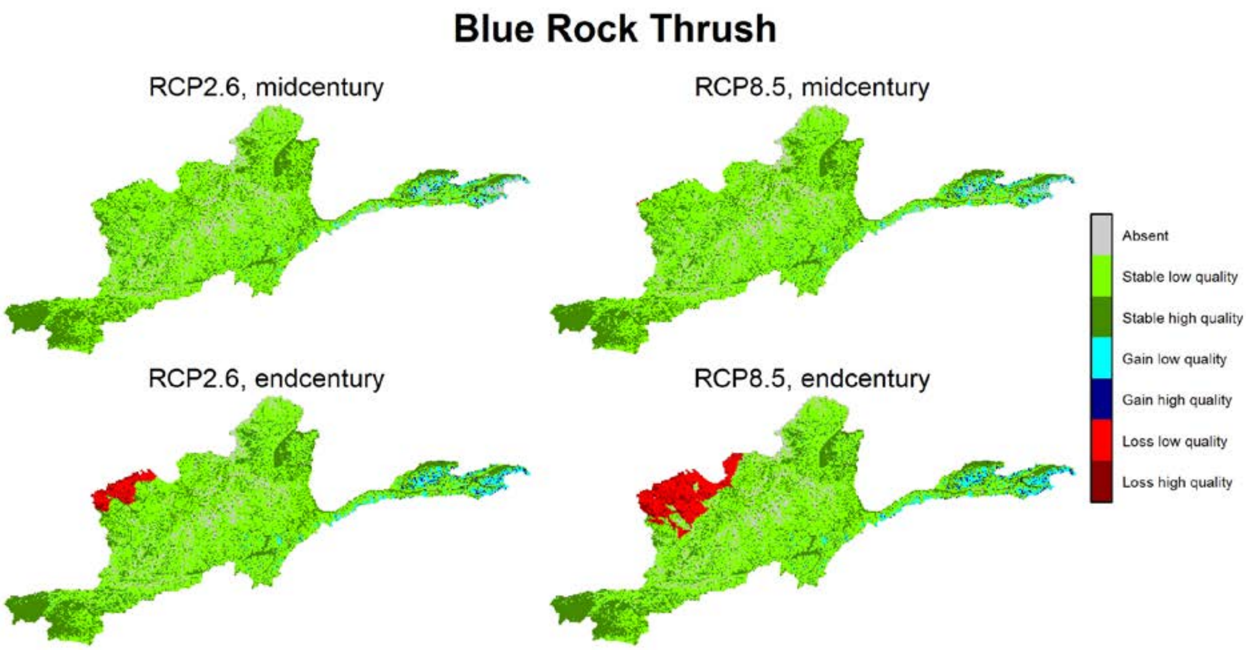

Figure 222. Changes in suitable habitat for Blue Rock Thrush (*Monticola solitarius*).

APPENDICES

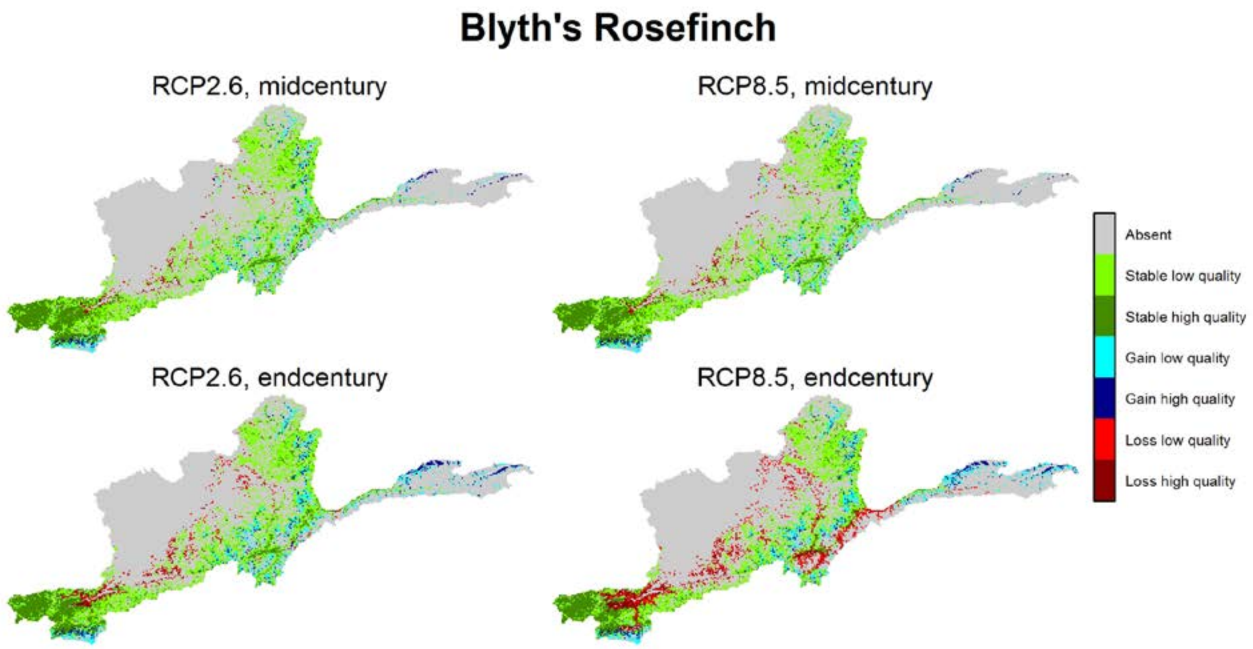

Figure 223. Changes in suitable habitat for Blyth's Rosefinch (*Carpodacus grandis*).

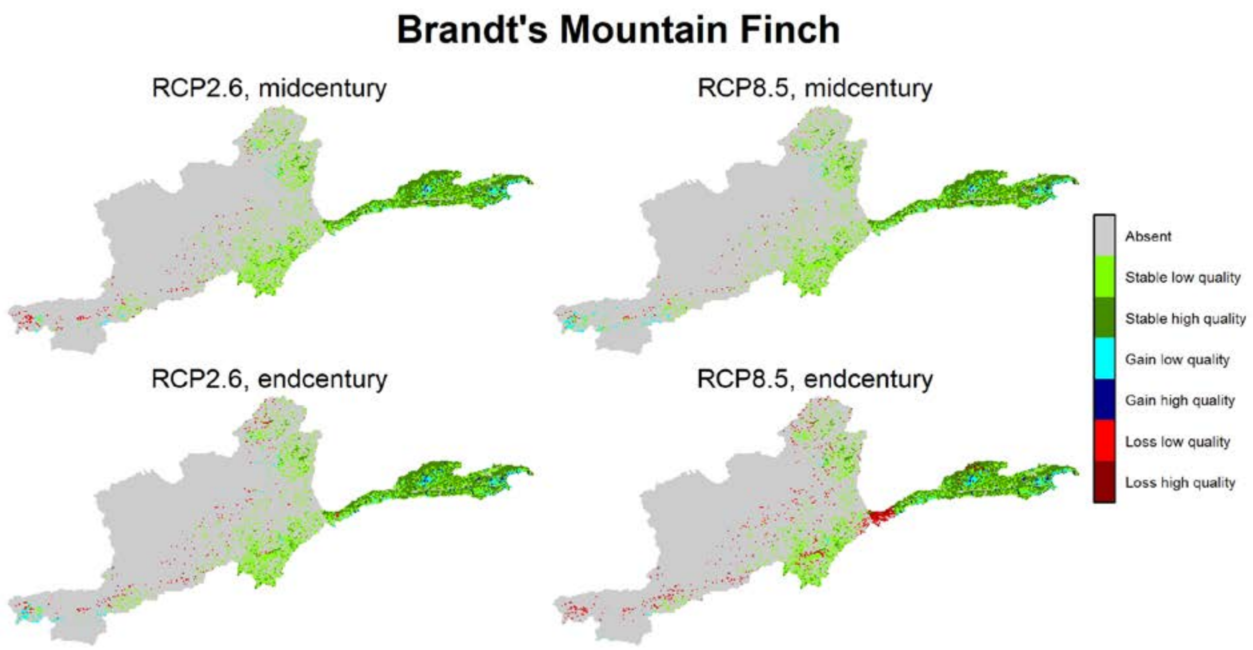

Figure 224. Changes in suitable habitat for Brandt's Mountain Finch (*Leucosticte brandti*).

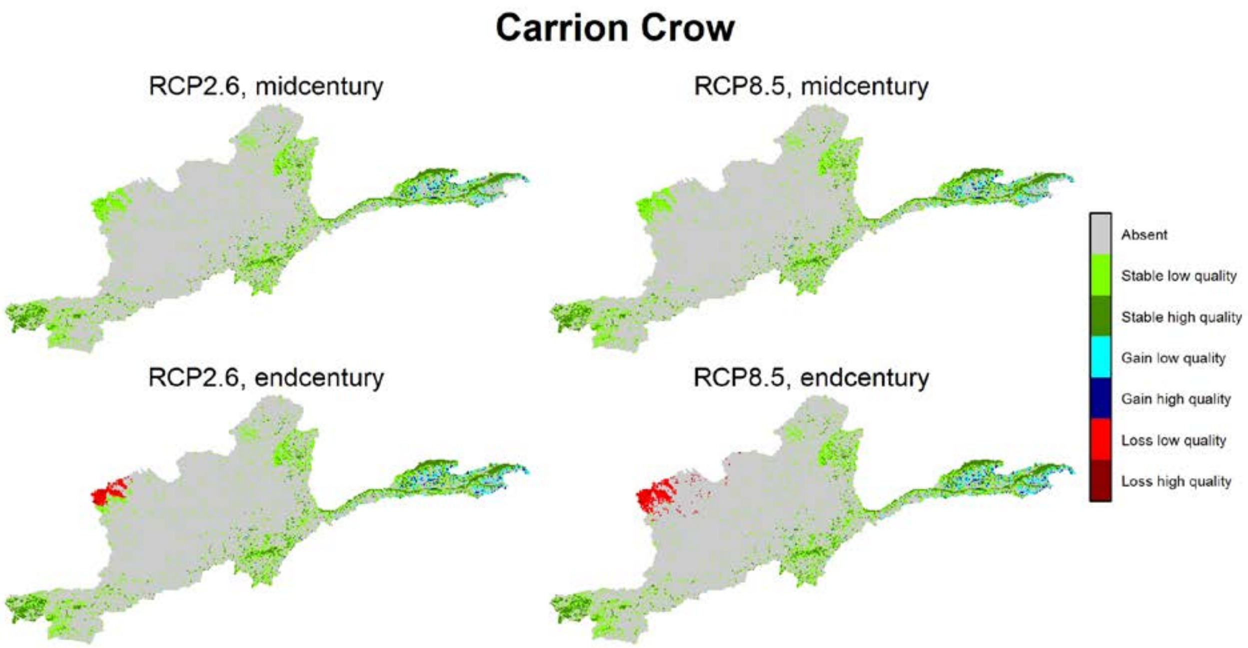

Figure 225. Changes in suitable habitat for Carrion Crow (*Corvus corone*).

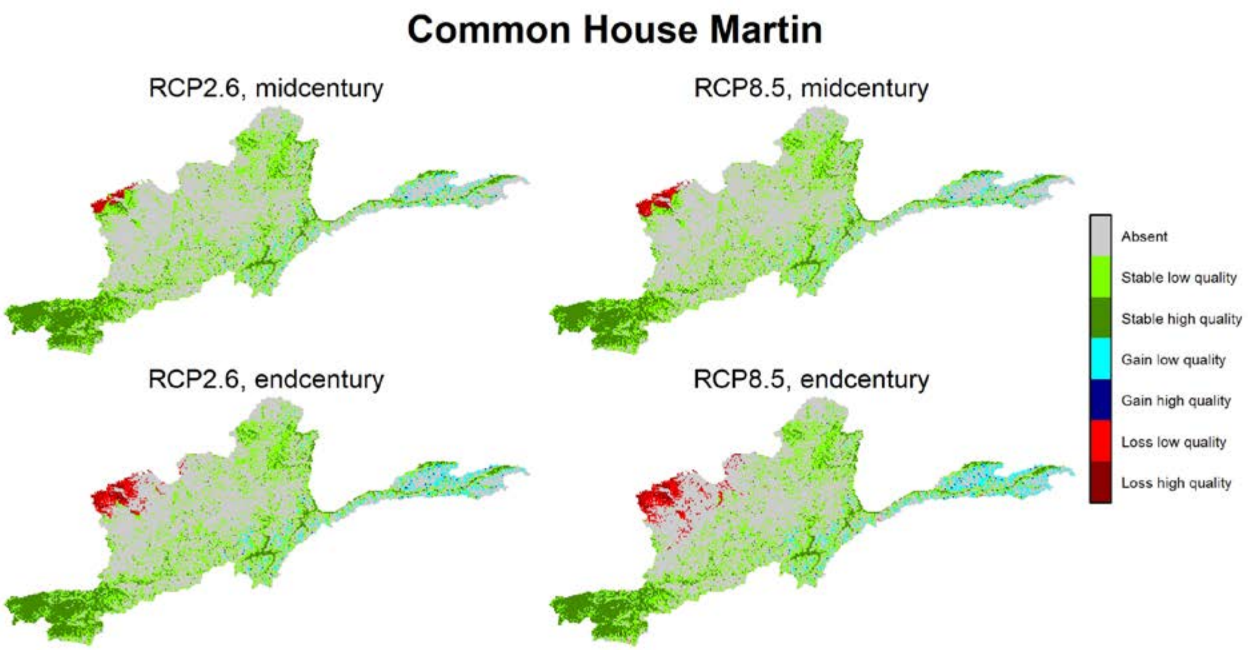

Figure 226. Changes in suitable habitat for Common House Martin (*Delichon urbicum*).

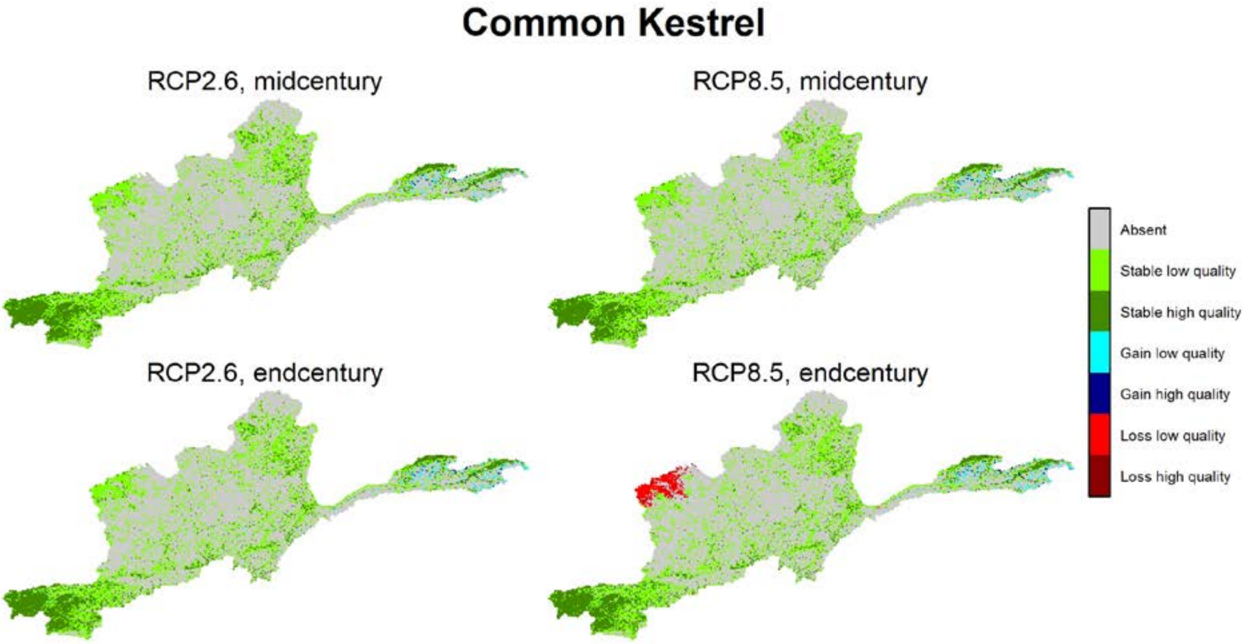

Figure 227. Changes in suitable habitat for Common Kestrel (*Falco tinnunculus*).

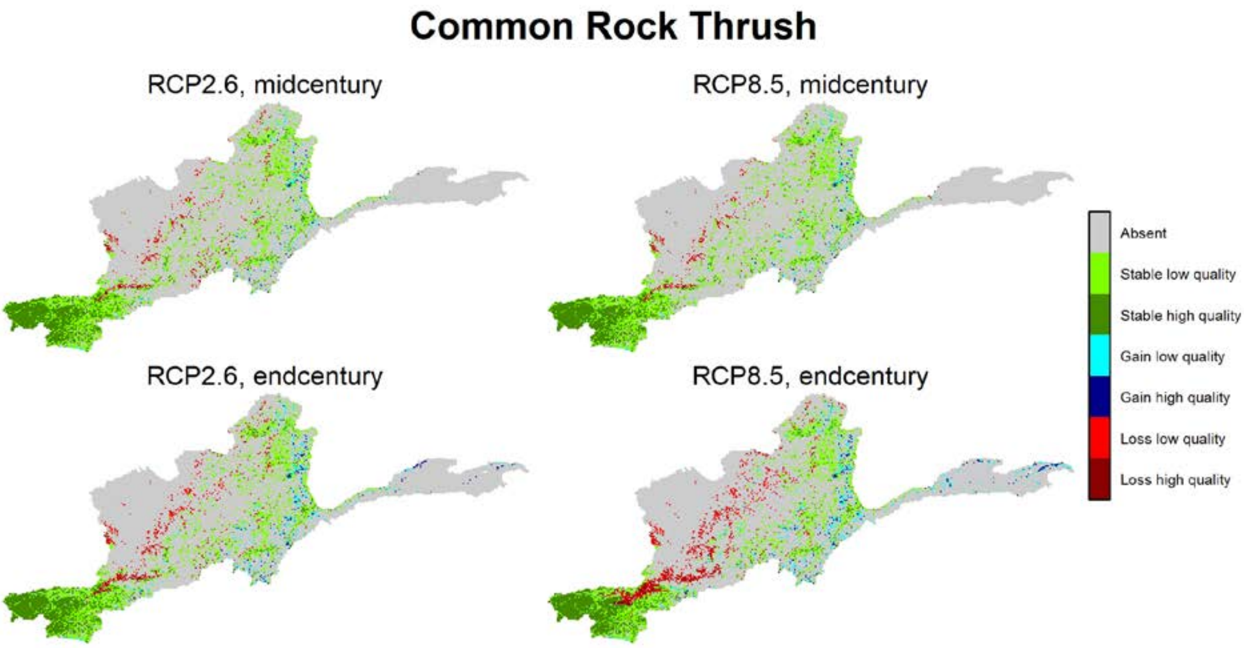

Figure 228. Changes in suitable habitat for Common Rock Thrush (*Monticola saxatilis*).

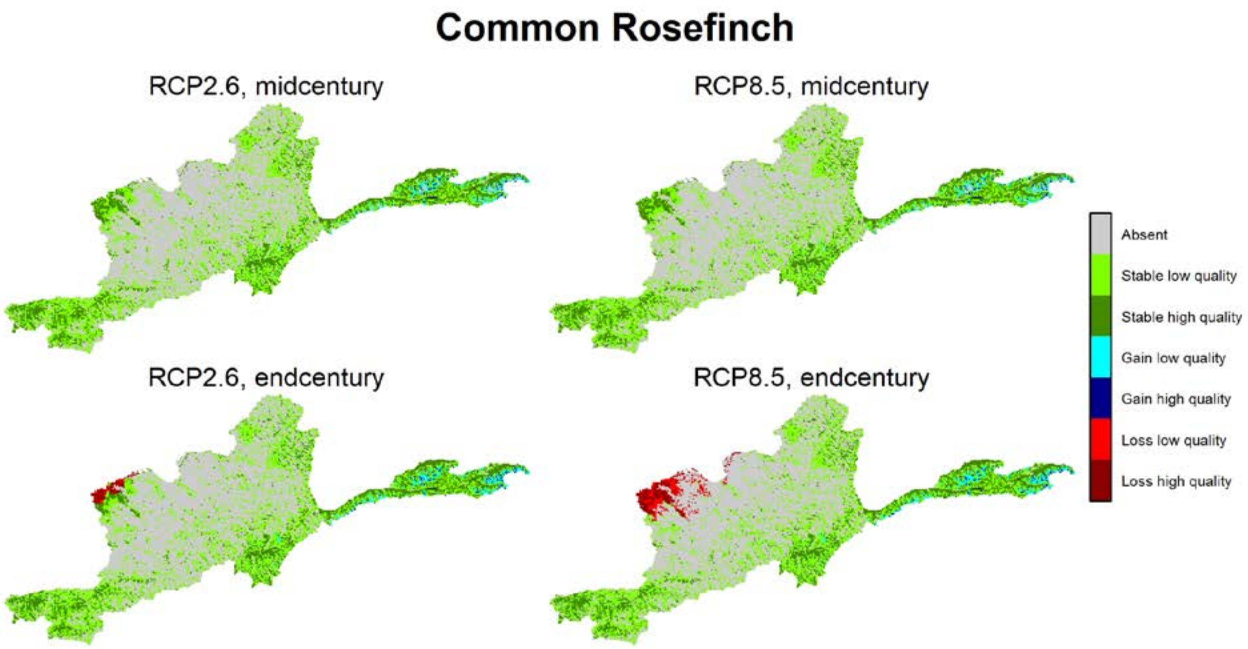

Figure 229. Changes in suitable habitat for Common Rosefinch (*Carpodacus erythrinus*).

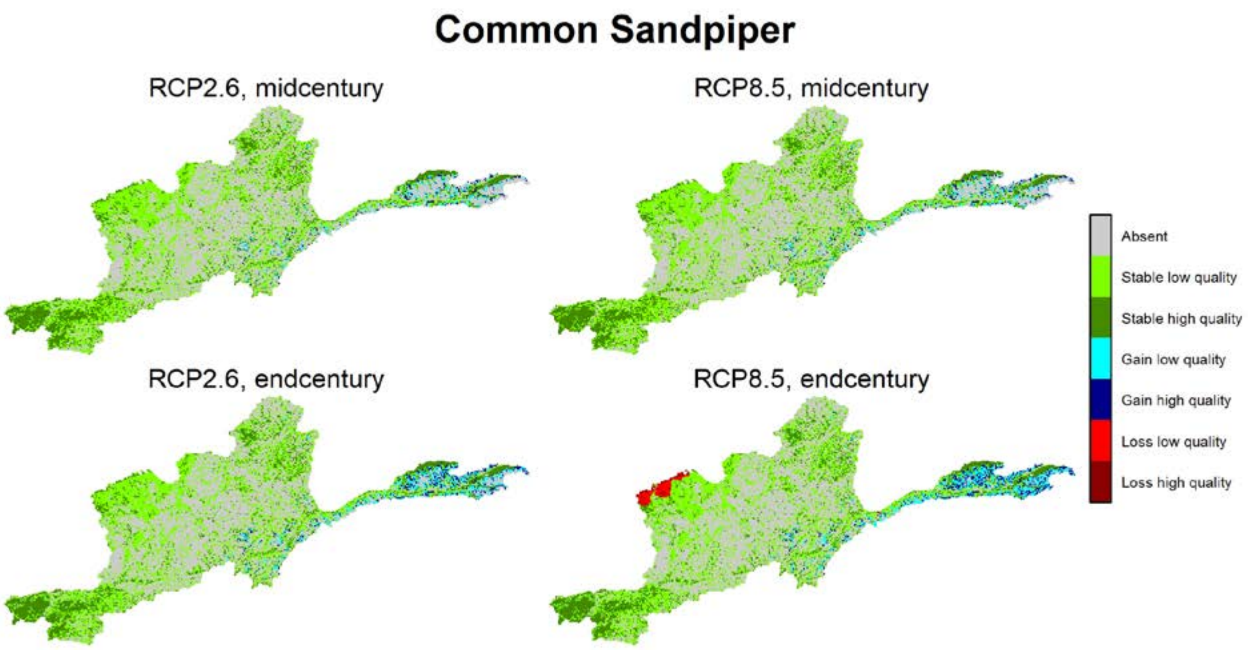

Figure 230. Changes in suitable habitat for Common Sandpiper (*Actitis hypoleucos*).

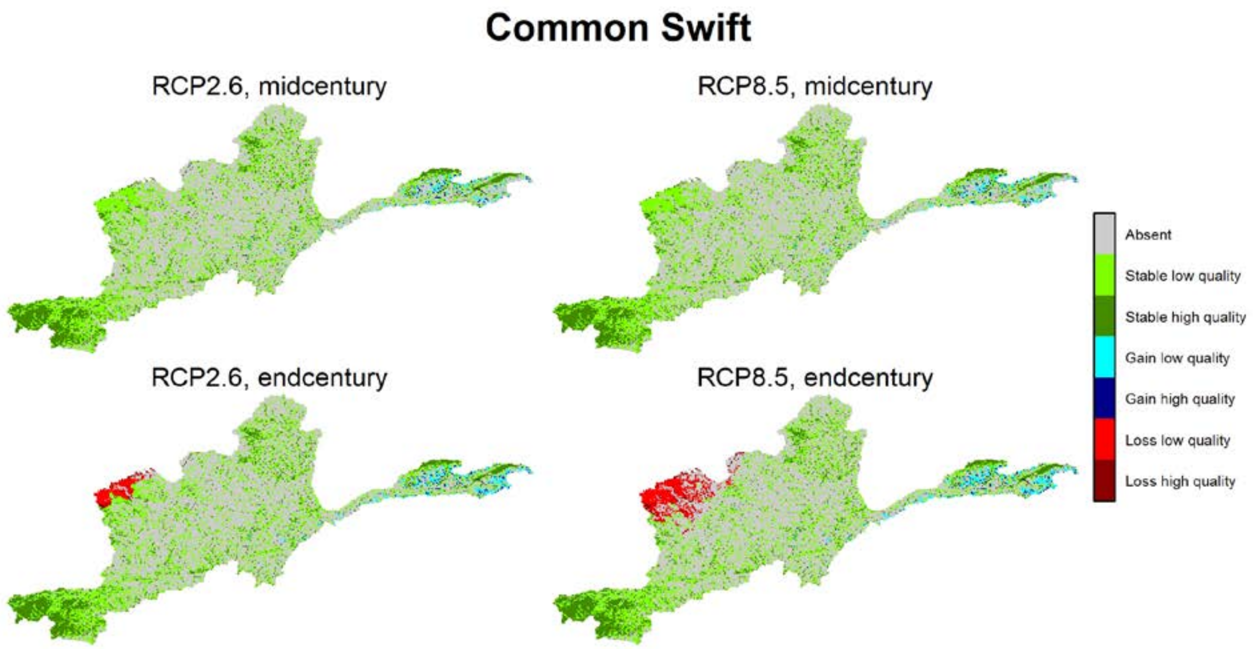

Figure 231. Changes in suitable habitat for Common Swift (*Apus apus*).

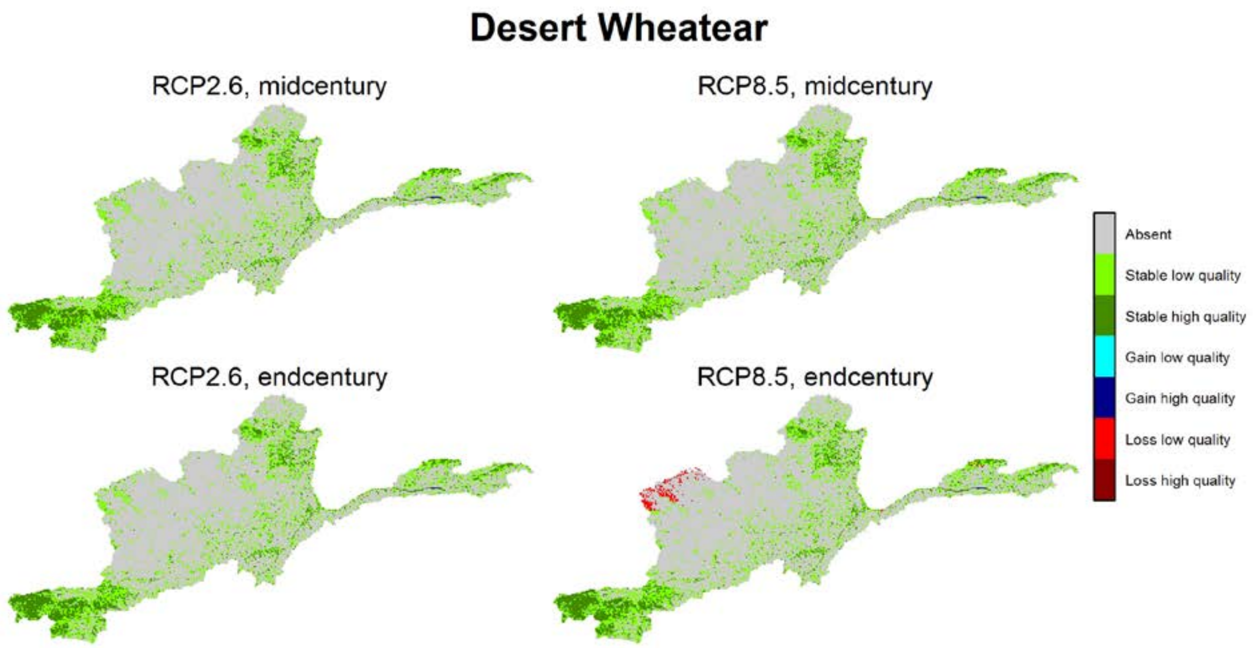

Figure 232. Changes in suitable habitat for Desert Wheatear (*Oenanthe deserti*).

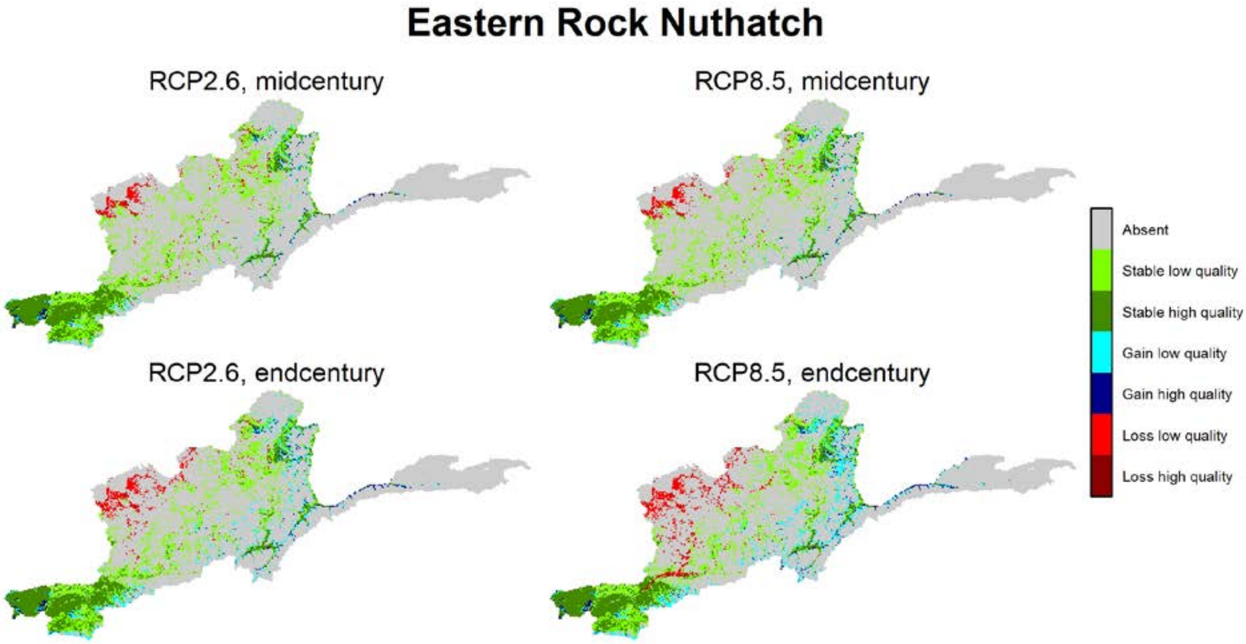

Figure 233. Changes in suitable habitat for Eastern Rock Nuthatch (*Sitta tephronota*).

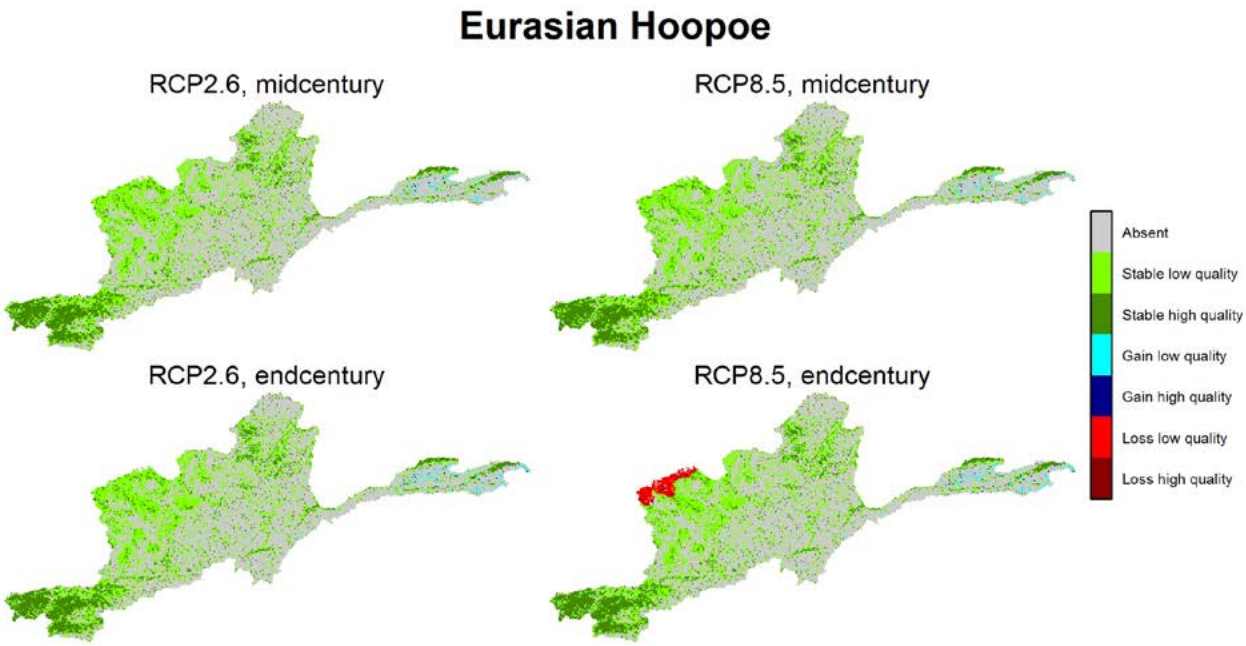

Figure 234. Changes in suitable habitat for Eurasian Hoopoe (*Upupa epops*).

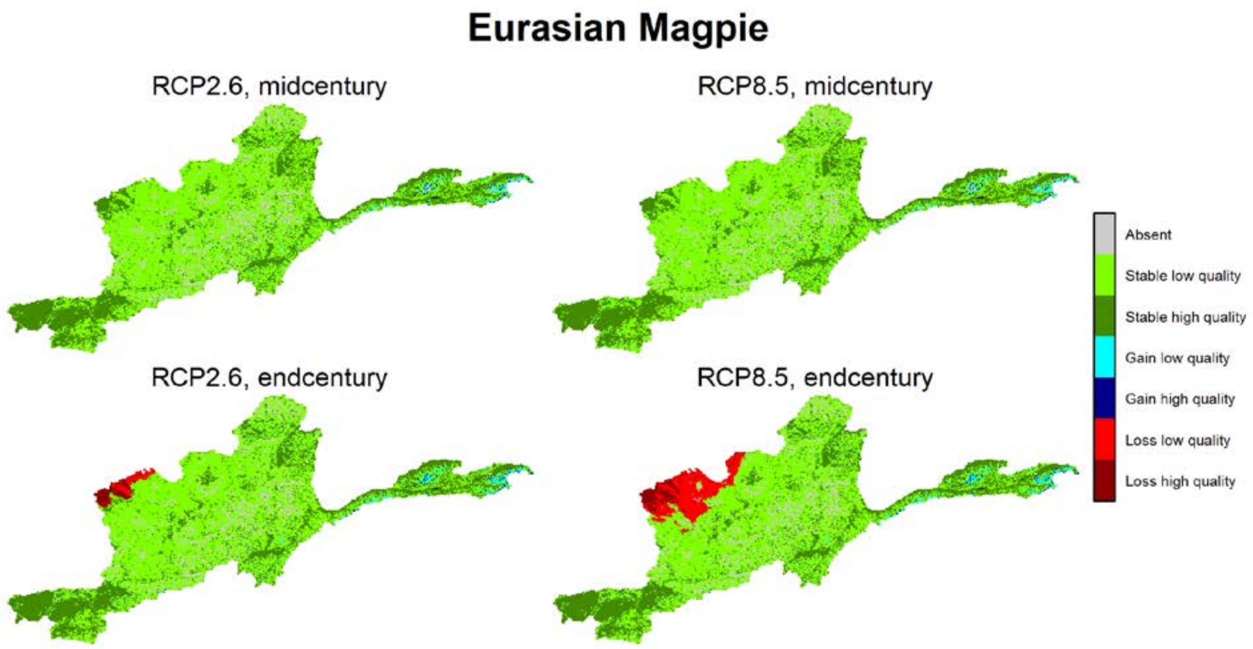

Figure 235. Changes in suitable habitat for Eurasian Magpie (*Pica pica*).

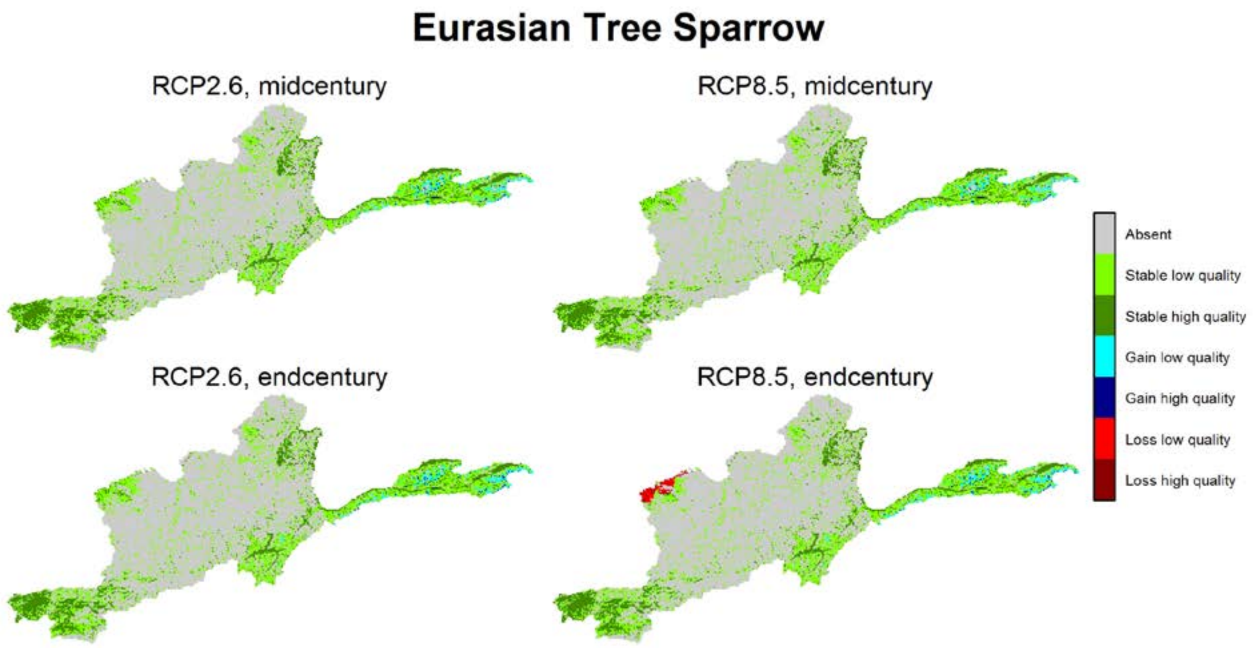

Figure 236. Changes in suitable habitat for Eurasian Tree Sparrow (*Passer montanus*).

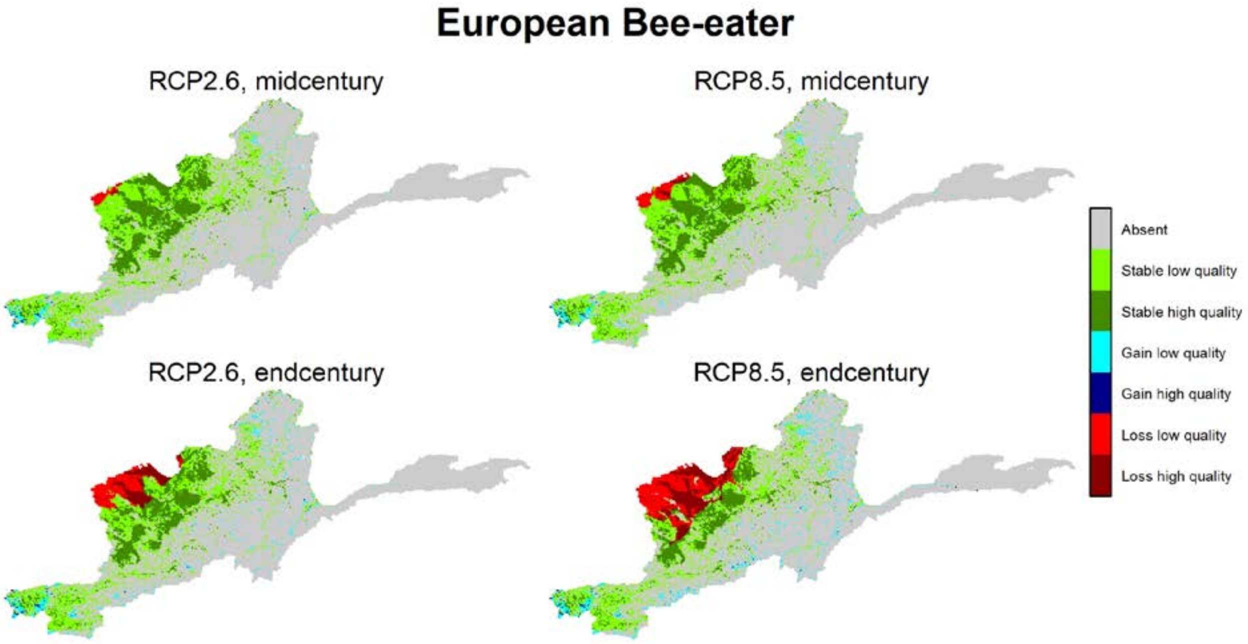

Figure 237. Changes in suitable habitat for European Bee-eater (*Merops apiaster*).

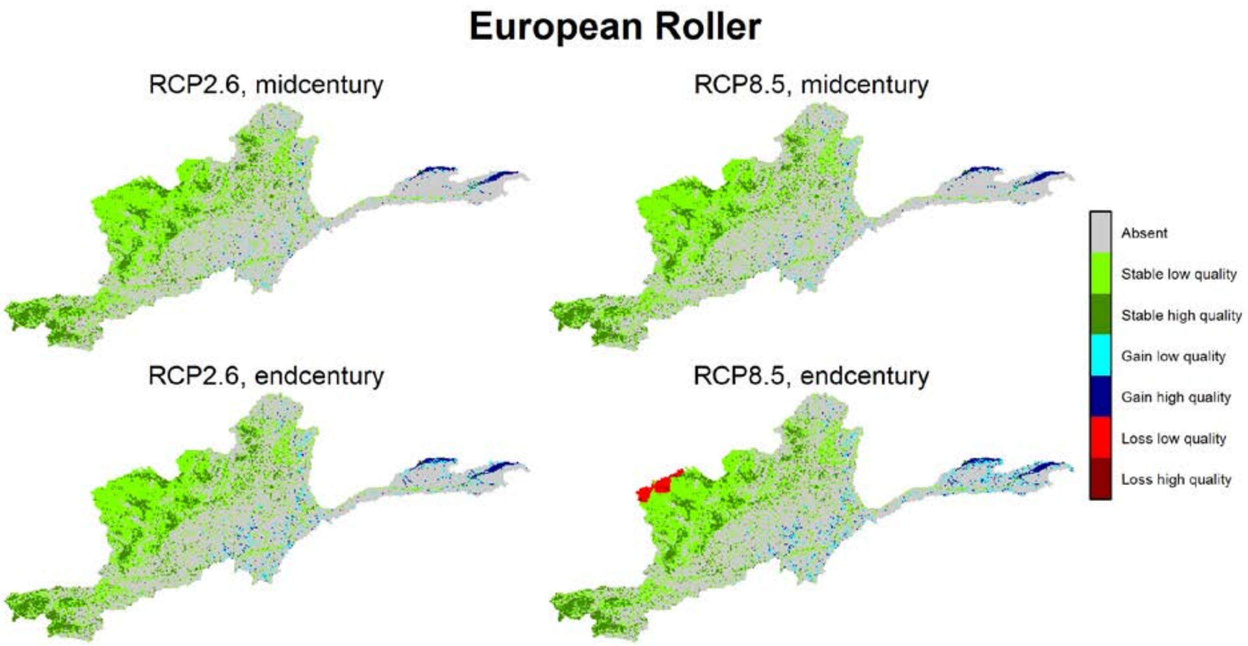

Figure 238. Changes in suitable habitat for European Roller (*Coracias garrulus*).

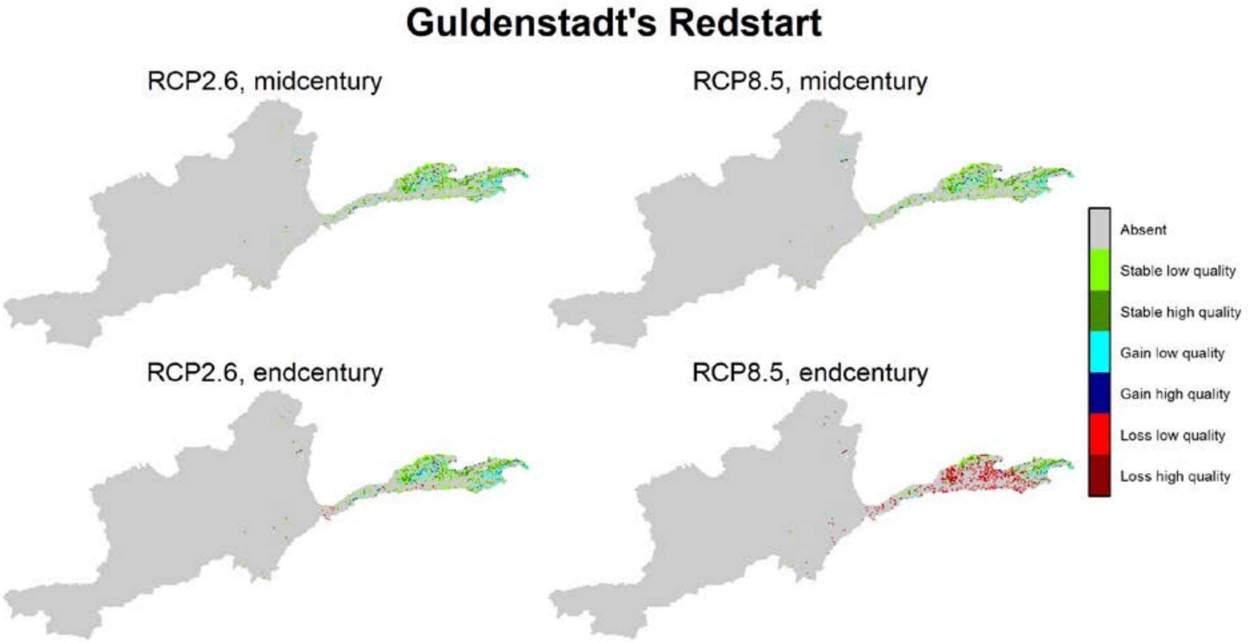

Figure 239. Changes in suitable habitat for Güldenstadt's Redstart (*Phoenicurus erythrogastrus*).

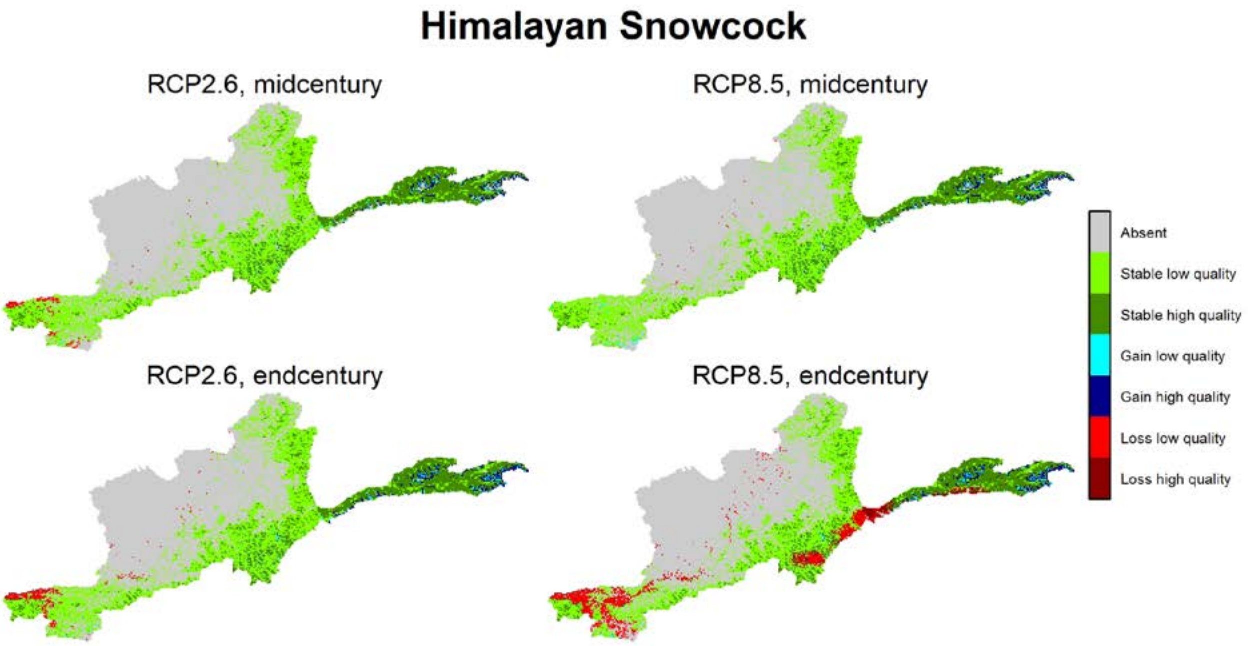

Figure 240. Changes in suitable habitat for Himalayan Snowcock (*Tetraogallus himalayensis*).

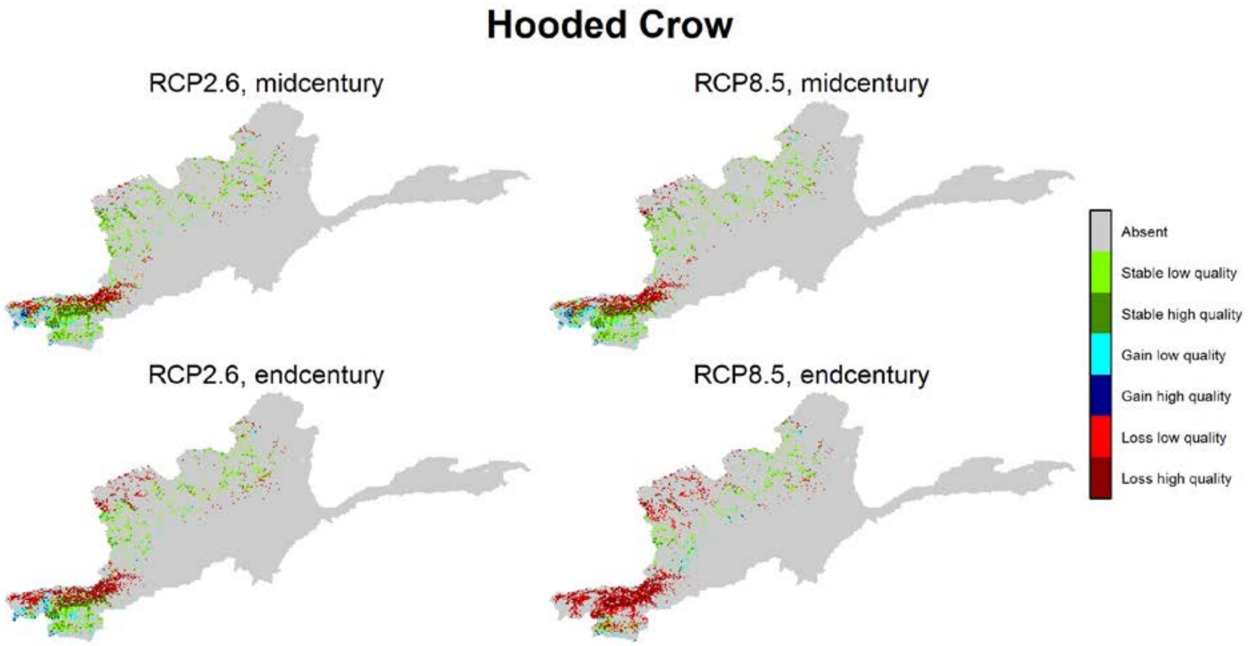

Figure 241. Changes in suitable habitat for Hooded Crow (*Corvus cornix*).

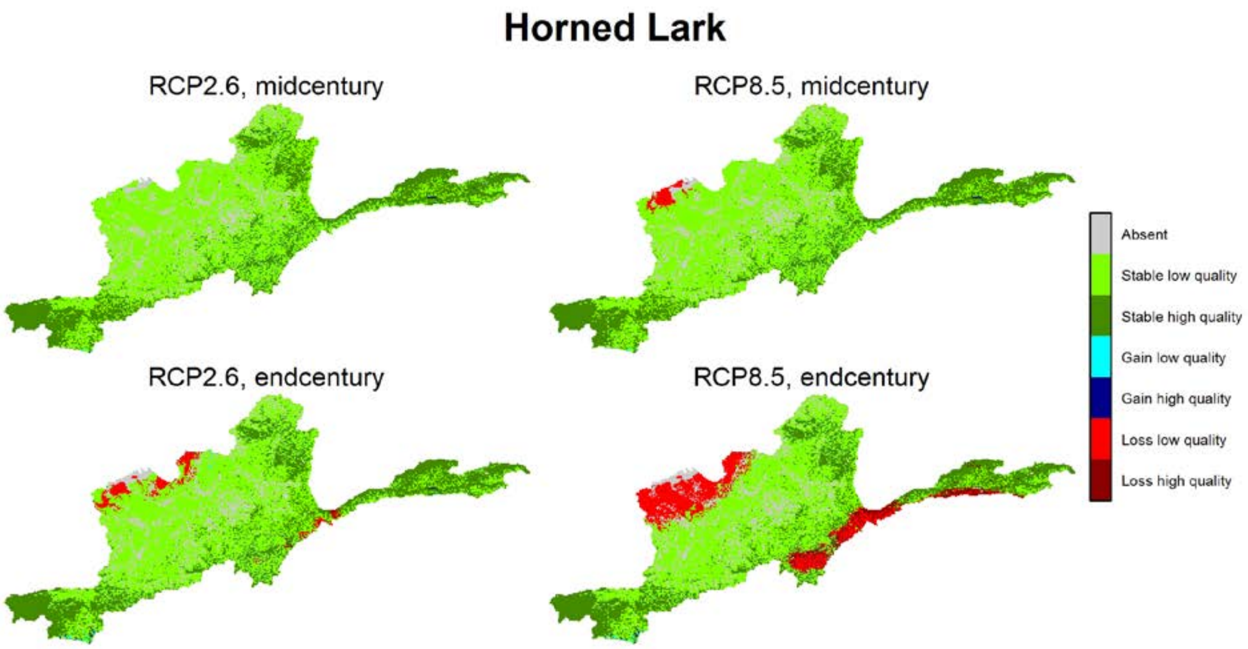

Figure 242. Changes in suitable habitat for Horned Lark (*Eremophila alpestris*).

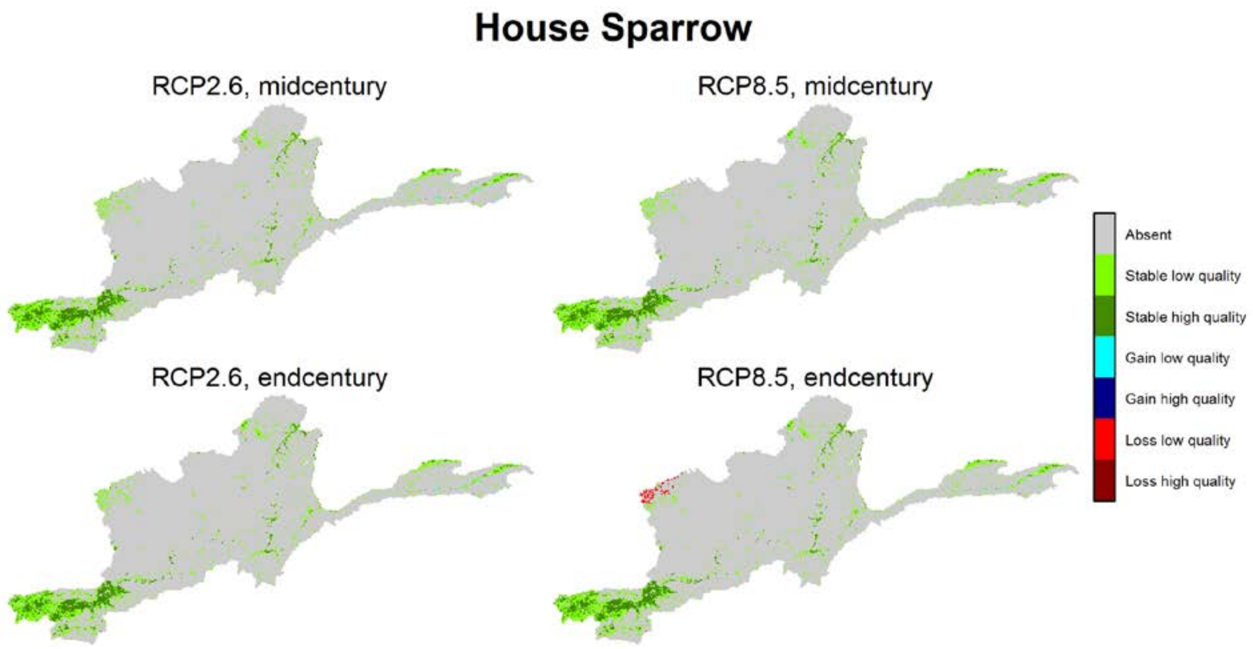

Figure 243. Changes in suitable habitat for House Sparrow (*Passer domesticus*).

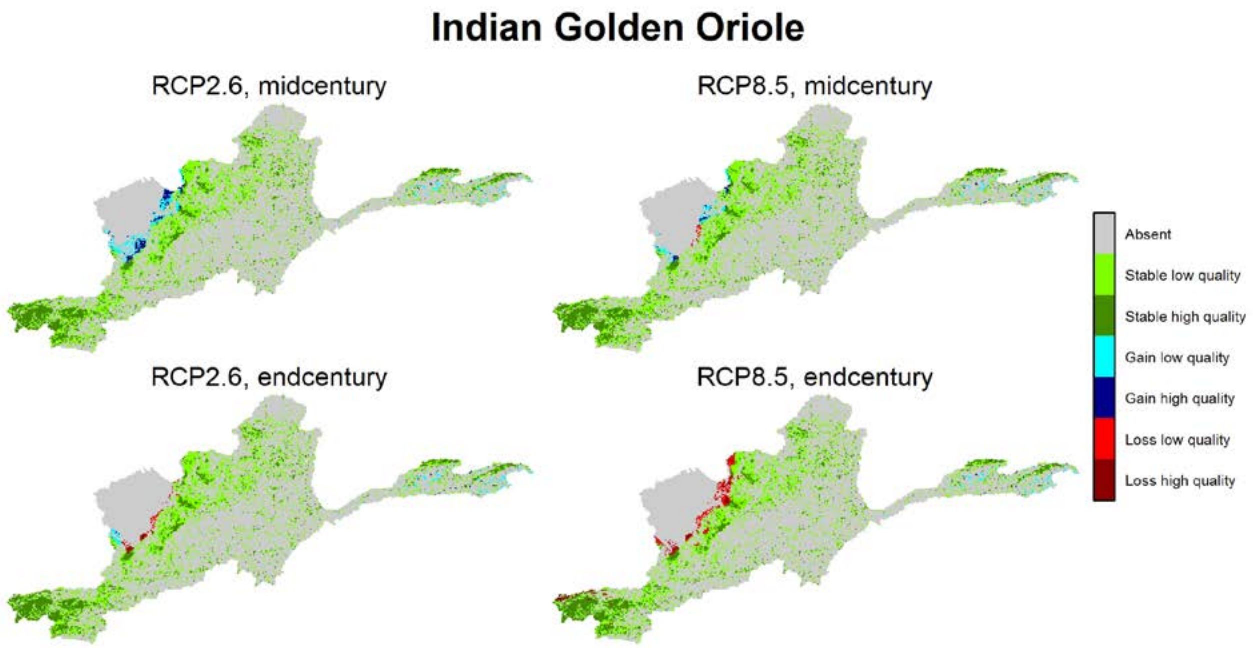

Figure 244. Changes in suitable habitat for Indian Golden Oriole (*Oriolus kundoo*).

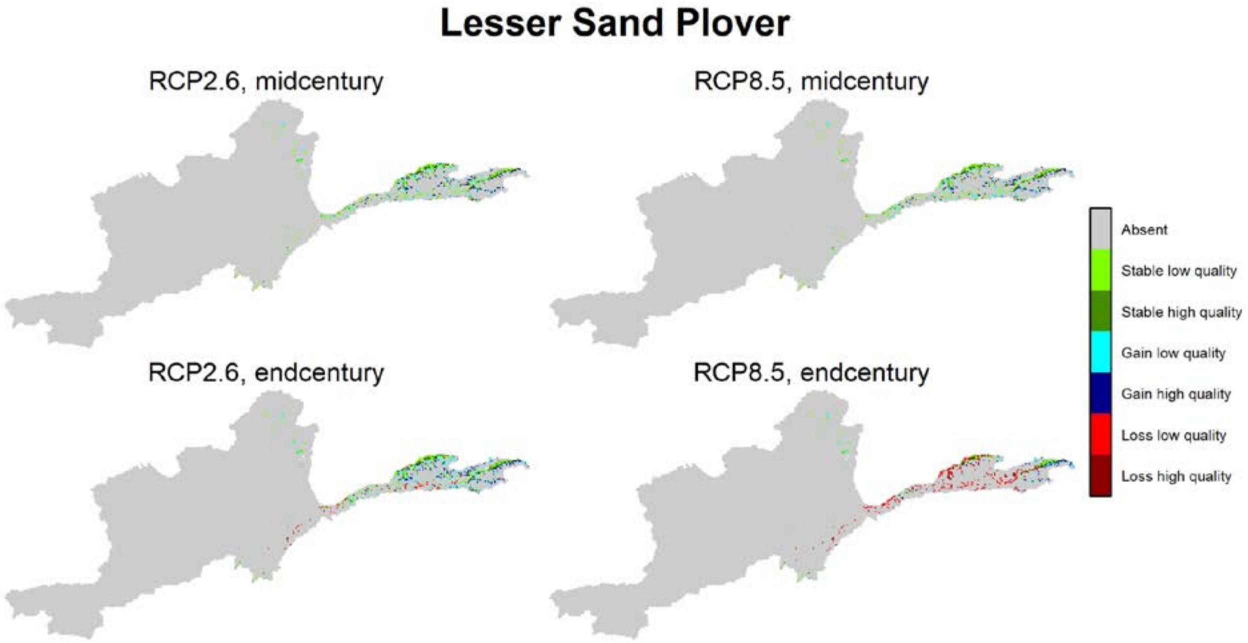

Figure 245. Changes in suitable habitat for Lesser Sand Plover (*Charadrius mongolus*).

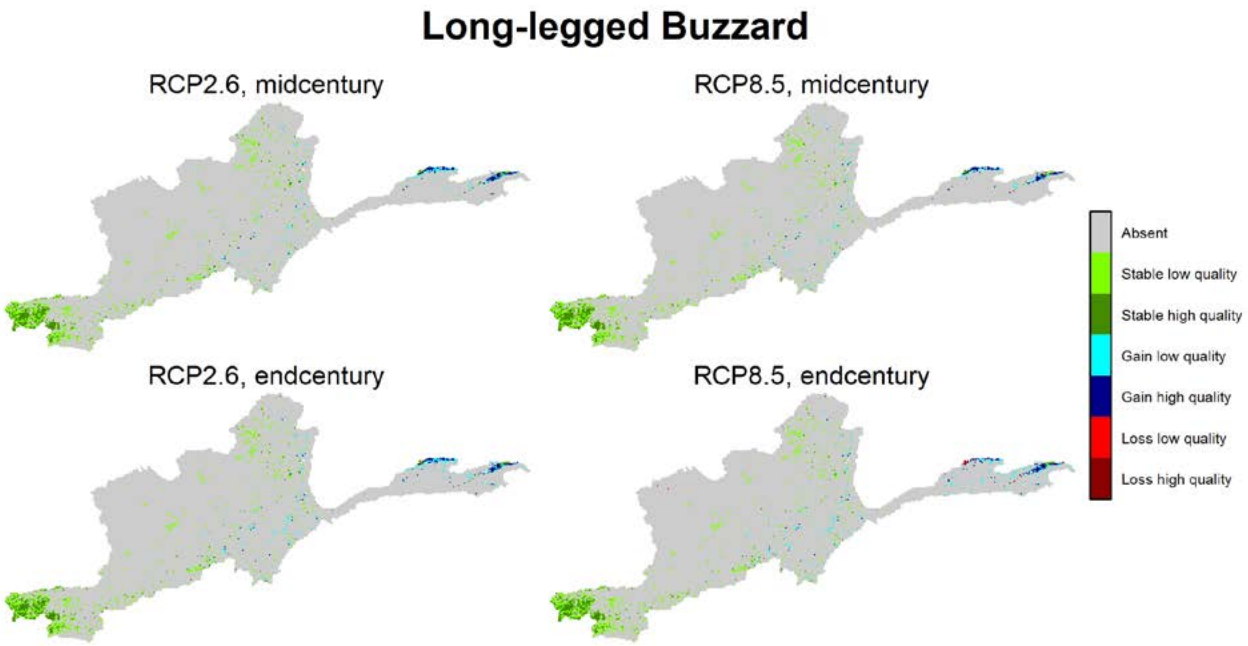

Figure 246. Changes in suitable habitat for Long-legged Buzzard (*Buteo rufinus*).

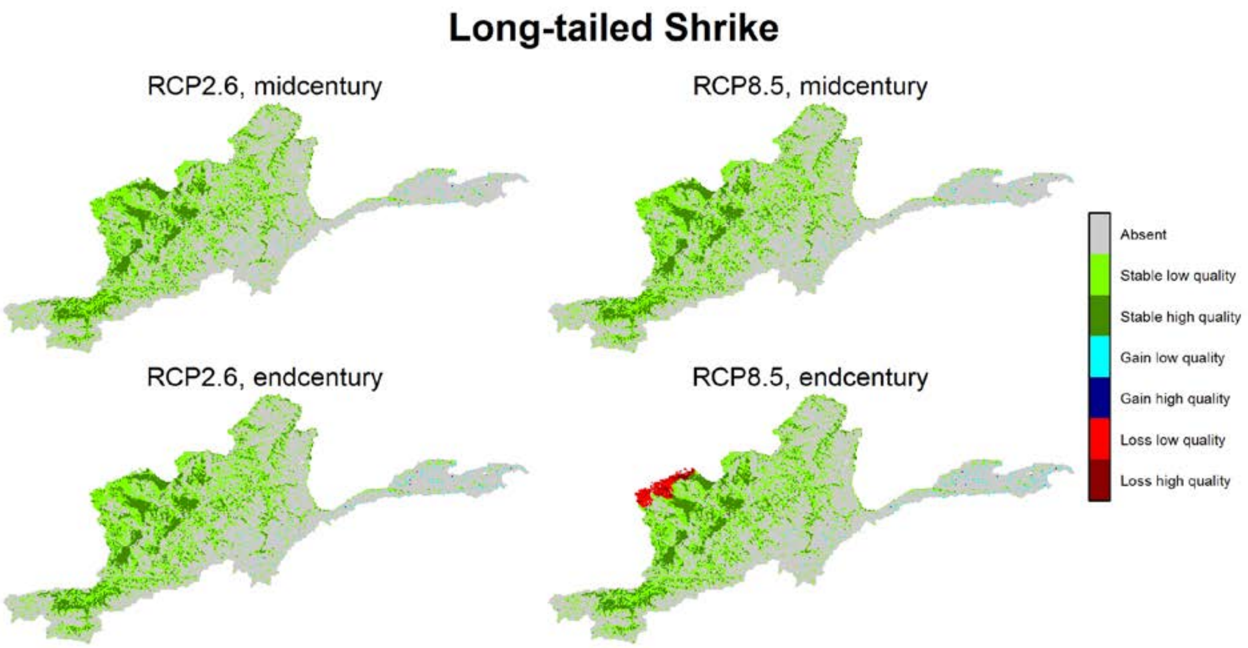

Figure 247. Changes in suitable habitat for Long-tailed Shrike (*Lanius schach*).

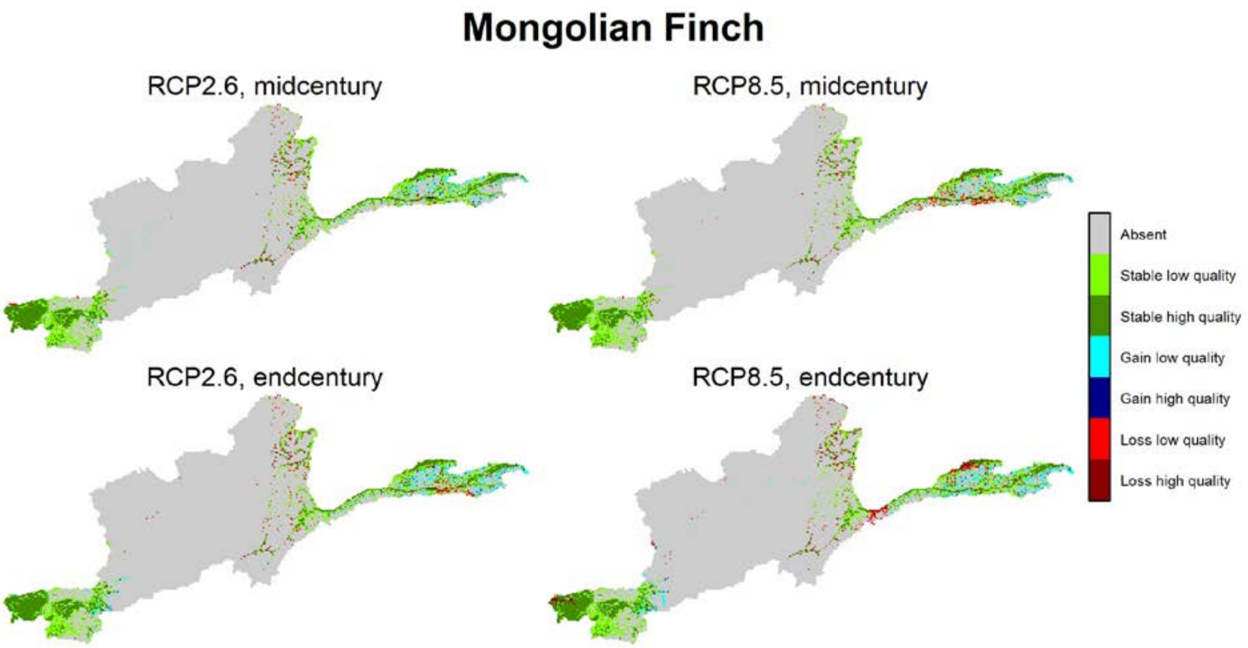

Figure 248. Changes in suitable habitat for Mongolian Finch (*Bucanetes mongolicus*).

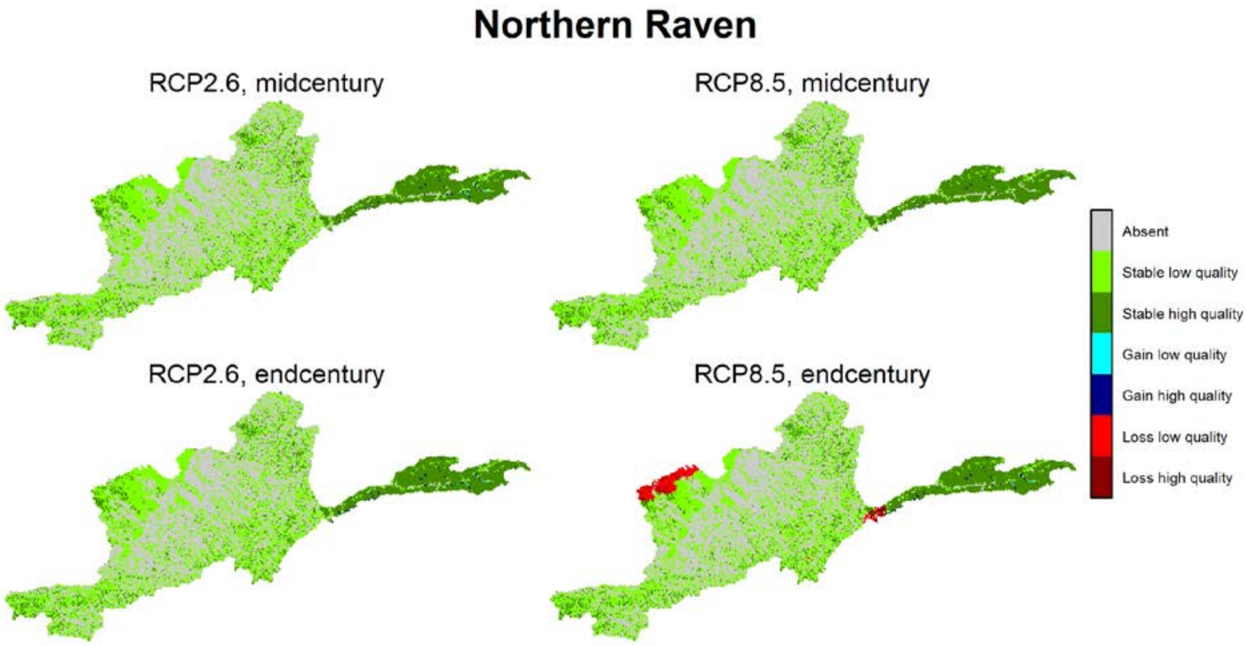

Figure 249. Changes in suitable habitat for Northern Raven (*Corvus corax*).

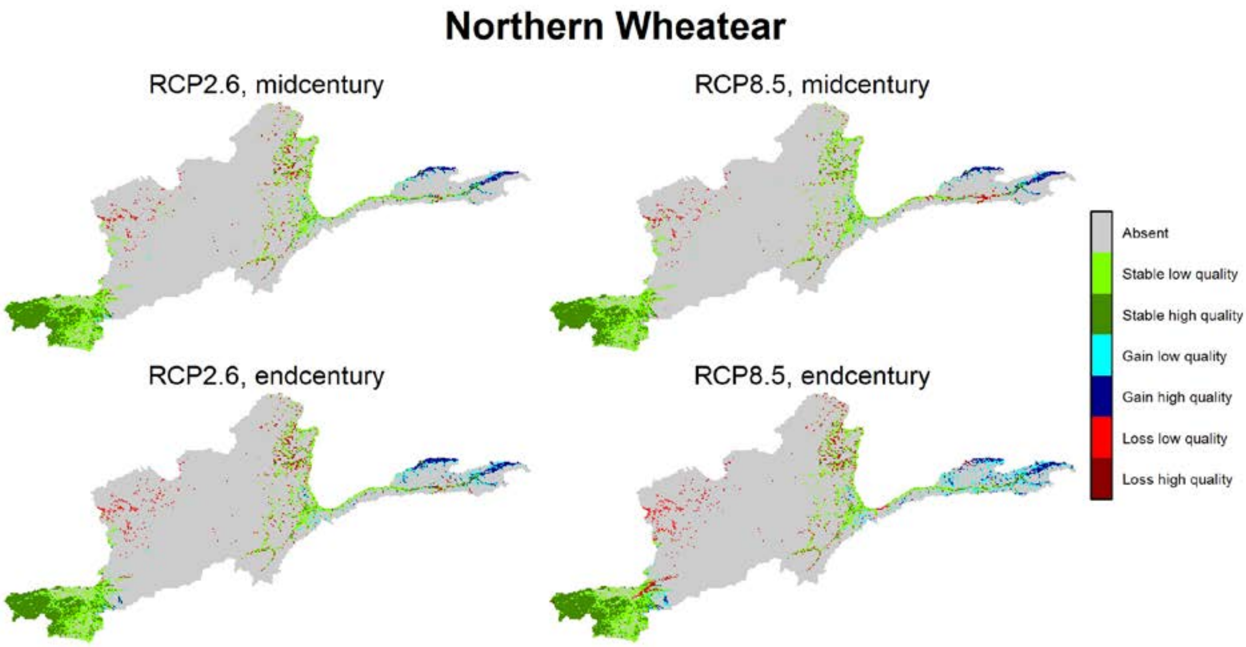

Figure 250. Changes in suitable habitat for Northern Wheatear (*Oenanthe oenanthe*).

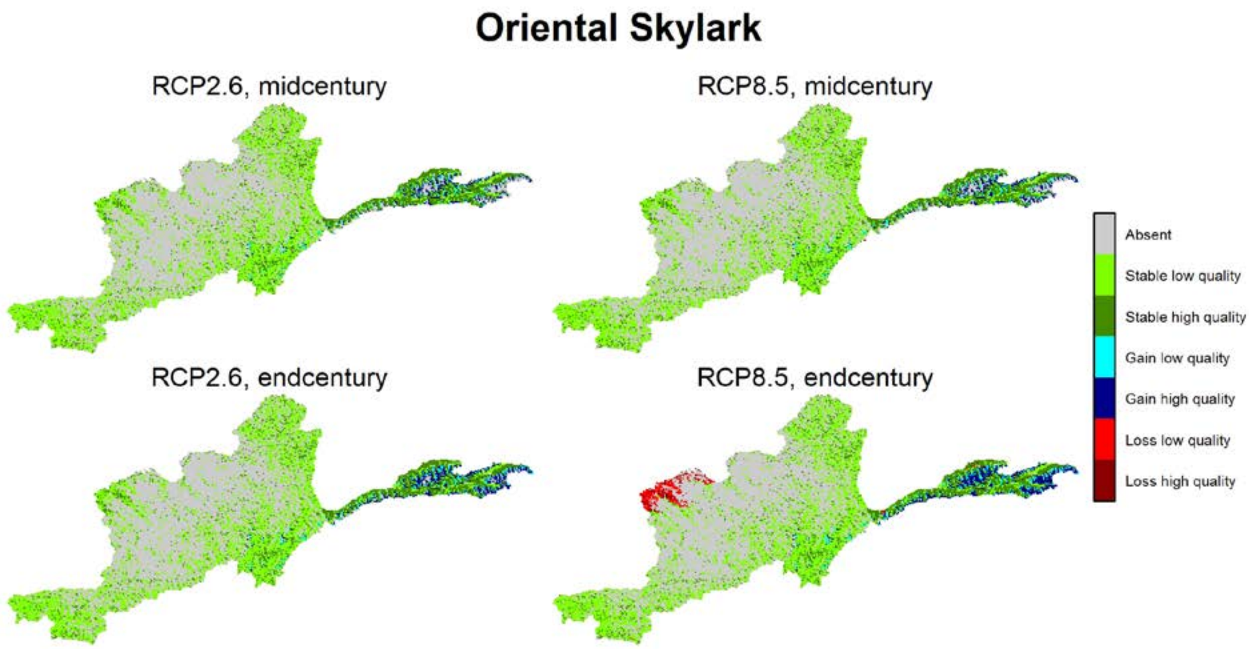

Figure 251. Changes in suitable habitat for Oriental Skylark (*Alauda gulgula*).

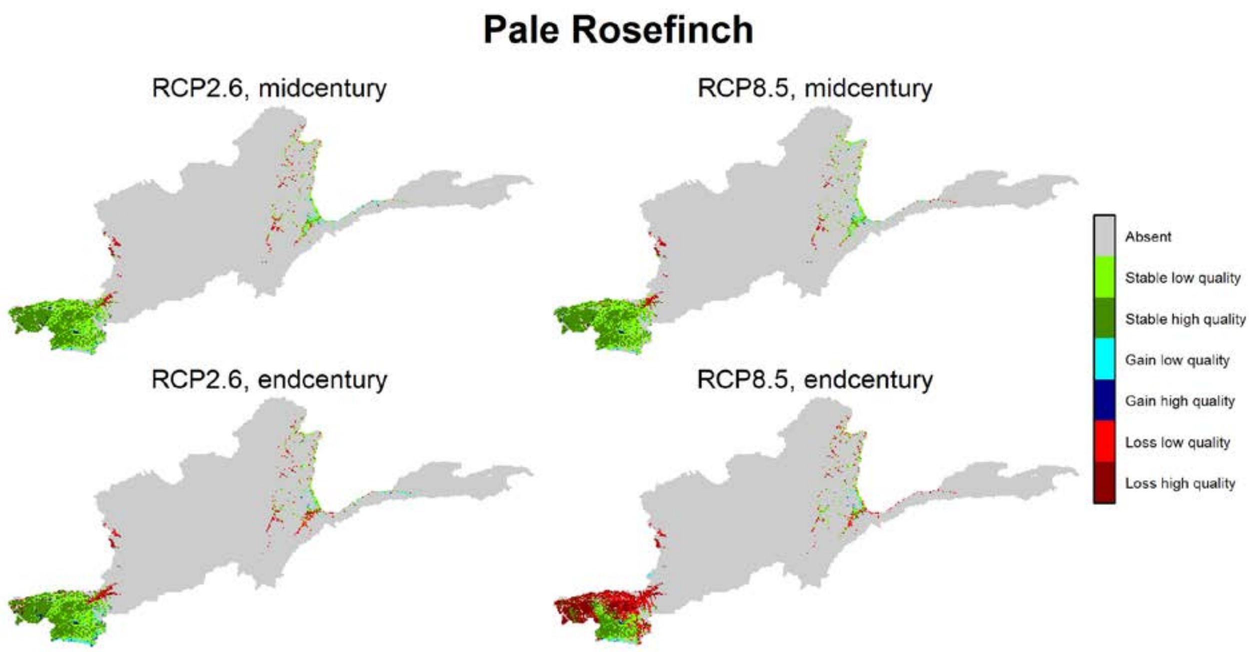

Figure 252. Changes in suitable habitat for Pale Rosefinch (*Carpodacus stoliczkae*).

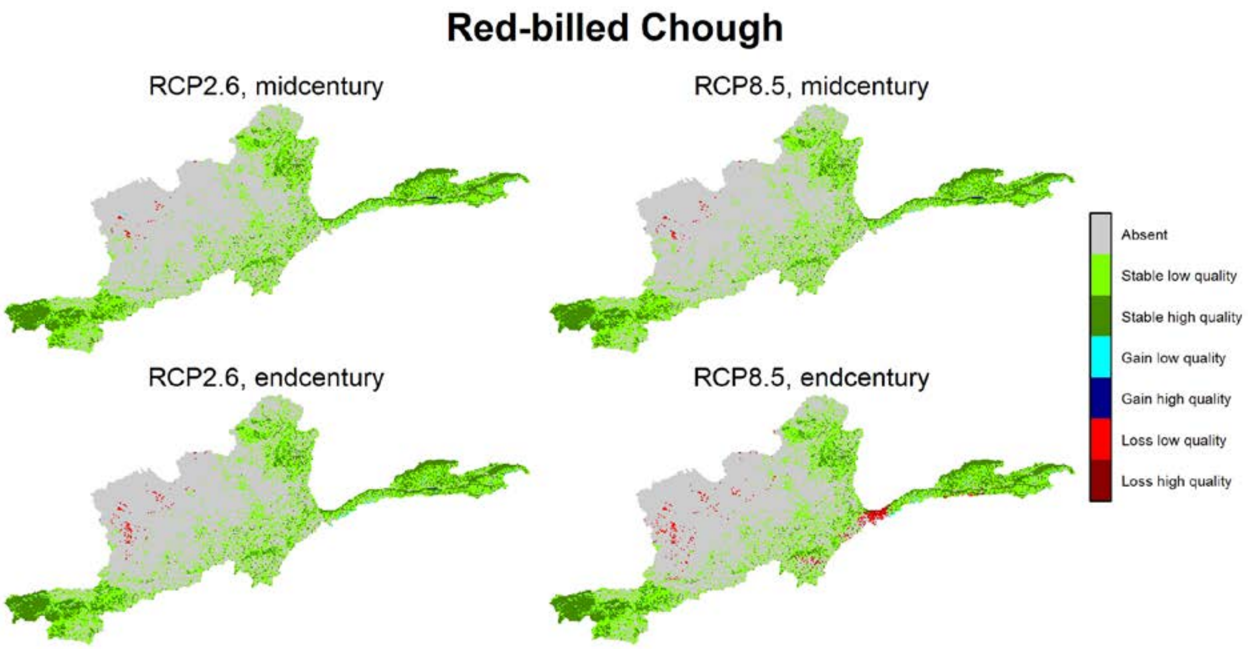

Figure 253. Changes in suitable habitat for Red-billed Chough (*Pyrrhocorax pyrrhocorax*).

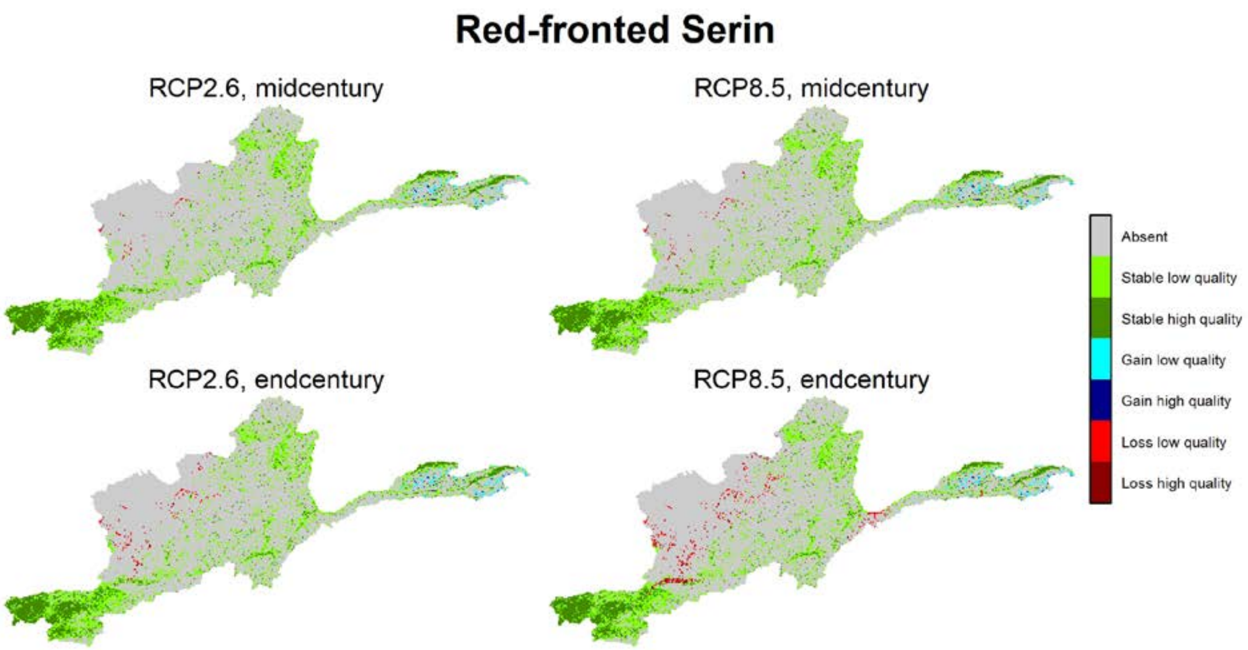

Figure 254. Changes in suitable habitat for Red-fronted Serin (*Serinus pusillus*).

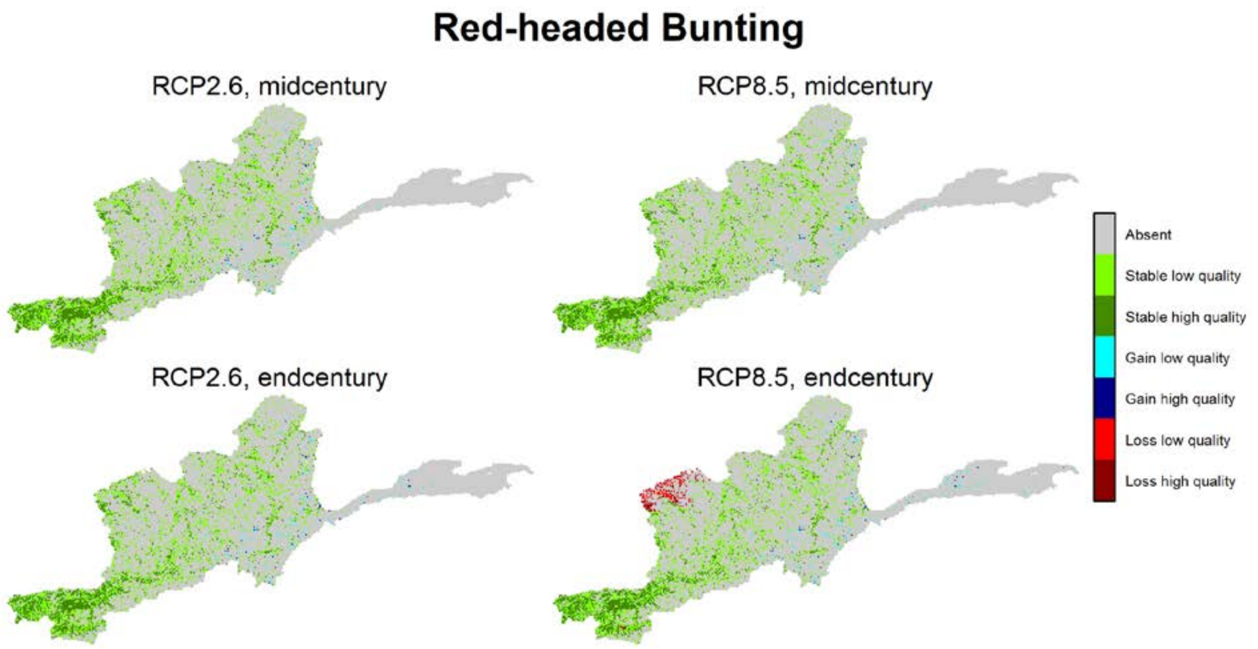

Figure 255. Changes in suitable habitat for Red-headed Bunting (*Emberiza bruniceps*).

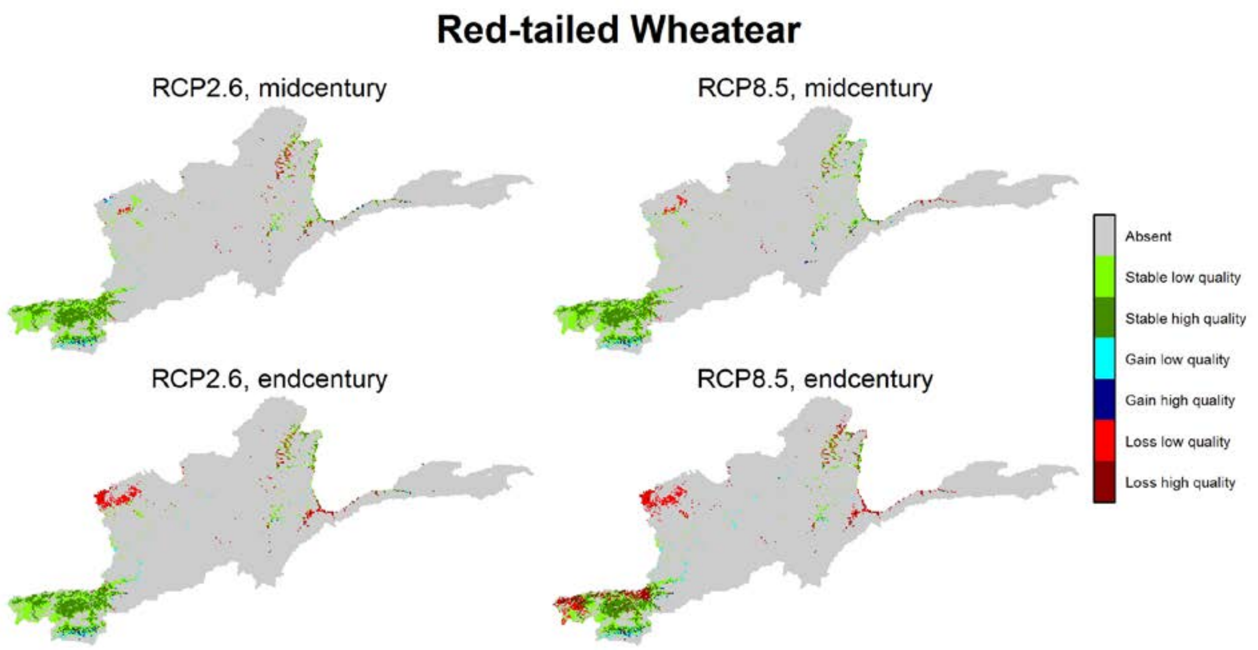

Figure 256. Changes in suitable habitat for Red-tailed Wheatear (*Oenanthe chrysopygia*).

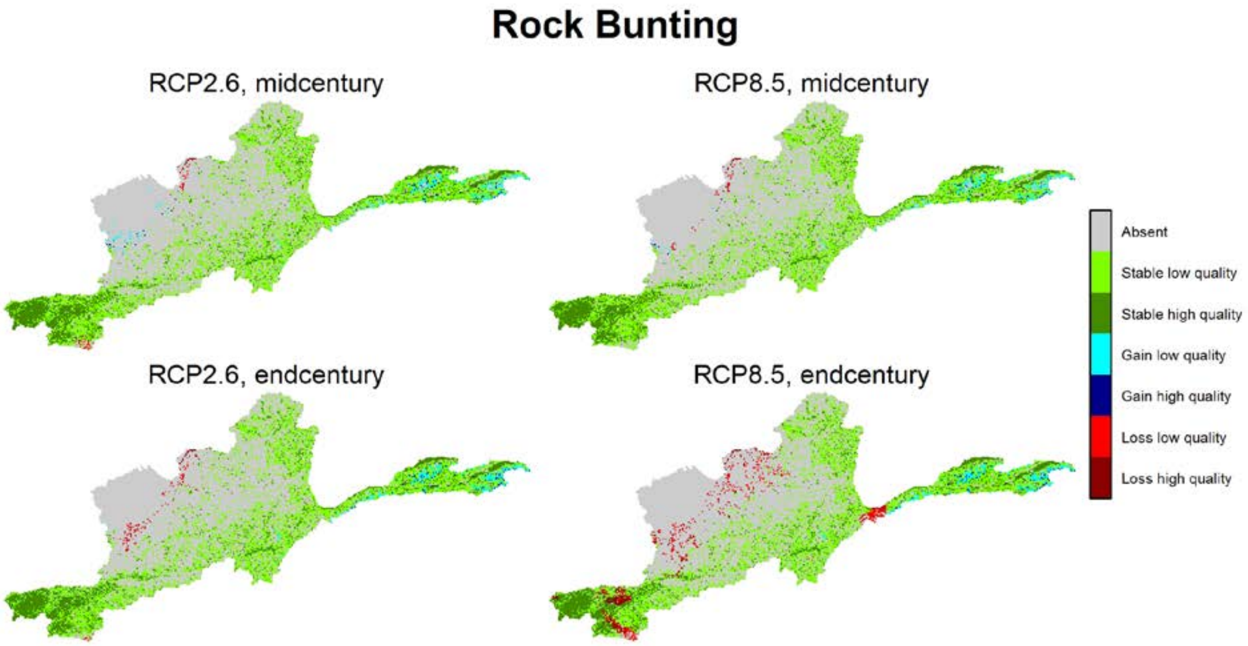

Figure 257. Changes in suitable habitat for Rock Bunting (*Emberiza cia*).

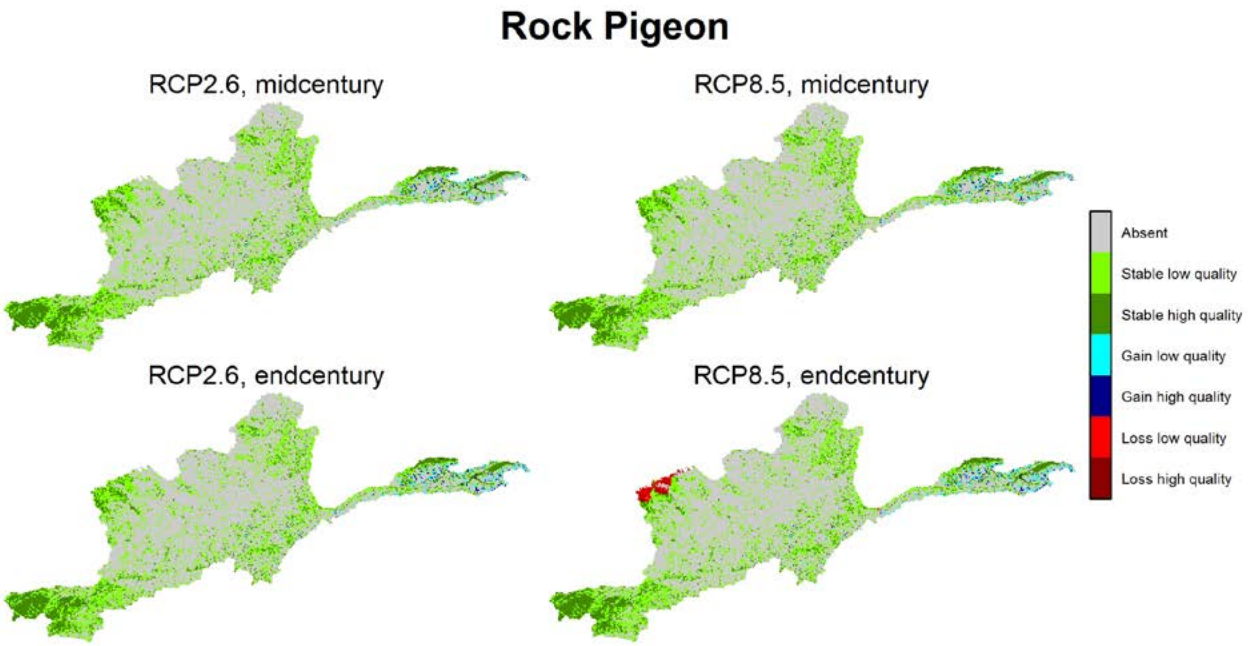

Figure 258. Changes in suitable habitat for Rock Pigeon (*Columba livia*).

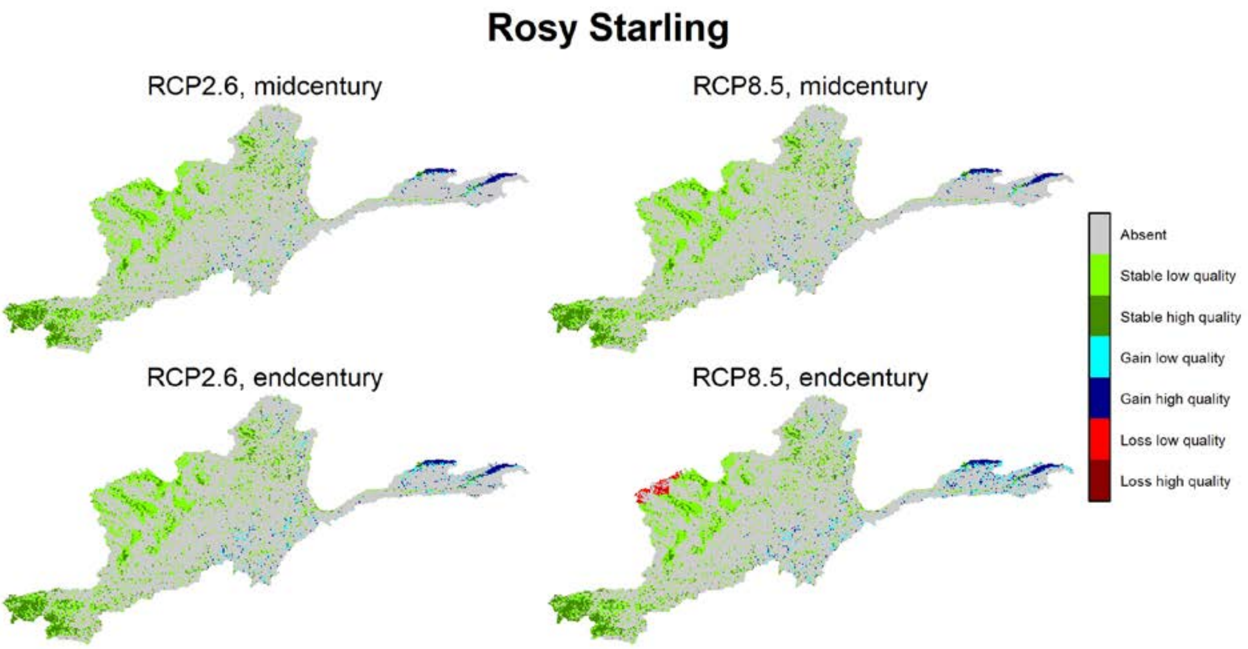

Figure 259. Changes in suitable habitat for Rosy Starling (*Pastor roseus*).

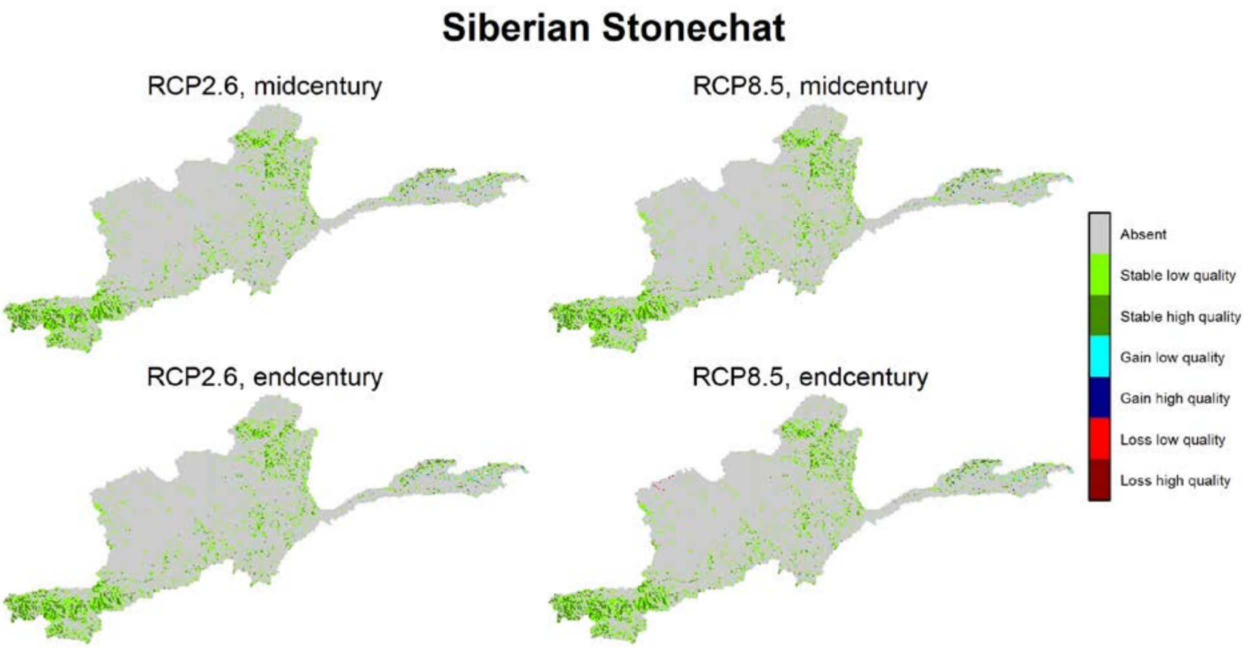

Figure 260. Changes in suitable habitat for Siberian Stonechat (*Saxicola maurus*).

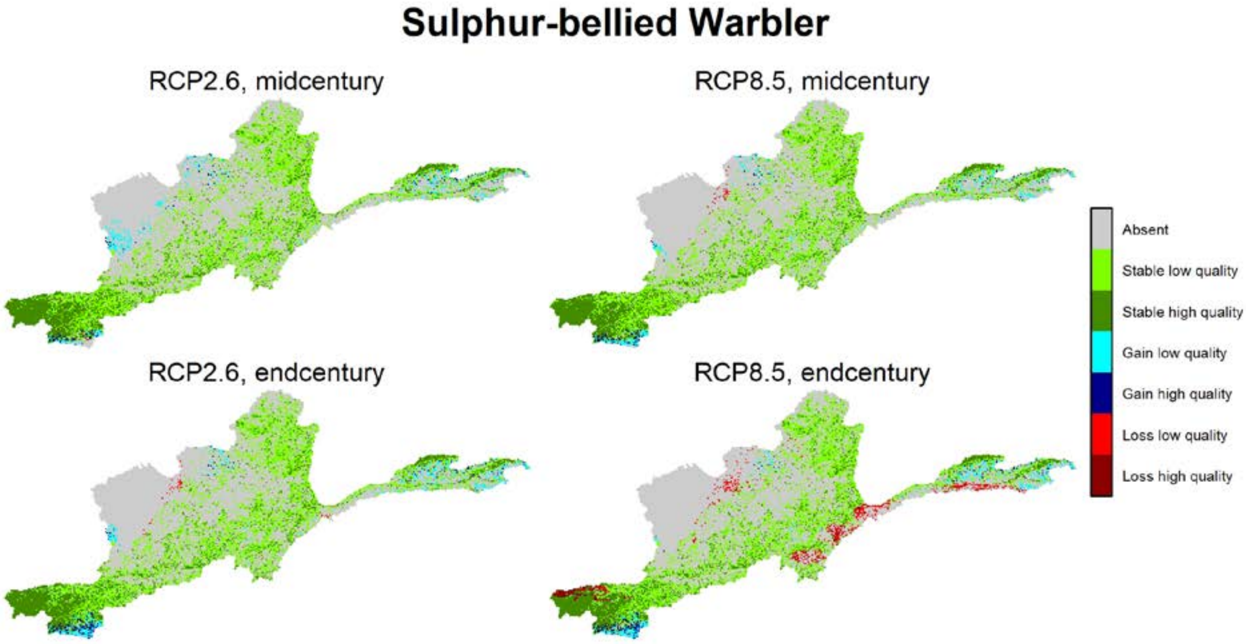

Figure 261. Changes in suitable habitat for Sulphur-bellied Warbler (*Phylloscopus griseolus*).

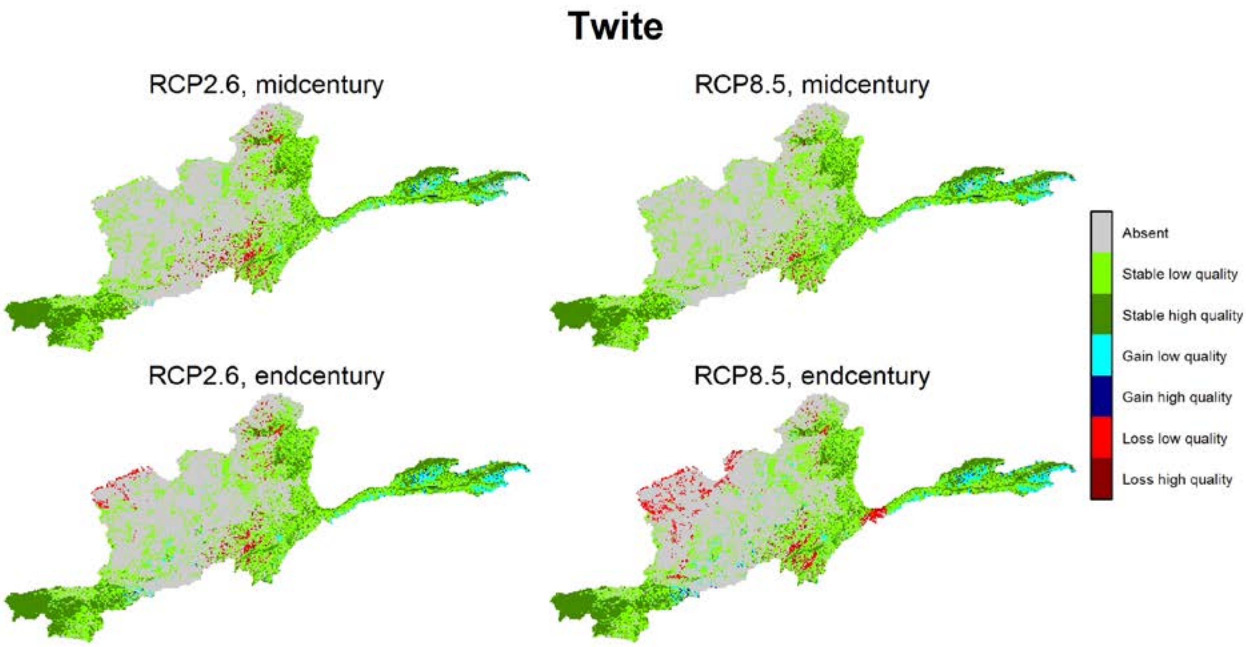

Figure 262. Changes in suitable habitat for Twite (*Linaria flavirostris*).

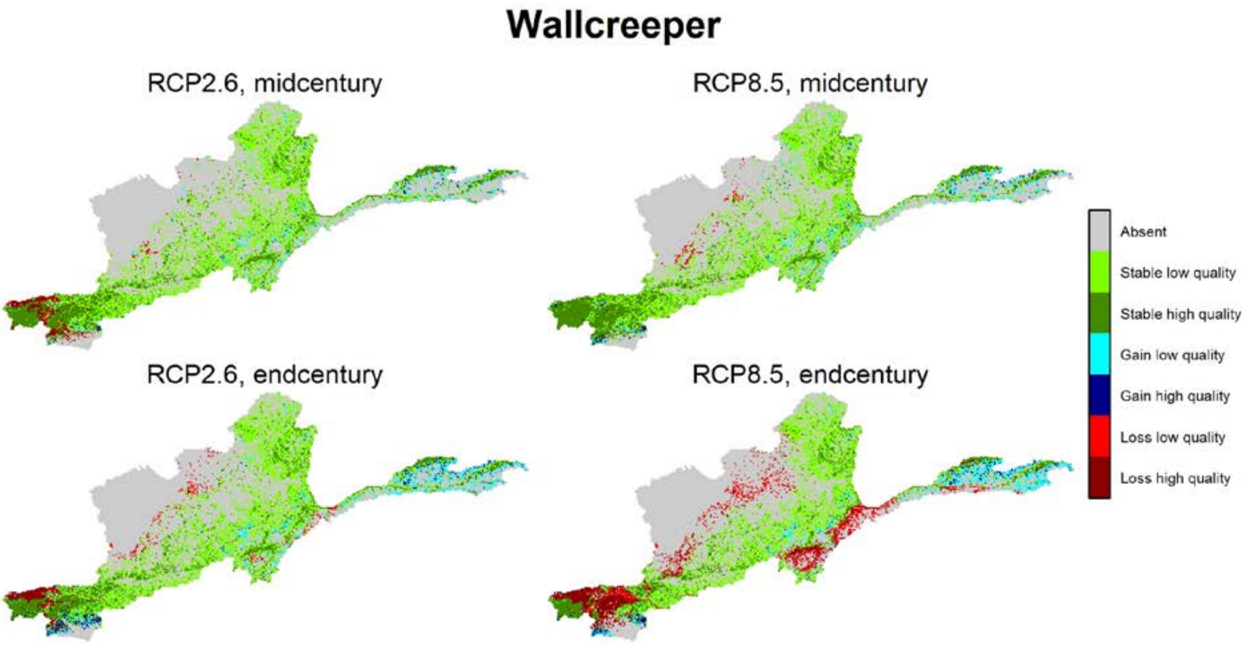

Figure 263. Changes in suitable habitat for Wallcreeper (*Tichodroma muraria*).

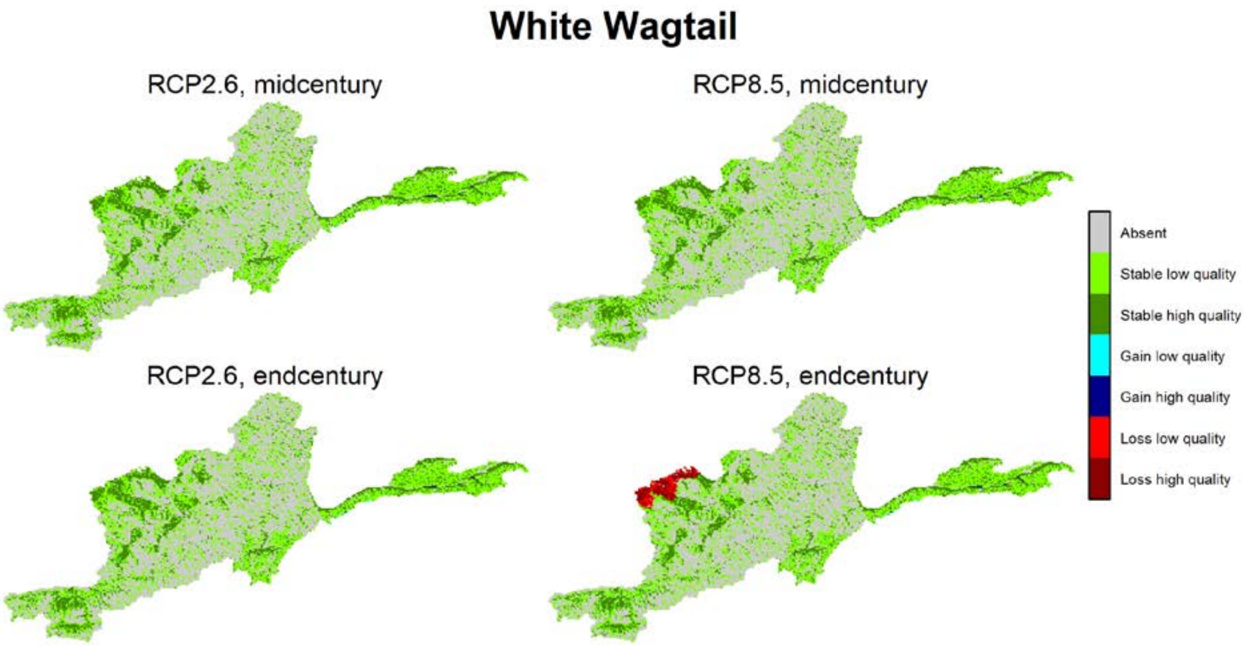

Figure 264. Changes in suitable habitat for White Wagtail (*Motacilla alba*).

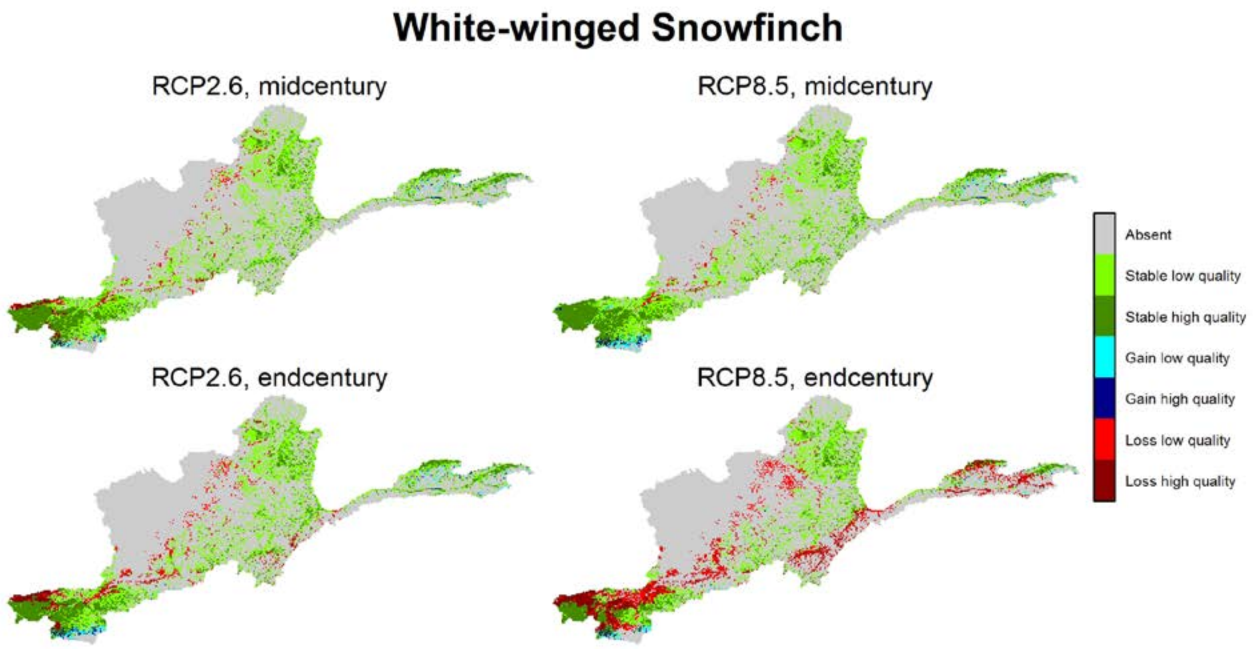

Figure 265. Changes in suitable habitat for White-winged Snowfinch (*Montifringilla nivalis*).

Mammal and Bird Species Sensitivity to Climate Change

S AC

Species selection

All bird and mammal species known to occur within the P-ARB were included in the analysis. To determine the species lists for each taxonomic group, IUCN range maps for birds and mammals were used to intersect with the P-ARB boundary. Range maps were then intersected with the P-ARB boundary to determine each species' geographic distribution within the study region. This process resulted in a total species pool of 103 mammal species and 273 bird species.

Ecological traits

Ecological traits related to distribution, demography, movement, reproduction, and specialization were obtained from primary literature and online databases for each species (Table 75). Descriptions of each trait are given below:

The number of ecoregions occupied was calculated by intersecting each bird and mammal range with a map of terrestrial ecoregions (Dinerstein et al. 2017) and counting the number of intersecting ecoregions.

Geographic range size was determined as global extent of occurrence as given by IUCN.

Median elevation was calculated using a 30 m SRTM digital elevation model and determining the median elevation value within each species' range.

Elevation range was calculated from the DEM as maximum elevation minus minimum elevation.

Median temperature was calculated using a 1 km gridded dataset of mean annual temperature (mean of 1979-2013) from CHELSA (Karger et al. 2017).

Temperature range was calculated from the mean annual temperature raster as maximum temperature minus minimum temperature.

Median precipitation was calculated using a 1 km gridded dataset of total annual precipitation (mean of 1979-2013) from CHELSA (Karger et al. 2017).

Precipitation range was calculated from the total annual precipitation raster as maximum precipitation minus minimum precipitation.

Age of sexual maturity, litter/clutch size, and body mass were obtained from an amniote life history database for birds and mammals (Myhrvold et al. 2015). For mammals, body mass data were supplemented by data from a database on generation length for mammals (Pacifici et al. 2013).

Diet breadth was obtained from a species-level foraging database for birds and mammals (Wilman et al. 2014). For mammals, data were supplemented from a species-level database of life history, ecology, and geography of mammals (Jones et al. 2009).

Generation length was obtained from the IUCN Red List (https://www.iucnredlist.org) for birds and from a database on generation length for mammals (Pacifici et al. 2013).

Habitat breadths were obtained from the. Two forms of habitat breadth were considered using the IUCN habitat typology. Broad and fine habitat breadths were determined by counting the number of habitats occupied by each species based on level 1 and level 2 habitat classifications, respectively.

Trophic level was obtained for mammals only from a species-level database of life history, ecology, and geography of mammals (Jones et al. 2009).

Table 75. Ecological traits and scoring system used to determine sensitivity to climate change for birds and mammals.

Trait	Birds	Mammals	Sensitivity score				
			Q1	Q2	Q3	Q4	Q5
No. ecoregions occupied	Yes	Yes	5	4	3	2	1
Geographic range size	Yes	Yes	5	4	3	2	1
Median elevation	Yes	Yes	1	2	3	4	5
Elevation range	Yes	Yes	5	4	3	2	1
Median temperature	Yes	Yes	5	4	3	2	1
Temperature range	Yes	Yes	5	4	3	2	1
Median precipitation	Yes	Yes	1	2	3	4	5
Precipitation range	Yes	Yes	5	4	3	2	1
Age of sexual maturity	Yes	Yes	1	2	3	4	5
Litter/clutch size	Yes	Yes	5	4	3	2	1
Body mass	Yes	Yes	5	4	3	2	1
Diet breadth	Yes	Yes	5	4	3	2	1
Generation length	Yes	Yes	1	2	3	4	5
Habitat breadth (broad – IUCN L1)	Yes	Yes	5	4	3	2	1
Habitat breadth (fine – IUCN L2)	Yes	Yes	5	4	3	2	1
Trophic level	No	Yes	1	2	3	-	-

Missing data

While most species had complete trait data, data were not available for all species. For birds, 14 species (0.05%) were missing clutch size and 127 species (46.5%) were missing sexual maturity data. For mammals, 47 species (45.6%) were missing diet breadth, 42 species (40.8%) were missing habitat breadth, 21 species (20.4%) were missing litter size, 54 species (52.4%) were missing sexual maturity, and 47 species (45.6%) were missing trophic level data. Missing data values were estimated by first using the Genus mean value. When data were missing for the entire Genus, data were filled using the Family mean value. When those data were missing, data were finally filled using the Order mean value.

Species sensitivity scoring

A scoring system, adapted from Butt and Gallagher (2018), was developed to relate ecological traits to species sensitivity under climate change. For birds and mammals separately, data for each trait were partitioned into quintiles. Sensitivity scores for each trait were then assigned based on the quintile following the scoring system shown in Table 75, where high values reflect greater sensitivity. Sensitivity scores were then summed across all traits per species to yield a final sensitivity score. For each taxonomic group, scores were then rescaled from 0 to 1 to aid interpretation, where 0 indicates low relative sensitivity and 1 indicates high relative sensitivity.

Full scores for each trait for each species, along with final sensitivity scores (raw values, prior to rescaling) are given in Table 76 for birds and Table 77 for mammals.

Species sensitivity mapping

Final sensitivity scores for each species were then applied to the geographic distribution of each species. To do this, vector maps of species ranges were rasterized to a 1 km grid, with each cell value for a given species equal to its sensitivity score. The final sensitivity maps shown in Figure 174 were calculated by summing all scores within each taxonomic group at the pixel level, and then rescaling those values from 0 to 1.

Table 76. Bird species trait and sensitivity scores.

Species	Ecoregion breadth	Range size	Med elev	Elev range	Med temp	Temp range	Med precip	Precip range	Maturity	Clutch size	Body mass	Diet breadth	Gen length	Hab breadth (broad)	Hab breadth (fine)	Sensitivity score
Accipiter badius	4	4	2	5	1	4	2	3	1	5	2	2	4	1	2	42
Accipiter nisus	3	2	3	4	5	1	3	5	4	2	2	5	5	1	1	46
Acridotheres tristis	2	2	2	2	1	2	5	1	1	2	2	1	2	1	2	28
Acrocephalus concinens	5	4	2	2	1	3	5	3	3	4	5	5	3	3	3	51
Acrocephalus dumetorum	4	3	1	4	4	5	4	5	3	3	5	3	3	1	2	50
Acrocephalus orinus	5	5	5	5	5	5	2	5	3	3	4	2	3	1	3	56
Acrocephalus scirpaceus	2	2	1	3	2	1	4	4	3	4	5	1	3	1	3	39
Acrocephalus stentoreus	5	4	3	5	1	5	1	5	3	3	4	2	3	1	3	48
Actitis hypoleucos	1	1	2	3	5	2	3	2	4	3	3	1	4	1	2	37
Aegypius monachus	2	3	4	4	4	1	1	5	5	5	1	5	5	1	3	49
Alauda arvensis	2	1	2	3	5	4	4	3	3	4	3	2	3	1	2	42
Alauda gulgula	4	4	4	2	2	2	1	2	3	5	3	3	3	1	3	42
Alcedo atthis	1	1	1	1	2	1	5	1	4	1	3	3	3	1	3	31
Alectoris chukar	2	2	4	1	2	1	1	2	1	1	1	2	2	2	3	27
Ammomanes deserti	3	2	3	5	1	5	1	5	3	4	4	3	2	1	3	45
Ammoperdix griseogularis	4	4	3	5	1	5	1	5	4	1	2	1	2	1	3	42
Anas platyrhynchos	1	2	2	4	2	1	4	1	4	1	1	1	4	3	3	34
Anser indicus	4	4	5	3	5	3	1	3	5	1	1	5	5	2	3	50
Anthus campestris	2	2	1	3	3	3	3	4	2	3	4	2	1	1	2	36
Anthus roseatus	4	4	5	2	5	5	2	5	2	4	4	5	1	2	3	53
Anthus rufulus	5	5	5	5	2	5	2	5	1	4	4	2	1	1	2	49
Anthus similis	5	5	3	4	1	3	1	3	2	5	4	3	1	1	2	43
Anthus spinoletta	3	4	4	4	5	5	2	4	1	2	4	1	1	2	3	45
Anthus trivialis	2	2	1	2	4	4	4	3	3	2	4	1	1	1	1	35
Apus affinis	4	5	3	2	1	2	2	5	5	5	4	5	5	1	2	51
Apus apus	1	1	2	1	3	1	3	3	5	5	3	5	5	1	1	40
Aquila chrysaetos	1	1	3	1	5	1	3	1	5	5	1	2	5	1	2	37
Ardea alba	1	1	3	1	3	1	3	1	5	4	1	1	5	3	3	36
Ardea cinerea	1	1	2	5	1	3	5	1	5	3	1	1	5	2	3	39
Ardea purpurea	3	3	1	4	2	3	4	4	5	3	1	1	5	2	3	44
Ardeola ralloides	4	4	1	5	2	4	3	4	5	3	2	2	4	3	3	49

APPENDICES

Species	Ecoregion breadth	Range size	Med elev	Elev range	Med temp	Temp range	Med precip	Precip range	Maturity	Clutch size	Body mass	Diet breadth	Gen length	Hab breadth (broad)	Hab breadth (fine)	Sensitivity score
Asio otus	1	1	2	3	4	3	4	2	3	2	2	5	5	1	1	39
Athene noctua	1	1	3	1	2	1	2	1	3	3	2	2	3	1	2	28
Aythya ferina	3	2	1	5	4	5	3	5	4	1	1	1	5	3	3	46
Aythya nyroca	3	3	1	4	3	3	3	4	1	1	1	1	5	3	3	39
Botaurus stellaris	1	1	1	4	4	2	3	4	5	1	1	2	4	3	3	39
Bubo bubo	1	1	3	1	4	1	3	3	5	5	1	2	5	1	1	37
Bucanetes githagineus	3	3	3	5	1	4	1	5	4	2	4	1	3	2	3	44
Bucanetes mongolicus	4	3	4	2	3	1	1	5	4	2	4	3	3	2	3	44
Burhinus oedicnemus	2	2	1	4	2	2	2	4	5	5	1	1	5	1	2	39
Buteo rufinus	3	2	2	2	2	1	1	4	5	5	1	3	5	1	2	39
Calandrella acutirostris	4	3	5	1	5	1	1	2	3	4	4	3	1	2	3	42
Calandrella brachydactyla	2	3	2	5	2	3	2	4	3	3	4	2	1	1	2	39
Calliope pectoralis	4	4	5	2	4	4	4	2	3	4	4	5	3	1	2	51
Caprimulgus europaeus	1	1	2	3	3	1	3	4	3	5	3	5	4	1	2	41
Carduelis caniceps	4	4	5	2	3	2	2	3	4	2	5	1	3	1	2	43
Carpodacus erythrinus	1	1	3	1	5	2	4	1	4	2	4	1	3	1	2	35
Carpodacus puniceus	4	4	5	2	5	4	2	2	4	2	3	2	3	2	3	47
Carpodacus rhodochlamys	4	4	4	3	5	3	1	3	4	2	3	2	3	1	3	45
Carpodacus rubicilla	4	4	5	3	5	4	2	2	4	2	3	1	3	1	2	45
Carpodacus rubicilloides	5	4	5	3	5	5	4	2	4	2	3	5	3	1	3	54
Carpodacus stoliczkae	5	5	5	5	3	5	1	5	4	2	4	3	3	1	3	54
Cecropis daurica	1	2	3	3	3	1	5	1	1	3	4	5	2	1	2	37
Cercotrichas galactotes	3	3	3	5	1	5	1	4	3	4	4	2	2	1	2	43
Certhia himalayana	4	5	5	5	3	5	5	1	3	2	5	3	1	1	2	50
Certhia hodgsoni	5	5	5	4	3	4	5	1	3	1	5	3	1	3	3	51
Cettia cetti	3	3	2	3	2	3	3	4	4	2	5	3	1	1	3	42
Charadrius alexandrinus	2	2	2	4	3	4	2	4	4	5	3	5	4	2	3	49
Charadrius dubius	1	1	2	3	4	1	4	2	5	3	3	5	4	1	2	41
Charadrius leschenaultii	4	3	4	4	3	4	1	5	5	5	2	3	4	1	3	51
Charadrius mongolus	3	3	5	1	5	2	2	2	4	5	3	5	4	1	3	48
Ciconia ciconia	3	3	1	5	2	5	5	5	5	3	1	1	5	2	3	49
Ciconia nigra	2	2	3	4	4	4	3	4	5	4	1	1	5	3	3	48

Species	Ecoregion breadth	Range size	Med elev	Elev range	Med temp	Temp range	Med precip	Precip range	Maturity	Clutch size	Body mass	Diet breadth	Gen length	Hab breadth (broad)	Hab breadth (fine)	Sensitivity score
Cinclus cinclus	1	2	4	1	4	2	4	1	3	2	3	3	3	3	3	39
Cinclus pallasii	2	2	3	1	3	2	5	1	3	2	2	5	2	3	3	39
Circaetus gallicus	4	4	1	5	1	4	5	1	5	5	1	3	5	1	2	47
Circus aeruginosus	3	2	1	4	3	4	4	4	5	2	1	1	5	3	3	45
Columba eversmanni	5	4	3	4	2	4	1	5	1	5	2	3	4	1	2	46
Columba leuconota	4	4	5	2	5	3	3	2	1	5	2	3	4	1	3	47
Columba livia	1	1	3	2	1	1	2	1	1	5	1	2	4	1	2	28
Columba oenas	4	3	1	4	3	5	4	4	3	5	2	2	4	1	1	46
Columba palumbus	3	3	3	3	2	2	5	3	3	5	1	2	4	1	1	41
Columba rupestris	3	2	4	1	5	4	2	3	1	5	2	2	4	1	3	42
Coracias garrulus	2	2	1	2	2	1	4	4	1	3	2	3	4	1	2	34
Corvus corax	1	1	3	1	5	1	3	2	5	2	1	1	5	1	2	34
Corvus corone	1	1	2	2	4	1	4	2	5	2	1	1	4	1	1	32
Corvus frugilegus	3	3	1	4	2	4	4	4	5	3	1	1	5	1	2	43
Corvus macrorhynchos	1	2	2	1	1	2	5	1	5	2	1	1	5	1	2	32
Corvus monedula	3	2	1	1	2	3	5	4	5	2	2	1	5	1	2	39
Coturnix coturnix	1	1	1	2	3	2	4	2	3	1	2	3	1	2	3	31
Cuculus canorus	1	1	2	1	4	1	4	1	4	1	2	3	4	1	2	32
Cyanecula svecica	2	1	1	2	5	4	3	4	4	1	5	1	3	1	1	38
Cyanistes cyanus	3	3	2	4	5	5	3	5	4	1	5	2	3	1	2	48
Delichon dasypus	3	4	4	1	4	3	5	2	4	3	4	5	3	2	3	50
Delichon urbicum	2	1	1	2	4	2	4	3	4	3	5	5	3	1	2	42
Dendrocopos leucopterus	5	4	3	5	2	5	1	5	4	2	3	1	4	1	2	47
Dicrurus leucophaeus	4	4	3	2	2	5	5	1	1	4	3	2	1	1	1	39
Dicrurus macrocercus	4	4	2	4	1	4	5	1	1	5	3	1	1	1	2	39
Emberiza bruniceps	4	3	2	4	2	4	1	5	3	2	4	2	1	1	3	41
Emberiza buchanani	4	4	4	5	3	3	1	5	3	2	4	2	1	1	3	45
Emberiza calandra	3	3	2	5	2	4	4	4	3	2	3	2	3	2	3	45
Emberiza cia	2	3	4	2	2	2	4	3	3	3	4	3	1	1	3	40
Emberiza schoeniclus	2	3	2	4	2	4	2	4	3	2	4	2	1	3	3	41
Emberiza stewarti	5	5	4	5	3	5	3	5	3	4	5	2	1	1	3	54
Enicurus scouleri	3	4	4	2	1	3	5	1	3	5	5	3	2	3	3	47

Species	Ecoregion breadth	Range size	Med elev	Elev range	Med temp	Temp range	Med precip	Precip range	Maturity	Clutch size	Body mass	Diet breadth	Gen length	Hab breadth (broad)	Hab breadth (fine)	Sensitivity score
Eremophila alpestris	2	2	4	1	3	2	1	2	3	4	3	3	3	1	2	36
Erythrogenys erythrogenys	5	5	4	2	1	4	5	2	1	5	3	2	5	2	3	49
Falco cherrug	2	2	3	4	4	3	2	5	5	3	1	3	4	1	2	44
Falco naumanni	2	2	3	3	3	2	2	5	4	3	2	5	4	1	2	43
Falco peregrinus	1	1	2	1	5	1	3	1	5	4	1	2	4	1	1	33
Falco subbuteo	1	1	2	3	4	2	4	2	4	5	2	3	4	1	2	40
Falco tinnunculus	1	1	3	1	3	1	4	1	4	2	2	3	4	1	1	32
Ficedula ruficauda	5	5	5	3	4	4	5	2	3	4	5	5	1	3	3	57
Ficedula tricolor	5	5	5	3	2	4	5	1	3	4	5	5	2	1	2	52
Fulica atra	1	1	1	1	3	1	4	1	4	1	1	1	4	3	3	30
Galerida cristata	1	1	3	2	1	1	2	3	4	3	3	2	2	1	2	31
Gallinago gallinago	3	1	1	4	5	4	3	3	4	3	2	2	3	2	3	43
Gallinula chloropus	1	1	2	1	1	1	5	1	3	1	2	1	4	3	3	30
Garrulus lanceolatus	5	5	4	3	2	5	5	3	3	3	2	1	5	1	3	50
Gelochelidon nilotica	2	3	2	4	2	2	1	5	5	5	2	1	5	3	3	45
Glareola pratincola	2	3	2	3	1	1	1	5	1	5	2	5	5	2	3	41
Gymnoris xanthocollis	5	4	3	4	1	2	1	5	1	4	4	1	1	1	2	39
Gypaetus barbatus	1	3	5	1	4	1	2	2	5	5	1	5	5	1	2	43
Gyps fulvus	3	4	4	3	2	1	2	5	5	5	1	5	5	1	3	49
Gyps himalayensis	3	3	5	2	5	3	2	2	5	5	1	5	5	2	3	51
Halcyon smyrnensis	2	3	1	1	1	3	5	1	3	1	2	2	2	2	2	31
Haliaeetus leucoryphus	4	4	1	2	1	1	5	1	5	5	1	1	5	3	3	42
Hieraaetus pennatus	3	3	3	5	3	3	3	5	5	5	1	3	5	1	2	50
Hippolais languida	4	4	4	5	1	5	1	5	3	2	5	5	2	1	2	49
Hirundo rustica	1	1	2	1	4	1	3	2	4	3	4	2	2	1	2	33
Hirundo smithii	5	5	4	5	1	3	2	3	1	3	5	5	3	1	2	48
Hydrophasianus chirurgus	4	4	3	3	1	3	5	2	5	3	2	3	3	3	3	47
Hypsipetes leucocephalus	3	4	3	1	1	3	5	1	1	5	3	1	1	1	2	35
Ibidorhyncha struthersii	3	3	5	1	4	3	3	2	5	3	2	3	5	3	3	48
Iduna pallida	3	3	3	3	2	2	3	4	4	5	5	3	2	1	2	45
Irania gutturalis	4	5	4	4	2	3	3	5	3	3	4	3	2	1	2	48
Ixobrychus minutus	2	2	1	2	3	2	3	3	5	2	2	3	3	1	3	37

APPENDICES

Species	Ecoregion breadth	Range size	Med elev	Elev range	Med temp	Temp range	Med precip	Precip range	Maturity	Clutch size	Body mass	Diet breadth	Gen length	Hab breadth (broad)	Hab breadth (fine)	Sensitivity score
Lagopus muta	3	2	3	4	5	5	2	3	1	1	1	2	3	3	3	41
Lanius excubitor	2	1	1	2	1	1	1	2	1	1	3	1	2	1	1	21
Lanius minor	3	3	1	5	3	4	3	4	1	1	3	3	2	1	2	39
Lanius phoenicuroides	4	3	3	4	2	1	1	5	3	1	4	2	2	1	2	38
Lanius schach	4	4	4	1	2	2	3	2	1	3	3	2	1	1	1	34
Lanius vittatus	5	5	4	5	1	3	1	5	1	3	4	2	2	1	2	44
Larus brunnicephalus	5	5	5	5	5	5	1	5	5	5	1	1	5	3	3	59
Larus genei	4	5	2	5	3	5	1	5	5	5	2	2	5	3	3	55
Larvivora brunnea	4	5	5	2	3	4	5	1	3	4	5	5	3	1	3	53
Leptopoecile sophiae	4	5	5	3	5	5	3	3	4	1	5	2	2	2	3	52
Lerwa lerwa	5	5	5	5	5	5	4	2	4	5	1	3	4	1	3	57
Leucosticte brandti	5	4	5	5	5	5	2	2	1	4	3	2	1	2	3	49
Leucosticte nemoricola	4	4	5	2	5	4	2	2	1	4	4	3	1	2	3	46
Linaria cannabina	2	2	1	3	3	2	5	4	3	2	4	2	3	1	2	39
Linaria flavirostris	2	3	5	2	5	4	1	3	3	1	5	2	3	1	3	43
Lophophorus impejanus	5	5	5	2	5	4	5	2	4	1	1	1	4	1	3	48
Luscinia megarhynchos	3	3	2	3	2	3	4	4	3	2	4	2	3	1	1	40
Marmaronetta angustirostris	4	5	1	5	1	5	1	5	1	1	1	2	4	3	3	42
Melanocorypha bimaculata	5	5	2	5	1	5	1	5	3	4	3	3	2	2	3	49
Melanocorypha calandra	3	3	3	5	1	5	3	4	3	3	3	2	2	2	3	45
Mergus merganser	3	1	3	4	5	4	4	4	5	1	1	1	5	3	3	47
Merops apiaster	2	2	2	2	2	1	3	4	3	1	3	5	4	1	1	36
Merops persicus	3	4	1	5	1	5	1	3	3	1	3	5	4	1	2	42
Microcarbo pygmaeus	5	5	1	5	2	5	1	5	5	1	1	5	5	2	3	51
Milvus migrans	1	1	2	2	4	1	3	4	5	5	1	1	5	1	1	37
Monticola cinclorhyncha	5	5	5	2	2	3	5	1	3	4	3	1	2	1	2	44
Monticola saxatilis	2	2	4	4	4	2	2	4	3	3	3	2	2	1	2	40
Monticola solitarius	1	2	3	1	2	2	5	1	3	3	3	1	2	1	2	32
Montifringilla nivalis	3	3	5	3	5	3	1	4	1	2	3	2	1	3	3	42
Motacilla alba	1	1	2	1	5	3	3	2	3	1	4	5	3	1	3	38
Motacilla cinerea	1	2	3	1	5	3	3	2	4	2	5	5	3	2	3	44
Motacilla citreola	2	2	4	1	5	3	3	2	3	2	4	5	3	1	3	43

Species	Ecoregion breadth	Range size	Med elev	Elev range	Med temp	Temp range	Med precip	Precip range	Maturity	Clutch size	Body mass	Diet breadth	Gen length	Hab breadth (broad)	Hab breadth (fine)	Sensitivity score
Motacilla flava	2	1	1	3	4	1	4	4	3	1	5	1	3	1	2	36
Muscicapa sibirica	2	3	3	1	5	2	4	1	3	4	5	5	1	2	2	43
Muscicapa striata	1	1	1	2	4	1	4	3	3	4	5	3	1	1	2	36
Mycerobas carnipes	3	4	5	3	4	2	2	1	1	5	3	2	3	2	3	43
Mycerobas icterioides	5	5	5	3	3	4	5	3	1	5	3	1	3	2	3	51
Myophonus caeruleus	5	5	5	3	4	2	2	3	3	3	2	2	3	2	2	46
Neophron percnopterus	3	3	3	1	1	1	2	3	5	5	1	1	5	1	2	37
Netta rufina	4	3	2	4	4	2	1	5	4	1	1	3	4	3	3	44
Nucifraga multipunctata	5	5	5	4	4	4	4	3	4	4	2	2	5	2	3	56
Nycticorax nycticorax	3	3	1	4	2	4	5	4	4	3	1	1	5	3	3	46
Oenanthe chrysopygia	5	5	4	5	2	4	2	5	2	2	4	1	3	1	2	47
Oenanthe deserti	3	3	4	1	3	1	1	4	2	2	4	3	3	1	2	37
Oenanthe finschii	5	5	3	5	1	5	1	5	2	1	3	2	3	1	2	44
Oenanthe isabellina	3	2	4	2	3	2	1	4	2	1	3	2	3	1	2	35
Oenanthe oenanthe	1	1	2	3	5	2	3	3	3	1	4	2	3	1	2	36
Oenanthe picata	4	4	4	3	1	2	1	3	2	3	4	3	3	1	3	41
Oenanthe pleschanka	3	2	4	3	4	3	2	3	2	1	4	3	3	1	2	40
Oriolus kundoo	4	4	4	2	2	3	2	3	4	4	2	1	1	2	3	41
Otus brucei	4	5	2	4	1	2	1	5	3	2	2	2	1	1	2	37
Otus scops	2	2	1	3	3	2	4	4	3	4	2	2	1	1	2	36
Panurus biarmicus	2	2	3	2	3	4	1	4	4	1	5	3	3	3	3	43
Parus major	1	1	2	1	3	1	4	1	4	1	5	1	3	1	1	30
Passer cinnamomeus	4	4	3	3	1	3	5	1	1	2	4	2	4	1	3	41
Passer domesticus	1	1	2	1	4	1	4	1	1	3	3	2	4	1	1	30
Passer hispaniolensis	3	4	3	5	1	4	1	4	3	2	4	2	4	1	1	42
Passer montanus	1	1	2	1	4	1	4	1	1	1	4	3	4	1	2	31
Pastor roseus	4	3	2	4	3	4	1	4	4	5	3	3	3	1	2	46
Pericrocotus ethologus	4	4	4	2	2	4	5	1	1	4	4	2	1	2	2	42
Pericrocotus roseus	5	5	4	2	1	2	5	1	1	4	4	5	1	2	3	45
Periparus ater	1	1	2	4	4	2	4	2	3	1	5	1	3	1	2	36
Periparus rufonuchalis	5	5	5	5	3	5	3	3	1	4	5	2	3	1	3	53
Petronia petronia	2	3	4	3	3	1	2	4	1	1	3	2	1	1	3	34

Species	Ecoregion breadth	Range size	Med elev	Elev range	Med temp	Temp range	Med precip	Precip range	Maturity	Clutch size	Body mass	Diet breadth	Gen length	Hab breadth (broad)	Hab breadth (fine)	Sensitivity score
Phalacrocorax carbo	2	3	2	4	4	3	3	4	5	4	1	2	5	3	3	48
Phasianus colchicus	3	3	3	4	3	3	4	2	1	1	1	1	4	1	3	37
Phoenicurus coeruleocephala	5	5	5	3	5	5	2	2	3	3	5	2	3	1	3	52
Phoenicurus erythrogastrus	3	4	5	1	5	4	1	2	3	3	4	3	3	1	3	45
Phoenicurus frontalis	5	5	5	5	5	5	5	2	3	4	5	5	3	1	2	60
Phoenicurus fuliginosus	3	3	3	1	1	3	5	1	3	4	4	2	2	3	3	41
Phoenicurus leucocephalus	5	5	3	3	1	4	5	4	3	4	3	2	2	3	3	50
Phoenicurus ochruros	1	2	4	1	3	2	3	1	3	2	5	2	3	1	2	35
Phoenicurus phoenicurus	2	2	1	4	4	2	4	3	3	1	5	3	3	1	1	39
Phylloscopus griseolus	4	3	4	4	4	2	1	5	3	2	5	5	1	1	3	47
Phylloscopus humei	3	4	4	2	5	3	2	2	3	2	5	5	1	1	2	44
Phylloscopus neglectus	5	5	4	5	1	5	2	5	3	4	5	5	1	1	2	53
Phylloscopus occipitalis	5	5	4	5	2	5	5	3	3	4	5	5	1	2	3	57
Phylloscopus sindianus	5	5	5	2	5	4	1	4	3	5	5	3	1	1	2	51
Phylloscopus trochiloides	3	3	1	1	4	3	4	2	3	2	5	2	1	1	2	37
Phylloscopus tytleri	5	5	5	3	4	4	5	3	3	2	5	5	1	3	3	56
Pica pica	1	1	2	1	4	1	4	1	5	1	2	1	5	1	1	31
Picus squamatus	5	5	4	3	1	2	2	3	3	1	2	3	4	1	2	41
Platalea leucorodia	3	3	2	5	3	5	2	4	5	4	1	1	5	3	3	49
Plegadis falcinellus	4	5	1	5	2	5	1	5	5	4	1	2	4	3	3	50
Podiceps cristatus	2	1	1	4	4	4	3	4	5	4	1	2	5	3	3	46
Podiceps nigricollis	2	4	4	3	1	2	3	5	5	4	1	2	5	3	3	47
Prunella collaris	1	2	4	1	5	1	3	2	3	4	3	2	3	1	2	37
Prunella fulvescens	3	4	5	3	4	4	1	2	3	4	4	2	3	1	3	46
Prunella rubeculoides	5	5	5	4	5	5	4	2	3	4	4	3	3	2	3	57
Pseudopodoces humilis	5	4	5	5	5	5	2	3	1	1	3	5	4	1	2	51
Ptyonoprogne rupestris	2	3	4	2	3	2	2	1	3	3	4	5	2	1	2	39
Pycnonotus leucogenys	5	5	4	2	2	5	5	2	1	5	3	1	1	1	3	45
Pyrgilauda theresae	5	5	5	5	3	5	2	5	1	4	4	3	1	2	3	53
Pyrrhocorax graculus	2	4	5	1	4	2	3	2	5	3	2	1	5	1	3	43
Pyrrhocorax pyrrhocorax	1	2	4	1	4	1	2	2	5	3	2	1	5	1	3	37

Species	Ecoregion breadth	Range size	Med elev	Elev range	Med temp	Temp range	Med precip	Precip range	Maturity	Clutch size	Body mass	Diet breadth	Gen length	Hab breadth (broad)	Hab breadth (fine)	Sensitivity score
Rallus aquaticus	1	2	1	2	3	2	4	3	3	1	2	1	3	3	3	34
Regulus regulus	1	2	1	2	4	3	5	2	3	1	5	5	1	2	3	40
Remiz coronatus	5	5	2	5	1	5	1	5	4	4	5	3	1	1	1	48
Rhodopechys sanguineus	4	4	4	4	2	2	2	5	4	2	3	2	3	2	3	46
Rhodospiza obsoleta	4	4	4	3	2	2	1	5	4	1	3	2	3	2	3	43
Riparia chinensis	5	5	4	5	1	5	3	5	4	5	5	5	1	1	3	57
Riparia diluta	3	2	4	5	5	3	2	1	4	3	5	5	1	2	2	47
Riparia riparia	1	1	2	4	5	1	3	1	4	3	5	5	1	2	2	40
Rostratula benghalensis	1	1	3	5	1	4	5	1	1	4	2	3	5	3	3	42
Saxicola caprata	4	4	3	2	1	1	1	4	4	4	5	3	1	1	2	40
Saxicola torquatus	1	1	3	1	5	1	3	1	4	1	5	1	1	1	1	30
Scotocerca inquieta	4	3	3	5	1	5	1	5	1	4	5	3	3	1	2	46
Serinus pusillus	4	4	5	2	4	3	2	3	1	3	5	5	2	1	3	47
Sitta cashmirensis	5	5	5	4	3	4	5	5	3	2	4	3	2	3	3	56
Sitta leucopsis	5	5	5	3	3	4	5	3	3	1	5	5	2	3	3	55
Sitta tephronota	4	4	4	4	2	2	2	5	3	1	3	3	2	2	3	44
Spatula clypeata	3	1	1	5	5	2	3	4	1	1	1	2	4	3	3	39
Spilopelia senegalensis	1	1	3	3	1	2	3	2	1	5	2	1	2	1	2	30
Sterna hirundo	1	1	2	1	4	2	3	2	5	5	2	2	5	3	3	41
Sternula albifrons	1	2	1	5	3	3	4	1	5	5	3	3	5	3	3	47
Streptopelia decaocto	1	1	1	1	2	1	4	1	3	5	2	1	4	2	2	31
Streptopelia orientalis	3	2	3	2	5	3	2	3	3	5	2	2	4	1	2	42
Streptopelia turtur	2	1	1	3	3	1	3	4	3	5	2	2	4	1	2	37
Strix aluco	2	2	1	2	3	3	5	3	3	5	1	2	5	1	1	39
Sturnia pagodarum	5	5	4	3	2	3	5	4	4	4	3	1	3	1	3	50
Sturnus vulgaris	2	1	1	4	4	1	4	3	4	1	2	1	3	1	2	34
Sylvia communis	2	2	1	3	3	3	4	3	3	2	5	2	2	1	2	38
Sylvia crassirostris	4	4	4	5	2	5	3	4	3	3	4	2	2	1	2	48
Sylvia curruca	2	1	1	1	4	1	4	3	3	2	5	1	2	1	2	33
Sylvia nana	4	3	3	4	2	5	1	5	3	4	5	2	2	1	3	47
Sylvia nisoria	3	2	1	4	3	4	4	4	3	2	4	3	2	1	2	42
Tachybaptus ruficollis	1	1	2	3	1	1	5	1	4	1	2	3	4	3	3	35

Species	Ecoregion breadth	Range size	Med elev	Elev range	Med temp	Temp range	Med precip	Precip range	Maturity	Clutch size	Body mass	Diet breadth	Gen length	Hab breadth (broad)	Hab breadth (fine)	Sensitivity score
Tachymarptis melba	2	3	4	1	1	2	4	2	5	5	2	5	5	1	1	43
Tadorna ferruginea	2	2	4	1	4	2	2	1	5	1	1	1	5	2	3	36
Tadorna tadorna	3	2	2	4	4	2	2	3	5	1	1	2	5	3	3	42
Tarsiger rufilatus	5	5	5	3	5	5	4	3	1	1	5	2	2	3	3	52
Terpsiphone paradisi	5	4	2	3	1	3	5	3	3	4	4	5	4	1	1	48
Tetraogallus himalayensis	4	4	5	3	5	4	2	3	1	1	1	3	4	2	3	45
Tetraogallus tibetanus	5	5	5	5	5	5	2	3	1	1	1	5	4	2	3	52
Tichodroma muraria	2	3	5	1	4	4	2	2	1	3	5	5	2	3	3	45
Tringa totanus	2	1	2	1	4	3	3	2	3	3	2	2	4	3	3	38
Trochalopteron lineatum	5	5	5	3	2	5	5	2	1	5	3	1	3	1	3	49
Trochalopteron variegatum	5	5	5	3	3	4	5	3	1	5	3	3	3	2	3	53
Troglodytes troglodytes	1	2	3	1	2	3	5	1	3	1	5	1	1	1	2	32
Turdus maximus	5	5	5	2	5	3	4	1	3	3	2	1	4	3	3	49
Turdus merula	2	2	1	3	3	2	5	3	3	3	2	1	4	1	1	36
Turdus viscivorus	2	2	1	2	4	3	4	3	3	4	2	1	4	1	1	37
Upupa epops	1	1	3	1	3	1	3	1	3	1	3	3	4	1	2	31
Vanellus indicus	2	3	1	5	1	5	5	1	5	3	2	5	5	2	3	48
Zapornia parva	4	3	1	4	3	5	4	4	1	1	3	2	1	3	3	42
Zapornia pusilla	2	2	2	4	4	4	3	3	1	1	3	1	1	3	3	37

Table 77. Mammal species trait and sensitivity scores.

Species	Ecoregion breadth	Range size	Med elev	Elev range	Med temp	Temp range	Med precip	Precip range	Maturity	Litter size	Body mass	Diet breadth	Gen length	Hab breadth (broad)	Hab breadth (fine)	Trophic level	Sensi-tivity score
Allactaga elater	4	3	1	5	2	5	1	5	2	2	4	1	1	2	3	2	43
Allactaga severtzovi	5	5	1	5	2	5	1	5	2	2	3	1	1	3	3	2	46
Allactaga williamsi	4	4	4	5	3	5	3	5	2	2	4	1	1	3	3	2	51
Alticola argentatus	4	4	5	3	4	3	2	4	1	1	4	3	1	1	3	1	44
Apodemus pallipes	4	4	5	3	4	3	3	3	1	1	3	1	1	3	3	2	44
Apodemus uralensis	3	2	1	3	4	4	4	3	1	1	4	1	1	1	3	2	38
Barbastella leucomelas	2	3	4	1	3	1	4	1	3	4	4	3	3	1	2	3	42
Blanfordimys afghanus	5	5	5	5	3	5	2	5	1	3	3	1	5	1	3	2	54
Blanfordimys bucharensis	5	5	4	5	3	5	3	5	1	3	3	1	5	3	3	2	56
Calomyscus baluchi	5	5	5	4	2	3	2	4	2	2	3	1	2	2	3	1	46
Canis lupus	1	1	2	1	5	1	3	2	5	1	1	3	5	1	1	3	36
Capra falconeri	5	5	5	5	4	5	4	5	5	4	1	3	4	1	2	1	59
Capra sibirica	4	4	5	3	5	4	1	3	5	5	1	3	5	1	3	1	53
Caracal caracal	1	1	3	4	1	5	4	3	4	3	1	3	4	1	2	3	43
Cervus hanglu	5	5	1	5	2	5	1	5	4	5	1	3	5	1	2	1	51
Cricetulus migratorius	2	2	3	3	4	2	2	3	1	1	4	2	1	1	2	2	35
Crocidura gmelini	4	4	4	3	3	1	2	4	1	3	5	1	1	2	3	3	44
Crocidura suaveolens	2	1	2	5	4	3	3	3	1	3	5	1	1	1	2	2	39
Crocidura zarudnyi	5	5	4	5	1	5	1	5	1	1	5	1	1	3	3	3	49
Dryomys nitedula	3	3	3	3	3	3	4	3	3	3	4	1	2	1	2	2	43
Ellobius tancrei	4	4	3	5	4	5	2	4	1	2	4	3	1	1	3	1	47
Eoglaucomys fimbriatus	5	5	5	4	5	4	5	3	4	2	2	1	2	3	3	2	55
Eptesicus gobiensis	4	3	4	2	4	2	1	4	3	4	5	3	4	1	3	3	50
Eptesicus serotinus	1	1	1	2	3	2	5	2	3	4	4	3	4	1	2	3	41
Felis chaus	1	2	1	3	1	4	5	1	4	3	1	2	3	1	1	3	36
Felis silvestris	1	1	3	3	1	1	3	3	3	3	2	1	5	1	1	3	35
Hemiechinus auritus	3	2	3	3	4	1	1	4	2	2	3	1	2	1	2	2	36
Herpestes auropunctatus	3	3	1	3	1	4	5	1	2	4	2	1	3	2	3	2	40
Hyaena hyaena	1	1	2	4	1	3	1	2	5	3	1	1	5	2	3	2	37
Hypsugo savii	2	3	3	3	2	2	4	3	1	4	5	3	3	1	2	3	44

APPENDICES

Species	Ecoregion breadth	Range size	Med elev	Elev range	Med temp	Temp range	Med precip	Precip range	Maturity	Litter size	Body mass	Diet breadth	Gen length	Hab breadth (broad)	Hab breadth (fine)	Trophic level	Sensi-tivity score
Hystrix indica	2	2	3	2	1	1	3	2	4	4	1	2	4	1	2	2	36
Jaculus blanfordi	5	4	3	5	1	5	1	5	2	2	4	2	2	3	3	2	49
Lepus capensis	1	1	2	1	1	1	1	4	2	3	2	3	2	1	2	1	28
Lepus tibetanus	4	4	4	2	3	1	1	4	2	3	2	3	2	1	3	1	40
Lutra lutra	1	1	2	1	5	1	4	1	5	4	1	1	5	1	1	3	37
Lynx lynx	1	1	2	1	5	2	4	2	5	3	1	3	5	1	1	3	40
Macaca mulatta	2	2	2	2	1	2	5	1	5	5	2	1	5	1	1	1	38
Marmota caudata	4	5	5	3	5	3	3	4	5	3	2	1	3	1	3	1	51
Marmota himalayana	4	4	5	2	5	3	3	2	5	2	1	1	3	1	2	1	44
Martes flavigula	2	3	2	1	2	3	5	1	5	3	2	1	4	1	2	3	40
Martes foina	1	1	3	1	4	1	4	2	5	2	2	1	4	1	2	3	37
Meles leucurus	2	1	2	2	5	3	3	3	4	3	2	1	4	1	2	3	41
Meles meles	3	2	1	5	4	4	4	2	4	3	1	1	4	1	1	3	43
Meriones libycus	3	2	2	4	1	3	1	4	2	2	3	1	2	1	3	1	35
Meriones meridianus	3	2	4	3	3	4	1	4	1	1	3	1	1	2	3	1	37
Meriones persicus	4	4	4	4	2	3	2	4	1	1	3	1	1	1	3	1	39
Meriones tamariscinus	4	4	2	3	4	4	1	5	1	2	3	1	1	1	2	1	39
Meriones zarudnyi	5	5	4	5	2	5	2	5	1	1	3	1	1	3	3	1	47
Microtus ilaeus	5	5	4	5	4	5	3	5	1	2	4	2	1	1	3	1	51
Miniopterus schreibersii	1	1	3	2	2	1	5	1	5	5	5	3	3	1	1	3	42
Moschus cupreus	5	5	5	4	5	4	2	4	4	4	1	3	4	1	3	1	55
Mus musculus	1	1	2	1	4	1	4	1	1	1	4	1	2	1	1	3	29
Mustela altaica	3	3	4	1	5	3	3	2	3	1	3	3	3	1	3	3	44
Mustela erminea	1	1	1	2	5	1	3	2	2	1	3	1	2	1	1	3	30
Mustela eversmanii	2	1	2	3	4	4	3	4	3	1	2	3	2	2	3	3	42
Mustela sibirica	2	1	2	1	5	2	4	1	3	1	2	1	3	1	1	3	33
Myotis blythii	2	2	3	4	3	3	4	3	4	5	4	3	4	1	1	3	49
Myotis bucharensis	5	5	4	4	3	4	3	4	3	5	5	3	4	3	3	3	61
Myotis emarginatus	3	3	2	3	3	2	5	3	4	5	5	3	4	1	2	3	51
Myotis muricola	2	3	2	2	1	2	5	1	3	5	5	3	4	2	3	3	46
Myotis nipalensis	3	3	4	1	3	2	2	2	3	5	5	3	4	1	1	3	45

Species	Ecoregion breadth	Range size	Med elev	Elev range	Med temp	Temp range	Med precip	Precip range	Maturity	Litter size	Body mass	Diet breadth	Gen length	Hab breadth (broad)	Hab breadth (fine)	Trophic level	Sensi-tivity score
Neodon juldaschi	5	5	5	4	5	4	2	5	1	3	4	2	1	1	3	2	52
Nesokia indica	3	3	3	3	1	1	1	3	2	2	3	1	2	1	2	1	32
Nyctalus leisleri	3	3	1	4	3	4	5	3	4	4	5	3	3	1	3	3	52
Ochotona macrotis	4	4	5	2	5	3	3	2	3	2	3	3	2	3	3	1	48
Ochotona roylei	5	5	5	2	5	4	4	2	3	3	3	3	2	3	3	1	53
Ochotona rufescens	4	4	4	5	2	4	2	4	1	1	3	3	2	1	3	1	44
Ochotona rutila	5	5	5	4	5	5	4	5	3	2	3	3	2	3	3	1	58
Otocolobus manul	2	2	4	1	5	1	2	2	3	1	2	3	3	1	3	3	38
Otonycteris hemprichii	4	4	3	2	2	1	1	3	3	4	4	3	3	1	2	3	43
Ovis ammon	5	5	5	4	5	5	1	5	4	5	1	3	5	1	3	1	58
Ovis orientalis	4	5	5	4	3	3	2	4	5	5	1	3	5	1	2	1	53
Panthera pardus	3	3	4	3	2	2	2	3	5	4	1	3	5	1	1	3	45
Panthera uncia	3	3	5	2	5	4	2	2	5	4	1	3	5	1	3	3	51
Paradoxurus hermaphroditus	1	2	1	1	1	2	5	1	4	3	2	1	5	1	1	2	33
Paraechinus hypomelas	4	4	4	5	1	4	1	4	2	2	3	1	2	1	3	2	43
Pipistrellus coromandra	2	3	1	2	1	2	5	1	2	4	5	3	3	1	2	3	40
Pipistrellus javanicus	3	4	1	1	1	3	5	1	2	4	5	3	3	1	2	3	42
Pipistrellus kuhlii	2	1	2	4	2	2	2	3	2	5	5	3	3	1	2	3	42
Pipistrellus pipistrellus	1	1	1	2	3	1	5	1	2	5	5	3	3	1	2	3	39
Pipistrellus tenuis	2	2	1	3	1	2	5	1	1	4	5	3	3	1	1	3	38
Prionailurus bengalensis	1	2	2	1	2	2	5	1	5	3	2	1	4	1	2	3	37
Rattus pyctoris	3	4	5	2	3	1	4	2	1	2	3	1	1	1	2	2	37
Rhinolophus blasii	3	3	4	5	2	4	3	3	4	5	5	3	5	1	2	3	55
Rhinolophus bocharicus	5	4	1	5	2	5	2	5	4	5	4	1	4	1	2	3	53
Rhinolophus ferrumequinum	1	2	3	1	2	2	5	2	5	5	4	3	5	1	2	3	46
Rhinolophus hipposideros	2	2	3	1	3	1	4	3	4	5	5	3	4	1	2	3	46
Rhinolophus lepidus	3	3	1	4	1	4	5	1	4	5	5	3	5	1	2	3	50
Rhinopoma hardwickii	5	5	5	5	4	5	3	5	3	5	4	3	3	1	2	3	61
Rhombomys opimus	3	3	3	4	3	2	1	5	2	1	3	3	1	1	2	1	38
Semnopithecus schistaceus	4	5	5	2	4	4	5	2	5	5	1	1	5	1	3	1	53

Species	Ecoregion breadth	Range size	Med elev	Elev range	Med temp	Temp range	Med precip	Precip range	Maturity	Litter size	Body mass	Diet breadth	Gen length	Hab breadth (broad)	Hab breadth (fine)	Trophic level	Sensi-tivity score
Sorex buchariensis	5	5	5	4	5	5	4	5	3	1	5	2	1	3	3	3	59
Spermophilopsis leptodactylus	5	4	1	5	2	5	1	5	4	2	2	1	2	3	3	2	47
Suncus etruscus	1	3	1	2	1	3	5	1	2	2	5	1	1	1	2	3	34
Sus scrofa	1	1	1	1	3	2	4	1	3	2	1	1	4	1	1	2	29
Tadarida teniotis	2	3	3	1	2	2	4	2	3	5	4	3	3	1	2	3	43
Ursus arctos	1	2	3	2	4	2	3	3	5	4	1	1	5	1	2	2	41
Ursus thibetanus	2	2	2	1	2	1	5	1	5	4	1	1	5	1	1	1	35
Vespertilio murinus	2	1	1	3	4	3	3	2	3	4	4	3	3	1	1	3	41
Vormela peregusna	3	2	3	5	3	3	2	4	4	1	2	2	2	1	2	3	42
Vulpes cana	4	4	4	4	1	4	1	4	4	4	2	1	2	2	3	2	46
Vulpes corsac	3	2	3	4	4	5	2	5	5	1	2	1	4	1	3	2	47
Vulpes vulpes	1	1	2	1	5	1	3	1	3	1	2	1	3	1	1	3	30

Appendix 7. Local Communities Supplementary Methods & Results

Number of Agroforestry Trees Grown and Owned

AC

Indicator overview

Agroforestry is a substantial livelihood system from the perspective of its contribution to food security, increasing biodiversity, and combating climate change. Agroforestry can help to fight poverty and hunger as it raises potential for improved soil fertility and higher yields allowing for more diverse food, livelihoods, and income. Also, trees can provide habitat for multiple wildlife species and allow those species to migrate across landscapes, providing conditions for their survival thus contributing to biodiversity. Moreover, agroforestry is seen as a key tool of mitigation and adaption to climate change due to the storage of large amounts of carbon, increasing resilience of households to climate-related shocks and erratic water supplies (Agroforestry Network 2018).

Households or communities that own fewer agroforestry trees likely have less income and lower income diversification, which equates to lower adaptive capacity. Thus, they are likely to be more vulnerable.

Methods overview

Number of agroforestry trees grown and owned are estimated from households' responses about the numbers and types of trees in their ownership. The data were taken from the QoL 2014 Survey where households were asked the question: "Does your household own any type of trees?" and, in case of positive answer, were asked: "Please indicate the number of the following types of trees that the household owns (list)". The proposed list of trees included: apricot, mulberry, apple, cherry, peach, pear, plum, walnut, poplar, willow, almond, nashpati, fig, pomegranate, grapes, sour cherry, and other. All fruit trees were then aggregated into one category group by summing up the numbers of trees. The group 'fruit trees' includes apricot, mulberry, apple, cherry, peach, pear, plum, walnut, almond, nashpati (pear), fig, pomegranate, grapes, and sour cherry. Poplar and willow, being non-food productive, were aggregated and summed up into a separate category group. Also, during data analysis obvious outliers, i.e., single households that reported or registered remarkably high quantities of trees, were removed from the sample. This was done to avoid substantial influence of those single large numbers on the mean population estimates that could unevenly enlarge and misrepresent mean values of the district/province population, overestimating the average household's tree ownership.

The tables provide estimates on the mean numbers of trees of the 'fruit trees' category and of the 'poplar and willow trees' category per household at the district and province levels. Additionally, the tables include estimates of the standard deviations of the two tree categories to analyze the average variability in the owned numbers of trees among households at the district and province levels.

Summary tables of indicator by district and province

Table 78. Numbers of trees per household by district.

Province	District	Code	Mean numbers of trees per household			
			Fruit trees	St Dev	Poplar & Willow	St Dev
Badakhshan	Baharak	1108	42	53.5	70.5	139.3
Badakhshan	Darwaz	1110	24.8	27.3	8.8	30.9
Badakhshan	Ishkashim	1107	3.3	7.8	70.4	110.1
Badakhshan	Jurm	1103	36.4	67.9	79	212.8
Badakhshan	Kuran Wa Munjan	1117	26.6	33.3	20.1	27.4
Badakhshan	Shighnan	1109	27.4	25.2	26.6	52.9
Badakhshan	Wakhan	1106	3.8	10.8	46.1	94.7
Badakhshan	Zebak	1105	5.7	7.9	42	57.1
Baghlan	Andarab	1307	70	86.1	29.7	51.6
Baghlan	Dahana-I-Ghori	1303	44.8	42.3	36.5	52.2
Baghlan	Doshi	1304	16.8	42.1	26.8	70.9
Baghlan	Kahmard	2803	53	66	44.8	105.6
Baghlan	Khinjan	1306	38.8	46.2	19	27.4
Baghlan	Tala Wa Barfak	1305	35.8	66.1	33.2	70.8
Bamyan	Bamyan City	2801	12.7	19	104.5	163.2
Bamyan	Shibar	2802	25.8	21.2	15	21.1
Takhar	Farkhar	1206	13.7	16.2	105	251.7
Takhar	Kalafgan	1207	8.6	10.1	32.9	61.3
Takhar	Rustaq	1208	17.5	32.8	22.1	60.3
Takhar	Taluqan	1201	15.4	29.1	49.5	147.9
Takhar	Warsaj	1205	34.1	35	20.3	29.2

Source: QoL

Table 79. Numbers of trees per household by province.

Province	Mean numbers of trees per household			
	Fruit trees	St Dev	Poplar & Willow	St Dev
Badakhshan	29.1	46.0	46.8	128.3
Baghlan	44.9	67.9	31.8	71.5
Bamyan	14.9	19.9	89.4	152.6
Takhar	17.4	30.4	40.5	128.5

Source: QoL

Results summary

Even though the obvious outliers (i.e., households that reported considerably higher amounts of trees in their ownership) were removed from the sample, there is still very high estimates of the standard deviation, especially for poplar and willow trees. This means that there is an uneven distribution of trees in the ownership among households. That is, few households own significantly large numbers of trees, whereas most of the households residing in the same district or province own far fewer than the estimated mean numbers.

Among four observed provinces, Baghlan province reported the largest mean number of fruit trees per household (44.9 per household), but the least mean number of poplar and willow trees (31.8 per household). Bamyan province reported the highest mean number of poplar and willow trees (89.4 per household) and the lowest mean number of fruit trees (14.9 per household). Badakhshan province reported the second largest mean numbers of both fruit trees and poplar and willow trees per household (29.1 and 46.8 per household, respectively). Takhar province reported the second lowest mean number of both fruit and poplar/ willow trees per household (17.4 and 40.5 per household, respectively). The results of standard deviation estimates suggest that few households residing in each province have plantings of poplar and willow trees.

Variability of fruit trees and ownership of those provide households with the possibility of higher diversification both in food/nutrition and income. However, high variation in the numbers among households indicates that the uneven distribution of the plantations might increase the vulnerability of those households that have lower access to and ownership of the trees.

Age of Household Members

AC

Indicator overview

Age is an important human development indicator as it emphasizes the opportunities and possibilities of the population. Younger and older populations have different needs and different impacts on the society and the economy.

The pool of young population may result in a demographic dividend once they are fully employed and thus contribute to economic development. Although an aging population may indicate improved well-being of the society, it also implies greater burden in the need for more care and medical treatment. A study "The Global Burden of Disease" reported that noncommunicable and chronic diseases are age-related and are increasing with age. Thus, older people tend to have additional health needs and higher health expenditures. Also, as older people require health and social care simultaneously while also not working, household income carries this costly burden resulting in lower available income, economic opportunities, and well-being in general (Browne and Millington 2015).

In rural regions, agriculture is an essential source of income, subsistence, and livelihood. Smallholder agriculture, being a labor-intensive economic activity, requires involvement of a number of workers. Typically, family members are the primary source of the labor force in these household agricultural activities. Thus, household age structure plays a role in both household and society respects. The predomination of the younger population in the household allows use of their work capabilities for income and well-being generation. At the same time, older members of the household require care of other family members, preventing them from generating income through work activities and bearing expenditures from the additional health-related needs.

Thus, households with higher mean ages likely have fewer income and employment opportunities, which reduces their adaptive capacity and results in their higher vulnerability.

Methods overview

The available data on age of household members was taken from two data sources: QoL 2014 Survey and the Demographic and Health Survey (DHS) 2015.

In the QoL Survey, households were asked about the age in completed years of the households' members. The table presents the median estimates of the age of the households' members at the district and province levels. The table also includes measures of the proportion of the young population (aged 0-15 years) and senior population (aged 66 years and above), estimated first at the household level and then aggregated to the district and province levels. Moreover, standard deviation measures were included to represent variability of different age groups in household composition at the district and province levels. Standard deviation was calculated from the percentage estimation of each age group at the household level.

DHS Survey data provide information on the age of the household members reported from the household responses. Furthermore, weights were applied to estimate the median age and proportion of the young population group (aged 0-15 years) and senior population group (aged 66 and above) at the province level. The table comprise data on the weighted median age and proportions of different age groups at the province level.

Summary tables of indicator by district and province

Table 80. Age of household members by district.

Province	District	Code	Age of household members					
			Median age	% aged 0-15	St Dev of % of children in hh	% aged 66+	St Dev of % of elderly in hh
Badakhshan	Baharak	1108	16	48.4	16.7	1.4	3.6
Badakhshan	Darwaz	1110	15	52	11.1	2.6	7.4
Badakhshan	Ishkashim	1107	18	47.6	13	1.5	2.8
Badakhshan	Jurm	1103	18	41.5	16.3	3.4	8.4
Badakhshan	Kuran Wa Munjan	1117	17	47.9	13.5	3.1	2.9
Badakhshan	Shighnan	1109	18	43.5	14.5	2	5.2
Badakhshan	Wakhan	1106	17	44.7	15.4	1.9	11.2
Badakhshan	Zebak	1105	15	50.2	11.8	2.5	8.6
Baghlan	Andarab	1307	15	50.2	15.7	3.2	8.5
Baghlan	Dahana-I-Ghori	1303	15	50.1	16	2.4	5.5
Baghlan	Doshi	1304	17	46.5	16.3	3	9
Baghlan	Kahmard	2803	15	51.9	15.8	1.7	6.3
Baghlan	Khinjan	1306	18	45.1	16.5	3.5	13.5
Baghlan	Tala Wa Barfak	1305	16	48.2	15.2	2.7	9.1
Bamyan	Bamyan City	2801	16	49.9	14.3	2.4	11.9
Bamyan	Shibar	2802	16	47.2	13.5	3.8	19.2
Takhar	Farkhar	1206	13	56.2	14.9	2.7	25.5
Takhar	Kalafgan	1207	13	55.9	13.9	1.8	17
Takhar	Rustaq	1208	15	51.4	17	2.9	11.5
Takhar	Taluqan	1201	15	52.5	17.4	1.6	10.8
Takhar	Warsaj	1205	15	51.5	14.3	3.9	14.2

Source: QoL

Table 81. Age of household members by province (QoL).

Province	Age of household members				
	Median age	% aged 0-15	St Dev of % of children in hh	% aged 66+	St Dev of % of elderly in hh
Badakhshan	17	46.3	14.2	2.4	11.2
Baghlan	16	48.8	14.4	2.7	13.3
Bamyan	16	49.4	13	2.6	13.2
Takhar	15	52.4	15	2.4	19.7

Source: QoL

Table 82. Age of household members by province (DHS).

Province	Age of household members		
	Median age	% aged 0-15	% aged 66+
Badakhshan	16	49	2
Baghlan	16	48	2
Bamyan	16	47	3
Takhar	16	47	3
Kunduz	16	48	2

Source: DHS

Results summary

Both QoL and DHS data sources report the average median age of the household members at 16 years at the province level. However, according to the QoL data, Takhar province has the highest proportion of the young population at 52.4% and one of the lowest proportions of the senior population at 2.4% at the household level, and a median household age of 15 years. The proportion of the senior population is estimated at 2-3% when calculated at the household level and the province level. At the district level, the proportion of different age groups has only moderate variation. In general, the proportion of working aged adults constitutes roughly half of the total population, with a few exceptions in some districts of Takhar province, where the young population marginally predominates.

The analysis demonstrates that, on average, the population of the observed regions has an even age distribution. A substantial proportion of the household members are of working age, whereas the young population constitutes almost half of the family composition. The low proportion of seniors in the population could indicate a relatively low life expectancy, which raises concerns about quality of life and health systems. Furthermore, the high proportion of younger individuals in the population could indicate poor family planning services, or a situation where children typically play an essential role in the labor capital within the household. Whereas this composition is similar to developing and under-developed countries more broadly, it differs from the typical composition of developed countries where the proportion of the young population is relatively lower, and the proportion of the senior population is relatively higher.

Sex of Household Members

AC

Indicator overview

In most under-developed and developing countries, women still face constraints to access good education, decent employment, and an equally paid income. Women are also largely employed in nonpaid housework, such as cooking, cleaning, raising children, and taking care of the elderly. These activities take most of their time and effort and constrain them from opportunities to be employed in jobs that earn income. Also, early marriages, especially in poor and rural areas, often force women to exit schools early, which prevents them from finishing their education, receiving a degree, and be more competitive for employment. Even employed women still receive unequal wages and have limited career opportunities compared to men.

Thus, households with greater proportions of women likely have less income, lower education, and fewer employment opportunities, which reduces their adaptive capacity and, as a result, increases their vulnerability.

Methods overview

The sex of the household members was estimated from the QoL 2014 Survey on the sex of the households' members and from the NSIA on the gender composition. The tables present data on the proportion of females at the district and province levels.

Summary tables of indicator by district and province

Table 83. Percent females in household by district.

Province	District	Code	% Females
Badakhshan	Baharak	1108	49.84
Badakhshan	Darwaz	1110	50
Badakhshan	Ishkashim	1107	49.06
Badakhshan	Jurm	1103	50.03
Badakhshan	Kuran Wa Munjan	1117	50.35
Badakhshan	Shighnan	1109	48.17
Badakhshan	Wakhan	1106	46.92
Badakhshan	Zebak	1105	46.12
Baghlan	Andarab	1307	50.84
Baghlan	Dahana-I-Ghori	1303	49.17
Baghlan	Doshi	1304	51.34
Baghlan	Kahmard	2803	50.36
Baghlan	Khinjan	1306	53.71
Baghlan	Tala Wa Barfak	1305	48.76
Bamyan	Bamyan City	2801	50.58
Bamyan	Shibar	2802	46.88
Takhar	Farkhar	1206	54.18
Takhar	Kalafgan	1207	48.94
Takhar	Rustaq	1208	50.35
Takhar	Taluqan	1201	51.26
Takhar	Warsaj	1205	55.95

Source: QoL

Table 84. Percent females in household by province (QoL).

Province	% Females
Badakhshan	49.34
Baghlan	50.56
Bamyan	50
Takhar	51.22

Source: QoL

Table 85. Percent females in household by province (NSIA).

Province	% Females
Badakhshan	49
Baghlan	49
Bamyan	49
Takhar	49
Kunduz	49

Source: NSIA

Results summary

The average composition of households is equally distributed among genders. Females comprise around half of the population. At the district level, there is minor variability in the household composition among districts, but on average province level estimates suggest roughly equal allocation. The national statistics agency reports data showing 49% of the population at the province level are females. While analysis of the QoL Survey data with a representative sample shows slight variability, Badakhshan province shows the least proportion of females in the household composition at 49%, and Baghlan and Bamyan provinces report about 50% each. Takhar province reports 51% of females in the household composition of the province. There is further difference at the district levels with the smallest female share at 46% in Wakhan and Zebak districts of Badakhshan province and Shibar district of Bamyan province. The largest female share of 56% is in Warsaj district of Takhar province. One possible explanation of the variation in the female share across districts might be the different extent of female migration resulting in this share's higher values in the districts where this migration is more widespread. But assessing this is not possible with the data provided.

Household Size

AC

Indicator overview

In rural areas, the number of household members is proportional to the labor endowment of a household, especially for household agricultural activities. Dependents, such as small children and elderly, decrease the possibility for higher household income and employment as they reduce per capita expenditures from the household income and require more social care, which is time and effort that could be spent on other work and income generating activities. Even though economies of scale would suggest that food consumption is not proportionally increasing with each household member, larger households with more dependents are in a more vulnerable situation given their restraints to income opportunities.

Moreover, large household size can negatively affect household access to and availability and quality of the safe drinking water, sanitation, and improved home facilities due to crowded conditions. This in turn is directly related to population well-being.

Methods overview

Household size was estimated from the data provided by households on their household composition. The data was taken from the QoL 2014 Survey where households were asked to provide information on the number of household members. The table provides data on the mean household size at the district and province levels. Standard deviation was measured to estimate variability in household size. Data from the DHS was also used, which provides information on household composition. The weighted mean household size was estimated at the province level.

Table 86. Mean household size by district.

Province	District	Code	Mean hh size	St Dev
Badakhshan	Baharak	1108	9.1	3.9
Badakhshan	Darwaz	1110	9	4.5
Badakhshan	Ishkashim	1107	10.6	5
Badakhshan	Jurm	1103	7.9	3.3
Badakhshan	Kuran Wa Munjan	1117	10.1	4.7
Badakhshan	Shighnan	1109	9	4.4
Badakhshan	Wakhan	1106	10.7	5.3
Badakhshan	Zebak	1105	9.8	4.7
Baghlan	Andarab	1307	8.5	3.7
Baghlan	Dahana-I-Ghori	1303	8.4	4.7
Baghlan	Doshi	1304	8	3.2
Baghlan	Kahmard	2803	8.9	3.6
Baghlan	Khinjan	1306	7.5	3.6
Baghlan	Tala Wa Barfak	1305	9.1	3.5
Bamyan	Bamyan City	2801	8.6	3.8
Bamyan	Shibar	2802	6.4	2.3
Takhar	Farkhar	1206	5.9	2.7
Takhar	Kalafgan	1207	6.6	3.1
Takhar	Rustaq	1208	6.9	3.4
Takhar	Taluqan	1201	6.6	2.8
Takhar	Warsaj	1205	6.2	2.6

Source: QoL

Table 87. Mean household size by province (QoL).

Province	Mean hh size	St Dev
Badakhshan	9.1	4.3
Baghlan	8.4	3.7
Bamyan	8.2	3.6
Takhar	6.6	3.1

Source: QoL

Table 88. Mean household size by province (DHS).

Province	Mean hh size
Badakhshan	7.5
Baghlan	7.3
Bamyan	7.9
Takhar	7.5
Kunduz	8.1

Source: DHS

Results summary

The results of the mean household size estimations from QoL and DHS show some differences that can be explained by different samples and weights of the datasets.

DHS data reports on the mean household size ranging from 7-8 persons among all observed provinces. According to the QoL data, the mean household size is estimated to be on average more than 8 people in the households of Baghlan and Bamyan provinces, in Takhar province the mean household size is 6-7 persons, while in Badakhshan mean household size is 9 persons per household. Standard deviation shows some, but not very high, variability in household size, which implies that the average household size is close to the mean. In some districts of Badakhshan province (e.g., Ishkashim, Kuran Wa Munjan, and Wakhan), the average household size exceeds 10 persons while the standard deviation estimate is also high representing higher variability in the numbers of persons among households. The smallest average households are registered in the districts of Takhar province, but are reported to be still large at 6 persons per household.

More people in the household can lead to a heavier burden on household income, reducing per capita funds and time and effort spent on non-income generating activities. Furthermore, larger household sizes result in crowding, which limits household members' access to sanitation, clean water, and home facilities. Also, larger households imply more expenditures on food, health, and other vital costs. Based on experience of Central Asian and many other developing countries, household size is almost always positively correlated with poverty rates at community, province, and national levels (Sattar et al. 2013).

Occupation of Household Members

AC

Indicator overview

Employment and earnings are key indicators of economic performance and are driving forces of economic development and social well-being. Human capital is an essential factor of labor productivity that requires improved health and skills of workers apart from the physical and institutional infrastructure, equipment, and technology. Earnings and employment-related income provide households with purchasing power and results in capacity for consumption of goods and services and the accrual of savings. This represents a measure of workers' standard of living and the quality of employment. In line with earnings, social protection also plays an important role in indicating quality of life, health security, and living conditions. Access to basic social security ensures primary health care and basic income security over the life cycle. From an inclusive employment perspective, women still tend to be underemployed, not equally paid, and limited in access to high-level decision-making positions, which constrains them from participating and influencing the economy and society and causes them to be unempowered. Additionally, unpaid housework and care provided mostly by women remains a major concern that must be addressed to build inclusive labor markets and advance the overall economy (ILO 2018).

Fighting unemployment is not the only concern for mitigating or eliminating vulnerability, since being employed does not guarantee the ability to escape from poverty. Poverty eradication is only possible through stable, well-paid, sustained, and inclusive employment. Human well-being goes far beyond vital livelihoods and requires social security, full and productive employment, and, importantly, decent work[7].

As a result, self-employment, work in the informal sector, daily wage earnings, and small and medium enterprises represent the highest risks of disruption and vulnerability for employees (UN Economic and Social Council 2020). This is because these sectors do not provide social protection, guarantees, or sustainable and stable incomes. This increases the vulnerability of employees and negatively impacts their living conditions.

Consequently, households with fewer occupations, unstable occupations, and occupations associated with little income generation likely have fewer opportunities to obtain necessary livelihoods, which reduces their adaptive capacity, resulting in higher vulnerability.

Methods overview

Occupation of household members was estimated from households' responses on the occupation of each household member. The data were taken from two data sources, QoL 2014 Survey and DHS 2015.

The QoL 2014 Survey includes data from participants who were asked to provide information on (i) the main occupation of the household members, and (ii) the second occupation of the household members from a list. The proposed occupations in the list included: (i) private sector employee, (ii) NGO employee, (iii) Government employee, (iv) daily wage earner (casual worker), (v) self-employed in non or off farm, (vi) agriculture, (vii) livestock, (viii) unemployed, job-seeking, (ix) housework, (x) student, (xi) retired, and (xii) other. To avoid calculating child labor and misrepresenting actual employment, all individuals aged 0-15 years and retired individuals were excluded from the sample. The table presents the shares of adults within three of the most commonly reported main occupations of the household members. Additional estimates include the share of individuals of all ages who are employed or study, and the share of individuals who reported to have a second occupation, including study. Other variables were calculated to estimate the shares of adults (excluding students) who reported to have both a primary job and a secondary job. The data were disaggregated at the district and province levels.

DHS data provides information on males' occupations at the province level. The table presents data on the share of males employed in particular sectors/positions and is disaggregated at the province level. Provincial disaggregation of the data for women is not available due to small numbers of respondents and an underrepresentation of women in the particular sector/position.

7. https://sdg-tracker.org/economic-growth

Results summary

Table 89. Adult employment and occupations by district.

Province	District	Code	% people all ages having main job or study	% people all ages having 2nd job or study	% Adults (>15 y.o.) reported their main occupation						% adults (>15 y.o.) having main job	% adults (>15 y.o.) having second job
Badakhshan	Baharak	1108	78%	46%	Housework	46.66	Agriculture	17.15	Self-employed in non or off farm	13.23	98%	58%
Badakhshan	Darwaz	1110	73%	55%	Housework	54.49	Agriculture	30.43	Government employee	5.8	96%	79%
Badakhshan	Ishkashim	1107	76%	31%	Housework	46.51	Agriculture	29.46	Self-employed in non or off farm	9.3	95%	29%
Badakhshan	Jurm	1103	80%	58%	Housework	45.43	Agriculture	20.93	Self-employed in non or off farm	9.93	96%	66%
Badakhshan	Kuran Wa Munjan	1117	73%	48%	Housework	43.1	Agriculture	31.03	Livestock	8.19	94%	67%
Badakhshan	Shighnan	1109	79%	46%	Housework	39.13	Agriculture	22.17	Government employee	11.52	96%	58%
Badakhshan	Wakhan	1106	74%	48%	Housework	49.82	Agriculture	32.86	Livestock	7.77	98%	61%
Badakhshan	Zebak	1105	79%	54%	Housework	48.57	Agriculture	39.05	Government employee	3.81	98%	57%
Baghlan	Andarab	1307	73%	27%	Housework	53.39	Agriculture	23.75	Government employee	7.82	95%	29%
Baghlan	Dahana-I-Ghori	1303	72%	18%	Housework	48.87	Agriculture	19.9	Self-employed in non or off farm	15.11	96%	24%
Baghlan	Doshi	1304	75%	20%	Housework	51.98	Agriculture	20.74	Self-employed in non or off farm	8.32	96%	27%
Baghlan	Kahmard	2803	74%	24%	Housework	48.51	Agriculture	29.42	Government employee	7.75	95%	36%
Baghlan	Khinjan	1306	77%	24%	Housework	51.25	Agriculture	15.3	Self-employed in non or off farm	11.03	94%	26%
Baghlan	Tala Wa Barfak	1305	75%	23%	Housework	50.29	Agriculture	21.05	Self-employed in non or off farm	9.75	95%	28%
Bamyan	Bamyan City	2801	74%	31%	Housework	51.4	Agriculture	29.69	Self-employed in non or off farm	4.93	96%	48%
Bamyan	Shibar	2802	75%	46%	Housework	47.18	Agriculture	34.51	No occupation	8.45	92%	59%
Takhar	Farkhar	1206	72%	18%	Housework	59.79	Agriculture	14.95	Livestock	9.79	99%	22%
Takhar	Kalafgan	1207	69%	16%	Housework	54.67	Agriculture	18.67	Daily wage earner (casual worker)	11.33	99%	17%
Takhar	Rustaq	1208	76%	15%	Housework	51.27	Agriculture	17.94	Self-employed in non or off farm	12.52	98%	17%
Takhar	Taluqan	1201	73%	27%	Housework	53.81	Agriculture	14.41	Self-employed in non or off farm	12.71	99%	22%
Takhar	Warsaj	1205	73%	12%	Housework	52.59	Agriculture	20	Daily wage earner (casual worker) / Self-employed in non or off farm	8.15	98%	12%

Source: QoL

Table 90. Adult employment and occupations by province.

Province	% adults (>15 y.o.) having main job	% adults (>15 y.o.) having second job	% Adults (>15 y.o.) reported their main occupation					
Badakhshan	96	65	Housework	45.96	Agriculture	24.74	Self-employed in non or off farm	7.09
Baghlan	95	30	Housework	51	Agriculture	22.23	Self-employed in non or off farm	8.5
Bamyan	95	52	Housework	50.73	Agriculture	30.46	Self-employed in non or off farm	4.7
Takhar	99	19	Housework	53.09	Agriculture	16.58	Self-employed in non or off farm	11.17

Source: QoL

Table 91. Male occupations by province.

Province	% Male occupation					
	Professional/ technical/ managerial	Clerical	Sales and services	Skilled manual	Unskilled manual	Agriculture
Badakhshan	10.8	0.5	6.8	7.1	29.9	45
Baghlan	15.3	3.7	19.9	21.8	10.8	28.5
Bamyan	6.6	1.6	8.7	7.9	20.9	54.3
Takhar	8.4	1.3	8.9	18.5	35.1	27.7
Kunduz	7.8	2.3	27.9	21.5	15.9	24.7

Source: DHS

Results summary

According to the data provided by the households of the QoL 2014 Survey, more than 95% of adults across all four observed provinces have a primary job, with more than 99% in Takhar province having a primary job. Having a second occupation is least represented in Takhar province with 19% of adults, and largest in Badakhshan province, where 65% of adults reported to have a second job.

About half of adult household members reported to be employed in housework. The second most popular occupation is agriculture, where 30% of adults in Bamyan, 24% of adults in Badakhshan, 22% of adults in Baghlan, and 17% of adults in Takhar are employed. The third most popular occupation of adult household members across all provinces is self-employed in non- or off-farm work. However, at the district level, the responses vary. The third post popular occupation among adults in Kuran Wa Munjan, Wakhan, and Farkhar districts reported to be in the livestock sector. In Darwaz, Shighnan, Zebak, Andarab, and Kahmard districts, the third most popular occupation is government employee. In Shibar district, about 8-9% of adults reported to not have any occupation. In Kalafgan and Warsaj districts of Takhar province, 11% and 8% of adults reported to be employed as casual workers with daily wage earnings, respectively.

DHS data on the males' occupation also suggest that most males are still employed in agriculture and unskilled manual labor. Kunduz and Baghlan provinces reported to have relatively high proportions of males employed in sales and the services sector (about 28% and 20%, respectively), and in skilled manual works (about 21-22%). Only a marginal share of males employed in professional/technical/managerial positions was reported with a relatively high proportion of 15.3 and 10.8 in Baghlan and Badakhshan provinces, respectively, and 6.6 in Bamyan province. The least represented employment sector is clerical, constituting the largest share of males at 3.7% in Baghlan province and the least at 0.5% in Badakhshan province.

Underrepresentation of women in overall employment is a particular concern. Although most working women reported to be employed in professional/technical/managerial, agriculture, and skilled manual occupations, the overall numbers are scarce. At the same time, within agriculture, empowering women through increases in their decision-making over agricultural production and incomes has been shown to improve both family health and nutrition outcomes (ICSU 2017).

The results of the analysis of household members' occupation reveals a high vulnerability of the population in the region. The vast majority of adults are employed in the agricultural sector or in unskilled manual jobs that do not provide sustained and well-paid earnings or social security. Moreover, the agricultural sector is highly dependent on suitable climate and seasonal weather conditions, which may not allow households to sustain their current income and livelihood level under climate change. Daily-wage earnings, work in the informal sector, or self-employment cannot ensure a stable income, decent working conditions, or help to improve a households' living conditions, which negatively impacts well-being and is risky and uncertain.

Community Livelihood Support Institutions

AC

Indicator overview

Community livelihood support institutions play a crucial role in local development. Local institutions work to meet the specific needs of the local population while respecting limits and local barriers. Livelihood support institutions can address needs at various levels, ranging from individual livelihoods to global causes of poverty. The local institutions and self-governance of communities are united by a shared reliance on a common resource given unique ecological and social conditions (Wahl 2016).

Community initiatives can help improve multiple dimensions of community well-being, including food security, healthcare, education, natural resource management, sustainable lifestyle and environment, inequality, and others.

From the perspective of food security, local institutions can contribute to sustainable food production by taking into account food sovereignty and agroecology, agricultural, social, culinary, and economic traditions. Through maintaining increased knowledge about growing food, they can assist with avoiding exploitative relationships between importers and exporters of food and reducing pollution due to transportation, processing, packaging, and preservation of food as well as promoting local jobs (Amate and Molina 2013).

From the perspective of healthcare, local institutions can take a more holistic approach to health and well-being, taking into account local lifestyles, the social and physical environment, and resource constraints, and thus provide higher level of overall health and well-being at lower financial and resource costs (Missoni 2015).

Reaching higher levels of quality education, local institutions can initiate activities and networks using ongoing emerging and fast-changing global learning processes, and can provision new skills and knowledge, taking into account local social organization and cultural specifications (Henfrey 2017). Institutions can accumulate globally acquired knowledge and practices and provide educational programs and trainings to meet the needs of the local society.

Community institutions are the best agents for action to facilitate water, land, and other natural resources management in a holistic way with respect to the specific local landscape, environment, and needs of the population . Local initiatives can promote a sustainable lifestyle through less energy-intensive and polluting settlements, at the same time meeting the needs of the local communities. Also, local production in food (Henfrey and Penha-Lopes 2015), energy and housing can reflect the social and environmental responsibility when considering climate change.

Finally, inequalities are best addressed by local community institutions. Inequalities can include those related to social and gender status and access to resources and public services, including education and healthcare.

Consequently, local institutions have transformative power to recognize and influence local population priorities and attitudes and to encourage change in behavior in favor of sustainable development and well-being and address local needs of the community (ICLEI 2015).

As a result, households with fewer community livelihood support institutions have fewer benefits and opportunities to obtain necessary livelihoods, which reduces their adaptive capacity and increases their sensitivity to climate change-related natural hazards resulting in their higher vulnerability.

Methods overview

Community livelihood support institutions were estimated through information on the number of institutions respondents have access to in the community. The data were taken from two surveys: QoL 2014 and the recent 2018 dataset of NSIA.

In the QoL 2014 Survey, respondents were asked about their membership or volunteering in groups or associations. The proposed list of groups and associations included: (i) Community Development Council (CDC)/CLDC, (ii) District Development Association (DDA), (iii) Parent-Teacher-Student Association (PTSA), (iv) School Management Committee (SMC), (v) Health/Hygiene committee, (vi) Agricultural cooperative(s), (vii) FFS and/or PTD, (viii) Livestock association, (ix) Non-formal vocational group, (x) Water user's association, (xi) Other Producer's Associations, (xii) Self-Help Group: Community Based Savings Groups, (xiii) Hashar, (xiv) Other shura (traditional organizations), (xv) Chamber of Commerce, and (xvi) Other. Respondents included separately both males and females who were asked to indicate their membership in each group/association from the list. The mean number of membership groups was calculated separately for males and females at the district and province levels. Standard deviation estimates were included to represent the variability of the numbers of groups in which males or females participate. In addition, the three most popular groups or associations were determined. The table presents data on the mean number of groups on which males and females reported their membership, standard deviations of the mean at the district and province levels, and the percentage participation of males and females in the three most reported groups at the district level.

NSIA data provide information for 2018 on the absolute numbers of basic and comprehensive medical centers, pharmacies, medical personnel, and medical professionals, hospitals, beds, post offices, fixed telephones (for 2017), users of family planning, and medical doctors specialists (for 2017). The absolute numbers of the above facilities and medical staff at the province levels were then divided by the provincial population of 2018 and 2017 accordingly and calculated per 100,000 people to represent the availability of and access to public services and facilities. The table represents the numbers per 100,000 people at the province level.

Summary tables of indicator by district and province

Table 92. Male participation in community groups or associations by district.

Province	District	Code	MALES participation in the community groups or associations							
			Mean no of groups	Std. Dev.	Group	Percent	Group	Percent	Group	Percent
Badakhshan	Baharak	1108	2.47	2.3	Hashar	89	Other shura (traditional organizations)	36	Community Development Council	32
Badakhshan	Darwaz	1110	1.49	1.2	Hashar	87	Other shura (traditional organizations)	17	Community Development Council	15
Badakhshan	Ishkashim	1107	3.8	3.4	Hashar	100	Community Development Council	48	Health/Hygiene committee	36
Badakhshan	Jurm	1103	1.73	1.3	Hashar	94	Other shura (traditional organizations)	39	Community Development Council	15
Badakhshan	Kuran Wa Munjan	1117	1.66	1.1	Hashar	96	Community Development Council	19	Other shura (traditional organizations)	16
Badakhshan	Shighnan	1109	2.2	1.5	Hashar	96	Other shura (traditional organizations)	44	Community Development Council	26
Badakhshan	Wakhan	1106	3.86	2.8	Hashar	96	Community Development Council	54	Other shura (traditional organizations)	42
Badakhshan	Zebak	1105	3.16	2.9	Hashar	94	Other shura (traditional organizations)	96	Community Development Council	36
Baghlan	Andarab	1307	1.94	1.6	Hashar	69	Other shura (traditional organizations)	29	Community Development Council	27
Baghlan	Dahana-I-Ghori	1303	1.03	1.3	Hashar	49	Community Development Council	21	Other shura (traditional organizations)	7
Baghlan	Doshi	1304	1.63	1.8	Hashar	56	Community Development Council	35	Other shura (traditional organizations)	12
Baghlan	Kahmard	2803	1.82	1.5	Hashar	90	Other shura (traditional organizations)	23	Community Development Council	23
Baghlan	Khinjan	1306	2.07	1.7	Hashar	84	Other shura (traditional organizations)	40	Community Development Council	36
Baghlan	Tala Wa Barfak	1305	1.99	1.4	Hashar	85	Other shura (traditional organizations)	33	Community Development Council	30
Bamyan	Bamyan City	2801	1.61	1.2	Hashar	83	Community Development Council	21	Other shura (traditional organizations)	17
Bamyan	Shibar	2802	1.26	0.8	Hashar	98	Community Development Council	7	Self Help Group	7
Takhar	Farkhar	1206	1.68	1.1	Hashar	80	Other shura (traditional organizations)	45	Community Development Council	28
Takhar	Kalafgan	1207	1.96	1.3	Hashar	89	Other shura (traditional organizations)	52	Community Development Council	22
Takhar	Rustaq	1208	1.54	1.3	Hashar	74	Community Development Council	28	Other shura (traditional organizations)	23
Takhar	Taluqan	1201	1.61	1.3	Hashar	79	Other shura (traditional organizations)	42	Community Development Council	20
Takhar	Warsaj	1205	1.48	1.6	Hashar	55	Community Development Council	38	District Dev Ass / Agricultural cooperative(s)	12

Source: QoL

Table 93. Female participation in community groups or associations by district.

Province	District	Code	FEMALES participation in the community groups or associations							
			Mean no of groups	Std. Dev.	Group	Percent	Group	Percent	Group	Percent
Badakhshan	Baharak	1108	1.33	1.8	Women's shura	46	Self Help Group	25	Health/Hygiene committee	12
Badakhshan	Darwaz	1110	1.04	0.7	Women's shura	86	Community Development Council	7	Hashar	5
Badakhshan	Ishkashim	1107	2.88	2.2	Women's shura	84	Health/Hygiene committee	48	Self Help Group / Other shura	28
Badakhshan	Jurm	1103	0.85	1.1	Women's shura	36	Non-formal vocational group	17	Self Help Group	15
Badakhshan	Kuran Wa Munjan	1117	1	0.8	Women's shura	80	Community Development Council	7	Non-formal vocational group	4
Badakhshan	Shighnan	1109	1.13	0.7	Women's shura	89	Self Help Group	10	Non-formal vocational group	4
Badakhshan	Wakhan	1106	2.44	1.8	Women's shura	98	Other shura (traditional organizations)	38	Community Development Council	30
Badakhshan	Zebak	1105	3.12	2.6	Women's shura	84	Health/Hygiene committee	60	Other shura	36
Baghlan	Andarab	1307	0.64	0.6	Women's shura	51	Non-formal vocational group	4	Community Development Council	2
Baghlan	Dahana-I-Ghori	1303	0.3	0.5	Women's shura	24	Self Help Group	2	Parent-Teacher-Student Associations	2
Baghlan	Doshi	1304	0.97	0.9	Women's shura	56	Community Development Council	13	Self Help Group	9
Baghlan	Kahmard	2803	0.27	0.7	Women's shura	12	Community Development Council	10	Hashar	2
Baghlan	Khinjan	1306	1.08	0.7	Women's shura	79	Self Help Group	11	Community Development Council	7
Baghlan	Tala Wa Barfak	1305	0.71	0.6	Women's shura	64	Hashar	3	Community Development Council	2
Bamyan	Bamyan City	2801	0.75	0.9	Women's shura	40	Self Help Group	14	Community Development Council	12
Bamyan	Shibar	2802	0.82	0.7	Women's shura	64	Parent-Teacher-Student Associations	6	Hashar/HealthHygiene committee	4
Takhar	Farkhar	1206	0.33	0.7	Women's shura	12	Other Producer's Association	5	Others	3
Takhar	Kalafgan	1207	0.22	0.4	Women's shura	14	Health/Hygiene committee	6	Other Producer's Association	2
Takhar	Rustaq	1208	0.27	0.6	Women's shura	13	Health/Hygiene committee	5	Hashar	4
Takhar	Taluqan	1201	0.1	0.3	Women's shura	5	Other Producer's Association	4	Self Help Group	1
Takhar	Warsaj	1205	0.66	1	Women's shura	14	Self Help Group	14	Hashar/HealthHygiene committee	12

Source: QoL

APPENDICES

Table 94. Participation in groups or associations by sex and province.

Province	MALES participation in the community groups or associations		FEMALES participation in the community groups or associations	
	Mean number of groups per hh	Std. Dev.	Mean number of groups per hh	Std. Dev.
Badakhshan	2.18	2	1.3	1.5
Baghlan	1.75	1.6	0.7	0.8
Bamyan	1.54	1.1	0.8	0.9
Takhar	1.6	1.3	0.2	0.6

Source: QoL

Table 95. Health facilities per capita by province.

Province	Numbers per 100,000 of population										
	Basic med centers	Compreh. med centers	Pharmacies	Med personel	Med profess	Hospitals	Beds	Post offices	Fixed tel.	Users of Family planning	MD specialists
Badakhshan	3.14	1.38	17.3	9.53	51.79	0.29	28.5	2.85	840.53	4963.54	1.32
Baghlan	2.46	1.74	35.71	11.36	47.17	0.31	32.64	1.53	1596.26	3260.83	1.7
Bamyan	4.81	2.09	17.98	16.09	84.65	0.84	51.21	1.67	136.54	5589.81	1.95
Kunduz	3.02	1.19	38.31	10.81	46.83	0.37	35.01	0.82	1028.93	3564.97	1.33
Takhar	3.42	1.14	28.94	12.43	44.12	0.47	25.72	1.99	266.02	2988.84	1.18

Source: NSIA

Results summary

Both men and women of Badakhshan province reported their largest participation in community groups or associations among the four observed provinces (mean of 2.18 groups for men and 1.3 groups for women). Men of other provinces reported their participation on average in at least 1-2 groups, while women of Bamyan, Baghlan and Takhar provinces reported lower participation in local groups, with an average membership in 0.8, 0.7, and 0.2 groups respectively. Thus, a substantial number of women do not participate in any local groups or associations.

Men who participated most are in Wakhan, Ishkashim, and Zebak districts of Badakhshan province, with average memberships in 3.86, 3.8, and 3.16 groups, respectively. Male membership in the fewest groups was reported in Dahana-I-Ghori district of Baghlan province, where men reported to participate on average in one group. The most popular group for men was reported to be Hashar in all districts, with variation of participation from at least more than half and up to 100% of men. The second and third most popular groups for male participation were Shuhra (traditional organization) and the Community Development Council (CDC)/CLDC in all districts. The only exceptions were reported by men of Ishkashim district, where the third most popular group was the Health/Hygiene committee (36% of men reported membership), Shibar district, where the third most popular group was the Self-Help Group: Community Based Savings Group (7% of men reported membership), and Warsaj district, where the third most popular groups were the District Development Association and Agricultural cooperative(s) (12% of men reported membership).

Women reported much less participation in the local groups or associations, and these numbers varied greatly among provinces. The most popular group for women among all districts was the women's Shuhra, accounting for the largest participation of 80-90% of women in Badakhshan province and the least participation of around 10% of women in Takhar province. The other group that reported the largest female participation is the Self-Help Group: Community Based Saving Group, with the largest participation of women of 25% in Baharak district, 28% of women in Ishkashim, and 15% of women in Jurm (all of Badakhshan province). The third most popular group is the Community Development Council, with the largest participation of 30% of women in Wakhan district of Badakhshan province, 13% and 10% of women in Doshi and Kahmard districts (both of Baghlan province), respectively, and 12% of women in Bamyan city.

Health/Hygiene Committee is another well-represented group for 60% of women in Zebak and 48% of women in Ishkashim districts, both of Badakhshan province. Although the groups vary among provinces on the number of participating women, there are several more groups popular among females, including other Shuhra (traditional organization), Non-formal Vocational Group, and Hashar.

The data show that the most popular local group for men is Hashar and for women is Women's Shuhra. Men are more represented in the membership of the Community Development Councils and other Shuhra (traditional organizations), while women are more represented in Self-Help Groups: Community Based Savings Group and Health/Hygiene Committee in some districts. Overall, female participation in the local groups and associations is not universal and is not as extensive as for men. Women are underrepresented both in the membership of particular groups and in the quantity of groups in general.

According to the NSIA data, Bamyan province has the most medical centers among the five observed provinces with 4.8 basic and 2.1 comprehensive per 100,000 people, while Badakhshan, Bamyan, and Takhar provinces have on average 3 basic and 1 comprehensive centers per 100,000 people. The proportion of medical personnel, medical professionals, hospitals, beds, users of family planning, and MD specialists are also substantially larger in Bamyan province. Badakhshan province reports the largest number of post offices at 2.85 per 100,000 people, Baghlan province reports the largest number of fixed telephones at 1596.3 per 100,000 people, and Kunduz province reports the largest number of pharmacies at 38.3 per 100,000 people. Although it is difficult to estimate the availability and accessibility of medical facilities, medical staff, and public services for each household of the province, the numbers per 100,000 people are relatively low, which raises concerns about the scarcity of essential services provided by local institutions for community life and well-being.

Underrepresentation of women in the local groups and associations highlights their likely limitations to access to decision-making and lower accountability of their interests and needs, which constrains their sustainable livelihoods and raises their vulnerability. The scarce medical services and facilities can result in poor well-being and restricted opportunities for households to improve their livelihoods and build a sustainable community. Limited access to basic health and communication services reduces adaptive capacity of the households and their ability to mitigate shocks, which raises their vulnerability.